# Phytochemical Studies of Bornean Myristicaceae and

# Clusiaceae Species and Evaluation of their

## **Antibacterial and Anticancer Activities**

by

## Maya Dawn Valmiki

University of East Anglia

Norwich Research Park, Norwich NR4 7TJ



Supervisor: Professor A. Ganesan

Second Supervisor: Dr. Pedro Ernesto de Resende

Thesis for the degree of Doctor of Philosophy

June 2025

© This copy of the thesis has been supplied on condition that anyone who consults it is understood to recognise that its copyright rests with the author and that use of any information derived therefrom must be in accordance with current UK Copyright Law. In addition, any quotation or extract must include full attribution.

## **Abstract**

Bacterial antimicrobial resistance has emerged as one of the most pressing global health threats. The inappropriate use of antibiotics has led to the growing ineffectiveness of many frontline treatments, escalating the need for novel therapeutic agents. Amongst the most promising, yet underexplored, sources of such agents are plant natural products, particularly those derived from biodiverse ecosystems, like the tropical rainforests of Borneo. These rainforests host a wealth of ethnomedicinal plants, traditionally used to treat infections and cancers, inferring a potential source for bioactive compounds. However, despite their cultural and medicinal significance, their phytochemical and pharmacological profiles remain largely uncharacterised.

This thesis presents the isolation, structural elucidation and biological evaluation of secondary metabolites from three previously unexplored Bornean plant species: Knema membranifolia, Gymnacranthera contracta (Myristicaceae) and Garcinia caudiculata (Clusiaceae). Here, chromatographic separation spectroscopic techniques (MS, 1D/2D NMR) were used to characterise one previously undescribed salicylic acid derivative, and twelve known phytochemicals, including seven additional salicylic acid-related compounds, two acetophenones, a resorcinol, a tocopherol derivative, and a fatty acid from the Myristicaceae family. From the Clusiaceae family, one previously undescribed hydroquinone methyl ester and five known metabolites were identified: a benzofuranone lactone, a flavonoid glycoside, a polyphenol, and two tocopherol derivatives. Several isolated compounds exhibited promising antibacterial effects, with compound 2.4 showing the most potent bactericidal activity against methicillin-resistant Staphylococcus aureus with an MIC of 2 μg/mL. In addition, compounds were assessed for their in vitro antifungal and anticancer activities.

In summary, this research identifies nineteen metabolites, including two new natural products (a salicylic acid derivative and a meroterpene named caudiquinol), from three chemically unresearched rainforest species, including *Knema membranifolia*, *Gymnacranthera contracta* and *Garcinia caudiculata*. Several compounds demonstrated significant antibacterial activity, particularly against drugresistant bacteria, evidencing the therapeutic potential of these plant species and their genera in modern medicine, particularly in the age of antimicrobial resistance.

#### **Access Condition and Agreement**

Each deposit in UEA Digital Repository is protected by copyright and other intellectual property rights, and duplication or sale of all or part of any of the Data Collections is not permitted, except that material may be duplicated by you for your research use or for educational purposes in electronic or print form. You must obtain permission from the copyright holder, usually the author, for any other use. Exceptions only apply where a deposit may be explicitly provided under a stated licence, such as a Creative Commons licence or Open Government licence.

Electronic or print copies may not be offered, whether for sale or otherwise to anyone, unless explicitly stated under a Creative Commons or Open Government license. Unauthorised reproduction, editing or reformatting for resale purposes is explicitly prohibited (except where approved by the copyright holder themselves) and UEA reserves the right to take immediate 'take down' action on behalf of the copyright and/or rights holder if this Access condition of the UEA Digital Repository is breached. Any material in this database has been supplied on the understanding that it is copyright material and that no quotation from the material may be published without proper acknowledgement.

# **Table of Contents**

Abstract		ii
Table of Content	S	iii
List of Figures		ix
List of Tables		xiii
List of Abbreviati	ions	xvi
Acknowledgeme	nts	xix
Conferences and	l Publications	XX
Chapter 1 – Intr	oduction	1
1.1. Natural	Product Drug Discovery	1
1.1.1. His	storical significance of terrestrial natural products	1
1.1.2. Eco	ological role of natural products – structural evolution	3
1.1.3. Maj	jor plant- derived bioactive compounds	6
1.2. The Glo	bal Burden of Microbial Infections	11
1.2.1. Ant	timicrobial resistance (AMR) – the need for new antimicrobial ag	ents11
1.2.1.1.	Significance of bacterial and fungal infections	11
1.2.1.2.	Antimicrobial resistance acquisition	12
1.2.1.3.	Antimicrobial resistance strategies: four biochemical mechanic	sms 14
1.2.1.4.	Resolving antimicrobial resistance	18
1.2.2. Clir	nically relevant bacterial species	19
1.2.2.1.	Staphylococcus aureus	19
1.2.2.2.	Enterococcus faecalis	19
1.2.2.3.	Escherichia coli	20
1.2.2.4.	Klebsiella pneumonia	20
1.2.2.5.	Salmonella enterica	21
1.2.2.6.	Pseudomonas aeruginosa	21
1.2.3. Clir	nically relevant fungal species	22
1.2.3.1.	Aspergillus fumigatus	22
1.2.3.2.	Candida albicans	23

1.3. T	Γhe Glo	bal Burden of Cancer	23
1.3.1.	. Leı	ukaemia	24
1.3.2.	. Lu	ng cancer	25
1.3.3.	. Me	lanoma	26
1.4. F	Plant Fa	amilies Used in This Study – Myristicaceae and Clusiaceae	26
1.4.1.	. My	risticaceae family	26
1.4	.1.1.	Distribution and botanical characterisation	26
1.4	.1.2.	Ethnomedicinal value	28
1.4	.1.3.	Phytochemical investigations	29
1.4.2.	. Clu	ısiaceae family	29
1.4	.2.1.	Distribution and botanical characterisation	29
1.4	.2.2.	Ethnomedicinal value	30
1.4	.2.3.	Phytochemical investigations	31
1.5. A	Aims ar	nd Objectives of Thesis	31
1.5.1.	. Air	n	31
1.5.2.	. Ob	jectives	32
1.6. F	Referer	nces	33
Chapter 2	2 – Lite	erature Review on Plant Species Sampled from Borneo -	Direction
of Future	Work		38
2.1. E	Biodive	ersity of Borneo – Myristicaceae and Clusiaceae	38
2.2. N	Myristi	caceae Species	41
2.2.1.	. Но	rsfieldia Genus (Myristicaceae)	41
2.2	2.1.1.	Horsfieldia Summary	45
2.2.2.	. Gyr	mnacranthera Genus (Myristicaceae)	46
2.2	2.2.1.	Gymnacranthera Summary	49
2.2.3	. Kn	ema Genus (Myristicaceae)	49
2.2	2.3.1.	Knema Summary	55
2.2.4.	. <i>My</i>	ristica Genus (Myristicaceae)	55
2.2.5.	. <i>My</i>	ristica summary	62

2.3.	Myri	sticaceae Family Summary	66
2.4.	Clus	siaceae Family	67
2.4	.1.	Garcinia genus (Clusiaceae)	67
2	2.4.1.1	. Garcinia Summary	80
2.4	1.2.	Mesua Genus (Clusiaceae)	81
2.4	1.3.	Kayea Genus (Clusiaceae)	82
2	2.4.3.1	. Kayea (Clusiaceae) Summary	85
2.4	1.4.	Calophyllum Genus (Calophyllaceae)	85
2	2.4.4.1	. Calophyllum (Clusiaceae) Summary	89
2.4	<b>.</b> .5.	Mammea Genus (Clusiaceae)	89
2.5.	Clus	siaceae Summary	. 100
2.6.	Myri	sticaceae and Clusiaceae Pharmacological Relevance	. 100
2.7.	Refe	rences	. 101
Chapte	er 3 – 1	Material and Methods	.113
3.1.	Lite	cature Review	.113
3.2.	Plan	t Material	. 113
3.2	2.1.	Myristicaceae plant species	.114
3.2	2.2.	Clusiaceae plant species	. 115
3.3.	Extr	action Processes	. 115
3.3	3.1.	Sequential plant extraction	.115
3	3.3.1.1	. Small scale	. 115
3	3.3.1.2	Large scale	. 116
3.3	3.2.	Non-sequential plant extraction	. 116
3.4.	Chro	omatographic Techniques	.116
3.4	.1.	Thin layer chromatography (TLC)	.116
3.4	.2.	Vacuum liquid chromatography (VLC)	. 117
3.4	.3.	Analytical High Performance Liquid Chromatography (HPLC)	.117
3.4	.4.	Preparative Thin Layer Chromatography (prep TLC)	.118
3.4	l.5.	Recycling preparative HPLC	.119

3.5. Sp	ectroscopic Methods for Structure Elucidation	119
3.5.1.	Liquid Chromatography Mass Spectrometry (LC-MS)	119
3.5.2.	Nuclear Magnetic Resonance spectroscopy (NMR)	120
3.5.3.	Infrared (IR) spectroscopy	121
3.5.4.	Ultraviolet-visible (UV-Vis) spectroscopy	122
3.5.5.	X-ray crystallography	122
3.5.5	.1. Crystallisation	123
3.5.5	.2. Single Crystal X-ray Diffraction (SCXD)	123
3.6. Bio	ological Evaluation	123
3.6.1.	Maintenance of bacterial strains	123
3.6.1	.1. Bacterial strains and growth conditions	123
3.6.1	.2. Cryopreservation	125
3.6.2.	Minimum Inhibitory Concentration (MIC) Determination	125
3.6.3.	Minimum Bactericidal Concentration (MBC) determination	127
3.6.4.	Inhibition Zone Determination – Disc Diffusion Assay	128
3.6.5.	AlamarBlue Assays	128
3.6.5	.1. Cancer Cell Cytotoxicity Assay	129
3.6.5	.2. Fungal Cell Cytotoxicity Assay	129
3.7. Re	ferences	130
Chapter 4 -	- Isolation, Structure Elucidation and Biological Activities of	Secondary
Metabolites	s from Myristicaceae	132
4.1. Int	roduction	132
4.1.1.	Knema membranifolia H.J.P.Winkl.	132
4.1.2.	Gymnacranthera contracta Warb	132
4.2. Re	sults and Discussions	133
4.2.1.	Structure elucidation - Knema membranifolia	133
4.2.1	.1. $6\Omega$ -Phenylalkylsalicylic acid, 10 carbon decyl linker, (4.1,	known)133
4.2.1	.2. $6\Omega$ -Phenylalkylsalicylic acid, 12 carbon decyl linker, (4.2,	known)136
4.2.1	.3. $6\Omega$ -Phenylalkylsalicylic acid, 16 carbon decyl linker, (4.3,	new) 140

6-Alkylacetophenone, 8 carbon phenyloctyl linker, (4.4, known)	143
6-Alkylacetophenone, 10 carbon phenyldecyl linker (4.5, known)	146
6-Alkylresorcinol, 10 carbon phenyldecyl linker (4.6, known)	149
acture elucidation - Gymnacranthera contracta	151
α-tocopherol quinone (4.7, known, isolation one)	151
Methyl oleate (4.8, known)	155
ni-purified Knema membranifolia fractions	157
Fraction 1 ( <b>4.1</b> / <b>4.9</b> )	157
Fraction 2 ( <b>4.10</b> / <b>4.11</b> )	162
Fraction 3 ( <b>4.11</b> / <b>4.12</b> )	167
Fraction 4 ( <b>4.13</b> / <b>4.14</b> )	170
nclusion	174
synthetic pathway of <i>Knema</i> compounds	174
logical activities of isolated compounds	177
Antibacterial Activities of Isolated Myristicaceae Compounds	178
Conclusion	184
Anticancer Activities of Isolated Myristicaceae Compounds	184
Conclusion	193
Antifungal Activities of Isolated Myristicaceae Compounds	193
Previous reports of biological activities	194
ces	194
ation, Structure Elucidation and Biological Activities of Second	lary
m Clusiaceae	198
ction	198
rcinia caudiculata Ridl./Garcinia grahamii Pierre	198
and Discussions	198
ucture elucidation - Garcinia caudiculata	198
5-hydroxy-7-(3,7,11,15-tetramethylhexadeca-2,6,10,11-tetraenyl- zofuranone (5.1, known)	
Caudiquinol (5.2, new)	202
	6-Alkylacetophenone, 10 carbon phenyldecyl linker (4.5, known) 6-Alkylresorcinol, 10 carbon phenyldecyl linker (4.6, known) 6-Alkylresorcinol, 10 carbon phenyldecyl linker (10 carbon phenyldec

5.2.1.3.	Alpha tocopherol quinone (4.7, known, isolation two)	207
5.2.1.4.	α-tocopherol (5.3, known)	208
5.2.1.5.	Isovitexin (5.4, known)	210
5.2.1.6.	Chlorogenic acid (5.5, known)	213
5.2.1.7.	Dioctyl phthalate – contaminant	217
5.2.2. Co	nclusion	220
5.2.3. Bio	synthetic pathway of Caudiquinol	220
5.2.4. Bio	logical activities of isolated compounds	223
5.2.4.1.	Antibacterial activities of isolated Clusiaceae compounds	223
5.2.4.2.	Anticancer activities of isolated Clusiaceae compounds	224
5.2.4.3.	Antifungal Activities of Isolated Clusiaceae Compounds	226
5.2.4.4.	Previous reports of biological activities	226
5.3. Conclus	sion	229
5.4. Referen	ces	230
Chapter 6 – Con	clusions	233
6.1. Future Ou	tlooks	239
Appendices		241
Appendix A: S	pectral data of natural products isolated from Myristicaceae	241
Appendix B: S	pectral data of natural products isolated from Garcinia	
caudiculata		277
Appendix C: B	iological evaluation of isolated compounds	291
Appendix D: P	ublished paper on newly reported <i>G. caudiculata</i> compounds	295

# List of Figures

Figure 1.1. Examples of specialised bioactive plant secondary metabolites5
Figure 1.2. Illustrations of mechanisms of horizontal gene transfer
Figure 1.3. Illustration of Gram-positive and Gram-negative cell wall structures15
<b>Figure 1.4.</b> The fruits, stems and leaves of <i>Myristica fragrans</i> (Myristicaceae)28
<b>Figure 1.5.</b> The fruits, stems and leaves of <i>Garcinia xanthochymus</i> (Clusiaceae)30
Figure 2.1. Taxonomic summary of 44 Bornean species of interest
<b>Figure 2.2.</b> Chemical structure of <b>1</b> isolated from <i>Horsfieldia grandis</i> (Hook. <i>f.</i> ) Warb.
Figure 2.3. Chemical structures of 2 and 3 isolated from Horsfieldia polyspherula45
<b>Figure 2.4.</b> Chemical structures of <b>4</b> and <b>5</b> isolated from <i>Gymnacranthera ocellata</i> R.T.A. Schouten
<b>Figure 2.5.</b> Chemical structures of <i>K. furfuracea</i> metabolites, including (A) lignans: 6, 7 and 8; (B) isoflavone 9 and (C) phenolic compounds 10 and 11
Figure 2.6. Chemical structures of (A) diterpene acid 12, (B) phenolic compounds 13, 14 and 15, (C) lignan, 16 and (D) flavan 17 isolated from <i>Knema glauca</i> (Blume) Warb.
<b>Figure 2.7.</b> Chemical structures of chlorophyll derivatives <b>18, 19, 20</b> and <b>21</b> isolated from <i>Knema curtisii</i> (King) Warb
<b>Figure 2.8.</b> Chemical structures of <b>(A)</b> acylphenol compounds <b>22</b> – <b>29</b> and <b>(B)</b> sitosterol ester <b>30</b> isolated from <i>Myristica maxima</i> Warb
Figure 2.9. Chemical structures of ω-phenyl fatty acids 31 – 33 isolated from Myristica villosa Warb60
<b>Figure 2.10.</b> Chemical structures of <b>(A)</b> amides <b>34</b> and <b>35</b> ; <b>(B)</b> flavone <b>36</b> , and <b>(C)</b> lignan <b>37</b> isolated from isolated from <i>Myristica lowiana</i> King
<b>Figure 2.11.</b> Chemical structures of xanthone <b>38</b> and triterpene <b>39</b> isolated from <i>Garcinia maingayi</i> Hook. <i>f.</i>
<b>Figure 2.12.</b> Chemical structures of <b>(A)</b> xanthones <b>40</b> – <b>42, 45</b> – <b>52, 63</b> and <b>65</b> ; <b>(B)</b> phloroglucinols <b>53</b> – <b>55</b> ; <b>(C)</b> depsidones <b>43, 44, 56, 57</b> ; <b>(D)</b> quinones <b>58</b> and <b>59 (E)</b>

flavonoid <b>60</b> ; ( <b>F</b> ) sterol <b>61</b> ; ( <b>G</b> ) triterpene <b>62</b> and ( <b>H</b> ) polycyclic polyprenylated acylphloroglucinol <b>64</b> , isolated from <i>Garcinia parvifolia</i> (Miq.)74
Figure 2.13. Chemical structures of (A) triterpenes 66 – 71; (B) flavonoids 72 and 73; (C) sesquiterpene, 74; (D) xanthones 75 – 80, 83 and (E) phenolic compounds 81 and 82, isolated from <i>Garcinia hombroniana</i> Pierre.
<b>Figure 2.14.</b> Chemical structures of xanthones <b>84</b> – <b>88</b> isolated from <i>G. penangiana</i> Pierre
Figure 2.15. Chemical structures of (A) benzophenones 89, 90 and 95; (B) xanthones 93 and 94; (C) sterol 91 and (D) fatty acid methyl ester 92, isolated from <i>Garcinia benthamiana</i> (Planch & Thiana) Pipoly
<b>Figure 2.16.</b> Chemical structures of coumarins <b>96</b> – <b>99</b> , isolated from <i>Kayea borneensis</i> P.F. Stevens.
<b>Figure 2.17.</b> Chemical structures of the chromanone acid <b>100</b> isolated from <i>Kayea</i> calophylloides P.F. Stevens
<b>Figure 2.18.</b> Chemical structures of <b>(A)</b> triterpenes <b>100</b> – <b>104</b> and <b>(B)</b> xanthone <b>105</b> , isolated from <i>Kayea myrtifolia</i> Baill.
Figure 2.19. Chemical structures of (A) coumarins 106 and 109; (B) xanthones 108, 110 – 113; (C) benzofuran 114; (D) phloroglucinols 115 and 116 and (E) terpene 107, isolated from <i>Calophyllum soulattri</i> Burm. Ex F.Mull
<b>Figure 2.20.</b> Chemical structures of chromanone acids <b>117</b> and <b>118</b> isolated from Calophyllum castaneum P.F. Stevens
Figure 2.21. Chemical structures of xanthones 119 and 12090
<b>Figure 3.1.</b> Locations within Sarawak on the island of Borneo where plant specimens were sampled from
Figure 3.2. Illustration of the broth microdilution assay used to determine the MIC.127
<b>Figure 4.1.</b> Chemical structures of lauric acid ( <b>a</b> ) and myristic acid ( <b>b</b> ) isolated from <i>Gymnacranthera contracta</i> Warb
Figure 4.2. COSY and HMBC correlations of compound 4.1
Figure 4.3. Mass spectrum of compound 4.1
<b>Figure 4.4.</b> Single crystal X-ray diffraction image generated of <b>4.2</b>
Figure 4.5. COSY and HMBC correlations of compound 4.2

Figure 4.6. Mass spectrum of compound 4.2.	140
Figure 4.7. COSY and HMBC correlations of compound 4.3.	141
Figure 4.8. Mass spectrum of compound 4.3.	143
Figure 4.9. COSY and HMBC correlations of compound 4.4.	144
Figure 4.10. Mass spectrum of compound 4.4.	146
Figure 4.11. Key COSY and HMBC correlations of compound 4.5.	147
Figure 4.12. Mass spectrum of compound 4.5.	148
Figure 4.13. COSY and HMBC correlations of compound 4.6	150
Figure 4.14. Mass spectrum of compound 4.6.	151
Figure 4.15. Structure of compound 4.7.	153
Figure 4.16. Mass spectrum of compound 4.7.	154
Figure 4.17. Structure of compound 4.8.	156
Figure 4.18. Mass spectrum of compound 4.8.	157
Figure 4.19. Structure of 4.9, with key COSY and HMBC correlations	159
Figure 4.20. <sup>1</sup> H NMR spectrum of 4.1/4.9 fraction.	161
Figure 4.21. Compound 4.9 mass spectrum in 4.1/4.9 fraction	161
Figure 4.22. Compound 4.1 mass spectrum in 4.1/4.9 fraction.	162
Figure 4.23. Structures of 4.10 and 4.11, with key COSY and HMBC correlations	164
Figure 4.24. Compound 4.11 mass spectrum in fraction 4.10/4.11	165
Figure 4.25. Compound 4.11 mass spectrum in fraction 4.10/4.11	166
Figure 4.26. Compound 4.10 mass spectrum in fraction 4.10/4.11	166
Figure 4.27. Compound 4.10 mass spectrum in fraction 4.11/4.12.	167
Figure 4.28. Structure of 4.12, with key COSY and HMBC correlations	168
<b>Figure 4.29.</b> Compound <b>4.11</b> mass spectrum in fraction <b>4.11/4.12</b>	169

<b>Figure 4.30.</b> Compound <b>4.12</b> mass spectrum in fraction <b>4.11</b> / <b>4.12</b>	.70
<b>Figure 4.31.</b> Compound <b>4.10</b> mass spectrum in fraction <b>4.11/4.12</b>	.70
Figure 4.32. Structures of 4.13 and 4.14, with key COSY and HMBC correlations 1	.72
<b>Figure 4.33.</b> Compound <b>4.13</b> mass spectrum in fraction <b>4.13</b> / <b>4.14</b>	.73
<b>Figure 4.34.</b> Compound <b>4.14</b> mass spectrum in fraction <b>4.13</b> / <b>4.14</b>	.74
Figure 4.35. Proposed biosynthesis of <i>Knema</i> phenyl-alkyl compounds1	.76
<b>Figure 4.36.</b> Dose-response curves of compounds <b>4.2</b> , <b>4.3</b> and <b>4.6</b> against A549 lung cancer cells in comparison to cisplatin	
Figure 5.1. Key COSY and HMBC correlations of compound 5.1	200
Figure 5.2. Mass spectrum of compound 5.1.	202
<b>Figure 5.2a.</b> Structures of known plant meroterpenoids, other than <b>5.1</b> and <b>5.1</b> , with an intact geranylgeranyl sidechain.	
Figure 5.3. Key COSY and HMBC correlations of compound 5.2	205
Figure 5.4. Mass spectrum of compound 5.2.	207
Figure 5.5. IR spectrum of compound 5.2.	207
Figure 5.6. Structure of compound 5.3	208
Figure 5.7. Key COSY and HMBC correlations of compound 5.4	:11
Figure 5.8. Mass spectrum of compound 5.4.	13
Figure 5.9. COSY correlations of compound 5.5	:15
Figure 5.10. Mass spectrum of compound 5.5.	:16
Figure 5.11. UV spectrum of compound 5.5	:16
Figure 5.12. Structure of the contaminant dioctyl phthalate2	<u>2</u> 19
<b>Figure 5.13.</b> Mass spectrum of <i>Bis</i> (2-ethylhexyl) phthalate	220
<b>Figure 5.14.</b> Proposed biosynthetic route of Caudiquinol ( <b>5.2</b> )	222

# List of Tables

Table 1.1. Plant derived compounds and their structures which are marketed as      antimicrobial agents.
Table 1.2. FDA approved anticancer drugs.    9
Table 2.1. Known bioactivity of crude extracts from species of the Myristicaceae         family.       62
<b>Table 2.2.</b> All known compounds isolated from species of interest (Figure 2.1) within the Myristicaceae family.       64
Table 2.3. Known bioactivity of crude extracts from species of the Clusiaceae family.         91
Table 2.4. All known compounds isolated from species of interest within the         Clusiaceae and Calophyllaceae family.       94
<b>Table 3.1.</b> Voucher specimen numbers and the corresponding Myristicaceae species.        114
<b>Table 3.2.</b> Voucher specimen numbers and the corresponding Clusiaceae species. 115
Table 3.3. HPLC method used during LC-MS analysis.    120
Table 3.4. Gram -positive and negative bacterial strains used during microbiological studies.       124
<b>Table 4.1.</b> <sup>1</sup> H, <sup>13</sup> C, COSY and HMBC NMR data of compound <b>4.1</b> (CDCl <sub>3</sub> , 500/126 MHz).
<b>Table 4.2.</b> <sup>1</sup> H, <sup>13</sup> C, COSY and HMBC NMR data of compound <b>4.2</b> (CDCl <sub>3</sub> , 500/126 MHz).
<b>Table 4.3.</b> <sup>1</sup> H, <sup>13</sup> C, COSY and HMBC NMR data of compound <b>4.3</b> (CDCl <sub>3</sub> , 500/126 MHz).
<b>Table 4.4.</b> <sup>1</sup> H, <sup>13</sup> C, COSY and HMBC NMR data of compound <b>4.4</b> (CDCl <sub>3</sub> , 500/126 MHz)
<b>Table 4.5.</b> <sup>1</sup> H, <sup>13</sup> C, COSY and HMBC NMR data of compound <b>4.5</b> (CDCl <sub>3</sub> , 500/126 MHz).
<b>Table 4.6.</b> <sup>1</sup> H, <sup>13</sup> C, COSY and HMBC NMR data of compound <b>4.6</b> (CDCl <sub>3</sub> , 500/126 MHz).

<b>Table 4.7.</b> <sup>1</sup> H and <sup>13</sup> C NMR data of <b>4.7</b>
<b>Table 4.8.</b> <sup>1</sup> H and <sup>13</sup> C NMR data of <b>4.8</b>
<b>Table 4.9.</b> <sup>1</sup> H, <sup>13</sup> C, COSY and HMBC NMR data of compound <b>4.9</b> from <b>4.1/4.9</b> fraction (CDCl <sub>3</sub> , 500/126 MHz)
<b>Table 4.10.</b> <sup>1</sup> H, <sup>13</sup> C, COSY and HMBC NMR data of compounds <b>4.10</b> and <b>4.11</b> (CDCl <sub>3</sub> , 500/126 MHz)
<b>Table 4.11.</b> <sup>1</sup> H, <sup>13</sup> C, COSY and HMBC NMR data of compounds <b>4.12</b> (CDCl <sub>3</sub> , 500/126 MHz)
<b>Table 4.12.</b> <sup>1</sup> H, <sup>13</sup> C, COSY and HMBC NMR data of compounds <b>4.13</b> / <b>4.14</b>
<b>Table 4.13.</b> <i>In vitro</i> antibacterial activity of Myristicaceae species measured using the broth microdilution assay to obtain the minimum inhibitory concentration (MIC) of each extract.
<b>Table 4.14.</b> MIC values of compounds <b>4.1</b> – <b>4.6</b> tested against Gram-negative bacterial strains.
<b>Table 4.15.</b> <i>In vitro</i> antibacterial activity, showing MIC (shaded) and MBC values (μg/mL), of isolated compounds <b>4.1</b> – <b>4.6</b> against <i>Staphylococcus aureus</i> 182
<b>Table 4.16.</b> <i>In vitro</i> antibacterial activities, displaying MIC (shaded) and MBC values $(\mu g/mL)$ , of isolated compounds <b>4.1</b> – <b>4.6</b> against susceptible <i>E. faecalis</i>
Table 4.17. Cytotoxic activity of isolated compounds against A549 lung cancer cells.
<b>Table 5.1.</b> <sup>1</sup> H, <sup>13</sup> C, COSY and HMBC NMR data of compound <b>5.1</b> (CDCl <sub>3</sub> , 600/150 MHz)
<b>Table 5.2.</b> <sup>1</sup> H, <sup>13</sup> C, COSY and HMBC NMR data of compound <b>5.2</b> (CDCl <sub>3</sub> , 500/126 MHz)
<b>Table 5.3.</b> $^{1}$ H and $^{13}$ C NMR data of compound <b>5.3</b> (CDCl <sub>3</sub> , 500/126 MHz)209
<b>Table 5.4.</b> <sup>1</sup> H, <sup>13</sup> C, COSY and HMBC NMR data of compound <b>5.4</b> (MeOH-d <sub>4</sub> , 600/150 MHz)
<b>Table 5.5.</b> <sup>1</sup> H, <sup>13</sup> C and COSY data of compound <b>5.5</b> (CD <sub>3</sub> OD, 500/126 MHz)215
<b>Table 5.6.</b> <sup>1</sup> H, <sup>13</sup> C and COSY data of the contaminant dioctyl phthalate compound (CD <sub>3</sub> OD, 500/126 MHz)

Table 5.7. In vitro antibacterial activity of Clusiaceae species.    22	13
<b>Table 5.8.</b> MIC values of compounds <b>5.1</b> , <b>5.2</b> and ampicillin positive control tested against Gram-negative and Gram-positive bacterial strains	24
Table 5.9. Cytotoxic activity of compounds 5.1 and 5.2 against A549 lung cancer cells      22	
Table 4.1. Structures of all compounds identified in this study, indicating the plan source	

## List of Abbreviations

% Percent

°C Degree Celsius

μg Microgram
 μL Microlitre
 μM Micromolar
 δ Chemical shift

2D Two Dimensional3D Three DimensionalABC ATP binding cassette

ACN Acetonitrile

ALL Acute Lymphocytic Leukaemia
AML Acute Myelogenous Leukaemia

AMR Antimicrobial Resistance

ATCC American Type Culture Collection

CD<sub>3</sub>OD Deuterated Methanol
 CDCl<sub>3</sub> Deuterated Chloroform
 CFU Colony-forming units

CLL Chronic Lymphocytic Leukaemia

**cm** Centimetre

CML Chronic Myelogenous Leukaemia

CoA Coenzyme A

**COSY** Correlation spectroscopy (NMR)

d Doublet (NMR)

DAD Diode array detectorDCM Dichloromethane

**dd** Doublet of Doublets (NMR)

**DEPT** Distortionless Enhancement of Polarisation Transfer (NMR)

**DMAPP** Dimethylallyl pyrophosphate

**DMSO** Dimethyl sulfoxide

DMT N,N-DimethyltryptamineDNA Deoxyribonucleic acid

**FDA** Food and Drug Administration

g Gram

GDP Gross Domestic ProductHAT Histone acetyltransferase

HIV Human Immunodeficiency Virus

**HMBC** Heteronuclear multiple-bond correlation spectroscopy

**HPLC** High Performance Liquid Chromatography

**Hz** Hertz

IC<sub>50</sub> Concentration inhibiting 50% of cell growth

IR Infra-red

**IPP** Isopentenyl diphosphate

J Spin-Spin coupling constant (Hz)

L Litre

LPS Lipopolysaccharidem Multiplete (NMR)m/z Mass-to-charge ratio

MBC Minimum Bactericidal Concentration

MDR Multi Drug Resistant

**MeOH** Methanol

MIC Minimum Inhibitory Concentration

mL MillilitremM Milimolar

MRSA Methicilin Resistant Staphylococcus aureus

MS Mass Spectrometry

MSSA Methicilin Susceptible Staphylococcus aureus

**NCTC** National Collection of Type Cultures

**nm** Nanometre

NMR Nuclear Magnetic Resonance
PBP Penicillin binding protein
PBP Penicillin Binding Protein
PBS Phosphate Buffer Saline
PKS Polyketide synthase

**PTFE** Polytetrafluoroethylene

**pTLC** Preparative Thin Layer Chromatography

**q** Quartet

Q-ToF Quadrupole - Time of Flight R+D Research and Development

s Singlet (NMR)

SCXD Single crystal X-ray diffraction

t Triplet (NMR)

TLC Thin Layer Chromatography

UK United Kingdom

**USA** United State of America

**USD** United States Dollar

UV Ultraviolet

**VLC** Vacuum Liquid Chromatography

WHO World Health Organisation

## Acknowledgements

Firstly, I would like to express my deep gratitude to my primary supervisor, Professor Ganesan, whose steady guidance and expertise in natural products have shaped both my research and my growth as a scientist. His depth of knowledge, intellectual generosity, as well as reassuring presence throughout my time at the university have been a constant source of support and inspiration.

I would also like to thank my secondary supervisor, Dr. de Resende, for his guidance and kindness throughout this project. From the very beginning, he guided me through the practical aspects of the lab with exceptional generosity, always taking the time to teach and encourage me. His comprehensive knowledge and reassurance never failed me, and for that, I remain deeply thankful.

My sincere thanks go to Professor Gibbons, whose vision and scientific insight were the foundation of this project. His guidance in shaping the rationale behind the research, and his continued support, even beyond formal obligations, have been a source of genuine inspiration throughout my doctoral journey.

I thank Dr. Teo Ping for his expertise in the collection and provision of the plant specimens used in this study. I extend my thanks to the staff at The University of East Anglia, including Dr. Wright and Dr. Morritt for their assistance with X-ray diffraction, Dr. Bidula and Dr. Storer for conducting the antifungal assays, and Dr. Sobolewski and Dr. Banerjee for the cytotoxicity assays. I thank Dr. Hill at the John Innes Centre for his support with LC-MS analyses. Special thanks to Mr Alroomi for his laboratory support towards this study. I express my appreciation to my colleagues for their dedication to natural product drug discovery, and for their stimulating scientific discussions and encouragement, which made this journey far more enjoyable and meaningful. I also thank Dr El-Demerdash for his valuable insight during our group meetings. I gratefully acknowledge that this project was made possible through funding from the UEA.

Finally, I would like to thank all of my siblings and friends for filling my PhD journey with laughter and warmth in their own ways. I could not have done it without each of you. I am grateful to my father, Dr. Valmiki, for his ongoing encouragement and advice. I thank my dogs, Mali and Wilma for the joyful presence they provided throughout. Thank you, Declan, for being a steady voice of reassurance, and for always reminding me to believe in myself. I am especially thankful to my mother, Dawn, for her practical wisdom and for being a constant source of strength and inspiration.

## **Conferences and Publications**

- The results obtained from the investigation of *Garcinia caudiculata* (Clusiaceae) have been published in Molecules. M. Valmiki, S. P. Teo, P. E. de Resende, S. Gibbons and A. Ganesan, *Molecules*, 2024, 29.
- UEA School of Chemistry, Pharmacy and Pharmacology Research Day, May 2022,
   2023 and 2024, Poster Presentation: Antibacterial and Phytochemical Study of
   Bornean Myristicaceae and Clusiaceae Species.
- 70<sup>th</sup> Gordon Research Conference on Natural Products and Bioactive Compounds,
   30<sup>th</sup> July 2024, New Hampshire, USA, Poster Presentation: Antibacterial and
   Phytochemical Study of Bornean Myristicaceae and Clusiaceae Species.
- 4<sup>th</sup> Annual Centre for Natural Products Discovery, 19<sup>th</sup> June 2023, Liverpool John Moores University, UK, Poster Presentation: Antibacterial and Phytochemical Study of Bornean Myristicaceae and Clusiaceae Species.
- International Congress on Natural Products Research, 13th July 2024, Kraków,
   Poland, Poster Presentation: Antibacterial and Phytochemical Study of Bornean
   Myristicaceae and Clusiaceae Species.

## **Chapter 1 – Introduction**

## 1.1. Natural Product Drug Discovery

Forged through millennia of evolutionary adaptation, natural products are among nature's most sophisticated gifts to humanity – complex bioactive compounds that have profoundly shaped the course of modern medicine. Their impressive chemical diversity and biological specificity have played a key role in medicine throughout human history, long before the advent of modern pharmaceuticals. As our understanding of biology and chemistry has deepened, so too has our capacity to explore, modify, and synthesise these molecules, using them as powerful tools for treating disease. Indeed, natural products have not only inspired countless synthetic and semi-synthetic drugs as described in 1.1.3, but have also shaped entire fields of therapeutic discovery, from antibiotics to anticancer agents.

## 1.1.1. Historical significance of terrestrial natural products

Health seeking behaviour, including the use of medicinal plants for self-medication, is an evolutionarily conserved trait observed across the animal kingdom and is deeply embedded in human history<sup>1</sup>. Some of the earliest evidence of this dates back to the Middle Palaeolithic period: pollen from *Ephedra* (Ephedraceae), a medicinal plant, was discovered at a 60,000-year-old Neanderthal burial site in Shanidar Cave<sup>2,3</sup>. The earliest evidence of long-term survival in hominins comes from a subspecies of *Homo erectus* dating to approximately 1.7 million years ago, which exhibited signs of chronic periodontal disease. Their extended survival suggests the possible use of antibacterial plants to mitigate infection and support longevity despite the high risk of disease-related complications<sup>4,5</sup>. Similarly, archaeological evidence from Iran, dating between 65,000 and 35,000 years ago, indicates that Neanderthals survived to advanced ages despite sustaining injuries that would likely have resulted in fatal infections without the use of anti-infective agents, possibly derived from medicinal plants<sup>4,6</sup>.

There is substantial evidence of medicinal plant use dating back to ancient Mesopotamia (~2600 B.C.), where early pharmacopoeial records documented

therapeutic applications of *Cupressus sempervirens* (cypress) and *Commiphora* species (myrrh) oils. Similarly, the Egyptian *Ebers Papyrus* (circa 2900 B.C.) describes over 700 plant-derived remedies, demonstrating a sophisticated understanding of natural therapeutics. A rich tradition of plant-based therapeutics also emerged in ancient China over successive centuries, as documented in classical texts such as the *Materia Medica* (1100 B.C.), the *Shennong Herbal* (~100 B.C.), and the *Tang Herbal* (659 A.D.), which collectively catalogued more than a thousand drugs and prescriptions. Greek scholars Theophrastus (~300 B.C.) and Dioscorides (circa 100 A.D.) documented many natural medicines, including properties of herbs, their collection, storage, and therapeutic applications. This knowledge was safeguarded throughout the Middle Ages by European monasteries, while Arab scholars used and integrated Greco-Roman medicinal practices with Chinese and Indian systems. This gave rise to the world's first privately owned pharmacies by the Arabs<sup>7,8</sup>.

The use of plants in traditional medicine has long been a crucial part of healthcare across diverse cultures. Systems such as Ayurveda, traditional Chinese medicine, Jami Siddha, and practices from indigenous groups like the Aztecs and Iboga have relied on plants for their healing properties<sup>9</sup>. This wealth of knowledge, passed down through generations of trial and error, has been instrumental in shaping modern pharmacology. Morphine, derived from *Papaver somniferum*, was the first natural plant product to enter the commercial market in 1826. Traditionally, poppies had been used for their analgesic properties, providing the requisite incentive for the development of morphine as a marketable therapeutic drug<sup>10</sup>. This was quickly followed by the introduction of aspirin, a semi-synthetic drug based on salicin from *Salix alba*, which had been used for centuries to alleviate pain, reduce inflammation, and treat fever<sup>11</sup>. Other plant-derived compounds such as cocaine from *Erythroxylon coca*, digitoxin from *Digitalis purpurea*, quinine from *Cinchona ledgeriana*, and pilocarpine from *Pilocarpus microphyllus*, were similarly pioneering in their drug applications (Figure 1.1)<sup>12,13</sup>. Another notable drug is the Pacific Yew tree (*Taxus brevifolia*), historically used for

ailments like diphtheria and fever, which became the source of paclitaxel, a now widely used anticancer drug (Figure 1.1)<sup>14</sup>.

Still today, despite the development of modern medicine and synthetic drugs, the World Health Organisation (WHO) has estimated that 80% of the world's population rely on plant-based traditional medicines for primary healthcare, and the same percentage of plant-derived FDA-approved drugs have their purposes related ethnopharmacological use<sup>15</sup>. The enduring connection between traditional knowledge and modern drug development stresses the continued relevance of natural products in this context during the search for new therapeutic agents. The use of plants in this way would not have been possible without their millions of years of natural evolution, during which they developed bioactive compounds to fulfil specific ecological roles and form plant defence systems.

#### 1.1.2. Ecological role of natural products – structural evolution

Through the intricate process of evolution, plants have developed tailored bioactive molecules, finely tuned to fulfil crucial ecological roles within their environments, for example morphine and myristicin. These phytochemicals are broadly categorised as either primary or secondary metabolites<sup>9</sup>. Primary metabolites hold lower structural diversity due to their role in basic life functions across all plants, including cell division and growth, glycolysis, the Krebs cycle and photosynthesis. Examples include proteins, sugars, amino acids, polysaccharides and nucleic acids.

Secondary metabolites are structurally diverse, species-specific phytochemicals which aid the adaptation and survival of plants within their habitats<sup>16</sup>. Since the evolution of angiosperms approximately 140 million years ago, plants have developed defense chemicals on account of their sessile nature, designed to enhance competition against other plants and to protect them against viruses, bacteria, fungi and herbivores<sup>16</sup>. Such metabolites are products of specialised biosynthetic pathways which use precursors obtained from primary metabolism to build specific structures. Therefore, biosynthetic

pathways determine the natural product classification of a compound. Natural product classes include alkaloids, lipids, phenolics, saponins and terpenoids. Figure 1.1 summarises compound classes of some bioactive plant compounds, categorised into their primary biosynthetic pathways<sup>17–18</sup>.

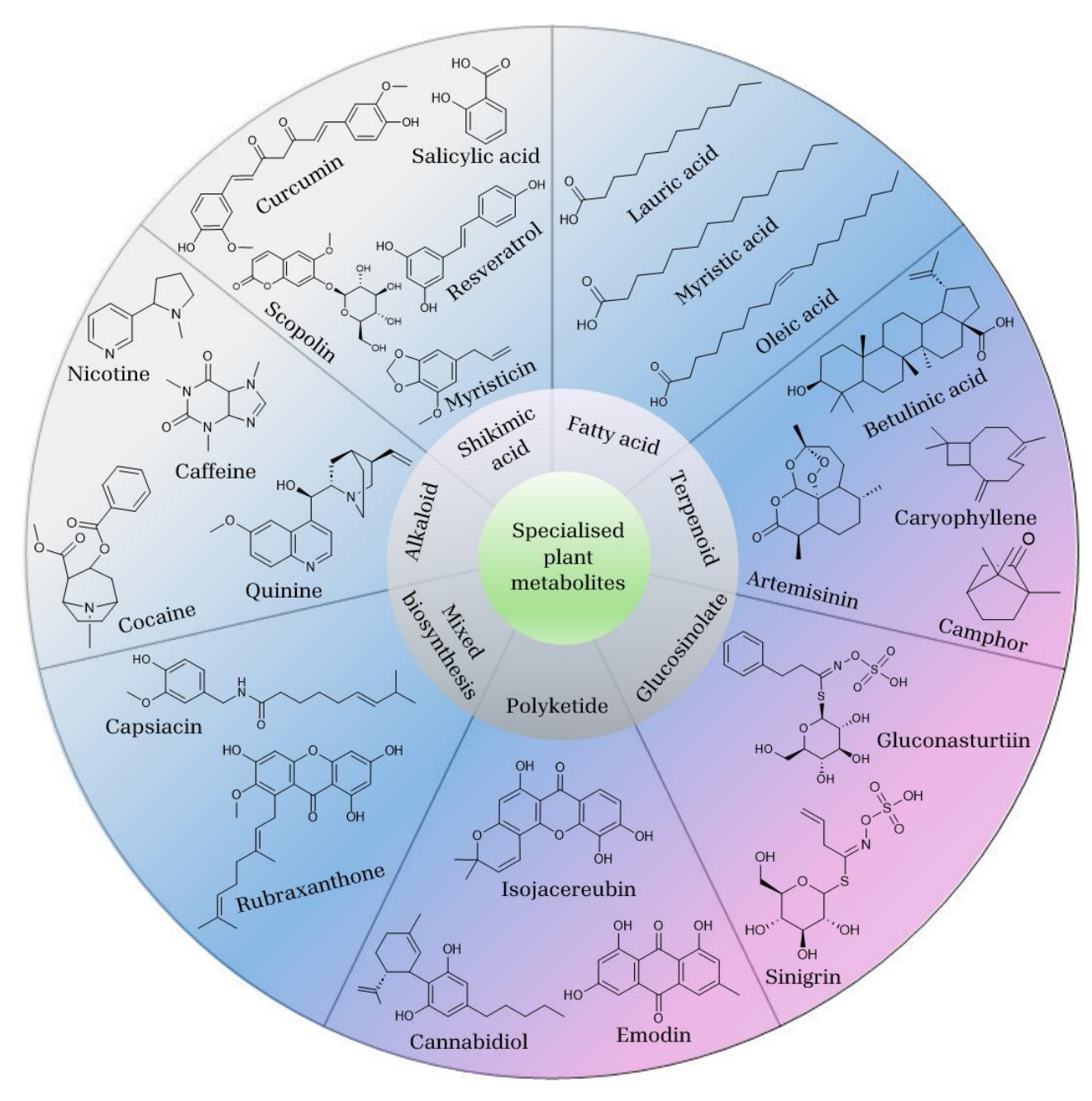


**Figure 1.1.** Examples of specialised bioactive plant secondary metabolites categorised by their primary biosynthetic pathways. This figure was adapted from Huang and Dudareva 2023<sup>17</sup>.

The adaptation of plants, the evolution of biosynthetic pathways and therefore a diverse array of bioactive natural products provide the scientific basis of why nature holds such medicinal value. As mentioned, this has been exploited by humans in ancient and modern medicine. The next section will report some notable plant natural products used as antimicrobial and anticancer treatments.

## 1.1.3. Major plant-derived bioactive compounds

One of the main threats to plant life is infection, therefore plants produce various secondary metabolites to protect themselves from microbial attacks. Many thousands of plant extracts have been screened for their antimicrobial activities. In addition, numerous plant derived compounds have displayed bactericidal activities (Table 1.1). These capabilities have been well-reviewed, however additional research is necessary with the majority of these, to fully understand the mechanisms of action and safety of their use as antimicrobial agents for humans<sup>19</sup>.

**Table 1.1.** Plant derived compounds and their structures which are marketed as antimicrobial agents. This table has been adapted from those by Khamaneh *et al.*, 2019 and Angelini 2024<sup>19.20</sup>.

Compound	Structure	Species (common name)	Active against	Drug delivery system
Berberine		Berberis vulgaris (Barberry)  Mahonia aquifolia (Oregon grape)	Bacteria, protozoa Bacteria	Soft gel 1000 mg Capsule 500 mg
Piperine		Piper nigrum (Black pepper)	Fungi, Lactob acillus, Micro coccus	

Eugenol	но	Syzygium aromaticum (Clove)	General	Capsule 500 mg
Berberine, hydrastine		Hydrastis canadensis (Goldenseal)	Bacteria, Giardia duodenale,	Solution 500 mg per dosage
Glabrol	НО	Glycyrrhiza glabra (Licorice)	S. aureus, M. tuberculosis	Capsule 450 mg
Allicin	S S	Allium cepa (Onion)	Bacteria, Candida	

The traditional use of plants in the treatment of tumours has laid the foundation for the discovery of numerous anticancer agents now employed in modern oncology. These compounds exhibit a broad spectrum of antineoplastic mechanisms, including the induction of apoptosis, immunomodulation, inhibition of angiogenesis, interference with oncogenic signalling pathways, antioxidant effects, and the enhancement of DNA repair processes<sup>21-24</sup>. Table 1.2 presents a selection of FDA-approved anticancer drugs derived from botanical sources, exemplifying the clinical significance of phytochemicals in cancer therapy.

**Table 1.2.** FDA approved anticancer drugs, including the source species and types of cancers treated by each drug.

Compound	Structure	Species source	Cancer application	Ref.
Paclitaxel	OH O	Pacific yew tree	Breast, ovarian, lung	25
Vinblastine	HO TO OH O	Madagascar periwinkle	Leukaemia, lymphoma	26
Vincristine	HO TO O O O O O O O O O O O O O O O O O	Madagascar periwinkle	Leukaemia, lymphoma	26

In parallel with these approved drugs, a number of plant-derived compounds, for example curcumin, have moved through clinical and preclinical studies, reflecting the ongoing interest in nature as a reservoir for structurally novel and pharmacologically potent anticancer scaffolds<sup>21</sup>. Given the escalating global cancer burden and the intersecting challenge of AMR, the search for new drugs remains a priority. The chemical diversity and evolutionary refinement of plant secondary metabolites position them as an essential resource in the pursuit of novel drugs for these worsening diseases.

#### 1.2. The Global Burden of Microbial Infections

## 1.2.1. Antimicrobial resistance (AMR) - the need for new antimicrobial agents

#### 1.2.1.1. Significance of bacterial and fungal infections

Antimicrobial resistance (AMR) is a leading cause of morbidity and mortality worldwide, posing a significant global health threat which is worsening at an alarming rate<sup>30</sup>. It is defined as the resistance of a microorganism to an antimicrobial agent to which it was originally susceptible<sup>30</sup>. The increasing prevalence of resistant bacterial strains has led to a reduction in viable treatment options, resulting in more severe infections, the requirement for additional treatments and prolonged hospitalisations. Once-treatable infections have become harder (or even impossible) to cure, leading to an increased morbidity from infections worldwide<sup>31</sup>.

In 2021, By 2050, 7.96 million deaths are estimated to be associated with antibiotic-resistant infections, which is an increase of 69% from 2021<sup>32</sup>. Beyond its impact on public health, AMR poses a substantial economic burden, costing an estimated up to 100 trillion USD of global economic loss in the next three decades, resulting in a significant worldwide GDP reduction<sup>33</sup>.

The timeline of AMR is short due to the fast-evolving nature of bacteria (relative to humans), which has rendered us in a worldwide crisis within less than a century. The earliest report of clinical AMR was in 1924, against the antimicrobial agent, arsphenamine, 14 years after its introduction and despite its limited use relative to modern-day antibiotics<sup>34</sup>. Penicillin was discovered in 1928 and was used widely by the mid-1940s, by which point, resistant *Escherichia coli* strains had already been discovered<sup>35</sup>. The rate of penicillin resistance increased rapidly within the next 20 years, with 80% of *Staphylococcus aureus* strains being resistant by the late 1960s<sup>36</sup>. The development and use of semi-synthetic penicillin derivatives such as methicillin caused a reduction in penicillin-resistant fatalities, however methicillin resistance emerged shortly after its introduction. Within 20 years, 29% of those admitted to hospital with *S. aureus* infections were infected with methicillin-resistant strains<sup>37</sup>.

The pattern of new antibiotic introduction and development of resistance is not only confined to those which are penicillin-derived, but applies to most of the (approximately 150) antibiotics that have been developed since penicillin<sup>38</sup>. Since the 1970s, no new classes of antibiotics have been discovered, therefore marking this the end of the "golden era" of antibiotics. The "discovery void" for antibiotic drugs has since then led to a lack of alternative treatments for resistant strains, whilst the accumulation of resistance to existing antibiotics continues. Paradoxically, during this reduction in drug development, knowledge on the mechanisms of antibiotic modes of action and bacterial resistance have developed significantly<sup>39</sup>.

#### 1.2.1.2. Antimicrobial resistance acquisition

AMR in bacteria can be acquired by either of two genetic mechanisms: a spontaneous mutation causing a change in DNA bases, or by the acquisition of new DNA via horizontal gene transfer. Horizontal gene transfer takes place by transduction, transformation or conjugation (Figure 1.3) <sup>40</sup>. All mechanisms result in bacteria gaining DNA, which induces resistance to an antimicrobial agent within that individual <sup>41,42</sup>. These resistance genes often exist on plasmids, which are circular extrachromosomal DNA molecules that can undergo autonomous replication. Plasmids allow the mobilisation of resistant genes by acquiring mobile genetic elements, including insertion sequences and transposons (Figure 1.3) <sup>43</sup>. Although self-adaptive mutations drive the creation of resistant genetic material, horizontal gene transfer has allowed the fast spread of this genetic material between a diversity of bacterial species and has therefore allowed such escalation of the AMR crisis <sup>39</sup>.

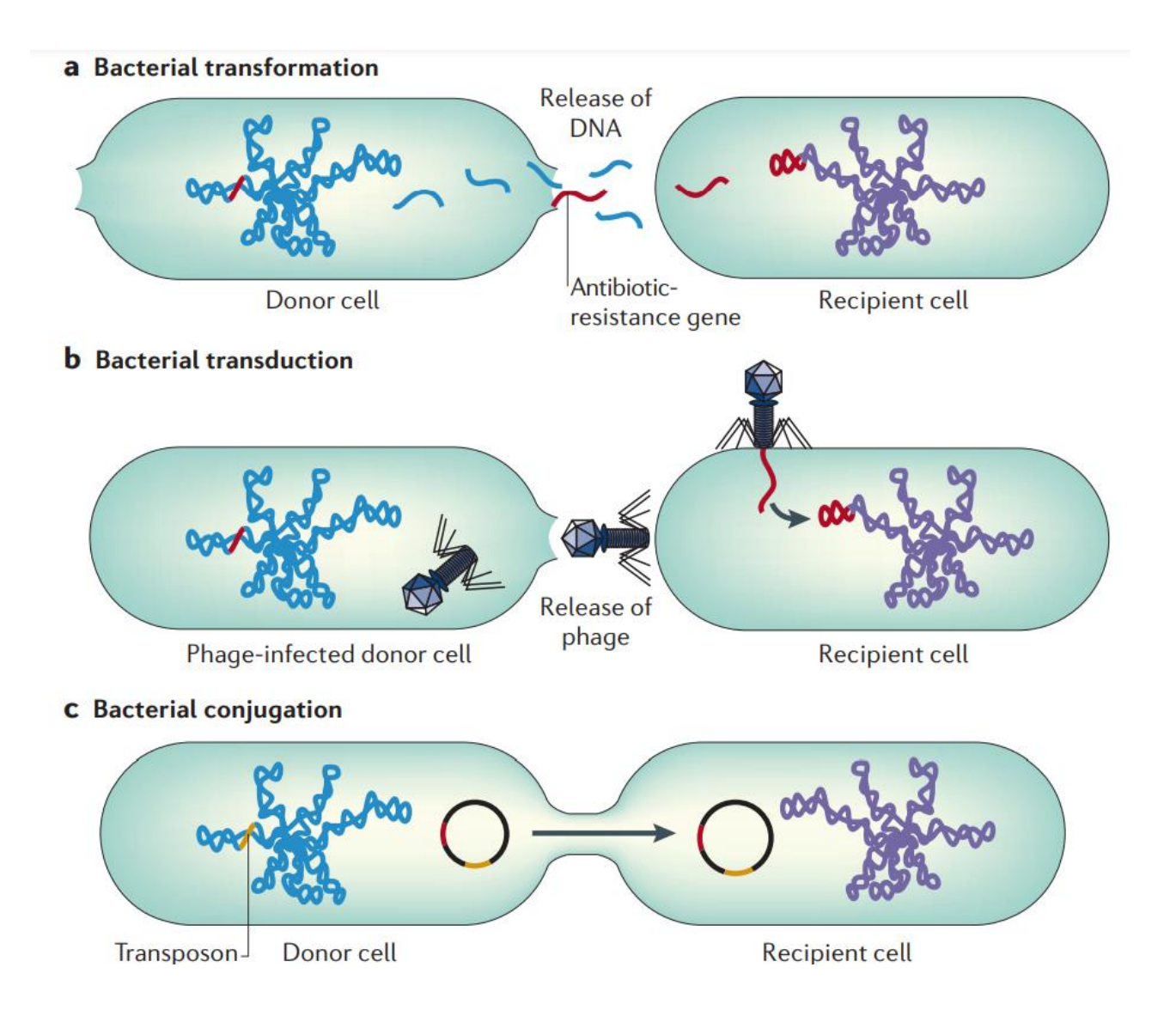
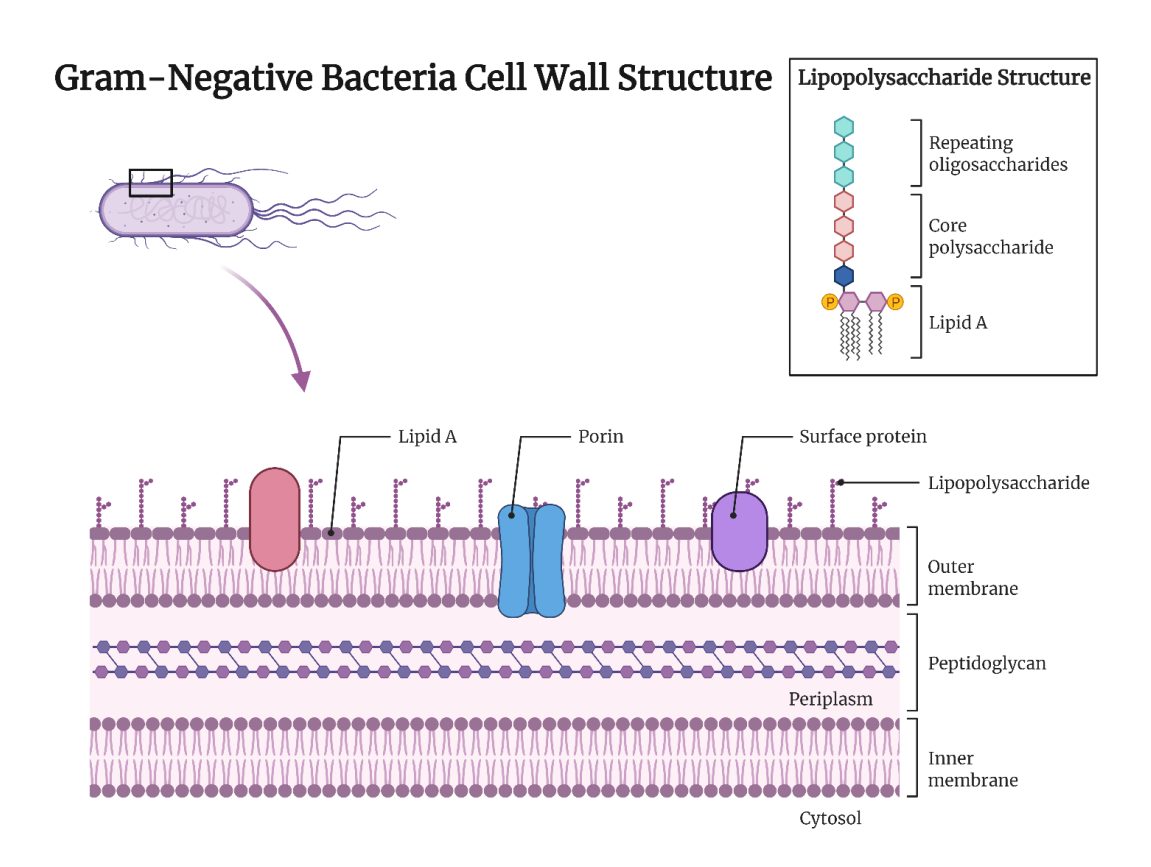


**Figure 1.2.** Illustrations of mechanisms of horizontal gene transfer including **(a)** transformation: the release of naked DNA upon lysis of the donor bacteria, which is taken by the recipient cell and integrated into the genome or plasmid; **(b)** transduction: bacteriophage vector mediates the transfer of resistance genes by infecting the recipient, followed by the donor, resulting in release of DNA into the donor cell (lysogeny) and **(c)** conjugation: the donor and recipient plasmids form a conjugation tube between two individuals, allowing resistant DNA to transfer from donor to recipient. Illustration by Lowy *et al.*, 2006<sup>44</sup>.

## 1.2.1.3. Antimicrobial resistance strategies: four biochemical mechanisms

Bacteria use a variety of biochemical mechanisms to manifest resistance to antimicrobial agents<sup>45</sup>. Gram-negative bacterial cell walls consist of three layers. The outermost layer is the outer membrane, which is comprised of a phospholipid bilayer that is surrounded by lipopolysaccharides (LPS). This outer membrane contains outer membrane proteins, such as porins, which allow the transportation of small molecules into the cell. Inside the outer membrane is a thin peptidoglycan cell wall. This is comprised of the repeated disaccharide unit, N-acetyl glucosamine-N-acetylmuramic acid, which provides cell structural integrity<sup>46</sup>. The third and innermost layer is the inner membrane, which is another phospholipid bilayer that also contains proteins, and is associated with multiple cellular processes<sup>47</sup>.

Gram-positive bacteria, including *S. aureus* and *E. faecalis*, differ from Gram-negative by their cell membranes. These lack an outer membrane and are surrounded by a layer of peptidoglycan, which is thicker than that present in Gram-negative bacteria. Further major Gram-positive cell wall components are long anionic polymers, named teichoic acids, which are threaded through the peptidoglycan layer (Figure 1.4)<sup>46</sup>.



## Gram-Positive Bacteria Cell Wall Structure

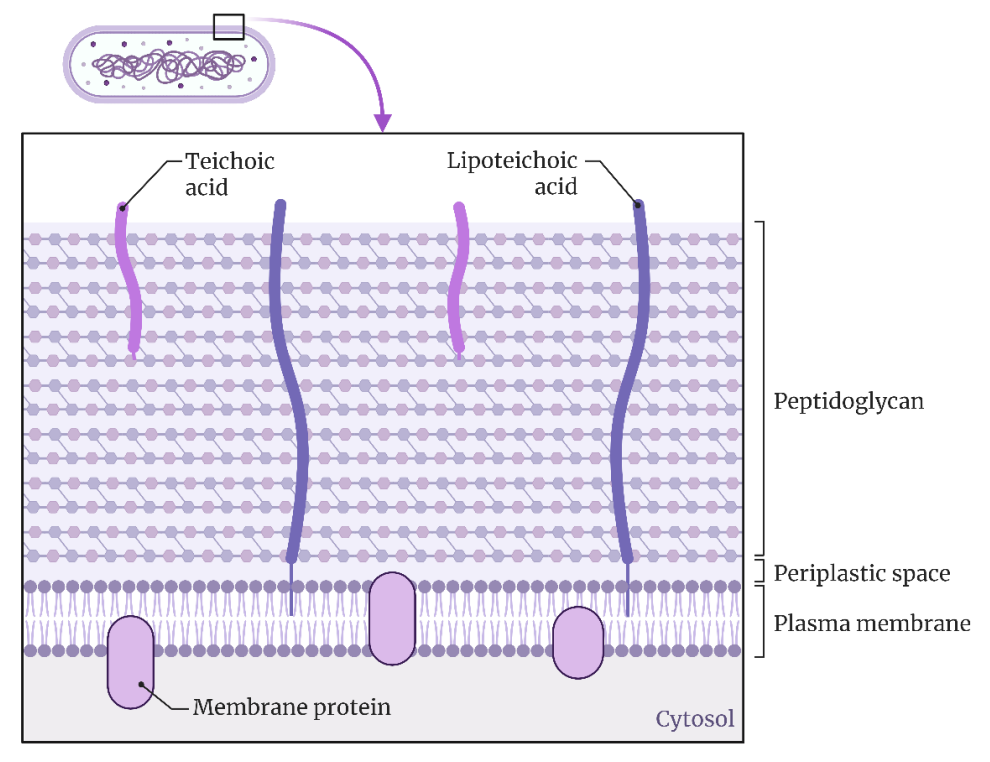


**Figure 1.3.** Illustration of Gram-positive and Gram-negative cell wall structures. This figure was created using Biorender<sup>48</sup>.

# 1) Decreased antibiotic accessibility

The hydrophobic LPS and outer membrane protein-containing bilayer of Gram-negative bacteria offer intrinsic resistance (innate resistance, which is genetically determined by chromosomal genes and shared by all genus members), acting as a barrier to multiple antibiotics<sup>31</sup>. These membrane components offer intrinsic resistance by inhibiting the diffusion of lipophobic solutes. However, they also allow penetration of lipophilic solutes, which utilise the lipid diffusion pathway, rendering them susceptible to these molecules<sup>49</sup>. Furthermore, the LPS component of Gram-negative cell membranes makes the passive diffusion of most small molecules difficult. Generally, small hydrophilic molecules translocate across the membrane via porins only<sup>50</sup>. The cell wall properties also give Gram-negative bacteria intrinsic resistance to glycopeptide (hydrophilic molecules which are too large to pass via porins) and lipopeptide (amphiphilic molecules which are unable to depolarise the Gram-negative cell membrane) antibiotics<sup>51,52</sup>.

# 2) Drug efflux

The Gram-positive cell wall morphology offers bacteria minimal resistance to the passive diffusion of small molecules<sup>50</sup>. Some Gram-positive and -negative bacteria possess efflux pumps, which are an element of their outer membranes and are categorised into five main families<sup>31</sup>. These provide intrinsic resistance by pumping toxic substances out of the cell, for example, the expulsion of  $\beta$ -lactams, tetracyclines and aminoglycosides from Gram-negative bacteria<sup>53</sup>. The tet(K) gene codes for tetracycline efflux pumps in *S. aureus*, strains including the clinical isolate *S. aureus* XU212 which overexpress this<sup>54</sup>. Similarly, *norA* gene is responsible for efflux activity associated with fluoroquinolone resistance and is found in *S. aureus* 1199B<sup>49,55</sup>. A further virulence factor of certain *S. aureus* strains, for example *S. aureus* RN4420, is the production of  $\beta$ -hemolysin, which hydrolyses sphingomyelin, a plasma membrane lipid, resulting in hemolytic activity<sup>56,57</sup>.

# 3) Alteration of antibiotic target

Another antibacterial resistance strategy is by modifying the antimicrobial agent's target. The adaptive nature of bacteria allows the upregulation or modification of drug targets, to induce desensitisation to the drug and therefore increase survival. One example used mainly by Gram-positive bacteria induces resistance to  $\beta$ -lactam drugs, and is achieved by altering the structure and/or number of penicillin binding proteins (PBPs). PBPs enable the peptidoglycan synthesis for Gram-positive cell walls, therefore  $\beta$ -lactams work by inhibiting this process<sup>31</sup>. *S. aureus* bacteria can utilise this mechanism. Here, the structure of PBP2a is altered via acquisition of the gene, *mecA*, which compromises or completely inhibits the drug binding ability of  $\beta$ -lactams <sup>43</sup>. This is the resistance mechanism of MRSA<sup>59</sup>.

More examples of target-altering resistance mechanisms of MRSA are against vancomycin (glycopeptide) and daptomycin (lipopeptide). These require either the acquisition of *van* genes for vancomycin resistance or mutations in genes such as the *mprF* for daptomycin, which result in changes to peptidoglycan precursors and cell membrane charges, respectively, ultimately causing alterations to the antibiotic target site<sup>60-62</sup>.

### 4) Chemical modification of drug

Some bacteria acquire the ability to produce enzymes which degrade or deactivate antibiotic agents by changing the chemical composition, either by drug degradation or the addition of chemical groups. A well-known example of this is  $\beta$ -lactamase enzymes, which hydrolyse drugs<sup>63</sup>. These are produced by Gram-negative bacteria including *E. coli*. Enzymes which catalyse the attachment of chemical groups to drugs may transfer phosphoryl, acetyl and adenyl groups. Aminoglycoside-modifying enzymes catalyse the phosphorylation and adenylation of aminoglycosides, rendering them unable to act on their target<sup>31,53</sup>.

# 1.2.1.4. Resolving antimicrobial resistance

Although AMR is a naturally occurring evolutionary process of microbes, the widespread and inappropriate use of antimicrobials by humans has caused its emergence at an unprecedented and accelerated rate, surpassing natural evolutionary trajectories<sup>64</sup>. Collingnon *et al.* performed a multivariable analysis of the socioeconomic and anthropologic factors which contribute to the AMR burden on human health. Here, findings suggested that an initiation of appropriate use of currently available antibiotics would not be sufficient to decrease the prevalence of AMR infections. The already-established worldwide prevalence of resistant bacteria means that inhibiting the transmission of AMR genes is a key aspect to resolving this issue, emphasising the need for more working antibiotics<sup>65</sup>.

There are three key variables involved in resolving antimicrobial resistance: sanitation, antimicrobial stewardship and novel antibiotics. Factors including improved sanitation and public healthcare worldwide would decrease dissemination of resistant genes and therefore contribute to the reduction of resistant infections<sup>65</sup>. These are multisectoral and multifaceted problems which develop at a slow rate, with high costs and dependence on government funding. For example, infrastructure for clean water, clean and spacious housing, improved agricultural practice, public engagement and clinical hygiene are vital here. Additionally, international collaboration is necessary to reduce AMR genes spreading via improved sanitation. These factors have a common interest which is to prevent the transmission of resistant genes – mostly transferred via conjugation through bacterial plasmids. Therefore, the prospect of plasmid-curing agents is also an important one<sup>66</sup>.

From an alternative perspective, the introduction of new antibacterial agents is another resolution to AMR. Providing however, that these are used optimally and therefore responsibly, e.g. the appropriate antibiotic prescribed (upon correct diagnosis), with the correct duration and dosage. Improving antimicrobial stewardship, which includes making AMR a political priority, by improving monitoring, increasing education of the public and considering healthcare professionals prescribing decisions. Artificial

intelligence has already begun to transform infectious disease management by enhancing diagnostic accuracy and accelerating drug discovery. Machine learning and deep learning approaches are increasingly employed to detect pathogens, predict resistance patterns, and support clinical decision-making in both diagnosis and treatment<sup>67</sup>. Combining the reduction of resistant gene spread with the introduction of novel antimicrobial agents may be the best strategy to tackle AMR<sup>68</sup>.

# 1.2.2. Clinically relevant bacterial species

Antibiotic-resistant strains of *Escherichia coli*, *Staphylococcus aureus*, *Klebsiella pneumoniae*, *Pseudomonas aeruginosa*, *Salmonella enterica* serotype Typhi, and *Enterococcus faecalis* ranked among the top twelve global causes of death from bacterial infections – placing first, second, third, sixth, eleventh, and twelfth, respectively. These pathogens therefore represent critical targets in the fight against AMR<sup>96</sup>.

### 1.2.2.1. Staphylococcus aureus

Staphylococcus aureus strains are Gram-positive cocci, which are common human commensals that colonise the axilla and nasal passages. However, *S. aureus* pathogenic strains possess virulence factors and can therefore cause infection<sup>70</sup>. *S. aureus* resistant-associated infections caused approximately 700,000 deaths worldwide in 2019<sup>69</sup>. The most problematic resistant strain of *S. aureus* is methicillin resistant *S. aureus* (MRSA), which is often indicative of multiple resistances<sup>70</sup>. MRSA infections alone hold a significant economic burden, with each infection treatment costing over \$18,000 USD ( $\sim$ £14,000 GPB) in and USA and almost £9000 ( $\sim$ £7,500) in Germany<sup>71,72</sup>.

### 1.2.2.2. Enterococcus faecalis

*Enterococcus faecalis* are Gram-positive cocci and are a commensal of the gastrointestinal tract. However, disruption of homeostasis between the host and bacteria, or translocation of bacteria to other organ systems may lead to disease<sup>73</sup>. *E. faecalis* infections accounted for approximately 200,000 AMR-associated deaths in 2019 and are therefore a significant burden on human health<sup>69</sup>.

#### 1.2.2.3. Escherichia coli

In 2019, resistant *Escherichia coli* strains were associated with approximately 800,000 deaths worldwide and responsible for an increased cost of £420 per patient treatment in 2012. This cost is in addition to the total annual cost of non-resistant *E. coli* bacteraemia infections of over £14 million in the UK alone<sup>69,74</sup>. Thus, drug-resistant *E. coli* is deemed a "critical priority" pathogen by the WHO<sup>75,76</sup>. The majority of pathogens listed as critical priority by the WHO are Gram-negative<sup>76</sup>. Their unique cell wall structure heightens their intrinsic and acquired resistance capabilities, as described above<sup>49</sup>.

### 1.2.2.4. Klebsiella pneumonia

Although *Klebsiella pneumoniae* exists as a commensal bacteria existing on humans, animals and in the environment, there are also several clinically significant pathogenic strains which have given rise to those which are multidrug resistant. This species is closely related to *Salmonella enterica* and *E. coli* and is a prevalent opportunistic pathogen in hospitals, accounting for approximately 30% of all Gram-negative bacterial infections<sup>77</sup>. Despite antibiotic intervention, hospital acquired pneumonia caused by *K. pneumoniae* is common and has mortality rates of over 50%. This increases and is a particular problem amongst vulnerable individuals, including neonates, leukaemia patients, and those with compromised immune systems<sup>78</sup>.

The subsequent increased use and reliance on antibiotics for K. pneumoniae infections has brought about the emergence and spread of multidrug resistant strains including those producing extended spectrum  $\beta$ -lactamases and those resistant to carbapenems. Such strains are particularly concerning and have been classified by the WHO as critical threats to global public health<sup>79</sup>. Like other bacterial species, the fast accumulation of resistant strains of K. pneumoniae highlights the urgency for novel antimicrobial strategies against these infections.

#### 1.2.2.5. Salmonella enterica

Salmonella enterica is a diverse Gram-negative bacterial species comprising over 2600 distinct serovars, differing in antigen expression and presentation. Pathogenic *S. enterica* which infect mammals are broadly classified into typhoidal or non-typhoidal serovars, which each possess unique virulence factors. As the name suggests, typhoidal *Salmonella* causes enteric fever, also known as typhoid<sup>80</sup>. This is caused by a few specialist *Salmonella* serotypes including Typhi and Paratyphi A and B. Typhoidal *Salmonella* is human-restricted and endemic to developing populations including those of Africa. Differing from non-typhoidal *Salmonella*, typhoidal *Salmonella* does not induce a high inflammatory response<sup>80</sup>.

Non-typhoidal *salmonella* causes morbidity worldwide but mortalities are highest in developing countries. Examples of these ubiquitous serovars are Typhimurium and Enteritidis, which induce severe intestinal inflammation, exploiting inflammatory derived metabolites for growth, causing self-limiting, acute gastroenteritis and watery diarrhea in hosts<sup>81</sup>. In addition, this infection is associated with short incubation periods and invasive extraintestinal infections. This *Salmonella* type is not restricted to humans, allowing bacterial reservoirs in livestock, produce and pets, facilitating widespread transmission<sup>80</sup>.

Complications are frequent with non-typhoidal *Salmonella* infections causing death in 15% of patients, constituting almost 155,000 deaths per annum<sup>82</sup>. The emergence of resistant *Salmonella* strains has exacerbated the challenge of treatment. Such strains were categorised as a "high" priority pathogen by the WHO in 2024, emphasising the need for novel drugs to target this growing problem<sup>79</sup>.

# 1.2.2.6. Pseudomonas aeruginosa

*Pseudomonas aeruginosa* is a Gram-negative bacteria which is widely distributed in the environment, commonly found in soil, water, and as part of the human microbiota, including the skin, throat, and gastrointestinal tract. Most *P. aeruginosa* infections

include those which are nosocomial and include pneumonia, urinary tract infections, wounds and sepsis<sup>83-87</sup>.

Due to the emergence of several resistant strains, *P. aeruginosa* infections are becoming increasingly difficult to treat. This bacterium is the second most common cause of ventilator associated pneumonia in the United States and is the fourth most common cause of nosocomial infections, accounting for 20% in the USA and Europe<sup>88,89</sup>. In addition, *P. aeruginosa* infections cause 75% of deaths in patients with severe burns<sup>90,91</sup>.

Although global resistance trends for carbapenem-resistant *P. aeruginosa* have shown a decline, prompting the WHO to reclassify it from a "critical" priority pathogen in 2017 to a "high" priority in 2024, the need for continued research and drug development remains essential due to its persistent clinical burden<sup>79</sup>.

### 1.2.3. Clinically relevant fungal species

Invasive fungal infections have a worldwide annual incidence rate of 6.5 million, causing 3.8 million deaths, 2.5 million of which were directly attributable to the fungal infection<sup>92</sup>. Fungal infections range from superficial to life threatening, with treatment failure being common with the use of current antifungal drugs. Antifungal resistance of fungi is rising, rendering fungal infections from *Aspergillus fumigatus* and *Candida albicans* recognised for unmet research and development needs, and higher as a public health burden, these pathogens are, in 2025, therefore recognised as "critical" priority by the WHO<sup>93</sup>.

# 1.2.3.1. Aspergillus fumigatus

A. fumigatus is a major opportunistic fungal pathogen, responsible for a range of infections that vary in severity depending on the host's immune status and pulmonary condition<sup>94</sup>. Invasive aspergillosis is amongst the most prevalent and severe fungal infections, with high incidence rates in patients with chronic obstructive pulmonary disease, those in intensive care units, individuals with leukaemia, lymphoma, or lung cancer, as well as recipients of hematopoietic stem cell transplants and those with

chronic pulmonary aspergillosis. Collectively, these conditions are associated with a crude annual mortality rate of approximately 85%<sup>92</sup>.

The rising antifungal resistance of A. fumigatus poses a significant global health threat. Triazole resistance, primarily driven by mutations in the cyp51A gene, has led to the emergence of pan-triazole-resistant strains, substantially limiting first-line treatment options. This growing resistance is particularly concerning in low- and middle-income countries, where antifungal susceptibility testing is not routinely available, further complicating effective disease management<sup>93</sup>.

#### 1.2.3.2. Candida albicans

Recent research has revealed the alarming impact of invasive *Candida* infections, with over 1.5 million cases reported annually, resulting in approximately 995,000 deaths — an alarming mortality rate of 66.3%<sup>92</sup>. The most common cause of invasive candidiasis is *Candida albicans*, which frequently presents as sepsis, often progressing to multiorgan failure and septic shock<sup>95,96</sup>.

The growing threat of *Candida* resistance exacerbates this issue, with strains exhibiting resistance to first line drugs such as echinocandins, as well as cases of multidrug resistance occurring against all four major classes of antifungal agents<sup>97-99</sup>. These alarming morbidity and mortality rates demonstrate the urgent need for novel antifungal therapies to combat resistance and improve patient outcomes.

# 1.3. The Global Burden of Cancer

Cancer is a hypernym which describes over 100 diverse pathologies and refers to a class of diseases whereby uncontrolled proliferation of cells occurs, creating a malignancy<sup>100</sup>. These neoplastic processes are governed by hallmark molecular and genetic alterations that facilitate tumour progression and therapeutic resistance<sup>100</sup>. Cancer remains the second leading cause of mortality worldwide, with incidence rates projected to increase by 78% between 2012 and 2035. This rising burden is predominantly attributed to demographic shifts, particularly an ageing global

population, as well as the increasing prevalence of carcinogenic lifestyle factors characteristic of western industrialised societies, including tobacco and alcohol consumption, obesity, physical inactivity, and chronic UV exposure<sup>101</sup>. These epidemiological and environmental determinants act synergistically, driving the escalating morbidity and mortality associated with malignant disease.

Whilst combinatorial chemistry and high-throughput screening have led to the discovery of numerous synthetic chemotherapeutic agents, natural products offer incomparable advantages in anticancer drug development. Various natural product derived compounds, including crude extracts, bioactive component enriched fractions, and structurally modified analogues, have demonstrated significant anticancer activity in both preclinical and clinical settings<sup>102</sup>. In fact, over 60% of clinically approved antineoplastic agents with high therapeutic efficacy have been sourced from natural origins, including terrestrial plants, marine organisms, and microorganisms<sup>103</sup>. These compounds exert their anticancer activity through diverse molecular mechanisms, including the induction of apoptosis, modulation of immune signalling pathways, and suppression of angiogenesis.

Examples of successful natural product-based chemotherapeutics include vincristine, paclitaxel, and topotecan. The vast chemical diversity inherent to natural products provides an invaluable reservoir of bioactive scaffolds for drug discovery, an approach that is gaining increasing recognition in the search for novel cancer therapeutics<sup>104</sup>. Given their structural complexity and unique biological activities, natural products hold high promise for the continued advancement of oncology treatments.

#### 1.3.1. Leukaemia

Leukaemias encompass a group of hematologic malignancies characterised by the uncontrolled proliferation of aberrant white blood cells. These dysfunctional leukocytes lack proper immune function and, by occupying space within the bone marrow, interfere with its capacity to produce substantial numbers of red blood cells,

platelets, and functional white blood cells. There are four main types of leukaemia: acute lymphocytic leukaemia (ALL); acute myelogenous leukaemia (AML); chronic lymphocytic leukaemia (CLL); and chronic myelogenous leukaemia (CML). These are categorised based on the type of white blood cells affected and the speed of progression<sup>103,105</sup>.

Leukaemia accounts for 2.5 and 3.5% of all cancer incidences and mortalities, respectively. Whilst there has been an overall decrease in leukaemia rates worldwide, some populations including Germany, United Kingdom, Japan, Korea and Canada have increasing incidence rates<sup>106</sup>. Leukaemia represents approximately a quarter of all cancer cases in children and is the second leading cause of death in those under 15 years of age<sup>107,108</sup>.

Plant-derived compounds play a crucial role in the treatment of hematologic malignancies. Amongst the earliest plant-based chemotherapeutics approved by the US FDA are the vinca alkaloids from *Catharanthus roseus* (Apocynaceae), vincristine and vinblastine, which are integral to combination therapies for lymphomas, including Hodgkin's disease, as well as acute lymphoblastic leukaemia. Additionally, etoposide, widely used for the management of various leukaemias and lymphomas, and teniposide, used either as a monotherapy or in conjunction with other chemotherapeutic agents for hematologic cancers, are both semi-synthetic derivatives of plant-based compounds of hematologic cancers, are both semi-synthetic derivatives properties highlights their potential in advancing leukaemia therapy. Continued exploration of these bioactive molecules is essential for developing novel, more effective treatment strategies.

# 1.3.2. Lung cancer

Lung cancer is the most common cancer in men, and in 2022, it accounted for approximately 2.5 million new cases and over 1.8 million deaths worldwide, making it the leading cause of cancer mortality. Lung cancer is divided into two main pathological groups: small cell and non-small cell lung cancer. The latter includes squamous and

large cell cancer, as well as lung adenocarcinoma. Lung cancer is responsible for 12.4% of cancers worldwide and 18.7% of cancer-related deaths<sup>110</sup>.

Natural products are fundamental to cancer therapy, with several bioactive compounds derived from plants demonstrating cytotoxic effects on lung cancer cells and modulating the tumour microenvironment. While several such compounds are under investigation but are not yet FDA-approved, promising candidates include galbanic acid from *Ferula assafoetida* (Apiaceae), jolkinolides A and B from *Euphorbia fischeriana* (Euphorbiaceae), parthenolide from *Tanacetum parthenium* (Asteraceae), and isogambogenic acid from *Garcinia hanburyi* (Clusiaceae)<sup>111-115</sup>.

In addition, several plant-derived compounds have successfully progressed to clinical use and received FDA approval for lung cancer treatment. For example, paclitaxel, etoposide and topotecan, a semi-synthetic analogue of camptothecin<sup>116-118</sup>. These compounds exemplify the immense potential of plant-derived molecules in advancing lung cancer therapeutics and underscore the need for continued exploration of natural product scaffolds in drug discovery.

#### 1.3.3. Melanoma

Melanoma is an aggressive malignancy arising from melanocytes, the melaninproducing cells of the epidermis. It ranks as the fifth most common cancer in men and
the sixth in women, and despite constituting only 4% of all skin cancer cases, it causes
75% of deaths from skin cancer. While early-stage melanoma can often be managed
effectively through surgical excision, prognosis declines precipitously with disease
progression. The limited efficacy of current therapeutic strategies in advanced cases is
a significant challenge, highlighting the urgent need for new treatment options<sup>119</sup>.

# 1.4. Plant Families Used in This Study - the Myristicaceae and the Clusiaceae

# 1.4.1. The Myristicaceae family

### 1.4.1.1. Distribution and botanical characterisation

The Myristicaceae (nutmeg) is a pantropical family of angiosperm trees distributed throughout Africa, Central and South America, North America, Asia and the Pacific

Islands. This family is often amongst the ten most common tree families present in lowland tropical forests ecoregions including karangas and marshes 120. The Myristicaceae belongs to the order Magnoliales and class Dicotyledonia. The family consists of approximately 21 genera (with each genus restricted to a specific continent) and 520 species, which are lowland rainforest and mainly understory trees 121,122. Members of Myristicaceae are distinguished by their small unisexual flowers - which have synandrium (androecium which is fused). These grow around a sterile central column to produce a sessile point which is surrounded by a single perianth, with an average of 3 tepals<sup>123</sup>. Most Myristicaceae species are dioecious, including the genera explored in this study: Gymnacranthera, Horsfieldia, Myristica and Knema. All species' fruits are leathery and oblong, with light orange to salmon-colored pericarps, measuring 1-12 cm long. Pericarps surround dark colored seeds which are covered by a bright orange or red aril<sup>124</sup>. Myristicaceae bark ranges from smooth to scaly. Further defining characteristics of Myristicaceae include watery red or pink sap produced by the bark when cut, and distinctive tree architecture 120. Leaves of the Myristicaceae species are mostly exstipulate and arranged alternately in two opposite rows. The leaf lamina is entire, with most species having a white to pale green underside (Figure 1.4). When Myristicaceae leaves are dried, the underside of all members of the Gymnacranthera, Knema and some of the Myristica remain waxy-white, whilst all of the Horsfieldia and some of the Myristica members have brown undersides. When dried, all species display raised veins on the underside only <sup>121</sup>.



**Figure 1.4.** The fruits, stems and leaves of *Myristica fragrans* (Myristicaceae)<sup>125</sup>.

### 1.4.1.2. Ethnomedicinal value

Myristicaceae species are of high ethnobotanical significance and species have been used as timber, food, poisons, medicines and hallucinogenic agents<sup>120</sup>. Four of the twenty-one Myristicaceae species are psychoactive, including the *Virola* genus and *Myristica fragrans* species which produce the indole alkaloid *N*,*N*-dimethyltryptamine (DMT) and the phenylpropenes myristicin, elemicin and safrole, respectively<sup>126,127</sup>. The psychomimetic properties of these species means that they are used during spiritual ceremonies<sup>128</sup>. In addition, *Virola theiodora* was used to poison arrow heads by the Yekwana Indians. Many members of the Myristicaceae hold ethnomedicinal value across the world, with 37 species having reported uses<sup>129</sup>. Many of which are associated with anti-microbial, anti-inflammatory and psychotropic properties. For example, *Osteophloeum platyspermum* is drunk or smoked in Brazil to treat respiratory disorders, infections and mental disorders<sup>130,131</sup>. *Virola surinamensis* is inhaled or drunk to treat inflammation, cancers and stomach disorders, and *Staudtia kamerunensis* var. *gabonensis* is drunk to treat dysentery, mental disorders and as an arrow poison antidote<sup>132,133</sup>.

### 1.4.1.3. Phytochemical investigations

Pharmacological investigations have revealed a spectrum of activity including anti-diabetic, anti-protozoal, anti-microbial, cytotoxic and immunomodulatory. In addition, many compounds have been isolated from the Myristicaceae species, including terpenes, fatty acids, alkanes, lignans, flavonoids, coumarins and indole alkaloids<sup>129</sup>. Barman *et al.* reviewed the phytochemicals, pharmacology and toxicity of the Myristicaceae family, demonstrating the bioactive potential of these species. This certainly warrants the investigation into under-explored members of the Myristicaceae, which is the case for many of the 26 Myristicaceae species in this review, which have been sampled from Borneo. These species belong to the *Horsfieldia, Gymnacranthera, Knema* or *Myristica* genera and their known traditional uses as well as their pharmacological and phytochemical studies are summarised in chapter 2.

# 1.4.2. The Clusiaceae family

### 1.4.2.1. Distribution and botanical characterisation

The Clusiaceae family (formally known as the Guttiferae) is comprised of approximately 15 genera and 800 species which are widely distributed throughout tropical regions <sup>134</sup>. The Clusiaceae genera of interest in this study (*Calophylum*, *Garcinia*, *Kayea*, *Mammea* and *Mesua*) are mainly distributed throughout the Indo-Malesian area <sup>135</sup>. These regions have a minimum average monthly temperature of 18 °C and high rainfall <sup>136</sup>. Here, the Clusiaceae are often associated with water courses, growing in lowland and sometimes lower montane environments, and generally occur in primary forests, peat swamps, or in black-water flood plains <sup>135,137</sup>. The Clusiaceae is a family of small to medium trees, shrubs or herbs which secrete resinous white–yellow viscous exudates. Some former Clusiaceae species have black or red glands which contain the bioactive metabolites hypericin or pseudohypericin, the active components of the medicinal plant, "St John's Wort" (*Hypericum perforatum*), which now belongs to the Hypericaceae family <sup>138</sup>. Leaves of species within the Clusiaceae family are usually entire, can be arranged either whorled or opposite, and are almost always estipulate (Figure 1.5). The Clusiaceae species are a mixture of monoecious and dioecious, depending on their genus. This

family's flowers are hypogynous and have bracteoles often present close beneath the calyx. Petals exist separated but imbricate or contorted in bud, and stigmas range from 1–12 in count. Fruits of this family are capsular, contain multiple seeds and have vertical dehiscence (slight splitting)<sup>135</sup>.



Figure 1.5. The fruits, stems and leaves of *Garcinia xanthochymus* (Clusiaceae)<sup>139</sup>.

### 1.4.2.2. Ethnomedicinal value

The Clusiaceae family is a rich source of bioactive metabolites, which explains their high ethnomedicinal value. For example, *Montrouziera cauliflora* is used as a laxative, *Moronobea coccinea* is used topically for wounds and skin infections, *Pentadesma butracea* treats infections, cardiovascular and digestive problems, diarrhoea, fever and for cosmetic purposes<sup>139</sup>, <sup>141</sup>. *Symphonia globulifera* is used to treat scabies and as an analgesic <sup>140</sup>. Many of the Clusiaceae species exert anti-inflammatory effects and have therefore been traditionally used with many inflammatory-associated disorders, covering a very wide spectrum of medicinal uses <sup>142</sup>. Clusiaceae is a family of high economic value, due to being used as building materials, for the production of commercially valuable gum or resin (*Garcinia*), in agriculture for production of edible

fruits and in medicine<sup>143</sup>. In addition, species are popular ornamental plants and have been commercialised due to this in several countries<sup>136</sup>.

# 1.4.2.3. Phytochemical investigations

The Clusiaceae is known phytochemically for biosynthesising the major compound classes: benzophenones, bioflavonoids, coumarins and xanthones. Of these, many polyisoprenylated benzophenones from Clusiaceae species have reported biological activities including cytotoxic, anti-inflammatory, anti-microbial and anti-oxidant<sup>114</sup>. The heterogeneity of species within this family has resulted in a particularly wide scope of uses. In chapter 2, the genera *Garcinia*, *Kayea*, *Calophyllum* (Calophyllaceae), *Mammea* and *Mesua* will be broadly described, and the literature on selected species of each genus will have reports on their phytochemistry and biological activity reviewed.

### 1.5. Aims and Objectives of Thesis

The rationale behind this study is based on the evidence that phytochemicals remain one of the most productive reservoirs of lead compounds in modern drug discovery. Despite their potential, the vast botanical diversity of Borneo is still largely untapped, with an estimated less than 5% having been previously investigated for their pharmacological properties. These species belong to genera (for example *Garcinia* and *Myristica*) with documented pharmacological and ethnomedicinal value, making them a compelling source of plants to investigate.

# 1.5.1. Aim

The main aim of this research was to isolate and characterise the natural products from previously unexplored species of the Myristicaceae (*Knema membranifolia*, *Gymnacranthera forbessi* and *Gymnacranthera contracta*) and the Clusiaceae (*Garcinia caudiculata*) families. This research primarily aimed to identify antibacterial compounds, while also evaluating the antifungal and anticancer potential of selected metabolites.

# 1.5.2. Objectives

- 1. To conduct a targeted comprehensive literature review, compiling all the published phytochemical and pharmacological data on each of the Myristicaceae and the Clusiaceae species collected from Borneo (Chapter 2).
- 2. To select unstudied species based on the preliminary literature review and perform small scale extractions for their initial screening against clinically relevant bacterial pathogens.
- 3. To scale up extractions which displayed antibacterial activities in preliminary screening assays.
- 4. To isolate both bioactive and co-occurring compounds as well as other metabolites from extracts displaying antibacterial activity, using various chromatographic techniques.
- 5. To elucidate the structures of novel and known isolated compounds using spectroscopic methods, including mass spectrometry (MS), and 1D and 2D nuclear magnetic resonance (NMR) techniques such as COSY, HSQC, and HMBC.
- 6. To evaluate the antifungal and anticancer activity of each isolated compounds which have not previously been explored for these properties.

### 1.6. References

- 1 J. Shurkin, *Proc Natl Acad Sci USA*, 2014, **111**, 17339–17341.
- 2 J. Lietava, *J Ethnopharmacol*, 1992, **35**, 263–266.
- 3 R. S. Solecki, Science, 1975, 190, 880-881.
- 4 K. Hardy, Revista Brasileira De Farmacognosia, 2020, 31, 1.
- D. Lordkipanidze, A. Vekua, R. Ferring, G. P. Rightmire, J. Agusti, G. Kiladze, A. Mouskhelishvili, M. Nioradze, M. S. Ponce De León, M. Tappen and C. P. E. Zollikofer, *Nature*, 2005, **434**, 717–718.
- 6 E. Trinkaus and M. R. Zimmerman, Am J Phys Anthropol, 1982, 57, 61–76.
- 7 G. M. Cragg and D. J. Newman, *Pure Appl Chem*, 2005, 77, 7–24.
- N. Chaachouay and L. Zidane, *Drugs Drug Candidates*, 2024, 3, 184–207.
- 9 S. Wangkheirakpam, in *Natural Products and Drug Discovery*, editors: S. C. Mandal, V. Mandal, T. Konishi, Elsevier, 2018, Chapter 2 Traditional and Folk Medicine as a Target for Drug Discovery, 29-56.
- M. Butnariu, C. Quispe, J. Herrera-Bravo, M. Pentea, I. Sarac, A. S. Küşümler, B. Özçelik, S. Painuli, P. Semwal, M. Imran, T. A. Gondal, S. Emamzadeh-Yazdi, N. Lapava, Z. Yousaf, M. Kumar, A. H. Eid, Y. Al-Dhaheri, H. A. R. Suleria, M. del M. Contreras, J. Sharifi-Rad and W. C. Cho, Oxid Med Cell Longev, 2022, 2022, 1–23.
- N. Tawfeek, M. F. Mahmoud, D. I. Hamdan, M. Sobeh, N. Farrag, M. Wink and A. M. El-Shazly, *Front Pharmacol*, 2021, **12**, 593856.
- 12 C. Veeresham, *J Adv Pharm Technol Res*, 2012, **3**, 200–201.
- 13 D. H. Boucher, *Bioscience*, 1991, **41**, 72–76.
- D. Juyal, V. Thawani, S. Thaledi and M. Joshi, J Tradit Complement Med, 2014, 4, 159–161.
- 15 D. A. Dias, S. Urban and U. Roessner, *Metabolites*, 2012, **2**, 303–336.
- 16 M. Wink, *Phytochemistry*, 2003, **64**, 3–19.
- 17 X. Q. Huang and N. Dudareva, *Curr Bio*, 2023, **33**, R473–R478.
- 18 R. A. Hussein and A. A. El-Anssary, in *Herbal Medicine*, ed. P. F. Builders, Salem Press, 2020, Chapter 2 Plant Secondary Metabolites: The Key Drivers of the Pharmacological Actions of Medicinal Plants, 14–30.
- 19 P. Angelini, *Antibiotics*, 2024, **13**, 746.
- B. Khameneh, M. Iranshahy, V. Soheili and B. S. Fazly Bazzaz, *Antimicrob Resist Infect Control*, 2019, **8**, 1–28.
- W. H. Talib, S. Daoud, A. I. Mahmod, R. A. Hamed, D. Awajan, S. F. Abuarab, L. H. Odeh, S. Khater and L. T. Al Kury, *Molecules*, 2022, 27, 1–41.
- 22 A. Rayan, J. Raiyn and M. Falah, *PLoS One*, 2017, **12**, e0187925.
- A. Tariq, S. Sadia, K. Pan, I. Ullah, S. Mussarat, F. Sun, O. O. Abiodun, A. Batbaatar, Z. Li, D. Song, Q. Xiong, R. Ullah, S. Khan, B. B. Basnet, B. Kumar, R. Islam and M. Adnan, *Phytother Res*, 2017, 31, 202–264.
- J. Iqbal, B. A. Abbasi, T. Mahmood, S. Kanwal, B. Ali, S. A. Shah and A. T. Khalil, *Asian Pac J Trop Biomed*, 2017, **7**, 1129–1150.
- 25 L. Zhu and L. Chen, *Cell Mol Biol Lett*, 2019, **24**, 1–11.
- 26 A. Paul, K. Acharya and N. Chakraborty, *S Afr J Bot*, 2023, **161**, 365–376.
- 27 A. Behera and S. Padhi, *Environ Chem Lett*, 2020, **18**, 1557–1567.
- 28 K. Avemann, R. Knippers, T. Koller and J. M. Sogo, *Mol Cell Biol*, 1988, **8**, 3026–3034.
- 29 C. C. Wu, T. K. Li, L. Farh, L. Y. Lin, T. S. Lin, Y. J. Yu, T. J. Yen, C. W. Chiang and N. L. Chan, *Science*, 2011, **333**, 459–462.

- 30 K. de Sousa Oliveira, L. A. de Lima, N. B. Cobacho, S. C. Dias and O. L. Franco, in *Antibiotic Resistance: Mechanisms and New Antimicrobial Approaches*, ed. K. Kon, M. Rai, Academic press, 2016, Chapter 2 Mechanisms of Antibacterial Resistance: Shedding Some Light on These Obscure Processes?, 19–35.
- 31 W. C. Reygaert, *AIMS Microbiol*, 2018, **4**, 482–501.
- 32 GBD 2021 Antimicrobial Resistance Collaborators, *The Lancet*, 2024, **404**, 1199–1226.
- 33 J. O'neill et al., Tackling Drug-Resistant Infections Globally: Final Report and Recommendations, Welcome Trust, London, 2016.
- 34 D. Stekel, *Nature*, 2018, **562**, page 192.
- 35 E. P. Abraham and E. Chain, *Nature*, 1940, **146**, DOI: 10.1038/146837a0.
- 36 F. D. Lowy, *Nature*, 2003, **111**, 1264–1273.
- A. L. Panlilio, D. H. Culver, R. P. Gaynes, S. Banerjee, T. S. Henderson, J. S. Tolson, W. J. Martone, *Infect Control Hosp Epidemiol*, 1992, **13**, 582–586.
- 38 M. Lobanovska and G. Pilla, *Yale J Biol Med*, 2017, **90**, 135–145.
- 39 K. Lewis, *Cell*, 2020, **181**, 29–45.
- T. G. Villa, L. Feijoo-Siota, A. Sánchez-Pérez, J. L. R. Rama and C. Sieiro. In *Horizontal Gene Transfer, an Overview of the Mechanisms Involved*, Springer, 2019, 3–76.
- 41 F. Le Roux and M. Blokesch, *Annu Rev Microbiol*, 2018, **72**, 89–110.
- 42 D. Sun, K. Jeannot, Y. Xiao and C. W. Knapp, *Front Microbiol*, 2019, **10**, 01933.
- 43 A. Carattoli, *Int J Med Microbiol*, 2013, **303**, 298–304.
- 44 E. Y. Furuya and F. D. Lowy, *Nat Rev Microbiol*, 2006, **4**, 36–45.
- 45 F. C. Tenover, Am J Med, 2006, 119, S3–S10.
- 46 T. J. Silhavy, D. Kahne and S. Walker, *Cold Spring Harb Perspect Biol*, 2010, 2, 1–16.
- 47 Z. Breijyeh, B. Jubeh and R. Karaman, Molecules, 2020, 25, 1–23.
- Biorender, Scientific Image and Illustration Software BioRender, www.biorender.com, (accessed 5 May 2025).
- 49 R. E. Impey, D. A. Hawkins, J. M. Sutton and T. P. Soares da Costa, *Antibiotics (Basel)*, 2020, **9**, 1–19.
- 50 M. F. Richter and P. J. Hergenrother, *Ann N Y Acad Sci*, 2019, **1435**, 18–38.
- V. Yarlagadda, G. B. Manjunath, P. Sarkar, P. Akkapeddi, K. Paramanandham, B. R. Shome, R. Ravikumar and J. Haldar, *ACS Infect Dis*, 2016, **2**, 132–139.
- 52 M. Vaara, *Microbiol Rev*, 1992, **56**, 395–411.
- T. Uddin, A. Chakraborty, A. Khusro, B. Zidan, S. Mitra, T. Bin Emran, K. Dhama, M. Ripon, M. Gajdács, M. Sahibzada, M. Hossain and N. Koirala, *J Infect Public Health*, 2021, **14**, 1750–1766.
- 54 S. Gibbons and E. E. Udo, *Phytother Res*, 2000, **14**, 139–140.
- E. C. J. Smith, G. W. Kaatz, S. M. Seo, N. Wareham, E. M. Williamson and S. Gibbons, *Antimicrob Agents Chemother*, 2007, **51**, 4480–4483.
- F. Vandenesch, G. Lina and T. Henry, Front Cell Infect Microbiol, 2012, 2, 12.
- G. Sakoulas, G. M. Eliopoulos, R. C. Moellering, C. Wennersten, L. Venkataraman, R. P. Novick and H. S. Gold, *Antimicrob Agents Chemother*, 2002, **46**, 1492–1502.
- 58 S. J. Peacock and G. K. Paterson, *Annu Rev Biochem*, 2015, **84**, 577–601.
- 59 W. Reygaert, *Clin Lab Sci*, 2009, **14**, 139–140.
- 60 G. Cox and G. D. Wright, *Int J Med Microbiol*, 2013, **303**, 287–292.
- 61 S. Stefani, F. Campanile, M. Santagati, M. L. Mezzatesta, V. Cafiso and G. Pacini, *Int J Antimicrob Agents*, 2015, **46**, 278–289.
- 62 A. Beceiro, M. Tomás and G. Bou, *Clin Microbiol Rev*, 2013, **26**, 185–230.
- 63 D. Rawat and D. Nair, *J Glob Infect Dis*, 2010, **2**, 263–274.
- 64 F. Prestinaci, P. Pezzotti and A. Pantosti, Pathog Glob Health, 2015, 109, 309–318.

- P. Collignon, J. J. Beggs, T. R. Walsh, S. Gandra and R. Laxminarayan, *Lancet Planet Health*, 2018, **2**, e389–e405.
- 66 M. M. C. Buckner, M. L. Ciusa and L. J. V. Piddock, FEMS Microbiol Rev, 2018, 42, 781–804.
- A. Cesaro, S. C. Hoffman, P. Das and C. de la Fuente-Nunez, *npj Antimicrob Resist*, 2025, **3**, 1–10.
- 68 U. Hofer, *Nat Rev Microbiol*, 2018, **17**, 3–3.
- 69 C. J. Murray et al., Lancet, 2022, **399**, 629–655.
- 70 T. Foster, in *Medical Microbiology*, 4<sup>th</sup> edition, University of Texas Medical Branch at Galveston, 1996, Chapter 12 *Staphylococcus*.
- G. A. Filice, J. A. Nyman, C. Lexau, C. H. Lees, L. A. Bockstedt, K. Como-Sabetti, L. J. Lesher and R. Lynfield, *Infect Control Hosp Epidemiol*, 2010, **31**, 365–373.
- 72 C. Hübner, N. O. Hübner, K. Hopert, S. Maletzki and S. Flessa, *Eur J Clin Microbiol Infect Dis*, 2014, 33, 1817–1822.
- 73 K. L. Mason, T. A. Stepien, J. E. Blum, J. F. Holt, N. H. Labbe, J. S. Rush, K. F. Raffa and J. Handelsman, *mBio*, **2**, e00065-11.
- N. R. Naylor, K. B. Pouwels, R. Hope, N. Green, K. L. Henderson, G. M. Knight, R. Atun, J. V. Robotham and S. R. Deeny, *PLoS One*, 2019, **14**, e0221944.
- E. Tacconelli, E. Carrara, A. Savoldi, S. Harbarth, M. Mendelson, D. L. Monnet, C. Pulcini, G. Kahlmeter, J. Kluytmans, Y. Carmeli, M. Ouellette, K. Outterson, J. Patel, M. Cavaleri *et al.*, *Lancet Infect Dis*, 2018, **18**, 318–327.
- WHO, WHO publishes list of bacteria for which new antibiotics are urgently needed, www.who.int/news/item/27-02-2017-who-publishes-list-of-bacteria-for-which-new-antibiotics-are-urgently-needed, (accessed 21 March 2025).
- 77 M. Adeolu, S. Alnajar, S. Naushad and R. S. Gupta, *Int J Syst Evol Microbiol*, 2016, **66**, 5575–5599.
- 78 Y. Li, S. Kumar, L. Zhang, H. Wu and H. Wu, *Open Med*, 2023, 18, 2–12.
- 79 WHO, WHO Bacterial Priority Pathogens List, 2024: bacterial pathogens of public health importance to guide research, development and strategies to prevent and control antimicrobial resistance, World Health Organization, Geneva, 2024.
- 80 O. Gal-Mor, E. C. Boyle, G. A. Grassl, C. López-Macías, L. L. Lenz, J. Health and R. Kumar, *Front Microbiol*, 2014, 5, 1 10.
- 81 V. J. McGovern and L. J. Slavutin, *Am J Surg Pathol*, 1979, **3**, 483–490.
- 82 G. Kumar, S. Kumar, H. Jangid and A. Shidiki, Front Microbiol, 2025, 16, 1524287.
- 83 Q. Shi, C. Huang, T. Xiao, Z. Wu and Y. Xiao, Antimicrob Resist Infect Control, 2019, 8, 1–9.
- A. Zawacki, E. O'Rourke, G. Potter-Bynoe, A. Macone, S. Harbarth and D. Goldmann, *Infect Control Hosp Epidemiol*, 2004, **25**, 1083–1089.
- M. Kim, S. Christley, N. N. Khodarev, I. Fleming, Y. Huang, E. Chang, O. Zaborina and J. C. Alverdy, *J Trauma Acute Care Surg*, 2015, **78**, 823–829.
- K. Shigemura, S. Arakawa, Y. Sakai, S. Kinoshita, K. Tanaka and M. Fujisawa, *Int J Urol*, 2006, 13, 538–542.
- 6. H. C. Furtado, P. A. d'Azevedo, A. F. Santos, A. C. Gales, A. C. C. Pignatari and E. A. S. Medeiros, *Int J Antimicrob Agents*, 2007, **30**, 315–319.
- A. Gomila, J. Carratalà, J. M. Badia, D. Camprubí, M. Piriz, E. Shaw, V. Diaz-Brito, E. Espejo, C. Nicolás, M. Brugués, R. Perez, A. Lérida, A. Castro, S. Biondo, D. Fraccalvieri, E. Limón, F. Gudiol, M. Pujol, X. Serra-Aracil, L. Mora, A. Cruz, E. Moreno, F. Aguilar, L. Pagespetit, N. Freixas, A. Navarro, L. Martin, C. Sanz, J. Cuquet, R. Vazquez, N. Arroyo, A. F. Lopez, S. Iftimie, J. Obradors and A. Marrón, *BMC Infect Dis*, 2018, **18**, 1–9.
- M. H. Kollef, J. Chastre, J. Y. Fagon, B. François, M. S. Niederman, J. Rello, A. Torres, J. L. Vincent, R. G. Wunderink, K. W. Go and C. Rehm, *Crit Care Med*, 2014, **42**, 2178–2187.

- 90 N. Sathe, P. Beech, L. Croft, C. Suphioglu, A. Kapat and E. Athan, *Infect Med*, 2023, 2, 178–194.
- 91 R. L. Bang, P. N. Sharma, S. C. Sanyal and I. Al Najjadah, *Burns*, 2002, **28**, 746–751.
- 92 D. W. Denning, *Lancet Infect Dis*, 2024, **24**, 428–438.
- WHO, Antifungal agents in clinical and preclinical development: overview and analysis, https://www.who.int/publications/i/item/9789240105140, (accessed 3 April 2025).
- 94 F. Bongomin, S. Gago, R. O. Oladele and D. W. Denning, J Fungi, 2017, 3, 57.
- 95 J. P. Richardson, *Pathogens*, 2022, **11**, 459–462.
- 96 C. Logan, I. Martin-Loeches and T. Bicanic, *Intensive Care Med*, 2020, 46, 2001–2014.
- 97 S. Costa-de-oliveira and A. G. Rodrigues, *Microorganisms*, 2020, **8**, 154–173.
- 98 P. G. Pappas, C. A. Kauffman, D. R. Andes, C. J. Clancy, K. A. Marr, L. Ostrosky-Zeichner, A. C. Reboli, M. G. Schuster, J. A. Vazquez, T. J. Walsh, T. E. Zaoutis and J. D. Sobel, *Clin Infect Dis*, 2015, **62**, 1–50.
- 99 J. Chatelon, A. Cortegiani, E. Hammad, N. Cassir and M. Leone, *Adv Ther*, 2019, **36**, 3308–3320.
- 100 Y. A. Fouad and C. Aanei, *Am J Cancer Res*, 7, 1016–1036.
- Jemal A, Bray F, Center MM, Ferlay J, Ward E, Forman D, CA Cancer J Clin, 2011, 61, 69–90.
- 102 Q. Y. Zhang, F. X. Wang, K. K. Jia and L. D. Kong, Front Pharmacol, 2018, 9, 1253.
- 103 C. Cotoraci, A. Ciceu, A. Sasu, E. Miutescu and A. Hermenean, *Molecules*, 2021, 26, 2709–2738.
- 104 P. S. Bhadury and J. Pang, Curr Org Chem, 2015, 19, 1460–1490.
- 105 T. Nemkov, A. D'Alessandro and J. A. Reisz, *Cancer Rep.*, 2018, **2**, 1139 1152.
- J. Huang, S. Chai Chan, C. Ho Ngai, V. Lok, L. Zhang, D. Eliseo Lucero-Prisno III, W. Xu, Z.-J. Zheng, E. Elcarte, M. Withers, M. C. S Wong, D. Kristjansson, W. M. Rashed, L.-P. DE Iii and Z. Z-j, Frontiers in Oncology, 2022, 12, 904292.
- National Cancer Institute, *Cancer Information Summaries* www.cancer.gov/types/leukemia/patient/child-all-treatment-pdq (accessed 20th April 2025).
- T. P. Whitehead, C. Metayer, J. L. Wiemels, A. W. Singer and M. D. Miller, *Curr Probl Pediatr Adolesc Health Care*, 2016, **46**, 317–352.
- 109 A. Paul, K. Acharya and N. Chakraborty, *S Afr J Bot*, 2023, **161**, 365–376.
- 110 S. Wang, L. Dong, X. Wang and X. Wang, *Open Med*, 2020, **15**, 190–197.
- 111 A. Vennepureddy, J.-P. Atallah and T. Terjanian, World J Oncol, 2015, 6, 429-436.
- F. Bray, M. Laversanne, S. Hyuna, J. Ferlay, R. L. Siegel, I. Soerjomataram and J. Ahmedin, *CA Cancer J Clin*, 2024, **74**, 229–263.
- 113 L. Shen, S. Q. Zhang, L. Liu, Y. Sun, Y. X. Wu, L. P. Xie and J. C. Liu, *Med Sci Monit*, 2017, **23**, 223–237.
- 114 W. H. Talib and L. T. Al Kury, *Biomed Pharmacother*, 2018, **107**, 1488–1495.
- 115 Y. Fan, A. Peng, S. He, X. Shao, C. Nie and L. Chen, *J Chemother*, 2013, **25**, 298–308.
- 116 G. M. Hashim, M. Shahgolzari, K. Hefferon, A. Yavari, S. Venkataraman, *Bioengineering*, 2025, 12, 56–63.
- 117 C. A. Dehelean, I. Marcovici, C. Soica, M. Mioc, D. Coricovac, S. Iurciuc, O. M. Cretu and I. Pinzaru, *Molecules*, 2021, **26**, 1109–1138.
- 118 J. Y. Jang, D. Kim, E. Im and N. D. Kim, *Int J Mol Sci*, 2025, **26**, 796–813.
- 119 L. E. Davis, S. C. Shalin and A. J. Tackett, Cancer Biol Ther, 2019, 20, 1399–1379.
- J. P. Janovec and R. García. In *Encyclopedia of Forest Sciences*, editors: J. Burley, J. Evans and J. A. Youngquist, Elsevier, Oxford, 2004, 1762.
- 121 L. Neo, K. Y. Chong, S. Y. Tan, C. Y. Koh, R. C. J. Lim, J. W. Loh, W. Q. Ng, W. W. Seah, A. T. K. Yee and H. T. W. Tan, *Nat S*, 2016, **9**, 69–138.
- 122 M. J. M. Christenhusz and J. W. Byng, *Phytotaxa*, 2016, **261**, 201–217.
- 123 H. Sauquet, Am J Bot, 2003, 90, 2193–1305.
- 124 J. H. Beaman, W. J. J. O. de Wilde and P. F. Stevens, *Kew Bull*, 2002, **57**, 251–252.

- T. M. A. Utteridge and G. L. C. Bramley (editors), *The Kew Tropical Plant Families Identification Handbook*, 2nd edition, Royal Botanic Gardens, Kew, Richmond, 2015.
- B. Holmstedt, J. E. Lindgren, T. Plowman, L. Rivier, R. E. Schultes and O. Tovar, *Bot Mus Lealf Harv Univ*, **3**, 215–235.
- 127 N. A. Alrashedy and J. Molina, *PeerJ*, 2016, 4, e2546.
- 128 B. C. Bennett and R. Alarcón, *Econ Bot*, **48**, 152–158.
- 129 R. Barman, P. K. Bora, J. Saikia, P. Kemprai, S. P. Saikia, S. Haldar and D. Banik, 2021, *Phytother Res*, 4632–4659.
- 130 D. J. Mckenna, G. H. N. Towers and F. S. Abbott, *J Ethnopharmacol*, **12**, 179–211.
- 131 R. E. Schultes, Bot Mus Lealf Harv Univ, 3, 271–275.
- D. Musuyu Muganza, B. I. Fruth, J. Nzunzu Lami, G. K. Mesia, O. K. Kambu, G. L. Tona, R. Cimanga Kanyanga, P. Cos, L. Maes, S. Apers and L. Pieters, *J Ethnopharmacol*, **141**, 301–308.
- 133 C. A. Hiruma-Lima, L. M. Batista, A. B. A. de Almeida, L. de Pietro Magri, L. C. dos Santos, W. Vilegas and A. R. M. S. Brito, *J Ethnopharmacol*, 2009, **122**, 406–409.
- 134 V. Kuete, N. Lall and T. Efferth, 2012, *Evid Based Complement Alternat Med*, **2012**, DOI: 10.1155/2012/535219.
- P. F. Stevens, in *The Families and Genera of Vascular Plants*, volume 9, ed. K. Kubitzki, Springer, Berlin, 2007, 48–66.
- O. C. Spaargaren and J. A. Deckers, in *Encyclopedia of Soils in the Environment*, Academic Press, Oxford, 2004, chapter Factors of Soil Formation/Climate, 512–520.
- 137 K. A. P. Diel, L. C. Marinho and G. L. von Poser, *J Ethnopharmacol*, 2022, **284**, 114745.
- 138 M. Shrivastava and L. K. Dwivedi, Int J Pharm Sci Res, 2015, 6, 1000–1007.
- 139 Kew Science, *Clusiaceae Lindl, Plants of the World Online*, Kew Science, www.powo.science.kew.org/taxon/urn:lsid:ipni.org:names:30000758-2/images, (accessed 9 April 2025).
- 140 U. B. Breitbach, M. Niehues, N. P. Lopes, J. E. Q. Faria and M. G. L. Brandão, *J Ethnopharmacol*, 2013, **147**, 180–189.
- 141 G. Alitonou, F. Avlessi, D. C. K. Sohounhloue, J. M. Bessière and C. Menut, *J Essent Oil Res*, 2010, **22**, 138–140.
- 142 U. Acuna, N. Jancovski and E. Kennelly, Curr Top Med Chem, 2009, 9, 1560–1580.
- M. S. De Melo, J. D. S. S. Quintans, A. A. D. S. Araújo, M. C. Duarte, L. R. Bonjardim, P. C. D. L. Nogueira, V. R. D. S. Moraes, J. X. De Araújo-Júnior, Ê. A. N. Ribeiro and L. J. Quintans-Júnior, *Evid Based Complement Alternat Med*, 2014, **2014**, 1–10.

# Chapter 2 – Literature Review on Plant Species Sampled from Borneo – Direction of Future Work

# 2.1. Biodiversity of Borneo - the Myristicaceae and the Clusiaceae

The island of Borneo has remarkable biodiversity due to its complex network of ecological niches spanning a range of tropical forest types. For perspective, a tropical rainforest in Sarawak (East Malaysia) has over 1000 different species of trees within a 50-hectare area<sup>1</sup>. Amongst this diverse flora, a variety of unexplored species grow, some of which belong to families known for their pharmacological activity, such as the Myristicaceae and Clusiaceae. Since ancient times, the Dayak Tribe (the native people of the Island of Borneo) have utilised natural forest products of the island, which has revealed the significant ethnomedicinal value of Bornean ecosystems. Such generational knowledge of the Dayak people is important to allow 1) the global recognition that it is imperative to conserve these rapidly diminishing ecosystems, and 2) the discovery of novel bioactive plant metabolites for the development of modern drugs – each of which is integral for the other<sup>2</sup>.

The Island of Borneo, herein referred to as Borneo, contains seven ecoregions which allow the growth of an extensive diversity of plant species. Ecoregions include those occurring on the lowland areas including (i) lowland rainforests; (ii) heath forests (kerangas); (iii) peat swamp forests; (iv) freshwater swamp forests (Southwest) and (v) mangrove forests (coastal areas). In addition, (vi) mountain highland rainforests also occur (central and northeast Borneo) as well as (vii) highland alpine meadows and bushes<sup>2,3</sup>. Occupying these ecoregions are a diversity of species, many of which are endemic to Borneo.

Species within the Myristicaceae and Clusiaceae plant families are known for their production of pharmacologically active compounds and medicinal value. However, many species described here have had no reports of their ethnomedicinal value or phytochemistry thus far. To guide the selection of target species for further investigation in this project, this literature review describes all current literature on 44

plant species of interest (sampled from different parts of Borneo) belonging to these families (Figure 2.1). The reported botanical characterisation, distribution, phytoconstituents and bioactivity of these Bornean plant species of interest will be described herein.

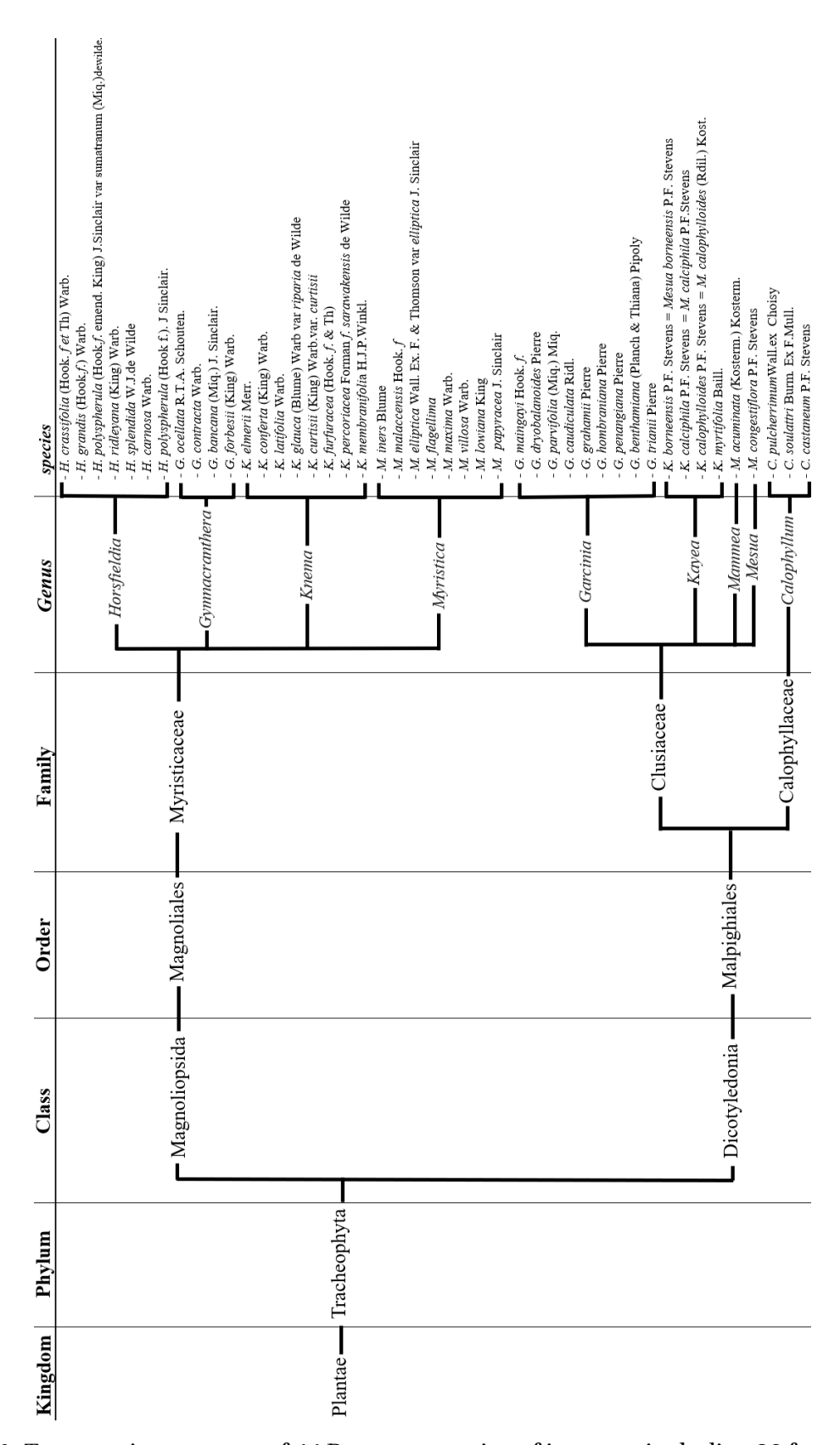


**Figure 2.1.** Taxonomic summary of 44 Bornean species of interest, including 26 from the Myristicaceae, 15 from the Clusiaceae and 3 from the Calophyllaceae (formally Clusiaceae).

### 2.2. The Myristicaceae Species

The distribution, botanical characterisation, ethnomedicinal value and a general overview of phytochemical investigations of the Myristicaceae family were briefly described in Chapter 1 (1.4.1). The following subchapter will summarise the phytochemical and biological investigations of each genus sampled for this study, followed by a comprehensive report of the biological and phytochemical investigations into each of the species to date.

# 2.2.1. Horsfieldia Willd. Genus (Myristicaceae)

The *Horsfieldia* is a genus within the Myristicaceae family consisting of evergreen trees native to South Asia, distributed across India to Malaysia, Borneo, Philippines, Papua New Guinea and Northern Australia<sup>4,5</sup>. The *Horsfieldia* is the second largest genus in the Myristicaceae family after *Myristica*, with approximately 100 species<sup>6,7</sup>. The *Horsfieldia* possess fruits which are significantly smaller than other genera within Myristicaceae. Some *Horsfieldia* species can also be distinguished by characteristic dark brown or dark red dots on leaf undersides. Inflorescences have three sections, are panicle-like and vary in shape and size throughout the genus<sup>8</sup>.

Many species in this genus are of high economic value. The *Horsfieldia* species are mostly known for the oil present in their seeds, which is used for biodiesel, and for their use as furniture and building materials<sup>9</sup>. There are reports of ethnomedicinal uses of the *Horsfieldia*, including of *H. glabra*, which is used in China, Indonesia and Thailand to treat sores and boils<sup>10</sup>. *H. irya* is used in Sri Lanka, Thailand, New Guinea and India to treat pimples, digestive disorders, ulcers and snake bites<sup>11-14</sup>. Furthermore, *H. kingii* is used in India as a stimulant, intoxicant and to treat dysentery<sup>15</sup>.

From these species collectively, compounds including phenols, lignans, fatty acids, flavonoids and alkaloids have been previously isolated<sup>12,13,16-20</sup>. Assessing the bioactivity of the *Horsfieldia* metabolites revealed antiprotozoal agents in *H. spicata*, which are procyanidin-like congeners (lacking a pedant aromatic ring) of myristinins, such as myristinin A (17) (Figure 2.6D)<sup>14</sup>. In addition, *H. irya* (Gaertn.) Warb. found in central

Kalimantan, Borneo, possesses antibacterial properties<sup>21</sup>. This genus seems to lack scientific studies on its bioactivity, considering the interesting spectrum of ethnomedicinal uses it has, as well as the pharmacologically promising family it belongs to.

# Horsfieldia crassifolia (Hook. f et Th) Warb.

Horsfieldia crassifolia is a tree which has been previously found in the peat-swamp forests in the Narathiwat province of Thailand and Brunei Darussalam, Borneo. This species has also been found in the Sabangau tropical peat-swamp forest in Central Kalimantan, Borneo, where the seeds are consumed by *Presbytis rubicunda* (Red langurs) $^{22\cdot26}$ . Like all the *Horsfieldia* members, *H. crassifolia* occurs in ecoregions which provide hot, wet climates with an average rainfall of ~2456 mm/year, average temperature of 27.2 °C and acidic soils $^{27}$ . *H. crassifolia* is the only member of the Myristicaceae which has leaves with brown undersides when fresh, and is one of four species within the *Horsfieldia* genus which has markings on its underside lamina $^{28,29}$ . In addition, this species has a two-lobed perianth, with lamina ranging from  $10-20 \times 3.5-7$  cm in size $^{30}$ . When dried, mature twigs can become hollow. A single phytochemical screening study on *H. crassifolia* as a plant in the Bornean orangutan's diet in Central Kalimantan revealed that fresh leaf samples were found to have 6.6% water, 3.2% protein and 3% (2.6% in dry leaves) lipid content $^{31}$ . However, this is the only chemical analysis of *H. crassifolia* present in the literature to date.

# Horsfieldia grandis (Hook.f.) Warb.

Horsfieldia grandis is a critically endangered 25 m tall understory tree with (usually) scaly and longitudinally fissured bark<sup>32</sup>. This species has been recorded in peat-swamp forests: the Nee Soon Swamp Forest (Singapore) as well as East Kalimantan, West Kalimantan, the Sentarum Lake National Park and the Semenggoh Forest Reserve, Sarawak (Borneo)<sup>30,33-37</sup>. In Sarawak, thrips inhabit *H. grandis* and are good pollinators for this species<sup>38</sup>. Twigs are 1–10 mm wide and densely hairy. Leaf buds are also very hairy and measure 7–15 mm long. This species' leaves are oblong shaped and green-brown in colour, measuring 12–40 × 5–20 cm with 8–19 pairs of secondary veins and

loosely spaced tertiary veins<sup>39,40</sup>. This species has an underside lamina covered in hairs giving it a woolly texture, with tertiary veins usually distinct in dried samples<sup>30</sup>.

Horsfieldia grandis is used traditionally, whereby the sap treats injured lips and the bark is used to treat sprains, by the Kedayan and the Iban ethnic groups, respectively, both from Sarawak, Borneo<sup>41,42</sup>. In addition, the Dayak tribe in Central Kalimantan use H. grandis as a medicinal plant during healing rituals and exorcisms<sup>43-45</sup>. The single phytochemical investigation of this species by Teo (2018) found H. grandis to contain an anti Gram-positive bacterial ( $IC_{50} > 16 \mu g/mL$ ) diterpene (E)-3-methyl-5-(2R,\*aR)-1,2,4a,5-tetramethyl-7-oxo-1,2,3,4,7,8,8a-octahydronaphthalene (STP17) (1) (Table 2.2, Figure 2.2)<sup>42</sup>.

**Figure 2.2.** Chemical structure of (*E*)-3-methyl-5-(2R,\*aR)-1,2,4a,5-tetramethyl-7-oxo-1,2,3,4,7,8,8a-octahydronaphthalene (**1**) isolated from *Horsfieldia grandis* (Hook.f.) Warb by Teo (2018)<sup>42</sup>.

Horsfieldia polyspherula (Hook f.). J Sinclair &

Horsfieldia polyspherula (Hook.f emend. King) J.Sinclair var. sumatrana (Miq.) dewilde.

This plant has been recorded in the Nee Soon Swamp Forest (Singapore) and Taman Negara Pahang, Kuala Tahan (Malaysia)<sup>46</sup>. This species is distributed in Malaysia, Borneo and Singapore<sup>4</sup>. The name *H. polyspherula* comes from the Latin *poly* meaning

many and *sphere* meaning globe/ball, which refers to its flowers resembling small balls. There are two varieties of *H. polyspherula*: *var. polyspherula* and *var. sumatrana*, which are distinguished by various characteristics from dry and fresh samples including fruit, bud and lamina size, and vein arrangement as described by Neo *et al.*, 2016<sup>30</sup>. This tree species reaches 40 m tall with striate bark, and branches measuring 2–5 mm across which are glabrous. Buds of this species are hairy, and flowers exist in clusters of up to 8. Leaves measure 7–28 × 2.5–9 cm with 6–15 pairs of raised secondary veins and faint tertiary veins. Dried leaves develop a brown lamina which varies in lightness and shape (from narrowly ovate [young leaves] to lanceolate)<sup>4,30</sup>.

In terms of phytochemistry of this species, Ismail *et al.* (2011)<sup>46</sup> found low flavonoid and low alkaloid content in *H. polyspherula* (*var. polyspherula*) stems after performing onsite chemical screening. In addition, crude extracts of an unspecified variety of *H. polyspherula* have *in vitro* antihyperglycaemic and antioxidant activity (Table 2.1)<sup>47</sup>. In terms of the chemotaxonomic differentiation of *H. polyspherula* varieties, there is no literature indicating this distinction. A recent study isolated nine phytochemicals from *H. polyspherula* (Hook f.) J. Sinclair. Here, an ethyl acetate and methanol extract of the bark displayed acetylcholinesterase and butyrylcholinesterase inhibition (Table 2.1).

Recent studies have performed the bioassay-guided isolation of benzoic acids, fatty acids and a sterol from *H. polyspherula*, where the known compounds 16-phenylhexadecanoic acid (2) and undecylbenzene (3) displayed acetylcholinesterase and butyrylcholinesterase inhibitory activity. Additional phytochemical analysis revealed the occurrence of flavonoids, phytosterols, steroids and triterpenoids in this species (Figure 2.3)<sup>48</sup>.

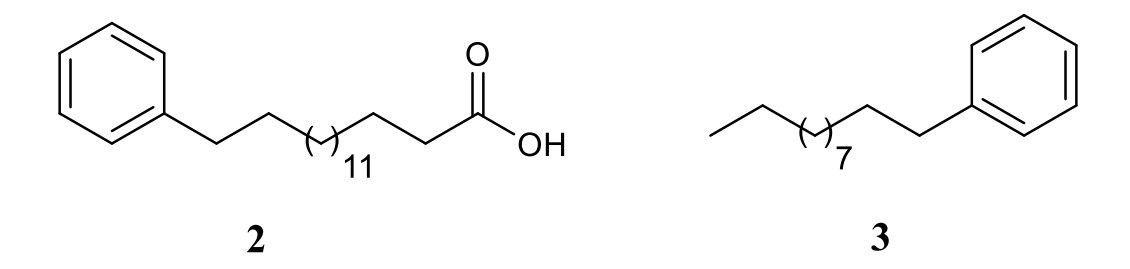


**Figure 2.3.** Chemical structures of 16-phenylhexadecanoic acid (2) and undecylbenzene (3) isolated from *Horsfieldia polyspherula*.

# Horsfieldia ridleyana (King) Warb.

This species has been recorded at Ayer Hitam Forest Reserve and Bukit Bauk (Peninsular Malaysia)<sup>49,50</sup>. *H. ridleyana* grows to 20 m tall in lowland forest in poor soils and produces edible fruits (as well as *H. amygdaliana* (Wall.) Warb which also produces edible seeds and arils)<sup>51-53</sup>.

# Horsfieldia splendida W.J.de Wilde.

*Horsfieldia splendida* is endemic to Borneo and is located in lowland mixed dipterocarp forests (whereby the dominant species belong to the family Dipterocarpaceae), kerangas forest and montane forests. This species usually occurs at altitudes under 600 m. As of 1998, this is a near-threatened species<sup>54</sup>.

### Horsfieldia carnosa Warb.

Like *H. splendida*, *H. carnosa* is also endemic to Borneo. It has been recorded in the Sentarum Lake National Park, West Kalimantan and Punggualas Peat Swamp Forest, Central Kalimantan, Borneo<sup>21,34,55</sup>. There is limited literature on the botanical characterisation of this species.

### 2.2.1.1. Horsfieldia Summary

Of the seven *Horsfieldia* species of interest from Borneo, one species (*H. grandis*) has a reported ethnomedicinal use, two species (*H. crassifolia* and *H. polyspherula* var. polyspherula) had a phytochemical screening study, and four species (*H. polyspherula* var. sumatrana, *H. ridleyana*, *H. splendida* and *H. carnosa*) have had neither of these.

Of these species, two have been evaluated for biological activity (*H. polyspherula* and *H. grandis*), both of which have had a bioactive compound isolated from it (Tables 2.2 and 2.3, Figure 2.2). Evidently, there are few reports of traditional uses of the Bornean *Horsfieldia* species in Figure 2.1, whilst several species of this genus have been well investigated, and their bioactive potential demonstrated. This indicates the medicinally promising secondary metabolites of this genus. In addition, *Horsfieldia* belongs to the Myristicaceae, which, as a family, produce a variety of bioactive metabolites and holds high pharmaceutical significance. This highlights a gap in the literature and suggests the need for further phytochemical and pharmacological investigations into the unexplored members of this genus.

# 2.2.2. Gymnacranthera Genus (Myristicaceae)

The *Gymnacranthera* (Myristicaceae) is a genus of flowering plants which are native to India, Malaysia, Borneo, Maluku, Indonesia, Philippines and Thailand. There are 7 accepted species in the *Gymnacranthera*, all of which have similar male and female flowers. Therefore, species have been distinguished on their vegetative features including leaf and fruit characteristics. The *Gymnacranthera* members always possess hairs on buds and have either smooth or slightly fissured bark with lenticels. Leaves have white undersides (with distinct tertiary veins) and glabrous upper surfaces. All *Gymnacranthera* are dioecious, with laciniate arils completely covering seeds. Important vegetative characteristics for species delimitation are well described by Shouten, 1986<sup>56</sup>.

One species of the *Gymnacranthera*, *G. farquhariana*, has a reported ethnomedicinal use in India for a variety of aliments, including infections<sup>57</sup>. The few studies on *Gymnacranthera* so far have found significant biological activity within this genus. Bhat (2016) found methanolic extracts of *G. farquhariana* to have antimicrobial and antioxidant properties<sup>58</sup>. Later, Bhat (2017) found the same species to have moderate cytotoxicity against breast cancer cells *in vitro*, whereby aqueous crude extractions caused a higher decrease in cell viability than methanolic<sup>57</sup>. This suggested that the presence of tannins, phenolics and resins in the methanolic extract enhanced the anti-

bacterial and anti-oxidative properties of this species<sup>58</sup>. Johns *et al.*, (1997) isolated the major (1,5-dimethoxy-3-(dimethylaminomethyl)indole) and minor (*N*-methyltetrahydro-β-carboline) alkaloids from *G. paniculata*<sup>59</sup>. In addition, *G. canarica* essential oil was found to have three main constituents: β-caryophyllene, linalool and α-humulene (with 58.1% of leaf oil constituents being sesquiterpene hydrocarbons)<sup>60</sup>. Finally, Teo isolated antibacterial compounds from *G. ocellata*, as reported below<sup>42</sup>. To date, these seem to be the only reports of the traditional use, specific phytochemistry and biological activity of the *Gymnacranthera*. The botanical characterisation and any phytochemical screening of the Bornean species of interest within this genus will be described.

# Gymnacranthera contracta Warb.

Information on this species investigated during this thesis is included chapter 4.0 results and discussions (section 4.1.2).

# Gymnacranthera ocellata R.T.A. Schouten

*Gymnacranthera ocellata* (formally *G. contracta*) is a species endemic to Borneo and is defined by the presence of woolly hairs on the bud surface throughout the plant's lifetime, with less lower leaf hair than other members of this genus. Twigs are flattened, covered with lenticels and have scars at the base from previous vegetative buds<sup>8,56</sup>. Teo (2018) previously isolated two compounds from *G. ocellata*: 4,4-(2*R*,3*S*)-2,3-dimethylbutane-1,4-diyl)bis-(2-methyoxyphenol) (STP14) (4) and its related compound STP15 (5), which both displayed moderate activity against Gram-positive bacterial strains (Table 2.2, Figure 2.4)<sup>42</sup>.

**Figure 2.4.** Chemical structures of 4,4-(2*R*,3*S*)-2,3-dimethylbutane-1,4-diyl)*bis*-(2-methyoxyphenol) (4) and 5 isolated from *Gymnacranthera* ocellata R.T.A. Schouten.

# Gymnacranthera ocellata R.P.A Schotten.

There is currently no available literature on this species.

# Gymnacranthera bancana (Miq.) J. Sinclair

*G. bancana* is a tree distributed through Borneo, Singapore and Malaysia, and grows in lowland and swamp forests at up to 250 m altitude<sup>28,61</sup>. This species grows 20 m high and has fruits arranged in clusters of up to eight<sup>62</sup>.

# Gymnacranthera forbesii (King) Warb

*Gymnacranthera forbesii* has 2 varieties: var. *forbesii* and var. *crassinervis*. Var. *forbesii* has a wider distribution, throughout Borneo, southern Thailand and Malaysia, whilst var. *crassinervis* is endemic to Borneo. Var. *crassinervis* can be distinguished from var. *forbesii* and other species by its thick twigs and orange – yellow nerves on leaf undersides. However, the distinction of varieties within this species can be difficult. Both *G. forbesii* varieties grow up to 40 m tall and have microscopic hairs on leaf undersides which are shed easily. Var. *forbesii* grows leaf lamina up to 15 cm long and shows distinct secondary veins on the underside<sup>56</sup>.

# 2.2.2.1. The Gymnacranthera Summary

There have been no reports on ethnomedicinal uses of the *Gymnacranthera* species in this review. Of the five Bornean *Gymnacranthera* species of interest, two (*G. ocellata* and *G. contracta*) have been phytochemically studied to the extent of isolating a compound, all of which were bioactive metabolites. Two species, *G. bancana* and *G. forbesii* have had no studies on their phytochemical constituents or their biological activity. This genus seems to be largely unexplored, not only throughout the species of interest in this study, but throughout all species. However, chemotaxonomy would suggest that investigating this Myristicaceae genus further for their bioactive phytoconstituents is a reasonable objective.

# 2.2.3. The *Knema* Genus (Myristicaceae)

There are a total of 93 species belonging to the *Knema*, which are distributed through Africa, southeast Asia, southern China and throughout Malaysia, Borneo and Australia<sup>63-66</sup>. *Knema* species are the dominant members of the tropical lowland forest ecoregions of Borneo<sup>67</sup>. When dried, members of this genus have a waxy-white underside, with densely arranged and distinct tertiary veins on lamina tops and undersides<sup>30</sup>.

The *Knema* species are popular in traditional medicines, with multiple reports across species. For example, *K. corlicosa* is used as a traditional medicinal salves and *K. glaucescens* is a traditional medication for abdominal pain in Sarawak<sup>68-70</sup>. In addition, *K. attenuata* Warb. is used in "Ashwagandadhi nei" (medicated ghee) to treat breathing and spleen disorders, as well as tastelessness<sup>71,72</sup>. Furthermore, *K. angustifolia* and *K. erratica* are used in India and Thailand to treat a mixture of dysentery, cancer, ulcers, or as skin tonics<sup>11,73,74</sup>. *K. globularia* and *K. tenuinervia* subsp. *setosa* are used in Thailand as a blood tonic and as a cancer treatment, respectively<sup>75,76</sup>. In addition, *K. laurina* is used in Malaysia to treat rheumatism, digestive disorders, inflammation and fevers<sup>77,78</sup>.

A variety of compounds have been isolated from the *Knema* genus, including acetophenones, alkyl/acyl resorcinols, flavonoids, lignans, phenylalkylphenols and substituted stilbenes. These have shown a spectrum of biological activity including antibacterial, antifungal, antinematodal, anti-inflammatory, anticancer and acetylcholinesterase inhibitory activity. Twelve of the 93 *Knema* species have been phytochemically and/or pharmacologically investigated thus far, with 97 compounds isolated from the *Knema* since 1978<sup>75</sup>. This is a well explored genus, with each species providing a distinct profile of bioactive secondary metabolites, making the investigation into unexplored *Knema* species an exciting prospect.

### Knema membranifolia H.J.P.Winkl.

Literature published on this species, which was used in this study, is summarised in Chapter 4.0 results and discussions (section 4.1.1).

### Knema furfuracea (Hook. f. & Th)

Knema furfuracea is distributed through Peninsular Malaysia, Singapore and Thailand. However, it is predominantly distributed in Yunnan, China. This species grows up to 25 m tall, with a trunk measuring up to 35 cm diameter at breast height (DBH)<sup>79</sup>. At all *K. furfuracea* locations, this species is used as a traditional medicine for the treatment of cancer, dysentery, pimples and mouth sores<sup>76</sup>. Multiple studies have investigated the phytochemistry of this species which have been summarised in Table 2.2. Fourteen compounds have been isolated from this species, including cardanols, coumarins, lignans and phenolic compounds (Table 2.2). Some of these display biological activities.

Rangkaew *et al.* investigated *K. furfuracea* for its antiproliferative effects on cancer cells *in vitro*. The arylnaphthalene lignan furfuracin (6) displayed no cytotoxicity, whilst lignans (+)-*trans*-1,2-dihydrodehydroguaiaretic acid (7) and fragransin A2 (8) displayed weak cytotoxicity in ovarian cancer cells, and the isoflavone biochanin A (9) displayed weak cytotoxicity against lung cancer cells (Figure 2.5)<sup>80</sup>. Additionally, phenolic compounds knerachalins A (10) and B (11) have shown antibacterial activity against *Staphylococcus aureus* and *S. pneumoniae* with minimum inhibitory concentration

(MIC) values of 8 μg/mL and 4 μg/mL, respectively (Figure 2.5C)<sup>81</sup>. Further phenolic compounds have been isolated in more recent studies, including similar flavonoids, lignans, as well as anacardic acids<sup>82</sup>. The essential oil composition of this species has also been analysed using GC/MS, revealing a total of 31 components<sup>83</sup>.

**Figure 2.5.** Chemical structures of *K. furfuracea* metabolites, including **(A)** lignans: furfuracin **(6)**, (+)-trans-1,2-dihydrodehydroguaiiaretic acid (7) and fragransin A2 **(8)**; **(B)** isoflavone biochanin A **(9)** and **(C)** phenolic compounds knerachalin A **(10)** and knerachalin B **(11)**, isolated from *Knema furfuracea* (Hook. *f*. & Th).

# Knema glauca (Blume) Warb. (var. riparia de Wilde)

Knema glauca is native to Indonesia, Malaya, Sumatra, Thailand and Borneo. This species can grow from 5 – 30 m tall, with branches extending often from the top half of its trunk. Traditionally, it is harvested for its timber and fruits8. A single study by Rangkaew et al., (2009) investigated the phytochemistry and bioactivity of K. glauca (variety unspecified). A new diterpene acid, glaucaic acid (12) was isolated, however biological activity of this has not been found thus far (Figure 2.6A). Some compounds and crude extracts from this species displayed antibacterial, anti-viral and anti-cancer activities 2.2). (Table 2.1, Table For example, malabaricone dodecanoylphloroglucinol (14) and 1-(2,4,6-trihydroxyphenyl)-9-phenylnonan-1-one (15) isolated from K. glauca displayed anti-bacterial activity against Mycobacterium tuberculosis with MIC values of 25, 50 and 100 µg/mL, respectively (Figure 2.6B).

Additionally compound **13** was active against the malarial parasite *Plasmodium falciparum* and **14** displayed antiviral activity against herpes simplex virus type 1 and (both  $IC_{50} = 3 \mu g/mL)^{80}$ . Lignans such as sesamin (**16**) have also been isolated from this species (Figure 2.7B). **16**, a major component of sesame seeds, is recognised for its beneficial role in cardiovascular disease, cancer and oxidative stress<sup>84,85</sup>. Flavonoids such as myristinin A (**17**) are also *K. glauca* metabolites (Figure 2.6D). This compound is a known DNA damaging and DNA-polymerase beta inhibitor<sup>86</sup>.

**Figure 2.6.** Chemical structures of **(A)** diterpene acid, glaucaic acid **(12)**, **(B)** phenolic compounds, malabaricone A **(13)**, dodecanoylphloroglucinol **(14)**, 1-(2,4,6-trihydroxyphenyl)-9-phenylnonan-1-one **(15)**, **(C)** lignan, sesamin **(16)** and **(D)** flavan, myristinin A **(17)** isolated from *Knema glauca* (Blume) Warb.

#### Knema elmerii Merr.

*Knema elmerii* is a species endemic to Borneo and has been recorded in Sarawak, East Malaysia where it grows at low elevations in clay soils<sup>37</sup>. This tree grows 5 – 15 m tall, occasionally has stilt roots and is characterised by silky indumentum on its leaf undersides and flaking twig bark. This species has spherical (globose) male buds and convex staminal discs. Some of these species' defining features are present in other *Knema* species, however this is the only species to possess all of these properties combined<sup>4</sup>. *K. elmerii* is on the IUCN Red List, but is of low concern as of 2019<sup>87</sup>.

# Knema conferta (King) Warb.

*Knema conferta* is native to Borneo, Peninsular Malaysia, Singapore and Thailand<sup>64</sup>. This lowland forest tree grows from 10 – 25 m tall and is similar to *K. laurina*, *K.oblongata* and *K. scortechini*<sup>88</sup>. Species are differentiated based on varying indumentums and male flower characteristics, described by Koster and Bass, 1981<sup>29</sup>. Therefore, however, during vegetative states this species may be difficult to identify. Similarly to *K. elmerii*, this species has a conservation status of low concern<sup>89</sup>.

# Knema latifolia Warb.

*Knema latifolia* is distributed in Sumatra (Malaysia), Borneo and Indonesia<sup>35,90-92</sup>. This is the dominant species of the Myristicaceae family in the Bulungan forest area in East Kalimantan, composing part of the understory at 25 – 35 m high<sup>93</sup>. Additionally, in the Bogani Nani Wartabone National Park, Indonesia, this species is a significant part of the diet for *Bubalus* spp. which feed on the leaves, as well as shelter for Orangutans in Kalimantan<sup>94,95</sup>.

## Knema curtisii (King) Warb.var. curtisii

Knema curtisii is a species distributed through Peninsula Malaysia, Thailand and mainly Borneo<sup>53,96,97</sup>. Four varieties of this species are described by de Wilde (2000)<sup>8</sup>: var. curtsii, var. amoena J Sinclair, var. arnosa J Sinclair and var. paludosa J Sinclair. K. curtsii var. curtisii has been identified in Thailand and Singapore, in addition to Borneo and Peninsular Malaysia<sup>4,30</sup>. K. curtisii var. curtisii is distinguished by a broadly elliptic lamina, with blunt or acute tapering tips and distinct secondary and tertiary veins<sup>30</sup>. K. curtisii grows up to 35 m tall with twigs reaching 1-2 mm across. Lamina are glossy dark brown to green, and are up to 10 cm long, with brown lamina midribs. Flowers have a 3-4 lobed penrith and are cream – pink inside, with male and female inflorescence consisting of 2 – 15 and 1 – 5 flowers, respectively<sup>8,30</sup>.

Ong *et al.*, (2009)<sup>98</sup> examined *K. curtisii* (variety unspecified) and revealed the photosensitising activity of its crude methanolic extracts. Extracts were subject to bioassay-guided fractionation to isolate four chlorophyll derived photosensitising

agents following the pheophorbide-a and -b core structures: pheophorbide-a methyl ester (18), hydroxy pheophorbide-a methyl ester (19), hydroxy pheophorbide-b methyl ester (20) and hydroxy purpurin 7-lactone dimethyl ester (21) (Figure 2.7, Table 2.2).

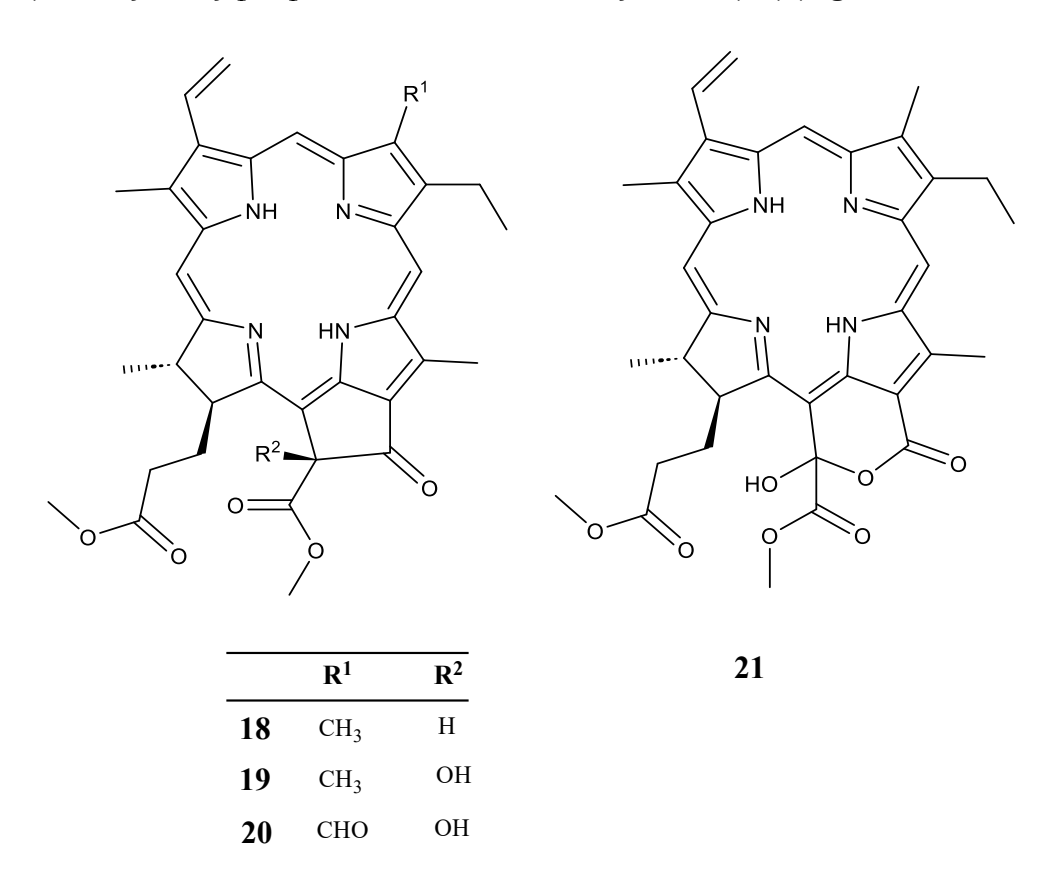


**Figure 2.7.** Chemical structures of chlorophyll derivatives, pheophorbide-a methyl ester (18), hydroxy pheophorbide-a methyl ester (19), hydroxy pheophorbide-b methyl ester (20) and hydroxy purpurin 7-lactone dimethyl ester (21) isolated from *Knema curtisii* (King) Warb.

### Knema percoriacea Forman f. sarawakensis de Wilde

Knema percoriacea J Sinclair species has three forms: forma percoriacea, forma fusca de Wilde and forma sarawakensis de Wilde, all of which are endemic to Borneo<sup>99,100</sup>. This species grows 5-25 m tall, extending twigs with a 3-6 mm diameter. Dry leaves are olive to brown on topside with distinct veins and measure  $7-25 \times 3-8$  mm. This species is closely related to *K. furfuracea*. *K. percoriacea* forma sarawakensis is defined by its papery leaves (which are larger than the other forma), brown – yellow hairs on twig, and apexes measuring 0.3-1 mm long. In addition, the flower indumentum of this forma partially sheds or is very easily rubbed off, making it the most similar forma of

this species to *K. furfuracea*<sup>8</sup>. Soares (2018) is the only report on the bioactivity of this species to date (Table 2.1). Here, hexane extracts of *K. percoriacea* displayed inhibition of R3888 (*IncW*) plasmid transfer<sup>101</sup>.

### 2.2.3.1. The Knema Summary

The literature published thus far on the *Knema* species shows very promising pharmacological potential of the genus as a whole. Of the 8 Bornean *Knema* species of interest in this study, only 1 (*K.* furfuracea) has reported ethnomedicinal uses, 3 have had bioactive compounds isolated from them (*K. furfuracea*, *K. glauca*, *K. curtisii*) and 1 has had only crude extracts bio-assayed (*K. percoriacea*). Two *Knema* species of interest (*K. elmerii* and *K.* latifolia) have no reported phytochemicals or biological activity. The *Knema* species which have been previously investigated for their pharmacologically valuable compounds and demonstrate the promising bioactive potential of the uninvestigated species of this genus.

### 2.2.4. The Myristica Gronov. Genus (Myristicaceae)

The genus *Myristica* includes 120 species and has the largest distribution of the genera within the Myristicaceae<sup>8</sup>. *Myristica* species exist through South Africa, Mauritius, Grenada, India, Sri Lanka, Singapore, New Guinea and are native to the Maluklu Islands (eastern Indonesia)<sup>102,103</sup>. This genus' centre of diversity is in the Malayan peninsula and New Guinea, where it can occur in montane forests<sup>8,67</sup>. The *Myristica* species are diecious trees with grey, brown to black bark and dark green leaves which usually dry into a white colour with loosely spaced reticulation. Fruits of the *Myristica* measure up to 10 cm long<sup>8,30</sup>. Inflorescences of this genus are of singular, and flowers are frequently fragrant. Fused androecium always create a pointed tip, and styles and stigmas are always small in the *Myristica* species<sup>8</sup>.

The *Myristica* is commonly known as the "nutmeg" genus due to the economically important nutmeg plant *Myristica fragrans* which produces the popular spice, nutmeg, harvested from its seed kernel inside the fruit, as well as the mace produced from the red aril. Nutmeg oil obtained from fruits and arils is also a popular component and is

used as a flavouring agent in food and drinks, and in perfumery and cosmetic industries. The *Myristica* metabolite trimyristin has multiple derivatives including myristic acid (5), myristic alcohol and glycerol, which are industrially important in many commercial products<sup>77</sup>. Nutmeg is a well-studied spice with multiple health benefits as well as adverse effects<sup>104,105</sup>.

Traditionally, the *Myristica* species have multiple ethnomedicinal uses. Many of these uses are shared between species. *M. fragrans* is used across Europe, Asia, Australasia and Africa to treat gastro-intestinal, inflammatory and mental disorders<sup>75,115-117</sup>. In India, *M. adamanica, M. beddomei* subsp. *ustulata* and *M. malabarica* are used to treat a mixture of fevers (particularly due to malaria infection), bleeding, skin infections and gastro-intestinal disorders, diabetes, respiratory infections, constipation, dysmenorrhea, vomiting, as an aphrodisiac and for spasmolytic problems<sup>73,77,106-113</sup>.

The mentioned *Myristica* species, as well as *M. argentea*, *M. cinnamomea*, *M. fatua* and *M. magnifica* have been extensively phytochemically explored, to reveal over 50 different compounds of a variety of classes including diaryl long-chain alkanes, indole alkaloids, lignans, long chain fatty acids, neolignans, phenylpropanoids and terpenes.<sup>77</sup>. Species of this genus have also displayed *in vitro* acetylcholinesterase and monoamine oxidase inhibition, *in vitro* and *in vivo* cytotoxic activity and antimicrobial activity against a range of bacteria and viruses<sup>77,114-121</sup>. *Myristica* has offered an exciting spectrum of bioactive secondary metabolites thus far, giving the unexplored species of this genus high pharmacological potential.

# Myristica iners Blume

*Myristica iners* is distributed in Singapore, Cambodia, Indonesia, Malaysia and Borneo<sup>122-126</sup>. This species grows up to 40 m tall, usually displaying buttress or stilt roots. Leaves dry into a brown- grey colour, lamina measure 7–24 × 1.5–10 cm and have 11 – 16 pairs of secondary veins. One of the distinctive characteristics of *M. iners* is inferred by its name, *iners*, which in Latin means inert, referring to the absence of seed aroma which is found in the other *Myristica* species. *M. iners* is a traditional medicine whereby

the bark is ingested to treat constipation and other ailments<sup>127</sup>. A recent study demonstrated the free radical scavenging activity of M. iners stem, revealing the significial antioxidant potential of this crude extract<sup>128</sup>.

## Myristica malaccensis Hook. f

This species is distributed in Borneo, Peninsular Malaysia, Indonesia and Sumatra $^{90,126,129-131}$ . *M. malaccensis* grows 7-35 m tall, has buttress roots (1-3 m tall) and extends twigs measuring 2-4 mm in diameter with hairs always under 1 mm. The trunk bark is smooth, greenish – grey – dark brown, with pale yellow inner bark. Leaves are thin and elliptic to oblong shaped, measuring  $10-30 \times 4-10$  cm with a dark olive upper surface and grey – brown lower surface. There are two subspecies of *M. malaccensis*: subsp. *malaccensis* and subsp. *papillosa* de Wilde, the latter displaying distinctive papillation (small bumps) on the lamina lower surface and being endemic to Borneo<sup>8</sup>.

# Myristica elliptica Wall, Ex Hook. f. & Thomson var. elliptica J. Sinclair

*Myristica elliptica* is distributed in Singapore, Borneo, Indonesia, Thailand and Malaysia, growing often in peat swamp forest ecoregions, along rivers and streams, at maximum altitudes of  $500 \text{ m}^{30,132\cdot134}$ . This species grows 6-40 m tall, extending straw-colored twigs which measure 2-4 mm in diameter and have short grey hairs (0.1-0.3 mm). Trunks can be branched from the base, and buttress roots can form. Fresh leaves are glossy green on the topside and dry into the same straw colour as twigs. These are elliptic shape (relating to the name *elliptica*) and measure  $9-32 \times 3-12 \text{ cm}^8$ . The fruit of this species is used as a spice. Additionally, the Shompen tribe of the Great Nicobar Islands (positioned among mainland India, Thailand, the Malay Peninsular and Java-Sumatra), applied crushed *M. elliptica* bark and seeds externally to treat skin diseases<sup>135-137</sup>.

#### Myristica maxima Warb.

*Myristica maxima* is distributed in Borneo, Singapore, Thailand and Malaysia<sup>8,138</sup>. This species grows up to 35 m tall, with buttress or stilt roots, grey – brown bark and extends twigs which measure 4 – 8 mm across. Leaves measure 16 – 40 x 6 – 20 cm, are membranous with 23 – 33 pairs of secondary veins, and very distinct tertiary veins on both the top and bottom sides<sup>8</sup>. This species is critically endangered. *M. maxima* is distinguished by its dense indumentum on the leaf underside and its black leaf colour when dried. The word "*maxima*" in Latin may refer to the large leaf size of this species<sup>30</sup>.

Two studies have isolated and described some bioactivity of M. maxima metabolites. From these investigations, ten acylphenol compounds including the sitosterol ester  $\beta$ -sitosteryl oleate (30), giganteone A (24), giganteone C (25), giganteone E (26), maingayic acid B (29), maingayone A (27), maingayone B (28), malabaricone A (13) (also isolated from K. glauca, Figure 2.6), malabaricone B (22), malabaricone C (23) (Figure 2.8, Table 2.2)<sup>139,140</sup>. Here, compounds 13 and 25 were cytotoxic against human prostate cancer cell lines, and compounds 26, 24, 25, 27 and 28 displayed potent DPPH free radical scavenging<sup>139</sup>. Later, compounds 23 and 24 displayed potent  $\alpha$ -glucosidase inhibitory activity of with IC<sub>50</sub> values of 59.6  $\mu$ M and 39.5  $\mu$ M, respectively<sup>139,140</sup>. Additional studies have demonstrated the anticancer activity of compound malabaricone A<sup>141,142</sup>. Compound 30 has been found as a potential modern-day ingredient in low cholesterol butter<sup>143,144</sup>.

**Figure 2.8.** Chemical structures of **(A)** acylphenol compounds malabaricone B **(22)**, malabaricone C **(23)**, giganteone A **(24)**, giganteone C **(25)** giganteone E **(26)**, maingayone A **(27)**, maingayone B **(28)**, maingayic acid B **(29)** and **(B)** sitosterol ester b-sitosteryl oleate **(30)** isolated from *Myristica maxima* Warb.

#### Myristica villosa Warb.

30

This species is distributed through Borneo, growing on primarily dry land and sometimes marsh forests at altitudes of  $20 - 1200 \,\mathrm{m}^{36,90}$ . *M. villosa* grows from  $1 - 40 \,\mathrm{m}$  tall, usually has stilt roots and extends twigs measuring  $5 - 10 \,\mathrm{mm}$  in diameter. The bark of this tree is often flakey, with red – brown under bark. This species is distinguishable by its clear indumentum on the leaf underside and its hairy and asymmetrical fruits<sup>8</sup>.

Voeks (2007) reported M. villosa as a useful species to the Dunsun ethnic group in Borneo<sup>145</sup>.

Soares (2018) investigated M. villosa conjugation inhibitors in bacteria and isolated three bioactive  $\omega$ -phenyl fatty acids: 11-phenylundecanoic acid (S70-1) (31), (Z)-13-phenyltridec-4-enoic acid (S70-2) (32) and 14-phenyltridecanoic acid (S70-3) (33) (Figure 2.9, Table 2.2). Using bioassay guided fractionation, these compounds were found to dose-dependently inhibit R388 plasmid transfer in *Escherichia coli*, by targeting bacterial conjugation machinery. Compound 32 displayed the lowest IC<sub>50</sub> of 17  $\mu$ M<sup>101</sup>.

**Figure 2.9.** Chemical structures of  $\omega$ -phenyl fatty acids, 11-phenylundecanoic acid (S70-1) (**31**), (*Z*)-13-phenyltridec-4-enoic acid (S70-2) (**32**) and 14-phenyltridecanoic acid (S70-3) (**33**) isolated from *Myristica villosa* Warb.

# Myristica lowiana King

*Myristica lowiana* is distributed through Singapore, Borneo and Malaysia, growing in peat and fresh water swamp forest ecoregions, at altitudes up to 800 m<sup>30,146,147</sup>. This

species grows up to 25 m tall, extending black twigs which measure 3-6 mm in diameter. Leaves of this species when dry, are glossy and light brown in colour, measure  $14-35\times3.5-11.5$  cm and have 15-22 pairs of secondary veins which are usually sunken<sup>8</sup>.

One phytochemical investigation by Kwapong (2016) isolated amides: 9-oxo-9-((3-phenylpropyl)amino)nonanoic acid (34) and 11-oxo-11-((3-phenylpropyl)amino)undecanoic acid (35); a flavone: 4', 7-dihydroxy-5-methoxyflavone (36), and a lignan: 8-(4-hydroxy-3-methoxyphenyl)-3-methoxy-6,7- dimethyl-5,6,7,8-tetrahydronaphthalen-2-ol (37) from *M. lowiana* and demonstrated the antibacterial and antiplasmid effects of the extract fractions containing these compounds (Table 2.1, Table 2.2, Figure 2.10)<sup>148</sup>.

**Figure 2.10.** Chemical structures of **(A)** amides: 9-oxo-9-((3-phenylpropyl)amino)nonanoic acid **(34)** and 11-oxo-11-((3-phenylpropyl)amino)undecanoic acid **(35)**; **(B)** flavone: 4', 7-dihydroxy-5-methoxyflavone **(36)**, and **(C)** lignan: 8-(4-hydroxy-3-methoxyphenyl)-3-methoxy-6,7-dimethyl-5,6,7,8-tetrahydronaphthalen-2-ol **(37)** isolated from *Myristica lowiana* King.

# Myristica papyracea J. Sinclair

This species is endemic to Borneo and grows in mixed dipterocarp forests at altitudes of up to 300 m. *M. papyracea* grows from 20 – 40 m tall, extending twigs which measure 4 – 8 mm in diameter. Leaves are thin and leathery and measure 6 – 44 x 8—18 cm. The upper surfaces of leaves are olive – brown and lower surfaces are yellow with no hairs and are papillose. This tree often has laterally compressed stilt roots up to 2 m high and is closely related to *M. maxima*. The two can be distinguished by the leaf underside colours when dry<sup>8</sup>. Soares (2018) <sup>101</sup> is the only report of the bioactivity of extracts from *M. papyracea*, whereby hexane extracts displayed inhibition of bacterial plasmid transfer (Table 2.1).

## 2.2.5. The *Myristica* summary

Of the eight Myristica (Myristicaceae) species of interest, only one (*M. flagellima*) seems to have no reports on its botanical characterisation, phytochemical constituents or biological activity. Three species (*M. elliptica, M, iners* and *M. villosa*) have only brief reports on their ethnomedicinal uses, one species (*M. papyracea*) has had the biological activity of its crude extracts demonstrated, and two species (*M. maxima* and *M. lowiana*) have been well investigated for their phytochemistry and biological activity, resulting in the isolation of several compounds. Outside of these selected species, many members of the Myristicaceae family have been well investigated for their pharmacological value and demonstrate the potential value of unexplored species within this family.

**Table 2.1.** Known bioactivity of crude extracts from species of the Myristicaceae family, including those from the genera *Horsfieldia*, *Gymnacranthera*, *Knema* and *Myristica*. IC<sub>50</sub>: 50% maximum inhibitory concentration; MIC: minimum inhibitory concentration.

Species	Part	Extract solvent/s	Biological	Biological activity	Reference
	used		assay		
Horsfieldia	Leaf,	Dichloromethane	α-amylase	Potent α-amylase	47
polyspherula	stem		and α-	$(IC_{50} = 1.6 - 2.4)$	
			glucosidase	mg/ml-1) and a-	
			inhibitory	glucosidase (IC $_{50}$ =	
				2.4 - 4.2  mg/mL-1	

Knema furfuraceae K. glauca	Stem  Leaf  Fruit  Leaf	Dichloromethane, methanol  Ethanol, dichloromethane Ethanol  Methanol	assay. DPPH free radical scavenging assay. MIC assay. Resazurin microplate assay. MTT cell viability assay.	hyperglycaemic). Free radical scavenger (antioxidant, IC <sub>50</sub> =1.6 µg/mL). Anti- S. aureus (MIC = 19 µg/mL). Cytotoxic against NCI-H187 (IC <sub>50</sub> = 0.9 µg/mL). Reduced cell viability (20 µg/mL) when exposed to 9.6 J/cm² of a broad- spectrum light. (Photosensitising	47 81 80 98
K. curtisii	Bark	Hexane	Conjugation inhibition assay (automated).	agent). Specific inhibitor of R3888 (IncW) plasmid transfer.	101
K. percoriacea	Bark	Chloroform, hexane, methanol	Conjugation inhibition assay (automated).	Specific inhibitor of R3888 (IncW) and pKM101 (IncN) plasmid transfer at 512 µg/mL.	101
Myristica villosa	Stem bark	Hexane	Conjugation inhibition assay.	pUB307 (IncP), R7K (IncW) plasmid inhibition ≤15%.	148
M. lowiana	Stem bark Bark	Chloroform Methanol	Conjugation inhibition assay. Conjugation inhibition assay (automated).	pUB307 (IncP) plasmid inhibition ≤15%. TP114 (Incl₂), pUB307 (IncP), R7K (IncW) plasmid inhibition.	148

activity

inhibitor (anti-

Specific inhibitor of R3888 (IncW) plasmid transfer at  $512 \ \mu g/mL$ .

**Table 2.2.** All known compounds isolated from species of interest (Figure 2.1) within the Myristicaceae family, including those from the genera *Horsfieldia*, *Gymnacranthera*, *Knema* and *Myristica*. PPAPs: polycyclic polyprenylated acylphloroglucinol.

Species	Part used	Compound Isolated	Туре	Reference
Horsfieldia grandis	Leaf	( <i>E</i> )-3-methyl-5-(2 <i>R</i> ,*a <i>R</i> )- 1,2,4a,5-tetramethyl-7-oxo- 1,2,3,4,7,8,8a- octahydronaphthalen (STP17) (1)	Diterpene	42
H. polyspherula	Stem bark	16-phenylhexadecanoic acid (2) Undecylbenzene (3)	Fatty acid	48
Gymnacranthera ocellata	Leaf	4,4-(2R,3S)-2,3- dimethylbutane-1,4- diyl)bis-(2- methyoxyphenol) (STP14) (4) 4,4-(2R,3S)-2,3- dimethylbutane-1,4- diyl)bis-(2-	Diterpene  Diterpene	42
Knema furfuraceae	Stem bark	methyoxyphenol) (STP15) (5) Dehydroguaiaretic acid (+)-trans-1,2- dihydrodehydroguaiaretic acid 8-hydroxy-(12- phenyldodecyl)isocoumari n	Neolignan Cardanol Isocoumarin	76
		3-(12- phenyldodecyl)phenol	Cardanol	

	Leaf	Furfuracin (6)	Arylnaphthale ne lignan	80
	Stem	(+)-trans-1,2-	Lignan	
	Stem	dihydrodehydroguaiaretic acid (7)	Lighan	
		Fragransin A2 (8)	Lignan	
		Biochanin A (9)	Isoflavone	
		Gingkolic acid	Alkylbenzoic acid	
		Anarcardic acid	Alkylbenzoic acid	
		2-hydroxy6-(12-	Phenylalkylbe	
		phenyldodecyl)benzoic acid	nzoic acid	
		2- hydroxy-6-(12-	Phenylalkylbe	
		phenyldodecen-8'Z-	nzoic acid	
		yl)benzoic acid		
	Leaf	Knerachelin A (10)	Phenylacylphe	81
		Knerachelin B (11)	nol	
K. glauca	Fruit	Glaucaic acid (12)	Diterpene acid	80
		1-(2,6-dihydroxyphenyl)	Acylphenol	
		tetradecan-1-one		
		Malabaricone A (13)		
		Dodecanoylphloroglucinol		
		(14)		
		1-(2,4,6-trihydroxyphenyl)-		
		9-phenylnonan-1-one (15)		
		Sesamin (16)	Lignan	
		Asarinin		
		Myristinin D	Flavan	
	Leaf	Myristinin A (17)		
	Stem	(±)-7,4'-dihydroxy-3'- methoxyflavan		
K. curtisii	Leaf	Pheophorbide-a methyl	Cyclic	98
		ester (18)	tetrapyrrole	
		Hydroxy pheophorbide-a	derivative	
		methyl ester (19)		
		Hydroxy pheophorbide-b		
		methyl ester (20)		
		Hydroxy purpurin 7-		
		lactone dimethyl ester (21)		
Myristica maxima		Malabaricone A (13)	Acylphenol	139

	Bark (dichlorom ethane)	Malabaricone B (22) Malabaricone C (23) Giganteone A (24) Giganteone C (25) Giganteone E (26) Maingayone A (27) Maingayone B (28) Maingayic acid B (29) b—sitosteryl oleate (30)		
M. villosa	Bark (hexane)	11-phenylundecanoic acid (S70-1) ( <b>31</b> ) ( <i>Z</i> )-13-phenyltridec-4-enoic acid (S70-2) ( <b>32</b> )	Phenylalkenoi c acid ω- phenylalkenoi c acid	101
		14-phenyltridecanoic acid (S70-3) ( <b>33</b> )	Phenylalkenoi c acid	
M. lowiana	Stem bark (hexane)	9-oxo-9-((3- phenylpropyl)amino)nonan oic acid (AK-16) (34)	Amide	148
	Stem bark (methanol)	11-oxo-11-((3- phenylpropyl)amino)undec anoic acid (AK-17) ( <b>35</b> )	Amide	
	Stem bark (hexane)	4', 7-dihydroxy-5- methoxyflavone (AK-15) (36)	Flavone	
	Stem bark (Chloroform) Bark (dichlorom ethane)	8-(4-hydroxy-3- methoxyphenyl)-3- methoxy-6,7- dimethyl- 5,6,7,8- tetrahydronaphthalen-2-ol (AK-18) (37)	Lignan	

# 2.3. The Myristicaceae Family Summary

The Myristicaceae family clearly displays high pharmaceutical potential. The extensively studied species from the genera *Gymnacranthera*, *Horsfieldia*, *Knema* and *Myristica* (particularly the latter two) demonstrate considerable biological activity. From a chemotaxonomic perspective, the reviewed literature of the Myristicaceae suggests that the unexplored species belonging to these genera, should be explored due

to their potential medicinal applications. The Myristicaceae species of interest have had compounds including lignans, terpenes, flavonoids and phenolic compounds isolated. The biological activity of these species seem to be antibacterial, anticonjugative and antioxidant.

### 2.4. The Clusiaceae Family

### 2.4.1. The Garcinia L. genus (Clusiaceae)

The *Garcinia* is a genus of small to medium sized of evergreen trees comprised of approximately 260 species which are distributed throughout Africa, tropical Asia, northeast Australia, west Polynesia and America. The *Garcinia* species are located commonly in rainforest lowland areas and are concentrated in Southeast Asia and West Africa. Species of this genus mostly lack scales on their buds, have leathery – papery leaves which are arranged oppositely (rarely whorled) and are usually glabrous. Flowers can range from solitary, fascicled to panicled, and possess 4 – 5 petals. Male flowers have 2 – 4 lobed stamens which are either free or joined together. All species' stigma are sessile and visible. Most members of this genus produce edible fruits and yellow latex and all genus members are dioecious<sup>149</sup>.

Traditional uses of the *Garcinia* genus are well-reported, with 17 species having recorded traditional uses across Malaysia and West Sumatra (Indonesia). These cover a spectrum of ailments including stomach-ache, fever, skin diseases, circulatory problems, skin infections and oedema<sup>150</sup>. Some *Garcinia* species are very well studied, for example, *Garcinia lucida* has over 270 different reports on its range of ethnomedicinal uses<sup>151</sup>. Additionally, phytochemical studies have found *Garcinia* species to contain benzoquinone, benzophenones, bioflavonoids, triterpenes and xanthones<sup>152-164</sup>. Some of these compounds have proven bioactivity including antiinflammatory, antibacterial, anti-HIV and anti-cancer<sup>171-174</sup>. *Garcinia* that are previously well studied due to their biological activity include *G. kola, G. cowa, G. atroviridis* and *G. indica*<sup>162-164</sup>. Although the *Garcinia* genus is the most well-studied Clusiaceae genus for its biological activity, there are still many unexplored species.

Evidence illustrates significant pharmaceutical potential of these species, which warrants the investigation of all *Garcinia* species.

#### Garcinia caudiculata Ridl., Garcinia grahamii Pierre

As this is one of the species chemically investigated during this thesis, the literature for this is reviewed in the results and discussions in Chapter 5 (section 5.1.1).

### Garcinia maingayi Hook. f.

*Garcinia maingayi* is distributed in Sumatra, Peninsular Malaysia and Borneo, growing on hill forests or lower montane, up to 900 m altitude  $^{165,166}$ . This species grows up to 21 m tall and has opposite arranged leaves which are dark green in colour, slightly elliptic – egg shaped, and measure  $14 - 19 \times 6.5 - 8.5$  cm. The midrib of leaves is only raised on the underside and leaves display fine resin ducts. When dry, leaves are black – brown in colour  $^{167}$ .

Traditionally in Malaysia and West Sumatra (Indonesia), *G. maingayi* leaf decoction is used as an anti-fever treatment. Jabit *et al.*, (2009)<sup>152</sup> studied the cytotoxic and NO inhibitory activity of *G. maingayi* methanolic extracts and found strong and selective cytotoxicity against MCF-7 breast cancer cells, as well as moderate NO inhibitory activity (Table 2.3). Extraction yields of 20.4% and 9.2% were obtained from the stem and leaf extractions, respectively. In addition, Ee *et al.* <sup>168,169</sup>, isolated a prenylated xanthone, 1,3,7-trihydroxy-2-(3-methylbut-2-enyl)-xanthone (38) and the triterpene stigmasterol (39) (Figure 2.11, Table 2.4). Recent studies have performed the isolation of 39 as well as the terpenoid sitosterol <sup>170</sup>. In addition, polyisoprenylated benzophenones, including the known *Garcinia* metabolite, garcinol, have been isolated from the stem bark of this species <sup>171,172</sup>.

**Figure 2.11.** Chemical structures of xanthone 1,3,7-trihydroxy-2-(3-methylbut-2-enyl)-xanthone (38) and triterpene stigmasterol (39) isolated from *Garcinia maingayi* Hook. *f*.

# Garcinia dryobalanoides Pierre

*Garcinia dryobalanoides* is endemic to Borneo and grows in montane, mixed dipterocarp and heath forests<sup>173,174</sup>. This species produces edible fruit, known to be eaten by the Lun Bawang ethnic group of Borneo<sup>90,175</sup>. Recent studies have revealed the presence of known fatty acids, triterpenoids and xanthones in the stem bark of this species, which displayed bacterial inhibition<sup>176,177</sup>.

# Garcinia parvifolia (Miq.)

*Garcinia parvifolia*, known as the "Brunei cherry" grows in Sumatra, Peninsular Malaysia, Singapore and Borneo, mostly in primary and secondary forests up to altitudes of 600 m. This species is a common tree, growing up to 33 m tall with thin dark green leathery leaves which measure  $5 - 15 \times 1.9 - 5.7$  cm. Leaf blades are elliptic and form a narrow point at the top. Dark resin ducts are also visible in this species, as well as faint venation on leaf undersides. Male flowers measure 7 - 10 mm wide with white colouring and female flowers measure 4 - 6 mm wide with yellow colouring. This species produces rust orange fruits which are elliptic, 7 mm wide and contain up to 8 pulp-covered seeds inside<sup>167</sup>.

The fruits of this species are a popular food. In traditional medicine, it is reported that *G. parvifolia* stem bark is soaked in water and the decoction is ingested <sup>178,179</sup>. Additionally, this species is a traditional treatment for malaria, due to the bioactive compound  $\alpha$ -mangostin (65) (Figure 2.12A)<sup>180</sup>. Although there are no specific disorders

this species is traditionally said to treat, many studies have investigated its chemistry and bioactivity<sup>181</sup>.

Phytochemical screening of Malaysian *G. parvifolia* revealed that the total phenolic content of fruit samples was (mg gallic acid equivalent (GAE)/g of dry weight (DW)) 7.2 in fruit pulp and 5.3 in peel. In addition, the total carotenoids (β-carotene equivalent, mg/100 g DW) was 3 in fruit pulp and 17 in the peel<sup>162,182</sup>. Screening *G. parvifolia* stem bark for total phenolic content in wet or dry granulated tablets found that the phenolic content was highest in dry tablets. Additionally, methanolic crude extracts of *G. parvifolia* in this study were highly hygroscopic, resulting in liquification at higher humilities<sup>178</sup>. Later phytochemical screening of this species has revealed the presence of alkaloids, carbohydrates, flavonoids, phenols, saponins, steroids, tannin and terpenoids in leaves and pericarps (Table 2.4)<sup>183,184</sup>. A recent phytochemical study of several *Garcinia* species fruits found *G. parvifolia* to contain 79% water, 0.4% ash, 18.3% carbohydrate, 0.9% crude protein, 1.1% crude fat and 5.3% crude fibre<sup>181</sup>.

Pharmacological investigations have shown that crude extracts from vegetative parts of *G. parvifolia* also display bioactivity including anti-plasmodial (strongest activities from root and stem bark extracts) and antibacterial activity (strongest activity from root and fruit extracts) (Table 2.3)<sup>180</sup>. Crude extracts have also exerted free radical scavenging, cytotoxicity, a-glucosidase inhibitory and antiviral activity *in vitro*, as well as *in vivo* hepatoprotective effects (Table 2.3)<sup>162,184,185</sup>. However, no antibacterial activity against MRSA was recorded with crude *G. parvifolia* extracts (MIC > 512 μg/mL)<sup>157</sup>. Multiple studies have isolated compounds from *G. parvifolia* and assed their bioactivity (Table 2.3)<sup>157,184,186</sup>. Pattalung *et al.*, (1988)<sup>287</sup> isolated the xanthone rubraxanthone (40) from *G. parvifolia* latex and found this to be a strong anti-bacterial and moderate anti-fungal (Table 2.4). Jantan *et al.*, (2002)<sup>188</sup> later isolated compound 40 as well as isocowanol (41) from *G. parvifolia* bark and identified these as platelet activating factor receptor binding inhibitors (Table 2.4, Figure 2.12A).

Xu et al., (1998)<sup>189</sup> first isolated the cytotoxic (against leukaemia, lung and fibrosarcoma cancer cell lines) xanthone, griffipavixanthone (42) from G. parvifolia, and two years later, isolated four depsidones, garcidepsidone A (43), garcidepsidone B (44) and garcidepsidones C - D from this species, three of which were cytotoxic against a leukaemia cell line<sup>190</sup> (Figure 2.12C, Table 2.4). Xu et al., later isolated xanthones parvixanthones A - C (compounds 45 - 47) as well as parvixanthones D - I (Figure 2.12A, Table 2.4)<sup>191</sup>. Rukachaisirikul et al. then isolated more xanthones, dulxanthone D (51), mangostinone (50), norathyriol (52), parvifolixanthones A (48), B (49) and C, and phloroglucinols, parvifoliols A - C (compounds 53 - 55) as well as parvifoliols D - G (Figure 2.12, Table 2.4). Also isolated, were depsidones parvifolidones A (56) and B (57) (2E,6E,10E)-(+)-4 $\beta$ -hydroxy-3-methyl-5 $\beta$ -(3,7,11,15and tetraprenyltoluquinone, tetramethylhexadeca-2,6,10,14-tetraenyl)cyclohex-2-en-1-one (58) (Figure 2.12, Table 2.4). All of these compounds except 52, 57, 58 displayed only weak anti-MRSA (the remaining displayed none) and all compounds displayed DPPH free radical scavenging <sup>192</sup>. In addition, 51 induces apoptosis via the intrinsic mitochondrial pathway in the HepG2 hepatocarcinoma cell line<sup>193</sup>.

More examples of isolated compounds from *G. parvifolia* include the benzoquinone derivative, parvifoliquinone (59), flavonoid nigrolineaisoflavone A (60),  $\beta$ -sitosterol (61), triterpene squalene (62), xanthones cowanin (63), clusianone (64) and  $\alpha$ -mangostin (65) (Figure 2.12, Table 2.4). More compounds isolated from this species can be found in Table 2.4. 59 and 60 have displayed weak anti-MRSA activity (MIC < 30  $\mu$ g/mL)<sup>157</sup>. These compounds have recognised moderate biological activities, for example 61 (anxiolytic, sedative, lipid lowering and hepatoprotective), 62 (drug carrier, antioxidant, cytotoxic) and 65 (cytotoxic, antioxidant)<sup>194-196</sup>. All of these have been well investigated for their biological activity, from nutritional and pharmaceutical aspects<sup>196-201</sup>.

Recent studies have reisolated gardepsidones A (43)<sup>202</sup> and B (44)<sup>203</sup> as well as related novel depsidones including parvidepsidone<sup>204</sup>. Recent investigations have also

demonstrated the  $\alpha$ -glucosidase inhibitory $^{202}$ , antioxidant, antimalarial $^{205}$  and cytotoxic $^{206}$  activities of  $\it G. parvifolia$ .

**(D)** 

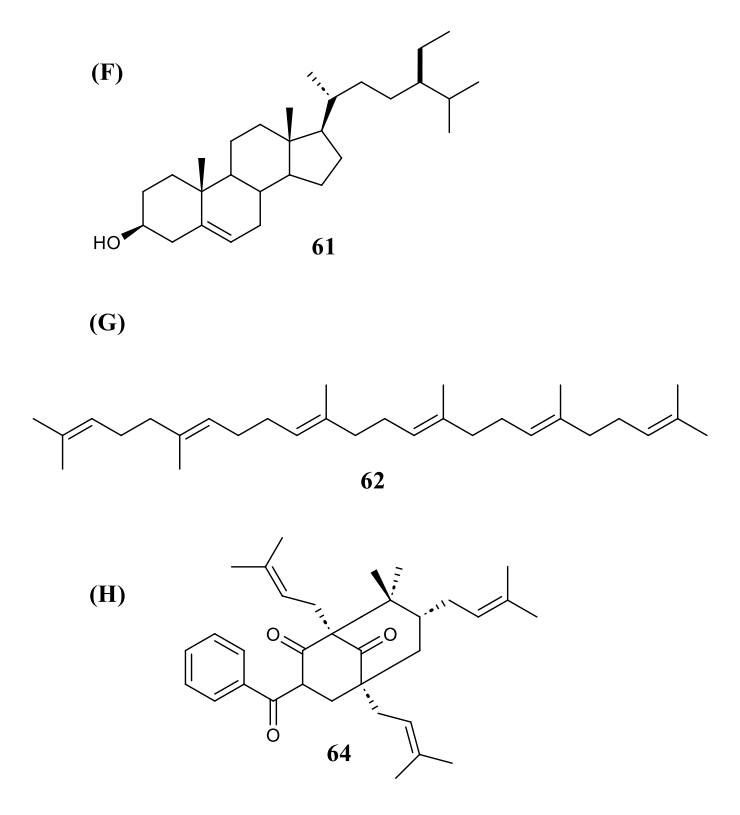


**Figure 2.12.** Chemical structures of **(A)** xanthones **40** – **42**, **45** – **52**, **63** and **65**; **(B)** phloroglucinols **53** – **55**; **(C)** depsidones **43**, **44**, **56**, **57**; **(D)** quinones **58** and **59 (E)** flavonoid **60**; **(F)** sterol **61**; **(G)** triterpene **62** and **(H)** polycyclic polyprenylated acylphloroglucinol **64**, isolated from *Garcinia parvifolia* (Miq.).

#### Garcinia hombroniana Pierre

*Garcinia hombroniana*, also known as the seashore mangosteen, is a widely distributed tree, growing in Borneo, Cambodia, Thailand, Vietnam, Andaman and the Nicobar Islands, but is native to Peninsula Malaysia. This species grows often in lowland forests and coastal regions, but also grows in highlands. *G. hombroniana* grows up to 6 m tall and 1.8 m in trunk DBH. Stems grow straight, with smooth, green young branches which become darker and covered with white latex with age. Leaves are bright green – yellow and fruits are light red and are a popular edible fruit<sup>207</sup>.

Traditionally, the roots of G. hombroniana are used to relieve itching and as a protective treatment after childbirth<sup>208,209</sup>. This species is well-studied in terms of bioactive metabolites, from classes including xanthones, flavonoids, triterpenes sterols (Figure

2.13, Table 2.4). Triterpenes largely dominate the secondary metabolites of G. hombroniana including for example, the cycloartane triterpene, (22Z,24E)-3βhydroxycycloart-14,22,24-trien-26-oic acid (69), friedolanostanes-type triterpenes such as (24E)-3α-hydroxy-17,14-friedolanostan-8,14,24-dien-26-oic acid (68), 3β acetoxy-9α-hydroxy-17,14-friedolanostan-14,24-dien-26-oic acid (70) and 3β, 23αdihydroxy-17,14-friedolanostan-8,14,24-trien-26-oic acid (71),well garcihombronanes B (66), C (67) and D – K(Figure 2.13A). Flavonoid glucosides have also been identified including vitexin (72) and isovitexin (73) and ionone glycosides (sesquiterpene) such as bluminol-C-9-O-β-D-apiofuranosyl-(1→6)-β-D-glucopyranoside (74) (Figure 2.13B,C). In addition, xanthones including garcihombronone A (75), B (76) and C – D, 57, gentisein (77), cheffouxanthone (78), bangangxanthone A (79), 1,3,5,7tetrahydroxy-2-(3,7-dimethyl-6-hydroxyocta-2-7-dien)xanthone (80).Phenolic compounds have also been isolated from this species including 4-hydroxybenzoic acid (81), 3,5,3',5'-tetrahydroxy-4-methoxybenzophenone (82) and euxanthone (83) (Table 4, Figure 2.13). Remaining examples of G. hombroniana metabolites from these classes are summarised in Table 4.

Isolated compounds from this species possess bioactivity including antibacterial (85 and 86) and low density lipoprotein (LDL) oxidation inhibition (82 and 83) $^{210,211}$ . Compounds found in Table 2.4 including 80, 71, garcihombronanes G and J, 66 and garcihombronane D displayed moderate acetylcholinesterase and butyrylcholinesterase inhibitory activity (Table 2.4) $^{212}$ . The most recent study of *G. hombroniana* bark extract revealed the antioxidant activity of an ethanolic extract $^{213}$ .

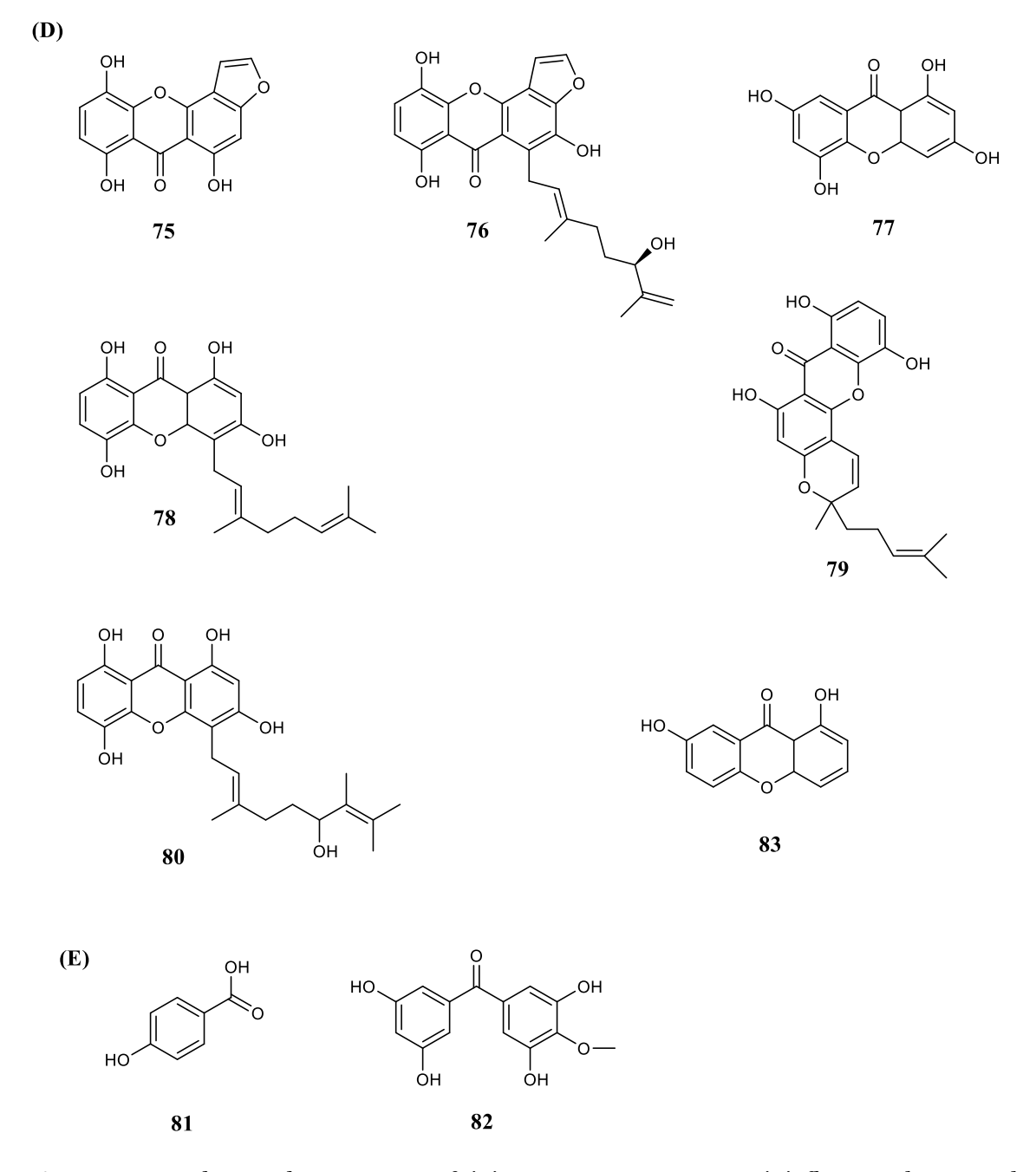


Figure 2.13. Chemical structures of (A) triterpenes 66 - 71; (B) flavonoids 72 and 73; (C) sesquiterpene, 74; (D) xanthones 75 - 80, 83 and (E) phenolic compounds 81 and 82, isolated from *Garcinia hombroniana* Pierre.

### Garcinia penangiana Pierre

*Garcinia penangiana* is distributed throughout Borneo, Sumatra and Peninsular Malaysia and grows in a mixture of lowland and hill forests up to 900 m. This tree grows up to 20 m tall, has dark brown bark and slightly red inner bark. Leaves are elliptic

shaped and measure  $13 - 16 \times 4 - 6$  cm, with leathery lamina which is dark brown – red on its topside and paler on the underside. The leaves of *G. penangiana* are distinct in that they turn reddish when dried, and have veins which are fine and closely arranged. In addition, male flower stamens form cruciform stamens when dry<sup>207</sup>.

Garcinia penangiana is traditionally used in Malaysia and West Sumatra to treat skin diseases and fever<sup>150</sup>. Jabit *et al.*, (2007)<sup>214</sup> isolated five compounds, four of which penangianaxanthone (84), cudratricusxanthone H (85), macluraxanthone C (86), gerontoxanthone C (87) displayed strong cytotoxicity toward breast, lung and prostate cancer cells lines (Table 2.4, Figure 2.14). (4-(1,1-dimethylprop-2-enyl)-1,3,5,8-tetrahydroxyxanthone (88) displayed weak cytotoxicity (Figure 2.14)<sup>214</sup>. Later, Jabit *et al.*, (2009) recorded the selective cytotoxicity of crude *G. penangiana* extracts against both breast and lung cancer cells, and moderate NO inhibitory activity (Table 2.3). Methanolic extractions yielded 8.1% and 5.5% from stems and leaves, respectively<sup>152</sup>. Although only Jabit *et al.* have explored the pharmaceutical potential of this species, its biological activity seems to be promising thus far, warranting further investigation.

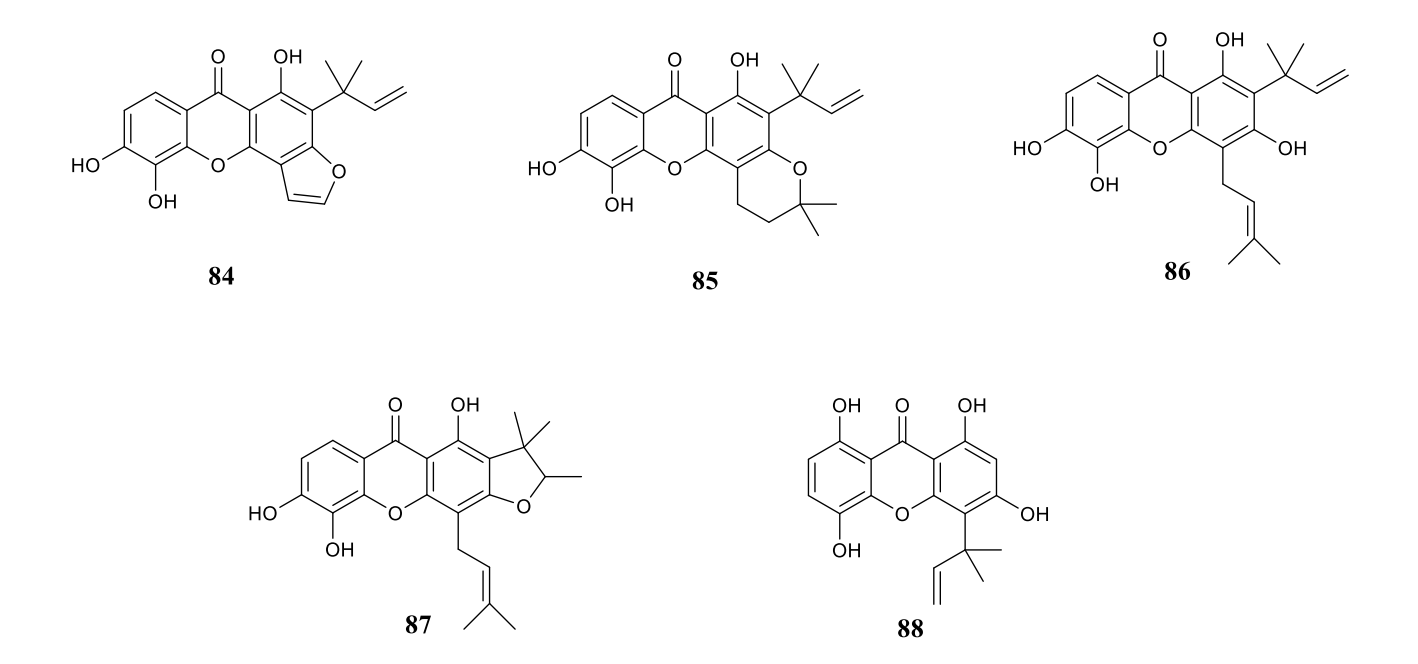


**Figure 2.14.** Chemical structures of xanthones, penangianaxanthone (84), cudratricusxanthone H (85), macluraxanthone C (86), gerontoxanthone C (87) and (4-(1,1-Dimethylprop-2-enyl)-1,3,5,8-tetrahydroxyxanthone (88) isolated from *G. penangiana* Pierre.

#### Garcinia benthamiana (Planch & Thiana) Pipoly

Garcinia benthamiana is a medium tree which grows up to 20 m tall, with a trunk measuring up to 40 cm DBH. The fruits of this species are edible, however there are no traditional uses reported for this plant thus far. See *et al.*,  $(2016)^{215}$  were the first to isolate (six) compounds including, for example, two benzophenones, benthamianone (89) and congestiflorone (90), two sterols, stigmasterol (39) and γ-sitosterol (91) as well as methyl palmitate (92), α-mangostin (65) and β-mangostin (93) from *G. benthamiana* (Table 2.4, Figure 2.11, Figure 2.15). In this study they identified only weak antibacterial activity in all extracts, a high total phenolic content and moderate free radical scavenging activity<sup>215</sup>. A year after this, the same group performed phytochemical screening and further bioassays using *G. benthamiana* and revealed the presence of flavonoids, glycosides and terpenoids in stem bark extracts. No saponins, tannins or alkaloids were detected. They did however, find the highest total phenolic content in the

ethyl acetate extract, which increased to the anti-oxidant potential of this extract (Table 2.3)<sup>216</sup>. More recently, See *et al.*<sup>217</sup> isolated eight compounds including xanthones, for example **70** and mangaxanthone B (**94**), benzophenones including mangaphenone (**95**), **89**, **90** and a sterol, **39** from *G. benthamiana* (Table 2.4). Of these, compounds **70**, **93**, **94** and **95** exhibited significant cytotoxicity on two breast cancer cell lines, with IC<sub>50</sub> values  $< 12 \mu M^{217}$ .

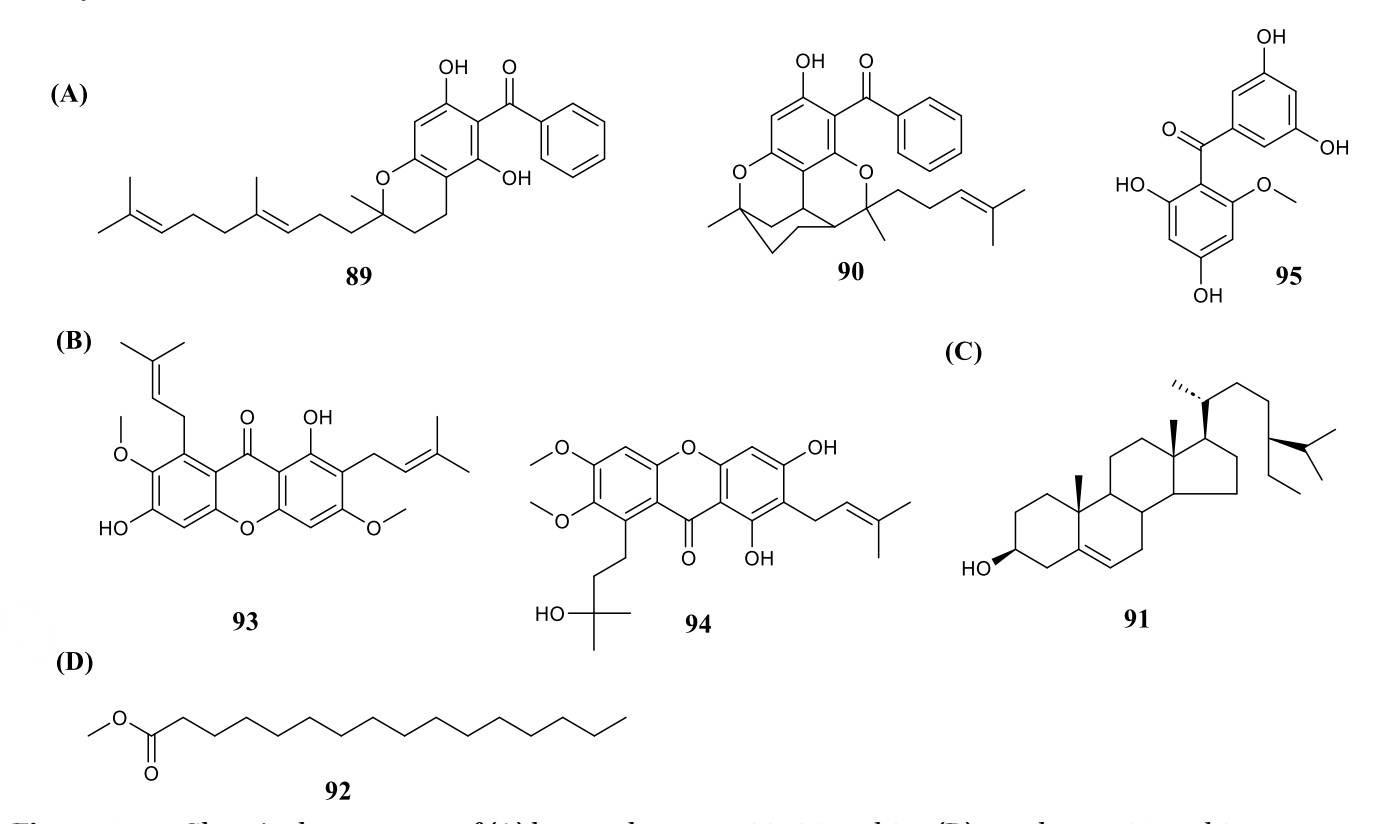


Figure 2.15. Chemical structures of (A) benzophenones 89, 90 and 95; (B) xanthones 93 and 94; (C) sterol 91 and (D) fatty acid methyl ester 92, isolated from *Garcinia benthamiana* (Planch & Thiana) Pipoly.

### Garcinia trianii Pierre

*Garcinia trianii* is a tree endemic to Borneo which grows in lower to upper montane forests at altitudes up to 1900 m<sup>165</sup>. This species is very morphologically similar to G. *maingayi* but has smaller flowers and leaves<sup>207</sup>.

### 2.4.1.1. The Garcinia Summary

The *Garcinia* genus contains species which have been well explored and produce compounds which exhibit a wide spectrum of bioactivities including cytotoxic,

antioxidant, hepatoprotective, antibacterial and anti-viral. Of the *Garcinia* species of interest in this study, four have no reports on their phytochemistry or biological activity (*Garcinia caudiculata*, *Garcinia dryobalanoides*, *Garcinia grahamii and Garcinia trianii*). One species has been investigated for the biological activity of its crude extracts but have had no compounds isolated from it. Four of the nine *Garcinia* species of interest (*Garcinia benthamiana*, *Garcinia hombroniana*, *Garcinia parvifolia and Garcinia penangiana*) have had compounds isolated, some of which displayed biological activities. The most well studied *Garcinia* species in this review are *G. parvifolia* and *G. hombroniana* which have secondary metabolomes mainly represented by xanthones and depsidones, and triterpenes, respectively. The compound types seem to make characteristic chemical profiles for each of these species, which suggests that the unexplored species of this genus may also offer novel metabolites and therefore bioactivities. This warrants investigation into species *Garcinia caudiculata*, *Garcinia dryobalanoides*, *Garcinia grahamii and Garcinia trianii* for their pharmaceutical potential.

### 2.4.2. The Mesua L. Genus (Clusiaceae)

The *Mesua* genus includes approximately 50 species which are distributed within Southeast Asia. The *Mesua* species were often misidentified as the *Kayea* species, due to their close relation, accounting for the synonymy of species names between these genera. Hence, most of the papers published thus far refer to the genus in the binomial *Kayea* species names as the *Mesua*, resulting in some confusion on which studies have been undertaken on which species. Phylogenetic analysis has confirmed that *Mesua* and *Kayea* are two separate genera<sup>218</sup>. The most well-studied *Mesua* species is *Mesua ferrea* Lin. This genus has been well investigated in terms of their phytochemistry, with about 170 secondary metabolites having been identified thus far from 13 different species. Phenolic xanthones and coumarins, and some sesquiterpenes, diterpenes and triterpenes have been isolated<sup>219-222</sup>. However, xanthone, coumarin and triterpene derivatives predominantly comprise the secondary metabolome of *Mesua* species<sup>219,223-229</sup>

#### Mesua congestiflora P.F. Stevens

*Mesua congestiflora* is a medium tree which is native to Indonesia and Borneo and grows in peat swap forest regions. This species can reach 15 m tall, contains yellow resins and produces black fruits<sup>230</sup>.

Mesua congestiflora is has been somewhat investigated in terms of phytochemistry, and similarly to other Mesua species, seems to produce mainly xanthones. Although, a benzophenone, congestiflorone (97) was isolated, which displayed cytotoxicity against lymphoma cells<sup>231</sup>. The activity of this isolated compound is demonstrated by another study which found M. congestiflora crude extracts to be inactive against several cancer cell lines, suggesting non-synergistic effects<sup>232</sup>. Crude extracts of this species have displayed significant anti-inflammatory activity. However, these extracts did not exceed activity of the main isolated compound, 97, emphasising the lack of synergism in M. congestiflora bioactivity and the value of 97<sup>233</sup>.

## 2.4.3. The Kayea Wall. Genus (Clusiaceae)

The genus *Kayea* belongs to the subfamily Calophylloideae and the family Clusiaceae. Approximately 75 species belong to the *Kayea*, however it is said that many more are still to be described<sup>234,235</sup>. All species which were formally classified as the *Mesua* genus have moved to the *Kayea* (except *Mesua ferrea* L.), explaining the synonyms listed below for each species. The *Kayea* species are distributed in tropical Asia, predominantly the Indo-Malaysia region. The *Kayea* are tree species which have coriaceous and glabrous leaves which are opposite. Inflorescences have singular large flowers which have four sepals. This genus produces fleshy fruits which contain up to four seeds each<sup>236</sup>.

The *Kayea* metabolites have been found to exhibit various pharmacological activities including anti-inflammatory, cytotoxic and anti-acetylcholinesterase<sup>229,237,238</sup>. Bioactive isolated coumarins from a particularly well investigated *Kayea* species, *K. assamica*, have exerted cytotoxic effects on human colon and epidermoid cancer cell lines<sup>239-241</sup>.

#### Kayea borneensis P.F. Stevens = Mesua borneensis P.F. Stevens

*Kayea borneesis* has been recorded in Central Kalimantan, Indonesia, but is native to Borneo and grows mostly in dipterocarp and sub-mountain forests on hillsides, up to 1100 m. This is an understory tree which grows to 39 m tall and 70 cm DBH. Leaves are glabrous, with clear secondary veins. Fruits are a red – brown in colour and are up to 40 mm in diameter<sup>24,242,243</sup>.

Tanjung *et al.*, <sup>227</sup> isolated three isoprenylated coumarin compounds from *K. borneensis:* mammea A/BA (**96**), mammea A/ AA cyclo D (**97**) and mesuol (**98**) (Figure 2.16, Table 2.4). Additionally, *K. borneensis* crude extracts exhibited anti-plasmodial and anti-oxidant activities, with isolated compounds displaying higher potency than crude extracts in all biological assays (Table 2.3)<sup>227</sup>. The isoprenylated 4-phenyl coumarin, mesucalophylloidin (**99**) (Figure 2.16)<sup>244</sup>.

**Figure 2.16.** Chemical structures of coumarins **96** – **99**, isolated from *Kayea borneensis* P.F. Stevens.

## Kayea calophylloides P.F. Stevens = Mesua calophylloides (Rdil.) Kost.

*Kayea calophylloides* is endemic to Borneo. Traditionally, decoction of the stem bark is used in to treat various diseases<sup>245</sup>. One phytochemical report of *K. calophylloides* is by Tanjung *et al.* (2018) who isolated four compounds from its stem bark (Table 2.4). Mesucalophylloidin (99) was found to be cytotoxic against murine leukaemia cell line ( $IC_{50} = 6.3 \mu g/mL$ ) (Figure 2.16)<sup>244</sup>. A further report has revealed the presence of chromanone acids, for example, calolongic acid (100) (Figure 2.17, Table 2.4).

**Figure 2.17.** Chemical structures of the chromanone acid, calolongic acid (**100**) isolated from *Kayea calophylloides* P.F. Stevens.

### Kayea calciphila P.F. Stevens = Mesua calciphila P.F. Stevens

*Kayea calciphila* is a species endemic to Borneo and grows up to 20 m tall and up to 106 cm DBH, with flaking bark brown coloured fruit with yellow sap $^{246}$ .

### Kayea myrtifolia Baill. = Mesua myrtifolia Baill.

*Kayea myrtifolia* is Endemic to Borneo, sampled only from Sarawak. However, there is no literature describing the detailed morphology of this species<sup>242</sup>. An early study isolated six compounds from the bark, including the triterpenoids similarenone (**101**), similarenol (**102**), taraxerol (**103**), betulinic acid (**104**) and the xanthone jacareubin (**105**) which was isolated from timber extracts (Figure 2.18, Table 2.4). Here, *K. myrtifolia* is referred to as *Mesua myrtifolia*, however it is recognised in this study that its secondary metabolome represented that of *Kayea*'s<sup>247</sup>.

**Figure 2.18.** Chemical structures of **(A)** triterpenes **100** – **104** and **(B)** xanthone **105**, isolated from *Kayea myrtifolia* Baill.

#### 2.4.3.1. The *Kayea* (Clusiaceae) Summary

Of the four Bornean *Kayea* species of interest, three have been scientifically investigated, either for the bioactivity of crude extracts (*K. calophyllodies*) or for their phytochemical constituents (*K. borneesis* and *K. myrtifolia*). The compound types isolated are mainly flavonoids, terpenes and xanthones. One species, *K. calciphila* has no studies investigating either of these. Generally, the *Kayea* seems to lack reports, however this may be due to confusion regarding nomenclature. Many early studies refer to *Kayea* as *Mesua*, therefore representing the *Kayea* as unexplored, and the *Mesua* as extensively researched. In this review, the binomial species name has been searched with both genera *Kayea* and *Mesua*. Nevertheless, there is still little exploration of these Bornean species.

## 2.4.4. The Calophyllum L. Genus (Calophyllaceae)

The *Calophyllum* is a large genus in the Clusiaceae family which includes approximately 200 species, distributed throughout tropical Asia, Africa, the Americans, Australia and the Pacific Islands<sup>248</sup>. However, the vast majority of these grow in the Indo-Malaysian region. There is some uncertainty regarding the classification of the *Calophyllum* genus, as it was moved from its former family, the Clusiaceae, and is now classified under the Calophyllaceae plant family by the Angiosperm Phylogeny Group classification system in 2009<sup>249,250</sup>. Therefore, much of the literature prior to this still refers to the Clusiaceae as the correct family for the *Calophyllum*, as this is a relatively recent divergence. However, the Calophyllaceae belongs to the order, Malpighiales, to which the Clusiaceae belongs too, inferring the similarities between these species (Figure 2.1)<sup>250</sup>.

The *Calophyllum* genus includes tree and shrub species, most of which are medium sized trees. *Calophyllum* habitats range from wet tropical forests (and even flooded areas, typically at lower altitudes) and higher, dryer areas too<sup>251</sup>. This genus is characterised by red bark which has diamond-shaped fissures. Leaves are oppositely arranged and possess alternating parallel veins. Fruits of *Calophyllum* contain a red

seed and thin outer layers of flesh. Species are monoecious, with sepals and petals arranged on flowers<sup>251,252</sup>.

The *Calophyllum* is a well-explored genus of in terms of bioactive metabolites. The *Calophyllum* species are widely used ethnomedicinal plants. Parts used include roots, bark, leaves and seeds for a variety chronic and acute conditions such as with ulcers, infections, inflammation, diabetes, eye diseases and gastrointestinal disorders<sup>248,251,253,254</sup>.

## Calophyllum pulcherrimum Wall. ex Choisy

Calophyllum pulcherrimum is a large tree species which grows up to 30 m tall, and is distributed throughout Cambodia, Peninsular Malaysia, Singapore, Thailand and Borneo<sup>255-257</sup>. The resin of this species is used traditionally in cancer treatment<sup>258</sup>. The only study investigating its biological activity assessed the free radical scavenging potential of crude extracts. Here, *C. pulcherrimum* extracts have exhibited antioxidant activity *in vitro* (Table 2.3)<sup>259</sup>.

# Calophyllum soulattri Burm. Ex F.Mull., (Calophyllum soulattri Burm.)

Calophyllum soulattri is a popular traditional medicine, particularly the seed oil which is used to treat skin infections, suggesting its anti-microbial properties<sup>260</sup>. In addition, root infusion is a traditional treatment for rheumatic pain<sup>248</sup>. The phytochemistry and biological activity of this species has been well-explored. Crude leaf, bark and root C. soulattri extracts have exhibited antimicrobial properties against multiple bacterial and protozoan species (Table 2.3)<sup>261</sup>. Insecticidal activity has also been recorded from crude C. soulattri extracts (Table 2.3)<sup>262,263</sup>. However, crude extracts lack anticancer and anti-inflammatory activity<sup>264</sup>.

Gunasekera *et al.*<sup>265</sup>, isolated coumarin alcohol, soulattrolide (**106**), a triterpene including taraxerol (**103**), sesterterpenoid taraxerone (**107**), sterol (**66**) and five xanthones including example 1,6-dihydroxy-5-methoxyxanthone (**108**) (Table 2.4, Figure 2.19). Of these, **106** is an inhibitor of human immunodeficiency virus (HIV) type

1 reverse transcriptase<sup>266</sup>. Ee *et al.* isolated a pyranocoumarin soulamarin (**109**) and eleven xanthones (isolated later by other teams) including example caloxanthone B (**110**) and rheediaxanthone A (**111**) from *C. soulattri* (Table 2.4)<sup>267</sup>. These compounds were later isolated again, as well as  $\beta$ -sitosterol (**61**) and it was found that all the formally isolated compounds were moderately cytotoxic against cancer cell lines including, cervix, colon, leukaemia, liver, lung, lymphoma, neuroblastoma, skin and stomach cancers<sup>20,268</sup>. Mah *et al.*, later isolated an additional two xanthones soulattrin (**112**) and phyllatrin (**113**) which showed a higher cytotoxicity against the same cell lines (Figure 2.19, Table 2.4)<sup>20</sup>. Further bioactive compounds isolated from *C. soulattri* include airlanggin A (**114**) and B (cytotoxic against murine leukaemia) and calosubellinone (**115**) and Garsubellin B (**116**) (cytotoxic against breast cancer cells)<sup>296,270</sup>.

Recent investigations into *Calophyllum soulattri* have led to the discovery of secondary metabolites, including a xanthone named soulaxanthone<sup>271,272</sup> and pyranoxanthones isolated from the stem bark<sup>273</sup>. Additionally, a range of known terpenoids and xanthones have been reported in this species within the last few years<sup>274,275</sup>. Crude extract studies have also demonstrated promising anti-obesity potential attributed to the metabolites of *C. soulattri*<sup>276</sup>.

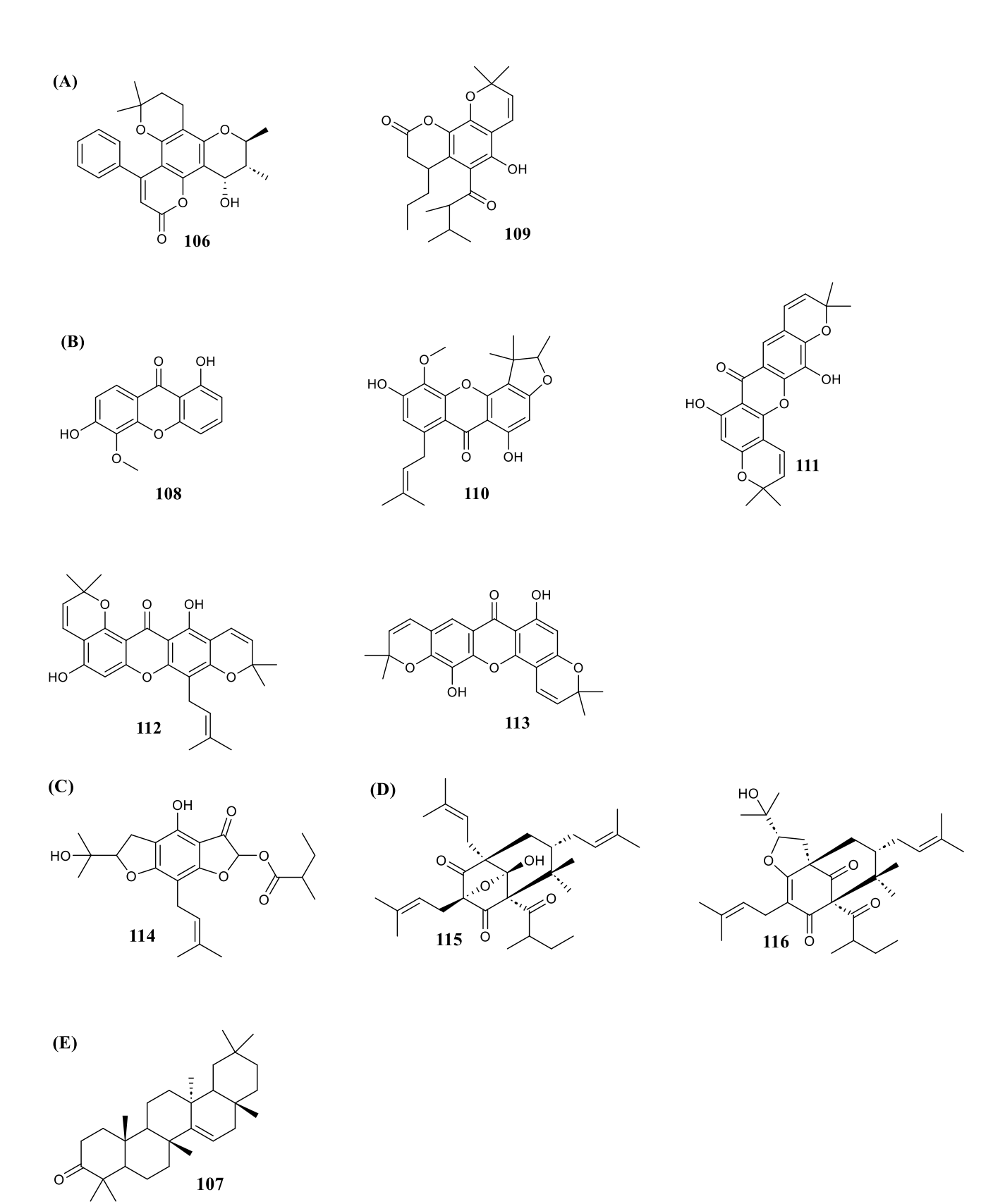


Figure 2.19. Chemical structures of (A) coumarins 106 and 109; (B) xanthones 108, 110 – 113; (C) benzofuran 114; (D) phloroglucinols 115 and 116 and (E) terpene 107, isolated from  $Calophyllum\ soulattri\ Burm.\ Ex\ F.Mull.$ 

### Calophyllum castaneum P.F. Stevens

Calophyllum castaneum is distributed within Borneo and grows at altitudes up to 500 m. This species reaches up to 30 m tall and 65 cm DBH. Fruits are approximately 20 mm in diameter and are green in colour<sup>248</sup>. Phytochemical investigations into *C. castaneum* revealed the presence of chromanone acids, isoblancoic acid (117) and blancoic acid (118), sterol  $\beta$ -sitosterol (66) and triterpenes friedelinol and friedelin (Figure 2.20, Figure 2.12F, Table 2.4). Compound 117 has shown cytotoxicity against brain and colorectal cancer cell lines *in vivo*<sup>277</sup>. In addition, crude extracts containing these compounds displayed antioxidant effects *in vitro* (Table 2.3)<sup>278,279</sup>.

**Figure 2.20.** Chemical structures of chromanone acids isoblancoic acid (117) and blancoic acid (118) isolated from *Calophyllum castaneum* P.F. Stevens.

## 2.4.4.1. The Calophyllum (Clusiaceae) Summary

All three Bornean *Calophyllum* species have had some biological investigation, one (*C. pulcherrimum*) having anti-oxidant crude extracts, and two (*C. soulattri* and *C. castaneum*) producing bioactive compounds, namely xanthones, coumarins, sterols and triterpenes. Despite only reviewing three *Calophyllum* species here, the metabolome seems to show a spectrum of compounds and biological activity, which makes this genus an interesting focus in the context of pharmaceutical applications.

### 2.4.5. The Mammea L. Genus (Clusiaceae)

The *Mammea* is a pantropical genus which contains approximately 75 species (roughly 30 of which are distributed throughout India and southeast Asia). Flowers possess two

sepals and 4 – 8 petals, which range from white to pink in colour and are all dioecious. Nectar glands do not occur in any members of this genus<sup>280</sup>. Traditionally, the *Mammea* is used to treat symptoms including stomach pains, fever, scabies as well as microbial infections<sup>305</sup>. Members of the *Mammea* genus are known to produce bioactive compounds including coumarins and xanthones, displaying biological activities such as cancer cell toxicity and anti-HIV activity<sup>282-284</sup>.

## Mammea acuminata (Kosterm.) Kosterm.

Despite the exploration of multiple members of the *Mammea* genus and the successful isolation of bioactive compounds, the species of interest in this review, *Mammea acuminata*, has had only two studies investigate its chemistry. Initially, Tosa *et al.*, isolated two new furanoxanthones (acuminol A (119) and B (120)) as well as four known xanthones from *M. acuminata*, and later isolated another new xanthone, 2,7-dihydroxyxanthone (Figure 2.21, Table 2.4)<sup>285,286</sup>. 2,7-dihydroxyxanthone did not show have antimalarial activity and the biological activity of 119 and 120 are still undetermined<sup>287</sup>. No biological activity of *M. acuminata* crude extracts have been analysed thus far.

Figure 2.21. Chemical structures of xanthones, acuminol A (119) and B (120).

**Table 2.3.** Known bioactivity of crude extracts from species of the Clusiaceae family, including those from the genera *Garcinia*, *Kayea*, *Mammea*, *Mesua* and *Calophyllum*. IC<sub>50</sub>: 50% maximum inhibitory concentration; LC<sub>50</sub>: 50% lethal concentration; MIC: minimum inhibitory concentration; GAE: gallic acid equivalent; CC<sub>50</sub>: 50% cytotoxicity concentration; MBC: minimum bactericidal concentration.

Species	Part used	Extract	Biological	Biological activity	Ref.
		solvent/s	assay		
Calophyllum	Stem bark	Methanol	DPPH free	Moderate free radical	278,
castaneum			radical scavenging	scavenging (IC <sub>50</sub> = 12	291
			assay.	μg/mL)	
C. pulcherrimum	Leaf	Ethanol	DPPH free	Moderate free radical	259
-			radical	scavenging ( $IC_{50}$ = 16.7	
			scavenging	$mg/L^{-1}$ )	
			assay.		
C. soulattri	Stem	Methanol,	Disk	Anti-bacterial against 25	261
	bark,	petrol,	diffusion	species and anti-protozoan	
	roots.	dichlorom	assay.	against one species.	
		ethane, ethyl			
		acetate.			
Garcinia	Bark	Water	In vitro	Anti- Babesia gibsoni (IC <sub>50</sub> =	290
benthamiana			anti-	16.3 μg/mL).	
			babesial		
			assay.		
	Stem bark	Ethyl	DPPH free	Free radical scavenger	216
		acetate	radical	(antioxidant, $IC_{50}$ = 60.8	
			scavenging	μg/mL <sup>-1</sup> ).	
			assay.		
		Methanol	Ferric	Strong reducing capacity	216
			reducing	(9.9 g GAE.100 g <sup>-1</sup> )	
			antioxidant		
			potential		
		C1.1 C	assay.		
		Chlorofor	β-carotene	Significant antioxidant	
		m, hexane	bleaching	activity.	
C	I c - £	Moth1	assay.	Crtatorio again-tIII CO	263
G. maingayi	Leaf	Methanol	MTT (cell	Cytotoxic against HL-60	200
			viability).	cells (IC <sub>50</sub> = 10 μg/mL).	
				Cytotoxic against HL-60 cells (IC <sub>50</sub> = 6 $\mu$ g/mL).	
				cens (10 <sub>50</sub> - σ μg/111L).	

G. parvifolia	Leaf, roots, stem bark Leaf, stem bark Leaf, roots, stem bark	Hexane Ethyl acetate Methanol	Griess assay (NO inhibitory). In vitro anti- Plasmodiu m falciparum assay.	NO inhibition (IC $_{50}$ = 33 $\mu g/mL$ ). Anti-plasmodial (IC $_{50}$ < 40 $\mu g/mL$ -1)	180
	Stem bark, roots, fruit.	Ethyl acetate, n- hexane	Disk diffusion evaluation.	Anti S. aureus (inhibition zones > 12 mm)	
	Stem bark	Ethyl acetate	Brine shrimp lethality test.	$LC_{50} = 1.5 \ \mu g/mL$	
	Periarp	Methanol	Disk diffusion evaluation. MIC assay.	S. aureus resistant (inhibition zone 11 mm).  Anti-S. aureus and -S. mercescens (MIC and MBC = 250 µg/mL).	183
	Stem bark	Ethyl acetate	DPPH free radical scavenging assay.	Free radical scavenger (antioxidant, $IC_{50} = 4.2$ ppm).	162- 164
	Leaves	Hexane	Cell viability (MTT).	Anti-viral (Vero cell), cytotoxic (CC <sub>50</sub> = $< 1.2$ µg/mL).	184
		Ethyl aetate	Viral inhibition assay.	75% Vero cell plaque inhibition at 125 µg/mL	200
		Chlorofor m	MIC assay.	Anti- Klebsiella pneumonia, Pseudomonas aeruginosa and Pseudomonas putida (MIC = 450 µg/mL)	288
	Twigs	Methanol	MIC assay.	Anti-S. aureus (MIC=>100 µg/mL).	185,2 88

	Bark Bark Leaves	20% methanoli c ethyl acetate Ethyl acetate	In vivo CCl <sub>4</sub> induced hepatotoxic ity model. Cell viability (LDH). $\alpha$ - Glucosidas e inhibitory activity assay.	Protection against CCl <sub>4</sub> -induced liver toxicity  Cytotoxic against MCF-7 and DBTRG cell lines.  α-glucosidase inhibitor at 16.4 μg/mL	185 289
G. penangiana	Leaf	Methanol	MTT (cell viability).	Cytotoxic against HL-60 cells (IC $_{50}$ = 5 $\mu$ g/mL). Cytotoxic against NCI-H460 cells (IC $_{50}$ = 8.2 $\mu$ g/mL)	152
	Stem		Griess assay (NO inhibitory).	NO inhibition (IC <sub>50</sub> = 33 $\mu$ g/mL).	
	Leaves	Methanol	Cell viability (MTT).	Cytotoxic against MCF-7 and H460 cell lines (IC $_{50}$ = 5 and 5 $\mu$ g/mL, respectively).	152
Kayea borneensis	Stem bark	Ethyl acetate	In vitro anti- Plasmodiu m falciparum	Anti-plasmodial (IC $_{50}$ =23.6 $\mu g/mL$ )	227
K. borneensis	Stem bark Leaves	n-hexane	DPPH free radical scavenging assay.	Moderate free radical scavening (IC $_{50}$ = 3575.3 $\mu g/mL$ )	227
		Ethyl acetate	DPPH free radical scavenging assay.	Moderate free radical scavenging (IC $_{50}$ = 1058.4 $\mu g/mL$ )	

Mesua	Roots	Ethyl	LPS-	Moderate NO inhibition,	233
congestiflora		acetate	induced NO	anti-inflammatory (58	
			production in RAW	μg/mL).	
			264.7 cells		

**Table 2.4.** All known compounds isolated from species of interest (Figure 2.1) within the Clusiaceae and Calophyllaceae family. PPAPs: polycyclic polyprenylated acylphloroglucinol.

Species	Part used	Compound Isolated	Type	Reference
Calophyllum castaneum	Stem bark (dichloro methane) Stem bark	Isoblancoic acid (117)  Blancoic acid (118)	Chromanone acid	278,279
	Stem bark	β-sitosterol (66)	Sterol	
	Stem bark	Friedelinol	Triterpenoid	278
	(methanol)	Friedelin		
C. soulattri	Bark	Soulattrolide (106) Taraxerol (103)	Coumarin alcohol Triterpenoid	265
	Timber	Taraxerone (107) β -sitosterol (61) 6-Deoxyjacreubin 1,6-Dihydroxy-5- methoxyxanthone (117)	Sesterterpenoid Sterol Xanthone	
		Euxanthone (90)		
		1-Hydroxy-5- methoxyxanthone		
		1,3,5-Trihydroxy-2- (3- methylbut-2- enyl)xanthone	Trihydroxyxantho ne	

	Stem bark	Soulamarin (118) Caloxanthone B (119) Caloxanthone C Pyranojacareubin Rheediaxanthone A (120) Macluraxanthone 4-hydroxyxanthone Brasixanthone B Trapezifolixanthone Macluraxanthone Brasixanthone Brasixanthone	Pyranocoumarin Xanthone	267 20,267,295,2 96 20,267 20,267
		Friedelin Stigmasterol	Triterpene	267 267
		β-sitosterol (66) Soulattrin (112)	Steroid Xanthone	268 20,296
	Stem bark	Phylattrin (113) Airlanggin A (114) Airlanggin B	Xanthone Isoprenylated benzofuran 3-ones	244
		Calosubellinone (115) Garsubellin B (116) Soulattrone A	Phloroglucinol (phenol) Phloroglucinol derivative Terpenoid	270
Garcinia benthamiana	Stem bark	Benthamianone (89) Congestiflorone (90) Stigmasterol (39) γ-sitosterol (91) Phloroglucinol	Benzophenone Benzophenone Sterol Sterol Benzentriol (phenol)	215
		Methyl palmitate (92) α-mangostin (65) β-mangostin (93) Mangosteno Mangaxanthone B (101)	Fatty acid methyl ester Xanthone	217

		Mangaphenone (102)	Benzophenone	
	Pericarp	Stigmasterol (39) Garcihombronane B (66)	Sterol Triterpene	293
G. hombroniana	Pericarp	Garcihombronane C ( <b>67</b> ) Garcihombronanes D – K (24 <i>E</i> )-3α-hydroxy-17,14- friedolanostan-8,14,24-dien-	Triterpene	293
		26-oic acid (68) $3\beta$ -Hydroxy-23-oxo-9,16- lanostadien-26-oic acid Methyl (24 $E$ )-3 $\alpha$ ,9,23- trihydroxy-17,14- friedolanostan-14,24-dien-		
		26-oate] Methyl (24 <i>E</i> )-3 <i>a</i> ,23- dihydroxy-17,14- friedolanostan-8,14,24-trien- 26-oate Methyl (24 <i>E</i> )-3 <i>a</i> ,23-		
		dihydroxy-17,14- friedolanostan-8,14,24-trien- 26-oate 3 <i>a</i> -Acetoxy-23-oxo-9,16-		
	Bark (dichloro methane)	lanostadien-26-oic acid (22 <i>Z</i> ,24 <i>E</i> )-3β-hydroxycycloart-14,22,24-trien-26-oic acid ( <b>69</b> ) 3β acetoxy-9α-hydroxy-17,14-friedolanostan-14,24-dien-26-oic acid	Triterpene	212
		3β acetoxy-9α-hydroxy- 17,14-friedolanostan-14,24- dien-26-oic acid ( <b>70</b> ) 3b, 23a-dihydroxy-17,14- friedolanostan-8,14,24-trien-		
	Leaves	26-oic acid (71) Monoacetate of garcihombronane I Methyl (25 <i>R</i> )- 3β-hydroxy-23- oxo-9,15-lanostadien-26- oate	Triterpene	394
		Vitexin (72) Isovitexin (73)	Flavonoid glucoside	

		Bluminol-C-9-O-β-D- apiofuranosyl-(1→6)-β-D- glucopyranoside ( <b>74</b> ) Vomifoliol-9-O-β-D - apiofuranosyl (1→6)-β-D- glucopyranoside	Sesquiterpene	
	Twigs	(22 <i>Z</i> , 24 <i>E</i> )-3β,9α-dihydroxy- 17,14-friedolanostan- 14,22,24-trien-26-oic acid	Triterpene	210
		Monoacetate of garcihombronane K	Sterol	
		Garcihombronane L	Sterol	
		Garcihombronone A (75)	Xanthone	
		Garcihombronone B ( <b>76</b> )	Xanthone	
		Garcihombronone C – D	Xanthone	
		Norathyriol (52)	Xanthone	
		Gentisein (77)	Xanthone	
		1,3,6,7-tetrahydroxy-8- prenylxanthone	Xanthone	
		Cheffouxanthone (78)	Xanthone	
		Bangangxanthone A (79)	Xanthone	
		Toxyloxanthone B	Xanthone	
		1,3,5,7- tetrahydroxy-2-(3,7-	Xanthone	
		dimethyl-6-hydroxyocta-2-7-		
		dien)xanthone (80)	D:(1 · 1	
		Volkensiflavone	Biflavonoid	
		Naringenin 7-O-β-D- glucuronide	Flavanone glucoside	
		Eriodictyol 7-O-β-D-	Flavanone	
		glucuronide	glucoside	
		4-hydroxybenzoic acid (81)	Phenol	
		Protocatechuic methyl ester	Phenol	
	Twigs (methanol)	3,5,3',5'-tetrahydroxy-4- methoxybenzophenone ( <b>82</b> )	Benzophenone	211
G. maingayi	Stem bark	1,3,7-trihydroxy-2-(3-	Prenylated	169
		methylbut-2-enyl)-xanthone	xanthone	
		(38) Stigmostorel (20)	Tritamons	169
		Stigmasterol (39)	Triterpene	
G. parvifolia	Latex (Methanol)	Rubraxanthone (40)	Xanthone	168,187,188, 192

# Bark

Bark	Isocowanol (41) Griffipavixanthone (42)	Xanthone Bixanthone	188 189 190
Leaves	Garcidepsidone A (43)	Depsidones	100
	Garcidepsidone B (44)		
	Garcidepsidone C and D		
Bark	Parvixanthones A (45)	Xanthone	191
	Parvixanthones B (46)		
	Parvixanthones C (47)		
	Parvixanthones D – I		
Twigs	Parvifolixanthone A (48) Parvifolixanthone B (49) Parvifolixanthone C Mangostinone (50) Dulxanthone D (51) 1,3,5,6- tetrahydroxyxanthone Norathyriol (52)		
	Parvifoliols A (53)	Phloroglucinol	
	Parvifoliol B (54)		
	Parvifoliol C (55)		
	Parvifoliols D – G		
	Parvifolidone A (56)	Depsidone	
	Parvifolidone B (57)		
	Garcidepsidone B (44)		
	(2 <i>E</i> ,6 <i>E</i> ,10 <i>E</i> )-(+)-4β-hydroxy- 3-methyl-5β-(3,7,11,15- tetramethylhexadeca- 2,6,10,14- tetraenyl)cyclohex-2-en-1- one (58)	Tetraprenyltoluqui none	
Leaves	Parvifoliquinone (59)	Benzoquinone derivative	157
	Nigrolineaisoflavone A (60)	Flavonoid	

	Leaves	b-sitosterol ( <b>61</b> ) Squalene ( <b>62</b> ) Friedelin-3β-ol Friedelin	Sterol Triterpene Triterpenoid Triterpenoid	288
	Stem bark (ethyl acetate)	1,6,7-trihydroxy-3- methoxyxanthone 3,8"-binaringenin	Xanthone Biflavonone	162-164
	Stem bark	Cowanin (63)	Xanthone	168
	Leaves	Clusianone (64)	PPAP	292
	Stem bark	α-Mangostin ( <b>65</b> )	Xanthone	178
	Pericarp	Garcihombronane B (66)	Triterpene	293
		Euxanthone (83)	Xanthone	
G. penangiana	Leaves	Penangianaxanthone (84)	Xanthone	314
penangiana		Cudratricusxanthone H (84)	Xanthone	
		Macluraxanthone C (85)	Xanthone	
		Gerontoxanthone C (86)	Xanthone	
		4-(1,1-Dimethylprop-2-enyl)- 1,3,5,8-	Xanthone	
***	G. 1 1	tetrahydroxyxanthone (87)		227
Kayea borneensis	Stem bark	Mammea A/BA (96) Mammea A/ AA cyclo D (97) Mesuol (98)	Isoprenylated coumarin	227
K. borneensis & K.	Stem bark	Mesucalophylloidin (99)	Isoprenylated 4- phenylcoumarin	244
calophylloides				
K. calophylloides	Stem bark	Mammea A/BA cyclo F	Isoprenylated 4-	20,244
cutophytiolides		Calolongic acid (100)	phenylcoumarin Chromanone acid	
K. myrtifolia	Bark	Isocalolongic acid Simiarenone (101) Simiarenol (102) Taraxerol (103) Betulinic acid (104)	Triterpene	247
	Timber	Oleanolic acid 3a-hydroxybauer-7-en-28- oic Jacareubin ( <b>105</b> )	Bauerene derivative Xanthone	

Mammea	Stem	Acuminol A (119)	Furanoxanthone	285
acuminata		Acuminol B (120)		
Mesua	Roots	α-mangostin ( <b>65</b> )	Xanthone	231
congestiflora		Congestiflorone (97)	Benzophenone	

# 2.5. The Clusiaceae Summary

The Clusiaceae family seems to be very well explored in terms of its biological activity. This may be because of the numerous reports on their ethnomedicinal value, as well as their wider distribution. There have been approximately 163 metabolites isolated from the 18 (only 10 of which have been investigated) species of interest in this study, many of which have biological activity including antimicrobial, cytotoxic and antioxidant. This illustrates the capacity that this family has to produce interesting and pharmacologically promising compounds. Most compounds are either triterpenes, or most predominantly, xanthones. Of the genera explored here, *Garcinia* and *Calophyllum* are particularly well studied, with emphasis on their anti-bacterial and anti-cancer metabolites.

### 2.6. Pharmacological Relevance of the Myristicaceae and the Clusiaceae

The Bornean Myristicaceae and Clusiaceae species explored in this review clearly illustrate the bioactive potential of all family members, including those which have not been scientifically investigated yet. Reviewing the literature on these species has evidenced the wide range of biosynthetic pathways and metabolites present. To compare the extent to which each family has been studied, 10/28 Myristicaceae and 10/18 Clusiaceae species of interest have been phytochemically investigated. 163 metabolites have been isolated from species of the Clusiaceae, 50 have been isolated from the Myristicaceae species of interest. Whilst this indicates the higher current pharmacological relevance of the Clusiaceae, the lack of Myristicaceae species exploration may make it seem this way. The collective metabolome of all Myristicaceae species certainly suggests the high pharmacological significance of this family too. Therefore, unexplored species hold high potential in the quest for novel bioactive

compounds. Borneo holds ecoregions which grow these species of interest, and the growing need for new pharmaceuticals warrants the conservation and investigation of its plant species.

### 2.7. References

- R. Condit, P. S. Ashton, P. Baker, S. Bunyavejchewin, S. Gunatilleke, N. Gunatilleke, S. P. Hubbell, R. B. Foster, A. Itoh, J. V. LaFrankie, H. S. Lee, E. Loses, N. Manokaran, R. Sukumar, T. Yamakura, *Science*, 2000, **288**, 1414–1418.
- F. R. Az-Zahra, N. L. W. Sari, R. Saputry, G. D. Nugroho, Sunarto, T. Pribadi and A. D. Setyawan, *Biodiversitas*, 2021, **22**, 4633–4647.
- 3 A. D. W. I. Setyawan, *Bioscience*, 2010, **2**, 97–108.
- 4 W. J. J. O. De Wilde, *Blumea: J Plant Taxon Plant Geogr*, 2002, **47**, 347–362.
- 5 L. E. Teo, G. Pachiaper, K. C. Chan, H. A. Hadi, J. F. Weber, J. R. Deverre, B. David and T. Sévenet, *J Ethnopharmacol*, 1990, **28**, 63–101.
- 6 C. N. Cai, H. Ma, X. Q. Ci, J. G. Conran, J. Li, J Syst Evol, 2019, **59**, 504–514.
- 7 J. E. Armstrong and T. K. Wilson, *Am J Bot*, 1978, **65**, 441–449.
- 8 J. H. Beaman, W. J. J. O. de Wilde and P. F. Stevens, Kew Bull, 2002, 57, 251.
- 9 C. Cai, J. Xiao, X. Ci, J. G. Conran and J. Li, *Plant Sys Evol*, 2021, **307**, 1–12.
- 10 C. Wiart, in *Ethnopharmacology of Medicinal Plants: Asia and the Pacific*, ed. L. E. Craker and Z. Gardner, New Jersey, 2007.
- 11 D. Banik and P. P. Bora, *Taiwania*, 2016, **61**, 141–158.
- M. J. Gonzalez, M. M. M. Pinto, A. Kijjoa, S. Kengthong, I. O. Mondanondra, A. Silva, G. Eaton and W. Herz, *Phytochemistry*, 2002, **61**, 995–998.
- 13 S. Wimalasena and E. Karunawansha, J Natl Sci Found, 1994, 22, 301–304.
- Z. Lu, R. M. Van Wagoner, C. D. Pond, A. R. Pole, J. B. Jensen, D. Blankenship, B. T. Grimberg,
   R. Kiapranis, T. K. Matainaho, L. R. Barrows and C. M. Ireland, *Org Lett*, 2013, 16, 346–349.
- 15 J. Barukial and J. N. Sarmah, Int J Med Arom Plants, 2011, 1, 203–211.
- 16 N. Chaichana, Curr J Appl Sci Technol, 2016, 9, 61–69.
- 17 B. Liu, Y. G. Chen, X. J. Tian and R. Zhan, *Nat Prod Res*, 2019, **35**, 1127–1133.
- 18 B. Liu, S. Z. Du, F. Kuang, Y. Liu, X. J. Tian, Y. G. Chen and R. Zhan, *Nat Prod Res*, 2019, **33**, 95–100.
- T. S. Kam, in *Alkaloids: Chemical and Biological Perspectives*, vol. 19, ed. S. W. Pelletier, Pergamon, Oxford, 1999, chapter 2 Alkaloids from Malaysian Flora, 285–435.
- 20 S. H. Mah, G. C. L. Ee, S. S. Teh and M. A. Sukari, *Pak J Pharm Sci*, 2015, **28**, 425–429.
- 21 Denny and T. Kalima, *Buletin Plasma Nutfah*, 2016, **22**, 137–148.
- D. A. Ehlers Smith, S. J. Husson, Y. C. Ehlers Smith and M. E. Harrison, *Am J Primatol*, 2013, 7, 848–859.
- 23 E. Mirmanto, *Biodiversitas*, 2009, **10**, 187–194.
- 24 J. S. Rahajoe, L. Alhamd, T. D. Atikah, B. A. Pratama, S. Shiodera and T. S. Kohyama, in *Tropical Peatland Ecosystems*, ed. M. Osaki and N. Tsuji, Springer, Tokyo, 2016, chapter Floristic Diversity in the Peatland Ecosystems of Central Kalimantan, 167–196.

- M. E. Harrison, N. Zweifel, S. J. Husson, S. M. Cheyne, L. J. D'Arcy, F. A. Harsanto, H. C. Morrogh-Bernard, A. Purwanto, Rahmatd, Santiano, E. R. Vogel, S. A. Wich and M. A. Van Noordwijk, *Biotropica*, 2015, **48**, 188–197.
- D. Prasetyo, M. Ancrenaz, H. C. Morrogh-Bernard, S. S. Utami Atmoko, S. A. Wich and C. P. Van Schaik, in *Orangutans: geographic variation in behavioural ecology and conservation*, Oxford University Press, New York, USA, 2009, chapter Nest Building in Orangutans, 269-277.
- 27 F. Y. C. Chai and V. M. LeMay, For Ecol Manage, 1993, **58**, 51–64.
- T. O'dempsey and P. T. Chew, *Proceedings of Nature Society, Singapore's Conference on 'Nature Conservation for a Sustainable Singapore'*, October 2011, 121–166.
- 29 J. Koster and P. Baas, *Blumea*, 1981, **27**, 115–173.
- 30 L. Neo, K. Y. Chong, S. Y. Tan, C. Y. Koh, R. C. J. Lim, J. W. Loh, W. Q. Ng, W. W. Seah, A. T. K. Yee and H. T. W. Tan, *Nat Singap*, 2016, **9**, 1–28.
- M. Rothwell, MSc thesis: Selection of tree species for cambium consumption by the Bornean orang-utan (Pongo pygmaeus wurmbii), Selwyn College, 2008.
- 32 G. W. H. Davison, P. K. L. Ng and H. C. Ho, Raffles Bull Zool, 2013, 43, 287–288.
- 33 L. L. Komara, D. N. Choesin and T. S. Syamsudin, *Biodiversitas*, 2016, 17, 531–538.
- 34 S. Randi, A. Manurung, and T. F. Siahaan, *Jurnal Hutan Lestari*, 2014, 2, 2338–3127.
- 35 E. Suzuki, Ecol Res, 1999, 14, 211-224.
- K. Kartawinata, H. Priyadi, D. Sheil, S. Riswan, S. Sist and Machfudh, in *A field guide to the permanent sample plots in the conventional logging blocks 28 & 29 at CIFOR Malinau research forest East Kalimantan*, Centre for International Forestry Research, Bogor, Indonisia, 2006, DOI: 10.17528/cifor/002014.
- A. Itoh, T. Yamakura, M. Kanzaki, T. Ohkubo, P. A. Palmiotto, J. V. LaFrankie, J. J. Kendawang and H. S. Lee, *For Ecol Manage*, 2002, **168**, 275–287.
- 38 K. Momose, T. Nagamitsu and T. Inoue, *Biotropica*, 1998, **30**, 444–448.
- 39 W. J. J. O. de Wilde, Flora Malesiana Series 1, Spermatophyta, 2000, 14, 1-632.
- 40 J. Sinclair, *Gard Bull*, 1975, **28**, 1–181.
- 41 P. K. Chai, in *Medicinal plants of Sarawak*, Lee Ming Press, Sarawak, 2006.
- 42 S. Ping Teo, PhD thesis: *Antibacterials from the Plants of the Tropical Rain Forests of Borneo*, University College London, 2018.
- Wardah and S. Sundari, *IOP Conference Series: Earth and Environmental Science*, 2019, **298**, DOI: 10.1088/1755-1315/298/1/012005.
- 44 E. Mulyoutami, R. Rismawan and L. Joshi, For Ecol Manage, 2009, **257**, 2054–2061.
- 45 H. Zahorka, *J Trop Ethnobiol*, 2020, **3**, 57–68.
- 46 Ismail. Hadiani Nor, R. Ahmad, N. Ahmat and F. Jaafar Mohd, report: *Chemical Diversity and Biological Activity of Endemic Plants of Kuala Keniam, Taman Negara Pahang*, unpublished, 1011, ir.uitm.edu.my/id/eprint/27131/ (accessed October 2022).
- 47 M. R. Mohamad Jemain, M. Nik Musa'adah, A. Rohaya, L. Abdul Rashid and I. Nor Hadiani, *J Trop For Sci*, 2011, **23**, 467–472.
- 48 M. Idris, M. N. Azmi, T. Parmusivam, U. Supratman, M. Litaudon and K. Awang, *Trop Life Sci Res*, 2024, **35**, 165.

- P. Lepun, H. I. Faridah and K. Jusoff, *Tree Species Distribution in Ayer Hitam Forest Reserve*, Proc. 3rd IASME/WSEAS Int. Conf. on Energy, Environment, Ecosystems and Sustainable Development, Agios Nikolaos, Greece, July 2007.
- 50 S. Tarn, *Gard Bull*, 1999, **51**, 257–308.
- 51 H. C. Ong, P. F. J. Mojiun and P. Milow, *Afr J Agric Res*, 2011, **6**, 1962–1965.
- 52 H. Kayang, *Indian J Trad Knowl*, 2007, **6**, 177–181.
- F. Hanum, A. Z. Ibrahim, S. Khamis, M. Nzare, P. Lepun, G. Rusea, J. J. Lajuni and A. Latiff, *Pertanika J Trop Agric Sci*, 2001, **21**, 63–78.
- W. J. J. O. de Wilda, *Horsfieldia splendida*, The IUCN Red List of Threatened Species 1998, www.iucnredlist.org/species/34601/9876655, (accessed 10 April 2025).
- F. Yusro, G. Hardiansyah, E. Erianto, Y. Mariani, A. Aripin, H. Hendarto and D. Nurdwiansyah, *Jurnal Biologi Tropis*, 2020, **20**, 245–255.
- 56 R. Schouten, Blumea, 1986, 31, 451–486.
- 57 R. Bhat P, *Adv Obes Weight Manag Control*, 2017, **6**, 167–171.
- 58 Chaithanneya and R. Bhat, *Biotechol Biochem Res*, 2016, **4**, 77–82.
- 59 S. R. Johns, J. A. Lamberton and J. L. Occolowitz, *Aust J Chem*, 1967, **20**, 1737–1742.
- B. Sabulal, R. Kurup, B. Sumitha and V. George, J Essent Oil Res, 2005, 19, 323–325.
- P. Faezah, I. Asmida, M. H. Siti Khairiyah, J. S. Norrizah and C. A. Nuraini, 2013 IEEE Business Engineering and Industrial Applications Colloquium, Malaysia, 2013, 845–850.
- J. Sinclair, in the Gardens' bulletin, Singapore, 1986, 23, Govt. print off, Singapore.
- P. Wilkie, G. Argent, E. Cambell and A. Saridan, *Biodivers Conserv*, 2004, 13, 694–708.
- 64 M. R. Siddiqi and T. K. Wilson, Bull Torrey Bot Club, 101, 354–362.
- N. Y. Sandwith, *Bulletin of Miscellaneous Information (Royal Gardens, Kew)*, **1939**, 1939, 545–563.
- 66 W. J. J. O. De Wilde, *Blumea*, 1979, **25**, 321–478.
- J. P. Janovec and R. García, in *Encyclopedia of Forest Sciences*, ed. J. Burley, J. Evans and J. A. Youngquist, Elsevier, Oxford, 2004, 1762.
- 68 L. M. Perry and J. Metzger, in *Medicinal Plants of East and Southeast Asia: Attributed Properties and Uses*, vol. 33, Brittonia, New Yok, USA, **1981**, 258–259.
- 69 G. F. Spencer, L. W. Tjarks and R. Kleiman, *J Nat Prod*, 1980, **43**, 724–730.
- 70 C. Wiart, in *Medicinal Plant of Asia-Pacific-Drugs for the Future?*, World Scientific Publishing Co. Pte. Ltd, Singapore, 2006.
- Vinayachandra and K. R. Chandrashekar, *J Herbs Spices Med Plants*, 2014, **20**, 183–195.
- 72 K. Ravikumar and D. K. Ved, in *Hundred Red Listed Medicinal Plants of Conservation Concern* in *Southern India*, 1st edition, Foundation for Revitalization of Local Health Traditions, Anugraha, Bangalore, **2000**, 136–138.
- 73 C. P. Khare, in *Indian Medicinal Plants*, Springer-Verlag, Germany, 2007.
- 74 M. Phadungkit, R. Rattarom and S. Rattana, J Med Plants Res, 4, 1269–1272.
- 75 W. M. N. H. W. Salleh and F. Ahmad, *Pharm Sci*, 2017, **23**, 249–255.
- 76 M. Pinto and A. Kijjoa, *Quim Nova*, 1990, **13**, 243–244.
- 77 R. Barman, P. K. Bora, J. Saikia, P. Kemprai, S. P. Saikia, S. Haldar and D. Banik, *Phytother Res*, 2021, **35**, 4632–4659.

- 78 I. Häke, S. Schönenberger, J. Neumann, K. Franke, K. Paulsen-Merker, K. Reymann, G. Ismail, L. bin Din, I. M. Said, A. Latiff, L. Wessjohann, F. Zipp and O. Ullrich, *J Neuroinflammation*, 2009, 7, DOI: 10.1186/1478-811X-7-S1-A77.
- 79 J. Ohtani, Y. Saitoh, J. Wu, K. Fukazawa and S. qun Xiao, *IAWA J*, **13**, 301-306.
- 80 N. Rangkaew, R. Suttisri, M. Moriyasu and K. Kawanishi, Arch Pharm Res, 2009, 32, 685–692.
- 81 A. Zahir, A. Jossang, B. Bodo, H. A. Hadi, H. Schaller and T. Sevenet, JNat Prod, 56, 1643–1647.
- 82 C. F. Wang, F. Kuang, W. J. Wang, L. Luo, Q. X. Li, Y. Liu and R. Zhan, *Results Chem*, 2021, 3, 100175.
- 83 A. S. Salihu and W. M. N. H. W. Salleh, *Riv Ital Sostanze Grasse*, 2024, **101**, 21–28.
- 84 S. Dalibalta, A. F. Majdalawieh and H. Manjikian, Saudi Pharm J, 2020, 28, 1276–1289.
- M. S. Wu, L. B. B. Aquino, M. Y. U. Barbaza, C. L. Hsieh, K. A. De Castro-Cruz, L. L. Yang and P. W. Tsai, *Molecules*, 2019, **24**, 4426.
- 86 D. J. Maloney, J. Z. Deng, S. R. Starck, Z. Gao and S. M. Hecht, *J Am Chem Soc*, **127**, 4140–4141.
- 87 Y. Isnaini, M. Magandhi and Sahromi, *AIP Conf. Proc.*, 2019, **2120**, DOI:10.1063/1.5115663.
- 88 J. F. Maxwell, *Nat His Bull Siam Soc*, 2001, **49**, 29–59.
- J. M. Salim, G. E. Lee, M. R. Salam, S. Shahimi, E. Pesiu, J. M. Jani, N. A. I. Horsali, R. Shahrudin, S. M. M. Nor, J. L. Chong, F. Mohamad, A. Raffi and D. Nikong, *PhytoKeys*, 2020, **160**, 7–43.
- 90 C. Ling and S. Julia, *Gard Bull Singapore*, 2012, **64**, 139–169.
- 91 R. P. J. de Kok, M. Briggs, D. Pirnanda and D. Girmansyah, *Trop Conserv Sci*, **8**, 28–32.
- 92 M. P. Austin and P. Greig-Smith, *J Ecol*, 1968, **56**, 827–844.
- J. Kuusipalo, Y. Jafarsidik, G. Ådjers and K. Tuomela, For Ecol Manage, 1996, 81, 85–94.
- 94 D. I. D. Arini and N. I. Wahyuni, J Penelit Kehutan Wallacea, 2016, 5, 91–102.
- 95 M. Sidiq, B. Nurdjali and M. Idham, J Hutan Lestari, 2015, 3, 322–331.
- 96 R. T. Kwatrina, Y. Santosa, M. Bismark and N. Santoso, in *AIP Conference Proceedings*, 2018, DOI: 10.1063/1.5061882.
- 97 S. Kitamura and P. Poonswad, *Trop Conserv Sci*, 2013, **66**, 608–636.
- 98 C. Y. Ong, S. K. Ling, R. M. Ali, C. F. Chee, Z. A. Samah, A. S. H. Ho, S. H. Teo and H. B. Lee, *J Photochem Photobiol B*, 2009, **96**, 216–222.
- 99 N. Raes, M. C. Roos, J. W. F. Slik, E. E. Van Loon and H. Ter Steege, *Ecography*, 2009, **32**, 180–192.
- 100 K. R. McConkey, F. Aldy, A. Ario and D. J. Chivers, *Int J Primatol*, 2002, **23**, 123–145.
- 101 S. Soares, PhD thesis: *Natural Products as Inhibitors of Bacterial Type IV Secretion systems*, University College London, 2018.
- G. Periasamy, A. Karim, M. Gibrelibanos, G. Gebremedhin and A. H. Gilani, in *Essential Oils in Food Preservation, Flavor and Safety*, ed. V. R. Preedy, Academic Press, 2016, Chapter 69 Nutmeg (Myristica fragrans Houtt.) Oils, 607–616.
- 103 D. J. Mabberly, in *Mabberley's Plant-book: A Portable Dictionary of Plants, their Classification and Uses*, Cambridge University Press, 1981.
- B. Beckerman and H. Persaud, Complement Ther Med, 46, 44–46.
- D. N. Weerakoon, R. T. Perera, R. M. Rajapaksha, J. A. Liyanage, *Int J Innov Sci Res*, 2021, 3, 1316–1320.
- 106 R. A. DeFilipps and G. A. Krupnick, *PhytoKeys*, 2018, **102**, 1–341.

- 107 N. A. Alrashedy and J. Molina, *PeerJ*, **4**, DOI:10.7717/peerj.2546.
- 108 G. S. Sonavane, V. P. Sarveiya, V. S. Kasture and S. B. Kasture, *Pharmacol Biochem Behav*, 2002, 71, 239–244.
- 109 T. Sharma, K. Abirami and M. P. Chander, *Indian J Plant Genet Res*, 2018, 31, 125–133.
- T. E. Sheeja, O. B. Rosana, V. P. Swetha, R. S. Shalini, S. Siju, R. Dhanya, P. R. Rahul and B. Krishnamoorthy, *Genet Resour Crop Evol*, 2014, **60**, 523–535.
- 111 H. Benzeid, F. Gouaz, A. H. Touré, M. Bouatia, M. O. B. Idrissi and M. Draoui, *J Toxicol*, 2018, **2018**, 4563735.
- P. K. Chelladurai, R. Ramalingam, C. Prem and K. Chelladurai, *J Pharmacogn Phytochem*, 2017, 6, 155–258.
- 113 S. Subha, K. Prudhviraj, M. V. Aanandhi, M. Shankar and M. Nishanthi, *Int J Phytopharm*, 2013, **4**, 18–23.
- 114 S. M. Abdul Wahab, Y. Sivasothy, S. Y. Liew, M. Litaudon, J. Mohamad and K. Awang, *Bioorg Med Chem Lett*, 2016, **26**, 3785–3792.
- E. B. Truitt, G. Duritz and E. M. Ebersberger, *Proceedings of the Society for Experimental Biology and Medicine*, 1963, **112**, 647–650.
- 116 O. A. Olajide, J. M. Makinde and S. O. Awe, *Pharm Biol*, 2000, **38**, 385–390.
- O. A. Olajide, F. F. Ajayi, A. I. Ekhelar, S. O. Awe, J. M. Makinde and A. R. A. Alada, *Phytotherapy Research*, 1999, **13**, 344–345.
- 118 S. P. Piaru, R. Mahmud and S. Perumal, *Int J Pharmacol*, 2012, **8**, 572 576.
- 119 B. Narasimhan and A. S. Dhake, *J Med Food*, 2006, **9**, 396–399.
- 120 G. Singh, P. Marimuthu, C. S. De Heluani and C. Catalan, J Food Sci, 2005, 70, 141–148.
- P. A. Mary Helen, T. A. Vargheese, J. J. Jeeja Kumari, M. R. Abiramy, N. Sajina and S. Jaya Sree, Int J Curr Pharm Rev Res, 2011, 2, 188–198.
- 122 H. Krisnawati, For Res Bull, 2003, **639**, 1–19.
- 123 I. Theilade, L. Schmidt, P. Chhang and J. A. McDonald, Nord J Bot, 2011, 29, 71-80.
- E. Ito, J. Toriyama, M. Araki, Y. Kiyono, M. Kanzaki, B. Tith, S. Keth, L. Chandararity and S. Chann, *Jpn Agric Res Q*, 2014, **48**, 195–211.
- 125 N. Turreira-García, D. Argyriou, P. hourin Chhang, P. Srisanga and I. Theilade, *Cambodian J Nat His*, 2017, **1**, 76–101.
- 126 K. Pearce, *Gard Bull*, 2005, **57**, 145–182.
- 127 N. Burusliam, *Chonburi Hosp J*, 2020, **45**, 230–240.
- 128 F. H. Lestari, H. R. Rija'i and H. Herman, *Proceeding of Mulawarman Pharmaceuticals Conferences*, 2022, **15**, 65–71.
- 129 L. Medway, *Biol J Linn Soc*, 1972, **4**, 117–146.
- A. Powling, A. Phillips, R. Pritchett, S. T. Segar, R. Wheeler and A. Mardiastuti, *Reinwardtia*, 2020, **14**, 265–286.
- 131 A. Zamri and J. W. F. Slik, *SciBru*, 2018, **17**, 6–122.
- A. B. Suwardi, Z. I. Navia, T. Harmawan, Syamsuardi and E. Mukhtar, *Biodiversitas*, 2020, **21**, 1850–1860.
- 133 M. Yanbuaban, T. Nuyim, T. Matsubara, T. Watanabe and M. Osaki, *Tropics*, 2007, **16**, 31–39.
- 134 U. J. I. Tahan, *Biodiversitas*, 2003, **4**, 112–117.

- R. Elanchezhian, R. Kumar, S. Beena and M. Suryanarayana, *Ind Trad Know*, 2007, **6**, 342–345.
- 136 A. Arun Waman, P. Bohra and S. Mane, Curr Agric Res J, 2018, **6**, 320–327.
- M. Y. Kamble, S. S. Mane, C. Murugan and I. Jaisankar, in *Biodiversity and Climate Change Adaptation in Tropical Islands*, ed. C. Sivaperuman, A. Velmurugan, A. K. Singh and I. Jaisankar, Academic Press, 2008, chapter 3 Diversity of Ethno-Medicinal Plants of Tropical Islands With Special Reference to Andaman and Nicobar Islands, 55–103.
- P. J. A. Kessler, in *Dipterocarp Forest Ecosystems: Towards Sustainable Management*, ed. A. Schulte and D. Schone, World Scientific Publishing, Singapore, chapter Not Only Dipterocarps: an Overview of Tree Species Diversity in Diterocarp Forest Ecosystems of Borneo, 1996, 74–101.
- M. A. Othman, Y. Sivasothy, C. Y. Looi, A. Ablat, J. Mohamad, M. Litaudon and K. Awang, *Fitoterapia*, 2016, **111**, 12–17.
- 140 Y. Sivasothy, K. H. Leong, K. Y. Loo, S. M. Adbul Wahab, M. A. Othman and K. Awang, *Nat Prod Res*, 2022, **36**, 1581–1586.
- 141 A. Manna, S. De Sarkar, S. De, A. K. Bauri, S. Chattopadhyay and M. Chatterjee, *Int Immunopharmacol*, 2016, **39**, 34–40.
- A. Manna, S. De Sarkar, S. De, A. K. Bauri, S. Chattopadhyay and M. Chatterjee, *Phytomedicine*, 2015, **22**, 7–8.
- 143 A. T. L. Nguyen, P. G. Boakye, S. S. Besong, P. M. Tomasula and E. S. Alamu-Lumor, *J Food Sci*, 2021, **86**, 404–410.
- 144 F. H. Mattson, S. M. Grundy and J. R. Crouse, *Am J Clin Nutr*, 1982, **35**, 697–700.
- 145 R. A. Voeks, *SJTG*, 2007, **28**, 7–20.
- 146 K. A. Hamzah, I. Parlan, A. R. Kassim, C. H. Hassan, G. Akeng and N. M. Said, *Trop Life Sci Res*, 2009, **20**, 15–27.
- P. Ismail, M. S. Nizam, I. Faridah-Hanum, H. Khali Aziz, I. Shamsudin, M. Samsudin and A. Latiff, *Malays For*, 2009, **20**, 15–17.
- 148 A. A. Kwapong, PhD thesis: *Natural product inhibitors of bacterial type-IV secretion systems and efflux pumps*, University College London, 2016.
- 149 E. J. H. Corner, in *Wayside Trees of Malaya*, 1st edn., volume 2, Singapore Government Printing Office, 1952.
- 150 I. H. Burkill, W. Birtwistle, F. Foxworthy, Scrivenor J B and Watson J G, *Nature*, 1936, **137**, 255–255.
- 151 N. M. Guedje, F. Tadjouteu, J. M. Onana, E. Nnanga Nga and O. Ndoye, *J Appl Biosci*, 2017, **109**, 10594–10608.
- 152 M. L. Jabit, F. S. Wahyuni, R. Khalid, D. A. Israf, K. Shaari, N. H. Lajis and J. Stanslas, *Pharm Biol*, 2009, **47**, 1019–1026.
- 153 P. G. Waterman and R. A. Hussain, *Biochem Syst Ecol*, 1983, **11**, 21–28.
- 154 V. Peres, T. J. Nagem and F. F. De Oliveira, *Phytochemistry*, 2000, **55**, 683–710.
- S. Ali, R. Goundar, S. Sotheeswaran, C. Beaulieu and C. Spino, *Phytochemistry*, 2000, **53**, 281–284.
- K. Matsumoto, Y. Akao, E. Kobayashi, T. Ito, K. Ohguchi, T. Tanaka, M. Iinuma and Y. Nozawa, *Biol Pharm Bull*, 2003, **26**, 569–571.

- 157 V. Rukachaisirikul, K. Trisuwan, Y. Sukpondma and S. Phongpaichit, *Arch Pharm Res*, 2008, **31**, 17–20.
- 158 K. Nakatani, N. Nakahata, T. Arakawa, H. Yasuda and Y. Ohizumi, *Biochem Pharmacol*, 2002, **63**, 73–79.
- Y. M. Lin, H. Anderson, M. T. Flavin, Y. H. S. Pai, E. Mata-Greenwood, T. Pengsuparp, J. M. Pezzuto, R. F. Schinazi, S. H. Hughes and F. C. Chen, *J Nat Prod*, 1997, **60**, 884–888.
- V. Rukachaisirikul, M. Kamkaew, D. Sukavisit, S. Phongpaichit, P. Sawangchote and W. C. Taylor, *J Nat Prod*, 2003, **66**, 1531–1535.
- O. Thoison, J. Fahy, V. Dumontet, A. Chiaroni, C. Riche, M. Van Tri and T. Sévenet, *J Nat Prod*, 2000, **63**, 441–446.
- 162 S. H. Ali Hassan, J. R. Fry and M. F. Abu Bakar, *Biomed Res Int*, 2013, **2013**, 138950.
- 163 O. A. Adaramoye, Afr Health Sci, 2012, 12, 498–506.
- 164 U. Acuna, N. Jancovski and E. Kennelly, *Curr Top Med Chem*, 2009, **9**, 1560 1580.
- 165 G. Repin, R. Majuakim, L. Suleiman, M. Nilus, R. Mujih, H. and Gunsalam, *J Trop Biol Conserv*, 2012, **9**, 2012.
- 166 C. L. Lim, M. Y. Siti-Munirah and R. Kiew, *Malay Nat J*, 2009, **61**, 143–189.
- 167 S. Y. Tan, C. Y. Koh, H. J. M. Siow, T. Li, A. Heyzer, H. F. Wong and H. T. W. Tan, in *100 Common Vascular Plants of the Nee Soon Swamp Forest, Singapore*, Raffles Museum of Biodiversity Research, Singapore, 2013.
- N. A. Muhammad, N. Basar and S. Jamil, J Sci Math Lett, 2019, 7, 44–51.
- 169 G. C. L. Ee, C. K. Lim, Y. L. Cheow and S. M.A, *Malay J Sci*, 2005, **24**, 183–185.
- S. A. Izaddin, N. Syuriati and K. Rafidah, *Faculty of Applied Sciences Universiti Teknologi MARA Negeri Sembilan*, https://ir.uitm.edu.my/id/eprint/68453/1/68453.PDF (accessed October 2022).
- S. Hartati, N. Artanti, L. Sari, T. Ernawati, J. Raya Serang -Jakarta, K. Limandang, kelurahan Kelodran and W. Serang Banten, *Res J Pharm Tech*, 2024, **17**, 3546–3552.
- 172 S. Arullappan, W. Fai Chu, L. C. Kiang, V. Jong, Y. Mian and S. K. Mow, *J Exp Bio and Agric Sci*, 2021, 9, 71–84.
- 173 J. H. Adam, J Trop For Sci, 2001, **13**, 76–92.
- 174 S. J. Davies and P. Becker, *J Trop For Sci*, 1996, **8**, 542–569.
- 175 A. Hoare, Borneo Res Bull, 2003, **34**, 94–120.
- N. F. Z. Zaine, N. H. Zamakshshari, A. N. Abd Halim, V. J. Yi Mian and N. Ngui Sing, *Nat Prod Res*, 2024, **26**, 1–7.
- N. H. Zamakshshari, N. F. Zafirah Zaine, D. N. A. A. Heilman, A. N. A. Halim, S. Phornvillay, Y. K. Wei, V. Jong Yi and F. B. Ahmad, *BJRST*, 2014, **14**, 80–87.
- 178 Faizatun and Syamsudin, *Int J Pharma Bio Sci*, 2010, 1, 1 6.
- P. W. Grosvenor, P. K. Gothard, N. C. McWilliam, A. Supriono and D. O. Gray, *J Ethnopharmacol*, 1995, **45**, 75–95.
- 180 Syamsudin, S. Kumala and B. Sutaryo, Asian J Plant Sci, 2007, 6, 972–976.
- A. B. Suwardi, Z. I. Navia, T. Harmawan, Nuraini, Syamsuardi and E. Mukhtar, in *IOP Conference Series: Materials Science and Engineering*, 2020, **725**, 012064.
- 182 H. E. Khoo, A. Azlan, K. W. Kong and A. Ismail, *Evid Based Complement Alternat Med*, 2016, **2016**, 7591951.

- A. R. Mohd Nasir and F. Jasnie, Int J Pharmacogn Phytochem Res, 2016, 10, 1625–1629.
- A. Adnan, Z. N. Allaudin, H. Hani, H. S. Loh, T. J. Khoo, K. N. Ting and R. Abdullah, *BMC Complement Altern Med*, 2019, **19**, 169.
- N. Jamila, N. Khan, A. A. Khan, I. Khan, S. N. Khan, Z. A. Zakaria, M. Khairuddean, H. Osman and K. S. Kim, *Afr J Tradit Complement Altern Med*, 2017, **14**, 374–382.
- A. P. Anu Aravind, L. N. Menon and K. B. Rameshkumar, in *Diversity of Garcinia Species in the Western Ghats: Phytochemical Perspective*, JNTBGRI, Thiruvananthapuram, 2016, chapter 2 Structural diversity of secondary metabolites in Garcinia species, 19–75.
- P. Pattalung, P. Wiriyachitra and M. Ongsakul, *J Sci Soc Thailand*, 1988, **14**, 67–71.
- 188 I. Jantan, M. M. Pisar, M. S. Idris, M. Taher and R. M. Ali, *Planta Med*, 2002, **68**, 1133–1134.
- 189 Y. J. Xu, S. G. Cao, X. H. Wu, Y. H. Lai, B. H. K. Tan, J. T. Pereira, S. H. Goh, G. Venkatraman, L. J. Harrison and K. Y. Sim, *Tetrahedron Lett*, 1998, **39**, 9103–9106.
- 190 Y. J. Xu, P. Y. Chiang, Y. H. Lai, J. J. Vittal, X. H. Wu, B. K. H. Tan, Z. Imiyabir and S. H. Goh, *J Nat Prod*, 2000, **63**, 1361–1363.
- 191 Y. J. Xu, Y. H. Lai, Z. Imiyabir and S. H. Goh, *J Nat Prod*, 2001, **64**, 1191–1195.
- 192 V. Rukachaisirikul, W. Naklue, S. Phongpaichit, N. H. Towatana and K. Maneenoon, *Tetrahedron*, 2006, **62**, 8578–8585.
- 193 Z. Tian, J. Shen, A. P. Moseman, Q. Yang, J. Yang, P. Xiao, E. Wu and I. S. Kohane, *Int J Cancer*, 2008, **122**, 31–8.
- 194 S. Babu and S. Jayaraman, *Eur J Pharmacol*, 2020, **131**, 110702.
- 195 S. K. Kim and F. Karadeniz, *Adv Food Nutr Res*, 2012, **65**, 223–233.
- 196 G. Chen, Y. Li, W. Wang and L. Deng, Expert Opin Ther Pat, 2018, 28, 415–427.
- 197 M. A. Lozano-Grande, S. Gorinstein, E. Espitia-Rangel, G. Dávila-Ortiz and A. L. Martínez-Ayala, *International Journal of Agronomy*, 2018, **2018**, 1829160.
- 198 J. Das, A. Sarkar and P. Ghosh, *New J Chem*, 2018, **42**, 6673–6688.
- 199 N. Chowchaikong, S. Nilwarangoon, N. Tanjapatkul, S. Laphookhieo and R. Watanapokasin, *J Med Assoc Thai*, 2017, **100**, S7–S12.
- I. Siridechakorn, W. Phakhodee, T. Ritthiwigrom, T. Promgool, S. Deachathai, S. Cheenpracha,U. Prawat and S. Laphookhieo, *Fitoterapia*, 2012, 83, 1430–1434.
- F. H. Z. Reis, G. L. Pardo-Andreu, Y. Nuñez-Figueredo, O. Cuesta-Rubio, J. Marín-Prida, S. A. Uyemura, C. Curti and L. C. Alberici, *Chem Biol Interact*, 2014, **212**, 20–29.
- 202 R. Ramadhan, K. Ul-Haq, P. Phuwapraisirisan, F. A. Puspitasari and H. Suwito, *Rasayan J Chem*, 2023, **16**, 1811–1817.
- 203 S. Egra, H. Kuspradini, I. W. Kusuma, I. Batubara, K. Yamauchi and T. Mitsunaga, *Med Chem Res*, 2023, **32**, 1658–1665.
- 204 H. Sri, M. Megawati and D. A. Lucia, *Nat Prod Sci*, 2022, **28**, 13–17.
- 205 M. Wijayanti, H. Ilmi, E. Kemalahayati, L. Tumewu, F. Y. Wardana, Suciati, A. F. Hafid and A. Widyawaruyanti, *J Basic Clin Physiol Pharmacol*, 2021, **32**, 839–844.
- S. Assyifa, A. H. Zulfa, A. R. Setiawan, M. Tanjung, T. S. Tjahjandarie and R. D. Saputri, *Adv J of Chem A*, 2025, **8**, 1309–1316.
- 207 M. Nazre, Genet Resour Crop Evol, 2010, 57, 1249–1259.

- 208 K. J. John, R. S. Kumar, C. P. Suresh, J. K. George and Z. Abraham, *Genet Resour Crop Evol*, 2008, 55, 183–186.
- 209 T. K. Lim, in *Edible Medicinal and Non-Medicinal Plants*, vol. 2 Fruits, Springer, Germany, 2012, chapter *Garcinia hombroniana*, 56–58.
- 210 S. Klaiklay, Y. Sukpondma, V. Rukachaisirikul and S. Phongpaichit, *Phytochemistry*, 2013, **85**, 161–166.
- 211 F. C. Saputri and I. Jantan, *Phytother Res*, 2012, **26**, 1845–1850.
- 212 N. Jamila, N. Khan, I. Khan, A. A. Khan and S. N. Khan, *Nat Prod Res*, 2016, **30**, 1388–1397.
- 213 Ismail, Mufidah, S. S. Mamada, Amrianto and Y. M. Evary, *J Exp Biol Agric Sci*, 2021, **9**, S280–S285.
- 214 M. L. Jabit, R. Khalid, F. Abas, K. Shaari, L. S. Hui, J. Stanslas and N. H. Lajis, *J Biosci*, 2007, **62**, 786–792.
- 215 I. See, G. C. L. Ee, S. S. Teh, S. H. Mah, R. A. Karjiban, S. Daud and V. Y. M. Jong, *Rec Nat Prod*, 2016, **10**, 355–361.
- 216 I. See, G. C. L. Ee, S. H. Mah, V. Y. M. Jong and S. S. Teh, *J Herbs Spices Med Plants*, 2017, **23**, 117–127.
- 217 I. See, G. C. L. Ee, V. Y. M. Jong, S. S. Teh, C. L. C. Acuña and S. H. Mah, *Nat Prod Res*, 2021, **35**, 6184–6189.
- 218 C. Rouger, S. Derbré and P. Richomme, *Phytochem Rev*, 2019, **18**, 317 342.
- W. M. Bandaranayake, S. S. Selliah, M. U. S. Sultanbawa and D. E. Games, *Phytochemistry*, **14**, 256–269.
- 220 G. C. L. Ee, C. K. Lim and A. Rahmat, Nat Prod Sci, 2005, 11, 220-224.
- 221 G. C. Ee, C. K. Lim, A. Rahmat and H. L. Lee, *Trop Biomed*, 2005, **22**, 99–102.
- 222 T. Karunakaran, G. C. L. Ee, S. S. Teh, S. Daud, S. H. Mah, C. K. Lim, V. Y. M. Jong and K. Awang, *Nat Prod Res*, 2016, **30**, 1591–1597.
- 223 S. Singh, A. Gray and P. Waterman, *Nat Prod Lett*, 1993, **3**, 53–58.
- T. Karunakaran, G. C. L. Ee, K. H. Tee, I. S. Ismail, N. H. Zamakshshari and W. M. Peter, *Phytochem Lett*, 2016, **17**, 131–134.
- 225 K. Awang, G. Chan, M. Litaudon, N. H. Ismail, M. T. Martin and F. Gueritte, *Bioorg Med Chem*, 2010, **18**, 7873–7877.
- 226 C. Rouger, S. Derbré, B. Charreau, A. Pabois, T. Cauchy, M. Litaudon, K. Awang and P. Richomme, *J Nat Prod*, 2015, **78**, 2187–2197.
- 227 M. Tanjung, R. D. Saputri, F. F. Fitriati and T. S. Tjahjandarie, J Biol Act Prod, 2016, 6, 95–100.
- 228 C. K. Lim, H. Subramaniam, Y. H. Say, V. Y. M. Jong, H. Khaledi and C. F. Chee, *Nat Prod Res*, 2015, **29**, 1970–1977.
- 229 S. S. Teh, G. C. L. Ee, S. H. Mah and Z. Ahmad, Med Chem Res, 2016, 25, 819–823.
- 230 W. Giesen, L. S. Wijedasa and S. E. Page, *Mires Peat*, 2018, **22**, 1–13.
- 231 G. C. L. Ee, S. S. Teh, H. C. Kwong, S. H. Mah, Y. M. Lim and M. Rahmani, *Phytochem Lett*, 2012, 5, 545–548.
- 232 S. S. Teh, G. C. L. Ee, S. H. Mah, Y. K. Yong, Y. M. Lim, M. Rahmani and Z. Ahmad, *Biomed Res Int*, 2013, **2013**, 517072.
- 233 S. S. Teh, G. C. L. Ee and S. H. Mah, *Med Chem Res*, 2017, **26**, 3240–3246.

- 234 P. F. Stevens, *Angiosperm Phylogeny Website*, Version 14, July 2017, mobot.org/MOBOT/research/APweb/P. F. Stevens (accessed November 2022).
- 235 F. N. Cabral, R. J. Trad, B. S. Amorim, J. R. Maciel, M. C. E. do Amaral and P. Stevens, *Mol Phylogenet Evol*, 2021, **157**, 107041.
- 236 C. Byrne, J. A. N. Parnell and K. Chayamarit, Thai Forest Bulletin (Botany), 46, 162–216.
- 237 J. S. Negi, V. K. Bisht, P. Singh, M. S. M. Rawat and G. P. Joshi, *J Appl Chem*, 2013, **2013**, 1–9.
- 238 S. S. Teh, G. C. L. Ee, S. H. Mah, Y. M. Lim and M. Rahmani, *Molecules*, 2012, **17**, 10791–10800.
- 239 K. H. Lee, H. B. Chai, P. A. Tamez, J. M. Pezzuto, G. A. Cordel, K. K. Win and M. Tin-Wa, *Phytochemistry*, 2003, **64**, 535–541.
- 240 N. N. Win, S. Awale, H. Esumi, Y. Tezuka and S. Kadota, *Bioorg Med Chem*, 2008, **16**, 8653–8660.
- 241 N. N. Win, S. Awale, H. Esumi, Y. Tezuka and S. Kadota, *Bioorg Med Chem Lett*, 2008, **18**, 4688–4691.
- 242 R. Govaerts, E. Nic Lughadha, N. Black, R. Turner and A. Paton, Sci Data, 2021, 8, 215.
- 243 E. Pesiu, *J Trop Biol Consererv*, 2019, **16**, 7–43.
- 244 M. Tanjung, F. Rachmadiarti, R. D. Saputri and T. S. Tjahjandarie, *Nat Prod Res*, 2018, **32**, 1062–1067.
- 245 K. Heyne, in *The Useful Indonesian Plants*, Research and Development Agency, The Ministry of Forestry, Indonesia, Jakarta, 1987.
- 246 I. Turner, W. J. Kress, R. A. DeFilipps, E. Farr, D. Y. Y. Kyi, J. H. Lace, R. Rodger, H. G. Hundley and U. C. K. Ko, *Syst Bot*, 2004, **29**, 462–463.
- 247 S. P. Gunasekera and M. U. S. Sultanbawa, J Chem Soc Perkin Trans 1, 1977, 6–10.
- 248 P. F. Stevens, Journal of the Arnold Arboretum, 1980, 61, 117–424.
- B. Bremer, K. Bremer, M. W. Chase, M. F. Fay, J. L. Reveal, L. H. Bailey, D. E. Soltis, P. S. Soltis,
  P. F. Stevens, A. A. Anderberg, M. J. Moore, R. G. Olmstead, P. J. Rudall, K. J. Sytsma, D. C. Tank,
  K. Wurdack, J. Q. Y. Xiang and S. Zmarzty, *Bot J Linn*, 2003, 141, 199–436.
- 250 D. M. Jin, J. J. Jin and T. S. Yi, Sci Rep, 2020, 10, 9091.
- S. Gupta and P. Gupta, in *Bioactive Natural Products in Drug Discovery*, Springer, Germany, chapter The Genus *Calophyllum*: a Review of Ethnomedicinal Uses, Phytochemistry and Pharmacology, 2020, 215–242.
- 252 J. Eckenwalder, *J Arnold Arbor*, 1980, **61**, 701–722.
- 253 E. Dorla, I. Grondin, T. Hue, P. Clerc, S. Dumas, A. Gauvin-Bialecki and P. Laurent, *S Afr J Bot*, 2019, **122**, 447–456.
- K. Yasunaka, F. Abe, A. Nagayama, H. Okabe, L. Lozada-Pérez, E. López-Villafranco, E. E. Muñiz,
   A. Aguilar and R. Reyes-Chilpa, *J Ethnopharmacol*, 2005, 97, 293–299.
- 255 I. M. Turner, Y. K. Wong, P. T. Chew and A. Bin Ibrahim, Biodivers Conserv, 1997, 6, 537–543.
- Purwaningsih and K. Kartawinata, in *IOP Conference Series: Earth and Environmental Science,* Species Composition and Structure of Forests in the Muara Kendawangan Nature Reserve, West-Kalimantan, Indonesia, 2018, **166**, DOI: 10.1088/1755-1315/166/1/012005.
- 257 L. Neo, A. T. K. Yee, K. Y. Chong, H. H. T. Yeo and H. T. W. Tan, NiS, 2014, 7, 93-109.
- 258 S. Sudarmono, *J Trop Life Sci*, 2018, **8**, 116–112.
- E. Septiana and P. Simanjuntak, Buletin Penelitian Tanaman Rempah dan Obat, 2018, 29, 59–68.

- G. Watt, in *A Dictionary of the Economic Products of India*, volume 2, Cambridge University Press, 2014.
- 261 M. R. Khan, M. Kihara and A. D. Omoloso, *Fitoterapia*, 2002, **73**, 741–743.
- E. Husni, F. Sri Wahyuni, H. Nurul Fitri, H. Nurul Fitri and E. Badriyya, *Pharmacogn J*, 2021, **13**, 362–367.
- 263 E. D. Y. Syahputra, D. Prijono, S. Manuwoto and L. K. Darusman, *Hayati*, 2006, **13**, 7–12.
- 264 S. Mah, S. Teh and G. Lian Ee, *Pharmacogn Mag*, 2019, **15**, 135–139.
- S. P. Gunasekera, G. S. Jayatilake, S. S. Selliah and M. U. S. Sultanbawa, *J Chem Soc Perkin 1*, 1977, 1505–1511.
- 266 T. Pengsuparp, M. Serit, S. H. Hughes, D. D. Soejarto and J. M. Pezzuto, *J Nat Prod*, 1996, **59**, 839–842.
- G. Cheng Lian Ee, S. H. Mah, S. S. Teh, M. Rahmani, R. Go and Y. H. Taufiq-Yap, *Molecules*, **16**, 9721-9727.
- 268 S. H. Mah, G. C. L. Ee, S. S. The, M. Rahmani, Y. M. Lim and R. Go, *Molecules*, 2012, **17**, 8303–8311.
- M. Tanjung, F. Rachmadiarti, A. Prameswari, V. Ultha Wustha Agyani, R. Dewi Saputri, T. Srie Tjahjandarie and Y. Maolana Syah, *Nat Prod Res*, 2018, **32**, 1493–1498.
- 270 C. K. Lim, S. Hemaroopini, Y. H. Say and V. Y. M. Jong, *Nat Prod Commun*, 2017, **12**, 1469–1471.
- D. N. A. Abang Heilman, N. H. Zamakshshari, V. J. Yi Mian, A. Y. Chee Hui, M. A. Lizazman and F. B. Ahmad, *Nat Prod Res*, 2024, 1–7.
- N. S. Widayani, D. Dono, Y. Hidayat, S. Ishmayana and E. Syahputra, Open Agric, 2023, 8, 1–12.
- 273 M. A. Lizazman, V. Jong and Y. Mian, preprint, 2024, Research Square.
- S. D. Marliyana, F. R. Wibowo, D. S. Handayani, T. Kusumaningsih, V. Suryanti, M. Firdaus and E. N. Annisa, *Jurnal Kimia Sains dan Aplikasi*, 2021, **24**, 108–113.
- 275 M. Salman Fareza, N. A. Choironi, S. Sri Sutji, M. P. Rini, V. Festihawa, I. S. Nur Fauzi and E. D. Utami, *Indones J Pharm*, 2021, **32**, 356–364.
- I. Fajriaty, H. Ih, I. Fidrianny, N. F. Kurniati, M. A. Reynaldi, I. K. Adnyana, R. Rommy, F. Kurniawan and D. H. Tjahjono, *Pharmaceuticals*, 2023, **16**, 191.
- 277 C. K. Lim, S. Y. Gan, V. Yi, M. Jong, C. O. Leong, C. W. Mai and C. F. Chee, *Pak J Pharm Sci*, 2019, **32**, 2183–2187.
- 278 K. Murugesu, MSc thesis: *Investigation of Phytochemicals from Calophyllum Castaneum for their Antioxidant Properties*, Universiti Tunku Abdul Rahman, 2014.
- J. Y. Lai, MSc thesis: *Investigation of potential antioxidants from the endemic plant of Sarawak, Calophyllum castaneum,* Universiti Tunku Abdul Rahman, 2014.
- 280 M. Dunthorn, *Pl Syst Evol*, 2004, **429**, 191–196.
- 281 J. C. Chapuis, B. Sordat and K. Hostettmann, J Ethnopharmacol, 1988, 23, 273–284.
- 282 L. Maikaeo, S. Sajjabut and P. Thepthong, *Thai J Pharmacol*, 2019, 41, 5–12.
- 283 H. Yang, B. Jiang, K. A. Reynertson, M. J. Basile and E. J. Kennelly, *J Agric Food Chem*, 2006, **54**, 4114–4120.
- J. J. Magadula, P. J. Masimba, R. B. Tarimo, Z. Msengwa, Z. H. Mbwambo, M. Heydenreich, D. Breard and P. Richomme, *Biochem Syst Ecol*, 2014, **56**, 65–67.

- 285 H. Tosa, M. Iinuma, K. I. Murakami, T. Ito, T. Tanaka, V. Chelladurai and S. Riswan, *Phytochemistry*, 2010, **45**, 133–136.
- 286 M. Iinuma, H. Tosa, T. Tanaka and S. Riswan, *Phytochemistry*, 1996, 42, 245–247.
- Amanatie, Jumina, Mustofa and Hanafi, in *IOP Conference Series: Materials Science and Engineering*, 2018.
- A. B. Salleh, MSc thesis: *Chemical constituents from the leaves of Garcinia Parvifolia*, University of Technology Malaysia, 2013.
- N. Triadisti, R. Sauriasari and B. Elya, *Pharmacog J* 2017, 4, 488–492.
- Subeki, H. Matsuura, M. Yamasaki, O. Yamato, Y. Maede, K. Katakura, M. Suzuki, Trimurningsih, Chairul and T. Yoshihara, *J Vet Med Sci*, 2004, **66**, 871–874.
- 291 C. R. Liao, Y. H. Kuo, Y. L. Ho, C. Y. Wang, C. S. Yang, C. W. Lin and Y. S. Chang, *Molecules*, **19**, 9515–9534.
- 292 S. Nagalingam, K. Wai-Ling and K. Teng-Jin, *Planta Medica Letters*, 2016, 3, e10-e13.
- V. Rukachaisirikul, A. Adair, P. Dampawan, W. C. Taylor and P. C. Turner, *Phytochemistry*, 2000, 55, 183–188.
- V. Rukachaisirikul, S. Saelim, P. Karnsomchoke and S. Phongpaichit, *J Nat Prod*, 2005, **68**, 1222–1225.
- 295 G. C. L. Ee, S. H. Mah, H. C. Kwong, S. S. Teh, M. I. Mohamed Tahir and S. Silong, 2011, *Acta Crystallogr Sect E Struct Rep Online*, **67**, 2607–2608.
- 296 S. Mah, G. Ee and S. Teh, *Planta Med*, 2014, **80**, P1L101.

# Chapter 3 - Material and Methods

#### 3.1. Literature Review

As there was a large collection of plants from Borneo, consisting of twenty-seven Myristicaceae and eighteen Clusiaceae species, the direction of this study was led by the findings of an initial literature review which determined the extent of phytochemical and biological studies of each species. Additionally, this review aided in the prediction of compound classes likely to be encountered within each genus, giving guidance during the identification of isolated metabolites. Such reviews allow a targeted approach, which mitigates redundancy of lab work, while increasing the likelihood of novel discoveries. This preliminary study reviewed all published literature on all the plants sampled to date, thereby revealing unstudied species and identifying gaps in the existing literature.

To achieve this, a systematic search of published literature was performed, using Google and Google Scholar, to identify reports of phytochemical composition and biological activities of each species sampled. Searches were conducted using the binomial name of each species. Additionally, the ethnomedicinal reports of each species and genus were gathered to provide insight into their traditional and historical significance, which informed the selection of species with higher therapeutic potential. Furthermore, a brief botanical characterisation and geographic distribution of each species was compiled. From the information gathered, previously unstudied species were selected for investigation.

## 3.2. Plant Material

Leaves of plants belonging to the Myristicaceae and the Clusiaceae families were identified and collected from various locations on the island of Borneo during fieldwork by Dr Stephen Teo Ping (Forest Department Sarawak, Malaysia). The plant material was air-dried for 1-2 weeks and ground into a powder. Plants were authenticated and submitted as voucher herbarium specimens by Dr Teo and deposited at the Forest Herbarium (SAR), the Forest Department Sarawak.

# 3.2.1. The Myristicaceae plant species

Twenty-seven Myristicaceae species in total were collected from various districts of Borneo (Figure 3.1) and were ultimately stored at The University of East Anglia, UK. From the species investigated during this work, leaves were collected and deposited as voucher specimens with numbers included in Table 3.1.



**Figure 3.1.** Locations within Sarawak on the island of Borneo where plant specimens were sampled from.

**Table 3.1.** Voucher specimen numbers and the corresponding Myristicaceae species, with the location of collection, of species which were used in phytochemical investigations.

Voucher specimen number	Species	Locality
S.18	Knema elmerii Merr.	Sungai Tengah,
		Matang
S.19	Horsfieldia polyspherula (Hook.f. emend.	Kpg Segulang, Bau
	King) J.Sinclair var sumatranum (Miq.)	
	dewilde	
S.26	Gymnacranthera contracta (King) Warb.	Lundu
S.31	Horsfieldia splendida W.J.de Wilde	Kerangas, Matang
S.33	Knema latifolia Warb.	Jln Stephen Yong,
		Batu Kawa
S.83	Knema membranifolia H.J.P.Winkl.	Lundu

# 3.2.2. The Clusiaceae plant species

A total of eighteen Clusiaceae species were collected from different districts of Borneo and subsequently stored at the University of East Anglia, UK. Leaves from the studied species were gathered and preserved as voucher specimens, with the corresponding numbers listed in Table 3.2.

**Table 3.2.** Voucher specimen numbers and the corresponding Clusiaceae species, with the location of collection, of species which were used in phytochemical investigations.

Voucher specimen	Species	Locality
number		
S.39	Calophyllum pulcherrimum Wall.ex Choisy	Jln Matang
S.48	Mesua calciphila P.F.Stevens	Semengoh
S.86	Garcinia caudiculata Ridl.	Lundu

#### 3.3. Extraction Processes

In preparation for extractions, dried plant material was ground into a finer powder using an electric grinder (Russell Hobbs, UK), before being extracted at a sample-to-solvent ratio of 1:10. During each extraction process, plant material was magnetically stirred (IKA Ltd, UK) with the solvent at room temperature. Next, plant material was separated from the solvent by vacuum-assisted filtration using filter paper (Fisher Scientific, UK). Extracts were concentrated under vacuum at 40 °C using a rotary evaporator, and the resulting residues were weighed.

## 3.3.1. Sequential plant extraction

### 3.3.1.1. Small scale

Small scale extractions were initially performed to allow screening of individual species for antibacterial activities. Here 10 g of *Calophyllum pulcherimum* (S.39), *Garcinia caudiculata* (S.86), *Gymnacranthera contracta* (S.26), *Horsfieldia polyspherula* (S.19), *Horsfieldia splendida* (S.31), *Knema membranifolia* (S.83) and *Mesua calciphila* (S.48) were extracted 3 times with 100 mL of each solvent including hexane, dichloromethane, methanol and water, whilst *Knema elmerii* (S.18) and *Knema latifolia* (S.33) were

extracted 2 times with 100 mL of each of the same solvents. Each extraction was performed for 24 hours, before concentrating. Following this, fresh solvent was added to the plant material for further extraction, and the resulting extracts were concentrated and weighed.

### **3.3.1.2.** Large scale

Extractions were scaled up to 100 g of fresh plant material and 1 L of solvent in active extracts (*Garcinia caudiculata, Gymnacranthera contracta* and *Knema membranifolia*). Here, the same extraction times, solvents and methods were used as the small-scale extractions for each species.

## 3.3.2. Non-sequential plant extraction

*Garcinia caudiculata* (S.86) was extracted for a third time using 300 g of fresh plant material with ethanol and ethyl acetate at a ratio of 1:1. Plant material was extracted three times at room temperature for 24 hours each time.

# 3.4. Chromatographic Techniques

### 3.4.1. Thin layer chromatography (TLC)

Thin-layer chromatography (TLC) is a widely used technique for the separation and visualisation of compounds in crude natural product extracts. A small sample is applied to a silica gel-coated plate, which serves as the stationary phase. The plate is then placed in a solvent system, where compounds migrate at different rates depending on their polarity and interaction with the mobile phase. Detection methods include UV light at various wavelengths or chemical reagents that react with specific functional groups, allowing for compound characterisation<sup>1</sup>.

Here, extracts were dissolved in dichloromethane (1 mg/mL) and applied as a thin line onto a 5 x 10 cm TLC plate coated with silica gel 60  $F_{254}$  (Merck, Germany). The mobile phase was developed in an appropriate solvent system depending on the sample. UV light at 254 nm and 365 nm (Fisher Scientific, UK) was used for visualisation of the bands on the plate. Chemical spray reagent vanillin-sulfuric acid was used for the detection of phenolics.

# 3.4.2. Vacuum liquid chromatography (VLC)

Vacuum liquid chromatography (VLC) is a method proposed by Targett *et al.*, <sup>2</sup> and was developed in response to the need for a more efficient alternative to traditional column chromatography. This technique functions as a liquid-solid preparative layer chromatography separation carried out in a column, with vacuum facilitating solvent flow. VLC employs step-gradient elution, with the column being run dry between the collection of each fraction. This is an economical and efficient technique for the initial fractionation of complex crude plant extracts<sup>3</sup>.

During this work, VLC was used to separate the crude dichloromethane, methanolic and ethyl acetate/methanol extracts of *G. caudiculata*, *G. contracta* and *K. membranifolia* using a silica stationary phase and less polar mobile solvents including hexane, ethyl acetate and methanol. Here, a glass column was packed with dry silica gel 60 PF<sub>254+366</sub> (Merck, UK). A mixture of the plant extract and silica was prepared (with silica added at the weight of the plant extract + 1 g), and this was added to the top of the packed silica column, separated by a filter paper. Two and a half grams (2.5 g) of *K. membranifolia* dichloromethane extract and 6 g of the methanol extract, 4.5 g of *G. caudiculata* dichloromethane extract, 14 g of the *G. caudiculata* ethyl acetate/methanol extract, and 4 g of the *Gymnacranthera contracta* dichloromethane extract were separated in each VLC.

Compounds were eluted with 100 – 0% hexane-ethyl acetate mixtures at increments of 5 mL, until the mixture reached 50 mL (50%) hexane and 50 mL (50%) ethyl acetate, then hexane was reduced at increments of 10 mL. The final fractions were eluted with methanol and ethyl acetate, at a ratio of 10:90 and 50:50. Fractions were concentrated under vacuum at 40 °C using a rotary evaporator and used in subsequent biological assays and chemical analysis.

# 3.4.3. Analytical High Performance Liquid Chromatography (HPLC)

Analytical high-performance liquid chromatography (HPLC) is a useful separation technique, which uses high-pressure pumping of a mobile phase through a column

packed with a stationary phase. This method is employed to determine the complexity of crude extract mixtures, assess the purity of isolated substances, and provide insight into chemical classification based on UV absorbance profiles<sup>4</sup>.

Crude extracts and VLC fractions were partly characterised, by determining the approximate number of components within extracts, using an analytical HPLC Agilent 1200 series, fitted with a reverse phase Agilent column (C18, 4.6 x 150 mm, 5  $\mu$ m) (Agilent Technologies, UK). This analytical HPLC was supplied with a binary solvent manager, sample manager and photodiode array detector. The solvent system consisted of ACN or MeOH mixed with  $H_2O$ , all containing 0.1% TFA to enhance separation. Both gradient and isocratic methods were used to find good separation and the flow rate was set to 1 mL/min during all runs.

# 3.4.4. Preparative Thin Layer Chromatography (prep TLC)

Preparative thin layer chromatography (prep TLC) is a technique which works by the same principle of analytical TLC, whereby compounds are separated due to partitioning of the sample analytes between the normal phase (stationary phase) and the non-polar solvent (mobile phase). Prep TLC was performed on antibacterial crude extracts (*G. caudiculata* and *K. membranifolia*) to separate compounds.

Crude extracts were dissolved in dichloromethane to achieve 20 mg/mL concentrations. Samples were spotted and layered along a line 1 cm from the bottom of a 20 x 20 cm normal-phase silica TLC plate (Phase Separations, UK) using a capillary tube (Fisher Scientific, UK) and placed into a large glass chamber containing a mobile phase of hexane: ethyl acetate at 80:20. The mobile phase was left to travel until the solvent front reached 1 cm from the top of the plate, and once developed, the plate was air dried inside a fume hood. The TLC plate was then viewed under UV light (254 nm and 365 nm) to locate separated extract fractions. The fractions at each band were recovered by desorption using dichloromethane, dried, and the yields were weighed.

# 3.4.5. Recycling preparative HPLC

Recycling preparative HPLC is a useful instrument and technique, which was used in this study to purify simplified fractions of plant extracts obtained from VLC separation. The term recycling refers to the sample travelling through the column before being directed back to the beginning of the column, in a closed loop system. With each cycle through the column, peak separation and resolution improve, during which process no additional solvent is used. Samples can be collected once the desired baseline resolution has been achieved<sup>5,6</sup>.

Recycling preparative HPLC was performed using a recycling LaboACE LC-5060 series HPLC instrument fitted with a reverse phase C18 column (20 × 500 mm, 10 μm, 120 Å), and guard column (JAI, Tokyo, Japan). The solvent system was composed of either MeOH and water or ACN and water (all containing 0.1%, HCO<sub>2</sub>H), with a flow rate of 10 mL/min. Here, a method was optimised for each sample by injecting 1 mL of 1 mg/mL concentration and checking peak definition with varying solvent proportions. Upon development of a suitable HPLC method, preparative-scale sample quantities were injected, and manual peak collection was performed. Collected peaks were concentrated using a rotary evaporator and nitrogen gas.

### 3.5. Spectroscopic Methods for Structure Elucidation

## 3.5.1. Liquid Chromatography Mass Spectrometry (LC-MS)

Mass spectrometry (MS) is a comprehensive and essential analytical technique for the identification of natural products. The liquid chromatography (LC) element of the instrument initially separates out different compounds (including impurities of almost-pure fractions) and these separated analytes are ionised by an ion source and converted into charged particles. In this study, a quadrupole mass analyser was used. This quadrupole consists of four parallel rods arranged in a square, which have radio frequency and direct current potentials applied to them, thus creating a dynamic electric field. Ions are then accelerated by the electric field, during which heavier ions travel at lower speeds and therefore travel smaller distances within a given time. The

velocity of the ion is measured by the ToF analyser, which assigns it a mass-to-charge ratio (x-axis) and a relative abundance of the detected ion as a percentage (y-axis), thus producing a mass spectrum<sup>7</sup>.

LC-QToF-MS/MS data were obtained using an Agilent 6546 Quadrupole Time-of-Flight Q-ToF mass spectrometer (Santa Clara, CA, USA) coupled with a 1290 UHPLC system. Samples were prepared by dissolving crude extracts or purified compounds in either MeOH or ACN (depending on the solvent system used in the method) at 0.1 mg/mL final concentration, and were filtered through a PTFE 0.2  $\mu$ m filter into 1.5 mL LC-MS amber vials (Fisher Scientific, UK). Sample LC was performed on a Phenomenex Kintex C18 column (100 × 2.1 mm, 2.6  $\mu$ m, 100 Å), using a gradient elution with a solvent system containing either MeOH or ACN and deionized water (containing 0.1% formic acid, HCO<sub>2</sub>H) over varying run times. A 5  $\mu$ L sample volume was injected by the autosampler. The HPLC method shown in Table 3.3 was used for the analysis of compounds.

**Table 3.3.** HPLC method used during LC-MS analysis.

Time (min)	H <sub>2</sub> O (%)	Acetonitrile (%)
0.00	95	5
5.00	5	95
5.50	5	95
5.60	95	5
8.00	95	5

LCMS data were viewed using ACD/Spectrus processor (version 2021.2.2, ACD/Labs), which revealed a range of ion adducts as described in the results Chapters 4 and 5. The potential monoisotopic masses of the analytes of interest, as revealed, were searched using the CAS SciFinder (2024) database.

## 3.5.2. Nuclear Magnetic Resonance spectroscopy (NMR)

Nuclear Magnetic Resonance spectroscopy (NMR) is the most effective technique for elucidating the structures of unknown molecules, providing the highest resolution spectroscopic method. NMR provides spectra consisting of distinct peaks that depend on the chemical environment of hydrogen or carbon atoms in a molecule; these arise

due to shielding and deshielding effects within the molecular environment. Experiments are classified into one-dimensional (1D) or two-dimensional (2D). 1D experiments include <sup>1</sup>H (proton) and <sup>13</sup>C (carbon) NMR. 2D NMR types include COSY (homonuclear correlation spectroscopy), HSQC (heteronuclear single quantum coherence) and HMBC (heteronuclear multiple bond correlation) which give additional structural information through correlation of proximal atoms<sup>8</sup>.

One- and two-dimensional NMR spectra were acquired using a 500 MHz Bruker spectrometer, except for compound **5.4** due to low compound amounts (using a Bruker AVIII 400 MHz with broadband probe (400 MHz)) (Billerica, MA, USA). Samples were dried thoroughly under nitrogen gas and dissolved in 300 µL of deuterated solvent, either CD<sub>3</sub>OD (deuterated methanol) or CDCl<sub>3</sub> (deuterated chloroform) (Merck, UK). These deuterated solvents acted as internal references for the calibration of each spectrum. <sup>1</sup>H and <sup>13</sup>C NMR experiments were run with 32 and 2000 scans, respectively. The spectra generated displayed peaks with chemical shifts expressed in parts per million (ppm), typically ranging from 0 to 15 ppm for <sup>1</sup>H NMR spectra and from 0 to 220 ppm for the <sup>13</sup>C NMR spectra. Coupling constants (*J* values) were reported in Hertz (Hz). Spectral data were viewed, processed and analysed using MestReNova 14.1 software.

## 3.5.3. Infrared (IR) spectroscopy

Infrared spectroscopy involves the interaction of infrared light (absorption, emission, and reflection) with molecules to reveal their functional groups. Infrared light irradiation induces molecular vibrations of bonds, causing vibrational transitions. Different bonds within the molecule vibrate at characteristic frequencies, thus producing a unique IR spectrum, from which peaks can be used to infer functional groups<sup>9</sup>. Although IR spectroscopy does not provide detailed molecular structural information, it is valuable analysis when used in conjunction with other spectroscopic techniques to add evidence for compound identification and characterisation.

During this study, IR absorbance spectra were recorded with a Perkin-Elmer FT-IR System Spectrum BX. IR spectra were obtained for compounds **5.1** and **5.2**. Samples

were prepared by dissolving approximately 0.5 mg of pure compound in a small amount of dichloromethane.

# 3.5.4. Ultraviolet-visible (UV-Vis) spectroscopy

UV-Vis spectroscopy is a helpful tool for the identification of functional groups when investigating conjugated systems within a molecule. It provides information about chromophores, functional groups and other structural features of organic compounds. The absorption of UV and visible light (200 nm to 800 nm) by a compound results in electronic excitation, with the wavelength and intensity of absorption providing information about the molecular structure. The  $\lambda_{max}$  (lambda max) is the wavelength at which maximum absorbance occurs, indicating the most intense electronic transition. This value provides helpful information for natural product characterisation<sup>10</sup>.

In this study, UV-visible absorption spectra for compounds **5.1** and **5.2** were recorded using a Perkin-Elmer (Shelton, CT, USA) UV/Vis Lambda 365 spectrophotometer within a wavelength range of 200–700 nm. Samples were prepared at a concentration of 250 µg/mL for this analysis. UV-Vis data for compounds were obtained during LC-MS analysis using an MS instrument equipped with a diode array detector (DAD), set to a UV-Vis range of 200–400 nm. Instrument specifications and sample preparation for this analysis followed the protocol outlined in Section 3.4.1.

### 3.5.5. X-ray crystallography

X-ray crystallography is a useful analytical technique in chemical characterisation, used to determine the atomic and molecular structure of crystalline compounds. When an incident X-ray beam interacts with the ordered lattice of a crystal, it undergoes diffraction in specific directions. By analysing the resulting diffraction pattern, including the angles and intensities of the scattered X-rays, a three-dimensional electron density map can be constructed. This allows for the determination of atomic positions, molecular geometry, and chemical bonding within the crystal structure, therefore elucidating the structure definitively<sup>11</sup>.

### 3.5.5.1. Crystallisation

Prior to X-ray crystallographic analysis, crystallisation of the molecule of interest was essential. To promote crystal formation, a concentrated solution of a purified compound was made in a mixture of MeOH and DCM, producing approximately 0.5 mL of a supersaturated solution. This solution was left at room temperature overnight with a pierced lid, to allow for slow solvent evaporation and gradual concentration of the sample. This crystallisation method was attempted with all purified fractions, however crystals suitable for single crystal X-ray diffraction were produced only for compound 4.2. Crystals were examined under a microscope to assess their quality and suitability for diffraction analysis.

### 3.5.5.2. Single Crystal X-ray Diffraction (SCXD)

Crystals suitable for single crystal X-ray diffraction (SCXD) must be unfractured, optically clear and ideally measure 150 – 200 microns. SCXD was carried out by Dr. Alexander Morritt at The School of Chemistry, Pharmacy and Pharmacology at The University of East Anglia.

## 3.6. Biological Evaluation

### 3.6.1. Maintenance of bacterial strains

## 3.6.1.1. Bacterial strains and growth conditions

Seven Gram-positive bacterial strains were used for antibacterial testing, including both susceptible and resistant phenotypes. Susceptible strains comprised *Staphylococcus aureus* (MSSA 25923) and *Enterococcus faecalis* (12697), while resistant strains included methicillin-resistant *Staphylococcus aureus* (MRSA 13363), *S. aureus* 1199B, *S. aureus* XU212, *S. aureus* RN4420, and *E. faecalis* 51299. In addition, five Gram-negative bacterial strains were tested, including susceptible strains *Escherichia coli* 10418, *Salmonella typhimurium* 14028S and *Pseudomonas aeruginosa* 10662, as well as multidrug-resistant *Klebsiella pneumoniae* 13443 and *E. coli* G69. Further details of these strains are provided in Table 3.4.

Table 3.4. Gram-positive and negative bacterial strains used during microbiological studies.

Strain	Source	Gram	Antibiotic	Note	Reference
			resistance		
Enterococcus faecalis 12967	NCTC	+	Susceptible	Control strain	17 <b>12</b>
Enterococcus faecalis 51299	ATCC	+	MDR	Standard strain	18 13
Escherichia coli 10418	NCTC	-	Susceptible	Control strain	19 <b>14</b>
Escherichia coli G69	Clinical isolate	-	MDR	Possible efflux pump activity.	20 <b>15</b>
Klebsiella pneumonia 13443	NCTC	-	Susceptible	Standard strain	21 <b>16</b>
MRSA 13373	NCTC	+	MRSA	Standard strain	13 <b>17</b>
MSSA 25923	Clinical isolate, ATCC.	+	MSSA	Control strain	12 <b>18</b>
Pseudomonas aeruginosa 10662	NCTC	-	Susceptible	Standard strain	22 19
Salmonella enterica subsp. enterica serovar Typhimurium str. 14028S	ATCC, environmental isolate	-	Susceptible	Standard strain	23 <b>20</b>
Staphylococcus aureus 1199B	Genetically modified, derived from clinical isolate.	+	Norfloxacin	Resistant: <i>NorA</i> efflux pump activity.	15 <b>21</b>
Staphylococcus aureus RN4220	Genetically modified, derived from clinical isolate.	+	MRSA	Virulent strain (hemolytic), derived from S. aureus NCTC8325-4.	16 22
Staphylococcus aureus XU212	Clinical isolate	+	Tetracycline	Resistant:  TetK efflux  pump activity.	14 23

Bacterial strains were stored at 4  $^{\circ}$ C on sloped nutrient agar (Merck, UK) in bijoux vials (Merck, UK) for up to 5 months in their stationary growth phase. Prior to use in biological

assays, strains were subcultured onto fresh nutrient agar (Merck, UK) and incubated for 24 h at 37 °C. All growth media and reagents were sterilised by autoclaving at 121 °C for 20 min (Prestige Medical, UK). Biological assays were conducted using aseptic technique within a laminar flow hood.

#### 3.6.1.2. Cryopreservation

Bacteria were cultured at 37 °C overnight, until the mid-exponential growth phase was reached. A single colony was picked from the agar plate and inoculated into 1 mL of LB, which was then incubated overnight at 37 °C. This liquid culture was cryopreserved by mixing equal volumes (500  $\mu$ L) of the bacterial culture and a sterile 50% (v/v) aqueous glycerol solution. A total volume of 1 mL was preserved in cryovials and stored at -80 °C for long-term preservation.

#### 3.6.2. Minimum Inhibitory Concentration (MIC) Determination

The minimum inhibitory concentration (MIC) is determined using the broth microdilution assay, which is the gold standard method for evaluating the susceptibility of bacterial strains to antimicrobial agents. The MIC is defined as the lowest concentration of an antibacterial compound, measured in mg/L (µg/mL), that completely inhibits visible bacterial growth under controlled *in vitro* conditions<sup>24</sup>. MIC assays are widely used in clinical laboratories to determine antimicrobial susceptibility in bacterial infections. In research settings, MIC determination is an essential tool for investigating antibiotic resistance mechanisms, identifying potential drug targets and assessing the efficacy of novel antimicrobial compounds<sup>25</sup>.

The MIC of plant extracts and compounds was determined in this study by the broth microdilution assay protocol described by Andrews<sup>25</sup>. For crude extract sample preparation, plant extracts were dissolved in DMSO (Merck, UK) to produce stock solutions (13 mg/mL) which were diluted in LB Miller (Luria Bertani Broth, Merck, UK) to obtain working concentrations of 1025  $\mu$ g/mL.

For pure compound sample preparation, compounds were dissolved in DMSO to obtain stock solutions of 13 mg/mL, which were diluted further to obtain working

concentrations of 256  $\mu$ g/mL. Working concentrations were then serially diluted to obtain a final concentration range from 128  $\mu$ g/mL to 0.13  $\mu$ g/mL. The antibiotic positive control, Ampicillin (Merck, UK), working solution was prepared from a 13 mg/mL stock solution too, to obtain a highest final concentration of either 512 or 1024  $\mu$ g/mL, depending on the bacteria.

Bacterial strains were prepared by selecting one colony (previously cultured on fresh agar for 24 h) and suspending it in Phosphate Buffered Saline (PBS) consisting of 137 mM NaCl and 3 mM KCl (Merck, UK), to achieve an inoculum density of 1 x 10<sup>8</sup> colony forming units (CFU)/mL. Standardisation of cell suspensions was completed following the Beer-Lambert law, by adjusting the optical density to 0.1 at 600 nm (Lambda Bio+UV-Vis Spectrophotometer, Perkin Elmer, UK) before being diluted 1:100 in LB prior to inoculation. Microdilution was performed using 96-well microtiter plates (Merck, UK) obtaining a final inoculum of 5 x 10<sup>5</sup> CFU/mL. Results were determined by visual inspection of the wells, whereby opaque or pelleted wells indicated bacterial growth. MIC values were defined as the lowest concentration of treatment at which wells were completely clear, indicating no bacterial growth (Figure 3.2). Experiments were performed with two biological repeats.

## 1. Serial dilution of test compound 2 32 16 1 64 8 128 0.5 0.25 0.125 (µg/mL) 2. Inoculation (5 x $10^5$ CFU/mL) 3. Incubation (37 °C overnight) Bacterial growth No growth MIC 4. Reading

**Figure 3.2.** Illustration of the broth microdilution assay used to determine the MIC. Figure adapted from De Resende, 2017 <sup>27</sup>.

## 3.6.3. Minimum Bactericidal Concentration (MBC) determination

While the MIC indicates the lowest concentration needed to inhibit bacterial growth, the MBC is the lowest concentration needed to achieve a ≥99.9% reduction of the initial bacterial population. MBC quantifications are mechanistic studies, as this value provides insight into the mode of action of the antimicrobial compound, distinguishing between bacteriostatic and bactericidal effects.

To determine the minimum bactericidal concentration (MBC) of compounds, the MIC was initially determined. From the 96-well plate, 20  $\mu$ L was removed from the well corresponding to the MIC, the well with the next highest concentration, and all wells containing lower concentrations, and was spread onto sterile agar plates. These

dilutions were spread before being incubated overnight at 37 °C. Two biological repeats of each experiment were performed.

### 3.6.4. Inhibition Zone Determination - Disc Diffusion Assay

The disk diffusion method was used to provide additional evidence of the antibacterial activity of G. caudiculata and K. membranifolia dichloromethane extracts. Here, nutrient agar (Merck, UK) was autoclaved and 20 mL was poured into sterile petri dishes and allowed to set at room temperature. Meanwhile, single colonies obtained from overnight cultures of MSSA 25923 and E. faecalis 12697 were suspended in PBS. Cell suspensions were standardised as they were in the broth microdilution assay, by adjustment of the optical density to 0.1 at 600 nm to achieve a cell density of 1 x 108 CFU/mL. Cell suspension (1 mL) was added to the set agar, dispersed to obtain complete coverage, and then left to dry at room temperature. Treatment samples were prepared by diluting extracts or positive control (ampicillin) in DMSO to achieve concentrations of 10 mg/mL. Sterile paper discs were saturated with 20 µL of the prepared treatment and ampicillin dilutions (resulting in a loading of 200 μg/disc), left to dry at 37 °C for 1 h and then placed onto the bacteria-covered agar. Positive antibiotic and vehicle controls were included on each agar plate<sup>28</sup>. Active samples were indicated by clear zones around the discs, indicating no bacterial growth. These zones of inhibition were defined as the whole diameter of clear zones<sup>29</sup>.

### 3.6.5. AlamarBlue Assays

Alamar Blue is a widely used assay for assessing cell viability based, on the reduction of resazurin (a non-fluorescent, blue oxidised dye) into resorufin, a pink, fluorescent reduced product. This redox conversion occurs in metabolically active cells, and the resulting fluorescence correlates with cell viability. Due to its water solubility, membrane permeability, stability in culture media, and non-toxic nature, resazurin is an effective indicator of cellular viability, making it suitable and popular for *in vitro* cytotoxicity and proliferation studies<sup>30</sup>.

### 3.6.5.1. Cancer Cell Cytotoxicity Assay

The cytotoxic effects of compounds isolated from *Gymnacranthera forbesii*, *Knema membranifolia* (Myristicaceae) and *Garcinia caudiculata* (Clusiaceae) were assessed using the AlamarBlue assay. The A549, SK-MEL-28, RAW 264.7 and HL-60 cancer cell lines were initially screened with purified fractions. Based on preliminary results, doseresponse analyses were conducted in A549 cells for selected compounds exhibiting significant cytotoxic activity. This work was carried out by Miss Salonee Banerjee at The University of East Anglia, School of Chemistry, Pharmacy and Pharmacology.

In brief, to obtain the IC $_{50}$  values of compounds, A549 cells were seeded at a density of  $5 \times 10^3$  cells/well in 96-well plates and incubated for 72 hours at 37 °C in a humidified 5% CO $_2$  atmosphere. Cells were then treated in triplicate with experimental compounds as well as cisplatin (positive control) and incubated for an additional 24 hours. Following incubation 10  $\mu$ L of 0.1 mg/mL resazurin (AlamarBlue) reagent was added to all wells (10% of total well volume) and incubated for 4 hours under the same conditions. Fluorescence intensity was then measured at an excitation and emission wavelength of 540 and 590 nm, respectively, using a microplate reader (CLARIOstar 0430, BMG LABTECH).

All compounds were initially screened at 10  $\mu$ M and 100  $\mu$ M across the four cell lines. Compounds **4.1**, **4.2**, **4.3**, **4.4**, **4.5**, **4.6**, **5.1** and **5.2**, which showed significant cytotoxicity, were selected for further dose-response analysis in A549 cells at concentrations ranging from 6.25 to 800  $\mu$ M.

#### 3.6.5.2. Fungal Cell Cytotoxicity Assay

Isolated compounds were assessed for their anti-fungal activity against *Aspergillus fumigatus* and *Candida albicans* using the AlamarBlue cell viability assay, completed by Dr Isabelle Storer from Dr Stefan Bidula's lab at The University of East Anglia, School of Chemistry, Pharmacy and Pharmacology.

Compounds were assessed using a microdilution assay at concentrations ranging from 0.13 to 32  $\mu$ g/mL. In brief, tested compounds (at 0.13 to 32  $\mu$ g/mL), amphotericin B (2

 $\mu$ g/mL, positive control), DMSO (vehicle control), and test fungal species *Aspergillus fumigatus* and *Candida albicans* at 1 x 10<sup>4</sup> CFU/mL, were incubated in RPMI-1640 growth medium (Gibco, UK) for 24 h 37 °C. Following this, 10  $\mu$ g/mL resazurin (Merck, UK) was added to each well and incubated for a further 24 h. Fluorescence intensity was quantified using a CLARIOstar plate reader (BMG Labtech, UK) as described by Middleton *et al.*<sup>31</sup>.

#### 3.7. References

- 1 M. Santiago and S. Strobel, *Methods in Enzymol*, 2013, **533**, 303–324.
- N. M. Targett, J. P. Kilcoyne and B. Green, J Org Chem, 1979, 44, 4962–4964.
- A. Maurya, K. Kalani, V. S. Chandra, R. Singh and A. Srivastava, *Org Med Chem Int J*, 2018, **7**, 1–3.
- 4 J. L. Wolfender, *Planta Med*, 2009, **75**, 719–734.
- JAI, What is Recycling Preparative HPLC?, www.jai.co.jp/english/products/hplc/index.html, (accessed March 7, 2025).
- 6 J. Sidana and L. K. Joshi, *Chromatogr Res Int*, 2013, **2013**, 1–7.
- 7 D. R. Allen and B. C. McWhinney, Clin Biochem Rev, 2019, 40, 135–146.
- 8 W. F. Reynolds, in *Pharmacognosy: Fundamentals, Applications and Strategy*, ed. S. Badal and R. Delgoda, Academic Press, 2017, chapter 29 Natural Product Structure Elucidation by NMR Spectroscopy, 567–596.
- 9 D. Shikha and R. Awasthi, *Int J Adv Res Chem Sci*, 2015, **2**, 38–45.
- S. Sinha, C. Jeyaseelan, G. Singh, T. Munjal and D. Paul, in *Basic Biotechniques for Bioprocess and Bioentrepreneurship*, ed. A. K. Bhatt, R. K. Bhatia and T. C. Bhalla, Academic Press, 2023, chapter 8 Spectroscopy Principle, types, and applications, 145–164.
- 11 M. S. Smyth and J. H. J. Martin, *Mol Pathol*, 2000, **53**, 8.
- Culture Collections, *Enterococcus faecalis*, www.culturecollections.org.uk/nop/product/enterococcus-faecalis-23, (accessed March 31, 2025).
- J. M. Swenson, N. C. Clark, D. F. Sahm, M. J. Ferraro, G. Doern, J. Hindler, J. H. Jorgensen, M. A. Pfaller, L. B. Reller, M. P. Weinstein, R. J. Zabransky and F. C. Tenover, *J Clin Microbiol*, 1995, 33, 3019–3021.
- 14 Culture collections, *Escherichia coli*, www.culturecollections.org.uk/nop/product/escherichia-coli-200, (accessed March 13, 2025).
- P. D. Stapleton, K. P. Shannon and G. L. French, Antimicrob Agents Chemother, 43, 1206–1210.
- 16 Culture collections, *Klebsiella pneumoniae*, www.culturecollections.org.uk/nop/product/klebsiella-pneumoniae-90, (accessed March 13, 2025).

- 17 Culture Collections, Staphylococcus aureus, www.culturecollections.org.uk/nop/product/staphylococcus-aureus-183, (accessed April 30, 2025).
- T. J. Treangen, R. A. Maybank, S. Enke, M. B. Friss, L. F. Diviak, D. K. David, S. Koren, B. Ondov, A. M. Phillippy, N. H. Bergman and M. J. Rosovitz, *Genome Announc*, 2014, **2**, e01110-14.
- 19 Culture collections, *Pseudomonas aeruginosa*, www.culturecollections.org.uk/nop/product/pseudomonas-aeruginosa-20, (accessed March 13, 2025).
- 20 UniProt, *Salmonella typhimurium* (strain 14028s / SGSC 2262) Proteomes, www.uniprot.org/proteomes/UP000002695, (accessed March 13, 2025).
- E. C. J. Smith, G. W. Kaatz, S. M. Seo, N. Wareham, E. M. Williamson and S. Gibbons, *Antimicrob Agents Chemother*, 2007, **51**, 4480–4483.
- B. N. Kreiswirth, S. Löfdahl, M. J. Betley, M. O'reilly, P. M. Schlievert, M. S. Bergdoll and R. P. Novick, *Nature*, 1983, **305**, 709–712.
- 23 S. Gibbons and E. E. Udo, *Phytother Res*, 2000, **14**, 139–140.
- N. Kadeřábková, A. J. S. Mahmood and D. A. I. Mavridou, *npj Antimicrobials and Resistance*, 2024, **2**, 1–9.
- B. Kowalska-Krochmal and R. Dudek-Wicher, *Pathogens*, 2021, **10**, 165–186.
- 26 J. M. Andrews, *J Antimicrob Chemother*, 2001, **48**, 5–16.
- P. E. de Resende, Thesis: *Antimicrobial and Resistance-Modifying Activities of LY2183240 Regioisomers*, University College London, 2017.
- 28 S. Arullappan, Z. Zakaria, D. Fredalina Basri, P. Baru, J. Padang Tembak, T. Intan, U. Kebangsaan Malaysia, J. Raja Muda Abdul Aziz and K. Lumpur, *Trop Life Sci Res*, 2009, **20**, 109–118.
- J. Hudzicki, *American Society for Microbiology*, Kirby-Bauer Disk Diffusion Susceptibility Test Protocol, 2009.
- 30 M. N. Dinh, M. Hitomi, Z. A. Al-Turaihi and J. G. Scott, *MethodsX*, 2024, **28**, 103024.
- G. Middleton, F. O. Mahamud, I. Storer, A. Williams-Gunn, A. Abdolrasouli, E. Barclay, A. Bradford, O. Steward, J. McColl, B. Lézé, N. van Rhijn, A. da Silva Dantas, T. Furukawa, D. Warren, Z. A. Waller and S. Bidula, *BioRxiv*, 2025, Preprint.

## Chapter 4 – Isolation, Structure Elucidation and Biological Activities of Secondary Metabolites from the Myristicaceae

#### 4.1. Introduction

Of the six Myristicaceae plant extracts extracted on a small scale and screened for their antibacterial activities, *K. membranifolia* and *G. contracta* exhibited notable activity (Section 4.2.6, Table 4.13). Consequently, these two species were selected for further phytochemical investigation using scaled-up extractions.

## 4.1.1. Knema membranifolia H.J.P.Winkl.

*Knema membranifolia* is endemic to Borneo and grows from 6 – 25 m tall, at up to 500 m altitude, extending twigs measuring 1.5 – 3 mm in diameter. Leaves are thin and leathery or membranous (thin, semi-transparent), measure 12 – 28 x 3.5 – 8.5 cm and dry to a pale brown to olive colour. Bark of this species flakes/peels easily and it's twigs resemble those of *K. curtisii*, however *K. curtisii* lacks flaking bark and differs in androecium<sup>1,2</sup>. To date, there have been no phytochemical or biological investigations into this species of plant.

#### 4.1.2. Gymnacranthera contracta Warb.

*Gymnacranthera contracta* is a tree endemic to Borneo which grows from 5 – 26 m tall<sup>3-</sup> Shukla and Blicher-Mathiesen (1993) evaluated the oils present in *G. contracta* seeds using high-performance size exclusion chromatography. Seeds were found to have 58.8% oil content, 82% of which were triglycerides, 0.4% were diglycerides, 0.1% were mono-glycerides and 17.6% were free fatty acids. Seeds contained a high amount of medium chain length fatty acids including lauric acid (a) and myristic acid (b) (Figure 4.1)<sup>6</sup>. Lauric acid has a wide spectrum of antimicrobial activities and is an anticancer, cardioprotective and anti-inflammatory agent<sup>7-11</sup>. Furthermore, myristic acid has displayed cytotoxic, anti-inflammatory and anti-microbial activity<sup>12-14</sup>. Other than these two fatty acids, there have been no other investigations into this species.

**Figure 4.1.** Chemical structures of lauric acid (a) and myristic acid (b) isolated from *Gymnacranthera contracta* Warb.

#### 4.2. Results and Discussions

### 4.2.1. Structure elucidation of compounds from Knema membranifolia

### 4.2.1.1. $6\Omega$ -Phenylalkylsalicylic acid, 10 carbon decyl linker, (4.1, known)

Compound **4.1** (2.5 mg) was isolated as a yellow amorphous solid from a DCM sequential extract. The molecular formula of this compound was confirmed as  $C_{23}H_{30}O_3$  (exact mass 354.2195) based on the Q-ToF mass spectrometry data in positive ionisation mode, which indicated a protonated base peak at [M+H]<sup>+</sup> at m/z 355.233 ( $\Delta$ : +16.9 ppm), followed by an ammonium ion [M+NH<sub>4</sub>]<sup>+</sup> at m/z 372.222 ( $\Delta$ : +16.9 ppm) and a sodium molecular ion [M+Na]<sup>+</sup> peak at m/z 377.205 ( $\Delta$ : -86.0 ppm). The <sup>1</sup>H together with the COSY NMR spectra revealed the distinct aromatic and aliphatic regions of **4.1**. The trisubstituted benzoic acid was suggested by the <sup>1</sup>H NMR signals at  $\delta_H$  7.26 ppm (H-4, doublet of doublets), 6.77 ppm (H-5, doublet of doublets) and 6.68 ppm (H-3, doublet of doublets). **4.1** contains two phenyl residues linked by a 10-carbon chain, one of which possesses no further substitution and the other is 1,2,6-substituted. The benzene in the benzoic acid core is trisubstituted at positions 1 (-COOH), 2 (-OH) and 6 (-C<sub>12</sub>H<sub>24</sub>-Ph) as observed in salicylic acid phenyl alkyl compounds<sup>15</sup>. Information from the COSY analysis demonstrated coupling of H-4 with H-3 and H-5, and H-5 with H-4. This confirmed a *meta*-coupling relationship between H-5 and H-3.

The HMBC suggested a correlation between the H-1' protons with C-6 and C-1, whilst the H-10' protons were strongly correlated with C-2", C-6" and C-1", indicating the proximity of these aliphatic protons to the phenolic and phenyl rings of this molecule,

respectively. HMBC analysis confirmed the assignment of C-1', 2', 9' and 10' in the aliphatic region. The 1D <sup>13</sup>C NMR spectrum displayed 10 clear carbon peaks in the aliphatic region. This alteration in hydrocarbon linker length between the other salicylic acid-derived compounds was confirmed through this, as well as through the mass spectrum of the compound.

Compound **4.1** was previously isolated initially from *K. elegans* seed oil and later from *K. laurina* stem bark<sup>15,16</sup>. The latter study was the first to report the NMR data of this compound, however to the best of my knowledge, 2D NMR analysis was not undertaken. It is worth noting that my NMR data are consistent with theirs except for the assignment of C-3 at  $\delta_{\rm C}$  122 ppm and C-5 at  $\delta_{\rm C}$  115 ppm which are swapped when comparing the spectral data (Table 4.1). The same occurs in compound **4.2**.

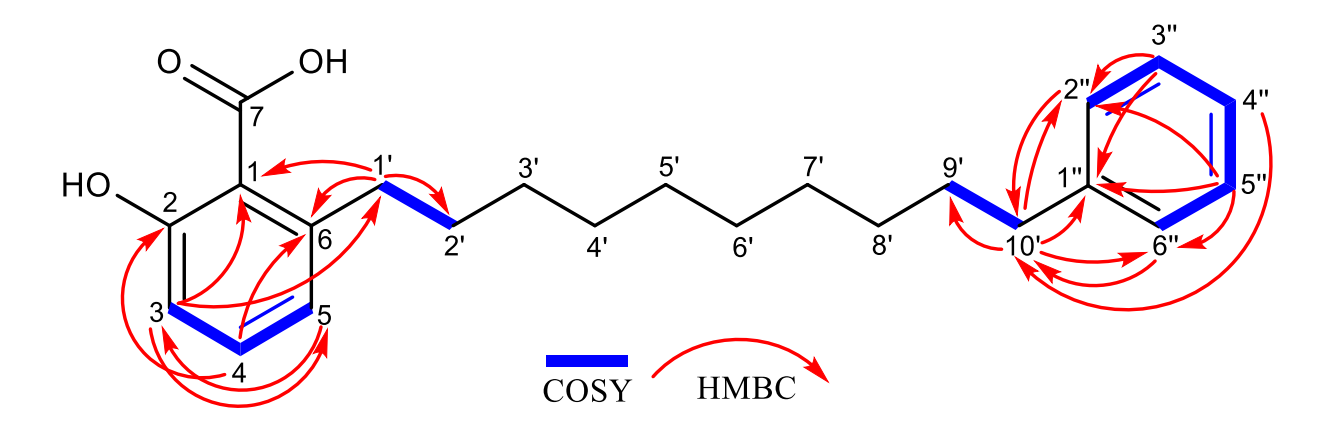


Figure 4.2. COSY and HMBC correlations of compound 4.1.

Table 4.1. <sup>1</sup>H, <sup>13</sup>C, COSY and HMBC NMR data of compound 4.1 (CDCl<sub>3</sub>, 500/126 MHz).

Position	δ <sub>c</sub> (ppm),	$\delta_{ m c}^{16}$	$\delta_{\rm H}$ , mult. ( <i>J</i> in Hz)	COSY	HMBC
	type				
1	110.6, C	110.5, C	-	-	1', 3
2	163.5, C	163.6, C	-	-	4
3	115.7, CH	115.8, CH	6.68, dd (7.5, 1.2)	4	5
4	135.0, CH	135.3, CH	7.26, dd (7.9, 1.8)	3, 5	-
5	122.6 <b>,</b> CH	122.7, CH	6.77, dd (8.4, 1.2)	4	3
6	147.5, C	147.6, C	-	-	1', 4
7	174.0, C	175.5, C	-	-	-
1'	$36.5$ , $CH_2$	$36.5$ , $CH_2$	2.89, t (7.5)	2'	3
2'	$32.1$ , $CH_2$	36.0, $CH_{\mid 2}$	1.46 - 1.58, $m$	1'	1'
3' to 8'	29.8, 29.7,	29.7, 29.6,	1.16 - 1.27, $m$	-	-
	29.63,	$\mathrm{CH}_2$			
	29.59,				
	29.5, 29.4,				
	$\mathrm{CH}_2$				
9'	$31.5$ , $CH_2$	$31.5$ , $CH_2$	1.46 - 1.58, $m$	10'	10'
10'	$36.0$ , $CH_2$	$36.5$ , $CH_2$	2.52, t (7.8)	9'	2", 6", 4"
1"	143.0, C	142.9, C	-	-	10', 5'',
					3"
2" and 6"	128.4, CH	128.2, CH	7.04 - 7.16, m	3", 5"	10', 5'',
					3"
3" and 5"	128.2, CH	128.4, CH	7.20, <i>d</i> (3.6)	2", 6",	-
				4"	
4"	125.5, CH	125.5, CH	7.04 - 7.16, m	3", 5"	-

 $<sup>^{16}\</sup>mbox{Reference}$  carbon chemical shifts of 2-hydroxy-6-(10-phenyldecyl)-benzoic acid measured in CDCl3.

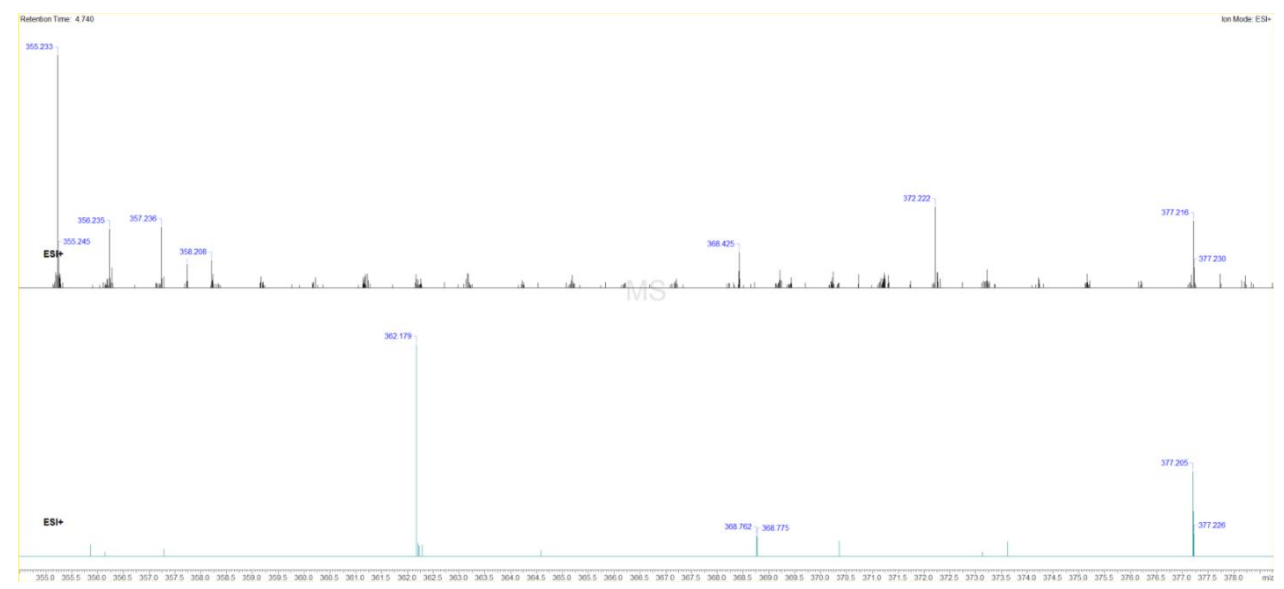


Figure 4.3. Mass spectrum of compound 4.1.

#### 4.2.1.2. $6\Omega$ -Phenylalkylsalicylic acid, 12 carbon decyl linker, (4.2, known)

Compound **4.2** (3.4 mg) was isolated as green crystals from a sequential dichloromethane extract. The structure of **4.2** was determined using single crystal X-ray diffraction (Figure 4.4) for the first time, and the molecular formula was established as  $C_{25}H_{34}O_3$  (exact mass 382.2508). Further confirmation of this structure was obtained based on the positive mode Q-ToF spectrum which displayed the protonated molecular ion [M+H]<sup>+</sup> at m/z 383.222 ( $\Delta$  = -96.54 ppm) and NMR spectra including <sup>1</sup>H, COSY, <sup>13</sup>C, HSQC and HMBC.

Structure elucidation using the spectroscopic methods mentioned above revealed **4.2** to be a known plant alkylsalicylic acid-type natural product, 2-hydroxy-6-(12-phenyldodecyl)-benzoic acid. **4.2** was a second compound containing two phenyl residues (linked by a 12-carbon chain), one of which is 1,2,6-substituted, producing a salicylic acid moiety. The <sup>1</sup>H and COSY NMR spectra displayed the remaining three aromatic proton splitting patterns with signals at  $\delta_{\rm H}$  7.31 – 7.37 ppm (H-4, multiplet),  $\delta_{\rm H}$  6.86 ppm (doublet of doublets, J = 8.4, 1.2 Hz) and  $\delta_{\rm H}$  6.76 ppm (doublet of doublets, J = 7.5, 1.2 Hz). These signals characterised the meta coupled H-3 and H-5, and the H-4 ortho coupling to H-3 and H-5. The terminal phenyl ring displayed a spin system of a

typical monosubstituted aromatic ring with signals at  $\delta_{\rm H}$  7.23 – 7.29 ppm (H-3" and 5", multiplet) and 7.14 – 7.19 ppm (H-2", H-4" and H-6", multiplet). In addition, the COSY spectrum displayed coupling in the aliphatic region, with  $\delta_{\rm H}$  2.96 ppm (H-1', triplet) and  $\delta_{\rm H}$  2.59 ppm (H-12', triplet) both coupling  $\delta_{\rm H}$  1.59 ppm (H-11' and H-2', quartet of doublets, J = 9.5, 8.5, 4.7 Hz) accounting for a total of four protons. The HSQC spectrum enabled the assignment of C-12' and C-1', thus allowing assignment of C-11' and 2'.

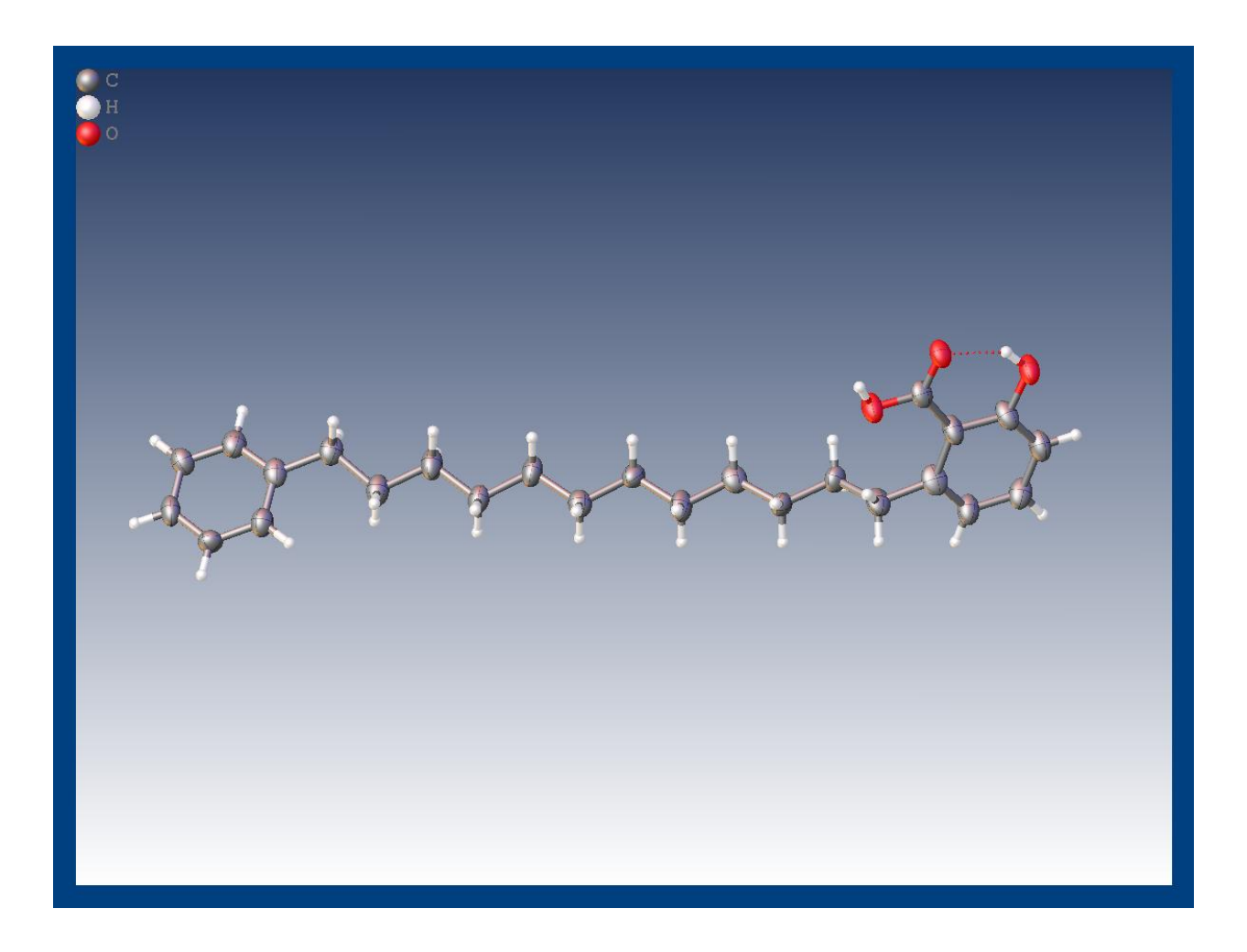


Figure 4.4. Single crystal X-ray diffraction image generated of 4.2.

Compound **4.2** was first identified in the seed oil of *K. elegans* and was later isolated from the stem bark of *K. furfuraceae*, with structure elucidation using NMR<sup>15,17</sup>. The carbon assignments obtained in the present study, based on HSQC and HMBC data, are largely consistent with those reported in the latter study, except for C-3, assigned at  $\delta_{\rm C}$  122.6 ppm in this study compared to 155.9 ppm previously, and C-5, assigned at 115.8 ppm here versus 122.7 ppm previously. Compound **4.2** has been found in the stem bark of other *Knema* species including *K. laurina*, *K. tenuinervia*, *K. glomerata* and from the roots of *Homalomena occulta* (Araceae)<sup>18-20</sup>. To the best of my knowledge, this thesis presents the first report of compound **4.2** isolated from plant leaves and the first record of its occurrence in *K. membranifolia*.

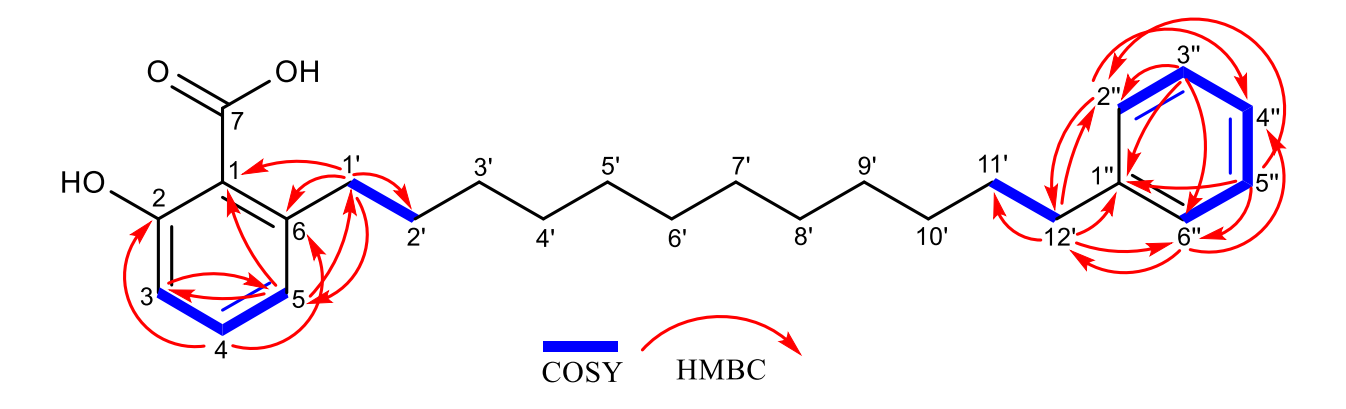


Figure 4.5. COSY and HMBC correlations of compound 4.2.

Table 4.2.  $^{1}$ H,  $^{13}$ C, COSY and HMBC NMR data of compound 4.2 (CDCl<sub>3</sub>, 500/126 MHz).

Position	δ <sub>C</sub> (ppm),	$\delta_{ m c}^{17}$	$\delta_{\rm H}$ , mult. ( <i>J</i> in Hz)	COSY	HMBC
	type				
1	110.5, C	110.5, C	-	-	1', 5, 3
2	163.6, C	163.6, C	-	-	4
3	115.8, CH	155.9, CH	6.76, dd (7.5, 1.2)	4	1, 5
4	135.1, CH	135.4, CH	7.31 - 7.37, m	3, 5	-
5	122.6, CH	122.7, CH	6.86, dd (8.4, 1.2)	4	1', 1, 3
6	147.5, C	147.8, C	-	-	1', 4
7	174.5, C	175.6, C	-	-	-
1'	36.5, CH <sub>2</sub>	36.4, CH <sub>2</sub>	2.96, t (7.5)	2'	5
2'	32.1, CH <sub>2</sub>	32.0, CH <sub>2</sub>	1.59, m	1'	1'
3' to 10'	29.8,	29.6, CH <sub>2</sub>	1.21 – 1.34, m	-	-
	29.60,				
	29.57,				
	29.52,				
	29.47,				
	29.3, CH <sub>2</sub>				
11'	31.5, CH <sub>2</sub>	31.5, CH <sub>2</sub>	1.59, <i>qd</i> (9.5, 8.5, 4.7)	12'	12'
12'	36.0, CH <sub>2</sub>	36.0, CH <sub>2</sub>	2.59, t (7.8)	11'	6", 2"
1"	143.0, C	142.9, C	-	-	12',
					3", 5"
2" and 6"	128.4, CH	128.2, CH	7.14 - 7.19, m	5", 3"	12',
					3", 5"
3" and 5"	128.2, CH	128.4, CH	7.23 - 7.29, $m$	2", 4",	-
				6"	
4"	125.6, CH	125.5, CH	7.14 – 7.19, m	5", 3"	2", 6"

 $<sup>^{17}\</sup>mbox{Reference}$  carbon chemical shifts of 2-hydroxy-6-(12-phenyldodecyl)-benzoic acid measured in CDCl3.

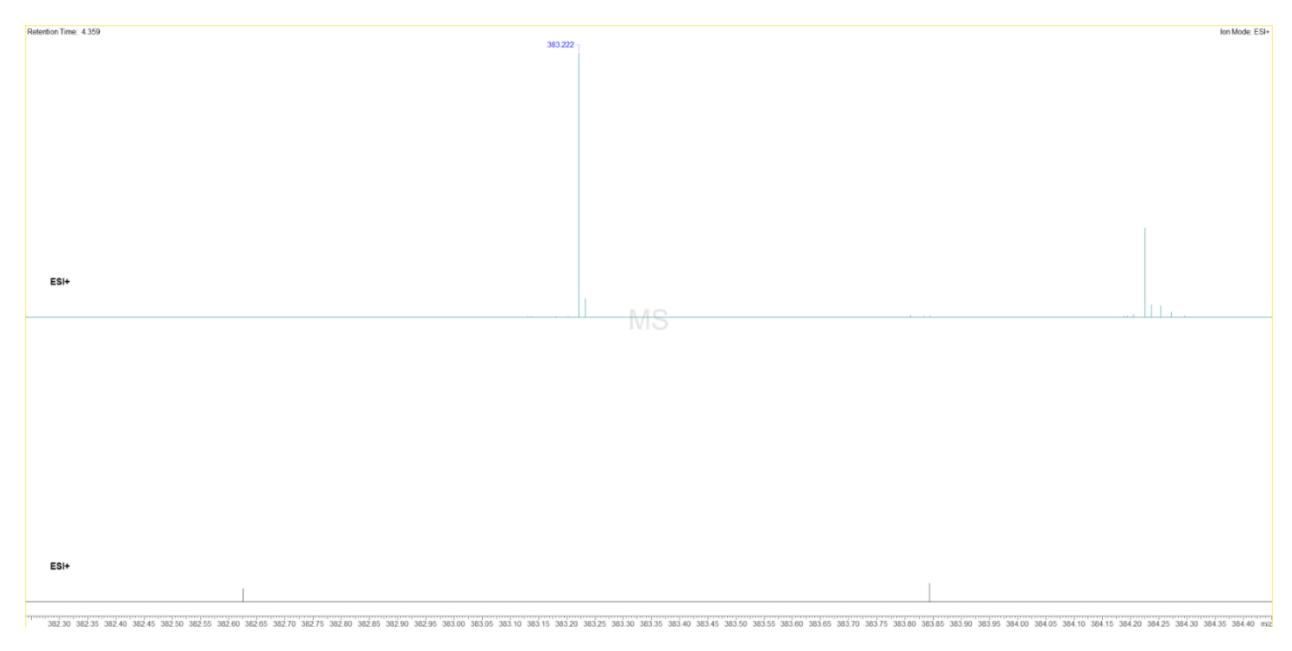


Figure 4.6. Mass spectrum of compound 4.2.

### 4.2.1.3. $6\Omega$ -Phenylalkylsalicylic acid, 16 carbon decyl linker, (4.3, new)

Compound **4.3** (9.4 mg) was isolated as green crystals and its molecular formula was established as  $C_{29}H_{42}O_3$  based on the positive mode Q-ToF mass spectral data, which revealed the protonated ion m/z at 439.177 ( $\Delta$ : +327.9 ppm). The length of the hydrocarbon linker of this compound was determined using the molecular weight and  $^{13}$ C data, which established the number of additional carbons present, compared to the other salicylic acid analogues.

As with previous compounds, observation of the  $^{1}H$  and COSY spectra revealed the substitution pattern of the benzoic acid and isolated phenyl ring of **4.3**. Here, the aromatic ring displayed three protons at  $\delta_{\rm H}$  6.69 ppm (H-3, doublet of doublets),  $\delta_{\rm H}$  7.28 ppm (H-4, doublet of doublets) and  $\delta_{\rm H}$  6.79 ppm (H-5, doublet of doublets), indicative of the meta positioning between H-3 and H-5, due to the lack of COSY correlation between these two protons. In addition, the absence of HMBC correlation between H-4 and C-6 confirmed the *para* orientation between the carboxyl group substitution and H-4, while the observed C-3/C-5 correlation indicated their meta positioning to C-6.

The remaining aromatic signals indicated a remaining monosubstituted terminal phenyl ring, supported by an integration value of 5 protons, and COSY correlations present between all protons H-1" to H-6". In addition, the carbons further downfield within the aliphatic region on the  $^{13}$ C spectra, at  $\delta_{\rm C}$  35.0 and 35.5 ppm, were correlated with either H-2" and H-6", or H-5, respectively, according to the HMBC spectrum, suggesting their locations at opposite ends of the chain. This, combined with the COSY data, delineated the phenylalkane and the benzoic acid of the compound and their positions on the linking hydrocarbon chain. The assignments of C-2' and C-15' were warranted by the HMBC correlations between the protons at  $\delta_{\rm H}$  2.86 – 2.93 ppm (H-1', multiplet) and H-16' protons at  $\delta_{\rm H}$  2.44 – 2.58 ppm (H-16', multiplet), respectively.

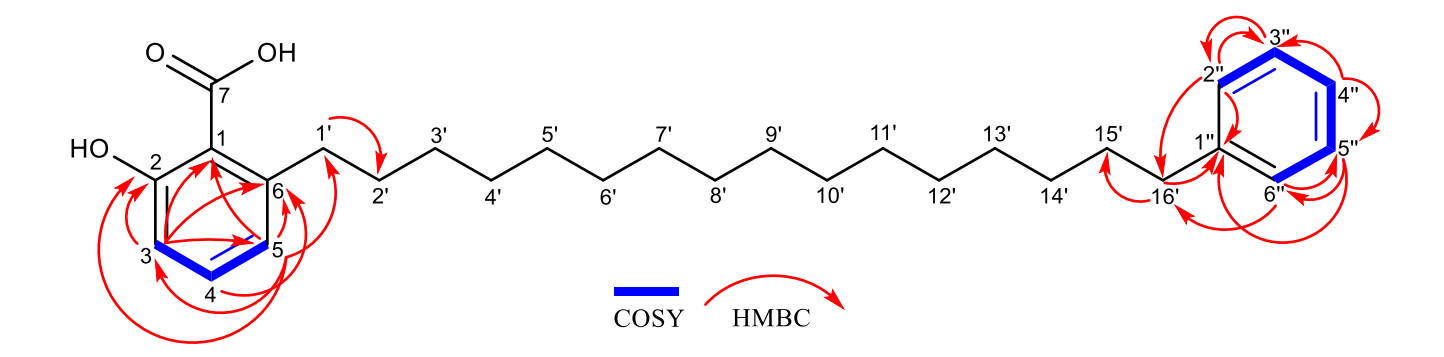


Figure 4.7. COSY and HMBC correlations of compound 4.3.

**Table 4.3.** <sup>1</sup>H, <sup>13</sup>C, COSY and HMBC NMR data of compound **4.3** (CDCl<sub>3</sub>, 500/126 MHz).

Position	$\delta_{\rm C}$ (ppm),	$\delta H$ , mult. ( $J$ in Hz)	COSY	HMBC
	type			
1	109.4, C	-	-	3, 5
2	162.6, C	-	-	3, 5
3	121.7, CH	6.69, dd (7.5, 1.2)	4	5
4	134.3, CH	7.28, dd (8.3, 7.5)	3, 5	-
5	114.8, CH	6.79, dd (8.3, 1.2)	4	3

6	146.7, C	-	-	3, 4, 5
7	174.5, C	-	-	
1'	35.5, CH <sub>2</sub>	2.86 – 2.93, m	3' to 14'	5
2'	32.9, CH <sub>2</sub>	1.52, <i>m</i>	-	1'
3' to 14'	30.9, 30.5,	1.21, m	-	-
	28.7, 28.64,			
	28.59, 28.6,			
	28.5, 28.4,			
	28.3, 28.0,			
	23.6, 21.7,			
	CH2			
15'	31.0, CH2	1.52, <i>m</i>	-	16'
16'	35.0, CH2	2.44 - 2.58, $m$	3' to 14'	2", 6"
1"	141.7, C	-	-	16", 2",
				6", 3", 5"
2" and 6"	127.4, CH	7.04 - 7.12, m	3", 5", 4"	2", 6", 4"
3" and 5"	127.2, CH	7.16 - 7.23, $m$	2", 6", 4"	2", 6", 4"
4"	124.5, CH	7.04 - 7.12, m	2", 6",	2", 6"
			3", 5"	

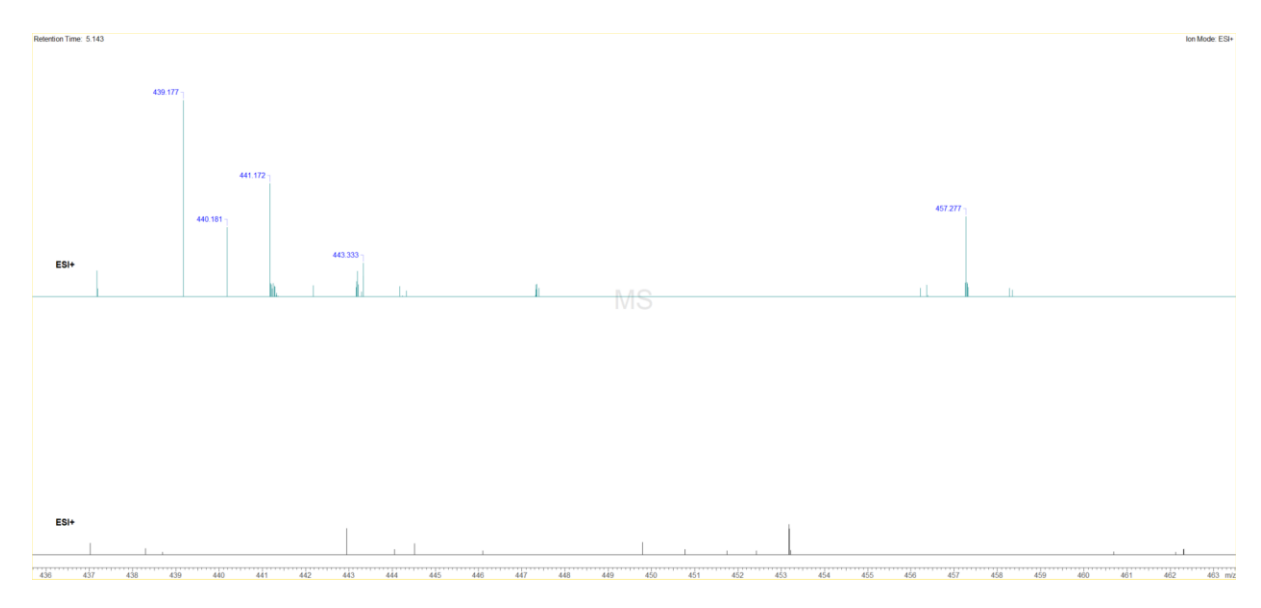


Figure 4.8. Mass spectrum of compound 4.3.

#### 4.2.1.4.6-Alkylacetophenone, 8 carbon phenyloctyl linker, (4.4, known)

Compound **4.4** (3.9 mg) was isolated as a viscous yellow oil from a methanol sequential extract. Its molecular formular was determined to be  $C_{22}H_{28}O_3$  ( $\Delta$  = 0.0 ppm), as established by positive mode Q-ToF mass spectrometry, which detected the protonated molecular ion at [M+H]<sup>+</sup> at m/z 341.212 (calculated 341.212).

The  $^1$ H spectrum of **4.4** revealed four aromatic signals. Two downfield multiplets at  $\delta_{\rm H}$  7.24 – 7.31 ppm (H-3" and H-5") and  $\delta_{\rm H}$  7.14 – 7.20 ppm (6", 2" and 4") corresponded to a terminal monosubstituted phenyl ring, with 2D COSY data confirming the characteristic spin system. The remaining aromatic protons appeared at  $\delta_{\rm H}$  6.24 (H-3, doublet) and  $\delta_{\rm H}$  6.26 (H-5, doublet, J = 2.5 Hz) indicative of *meta*-coupled protons on a 1,2,4,6-tetrasubstituted benzene ring. These signals were assigned via HSQC correlations between H-5 and C-5 ( $\delta_{\rm C}$  110.7 ppm) and H-3 and C-3 ( $\delta_{\rm C}$  101.6 ppm).

Further structural features were inferred from HMBC correlations: protons from the acetophenone methyl group displayed correlations to both a quaternary aromatic carbon (C-1,  $\delta_{\rm C}$  115.5 ppm) and the ketone carbon (C-7,  $\delta_{\rm C}$  204.3 ppm), confirming a COCH<sub>3</sub> moiety at C-7. The *meta*-arrangement of hydroxyl substituents on C-2 and C-4 and an aliphatic side chain on C-6 was also suggested by HMBC data.

The position of the aliphatic chain was established through HMBC correlations between H-1' and C-1, C-6 and C-4. The HMBC revealed that these protons were also correlated with C-2', allowing the assignment of  $\delta_{\rm C}$  32.38 ppm to this carbon. Additional correlations between H-8' and C-7', as well as between H-8' and the aromatic carbons of the terminal phenyl ring, allowed complete assignment of the terminal aliphatic segment.

Compound **4.4** was originally reported as kneglomeratanone A, isolated from the stem bark of K.  $glomerata^{20}$ . This compound was later isolated from the roots of the same species<sup>21</sup>. This is the first report of **4.4** isolated from K. membranifolia and the first instance of its occurrence in the leaf material of any Knema species.

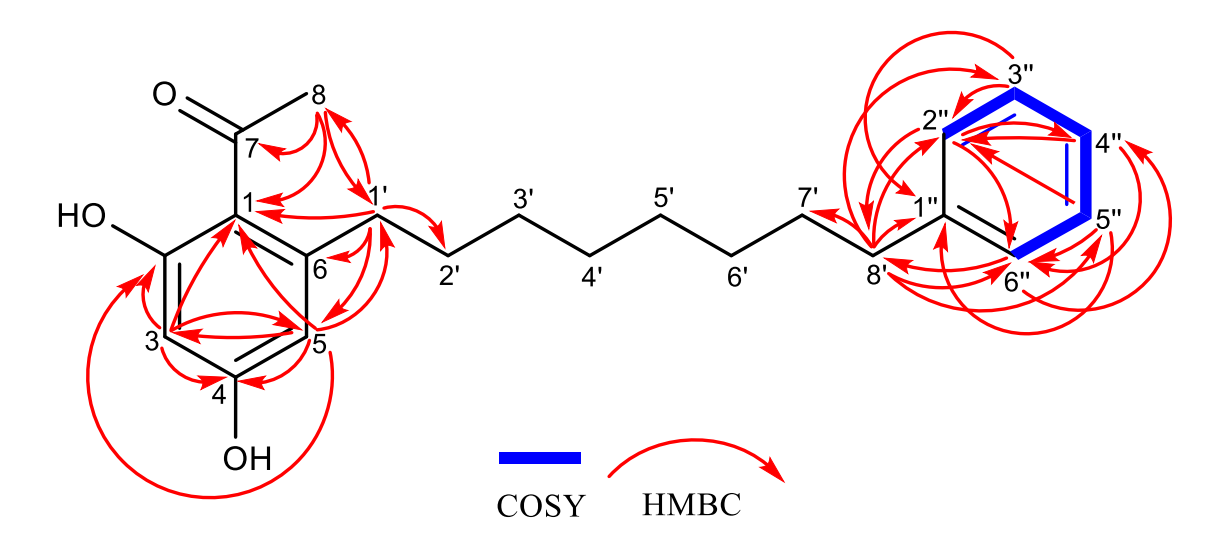


Figure 4.9. COSY and HMBC correlations of compound 4.4.

Table 4.4. <sup>1</sup>H, <sup>13</sup>C, COSY and HMBC NMR data of compound 4.4 (CDCl<sub>3</sub>, 500/126 MHz).

Position	δ <sub>C</sub> (ppm),	$oldsymbol{\delta_{\mathrm{c}}}^{20}$	$\delta_{\rm H}$ , mult. ( <i>J</i> in Hz)	COSY	HMBC
	type				
1	115.5, C	115.2, C	-	-	8, 5, 3, 1'
2	166.1, C	165.8, C	-	-	5, 3
3	101.8, CH	101.6, CH	6.24, d (2.5)	-	5
4	160.9, C	160.8, C	-	-	3, 5
5	110.7, CH	110.6, CH	6.26, d (2.5)	-	3, 1'
6	147.9, C	147.8, C	-	-	-
7	204.3, C	204.2, C	-	-	-
8	32.35, CH <sub>3</sub>	32.2, CH <sub>3</sub>	2.64, s	-	1'
1'	36.5, CH <sub>2</sub>	36.3, CH <sub>2</sub>	2.78 - 2.87, m	-	8, 5
2'	32.38, CH <sub>2</sub>	31.5, CH <sub>2</sub>	1.53 - 1.65, $m$	-	1'
3' to 6'	29.8, 29.52,	29.7, 29.2,	1.23 - 1.38, $m$	-	-
	29.46, 29.4,	29.3, 29.4,			
	$\mathrm{CH}_2$	$\mathrm{CH}_2$			
7'	31.6, CH <sub>2</sub>	31.2, CH <sub>2</sub>	1.53 - 1.65, $m$	-	8'
8'	36.1, CH <sub>2</sub>	36.0, CH <sub>2</sub>	2.60, t (8.8, 6.8)	-	2", 4", 6"
1"	143.0, C	142.7, C	-	-	8', 5", 3"
2" and 6"	128.5, CH	128.2, CH	7.14 - 7.20, m	3", 5"	8', 3", 4",
					5"
3" and 5"	128.4, CH	128.3, CH	7.24 – 7.31. <i>m</i>	2", 4", 6"	8'
4"	125.7, CH	125.5, CH	7.14 - 7.20, m	3", 5"	6", 2"

 $<sup>^{20}\</sup>mbox{Reference}$  carbon chemical shifts of 2,4-dihydroxy-6-(10-phenyldecyl)-acetophenone measured in CDCl $_3$ .

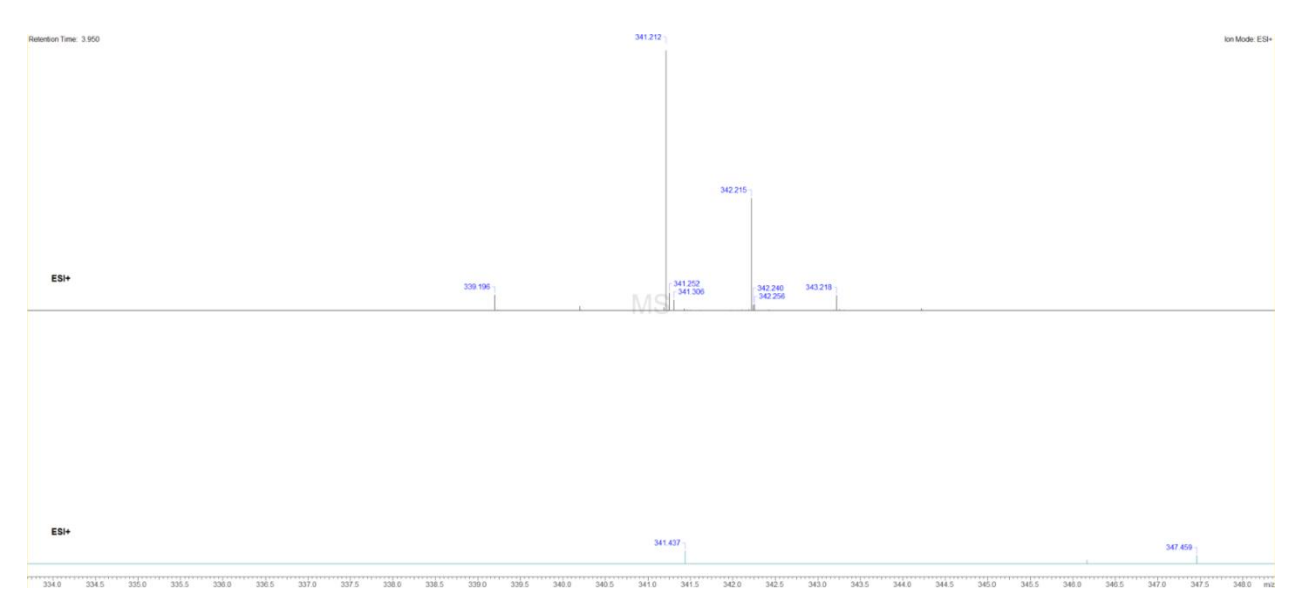


Figure 4.10. Mass spectrum of compound 4.4.

#### 4.2.1.5. 6-Alkylacetophenone, 10 carbon phenyldecyl linker (4.5, known)

Compound **4.5** (3 mg) was isolated as a green powder. The molecular formula of **4.5** was determined as  $C_{24}H_{32}O_3$  ( $\Delta$  = 0.0 ppm) based on the positive mode Q-ToF MS, which revealed a protonated [M+H]<sup>+</sup> ion at m/z at 368.235. The compound was identified as a second acetophenone analogue, distinguished by an additional carbon in the saturated hydrocarbon chain compared to compound **4.4**. This modification was evident from both the mass spectral data and the <sup>13</sup>C NMR spectrum, which displayed eleven signals in the aliphatic region, including a signal at  $\delta_{\rm C}$  32.35 ppm assigned to the terminal methyl carbon (C-8).

Due to the limited yield of **4.5**, the 2D NMR experiments revealed limited correlations. The  $^{1}$ H spectra displayed a peak at  $\delta_{\rm H}$  6.25 ppm (broad doublet, J = 2.6 Hz) which lacked an HSQC correlation to carbons C-3 and C-5, however it was concluded that this merged peak represents the two remaining protons on the phenolic ring. In addition, the HMBC correlation of this aromatic proton signal to 1' infers their location in the acetophenone ring, as COSY correlations confirmed the assignment of all other proton signals. Unlike the HMBC spectra for compound **4.4**, the hydroxyl protons displaying a combined singlet at  $\delta_{\rm H}$  12.96 ppm showed a correlation between neighbouring carbons C-3, C-2

and C-1. There was also no HSQC signal observed for C-1', C-10' or C-8, however comparing the chemical shifts of **4.5** to **4.4** and previous reports of **4.4**, elucidated the structure as the known compound, 2,4-dihydroxy-6-(10-phenyldecyl)-acetophenone, an acetophenone with a 10-carbon linker and a terminal phenyl. Owing to the absence of HSQC correlations for certain carbons, those data have not been included in Table 4.5. 2,4-dihydroxy-6-(10-phenyldecyl)-acetophenone was previously isolated from the stem bark of *K. laurina*, and *K. glomerata*<sup>18,20</sup>.

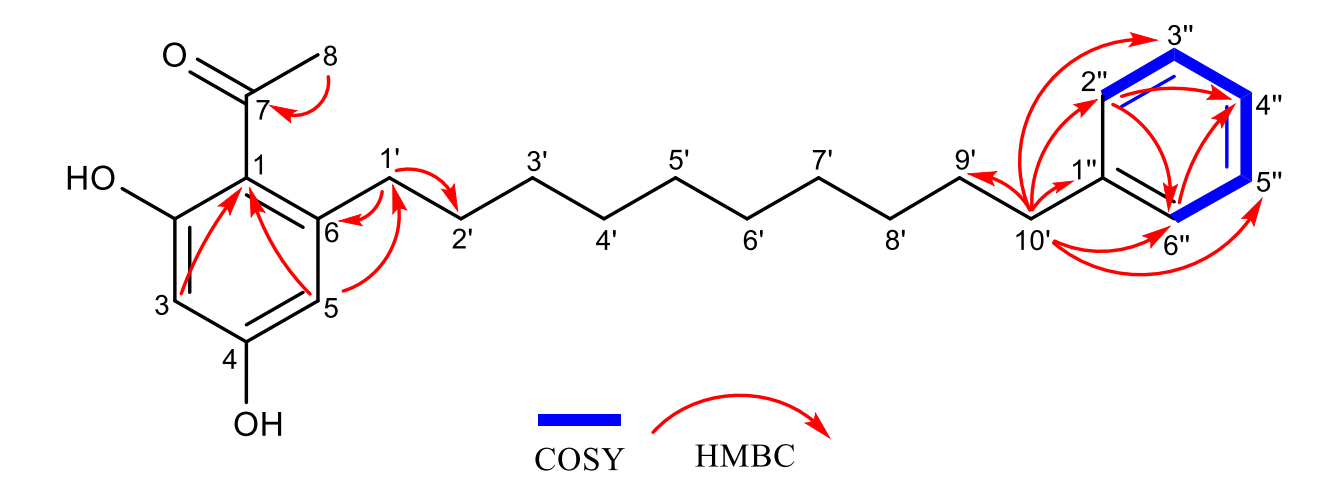


**Figure 4.11.** Key COSY and HMBC correlations of compound **4.5**.

Table 4.5. <sup>1</sup>H, <sup>13</sup>C, COSY and HMBC NMR data of compound 4.5 (CDCl<sub>3</sub>, 500/126 MHz).

Position	$\delta_{\rm C}$ (ppm), type	$\delta_{ m c}^{18}$	$\delta_{\rm H}$ , mult. ( <i>J</i> in Hz)	COSY	HMBC
1	115.5, C	115.0, C	-	-	5, 3, 2
2	166.9, C	165.7, C	-	-	2
3	101.8, CH	110.9, CH	6.23 - 6.27, $m$	-	2
4	160.9, C	161.4, C	-	-	-
5	110.6, CH	101.6, CH	6.23 - 6.27, $m$	-	-
6	148.0, C	147.9, C	-	-	1'
7	204.3, C	204.5, C	-	-	8

8	32.35, CH <sub>3</sub>	32.0, CH <sub>3</sub>	-	-	-
1'	36.5, CH <sub>2</sub>	36.3, CH <sub>2</sub>	-	2'	5
2'	32.41, CH <sub>2</sub>	32.2, CH <sub>2</sub>	-	1'	-
3' to 8'	31.1, 29.8,	29.6, 29.4,	1.21 - 1.39, $m$	-	-
	29.64, 29.61,	29.3, CH <sub>2</sub>			
	29.5, 29.4, CH <sub>2</sub>				
9'	31.6, CH <sub>2</sub>	31.4, CH <sub>2</sub>	-	10'	10'
10'	36.1, CH <sub>2</sub>	35.9, CH <sub>2</sub>	-	9'	-
1"	143.1, C	142.8, C	-	-	10'
2" and	128.5, CH	128.3, CH	7.15 - 7.20, m	3", 5"	10'
6"					
3" and	128.4, CH	128.2, CH	7.24 - 7.29, m	2", 6", 4"	10'
5"					
4"	125.7, CH	125.5, CH	7.15 - 7.20, m	3", 5"	2", 6"

 $<sup>^{18}\</sup>mbox{Reference}$  carbon chemical shifts of 2,4-dihydroxy-6-(10-phenyldecyl)-acetophenone measured in CDCl\_3.

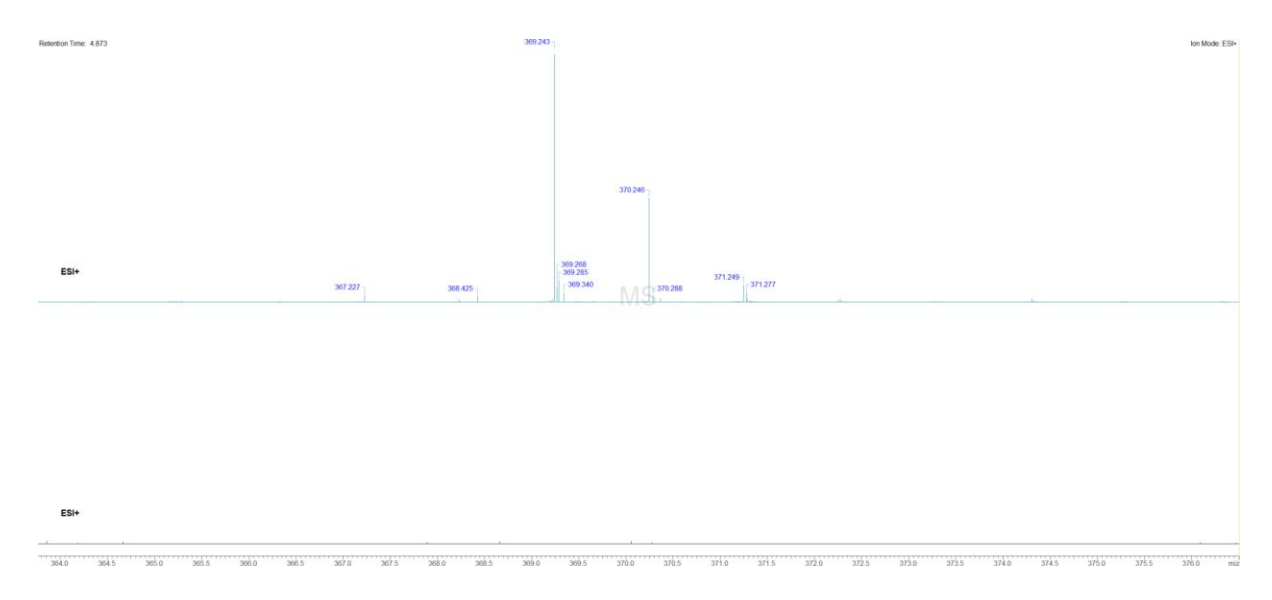


Figure 4.12. Mass spectrum of compound 4.5.

#### 4.2.1.6. 6-Alkylresorcinol, 10 carbon phenyldecyl linker (4.6, known)

Compound **4.6** (3.8 mg) was isolated as a yellow oil, and its molecular formula was established as  $C_{22}H_{30}O_2$  ( $\Delta$  = -2.4 ppm) using positive-mode Q-ToF mass spectrum, which revealed a protonated [M+H]<sup>+</sup> at m/z 327.232. The <sup>1</sup>H NMR spectrum of **4.6** exhibited an aromatic region consistent with previously isolated acetophenone derivatives. Signals characteristic of a monosubstituted phenyldecyl moiety were observed, with multiplets at  $\delta_H$  7.06 – 7.14 ppm (H-2", H-6", H-4") and  $\delta_H$  7.18 – 7.22 ppm (H-3", H-5") representing the terminal phenyl group.

A broad singlet at 6.16 ppm was attributed to three remaining protons (H-1, H-3, H-5) on the 2,4,6-trisubstituted resorcinol core. The similarity in chemical shifts caused these protons to appear as overlapping signals, rather than three distinct peaks with any multiplicity observed, thus only partially delineating the ring pattern from solely  $^1\text{H}$  spectrum. However, the occurrence of two quaternary carbons ( $\delta_{\text{C}}$  115.6 ppm, C-2, C-4) and two CH carbons ( $\delta_{\text{C}}$  107.0 ppm, C-1, C-5) at equivalent values, suggested the C-6 positioning of the alkyl chain, making a symmetrical substitution pattern on the aromatic ring. This allowed the prediction that of the three remaining proton signals, H-1 and H-5 would have a shared signal, and H-3 would appear at a similar chemical shift, explaining the broad singlet. This broad singlet is consistent with this compound reported in the literature.

Another concurring  ${}^{1}H$  signal to the literature is at  $\delta_{H}$  4.80 ppm, which represents the two OH protons  ${}^{22}$ . This compound was therefore identified as the previously reported 5-(10'-phenyldecyl)-resorcinol, an alkylresorcinol with a saturated 10-carbon chain terminating in a phenyl group.

Due to the low yield and associated weak resolution of the 2D NMR spectra, the HSQC signals did not clearly correlate C-1 with a proton signal, however a weak signal was observed correlating C-3 and C-5 to this broad singlet. The HMBC also lacked correlations of the aromatic protons in the resorcinol ring, however H-1' protons did correlate with carbons C-6 and C-2'.

To the best of my knowledge, the <sup>13</sup>C and 2D NMR data for this compound have not been previously reported. The first identification of **4.6** was made based on mass spectrometry data, where it was isolated from *K. elegans* stem bark<sup>16</sup>. Du *et al.*, later reported <sup>1</sup>H NMR data for this compound, identified within the sap of *Melanorrhoea usitate* (Anacardiaceae)<sup>24</sup>. **4.6** was also isolated from both the stem bark *K. glomerata* and leaves of *Dendrosenecio kilimanjari* (Asteraceae)<sup>20,23</sup>.

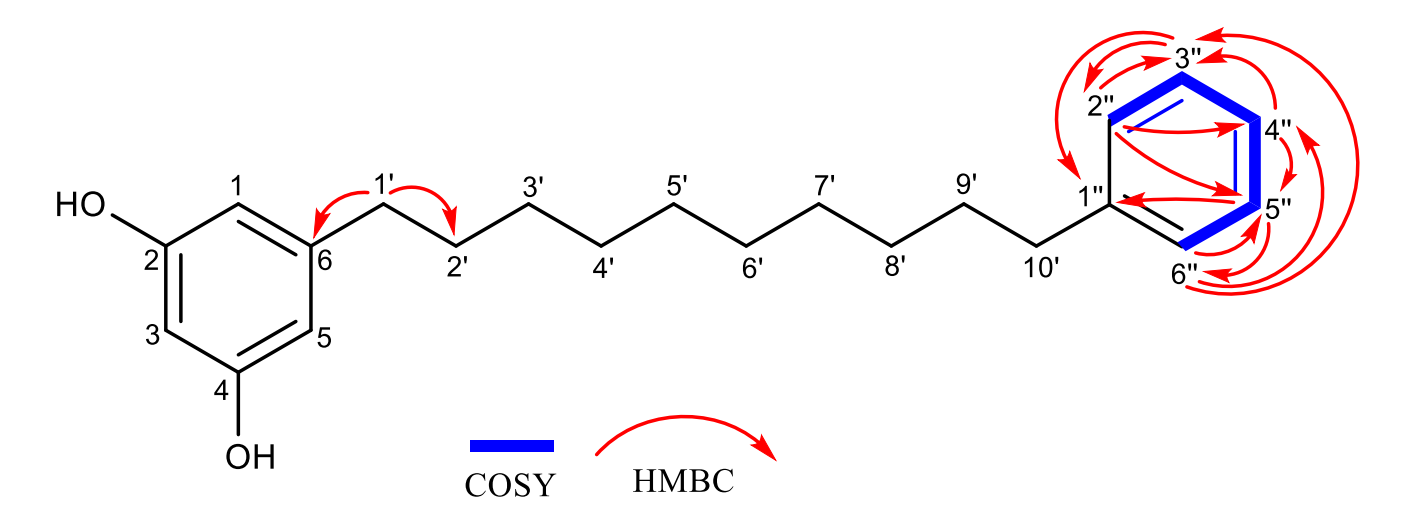


Figure 4.13. COSY and HMBC correlations of compound 4.6.

Table 4.6. <sup>1</sup>H, <sup>13</sup>C, COSY and HMBC NMR data of compound 4.6 (CDCl<sub>3</sub>, 500/126 MHz).

Position	$\delta_{\rm C}$ (ppm), type	$\delta_{\rm H}$ , mult. ( <i>J</i> in Hz)	COSY	HMBC
1	107.0, CH	6.16 m	-	-
2	155.6, C	-	-	-
3	99.1, CH	6.16, <i>m</i>	-	-
4	155.6, C	-	-	-
5	107.0, CH	6.16, <i>m</i>	-	-
6	145.1, C	-	-	1'
1'	35.0, CH <sub>2</sub>	2.52, t (7.5)	-	-
2'	$30.5$ , $CH_2$	1.44 - 1.57, m	-	1'

3' to 8'	28.51, 28.50,	1.22, dd (18.1, 9.2)	-	-
	28.47, 28.4,			
	28.3, 28.2, CH <sub>2</sub>			
9'	$30.0$ , $CH_2$	1.44 - 1.57, m	-	-
10'	$34.8$ , $CH_2$	2.41, <i>t</i> (7.7)	-	-
1"	141.9, C	-	-	3", 5"
2" and 6"	127.4, CH	7.06 - 7.14, m	3"', 5"	3", 5"
3" and 5"	127.2, CH	7.18 - 7.22, m	2", 4",	2", 6",
			6"	4"
4"	124.5, CH	7.06 – 7.14, <i>m</i>	3"", 5"	2", 6"

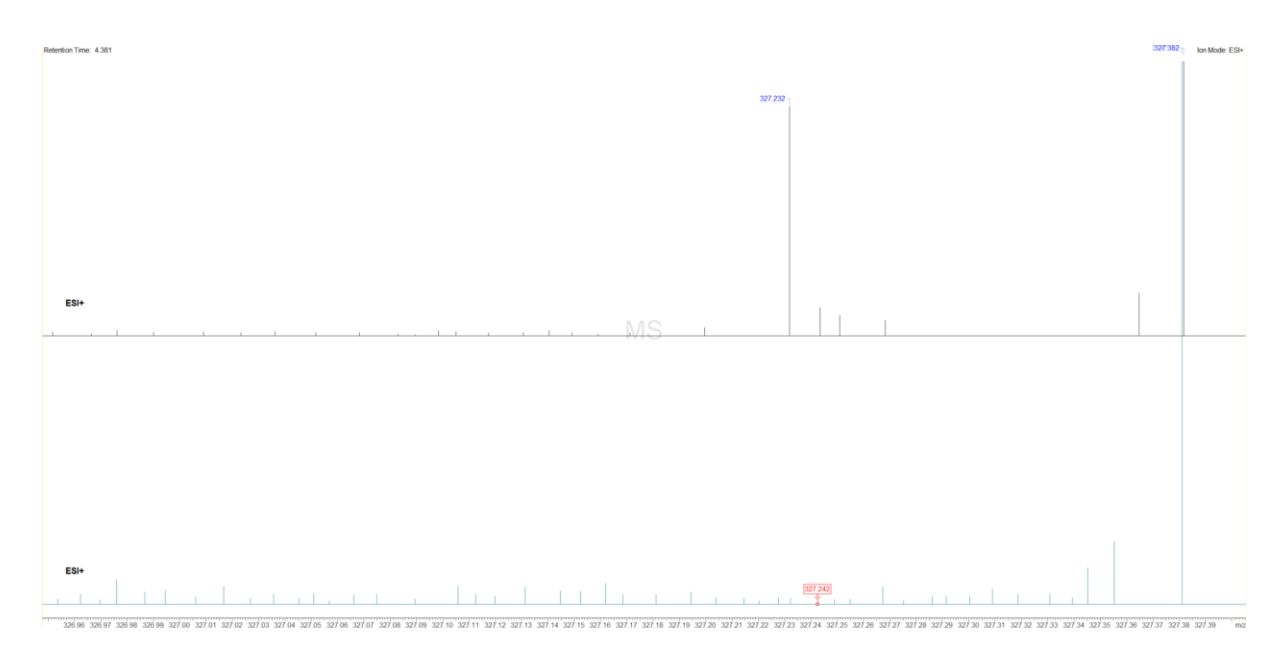


Figure 4.14. Mass spectrum of compound 4.6.

# 4.2.2. Structure elucidation of compounds from *Gymnacranthera contracta*

## 4.2.2.1. α-Tocopherol quinone (4.7, known, isolation one)

Compound **4.7** was isolated as a yellow crystal at 3.7 mg from a dichloromethane extract. The molecular formula was established as  $C_{29}H_{50}O_3$  ( $\Delta$  = -2.2 ppm) using positive mode Q-ToF MS analysis, which recorded the base and molecular ion peak at [M+H]<sup>+</sup> at

m/z 447.383. The  $^{1}H$  spectrum was characteristic of a tetraalkyl benzoquinone, displaying three methyl groups on the quinone ring with one methyl at  $\delta_{\rm H}$  2.04 ppm (5-Me, singlet) and two methyls at  $\delta_{\rm H}$  2.01 ppm (2-Me, 3-Me, singlet). Due to the full substitution of this quinone ring, no aromatic protons were observed; only a small singlet at  $\delta_{\rm H}$  8.10 ppm indicated the hydroxyl group at C-3'.

The  $\lambda_{\text{max}}$  at 234 nm was also typical of a quinonoid group. The methyl germinal to the hydroxyl group at C-3' displayed a <sup>1</sup>H signal at  $\delta_{\text{H}}$  1.23 ppm (3'-Me, singlet). The remaining four methyl groups displayed three signals at  $\delta_{\text{H}}$  0.86 ppm (11'-Me, doublet, J = 1.1 Hz), 0.86 ppm (7'-Me, doublet, J = 1.1 Hz) and 0.84 ppm (15'- and 16'-Me, doublet, J = 6.6 Hz). The <sup>13</sup>C NMR spectrum distinctly exhibited aliphatic signals characteristic of a phytol-like chain. As this compound was successfully identified in this study using MS, UV, <sup>1</sup>H and <sup>13</sup>C NMR data, 2D experiments were not necessary; therefore, the proton signals in Table 4.7 were assigned based on direct comparison with the literature. Comparison of the spectral data with the literature supported the conclusion that this was the known compound, 2,3,5-trimethyl6(3"-hydroxy)-phytyl-1,4-benzoquinone, commonly known as the vitamin E derivative,  $\alpha$ -tocopherol quinone<sup>24</sup>.

To the best of my knowledge, this study presents the first report of **4.7** being isolated from the Myristicaceae family. Quinones and tocotrienols bearing isoprenoid side chains have previously been identified in *Iryanthera juruensis* (Myristicaceae), highlighting biosynthetic capabilities for **4.7**<sup>25</sup>. The discovery of **4.7** broadens the known chemical diversity of Myristicaceae species and also emphasises the potential of this family as a reservoir of biologically significant natural products.

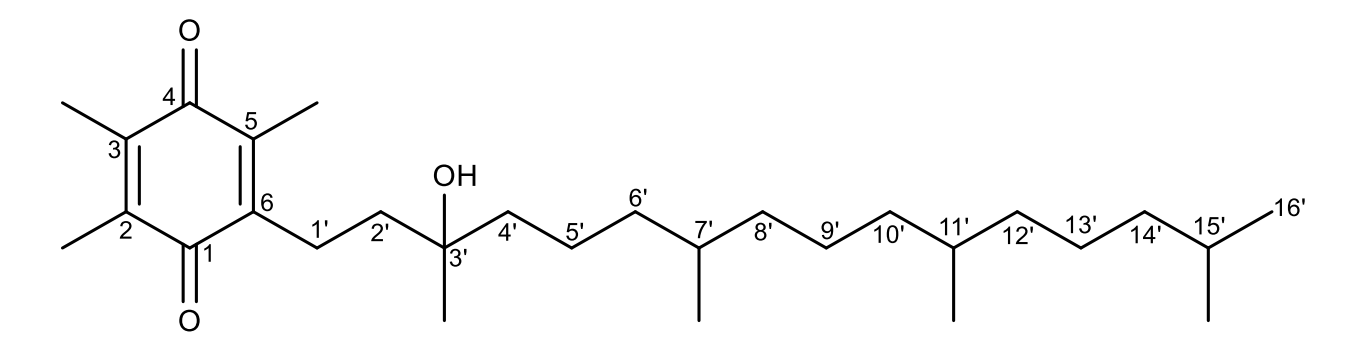


Figure 4.15. Structure of compound 4.7.

**Table 4.7.** <sup>1</sup>H and <sup>13</sup>C NMR data of **4.7**.

Position	$\delta_{\rm C}$ (ppm), type	$\delta_{ m c}^{24}$	$\delta_{\rm H}$ , mult. ( <i>J</i> in Hz)
1	187.4, C	187.2, C	-
2	140.3, C	140.2, CH	-
2- Me	12.45*, CH <sub>3</sub>	12.3*, CH <sub>3</sub>	2.01, s
3	140.6, C	140.4, CH	-
3- Me	12.12*, CH <sub>3</sub>	12.0*, CH <sub>3</sub>	2.01, s
4	187.9, C	187.7, C	-
5	140.7, C	140.5, C	2.04, s
5- Me	12.53*, CH <sub>3</sub>	12.4*, CH <sub>3</sub>	-
6	144.6, C	144.4, C	-
1'	21.6, CH <sub>2</sub>	21.4, CH <sub>2</sub>	2.51 - 2.58, m
2'	40.4, CH <sub>2</sub>	40.3, CH <sub>2</sub>	-
3'	72.8, C	72.7, CH	-
3' – Me	26.7, CH <sub>3</sub>	26.6, CH <sub>3</sub>	1.23, s
4'	42.4, CH <sub>2</sub>	42.3, CH <sub>2</sub>	-
5'	21.5, CH <sub>2</sub>	21.3, CH <sub>2</sub>	-
6'	37.8, CH <sub>2</sub>	37.6, CH <sub>2</sub>	-

7'	33.0, CH	32.8, CH	-
7'- Me	19.85, CH <sub>3</sub>	19.7, CH <sub>3</sub>	0.86, <i>d</i> (1.1)
8'	29.9, CH <sub>2</sub>	37.42, CH <sub>2</sub>	-
9'	24.7, CH <sub>2</sub>	24.5, CH <sub>2</sub>	-
10'	37.6, CH <sub>2</sub>	37.42, CH <sub>2</sub>	-
11'	32.9, CH <sub>2</sub>	19.74, CH <sub>2</sub>	-
11'- Me	19.90, CH <sub>3</sub>	19.74, CH <sub>3</sub>	0.86, <i>d</i> (1.1)
12'	37.4, CH <sub>2</sub>	37.3, CH <sub>2</sub>	-
13'	25.0, CH <sub>2</sub>	24.8, CH <sub>2</sub>	-
14'	39.5, CH <sub>2</sub>	39.4, CH <sub>2</sub>	-
15'	28.13, CH	28.0, CH	-
15'- Me	22.8, CH <sub>3</sub>	22.61, CH <sub>3</sub>	0.84, d (6.6)
16'- Me	22.9, CH <sub>2</sub>	22.61, CH <sub>3</sub>	0.84, d (6.6)

 $<sup>^{24}</sup> Reference$  carbon chemical shifts of  $\alpha\text{-tocopherol}$  quinone measured in CDCl $_3$ . \*indicates exchangeable signals.

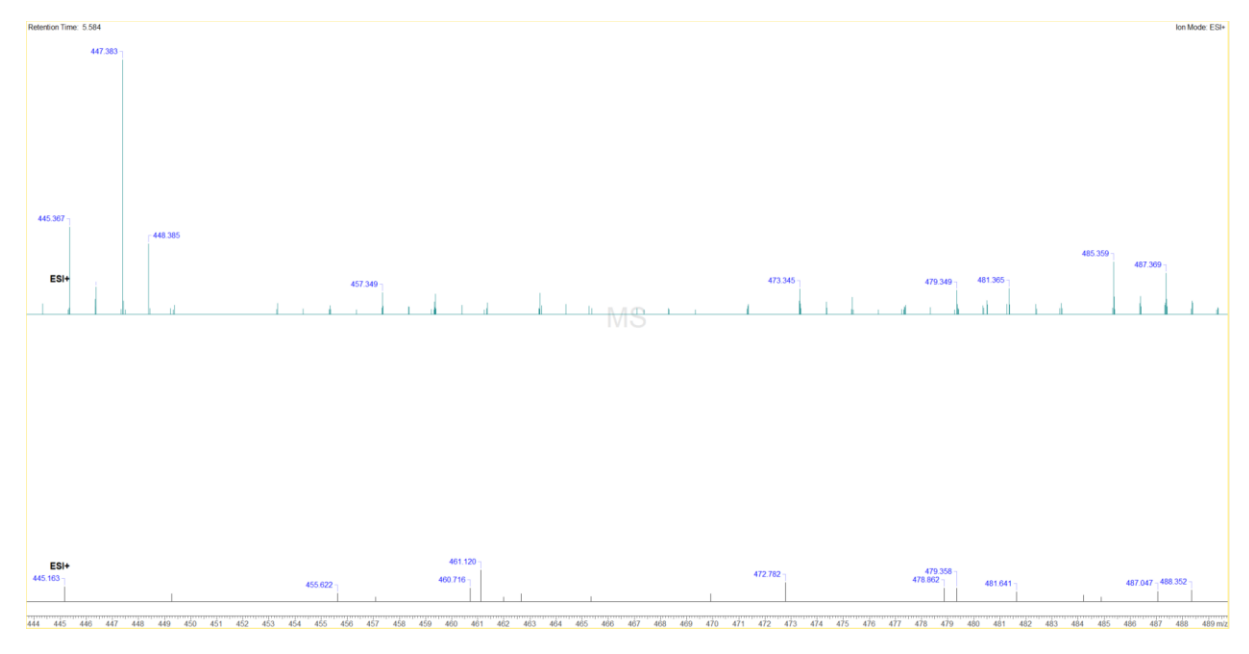


Figure 4.16. Mass spectrum of compound 4.7.

### 4.2.2.2. Methyl oleate (4.8, known)

Compound **4.8** was isolated as a yellow oil at 2 mg from a DCM extract of *G. contracta*. Q-ToF MS analysis established the molecular formula as  $C_{19}H_{36}O_2$  ( $\Delta$  = -3.36 ppm), indicated by the molecular ion peak [M+H] $^+$  at m/z 297.279 (Figure 4.18). The  $^1$ H NMR spectrum displayed a clear signal for the vinylic protons on C-10 and C-11, which were represented by a multiplet at  $\delta_{\rm H}$  5.21 – 5.44 ppm. The alkene could not be distinguished between trans or cis, as the relevant coupling constants could not be extracted due to overlapping and complex multiplet signals in the  $^1$ H NMR spectrum. Following this downfield signal, the methyl protons of the ester group at C-1 appeared as a singlet at  $\delta_{\rm H}$  3.47 ppm, whereas the terminal methyl group showed the lowest chemical shift as a multiplet at  $\delta_{\rm H}$  0.80 – 0.92 ppm. A distinct multiplet was observed at  $\delta_{\rm H}$  2.26 – 2.37 ppm, representing the most deshielded methylene protons at C-3, whilst another individual signal represented the adjacent methylene protons on C-4 ( $\delta_{\rm H}$  1.56 – 1.66 ppm, multiplet, 2H). The remaining 20 methylene protons on the saturated chain were represented by a multiplet in the aliphatic region  $\delta_{\rm H}$  1.97 – 2.04 ppm (Table 4.8).

The  $^{13}$ C NMR spectrum displayed one carbonyl ( $\delta_{\rm C}$  178.5 ppm, C-2) and two olefinic carbons ( $\delta_{\rm C}$  130.2 and 129.9 ppm, C-10, C-11). The C-1 ester methyl carbon appeared at  $\delta_{\rm C}$  50.9 ppm, followed by the alkyl chain carbon signals which clustered between  $\delta_{\rm C}$  22 – 35 ppm. The lowest chemical shift carbon was observed at  $\delta_{\rm C}$  14.3 ppm, representing the terminal methyl C-19. By comparison with the literature, this compound displayed characteristic  $^{1}$ H and  $^{13}$ C NMR chemical shifts and was therefore identified as methyl oleate, a fatty acid methyl ester  $^{26}$ .

Compound **4.8** is a known compound which has not been previously isolated from the genus *Gymnacranthera*.

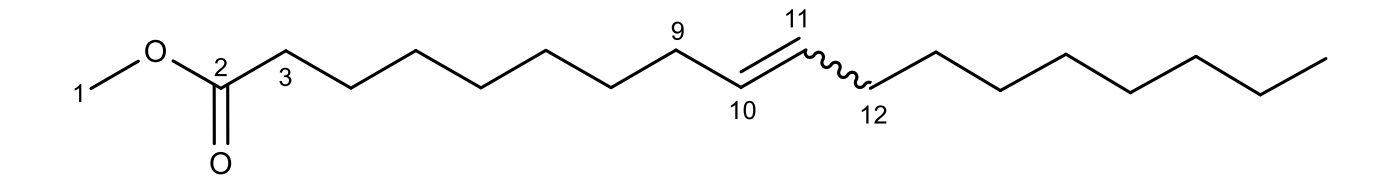


Figure 4.17. Structure of compound 4.8.

**Table 4.8.** <sup>1</sup>H and <sup>13</sup>C NMR data of **4.8**.

Position	$\delta_{\rm C}$ (ppm), type	$\mathbf{\delta_{c}}^{26}$	$\delta_{\rm H}$ , mult. ( <i>J</i> in Hz)
1	50.9, CH <sub>3</sub>	51.4, CH <sub>3</sub>	3.47, s
2	178.5, C	174.2, C	1.22 - 1.34, m
3	34.0, CH <sub>2</sub>	34.0, CH <sub>2</sub>	2.26 - 2.37, m
4	24.9, CH <sub>2</sub>	24.9, CH <sub>2</sub>	1.56 – 1.66, <i>m</i>
5	29.22, $\mathrm{CH}_2$	29.0, $\mathrm{CH}_2$	1.22 - 1.34, m
6	$29.38$ , $CH_2$	29.14, CH <sub>2</sub>	1.22 – 1.34, <i>m</i>
7	29.49, CH <sub>2</sub>	29.11, CH <sub>2</sub>	1.22 - 1.34, m
8	$27.29$ , $CH_2$	$27.1$ , $CH_2$	1.22 – 1.34, <i>m</i>
9	29.80, CH <sub>2</sub>	29.7, CH <sub>2</sub>	1.97 – 2.04, <i>m</i>
10	130.2, CH	129.9, CH	5.21 – 5.44, m
11	129.9, CH	129.7, CH	5.21 – 5.44, <i>m</i>
12	29.82, CH <sub>2</sub>	29.7, CH <sub>2</sub>	1.97 – 2.04, <i>m</i>
13	27.34, CH <sub>2</sub>	$27.2$ , $CH_2$	1.22 – 1.34, <i>m</i>
14	29.49, CH <sub>2</sub>	29.5, CH <sub>2</sub>	1.22 – 1.34, <i>m</i>
15	29.7, CH <sub>2</sub>	29.3, CH <sub>2</sub>	1.22 – 1.34, <i>m</i>
16	29.77, CH <sub>2</sub>	29.6, CH <sub>2</sub>	1.22 – 1.34, m
17	32.1, CH <sub>2</sub>	31.8, CH <sub>2</sub>	1.22 – 1.34, m
18	22.8, CH <sub>2</sub>	22.6, CH <sub>2</sub>	1.22 – 1.34, m
19	14.3, CH <sub>3</sub>	14.0, CH <sub>3</sub>	0.80 - 0.92, m

 $<sup>^{26}</sup>$ Reference carbon chemical shifts of  $\alpha$ -tocopherol quinone measured in CDCl<sub>3</sub>.

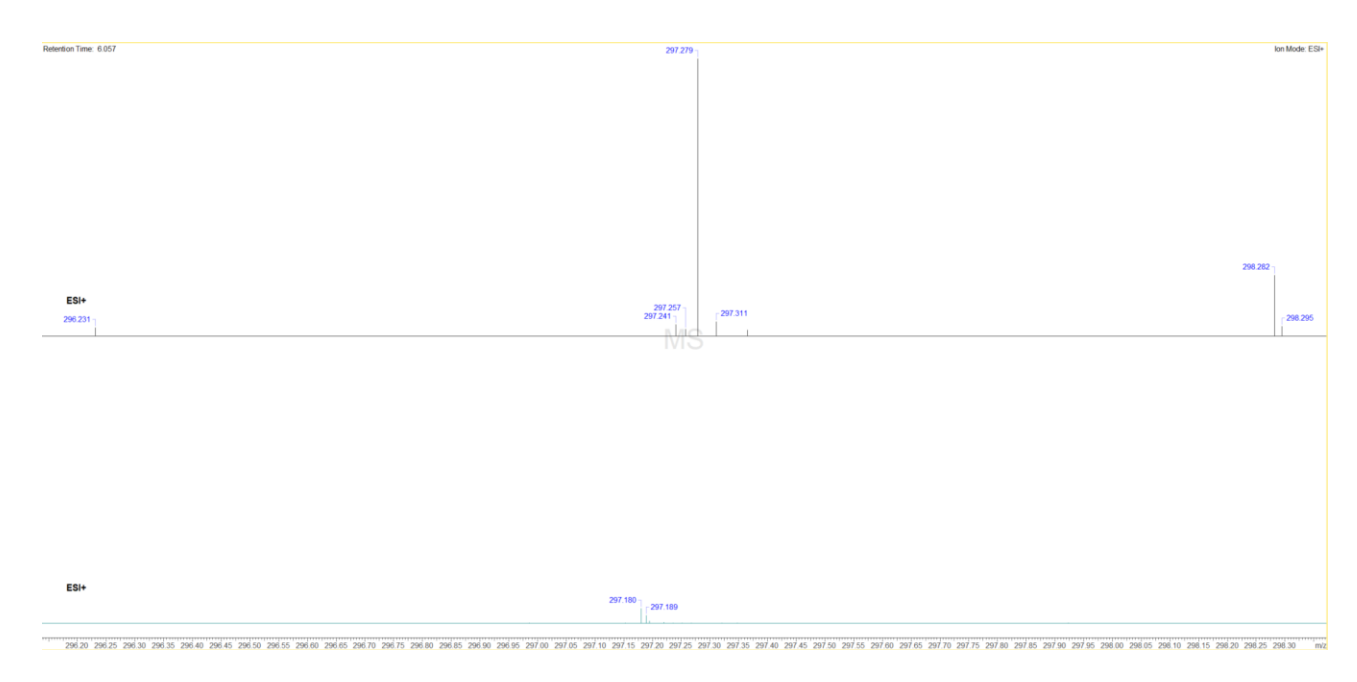


Figure 4.18. Mass spectrum of compound 4.8.

## 4.2.3. Semi-purified Knema membranifolia fractions

In addition to the previously described isolates, chromatographic separation of the *K. membranifolia* DCM extract yielded several semi-purified fractions, each containing predominantly mixtures of two structurally related compounds. Due to their low yields and close structural similarities, complete separation was not feasible. Nevertheless, spectral data were sufficient to allow tentative structural assignments.

The  $^{13}$ C and  $^{1}$ H NMR spectroscopy were used to identify key functional groups within these mixtures. Variations in alkyl chain lengths were inferred primarily from mass spectrometry, based on differences in m/z values. Although these fractions did not exhibit significant biological activity, the chemical profiles were deemed noteworthy and are thus reported here. Owing to the low abundance and partial purity of these samples, the proposed structures should be considered tentative.

#### **4.2.3.1. Fraction 1 (4.1/4.9)**

Fraction 1 was obtained at a yield of 7 mg. LC-MS analysis revealed two distinct peaks in the total absorbance chromatogram. Corresponding positive ionisation Q-ToF data supported the presence of the previously elucidated compound **4.1** and a known

anacardic acid, identified as compound **4.9**. Mass spectrometry data indicated a [M+H]<sup>+</sup> ion at m/z 355.227 ( $\Delta$ : 0 ppm) for compound **4.1**, while a second, less abundant peak in both the total ion and absorbance chromatograms corresponded to the [M+H]<sup>+</sup> ion of compound **4.9** at m/z 347.258 ( $\Delta$ : 0 ppm) (Figures 4.21, 4.22). Based on this, compound **4.9** was assigned the molecular formula  $C_{22}H_{34}O_3$ .

The one- and two-dimensional NMR spectra of the mixture were consistent with compound **4.1**, although several additional minor resonances were observed. Notably,  $^{1}$ H signals appeared at  $\delta$  5.31 – 5.40 ppm (alkene protons),  $\delta$  1.97 – 2.06 ppm (allylic protons), and  $\delta$  0.84 – 0.92 ppm (methyl triplet) (Figure 4.20), consistent with the presence of compound **4.9**.

HSQC correlations were observed between the alkene carbons at  $\delta$  130.04 ppm and alkene protons resonating at  $\delta$  5.31 – 5.40 ppm. HMBC correlations were also detected between these alkene protons and carbons at  $\delta$  27.35 and  $\delta$  27.06 ppm, as well as between the alkene carbons and the multiplet at  $\delta$  1.97 – 2.06 ppm, corresponding to the four methylene protons adjacent to the olefinic region. Six carbon signals were presumed to be overlapped within the methylene envelope around  $\delta$  29 ppm, characteristic of the long aliphatic chain of compound **4.1**. In addition, weaker signals were observed at  $\delta$  130.2, 130.0, 35.96, 32.11, 31.93, 27.34, 27.07, 22.84, and 14.27 ppm, accounting for the remaining carbon atoms.

The proposed HMBC correlations are summarised in Figure 4.19. Based on these spectroscopic data, the compound was tentatively identified as ginkgolic acid (15:1), a known anacardic acid characterised by a C15 aliphatic side chain bearing a double bond between C-8' and C-9' (Figure 4.19)<sup>27</sup>.

Figure 4.19. Structure of 4.9, with key COSY and HMBC correlations.

Table 4.9.  $^{1}$ H,  $^{13}$ C, COSY and HMBC NMR data of compound 4.9 from 4.1/4.9 fraction (CDCl<sub>3</sub>, 500/126 MHz)

Position	$\delta_{\rm c}$ (ppm), type	$\mathbf{\delta_c}^{27}$	$\delta_{\rm H}$ , mult. ( $J$ in Hz)	COSY	HMBC
1	110.5, C	110.4, C	-	-	-
2	163.8, C	163.6, C	-	-	-
3	116.0, CH	115.8,	6.86, dd (8.3, 1.2)	-	-
		СН			
4	135.4, CH	135.4,	7.35, dd (8.3, 7.5)	-	-
		СН			
5	122.9 <b>,</b> CH	122.7,	6.77, dd (7.5, 1.3)	-	-
		СН			
6	147.8, C	147.8, C	-	-	-
7	175.3, C	176.2, C	-	-	-
1'	$36.0$ , $CH_2$	36.4, CH <sub>2</sub>	2.91 - 3.00, m	-	-
2'	$32.1$ , $CH_2$	32.0, CH <sub>2</sub>	-	-	-
3', 4', 5',	29.1 – 29.9,	29.8,	1.18 – 1.41, <i>m</i>	-	-
6', 11',	$\mathrm{CH}_2$	29.7,			
12'		29.7,			
		29.6,			
		29.6,			

		29.5,			
		29.4,			
		29.3, CH <sub>2</sub>			
7'	27.1, CH <sub>2</sub> *a	26.9,	1.97 - 2.06, m	8'-	8'
		$\mathrm{CH_{2}}^{ullet}$			
8'	130.2, CH*b	129.9,	5.31 - 5.40, $m$	7', 9'	7'
		CH*			
9'	130.0, CH*b	129.8,	5.31 - 5.40, m	10', 8'	10'
		CH*			
10'	27.3, CH <sub>2</sub> *a	27.2,	1.97 - 2.06, m	9'	9'
		$\mathrm{CH_{2}}^{\star}$			
13'	$31.9$ , $\mathrm{CH}_2$	31.9, CH <sub>2</sub>	-	-	-
14'	$22.8$ , $CH_2$	22.3, CH <sub>2</sub>	1.18 - 1.41, $m$	-	15'
15'	$14.3$ , $\mathrm{CH}_2$	14.0, CH <sub>2</sub>	0.84 - 0.92, m	-	-

<sup>\*</sup>Coded indicates interchangeable signals.  $^{27}Reference$  carbon chemical shifts of  $\alpha\text{-tocopherol}$  quinone measured in CDCl $_3$ .

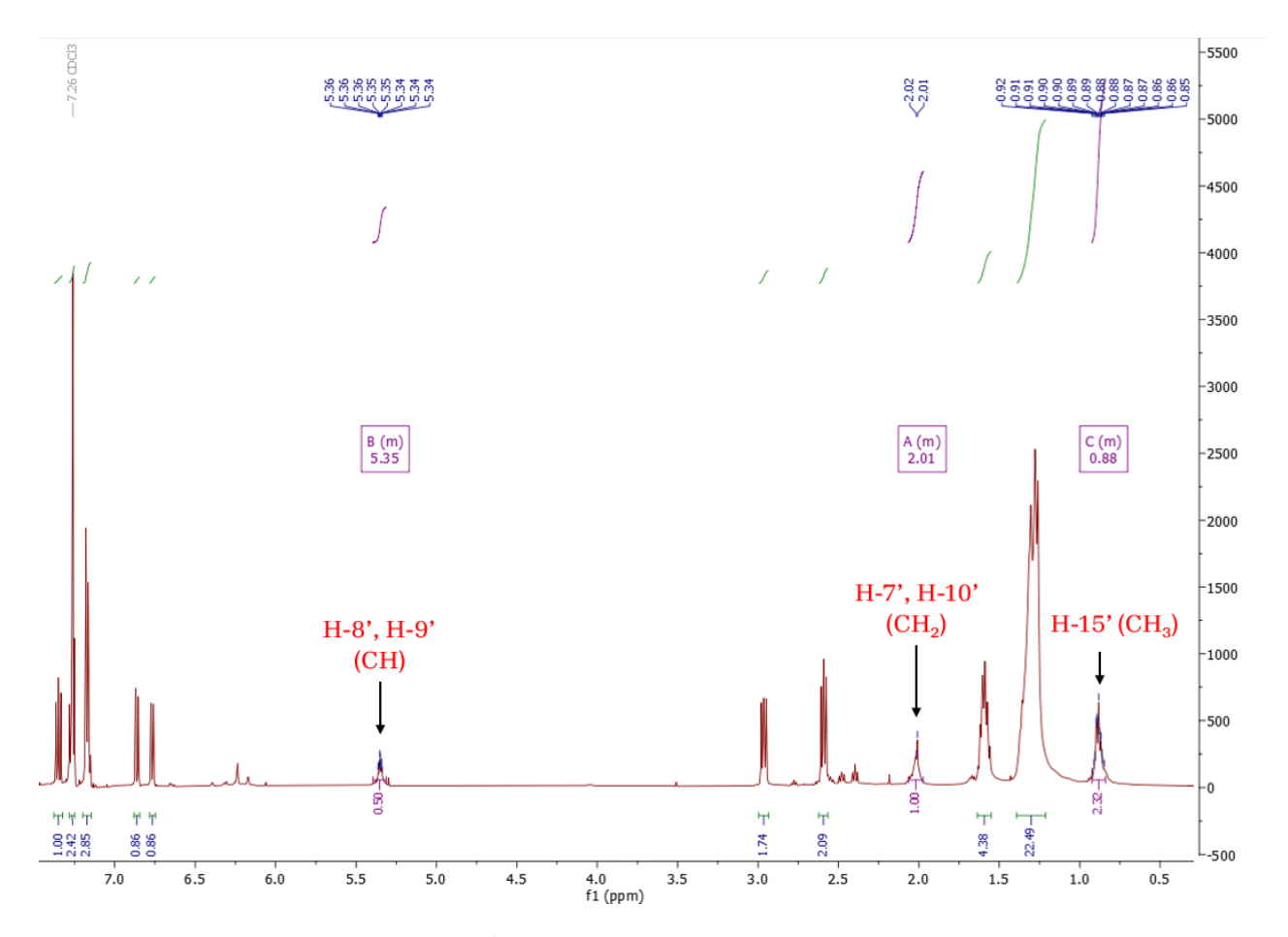


Figure 4.20. <sup>1</sup>H NMR spectrum of 4.1/4.9 fraction.

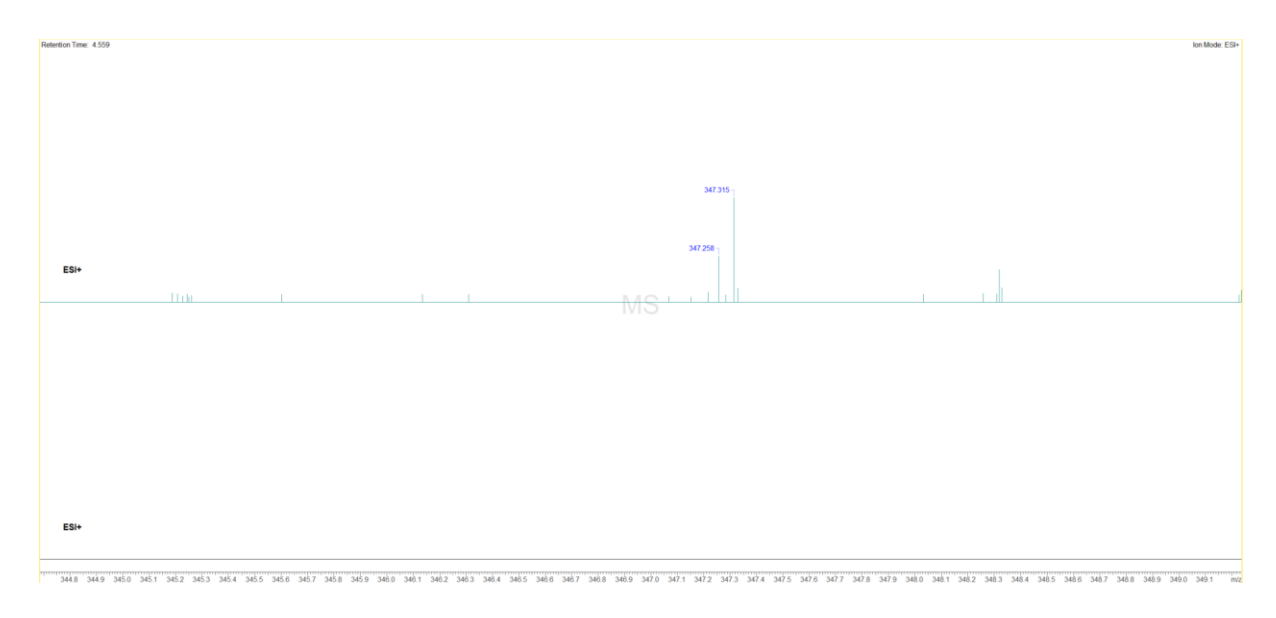


Figure 4.21. Compound 4.9 mass spectrum in 4.1/4.9 fraction.

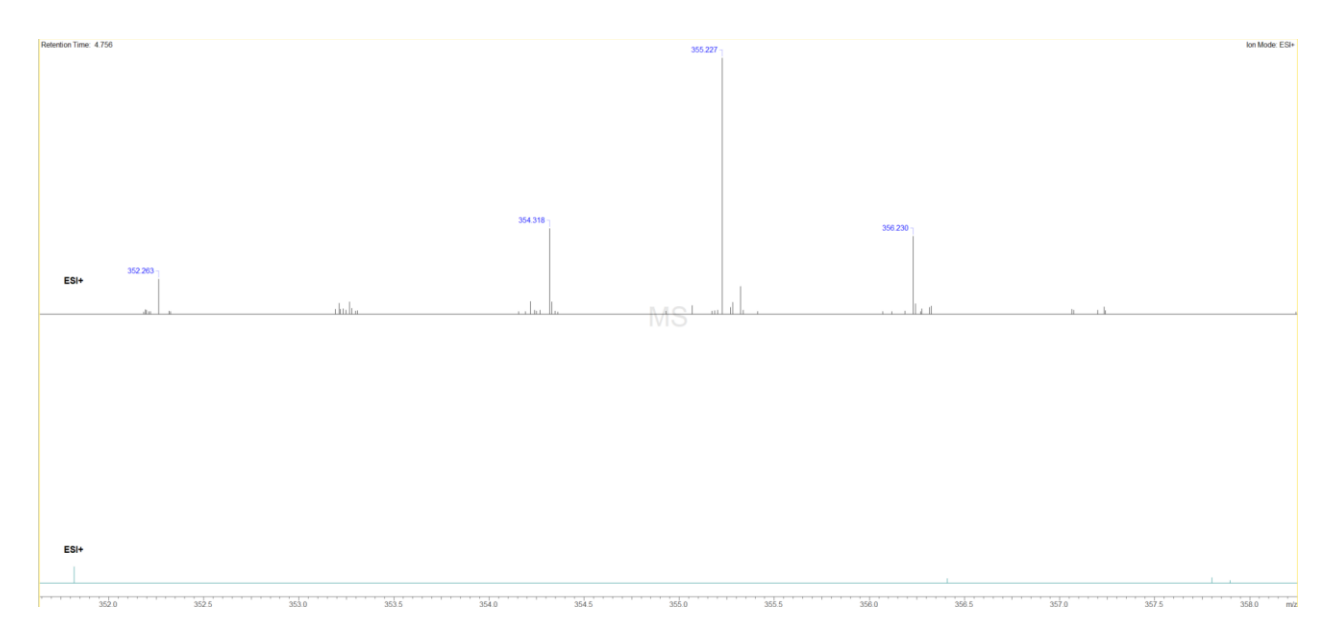


Figure 4.22. Compound 4.1 mass spectrum in 4.1/4.9 fraction.

### **4.2.3.2. Fraction 2 (4.10/4.11)**

For compounds **4.10** and **4.11**, the presence of a mixture was indicated by LC-MS data, which exhibited two closely eluting peaks on the total absorbance chromatogram, each corresponding to distinct molecular ions. Based on positive ionisation mode Q-ToF data, the molecular formulas of the two components were tentatively proposed. Compound **4.10** displayed molecular ions at [M+H] $^+$  at m/z 375.270 ( $\Delta$  = -26.6 ppm), [M+2H] $^+$  at m/z 376.290 ( $\Delta$  -18.6 ppm), and [M+3H] $^+$  at m/z 377.309 ( $\Delta$  = 10 ppm), supporting the assignment of the molecular formula  $C_{24}H_{38}O_3$  (Figures 4.26, 4.27). Compound **4.11** exhibited ions at [M+H] $^+$  m/z 405.337 ( $\Delta$  = 51.8 ppm), [M+NH<sub>4</sub>] $^+$  m/z 422.368 ( $\Delta$  = 37 ppm), and [M+Na] $^+$  m/z 427.319 ( $\Delta$  = 49 ppm), consistent with the proposed molecular formula  $C_{26}H_{44}O_3$  (Figures 4.24, 4.25).

The <sup>13</sup>C and <sup>1</sup>H NMR data indicated the presence of a mixture of compounds. This mixture comprised two alkyl salicylic acid derivatives lacking a terminal phenyl group, as suggested by the <sup>1</sup>H NMR spectrum. The shared aromatic signals in both the <sup>13</sup>C and <sup>1</sup>H NMR spectra indicated that these compounds possessed identical functional groups and differed only in their chain length and degree of saturation. The <sup>1</sup>H NMR spectrum

exhibited a weak alkene signal integrating into two protons, alongside two methyl resonances in the aliphatic region. Two  $\mathrm{CH_2}$  carbon signals at  $\delta$  27.3 and 27.1 ppm showed HMBC correlations with alkene carbons at approximately  $\delta$  130.04 and 130.00 ppm, supporting the assignment to **4.10** (Table 4.10, figure 4.23). Compound **4.10** was assigned the structure of a 17-carbon anacardic acid with one double bond, and **4.11** was assigned a 19-carbon anacardic acid with a saturated chain.

Although the precise positioning of the double bond is not confirmed by the current data, **4.10** and **4.11** have been previously isolated as a mixture<sup>28</sup> from *Ozoroa insignis* (Anacardiaceae), suggesting the likelihood of these being biosynthesised alongside each other<sup>28</sup>. However, other analogues of **4.10**, differing in saturation position, have been reported from *Knema* species, also making these structures possible<sup>29</sup>. Structural differences between **4.10** and **4.11**, namely a two-carbon variation in chain length and one double bond in saturation, account for their very similar chromatographic properties and the resulting difficulty separating these compounds. Compounds **4.10** and **4.11** were isolated in small combined quantities (3.7 mg) and exhibited no detectable antibacterial or anticancer activity, rendering further separation unjustified. To the best of my knowledge, compound **4.11** represents a novel isolation from Myristicaceae, whereas compound **4.10** has been previously reported from *Knema*. While the structural assignments regarding chain length and saturation remain tentative, the biosynthetic potential of *Knema* to produce these compounds is evident, as is their likelihood of occurring in an inseparable mixture.

 $\textbf{Figure 4.23.} \ \textbf{Structures of 4.10} \ \textbf{and 4.11}, \ \textbf{with key COSY and HMBC correlations}.$ 

Table 4.10.  $^{1}$ H,  $^{13}$ C, COSY and HMBC NMR data of compounds 4.10 and 4.11 (CDCl<sub>3</sub>, 500/126 MHz).

Position	$\delta_{\rm c}$ (ppm), type	$\delta_{\rm H}$ , mult. ( $J$ in Hz)	COSY	HMBC
1	110.6, C	-	-	1', 5, 3
2	163.7, C	-	-	4
3	116.0, CH	6.76, m	4, 5	-
4	135.4, CH	7.34, dd (11.4, 7.8)	3, 5	-
5	122.8 <b>,</b> CH	6.86, m	4, 3	1', 3
6	147.8, C	-	-	1'
7	175.3, C	-	-	-
1'	36.0, CH <sub>2</sub>	2.91 - 3.03, $m$	2'	5

2'	31.2*, 32.1*,	1.51 - 1.70, m	1'	-
	$\mathrm{CH}_2$			
Compound <b>4.10</b> (4' – 8',	29.0 – 30.0,	0.88, q (7.3)	-	-
13' – 15'), compound	$\mathrm{CH}_2$			
<b>4.11</b> (3' – 17')				
Compound <b>4.10</b> (15'),	31.9*a, 32.1*a	-	-	17',
compound <b>4.11</b> (17')				19'
Compound <b>4.10</b> (16'),	22.8*b, 22.5*b	0.88, m	-	-
compound <b>4.11</b> (18')				
Compound <b>4.10</b> (17'),	14.3*°, 14.1*°	0.88, m	-	-
compound <b>4.11</b> (19')				
9'	27.1, CH <sub>2</sub> *d	1.95 - 2.09, m	10'	10'
11'	130.2, CH*e	5.34, <i>t</i> (4.8)	12'	12'
10'	130.0, CH*e	5.34, <i>t</i> (4.8)	9'	9'
12'	27.3, $\mathrm{CH_2}^{\star\mathrm{d}}$	1.95 - 2.09, m	11'	11'

<sup>\*</sup>Coded signals represent interchangeable values. Red signals show those belonging to **4.10** exclusively, whilst black signals display shared signals, unless stated otherwise.

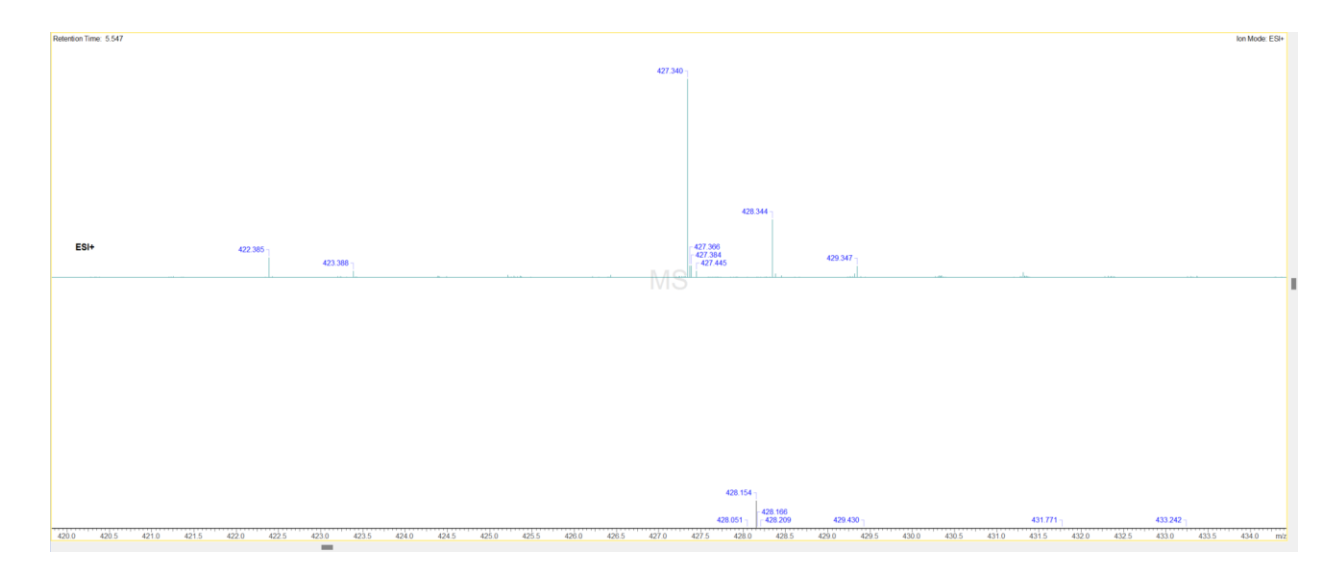


Figure 4.24. Compound 4.11 mass spectrum in fraction 4.10/4.11.

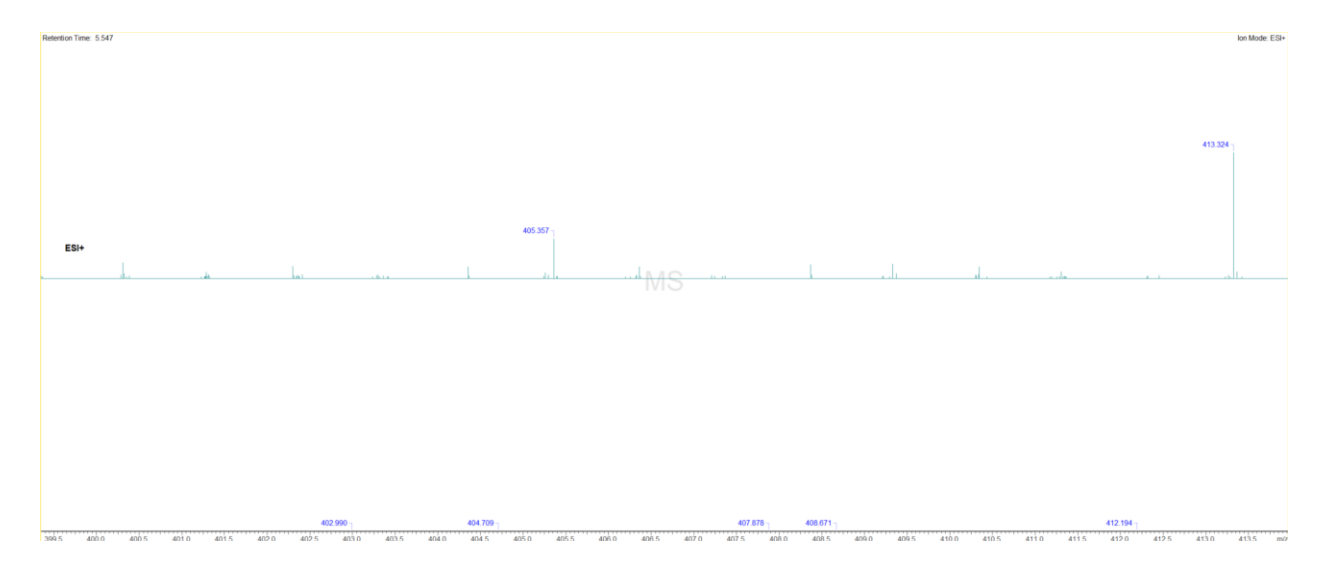


Figure 4.25. Compound 4.11 mass spectrum in fraction 4.10/4.11.

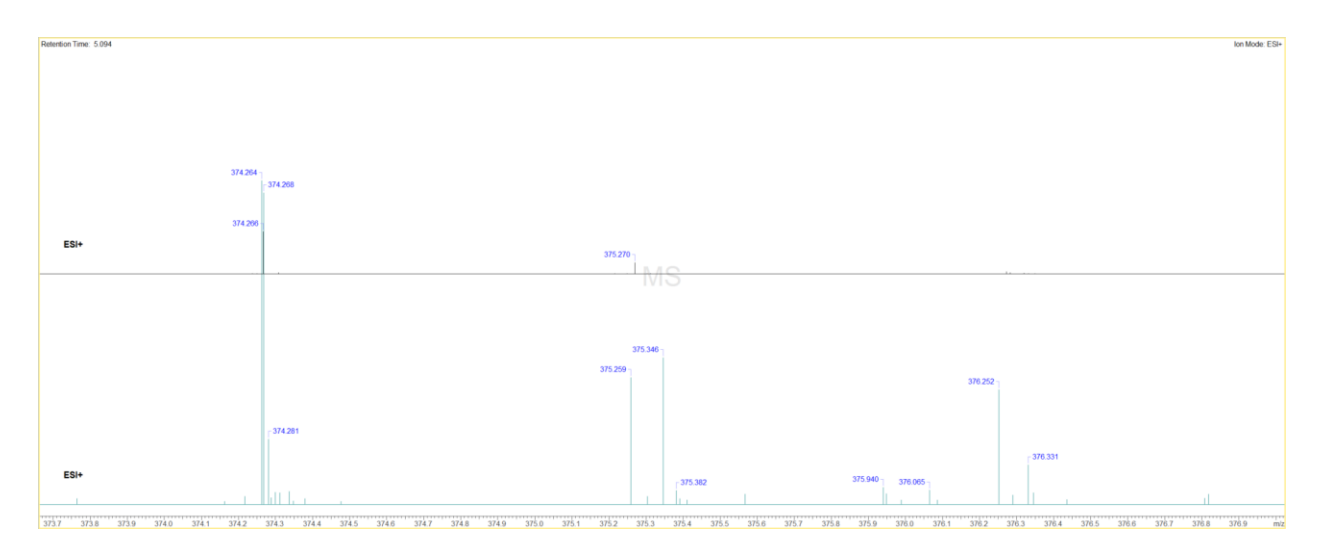


Figure 4.26. Compound 4.10 mass spectrum in fraction 4.10/4.11.

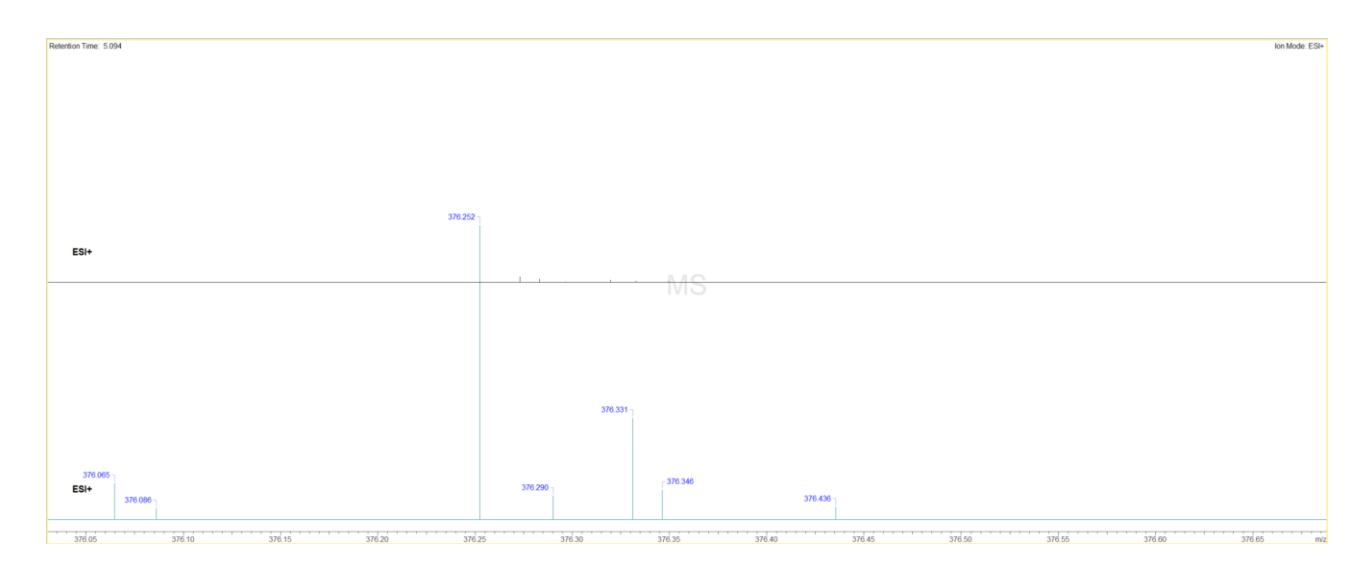


Figure 4.27. Compound 4.10 mass spectrum in fraction 4.11/4.12.

## 4.2.3.3. Fraction 3 (4.11/4.12)

Fraction three yielded 10 mg of a mixture containing two different compounds. LC-MS analysis revealed one dominant peak on the total absorbance and total ion chromatograms, accompanied by a minor peak eluting at a slightly earlier retention time. Positive ionisation mode Q-ToF data indicated these corresponded to two separate compounds. One compound exhibited molecular ions of [M+NH<sub>4</sub>] $^+$  at m/z 427.340 ( $\Delta$ : 49.1 ppm) and [M+K] $^+$  at m/z 443.335 ( $\Delta$ : 36.1 ppm), leading to the proposition of the molecular formula  $C_{26}H_{44}O_3$ . Combined with supporting 1D and 2D NMR data, this led to the tentative identification of **4.11** (an anacardic acid bearing a saturated 19-carbon alkyl chain). The NMR data for **4.11** are listed in Table 4.11. The second compound in the mixture displayed molecular ions of [M+H] $^+$  at m/z 459.378 ( $\Delta$ : 2.2 ppm) and of [M+2H] $^+$  at m/z 460.378 ( $\Delta$ : 10.9 ppm), leading to the proposition of the molecular formula  $C_{30}H_{50}O_3$  (Figures 4.29 – 4.31).

The  $^{1}$ H NMR spectrum exhibited a clear alkene signal at  $\delta$  5.25 – 5.45 ppm, as well as a multiplet at  $\delta$  1.98 – 2.10, corresponding to protons adjacent to the double bond. However, due to the complex multiplet signal, the couple and therefore cis/trans configuration could not be confidently established. The  $^{13}$ C NMR spectrum showed alkene carbon resonances at  $\delta$  130.0 ppm (assigned to C-10 and C-11). Based on these spectroscopic features, in conjunction with mass spectrometry data, the compound

was tentatively identified as **4.12** – a previously undescribed unsaturated anacardic acid with a 23-carbon chain with an unconfirmed double bond position. The saturated analogue of this compound has been previously reported from the Anacardiaceae family<sup>28</sup>.

Table 4.11 and Figure 4.28 present the  $^1$ H and  $^{13}$ C NMR assignments along with observed HMBC and COSY correlations. Most of the carbons of **4.11** and **4.12** are represented by carbon chemical shifts within 0.2 ppm between compounds, and are thus considered interchangeable, therefore representative values have been included in Table 4.11. The alkane carbon signals in the  $\delta$  29.0 – 30.0 ppm region displayed overlap and are reported as a range. A complete  $^{13}$ C spectrum with labelled resonances is included in Appendix A.58.

Figure 4.28. Structures of 4.12, with key COSY and HMBC correlations.

Table 4.11. <sup>1</sup>H, <sup>13</sup>C, COSY and HMBC NMR data of compounds 4.12 (CDCl<sub>3</sub>, 500/126 MHz).

Position	$\delta_{\rm C}$ (ppm), type	$\delta_{\rm H}$ , mult. ( <i>J</i> in Hz)	COSY	HMBC
1	110.7, C	-	-	5, 3, 1'
2	163.7, C	-	-	4
3	116.7, CH	6.76, dd (7.6, 1.2)	4, 5	5
4	135.4, CH	7.34, dd (8.3, 7.5)	3, 5	-
5	122.8 <b>,</b> CH	6.85, dd (8.3, 1.3)	3, 4	3

6	147.8, C	-	-	4, 1'
7	175.3, C	-	-	-
1'	36.6, CH <sub>2</sub>	2.90 - 3.02, $m$	2'	5
2'	$32.2$ , $CH_2$	2.33 - 2.48, m	1'	-
3'-8',	29.8 – 30.0,	1.10 - 1.47, $m$	-	-
13' – 20'	$\mathrm{CH}_2$			
9'	27.1, CH <sub>2</sub> *	1.98 - 2.10, m	10'	-
10'	130.2, CH*a	5.25 - 5.45, $m$	9'	9'
11'	130.0, CH*a	5.25 - 5.45, $m$	12'	12'
12'	27.3, CH <sub>2</sub> *	1.98 - 2.10, m	11'	11'
21'	$32.2$ , $CH_2$	1.10 - 1.47, $m$	-	23'
22'	$22.8$ , $\mathrm{CH}_2$	1.10 - 1.47, $m$	-	23'
23'	14.3, CH <sub>2</sub>	0.79 - 0.95, m	-	

<sup>\*</sup> Indicates interchangeable signals.



 $\textbf{Figure 4.29.} \ \textbf{Compound 4.11} \ mass \ spectrum \ in \ fraction \ \textbf{4.11/4.12}.$ 

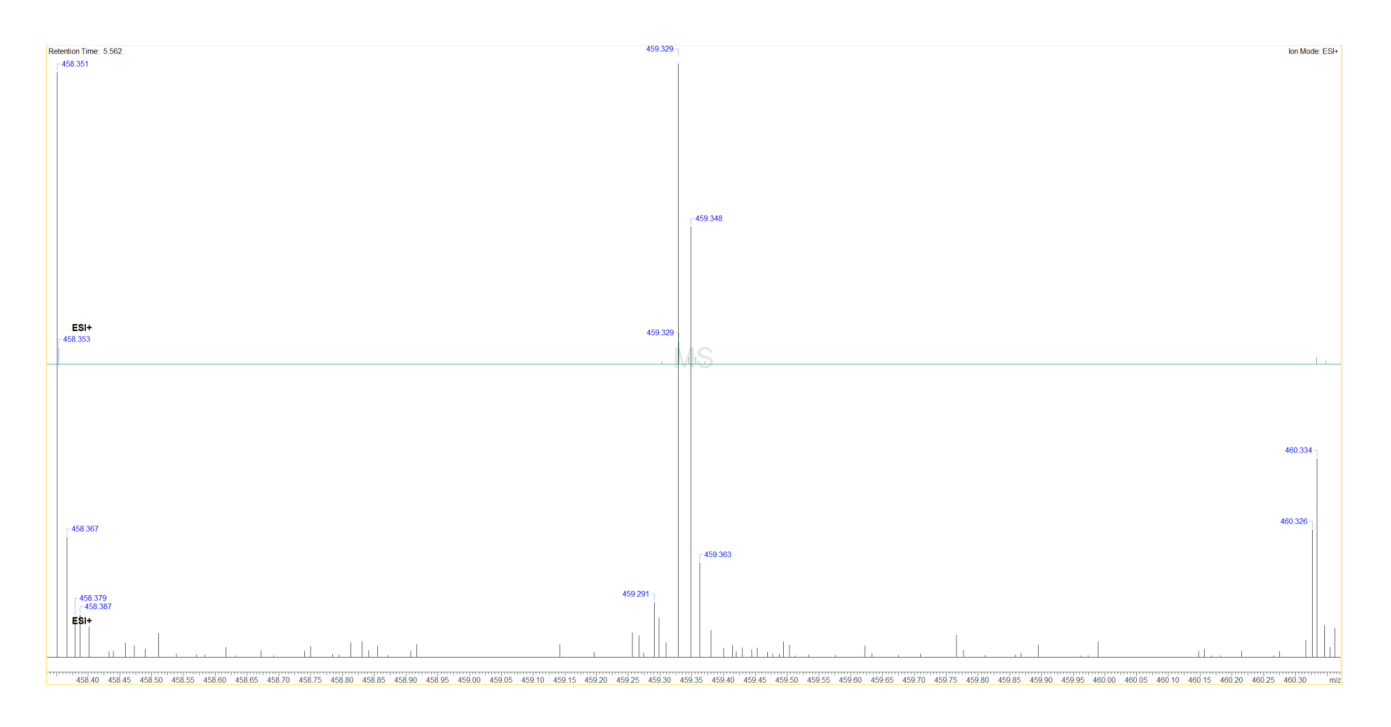


Figure 4.30. Compound 4.12 mass spectrum in fraction 4.11/4.12.

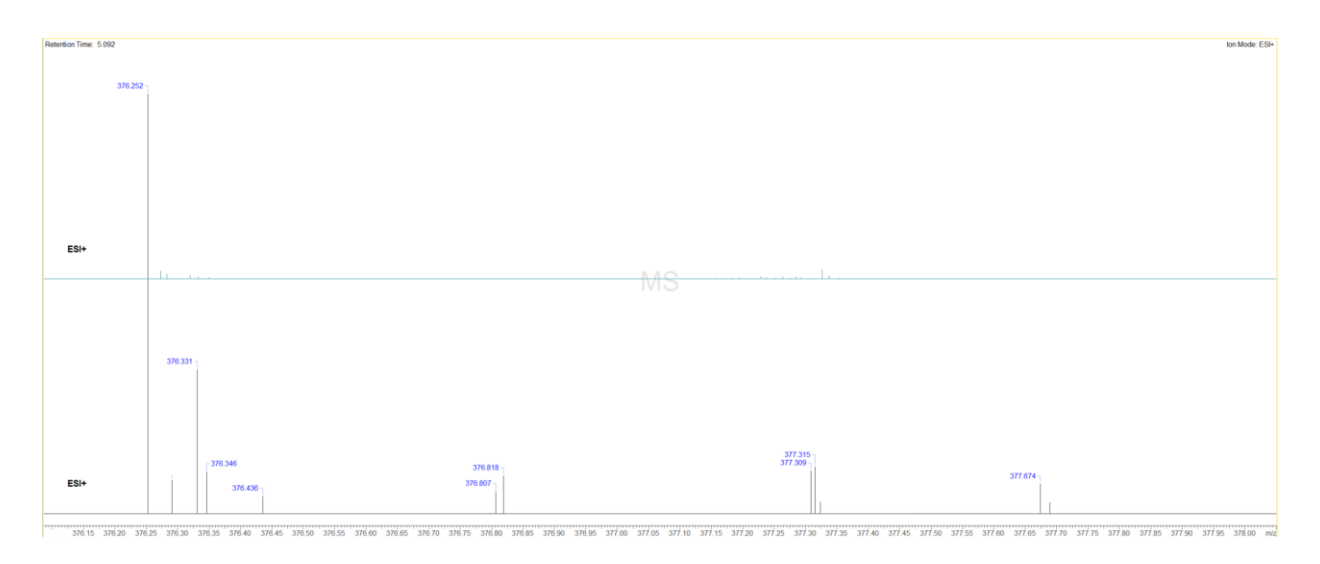


Figure 4.31. Compound 4.10 mass spectrum in fraction 4.11/4.12.

# **4.2.3.4. Fraction 4 (4.13/4.14)**

Fraction 4 was obtained at a yield of 3 mg and was determined to be a mixture of two structurally related compounds. Initial LC-MS analysis revealed two closely eluting peaks on both the total ion chromatogram and total absorbance chromatogram. The

compound corresponding to the less abundant peak exhibited a molecular ion at m/z 319.223 ([M+H]<sup>+</sup>,  $\Delta$  = 9.7 ppm) in the positive ionisation mode Q-ToF mass spectrum, consistent with the molecular formula  $C_{20}H_{30}O_3$ . This compound is herein referred to as **4.13**.

These signals showed correlations with the alkene carbons at  $\delta$  130 ppm in the HSQC and HMBC spectra, respectively. The aromatic regions in both the  $^{1}$ H and  $^{13}$ C NMR spectra were consistent with an anacardic acid lacking a terminal phenyl ring, indicating structural similarity to other members of the series, with the key differences residing in the alkene region.

Additionally, the spectra showed two distinct methyl signals in both  $^{1}$ H and  $^{13}$ C NMR, each attributed to one of the two compounds present in the mixture. The combined NMR data are summarised in Table 4.12. Carbon signals that differed by less than 0.5 ppm between the two compounds have been reported as a representative single value. The methylene carbons in the  $\delta$  29.0 – 30.0 ppm range were grouped, as individual assignments could not be confidently resolved due to overlap (Table 4.12).

Based on the spectroscopic evidence, **4.13** was tentatively assigned the structure of an anacardic acid bearing a 13-carbon alkyl chain with one double bond, while **4.14** was assigned as a saturated anacardic acid with a 16-carbon alkyl chain (Figure 4.32). Although the precise position of the double bond in **4.13** could not be definitively established from the available data, it is proposed to lie between C-8' and C-9'. This assignment is supported by prior isolation of a structurally analogous 13-carbon anacardic acid from the *Knema* species<sup>30</sup>.

Compound **4.14**, on the other hand, has been previously reported in *Ginkgo biloba*, a species known to share several secondary metabolites with *Knema*, thus reinforcing the plausibility of *K. membranifolia* biosynthesising this compound<sup>31</sup>.

Figure 4.32. Structures of 4.13 and 4.14, with key COSY and HMBC correlations.

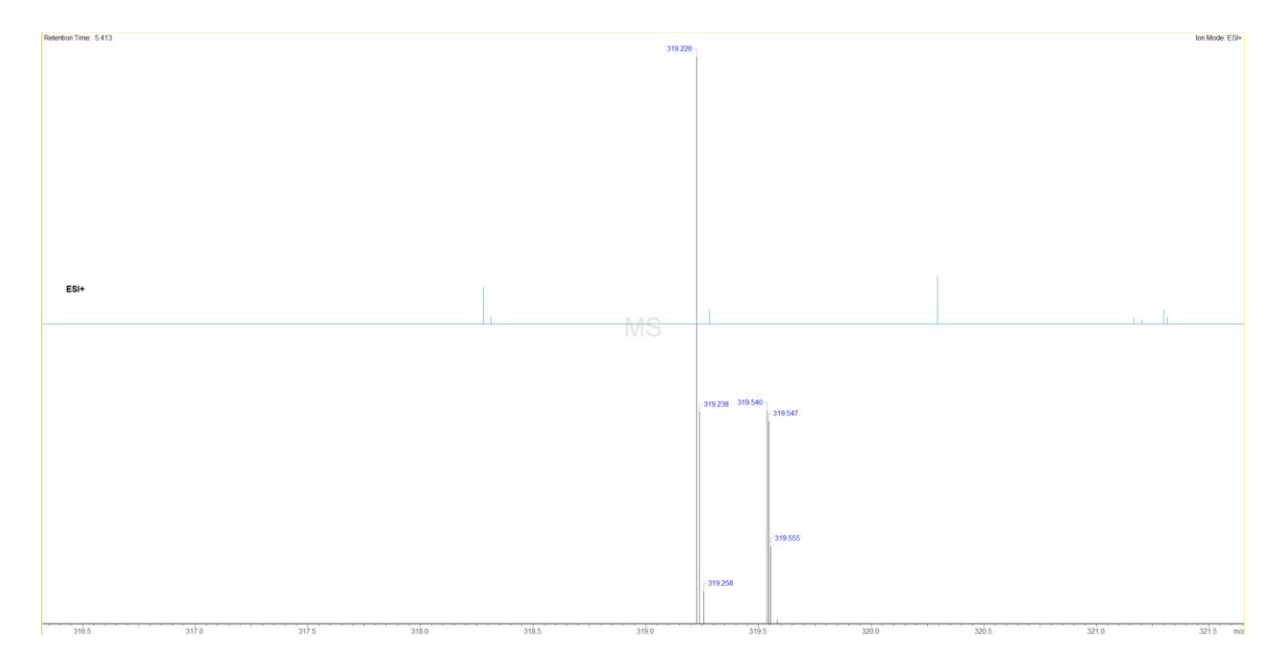
COSY HMBC

 $\textbf{Table 4.12.} \ ^{1}\text{H, } ^{13}\text{C, COSY and HMBC NMR data of compounds 4.13/4.14 (CDCl}_{3}, 500/126 \ \underline{\text{MHz}}\text{)}.$ 

Position	$\delta_{\rm C}$ (ppm), type	$\delta_{\rm H}$ , mult. ( <i>J</i> in Hz)	COSY	HMBC
1	110.5, C	-	-	-
2	163.8, C	-	-	-
3	116.0, CH	6.76, t (8.5)	4, 5	-
4	135.5, CH	7.34, td (11.4, 7.8)	3, 5	-
5	122.8 <b>,</b> CH	6.86, <i>d</i> (8.3)	4, 3	-
6	147.8, C	-	-	-
7	175.3, C	-	-	-
1'	36.7, CH <sub>2</sub>	2.91 - 3.03, m	2'	-
2'	$32.2$ , $CH_2$	1.51 - 1.70, m	1'	-
Compound 4.13	29.0 – 30.0, CH <sub>2</sub>	1.06 - 1.45, $m$	-	-
(3' – 6'),				
compound 4.14				
(3' – 13')				
Compound 4.13	31.9, CH <sub>2</sub>	-	-	-
(11'), compound				
<b>4.14</b> (14')				

Compound 4.13	$22.8$ , $CH_2$	0.88, q $(7.3)$	-	-
(12'), compound				
<b>4.14</b> (15')				
Compound 4.13	14.2, CH <sub>3</sub>	0.88, q $(7.3)$	-	-
(13'), compound				
<b>4.14</b> (16')				
7'	27.1, CH <sub>2</sub> *	1.95 - 2.09, $m$	10'	10'
8'	130.04, CH*a	5.34, <i>t</i> (4.8)	12'	12'
9'	130.01, CH*a	5.34, <i>t</i> (4.8)	9'	9'
10'	27.4, CH <sub>2</sub> *	1.95 - 2.09, $m$	11'	11'

<sup>\*</sup>Coded signals represent interchangeable values. Signals in red represent those belonging to **4.13** and all others are shared unless stated otherwise



 $\textbf{Figure 4.33.} \ \textbf{Compound 4.13} \ \textbf{mass spectrum in fraction 4.13/4.14}.$ 

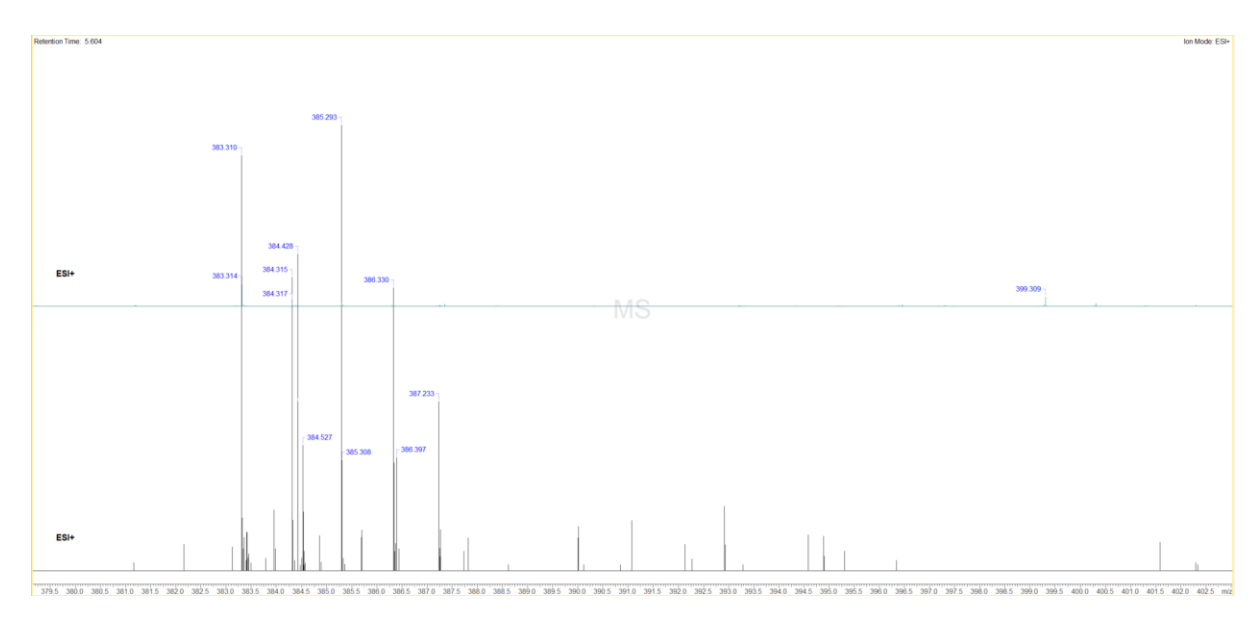


Figure 4.34. Compound 4.14 mass spectrum in fraction 4.13/4.14.

#### 4.2.4. Conclusion

Through detailed spectroscopic analysis, including 1D and 2D NMR and X-ray crystallography, this study marks the first phytochemical investigation of *K. membranifolia*. Six compounds were isolated, including one previously undescribed natural product, **4.3**. Furthermore compounds were identified across fractions 1 - 4, primarily differing in chain length and unsaturation. Despite occurring as inseparable mixtures, spectral data enabled tentative structural proposals, contributing information to the metabolic profile of *K. membranifolia*.

Amongst the key contributions, the full 2D NMR data of **4.1** and the crystal structure of **4.2** are reported here for the first time, as well as the carbon and 2D NMR data of **4.6**. Furthermore, α-tocopherol quinone is identified for the first time in the Myristicaceae family. These findings infer the biosynthetic potential of *K. membranifolia* (and the Myristicaceae family).

## 4.2.5. Biosynthetic pathway of *Knema* compounds

The biosynthesis of the alkylsalicylic acid compounds is proposed to involve a Type III polyketide synthase using hydrocinnamyl CoA as a starter unit. This would undergo successive Claisen condensation reactions with malonyl-CoA extender units, followed

by saturation of the ketone groups by a cycle of reduction, dehydration and reduction, as in fatty acid biosynthesis. With the final three extensions, however, the ketones are retained to give a polyketide terminus as illustrated for the alkylsalicylic acid with a 16-carbon linker (compound **4.15**, Figure 4.35). This undergoes an aldol reaction to give intermediate **4.16** followed by dehydration to give the resorcinol **4.17**. From this common precursor, further tailoring reactions to form cardol **4.18** (decarboxylation), cardanol **4.19** (reduction, decarboxylation), salicylic acid **4.20** (reduction, decarboxylation, oxidation) or urushiol **4.21** (reduction, hydrolysis)<sup>32</sup>.

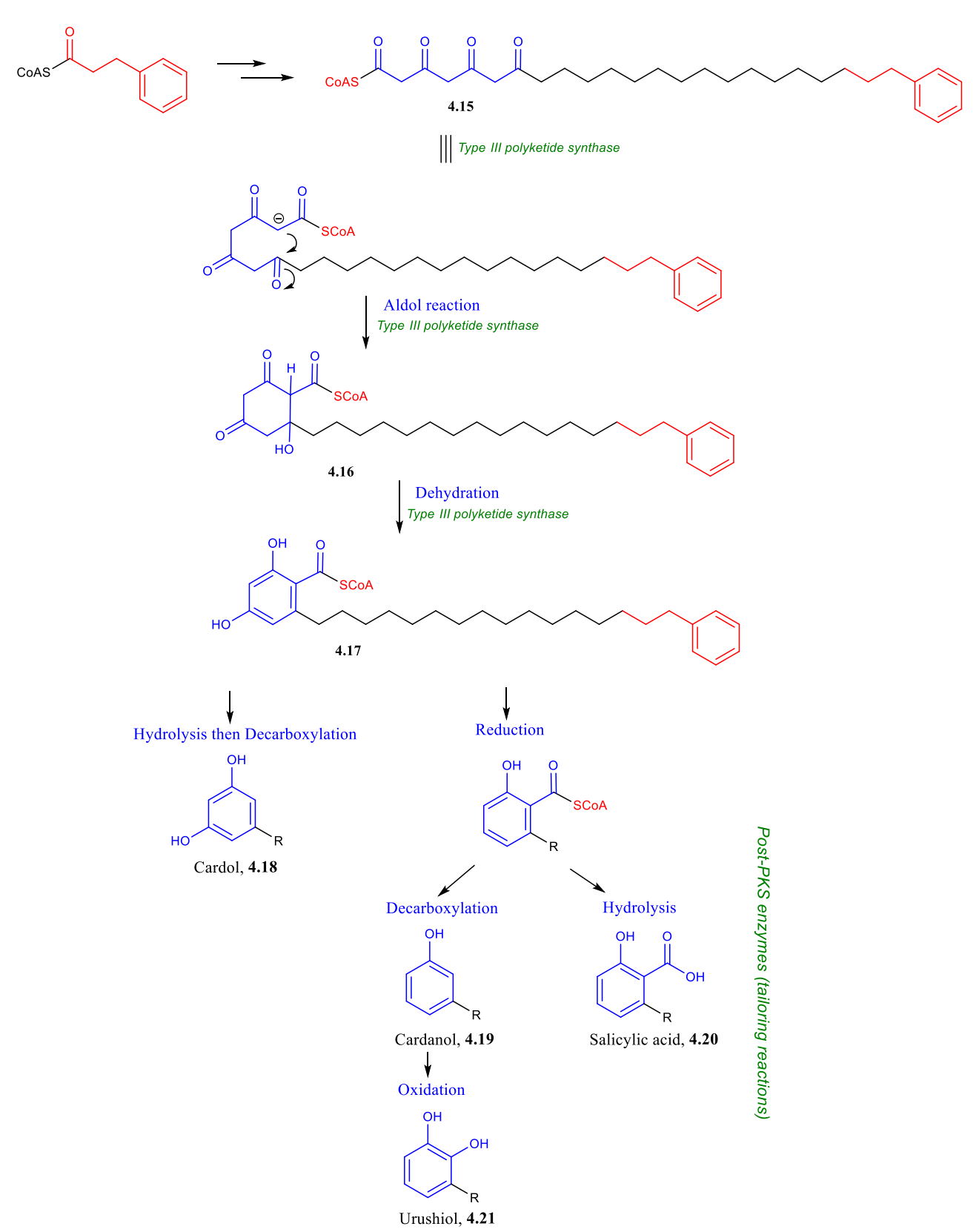


**Figure 4.35.** Proposed biosynthesis of Knema phenyl-alkyl compounds. R = 16 carbon alkyl chain with terminal phenyl.

# 4.2.6. Biological activities of isolated compounds

Among the six Myristicaceae species subjected to small-scale extraction and antimicrobial screening, two exhibited measurable antibacterial activity against MSSA (MIC <  $128 \, \mu g/mL$ , Table 4.13). As outlined above, the phytochemistry of these bioactive species was subsequently examined in greater detail. The unexplored antibacterial, anticancer and antifungal activities of isolated compounds from these species was investigated.

**Table 4.13.** *In vitro* antibacterial activity of Myristicaceae species measured using the broth microdilution assay to obtain the minimum inhibitory concentration (MIC) of each extract.

		MIC (µg/mL)		
Species	Extracting solvent	MSSA 25923	E. coli 10418	
Horsfieldia splendida	Hexane	>512	>512	
	Dichloromethane	512	>512	
	Methanol	512	>512	
Horsfieldia polyspherula	Hexane	512	>512	
	Dichloromethane	256	>512	
	Methanol	>512	>512	
Knema elmerii	Hexane	>512	>512	
	Dichloromethane	>512	>512	
	Methanol	>512	>512	
Knema latifolia	Hexane	>512	>512	
	Dichloromethane	>512	>512	
	Methanol	>512	>512	
Knema membranifolia	Hexane	128	>512	
	Dichloromethane	32	>512	
	Methanol	64	>512	
Gymnacranthera contracta	Hexane	128	>512	
	Dichloromethane	64	>512	
	Methanol	128	>512	

## 4.2.6.1. Antibacterial Activities of Isolated Myristicaceae Compounds

## K. membranifolia compound inactivity against Gram-negative bacterial strains

Despite all crude extracts being inactive against susceptible Gram-negative species, purified compounds were still screened on the basis that antagonism and/or concentration of compounds within the crude mixture were decreasing antibacterial effects. All purified compounds were screened against susceptible (*Escherichia coli* 10418, *Salmonella typhimurium* 14028S and *Pseudomonas aeruginosa* 10662) and multidrug resistant (*Klebsiella pneumonia* CPE16 and *Escherichia coli* G69) Gramnegative bacterial strains. All compounds had an MIC >128 μg/mL (with two biological repeats) and were therefore not investigated further within these strains.

**Table 4.14.** MIC values of compounds **4.1** – **4.6** tested against Gram-negative bacterial strains.

Bacterial strain	<b>Compounds 4.1 – 4.6</b>
Escherichia coli 10418	>128
Escherichia coli G69	>128
Salmonella typhimurium 14028S	>128
Pseudomonas aeruginosa 10662	>128
Klebsiella pneumonia CPE16	>128

### K. membranifolia compound activity against MSSA and MRSA

Moderate to strong activity against Gram-positive bacteria was exhibited by the *Knema* compounds isolated during this study. All isolated salicylic acid compounds displayed an extent of antibacterial activity against MSSA (Table 4.15). Compound **4.1** exhibited the lowest activity of the three (MIC =  $128 \, \mu g/mL$ ), followed by **4.3** (MIC =  $16 \, \mu g/mL$ ) and finally **4.2** (MIC 4 =  $\mu g/mL$ ). These data suggest that the linking alkane chain between the phenolic and phenyl ends of the molecule influences anti-MSSA activity. In future studies, to further investigate this effect, a 14-carbon linker salicylic acid-type compound should be assessed for its antibacterial activities, however this theoretical compound has not yet been discovered. The MBC values of **4.1** and **4.2** against MSSA were determined as 128 and 8  $\mu g/mL$ , respectively. However, the MBC of **4.3** was >32  $\mu g/mL$  and therefore unquantified, inferring that the additional two alkane carbons not

only decrease the MIC, but alter the mechanism of action, potentially rendering this compound bacteriostatic only. It is also worth noting that the importance of alkane chain length is demonstrated in the acetophenone compounds against all the *S. aureus* strains, whereby an increase of two carbons alters the compounds from moderately active to inactive (Table 4.15).

Interestingly, this effect is not shown in **4.3** against MRSA, where bactericidal activity is quantified at 8  $\mu$ g/mL, suggesting a difference in mechanism of action against strains MSSA and MRSA. In contrast, the pattern which shows **4.2** having the highest activity, which then decreases with increasing or decreasing alkane chain length, is maintained in the MRSA strain (with **4.1**, **4.2** and **4.3** possessing MIC values of 32, 2 and 8  $\mu$ g/mL), emphasising the importance of alkane length and suggesting similar modes of action of these compounds between the two strains.

In addition, studies have shown that **4.2** and **4.1** lacking the terminal phenyl have an MIC of 6  $\mu$ g/mL against MRSA, inferring the importance of this phenyl group, which causes a 3- or 5-fold increase, respectively, in anti-MRSA activity<sup>33</sup>. Kubo *et al.* determined the MIC of these compounds against the Gram-positive *Steptococcus mutans* 25175 at 2  $\mu$ g/mL. The terminal phenyl in **4.2** is likely to have the same enhancing effect on anti-*S. mutans* activity, warranting future investigations of compound **4.2** into this strain<sup>34</sup>. Green *et al.*, tested a range of synthesised and natural anacardic acids with variations in the hydrophobic tail portions and found that these parts of the compounds are correlated with antibacterial activities due the ability to readily disrupt membrane integrity. Here, 6-(4',8'-dimethylnonyl)salicylic acid displayed the lowest MIC at 0.39  $\mu$ g/mL against MRSA, with the others ranging from 6 – 100  $\mu$ g/mL, revealing that **4.2** found in this study is amongst the most potent anacardic acid-related compounds<sup>35</sup>.

Surprisingly, activity of the salicylic acid-related compounds isolated in this study are more potent against the MRSA than the MSSA. The MRSA 13373 used in this study contains the *mecA* gene, which encodes a low affinity penicillin binding protein (PBP2A),

thus reducing  $\beta$ -lactam effectiveness<sup>36</sup>. The results of this study suggest the absence of interaction between salicylic acid compounds and PBP2A, eliminating the possibility of PBP2A binding in their modes of action. Contrastingly, **4.4** displayed higher activity (MIC = 8  $\mu$ g/mL) against the MSSA than the MRSA (MIC = 16  $\mu$ g/mL), suggesting potential interaction of this compound with PBP2A, thus reducing the activity in the MRSA (Table 4.15).

# K. membranifolia compound activity against further resistant S. aureus strains

Compounds **4.1** and **4.3** lacked antibacterial activities against the other resistant *S. aureus* strains tested (MIC >128 µg/mL), whilst compound **4.2** displayed bactericidal activity at 8, 4 and 32 µg/mL against *S. aureus* RN4220, *S. aureus* 1188B and *S. aureus* XU212, respectively. *S. aureus* RN4220 contains the plasmid pUL5054, carrying the gene encoding the *MsrA* macrolide efflux protein<sup>37</sup>. These macrolide-specific efflux pumps are ATP-binding cassette (ABC) transport proteins which facilitate the energy-dependent efflux of macrolides to outside the bacterial cell<sup>38</sup>. The variation of MIC values of **4.2** throughout these strains highlights its relationship with their efflux pumping abilities.

S.~aureus~1199B overexpresses the NorA gene resulting in greater quantities of the NorA protein, which mediates the efflux of fluoroquinolones, as well as other structurally diverse compounds, to outside the bacterial cell<sup>39,40</sup>. Compound **4.2** and **4.4** displayed strong antibacterial activities (MIC = 4 and 32  $\mu$ g/mL, respectively), suggesting that the NorA protein is unable to efflux these compounds, however, does efflux the others tested (MIC >128  $\mu$ g/mL). Compound **4.6** is inactive exclusively against S.~aureus~1199B, suggesting that this structure potentially offers high affinity to the NorA efflux protein. The NorA's substrate binding pocket contains several aromatic residues and has ~65% lipophilic residues, making it likely to bind to aromatic compounds<sup>41,42</sup>.

S. aureus XU212 possesses the *TetK* gene, encoding tetracycline efflux proteins, thus inferring tetracycline resistance<sup>43</sup>. Compounds **4.2**, **4.4** and **4.6** displayed MIC values of 16, 4 and 4 µg/mL, respectively. Here, the efflux ability of the tetracycline efflux proteins

does not follow the same pattern as that of the *NorA* protein, with **4.2** potentially being effluxed at the highest rate.

The higher activity of **4.3** in the MSSA and MRSA compared with all three resistant strains RN4220, 1199B and XU212, suggests that these efflux pumps may be expelling this compound from within the cell, thus reducing its antibacterial activity. This emphasises the importance of the alkane chain linker of this compound. The fact that **4.1** has low activity against MSSA and the resistant efflux pump-possessing strains, versus moderate activity against MRSA (*MecA*-containing), suggests higher affinity to PBP2a than the PBPs present in MSSA<sup>44</sup>.

Compound **4.4** displays moderate activity against all *S. aureus* strains, whilst **4.5** displays none, demonstrating the importance of the additional two carbons in the alkane linker in this compound as well as in compounds **4.1** to **4.3**. The antibacterial activities of **4.4** are strongest against *S. aureus* XU212 (MIC 4 µg/mL). This is the same activity of **4.6**, and lower than activity of **4.2** within this strain. Compounds **4.6** and **4.4** are similar in the OH positionings meta to the C-6 alkane chain substitution, which could influence their activities. Based on structure, the acetophenone functional group positioning on **4.4** allows antibacterial activities of the compound, providing the alkane chain is only 8 carbons long. The antibacterial activities are similar within **4.4** and **4.6**, which highlights the importance of chain length and this substitution (providing the mechanisms of action are the same). For a deeper understanding of the SAR of these compounds, the resorcinols, salicylic acids and acetophenones with linkers of 8, 10 and 12 carbons should be investigated against each strain, to provide a comprehensive structure-antibacterial relationship report of these three compound types.

**Table 4.15.** *In vitro* antibacterial activity, showing MIC (shaded) and MBC values (μg/mL), of isolated compounds **4.1** – **4.6** against susceptible (MSSA 25923) and resistant strains of *Staphylococcus aureus*; MSSA: methicillin susceptible *Staphylococcus aureus*; MRSA: methicillin resistant *Staphylococcus aureus*; MIC: minimum inhibitory concentrations; MBC: minimum bactericidal concentration.

Compound		SSA 5923		RSA 3373		ireus 4220	S. au 119	reus 99B	S. au XU:	reus 212
4.1	128	128	32	32	>128	n.t.	>128	n.t.	>128	n.t.
4.2	4	8	2	2	8	8	4	4	16	32
4.3	16	>32	8	8	>128	n.t.	>128	n.t.	>128	n.t.
4.4	8	>16	16	32	8	8	32	>64	4	8
4.5	>128	n.t.	>128	n.t.	>128	n.t.	>128	n.t.	>128	n.t.
4.6	16	32	16	32	16	16	>128	n.t.	4	8
Ampicillin	>0.13	-	>0.13	-	>0.13	-	>0.13	-	>0.13	-

## K. membranifolia compound activity against Enterococcus faecalis strains

Compounds **4.1** – **4.6** were tested for their antibacterial activities against *E. faecalis*. Like the activity against *S. aureus*, **4.2** displayed the strongest activity, with MIC values of 4 and 2 µg/mL against the susceptible and resistant strains of *E. faecalis*, respectively. The optimal alkane chain length in the salicylic acid compounds was at 12 carbons, whilst either increasing or decreasing this length decreases activity, as aforementioned. Similarly, the increase in chain length between compounds **4.4** and **4.5** renders this compound inactive, matching the antibacterial trend occurring against the *S. aureus* (Table 4.16). The MIC of **4.1** displayed the largest difference between the two *E. faecalis* strains, suggesting that the resistance gene renders this strain more susceptible to the compound.

The mechanisms of action of all *Knema* compounds may be similar across the two *Enterococcus* species tested, as suggested by the consistent order of antibacterial potency observed among the compounds (Tables 4.15, 4.16). *E. faecalis* 51299 possesses the *vanB* gene, which confers vancomycin resistance by enabling an

alternative biosynthetic pathway during the production of peptidoglycan precursors, resulting in precursors which have low affinity to vancomycin. Vancomycin is a cell wall synthesis inhibitor that forms hydrogen bonds with the alanine region of Lipid II, a native peptidoglycan precursor. This binding prevents PBPs to cross linking Lipid II into mature peptidoglycan, thus compromising cell envelope integrity and causing cell death through osmotic stress. Therefore, the altered precursors with reduced vancomycin binding render the antibiotic ineffective<sup>45,46</sup>.

For all *Knema* compounds tested, antibacterial activity against susceptible *E. faecalis* was equal to or lower than that against the resistant strain. This suggests that their mode of action does not involve binding to native peptidoglycan precursors to inhibit cell wall synthesis. As mentioned above, a comprehensive SAR study of these compounds, including all compound classes with 8 to 16 carbon alkane linkers, is necessary to begin to properly speculate how linker lengths and functional groups affect antibacterial activities.

**Table 4.16.** *In vitro* antibacterial activities, displaying MIC (shaded) and MBC values (μg/mL), of isolated compounds **4.1** – **4.6** against susceptible (*E. faecalis* 12967) and resistant (*E. faecalis* 51299) strains of *Enterococcus faecalis* (n=2). MIC: minimum inhibitory concentrations; MBC: minimum bactericidal concentration.

Compound	E. faecalis 12967		E. faecalis 5129	
4.1	128	128	32	32
4.2	4	8	2	2
4.3	16	>32	8	8
4.4	8	>16	16	32
4.5	>128	n.t.	>128	n.t.
4.6	16	32	16	32
Ampicillin	>0.13	n.t.	>0.13	n.t.

#### **4.2.6.2. Conclusion**

Section 4.2.6 evaluates *K. membranifolia* compounds for their antibacterial activity, with a particular focus on Gram-positive pathogens, including MRSA and *E. faecalis* strains. Although crude extracts displayed no activity against Gram-negative bacteria, the screening of purified compounds revealed notable and selective effects against Gram-positive strains, particularly by the salicylic acid derivatives. Compound **4.2** consistently exhibited the highest potency, with bactericidal activity observed at low micromolar concentrations against MRSA and vancomycin-resistant *E. faecalis*, placing it amongst the most active natural salicylic acid analogues reported to date.

Structure-activity relationships observed across the isolated compounds indicate a clear influence of alkane chain length and functional group arrangement on antibacterial potency. A 12-carbon linker appears optimal, with aromatic group and chain length deviations either diminishing activity or potentially shifting the mode of action. Differential activity across resistant strains suggests specific interactions with known resistance mechanisms, including efflux pumps and modified target proteins such as PBP2A and *NorA*.

## 4.2.6.3. Anticancer Activities of Isolated Myristicaceae Compounds

This study aimed, in part, to investigate the anticancer potential of compounds which were isolated from the Myristicaceae and Clusiaceae families. Although anticancer activity did not directly guide the phytochemical investigations, pure compounds were evaluated *in vitro* against common cancer cell lines in Dr. Sobolewski's laboratory at the School of Chemistry, Pharmacy, and Pharmacology, University of East Anglia (UEA) by Dr Salonee Banerjee.

Initially, compounds **4.1** – **4.6**, were screened at 10  $\mu$ M and 100  $\mu$ M against A549, SK-MEL28, HL60, and RAW264.7 cancer cells. Results for this are shown in Appendix C, Figure C2 to C5. Here, compounds **4.1**, **4.2**, **4.3**, **4.4** and **4.6** were active against A549 cells, inhibiting growth at 100  $\mu$ M. This preliminary screening identified these compounds as candidates for further investigation. Subsequently, dose-response

curves were generated for these compounds in A549 cells over a concentration range from 6.26  $\mu$ M to 800  $\mu$ M, enabling further assessment of their cytotoxic potential. IC<sub>50</sub> values were calculated and are displayed in Table 4.17.

### Anticancer activity of compounds 4.1 – 4.3

The structure-activity relationship of the three salicylic acid derivatives against A549 lung cancer cells revealed a correlation between hydrocarbon chain length and cytotoxicity. Compound **4.2** (12-carbon linker,  $IC_{50} = 22.07 \mu M$ ) exhibited the highest potency, followed by compound **4.3** (16-carbon linker,  $IC_{50} = 43.19 \mu M$ ), while compound **4.1** (10-carbon linker,  $IC_{50} = 111.80 \mu M$ ) was the least effective. These data suggest that the hydrocarbon chain length and therefore hydrophobicity of these compounds play a role in their mechanism of action against A549 cells. Given that the C12 derivative was more effective than cisplatin ( $IC_{50} = 31.11 \mu M$ ), this compound demonstrates promising anticancer potential.

**Table 4.17.** Cytotoxic activity of isolated compounds against A549 lung cancer cells, displaying IC<sub>50</sub> values obtained using an AlamarBlue *in vitro* assay (n=3).

Compound	IC <sub>50</sub> (μΜ)
4.1	111.80
4.2	22.07
4.3	43.19
4.6	35.53
4.4	70.30
4.1/4.4	60.31
4.13/4.14	235.00
Cisplatin	18.57

#### Acetophenone and alkylresorcinol anticancer activity

Of the acetophenones isolated, **4.4** (8 carbon linker) was the only one to cause a decrease in fluorescence (p < 0.001) at 100  $\mu$ M during the initial screening. **4.4** was investigated further and displayed an IC<sub>50</sub> value of 70.30  $\mu$ M, highlighting the importance of the reduction in chain linker length by two carbons. Similarly to the salicylic acid

compounds, a 10-carbon linker is not optimal for cytotoxicity, however it is unknown weather an acetophenone with a 12-carbon linker enhances or decreases activity, as this compound is undiscovered and therefore untested.

The second most potent compound was **4.6** (IC<sub>50</sub> = 35.53  $\mu$ M). Interestingly, the 10-carbon linker length here offers cytotoxic activity, whereas this linker length was not optimal within the salicylic acids. These trends within the salicylic acids and acetophenones with 10-carbon linker chains infer the potential cytotoxic activity of a 12-carbon linker resorcinol. This was proven to be true by a previous study which found higher cytotoxicity of the 12-carbon linker resorcinol (LC<sub>50</sub> = 9.8  $\mu$ M) than the 8-carbon linker compound<sup>20</sup>.

Figure 4.36 displays the fluorescence intensity of cells treated with the compounds with IC $_{50}$  values less than 50  $\mu$ M. Here, **4.2** is the only compound to display a lower fluorescence intensity to the untreated control at every concentration point, whilst the cisplatin control displays this difference, with less statistical significance, within the top three concentrations. Although cisplatin has a lower half-maximal inhibitory concentration, **4.2** and **4.6** initiate a response at lower concentrations than the control.

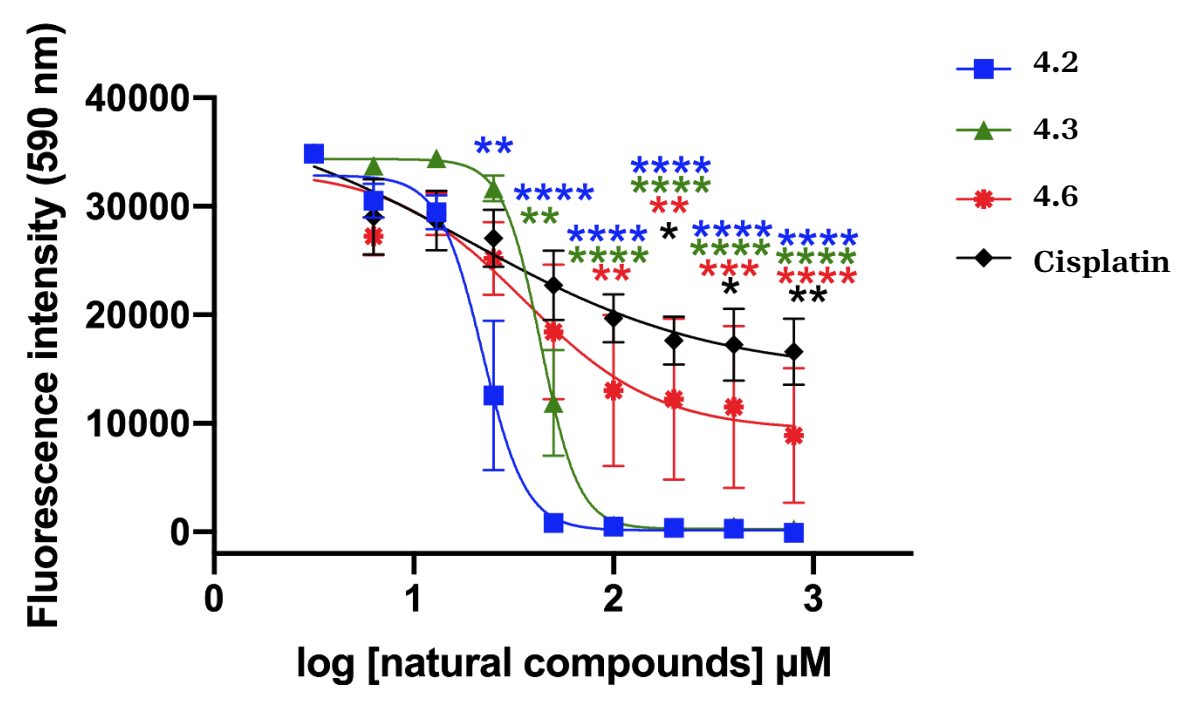


**Figure 4.36.** Dose-response curves of compounds **4.2**, **4.3** and **4.6** against A549 lung cancer cells in comparison to cisplatin. All values are expressed as mean +/- standard deviation; n = 3; \*\*\*\* p < 0.0001, \*\*\* p < 0.001, \*\*\* p < 0.01 and \*p < 0.05 at each concentration point when compared to untreated control cells.

#### Previous cytotoxic reports on compounds isolated from K. membranifolia

Studies have previously investigated the cytotoxicity of known compounds isolated from *K. membranifolia* during this study. Zeng *et al.*, previously investigated the *in vitro* anticancer activities of **4.2** (ED<sub>50</sub> values of 15, 3 and 3 μg/mL), **4.6** (ED<sub>50</sub> values of 3 μg/mL), **4.4** (ED<sub>50</sub> values of 4, 3 and 19 μg/mL) and **4.5** (ED<sub>50</sub> values of 3, 3 and 4 μg/mL) against A-549, MCF-7 and HT-29 cancer cell lines, respectively. During this study however, the positive control doxorubicin was significantly more active than the tested compounds, inferring limited cytotoxicity against cancer cells of these compounds.

The mutual cell line tested in this study was the A549 lung cancer cells, where the lowest EC<sub>50</sub> value translating to 9.6  $\mu$ M was exhibited by **4.6**, followed by compound **4.5** at 10.8  $\mu$ M and finally compound **4.2** at 39.2  $\mu$ M. Interestingly, the order of potency did not follow the same trend in this study, where the most potent compound was **4.2**,

followed by **4.6** and finally the **4.5**. While different methodologies may influence exact values, overall trends are expected to remain consistent. Notably, in the previous study, **4.6** and **4.5** exhibited similar potency, whereas in this study, **4.5** showed a two-fold increase in IC<sub>50</sub> value. This discrepancy emphasises the need for further investigation to fully understand the structure-activity relationships and reproducibility of these compounds' cytotoxic effects.

Zeng *et al.* also investigated the potential antineoplastic properties of these compounds by assessing their ability to inhibit crown gall tumour growth on potato discs. They reported inhibition rates of 61% for **4.2**, 62% for **4.6**, 38% for **4.4**, and 30% for **4.5**, demonstrating the antineoplastic potential of **4.2** and **4.6**. Although this study uses a distinct and different *in vitro* model for evaluating anticancer activity, the observed trend aligns with the findings presented in this thesis<sup>20</sup>.

To further evaluate their toxicity, a brine shrimp lethality assay was performed, where all compounds displayed potent activities with **4.2**, **4.6**, **4.4** and **4.5** displaying  $LC_{50}$  values of 1.24, 0.47, 0.37 and 0.18 µg/mL, respectively. Surprisingly, the trend in toxicity was reversed in this assay, but aligned with the mammalian cell *in vitro* assay, with **4.5** being the most potent and **4.2** being the least<sup>20</sup>.

Although these compounds have been previously tested against the A549 cancer cell line, this study is the first to report their activity against SK-MEL28, HL60, and RAW264.7 cancer cells. Additionally, this work provides a more comprehensive structure-activity relationship analysis by examining three salicylic acids with varying chain lengths in the same biological assay. The inconsistencies observed in activity from previous reports reinforce the importance of revisiting this work. Only *in vitro* screening assays of some of the compounds isolated in this thesis have been previously performed, and no mechanistic studies of salicylic acids with terminal phenyl groups have yet been undertaken.

### Previously reported anticancer mechanisms of anacardic acids

Previous studies have primarily examined the cytotoxic mechanisms of anacardic acids which lack the terminal phenyl group. This form is commonly referred to as anacardic acid, the most common of which features a 15-carbon alkyl side chain and constitutes 65% of cashew (*Anacardium occidentale*) nutshell extract<sup>47</sup>. Other natural compounds and synthetic derivatives from this, possessing side chains varying in length and saturation, have been explored for their anticancer properties, revealing that activity is largely due to mediation of histone acetyltransferases (HATs).

HATs are a class of enzymes responsible for catalysing histone acetylation, which in turn influences gene expression. HATs are categorised into three families: GCN5-related N-acetyltransferase, MYST (Moz, Ybf2/Sas3, and Tip60), and p300/CBP (CREB-binding protein). Among them, CBP/p300 is one of the most researched transcriptional co-activators due to its involvement in various cellular functions. Abnormalities in its function are linked to several major human diseases, including cancer, diabetes, viral infections, and asthma<sup>48</sup>.

Natural anacardic acids, including those which lack the terminal phenyl are known to inhibit P300 and P300/CBP associated factor (PCAF)<sup>49</sup>. Molecular modelling revealed that the salicylate moiety mimics the pyrophosphate group of CoA, forming hydrogen bonds with various chemical groups. In addition, the hydrocarbon chain remained in the pantothenic acid binding pocket, eliminating the importance of chain length and unsaturation. To assess this, synthetic derivatives of these were investigated, which found that a derivative containing an additional benzyl group and a *cis*-double bond significantly inhibited HAT activity by 50% *in vitro* in HepG2 liver cells (2-fold more than the 15-carbon saturated anacardic acid). Interestingly, there was no difference in activity between the 10- and 15-carbon chain saturated anacardic acids (which lack the terminal phenyl), whereas an increase in chain length by 2 carbons (4.1 vs 4.2) and 4 carbons (4.2 vs 4.3) rendered the molecule inactive or halved the IC<sub>50</sub> against A549 cells, respectively, in this study (Table 4.17). However, literature shows that introduction of

an aromatic ring within the chain did not affect HAT activity either<sup>50</sup>. These comparisons suggest that compound **4.2**, which possesses a terminal phenyl, may inhibit HAT activity, and that its chain length may be more important for activity than in regular anacardic acid compounds. However, this cannot be definitively deduced from the currently available data.

Further anticancer mechanisms of anacardic acids have been linked to HAT inhibition. These include reduced autophosphorylation of serine 2056, leading to DNA-PKcs enzyme inhibition; radiosensitisation of cancer cells; histone H3K9 hypoacetylation, affecting gene regulation; and antitumour activity mediated through NF-κB inhibition<sup>51-54</sup>. These findings suggest that HAT inhibition may contribute to the anticancer effects of salicylic acids examined in this study, although mechanistic studies are limited.

While anacardic acids have been extensively studied for their role in HAT inhibition, other anticancer mechanisms have also been explored. *In silico* studies suggest that anacardic acids selectively enhance aurora kinase activity, promoting histone H3 phosphorylation<sup>55</sup>. Additionally, the saturated anacardic acid (17:1) isolated from *Geranium* (Geraniaceae) exhibited cytotoxicity against BT-20 breast carcinoma cells, inhibiting proliferation of estrogen receptor alpha-positive breast cancer cells, disrupting cell cycle progression by reducing estrogen receptor-DNA interactions, and suppressing estrogen receptor-mediated transcription<sup>56</sup>.

### Previously reported anticancer mechanisms of alkyresorcinols

Alkylresorcinols (ARs) exert antitumour effects by damaging tumour cell DNA and inhibiting its repair, leading to increased genetic toxicity and cell death. This disruption prevents the growth of new cancer cells<sup>57,58</sup>. Recent studies suggest that natural plant compounds, including flavonoids and polyphenols, can trigger apoptosis and autophagy pathways, promoting tumour cell death and limiting their proliferation<sup>59</sup>.

Oskarsson and Ohlsson found that ARs affect steroid hormone production in human adrenocortical H295R cells by reducing testosterone synthesis and decreasing estradiol, cortisol, and aldosterone secretion. They found that this may be a result from CYP17

enzyme inhibition, which disrupts androgen and glucocorticoid synthesis while slightly increasing aldosterone production. As CYP17 is crucial for steroid hormone synthesis and a key target in prostate cancer treatment, AR-mediated CYP17 inhibition could be a potential strategy to limit androgen-dependent prostate cancer cell growth<sup>60</sup>. In addition, due to their high lipophilicity, ARs are believed to influence steroid hormone production by accumulating in lipid-rich tissues, including adipose tissue, testes, ovaries, and the adrenal cortex, which play key roles in steroidogenesis and therefore may play a role in chemoprevention<sup>61</sup>.

ARs have been associated a decreased risk in colorectal cancer in epidemiological studies, whereby an inverse correlation between AR blood plasma levels and risk of colon cancer development was observed in those with consistently high AR intake<sup>62,63</sup>.

In terms of *in vitro* studies, Sanchez *et al.* found that five natural ARs exhibited significantly greater cytotoxicity (9-fold higher) than adriamycin against MCF-7, H-460, and SF-268 cancer cell lines. These findings align with previous research showing the antiproliferative effects of 14 ARs isolated from a tropical tree on breast, lung, and central nervous system carcinoma cells<sup>67</sup>.

*In vitro* studies on HepG2 and Hep3B hepatocarcinoma cells showed that five ARs isolated from *L. molleoides* leaves induced DNA fragmentation and nuclear condensation (hallmarks of apoptosis) within 24 hours. Notably, cell death occurred independently of p53<sup>62</sup>. Research has consistently shown ARs to inhibit tumour cell growth, including ovarian, prostate, breast, and cervical cancer cells<sup>65-67</sup>. These findings suggest ARs may serve as promising adjuvants in cancer therapy.

To conclude the anticancer activities of AR compounds, their precise mechanisms remain unclear due to their multiple targets and complex biochemical interactions. They appear to induce apoptosis through DNA fragmentation and nuclear condensation, particularly in cells already damaged by genotoxic agents<sup>58,64</sup>. Meanwhile, some studies highlight their antioxidant properties, reducing ROS levels and inhibiting free radical-producing enzymes<sup>68,69</sup>. Despite their evident anticancer potential, further research is

needed to clarify the anticancer molecular mechanisms of ARs. Due lack of literature reports on specific molecular targets of ARs, it is difficult to evaluate which part of the molecular structure of **4.6** is responsible for activity in this study.

### Previously reported anticancer mechanisms of acetophenones

Many compounds which possess the acetophenone functional group exhibit anticancer properties, with some mechanistic studies providing insight into their mode of action. For example, the acetophenone xanthoxyletin suppresses the proliferation of human oral squamous carcinoma cells and induces apoptosis, autophagy, and cell cycle arrest through modulation of the MEK/ERK signalling pathway<sup>70</sup>. Most studies have focused on *in vitro* screening for antiproliferative abilities of acetophenones, displaying effects against multiple cancer cell lines including lung (A-549, NCI–H460), leukaemia (L1210, NALM6, Jurkat, HPB-ALL, K562, PBMNC), lymphoma (P-388), colon (HCT116, HT29), cervical (HeLa), liver (Hep-G2, Hep-3B) and stomach (AGS)<sup>71-75</sup>.

Among acetophenones, apocynin is particularly well studied<sup>76</sup>. Lirdprapamongkol *et al.* highlighted the importance of the carbonyl group in the acetophenone apocynin in its inhibitory effects of cell migration, where the ketone group was essential for this activity. Apocynin inhibited A-549 cell migration and selectively suppressed Akt phosphorylation in hepatocyte growth factor (HGF) signaling without affecting Met or Erk phosphorylation. An *in vitro* lipid kinase assay revealed that apocynin directly inhibited PI3K activity, inferring this as the mechanism behind its anti-migratory effects. The presence of an aldehyde or ketone group in the vanillin structure was essential for this inhibition. Additionally, apocynin reduced angiogenesis, revealed by the chick chorioallantoic membrane assay<sup>76,77</sup>. These structural-activity relationship studies and findings suggest that **4.4**, isolated in this study, may exhibit similar mechanisms amongst A-549 cells.

#### Previously reported biological activities of 4.7

Compound **4.7** was isolated during this study from both *G. caudiculata* (Clusiaceae) as well as *Gymnacranthera contracta* (Myristicaceae). This compound has been

previously investigated for its anticancer and antibacterial activities. *In vitro* antibacterial studies of **4.7** have been carried out, demonstrating lack of antibacterial properties of this compound. Ling *et al.*, assessed antibacterial activities against Grampositive and -negative bacteria including *B. subtilis, Micrococcus tetragenus, E. coli* and *P. fluorescens* with MIC values >1000 μg/mL<sup>78</sup>. However, moderate antibacterial activity was observed in another study with **4.7** displaying an MIC of 25 μg/mL against *Mycobacterium tuberculosis*<sup>79</sup>. A more recent study determined the MIC value of **4.7** against *S. aureus, Bacillus subtilis* and *Mycobacterium smegmatis* and determined this compound inactive against these strains<sup>80</sup>. Regarding anti-cancer activities, **4.7** has displayed moderate *in vitro* cytotoxicity against lung, breast, bladder, cervical and pancreatic cancer<sup>81</sup>.

## Previously reported biological activities of 4.8

Compound **4.8** has been investigated for its antibacterial properties, demonstrating significant inhibitory activity against *E. coli* and *K. pneumoniae*. However, its cytotoxicity against A549 lung carcinoma cells appears to be limited<sup>82</sup>.

## **4.2.6.4.** Conclusion

This study has identified multiple cytotoxic compounds from Myristicaceae species displaying significant *in vitro* anticancer activity. Compound **4.2** emerged as the most potent and consistent compound across assays (responsible for the activity of *K. membranifolia* recorded in the initial screening assay), while **4.6** also showed promising effects. Structure-activity trends within the salicylic acids and resorcinols suggest side chain length plays a crucial role in modulating activity. Though limited mechanistic data exist for these compound classes with terminal phenyl groups, available literature provides plausible biological pathways, particularly HAT inhibition and steroidogenic disruption.

#### 4.2.6.5. Antifungal Activities of Isolated Myristicaceae Compounds

The isolated Myristicaceae-derived compounds **4.1** – **4.6** were evaluated for antifungal activity against the critical priority pathogens *Aspergillus fumigatus* and *Candida* 

albicans using an *in vitro* AlamarBlue cell viability assay. This screening assessed the potential toxicity of these compounds against fungal cells. With the exception of compound **4.2**, none exhibited detectable antifungal activity. Compound **4.2** demonstrated moderate activity, reducing fungal cell viability to 62% at a concentration of 32  $\mu$ g/mL (Appendix C, Figure C6, presenting dose-response data for all tested compounds).

## 4.2.6.6. Previous reports of biological activities

Previous biological investigations (outside of bacterial and cancer cell cytotoxicity which are described in sections 4.2.6.2 and 4.2.6.3) of compounds isolated from *Knema* during this study are limited. Only one study by Tian *et al.*, assessed the potential of compound **4.2** in the treatment of Alzheimer's disease, by investigating its  $\beta$ -site amyloid precursor protein cleaving enzyme (BASE) inhibitory activity. **4.2** displayed potent inhibitory activity, at 7.7  $\mu$ M<sup>19</sup>. To the best of my knowledge, compound **4.1** has not had any biological activities previously reported.

#### 4.3. References

- J. H. Beaman, W. J. J. O. de Wilde and P. F. Stevens, Kew Bull, 2002, 14, 251.
- J. Kuusipalo, Y. Jafarsidik, G. Ådjers and K. Tuomela, For Ecol Manage, 1996, 81, 85–94.
- M. Siregar and E. N. Sambas, *Proceedings of the International Symposium on Tropical Peat Lands*, Floristic Composition of Peat Swamp Forests in Mensemat-Sambas, West Kalimantan, Hokkaido University & Indonesian Institute of Sciences, 1999, 153–164.
- D. Astiani, H. A. Ekamawanti, W. Ekyastuti, T. Widiastuti, G. E. Tavita and M. A. Suntoro, *Biodiversitas*, 2021, **22**, 2571–2578.
- 5 C. Ling and S. Julia, *Gard Bull Singapore*, 2012, **64**, 139–169.
- 6 V. K. S. Shukla and U. Blicher-Mathiesen, Fett Wiss Technol, 1993, 95, 367–369.
- M. Matsue, Y. Mori, S. Nagase, Y. Sugiyama, R. Hirano, K. Ogai, K. Ogura, S. Kurihara and S. Okamoto, *Cell Transplant*, 2019, **28**, 1528–1541.
- 8 L. Borrelli, L. Varriale, L. Dipineto, A. Pace, L. F. Menna and A. Fioretti, *Front Microbiol*, 2021, **12**, 620798.
- 9 W. C. Huang, T. H. Tsai, L. T. Chuang, Y. Y. Li, C. C. Zouboulis and P. J. Tsai, *J Dermatol Sci*, 2014, **73**, 232–240.
- 10 E. H. M. Temme, R. P. Mensink and G. Hornstra, *Am J Clin Nutr*, 1996, **63**, 897–903.
- 11 R. Lappano, A. Sebastiani, F. Cirillo, D. C. Rigiracciolo, G. R. Galli, R. Curcio, R. Malaguarnera, A. Belfiore, A. R. Cappello and M. Maggiolini, *Cell Death Discov*, 2017, **3**, 17063.
- A. Intisar, L. Zhang, H. Luo, J. B. Kiazolu, R. Zhang and W. Zhang, *Afr J Tradit Complement Altern Med*, 2012, **10**, 53–59.

- 13 S. Liu, W. Ruan, J. Li, H. Xu, J. Wang, Y. Gao and J. Wang, *Mycopathologia*, 2008, **166**, 93–102.
- 14 S. Virshette, M. Patil and A. Somkuwar, *J Pharmacogn Phytochem*, 2019, **8**, 1541–1546.
- 15 G. F. Spencer, L. W. Tjarks and R. Kleiman, *J Nat Prod*, 1980, **43**, 724–730.
- M. J. T. G. Gonzalez, C. J. C. DeOliveira, J. O. Fernandes, A. Kijjoa and W. Herz, *Phytochemistry*, 1996, **43**, 1333–1337.
- 17 M. M. M. Pinto, A. Kijjoa, I. on Mondranondra, A. B. Gutiérrez and W. Herz, *Phytochemistry*, 1990, **29**, 1985–1988.
- 18 A. Kijjoa, M. J. T. G. Gonzalez, M. M. M. Pinto, I. O. Monanondra and W. Herz, *Planta Med*, 1991, **57**, 575–577.
- 19 X. Y. Tian, Y. Zhao, S. S. Yu and W. S. Fang, *Chem Biodivers*, 2010, 7, 984–992.
- 20 L. Zeng, Z.-M. Gu, X.-P. Fang and J. L. Mclaughlin, *J Nat Prod*, 1994, **57**, 376–381.
- U. Sriphana, C. Yenjai and M. Koatthada, *Phytochem Lett*, 2016, **16**, 129–133.
- 22 Y. Du and R. Oshima, *J Chromatogr A*, 1985, **318**, 378–383.
- 23 T. Sorensen, M. Benn, S. Lynds and E. B. Knox, *Arkivoc*, 2009, **2009**, 17–22.
- 24 H. Sung, O. Lee, L. K. Son, N. S. Park, M. R. Kim, J. G. Kim and D. C. Moon, *Arch Pharm Res*, 1999, **22**, 633–637.
- D. H. S. Silva, F. C. Pereira, M. V. B. Zanoni and M. Yoshida, *Phytochemistry*, 2001, 57, 437–442.
- 26 F. L. Wu, B. P. Ross and R. P. McGeary, Eur J Org Chem, 2010, 2010, 1989–1998.
- B. E. Rivero-Cruz, N. Esturau, S. Sanchez-Nieto, I. Romero, I. Castillo-Juárez and J. F. Rivero-Cruz, *Nat Prod Res*, 2011, **25**, 1282–1287.
- T. D. Christelle, H. Hussain, E. Dongo, J. M. B. Hermine, I. Ahmed and K. Krohn, *Nat Prod Commun*, 2011, **6**, 1133–1134.
- 29 A. S. Salihu and W. M. N. H. W. Salleh, Vietnam J Chem, 2023, 61, 397-411.
- 30 W. M. N. H. W. Salleh, M. Z. A. Anuar, S. Khamis, M. A. Nafiah and M. D. Sul'ain, *Nat Prod Res*, 2019, **35**, 2279–2284.
- S. Ghosal, R. Sundaram, A. V. Muruganandam, S. K. Singh, K. S. Satyan, S. K. Bhattacharya, V. Saravanan and N. Mishra, *Indian J Chem*, 1997, **38**, 257–263.
- D. J. Schultz, N. S. Wickramasinghe and C. M. Klinge, in *Recent Advances in Phytochemistry*, Elsevier, 2006, **40**, 131–156.
- 33 H. Muroi, K. I. Nihei, K. Tsujimoto and I. Kubo, *Bioorg Med Chem*, 2004, **12**, 583–587.
- 34 I. Kubo, K. I. Nihei and K. Tsujimoto, *J Agric Food Chem*, 2003, **51**, 7624–7628.
- 35 I. R. Green, F. E. Tocoli, S. H. Lee, K. ichi Nihei and I. Kubo, *Bioorg Med Chem*, 2007, **15**, 6236–6241.
- 36 C. L. C. Wielders, A. C. Fluit, S. Brisse, J. Verhoef and F. J. Schmitz, *J Clin Microbiol*, 2002, **40**, 3970.
- 37 S. Gibbons, M. Oluwatuyi and G. W. Kaatz, *J Antimicrob Chemother*, 2003, **51**, 13–17.
- 38 K. D. Ambrose, R. Nisbet and D. S. Stephens, Antimicrob Agents Chemother, 2005, 49, 4203.
- 39 G. W. Kaatz and S. M. Seo, *Antimicrob Agents Chemother*, 1995, **39**, 2650–2655.
- 40 P. N. Markham, E. Westhaus, K. Klyachko, M. E. Johnson and A. A. Neyfakh, *Antimicrob Agents Chemother*, 1999, **43**, 2404–2408.
- D. N. Brawley, D. B. Sauer, J. Li, X. Zheng, A. Koide, G. S. Jedhe, T. Suwatthee, J. Song, Z. Liu, P. S. Arora, S. Koide, V. J. Torres, D. N. Wang and N. J. Traaseth, *Nat Chem Biol*, 2022, **18**, 706.

- 42 K. A. Klyachko, S. Schuldiner and A. A. Neyfakh, *J Bacteriol*, 1997, **179**, 2189–2193.
- 43 S. Gibbons and E. E. Udo, *J Antimicrob Chemother*, 2000, **14**, 139–140.
- 44 A. Wada and H. Watanabe, *J Bacteriol*, 1998, **180**, 2759–2765.
- 45 H. S. Gold, Clin Infect Dis, 2001, **33**, 210–219.
- 46 P. J. Stogios and A. Savchenko, *Protein Sci*, 2020, **29**, 654–669.
- 47 F. B. Hamad and E. B. Mubofu, *Int J Mol Sci*, 2015, **16**, 8569–8590.
- 48 F. J. Dekker and H. J. Haisma, *Drug Discov Today*, 2009, **14**, 942–948.
- 49 K. Balasubramanyam, V. Swaminathan, A. Ranganathan and T. K. Kundu, *J Biolog Chem*, 2003, **278**, 19134–19140.
- 50 M. Ghizzoni, A. Boltjes, C. De Graaf, H. J. Haisma and F. J. Dekker, *Bioorg Med Chem*, 2010, **18**, 5826–5834.
- 51 R. T. Cate, P. Krawczyk, J. Stap, J. A. Aten and N. A. Franken, *Oncol Lett*, 2010, 1, 765–769.
- 52 Y. Sun, X. Jiang, S. Chen and B. D. Price, *FEBS Lett*, 2006, **580**, 4353–4356.
- 53 B. Sung, M. K. Pandey, K. S. Ann, T. Yi, M. M. Chaturvedi, M. Liu and B. B. Aggarwal, *Blood*, 2008, **111**, 4880–4891.
- J. Tan, B. Chen, L. He, Y. Tang, Z. Jiang, G. Yin, J. Wang and X. Jiang, *Chin J Cancer Res*, 2012, **24**, 275–283.
- A. H. Kishore, B. M. Vedamurthy, K. Mantelingu, S. Agrawal, B. A. A. Reddy, S. Roy, K. S. Rangappa and T. K. Kundu, *J Med Chem*, 2008, **51**, 792–797.
- D. J. Schultz, N. S. Wickramasinghe, M. M. Ivanova, S. M. Isaacs, S. M. Dougherty, Y. Imbert-Fernandez, A. R. Cunningham, C. Chen and C. M. Klinge, *Mol Cancer Ther*, 2010, **9**, 594–605.
- 57 S. R. Starck, J. Z. Deng and S. M. Hecht, *Biochemistry*, 2000, **39**, 2413–2419.
- 58 K. Gasiorowski, A. Kulma, K. Skórkowska and B. Brokos, Cell Mol Biol Lett, 2001, 6, 649–675.
- 59 L. Liu, K. M. Winter, L. Stevenson, C. Morris and D. N. Leach, *Food Chem*, 2012, **130**, 156–164.
- A. Gsur, G. Bernhofer, S. Hinteregger, S. Haidinger, G. Schatzl, S. Madersbacher, M. Marberger, C. Vutuc and M. Micksche, *Int J Cancer*, 2000, **87**, 434–437.
- 61 A. Oskarsson and Å. Ohlsson Andersson, Nutr Cancer, 2016, 68, 978–987.
- M. D. Knudsen, C. Kyro, A. Olsen, L. O. Dragsted, G. Skeie, E. Lund, P. Åman, L. M. Nilsson, H.
   B. Bueno-De-Mesquita, A. Tjonneland and R. Landberg, Am J Epidemiol, 2014, 179, 1188–1196.
- C. Kyrø, A. Olsen, R. Landberg, G. Skeie, S. Loft, P. Åman, M. Leenders, V. K. Dik, P. D. Siersema, T. Pischon, J. Christensen, K. Overvad, M. C. Boutron-Ruault, G. Fagherazzi, V. Cottet, T. Kühn, J. Chang-Claude, H. Boeing, A. Trichopoulou, C. Bamia, D. Trichopoulos, D. Palli, V. Krogh, R. Tumino, P. Vineis, S. Panico, P. H. Peeters, E. Weiderpass, T. Bakken, L. A. Åsli, M. Argüelles, P. Jakszyn, M. J. Sánchez, P. Amiano, J. M. Huerta, A. Barricarte, I. Ljuslinder, R. Palmqvist, K. T. Khaw, N. Wareham, T. J. Key, R. C. Travis, P. Ferrari, H. Freisling, M. Jenab, M. J. Gunter, N. Murphy, E. Riboli, A. Tjønneland and H. B. Bueno-De-Mesquita, *J Natl Cancer Inst*, 2014, 106, djt352.
- 64 L. Barbini, P. Lopez, J. Ruffa, V. Martino, G. Ferraro, R. Campos and L. Cavallaro, *World J Gastroenterol*, 2006, **12**, 5959–5963.
- V. S. P. Chaturvedula, J. K. Schilling, J. S. Miller, R. Andriantsiferana, V. E. Rasamison and D. G. I. Kingston, *J Nat Prod*, 2002, **65**, 1627–1632.
- 66 K. Isao, O. Masamitsu, V. Paulo and K. Sakae, *J Agric Food Chem*, 1993, **41**, 1012–1015.

- 67 T. H. Chuang and P. L. Wu, *J Nat Prod*, 2007, **70**, 319–323.
- 68 Â. Luís, F. Domingues and A. Paula Duarte, *Mini Rev Med Chem*, 2016, **16**, 851–854.
- 69 A. A. Zabolotneva, O. P. Shatova, A. A. Sadova, A. V. Shestopalov and S. A. Roumiantsev, *J Nutr Metab*, 2022, **2022**, 4667607.
- 70 Q. Wen, K. Luo, H. Huang, W. Liao and H. Yang, Med Sci Monit, 2019, 25, 8025–8033.
- 71 K. Du, Z. Zhang, D. Jing, Y. Wang, X. Li and D. Meng, *Phytochemistry*, 2022, **203**, 113382.
- 72 T. H. Giap, H. T. Thoa, V. T. K. Oanh, N. T. M. Hang, N. H. Dang, D. N. Thuc, N. Van Hung and L. N. Thanh, *Nat Prod Commun*, 2019, **14**, 1–5.
- 73 C. Ito, M. Hosono, H. Tokuda, T.-S. Wu and M. Itoigawa, *Nat Prod Commun*, 2016, **11**, 1299–1302.
- 74 T. S. Wu, M. Ling Wang, T. T. Jong, A. T. McPhail, D. R. McPhail and K. H. Lee, *J Nat Prod*, 1989, **52**, 1284–1289.
- P. Panyasawat, A. Wisetsai, R. Lekphrom, T. Senawong and F. T. Schevenels, *Nat Prod Res*, 2022, **36**, 2743–2752.
- H. Ahmadpourmir, H. Attar, J. Asili, V. Soheili, S. F. Taghizadeh and A. Shakeri, *Nat Prod Bioprospect*, 2024, **14**, 1–36.
- 77 K. Lirdprapamongkol, J. P. Kramb, T. Suthiphongchai, R. Surarit, C. Srisomsap, G. Dannhardt and J. Svasti, *J Agric Food Chem*, 2009, **57**, 3055–3063.
- 78 T. J. Ling, W. W. Ling, Y. J. Chen, X. C. Wan, T. Xia, X. F. Du and Z. Z. Zhang, *Molecules*, 2010, **15**, 8469–8477.
- 79 J.-J. Chen, W.-J. Lin, P.-C. Shieh, I.-S. Chen, C.-F. Peng and P.-J. Sung, *Chem Biodivers*, 2010, 7, 717–721.
- 80 H. T. Nguyen, D. V. Ho, H. Q. Vo, A. T. Le, H. M. Nguyen, T. Kodama, T. Ito, H. Morita and A. Raal, *Pharm Biol*, 2017, **55**, 787–791.
- A. Hamed, M. El Gaafary, L. Fumiko Yamaguchi, H. G. Stammler, L. M. Salih, D. Ziegler, T. Syrovets and M. J. Kato, *Nat Prod Res*, 2024, **19**, 1–7.
- N. Padmini, N. Rashiya, N. Sivakumar, N. D. Kannan, R. Manjuladevi, P. Rajasekar, N. M. Prabhu and G. Selvakumar, *Microb Pathog*, 2020, **148**, 104446.

# Chapter 5 – Isolation, Structure Elucidation and Biological Activities of Secondary Metabolites From Clusiaceae

#### 5.1. Introduction

Of the three species subjected to small-scale extraction and antibacterial screening, *Garcinia caudiculata* was the only one to exhibit activity. Consequently, a larger-scale extraction was undertaken to investigate its phytochemistry in greater detail. This chapter first presents the chemical analysis of this species, followed by an evaluation and discussion of the biological activities of the isolated compounds.

# 5.1.1. Garcinia caudiculata Ridl./Garcinia grahamii Pierre

*G. caudiculata*, also known as *G. grahamiii*, is a tree endemic to Borneo, growing in mixed diterocarp forests to elevations up to 334 m<sup>1,2</sup>. The identification of the species *G. caudiculata* is based on a holotype<sup>3</sup>. No previous biological or phytochemical investigations of this species have been undertaken.

#### 5.2. Results and Discussions

#### 5.2.1. Structure elucidation - Garcinia caudiculata

# 5.2.1.1.5-hydroxy-7-(3,7,11,15-tetramethylhexadeca-2,6,10,11-tetraenyl-2(3*H*)-benzofuranone (5.1, known)

Compound **5.1** was isolated as a yellow oil at 7.4 mg from a dichloromethane extract. The molecular formula was established as  $C_{28}H_{38}O_3$  ( $\Delta$  = -2.2 ppm) using positive mode Q-ToF MS, which displayed the protonated molecular ion [M+H]<sup>+</sup> at m/z 423.289.

The <sup>1</sup>H NMR spectrum of **5.1** revealed one aromatic signal at  $\delta_{\rm H}$  6.63 – 6.55 ppm (H-5, H-3, multiplet) which represented the two aromatic methines, with 2D HSQC correlations to the only two non-quaternary aromatic carbons C-5 and C-3. This, along with the <sup>13</sup>C spectra which revealed four remaining quaternary carbons at  $\delta_{\rm C}$  147.0, 123.8, 152.4 and 126.1 ppm, suggested the presence of a 1,2,4,6-tetrasubstituted aromatic ring. A doublet at  $\delta_{\rm H}$  3.71 ppm (H-2', doublet, J = 19.5 Hz) represented an additional benzyl group which displayed HMBC correlations to the carbonyl at C-1', and the quaternary aromatic carbons C-1 and C-2, revealing the presence of the butanolide carboxyl.

The <sup>1</sup>H NMR also revealed the presence of four olefinic protons at  $\delta_{\rm H}$  5.28 ppm (H-8, triplet, J = 6.8 Hz) and  $\delta_{\rm H} 5.06 - 5.14$  ppm (H-12, H-16, H-20, multiplet). In addition, the  $^{13}$ C and  $^{1}$ H spectra displayed eight olefinic carbons at  $\delta_{\rm C}$  120.6 (C-8), 137.9 (C-9), 124.5 (C-12), 135.4 (C-13), 124.4 (C-16), 135.2 (C-17), 124.1 (C-20) and 131.5 ppm (C-21), twelve allylic protons  $\delta_H$  1.94 – 2.14 (H-10, -11, -14, -15, -18 and -19, multiplet), five vinylic methyls represented by <sup>1</sup>H singlets at  $\delta_{\rm H}$  1.71 ppm (H-1", CH<sub>3</sub>), 1.68 ppm (H-22, H-3"/2", CH<sub>3</sub>) and 1.59 ppm (H-4", H-3"/2", CH<sub>3</sub>) and five methyl carbons in the <sup>13</sup>C spectrum. These spectra were characteristic of four C-5 isoprene units forming a C<sub>20</sub> geranylgeranyl sidechain. The <sup>1</sup>H and <sup>13</sup>C NMR chemical shifts and overall spectral patterns were consistent with reported data for the all-trans geranylgeranyl chain. Given that naturally occurring geranylgeranyl groups are known to adopt an all-trans configuration, the double bonds are likely to be trans by comparison and exact matches with literature values. However, from these data alone, coupling constants for the olefinic protons could not be extracted due to overlapping multiplets, and have therefore not been definitively assigned (Figure 5.1). The presence of an additional benzyl group was indicated by a <sup>1</sup>H doublet at  $\delta_{\rm H}$  3.33 ppm (H-7, doublet, J = 7.2 Hz), which displayed HMBC correlations to aromatic carbons C-5, C-6 and C-1 as well as carbons in the attached chain at C-8 and C-9. In addition, the H-8 olefinic proton displayed 2D COSY correlations to these benzylic protons, suggesting it's positioning on the geranylgeranyl group attached to the aromatic ring.

Spectral data obtained in this study were closely compared to previously published data, showing a close match. Some  $^{1}$ H signals displayed differences, for example the aromatic protons in both previous reports were reported as a singlet representing two protons, whereas this report has identified a multiplet ( $\delta_{H}$  6.63 – 6.55 ppm) comprised of two overlapping doublets corresponding to these aromatic protons. Similarly to previous reports, the methyl at 1" appeared as an individual singlet. However, the previously reported shared methyl singlet representing nine protons at H-4", H-3" and H-2" (leaving the third singlet to represent the H-22 methyl) suggests a different assignment to this report<sup>4,5</sup>. The integration of the spectra in this study shows two singlets

representing six protons each at  $\delta_H$  1.59 and 1.68 ppm, with each showing an HSQC correlation to C-4" and C-22, respectively. Thus, leaving the methyls at H-3" and H-2" each belonging to either of these signals, however due to their proximity in  $\delta_C$ , this assignment could not be absolute.

Compound **5.1** was initially isolated from the fruits of *Iryanthera grandis* (Myristicaceae), where it was characterised based on the <sup>1</sup>H NMR and MS data<sup>5</sup>. It was later identified from the stems of *Rhus chinensis* of the Anacardiaceae family, where it was characterized using MS, <sup>1</sup>H and <sup>13</sup>C NMR <sup>4</sup>. This is the first study to identify **5.1** from the Clusiaceae family, as well as report the 2D NMR data, these data were published<sup>6</sup>.

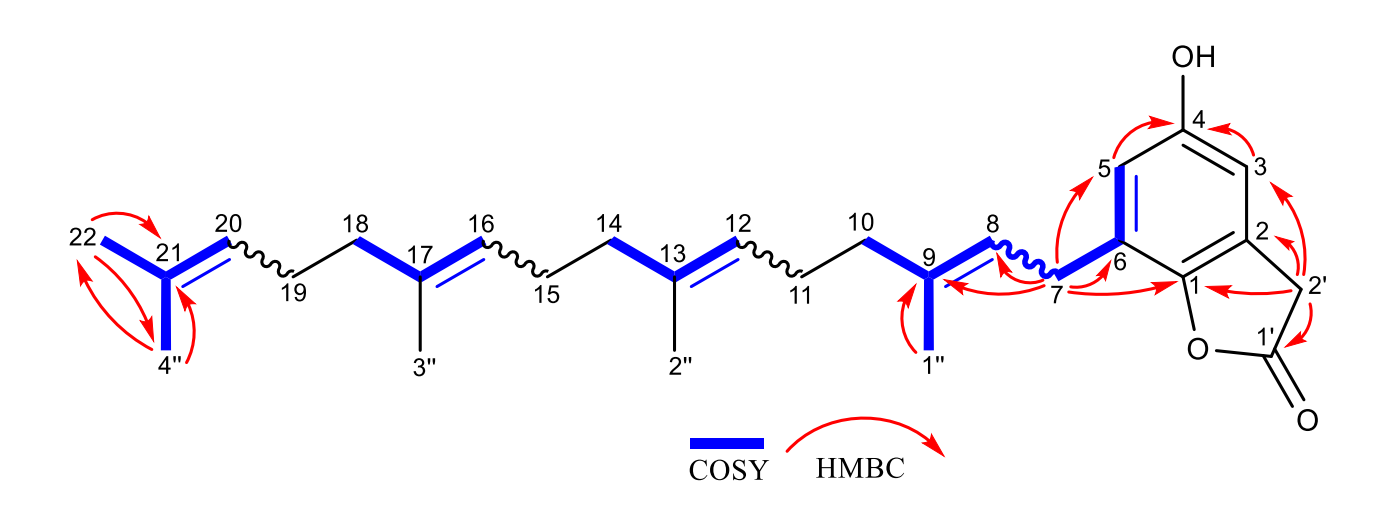


Figure 5.1. Key COSY and HMBC correlations of compound 5.1.

Table 5.1. <sup>1</sup>H, <sup>13</sup>C, COSY and HMBC NMR data of compound 5.1 (CDCl<sub>3</sub>, 600/150 MHz).

Position	$\delta_{\rm c}$ (ppm), type	$\delta_{ m c}{}^{4}$	$\delta_{\rm H}$ , mult. ( <i>J</i> in Hz)	COSY	HMBC
1	147.0, C	146.8, C	-	-	2', 7
2	123.8, C	123.6, C	-	-	2'
3	109.3, CH	109.2, CH	6.63 - 6.55, $m$	-	2'
4	152.4, C	152.3, C	-	-	5, 3
5	115.5, CH	115.4, CH	6.63 – 6.55, <i>m</i>	7	7

6	126.1, C	125.9, C	-	-	7
7	$27.9$ , $\mathrm{CH}_2$	27.7, CH <sub>2</sub>	3.33, d (7.2)	8, 5, 1"	-
8	120.6, CH	120.4, CH	5.28, t (6.8)	7	7
9	137.9, C	137.5, C	-	-	1", 7
10	39.9*, CH <sub>2</sub>	39.7, CH <sub>2</sub>	1.94 - 2.14, $m$	12	-
11	$26.9$ , $CH_2$	26.7, CH <sub>2</sub>	1.94 - 2.14, $m$	12	-
12	124.5, CH	124.4, CH	5.06 – 5.14, <i>m</i>	10, 11, 14	-
13	135.4, C	135.2, C	-	-	-
14	39.9*, CH <sub>2</sub>	39.7, CH <sub>2</sub>	1.94 - 2.14, m	12, 16	-
15	$26.6$ , $CH_2$	26.0, CH <sub>2</sub>	1.94 - 2.14, $m$	16	-
16	124.4, CH	124.2, CH	5.06 – 5.14, <i>m</i>	14, 15, 18	-
17	135.2, C	135.0, C	-	-	-
18	$39.8$ , $\mathrm{CH}_2$	39.7, CH <sub>2</sub>	1.94 - 2.14, m	20, 16	-
19	$26.8, \mathrm{CH}_2$	26.5, CH <sub>2</sub>	1.94 – 2.14, <i>m</i>	20	-
20	124.1, CH	124.0, CH	5.06 – 5.14, <i>m</i>	18, 19, 4", 22	-
21	131.5, C	131.3, C	-	-	22, 4"
22	25.6, CH <sub>3</sub>	25.7, CH <sub>3</sub>	1.68, s	20	-
1'	174.7, C	174.6, C	-	-	2'
2'	34.1, CH2	33.9, CH <sub>2</sub>	3.71, d (19.5)	-	-
1"	16.3, $CH_3$	16.2, CH <sub>3</sub>	1.71, s	7	-
2"	16.21*, CH <sub>3</sub>	16.0, CH <sub>3</sub>	1.59*, s	-	-
3"	16.16*, CH <sub>3</sub>	16.0, CH <sub>3</sub>	1.68*, s	-	-
4"	17.8, CH <sub>3</sub>	17.6, CH <sub>3</sub>	1.59, s	20	-

 $<sup>\</sup>overline{\,^4\!Reference}$  carbon chemical shifts of  $\alpha\text{-tocopherol}$  quinone measured in CDCl3.

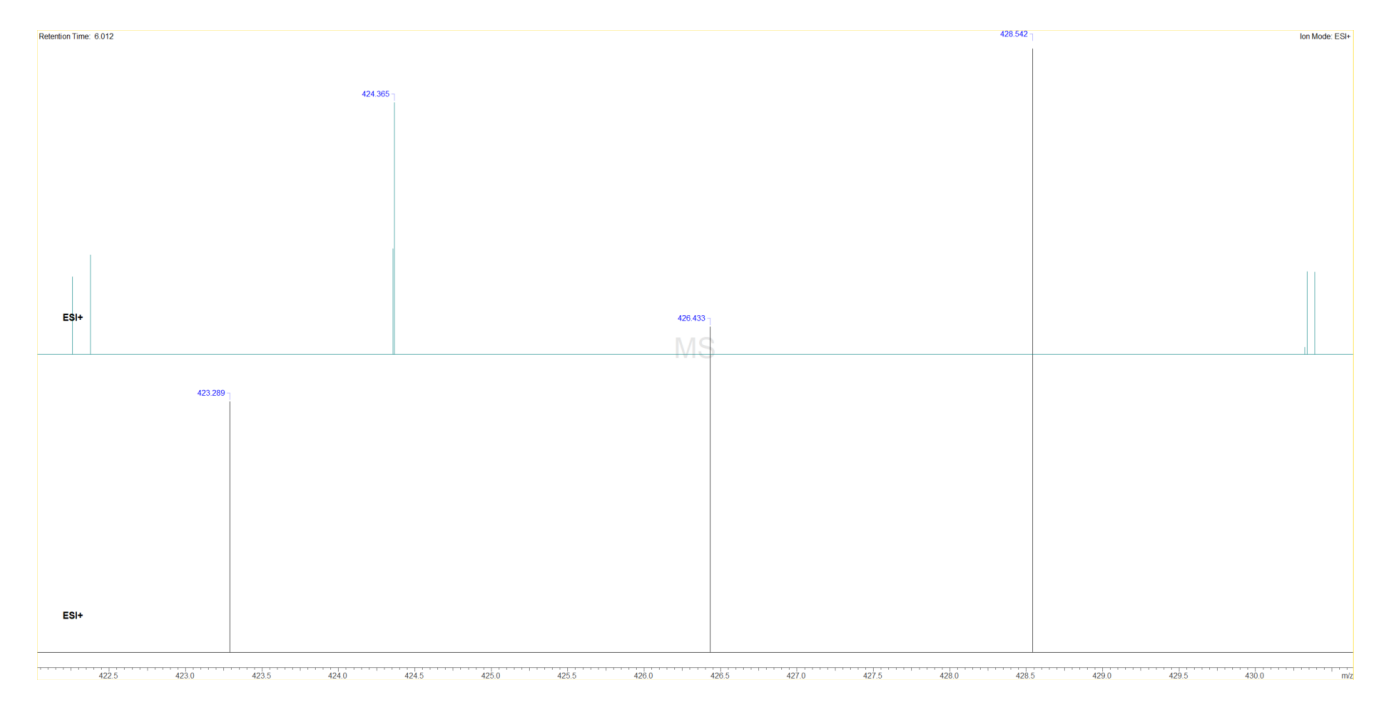


Figure 5.2. Mass spectrum of compound 5.1.

# **5.2.1.2.** Caudiquinol (**5.2**, new)

Compound **5.2** was isolated as a yellow oil at 6 mg and its molecular formula was established as  $C_{29}H_{42}O_4$  from the molecular ion [M+H]<sup>+</sup> at m/z 455.316 ( $\Delta$  = 0 ppm), which was revealed in the positive mode Q-ToF mass spectrum. An additional adduct displayed a molecular ion peak of [M+NH<sub>4</sub>]<sup>+</sup> at m/z 472.343 ( $\Delta$  = -2.1 ppm). The <sup>1</sup>H and <sup>13</sup>C NMR spectra indicated a  $C_{20}$  geranylgeranyl sidechain in **5.2**, displaying the same olefinic proton and carbon signals, as well as the twelve allylic protons, five vinylic methyls and five methyl carbons as compound **5.1**. The NMR data were consistent with literature data for an all-trans geranylgeranyl chain. As naturally occurring geranylgeranyl groups typically adopt this configuration, the double bonds are most likely trans. However, coupling constants for the olefinic protons could not be determined due to overlapping multiplets (Figure 5.2). In addition, compound **5.2** displayed IR absorptions at 3387 and 1714 cm<sup>-1</sup> inferring the presence of OH and C=O functional groups (Figure 5.5).

Similarly to compound **5.1**, the  $^1$ H spectrum revealed two aromatic protons at  $\delta_{\rm H}$  6.41 ppm (H-5, doublet, J = 3.1 Hz) and  $\delta_{\rm H}$  6.50 ppm (H-3, doublet of doublets, J = 5.7, 2.8 Hz) which displayed 2D COSY correlations only to each other, inferring a tetrasubstituted aromatic benzene ring with two remaining protons positioned in a meta relationship. Two benzyl groups were suggested by  $\delta_{\rm H}$  3.53 ppm (H-1', singlet) and  $\delta_{\rm H}$  3.27 ppm (H-7, doublet, J = 7.0 Hz), of which H-7 displayed HMBC correlations to C-5, C-6 and C-7, suggesting its positioning on the aromatic ring, therefore, the two OH group positions were narrowed down to either C-1 and C-4 or C-1 and C-2. The HMBC correlation of H-7 to C-1 (which possessed a downfield chemical shift of  $\delta_{\rm C}$  147.0 ppm, indicating an OH substitution) suggested the C-1 positioning of this OH group. Therefore, the para positioning of the hydroxyl groups and C-2 positioning of the additional benzyl were confirmed. The occurrence of a methyl singlet at  $\delta_{\rm H}$  3.66 ppm (H-3', singlet), which correlated with a carbon at  $\delta_{\rm C}$  52.5 ppm suggested the presence of a methoxy group.

HMBC analysis correlated H-3' to the carbonyl at C-2', suggesting the opening of the butanolide carboxyl into either a phenolic ether or an open ring lactone. The HMBC correlation between H-1' and the carbonyl at C-2' confirmed the latter, whilst  $^3J$  coupling observed between the methoxy group and the carbonyl, as well as appearance of the pseudo-molecular ion described above, enabled the conclusive elucidation of **5.2** as a new methyl ester, which was named caudiquinol<sup>6</sup>.

Caudiquinol is a meroterpenoid, whereby Greek-derived the prefix "*mero*-" means "fragment" or "partial". Therefore, meroterpenoids are compounds containing a partial terpene region, and in the case of **5.2**, a geranylgeranyl chain. This compound class is mostly reported from fungi and marine organisms, whilst far less have been identified from plants<sup>7</sup>. Meroterpenoids similar to **5.2**, consisting of different length sidechains (C10 or C20) built from isoprene units have been previously found throughout different plant families. Of these, there have been only four others (Figure **5.1a**) identified to date<sup>4,6,8-10</sup>.

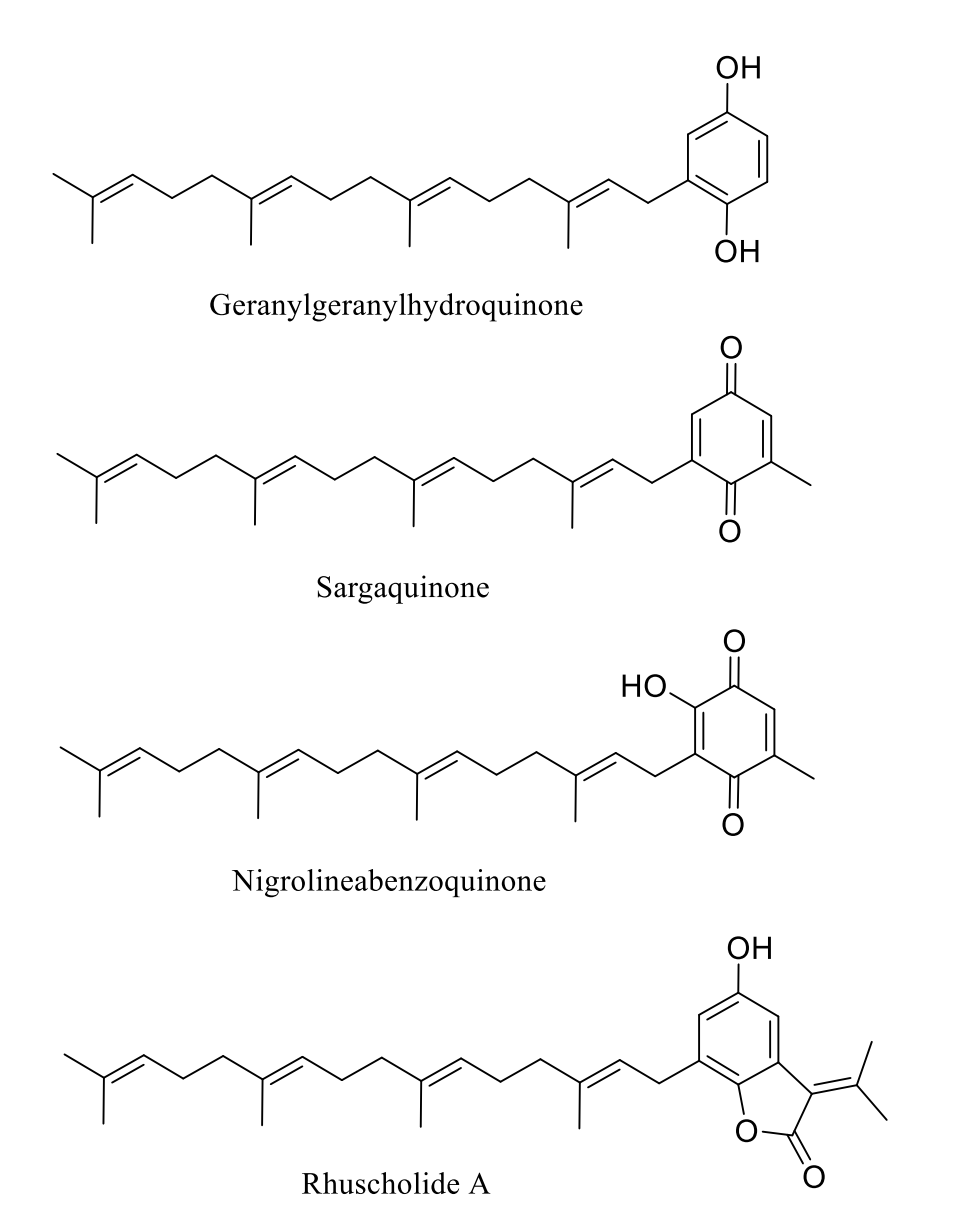


**Figure 5.2a.** Structures of known plant meroterpenoids, other than **5.1** and **5.1**, with an intact geranylgeranyl sidechain.

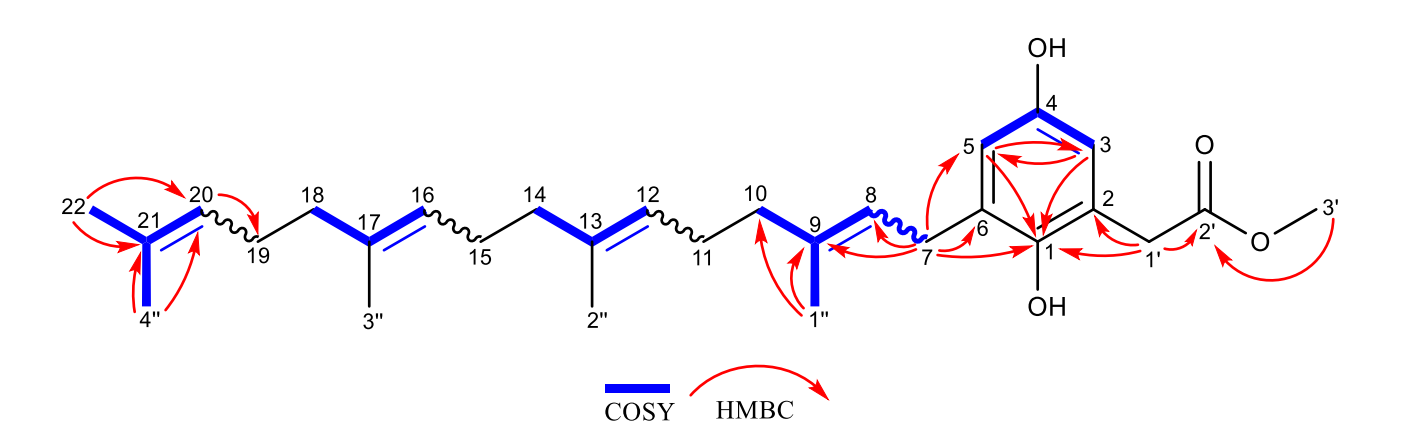


Figure 5.3. Key COSY and HMBC correlations of compound 5.2.

Table 5.2. <sup>1</sup>H, <sup>13</sup>C, COSY and HMBC NMR data of compound 5.2 (CDCl<sub>3</sub>, 500/126 MHz).

Position	$\delta_{\rm C}$ (ppm), type	$\delta_{H}$ , mult. (J in Hz)	COSY	HMBC
1	147.0, C	-	-	1', 7,
•	147.0, 0			3, 5
2	121.5, C	-	-	1'
3	115.0, CH	6.50, dd (5.7, 2.8)	5	5
4	149.0, C	-	-	-
5	115.9, CH	6.41, <i>d</i> (3.1)	3	7, 3
6	131.3, C	-	-	7
7	$29.2, \mathrm{CH}_2$	3.27, d (7.0)	8, 1"	-
8	121.6, CH	5.23, <i>dddd</i> (10.1, 8.8, 4.4, 3.0)	7	7, 1"
9	138.0, C	-	-	7, 1"
10	$37.2$ , $CH_2$	2.09 – 1.86, m	12, 1"	1"
11	$26.5$ , $\mathrm{CH}_2$	2.09 – 1.86, <i>m</i>	12, 1"	12
12	122 0 CH	5.03, qdt (7.1, 2.9, 1.5)	10, 11,	-
12	123.9, CH		14	
13	135.3, C	-	-	2"
14	39.69, CH <sub>2</sub>	2.09 – 1.86, m	12, 16	2"
15	$26.6$ , $\mathrm{CH}_2$	2.09 – 1.86, <i>m</i>	16	16

16	124.2, CH	5.03. <i>qdt</i> (7.1, 2.9, 1.5)	14, 15,	-
124.2, 011			18	
17	135.0, C	-	-	-
18	39.73, CH <sub>2</sub>	2.09 - 1.86, m	16, 20	-
19	26.7, CH <sub>2</sub>	2.09 – 1.86, m	20	20
20	124.4, CH	5.03, qdt (7.1, 2.9, 1.5)	18, 19	22, 4"
21	130.6, C	-	-	4", 22
22	25.6, CH <sub>3</sub>	1.52, s	-	-
1'	39.75, CH <sub>2</sub>	3.53, s	-	-
2'	173.9, C	-	-	3', 1'
3'	52.5, CH <sub>3</sub>	3.66, s	-	-
1"	16.3, CH₃	1.66, s	10, 11,	-
1	10.3, C113		8	
2"	16.2, CH <sub>3</sub>	1.52, s	-	12
3"	16.2, CH <sub>3</sub>	1.61, s	-	16
4"	17.8, CH <sub>3</sub>	1.52, s	-	-

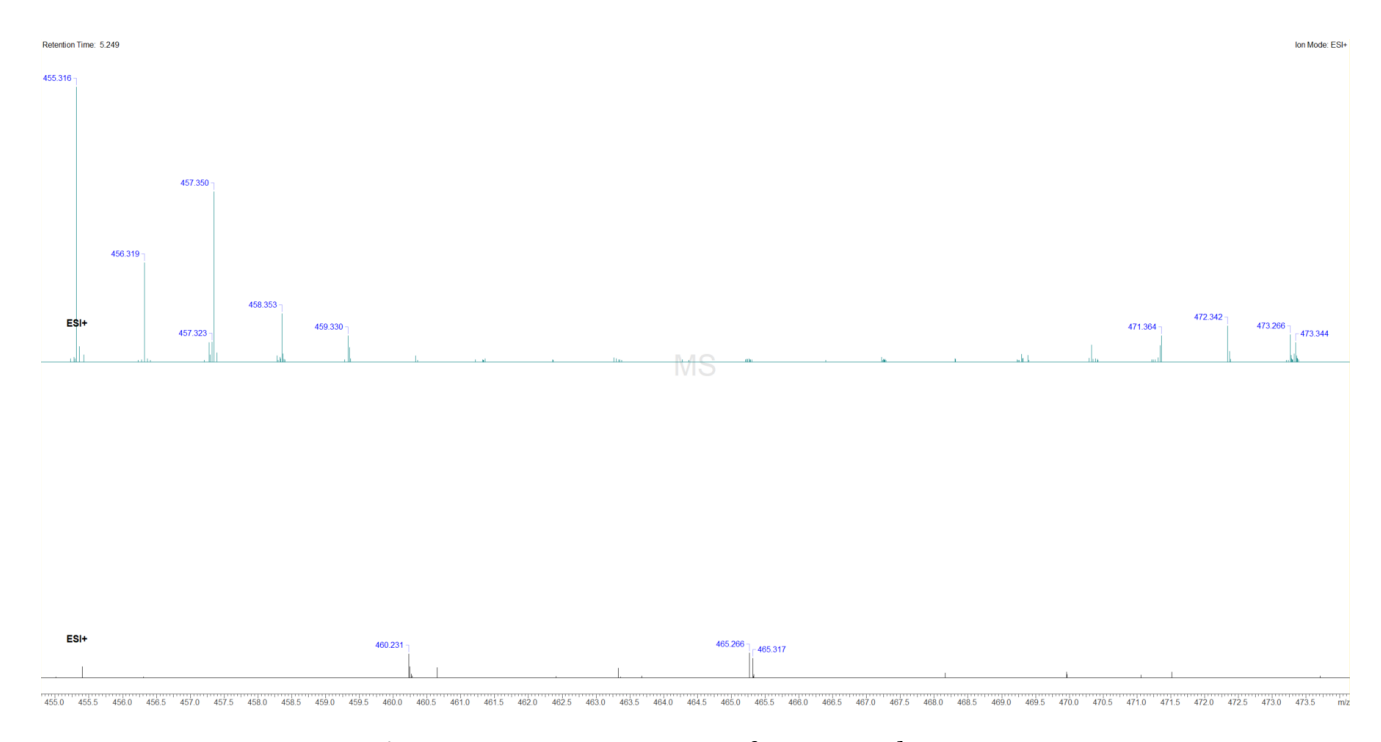


Figure 5.4. Mass spectrum of compound 5.2.

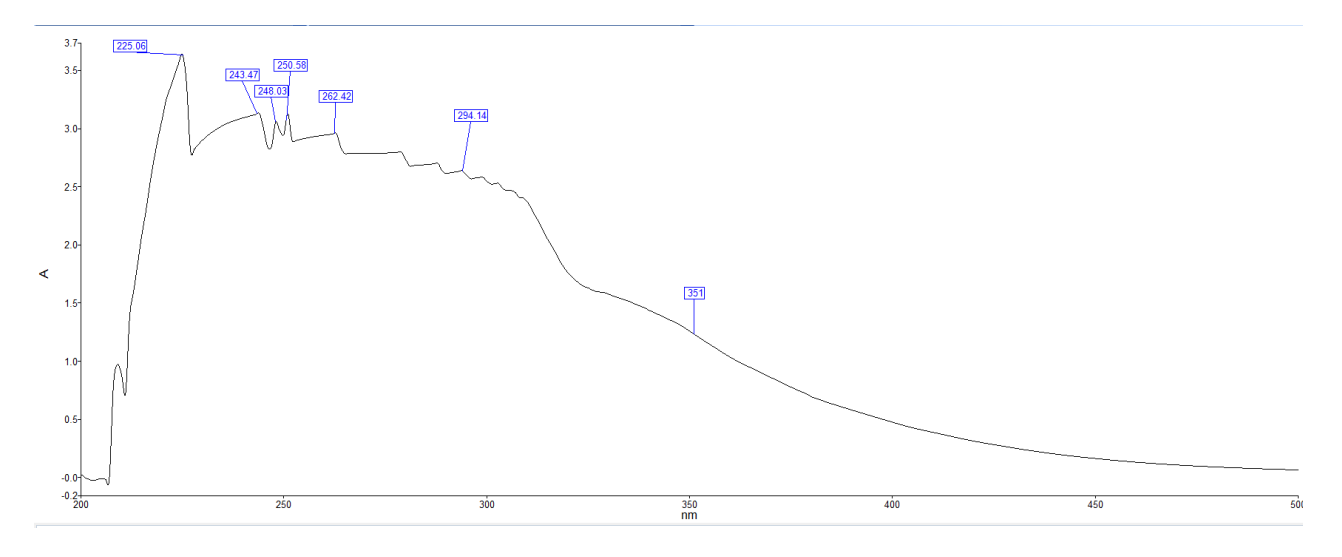


Figure 5.5. IR spectrum of compound 5.2.

# 5.2.1.3. Alpha tocopherol quinone (4.7, known, isolation two)

NMR spectra for the second isolation of compound **4.7** is found in appendix B (Figure B13 and Figure B14).

# **5.2.1.4.** α-Tocopherol (**5.3**, known)

Compound **5.3** was isolated as a yellow oil at 4 mg from an ethyl acetate/methanol extraction. The molecular formula was established as  $C_{29}H_{50}O_2$  ( $\Delta$  = 4.6 ppm) based on the [M+1]<sup>+</sup> ion at m/z 431.379 observed in the mass spectrum. The <sup>1</sup>H NMR spectrum lacked aromatic signals due to the presence of the chromanol ring. Here, the phenolic ring was fully substituted, with methyl groups at positions C-1, C-3 and C-4, displaying <sup>1</sup>H signals at  $\delta_H$  1.26 ppm (C-1 Me, singlet) and  $\delta_H$  2.11 ppm (C-3 Me and C-4 Me, singlet). The remaining protons in the chromanol ring were observed at <sup>1</sup>H signals at  $\delta_H$  2.60 ppm (H-1', triplet, J = 6.9 Hz),  $\delta_H$  1.74 – 1.83 ppm (H-2', multiplet) and  $\delta_H$  1.23 ppm (C-3' Me, singlet).

The  $^{13}$ C NMR spectra confirmed the presence of the phytyl chain, evidenced by carbon resonances observed in the aliphatic region. The four methyl substituents, initially inferred from the  $^{1}$ H NMR spectra, were detected in the  $^{13}$ C NMR spectra at  $\delta_{\rm C}$  24.0, 19.9, 19.8, 22.8, and 22.9 ppm, whilst the upfield-most signals at  $\delta_{\rm C}$  11.4, 12.4 and 11.9 ppm represented methyl substituents positioned on the aromatic ring. The spectral data recorded here were directly compared to those in the literature, showing a clear match. Based on the MS,  $^{1}$ H and  $^{13}$ C NMR data, this compound was identified as the known compound,  $\alpha$ -tocopherol (vitamin E).

Figure 5.6. Structure of compound 5.3.

**Table 5.3.**  $^{1}$ H and  $^{13}$ C NMR data of compound **5.3** (CDCl<sub>3</sub>, 500/126 MHz).

Position	$\delta_{\rm C}$ (ppm), type	$oldsymbol{\delta}_{ m C}^{11}$	$\delta_{\rm H}$ , mult. ( $J$ in Hz)
1	118.6, C	118.5, C	-
1- Me	11.4, CH <sub>3</sub>	11.3, CH <sub>3</sub>	2.16, s
2	144.7, C	144.5, C	-
3	121.1, C	121.0, C	-
3- Me	12.4, CH <sub>3</sub>	12.2, CH <sub>3</sub>	2.11, s
4	122.8, C	122.6, C	-
4- Me	11.9, CH₃	11.8, CH <sub>3</sub>	2.11, s
5	145.7, C	145.6, C	-
6	117.5, C	117.3, C	-
1'	$20.9$ , $\mathrm{CH}_2$	$20.8$ , $CH_2$	2.60, t (6.9)
2'	31.7, CH <sub>2</sub>	31.5, CH <sub>2</sub>	1.74 - 1.83, $m$
3'	74.7, C	74.5, C	-
3' - Me	$24.0$ , $\mathrm{CH_3}$	23.8, CH <sub>3</sub>	1.23, s
4'	40.0, CH <sub>2</sub>	38.8, CH <sub>2</sub>	1.24 - 1.62, $m$
5'	$21.2$ , $CH_2$	21.1, CH <sub>2</sub>	1.24 - 1.62, $m$
6'	37.62*, CH <sub>2</sub>	37.6, CH <sub>2</sub>	1.24 - 1.62, $m$
7'	32.9, CH	32.7, CH	1.24 - 1.62, $m$
7'- Me	19.9*, CH <sub>3</sub>	19.7*, CH <sub>3</sub>	0.82 - 0.89, $m$
8'	$37.37$ , $\mathrm{CH}_2$	37.3, CH <sub>2</sub>	1.24 - 1.62, $m$
9'	24.6, CH <sub>2</sub>	24.5, CH <sub>2</sub>	1.24 - 1.62, m
10'	$37.4$ , $CH_2$	37.4, CH <sub>2</sub>	1.24 - 1.62, m
11'	33.0, CH	32.8, CH	1.24 - 1.62, m
11'- Me	19.8*, CH <sub>3</sub>	19.7*, CH <sub>3</sub>	0.82 - 0.89, m
12'	37.6, CH <sub>2</sub>	37.5, CH <sub>2</sub>	1.24 - 1.62, m
13'	$25.0$ , $CH_2$	25.8, CH <sub>2</sub>	1.24 - 1.62, m
14'	39.9, CH <sub>2</sub>	39.4, CH <sub>2</sub>	1.24 – 1.62, <i>m</i>

15'	28.1, CH	28.0, CH	1.24 - 1.62, $m$
15'- Me	22.8, CH <sub>3</sub>	22,6, CH <sub>3</sub>	0.82 - 0.89, m
16'- Me	22.9, CH <sub>3</sub>	22.7, CH <sub>3</sub>	0.82 - 0.89, m

<sup>&</sup>lt;sup>11</sup>Reference carbon chemical shifts of α-tocopherol quinone measured in CDCl<sub>3</sub>.

#### 5.2.1.5. Isovitexin (5.4, known)

Compound **5.4** was isolated as a yellow amorphous powder (3 mg). The molecular formula was established as  $C_{21}H_{20}O_{10}$  ( $\Delta$  = 0.0 ppm) using positive ionisation Q-ToF MS, which revealed the base peak representing the [M+H]<sup>+</sup> ion at m/z 433.114, and another molecular ion peak at [M+Na]<sup>+</sup> at m/z 445.095.

The  $^{1}$ H and COSY spectrum revealed two aromatic proton signals representing the protons of the AA'BB' coupling system in the B ring of the flavone core:  $\delta_{\rm H}$  7.86 ppm (H-2', H-6', doublet, J = 8.9 Hz) and  $\delta_{\rm H}$  7.86 ppm (H-3', H-5', doublet, J = 8.9 Hz). The remaining signals in the  $^{1}$ H aromatic region represented the two protons of the flavone aglycone at  $\delta_{\rm H}$  6.62 ppm (H-3, singlet) and  $\delta_{\rm H}$  6.52 ppm (H-8, singlet).

The glycosidic region showed upfield multiplets with COSY and HMBC correlations. A signal at  $\delta_{\rm H}$  4.89 ppm (H-1", doublet, J = 9.9 Hz) represented the anomeric proton attached to the C-sugar unit. This proton was the only glycoside HMBC correlation to the flavone core, to C-6 and C-7, indicating that the C-Glucose moiety was attached at C-6.

The DEPT-Q spectrum revealed eight quaternary carbon signals corresponding to nine carbons within the aromatic regions. Here, one carbonyl was observed at  $\delta_{\rm C}$  184.2 ppm (C-4) and the remaining quarternaries at  $\delta_{\rm C}$  166.4 (C-2), 165.1 (C-7), 163.0 (C-4'), 158.9 (C-9), 123.3 (C-1'), 109.4 (C-6) and 105.3 ppm (C-5, C-10). The remaining four aromatic signals revealed six protonated aromatic carbons at  $\delta_{\rm C}$  129.6 (C-2', C-6'), 117.2 (C-5', 3'), 104.1 (C-3) and 95.4 ppm (C-8).

The HMBC correlations occurring only from H-8 ( $\delta_{\rm H}$  6.52 ppm) to C-7, C-6, C-5, C-4, C-10, C-9 and C-2, and from H-3 ( $\delta_{\rm H}$  6.62 ppm) to C-4 and C-10, confirmed the proton positions at 8 and 3.

The spectroscopic data obtained showed consistency upon careful comparison with the literature, allowing the conclusive characterisation of **5.4** as the known apigenin-6-C-glucoside, also known as isovitexin<sup>12</sup>.

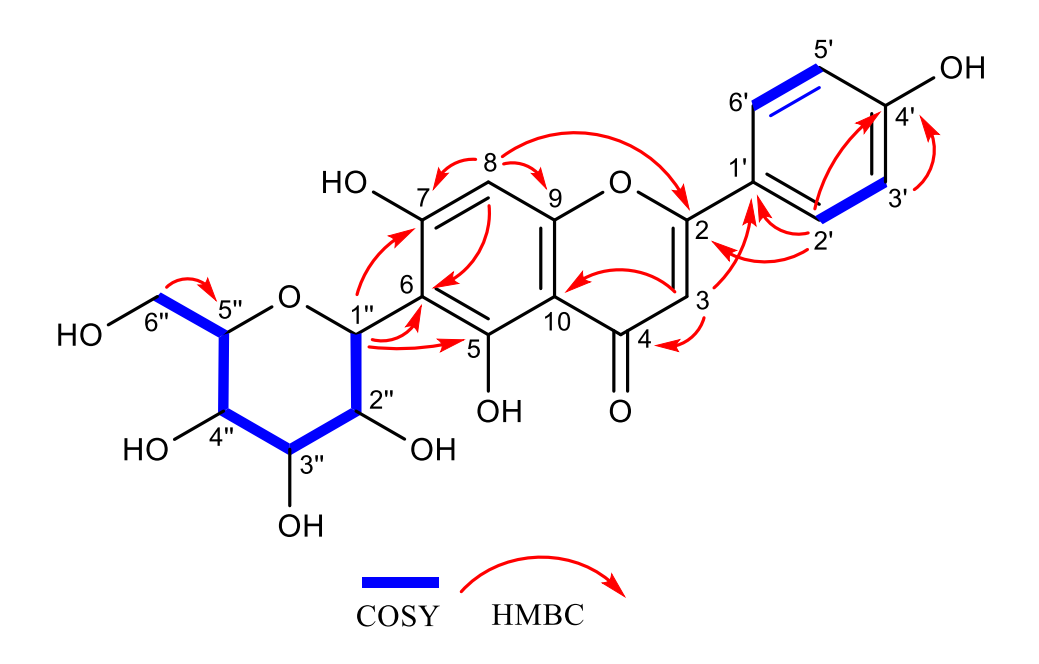


Figure 5.7. Key COSY and HMBC correlations of compound 5.4.

Table 5.4. <sup>1</sup>H, <sup>13</sup>C, COSY and HMBC NMR data of compound 5.4 (MeOH-d<sub>4</sub>, 600/150 MHz).

Position	$\delta_{\rm C}$ (ppm), type	$\mathbf{\delta_{c}}^{12}$	$\delta_{\rm H}$ , mult. ( <i>J</i> in Hz)	COSY	HMBC
1	-	-	-	-	-
2	166.4, C	166.0, C	-	-	8, 2', 6'
3	104.1, CH	103.6, CH	6.62, s	-	-
4	184.2, C	183.8, C	-	-	3, 8
5	105.3, C	-	-	-	3, 8
6	109.4, C	109.5, C	-	-	8, 1"
7	165.1, C	163.0, C	-	-	8, 1"
8	95.4, CH	95.7, CH	6.52, s	-	-
9	158.9, C	158.8, C	-	-	8
10	105.3, C	104.6, C	-	-	3, 8

1'	123.3, C	123.0, C	-		-	3', 5', 3
2'	129.6, CH	129.4, CH	7.86, d (8.9)	3'		-
3'	117.2, CH	117.1, CH	6.94, d (8.8)	2'		-
4'	163.0, C	162.0, C	-		-	2', 6', 3', 5'
5'	117.2, CH	117.1, CH	6.94, d (8.8)	6'		2', 6'
6'	129.6, CH	129.4, CH	7.86, d (8.9)	5'		-
1"	75.5, CH	75.4, CH	4.89, d (9.9)		-	3", 4"
2"	72.7, CH	72.5, CH	4.16, t (9.2)		-	-
3"	80.2, CH	80.3, CH	3.48, m		-	1", 4"
4"	71.9, CH	71.7, CH	3.48, <i>m</i>		-	1", 6"
5"	82.8, CH	82.6, CH	3.42, m		-	1", 6", 3", 4"
6"	63.0, CH <sub>2</sub>	62.8, CH <sub>2</sub>	3.87, dd (12.1, 2.3),		-	-
			3.74, dd (12.2, 5.4)			

 $<sup>^{12}</sup> Reference$  carbon chemical shifts of chlorogenic acid measured in MeOH-d\_4.

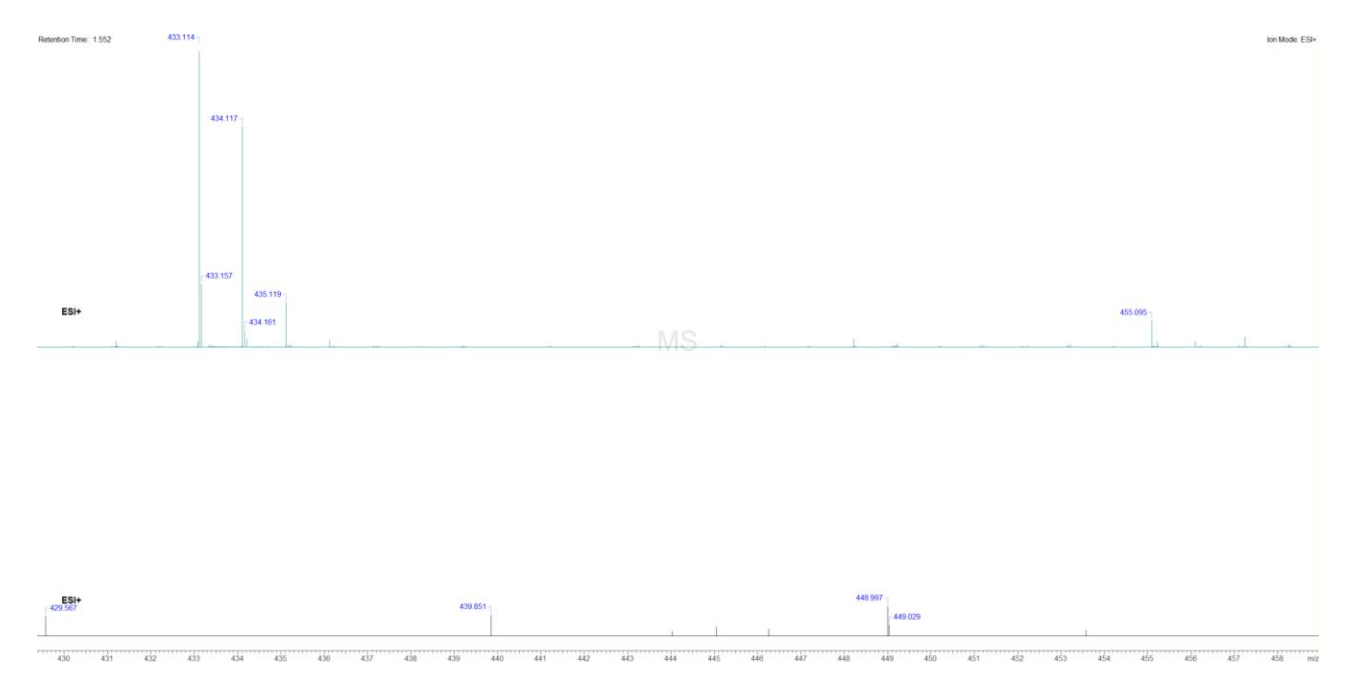


Figure 5.8. Mass spectrum of compound 5.4.

# 5.2.1.6. Chlorogenic acid (5.5, known)

Compound **5.5** was isolated as a white amorphous solid at 2.7 mg from an ethyl acetate/methanol extract. Q-ToF mass spectrometry analysis revealed a protonated base peak [M+H] $^+$  at m/z 355.103 ( $\Delta$  = 0.0 ppm) and a sodium adduct [M+Na] $^+$  at m/z 377.085 ( $\Delta$  = 0.0 ppm), allowing the establishment of the molecular formula as  $C_{16}H_{18}O_{9}$ . The UV spectrum of **5.5** was consistent with the literature, showing two absorption maxima: a lower intensity peak at 218 nm and the second with higher intensity at 326 nm (Figure 5.11) $^{13}$ .

The  ${}^{1}$ H spectrum displayed aromatic proton signals attributed to the 1,3,4-trisubstituted benzene ring of the caffeic acid moiety. Here, three aromatic protons were observed at  $\delta_{\rm H}$  7.05 ppm (H-6', doublet, J = 2.0 Hz),  $\delta_{\rm H}$  6.95 ppm (H-2', doublet of doublets, J = 8.2, 2.1 Hz) and  $\delta_{\rm H}$  6.78 ppm (H-5', doublet, J = 8.2 Hz). The 2D COSY NMR spectrum displayed clear *ortho*-coupling between the H-5' and H-6' and a correlation was also observed between the para positioned protons at H-5' and H-2', evidencing their proximity in the aromatic region.

The olefinic protons of the caffeoyl group resonated on the  $^1\text{H}$  spectrum at  $\delta_{\text{H}}$  7.56 ppm (H-7', doublet, J = 15.9 Hz) and 6.26 ppm (H-8', doublet, J = 15.9 Hz), and displayed *trans*-coupling to one another, revealing the trans-disubstituted ethylene moiety, shown by the COSY correlations. The most deshielded protons displayed resonances representing the quinic acid portion of **5.5**. Here, the hydroxylated methine protons appeared as individual signals at  $\delta_{\text{H}}$  5.33 ppm (H-5, quintet, J = 3.9 Hz),  $\delta_{\text{H}}$  4.17 ppm (H-3, triplet of doublets, J = 3.3, 2.8 Hz) and  $\delta_{\text{H}}$  3.72 ppm (H-4, doublet of doublets, J = 8.4, 3.1 Hz). 2D COSY correlations also revealed coupling between H-5 and H-4. Due to the low compound quantity and thus spectral resolution, these were the only 2D experiment signals visible. Therefore, HSQC assignments were made by comparison with literature values.

The  $^{13}$ C NMR spectrum of **5.5** revealed 16 carbon atoms, including two carbonyl groups at  $\delta_{\rm C}$  168.7 ppm (C-7) and  $\delta_{\rm C}$  164.5 ppm (C-9'), which appeared slightly upfield compared to literature values. Two hydroxyl-substituted aromatic carbons were present at  $\delta_{\rm C}$  149.6 ppm (C-4') and  $\delta_{\rm C}$  146.8 ppm (C-3'), whilst the remaining aromatic signals ranged from  $\delta_{\rm C}$  115.3 to 127.8 ppm (C-1', 2', 5' and 6'). The olefinic of the caffeoyl moiety speared at  $\delta_{\rm C}$  147.1 ppm (C-7') and  $\delta_{\rm C}$  115.2 ppm (C-8'), while the remaining upfield carbon signals, including the hydroxyl-bearing methine and methylene (-CH<sub>2</sub>), comprised the quinic acid core.

Through detailed analysis of the spectral data and comparison with previously published data, compound **5.5** was identified as the known compound 5-caffeoylquinic acid, commonly known as chlorogenic acid<sup>14,15</sup>.

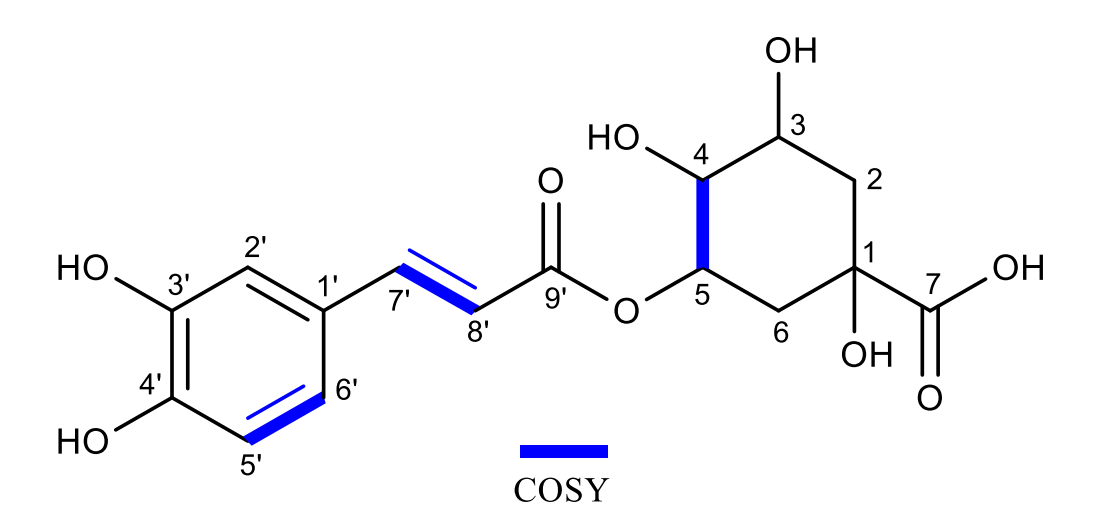


Figure 5.9. COSY correlations of compound 5.5.

**Table 5.5.**  $^{1}$ H,  $^{13}$ C and COSY data of compound **5.5** (CD<sub>3</sub>OD, 500/126 MHz).

Position	$\delta_{\rm C}$ (ppm), type	$\delta_{\mathrm{C1}}^{14}$	$\delta_{\rm H}$ , mult. ( <i>J</i> in Hz)	COSY
1	76.2, C	74.7, C	-	-
2	38.8, CH <sub>2</sub>	37.3, CH <sub>2</sub>	$2.04^*$ , $m$	-
3	71.3, CH	70.5, CH	4.17, td (3.3, 2.8)	-
4	73.5, CH	72.1, CH	3.72, dd (8.4, 3.1)	5
5	72.0, CH	70.6, CH	5.33 q (3.9)	4
6	38.2, CH <sub>2</sub>	36.8, CH <sub>2</sub>	2.11 - 2.26*, m	-
7	168.7, C	175.6, C	-	-
1'	127.8, C	126.4, C	-	-
2'	115.3, CH	113.9, CH	6.95, dd (8.2, 2.1)	-
3'	146.8, C	145.3, C	-	-
4'	149.6, C	148.1, C	-	-
5'	116.5, CH	115.1, CH	6.78, d (8.2)	6'
6'	123.0, CH	121.6, CH	7.05, d(2.0)	5'
7'	147.1, CH	145.7, CH	7.56, d (15.9)	8'
8'	115.2, CH	113.8, CH	6.26, d (15.9)	7'
9'	164.5, C	167.3, C	-	-

\*Indicates interchangeable values.  $^{\rm 14}Reference$  carbon chemical shifts of chlorogenic acid measured in CD\_3OD.

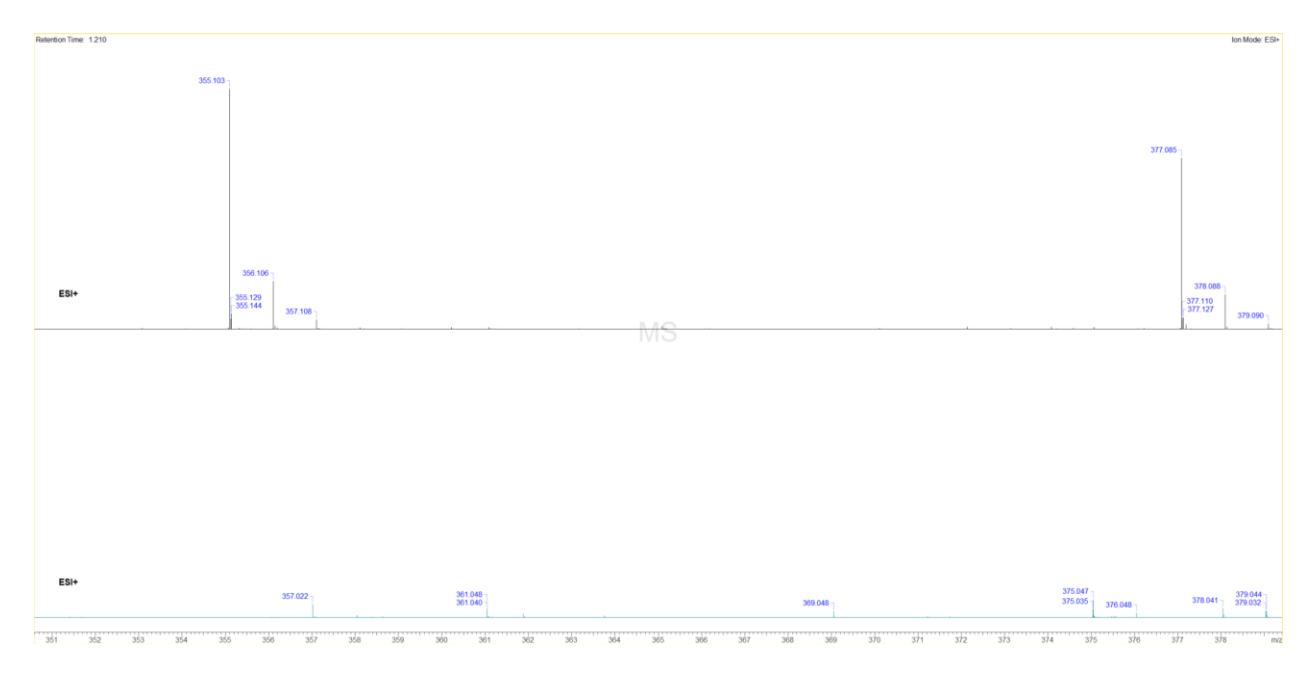


Figure 5.10. Mass spectrum of compound 5.5.

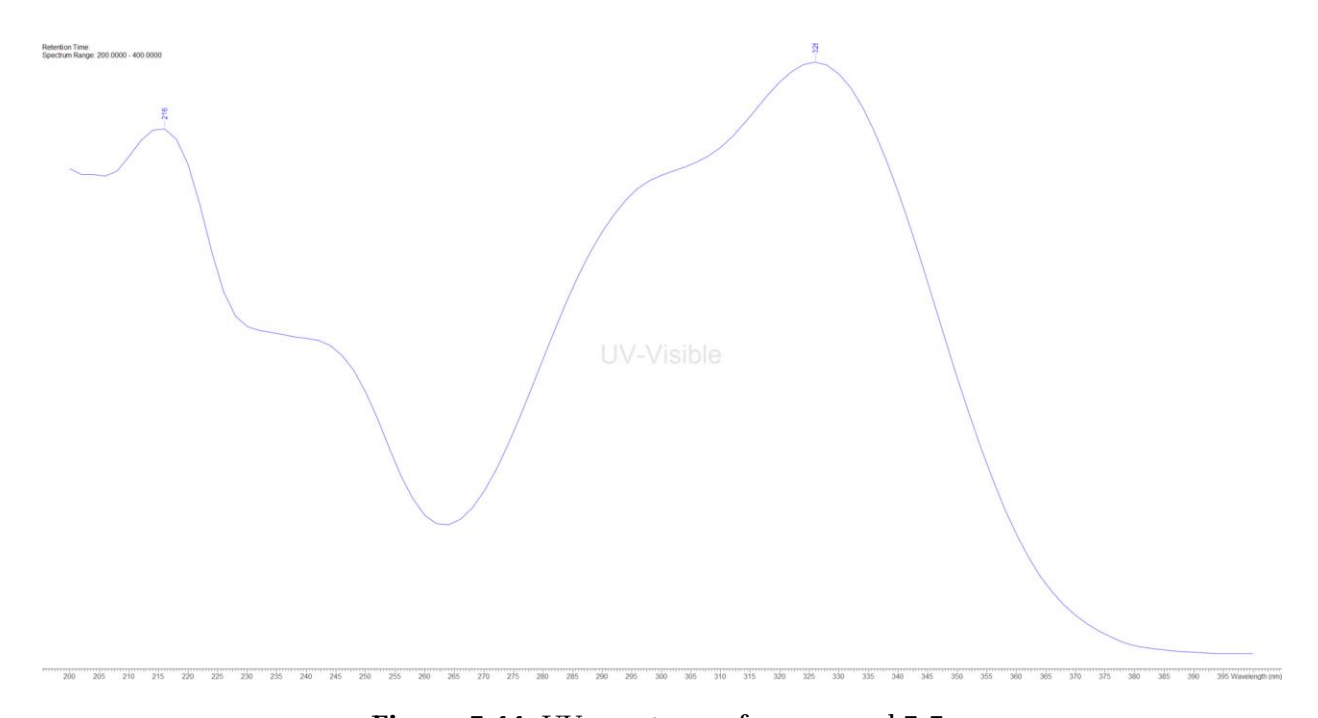


Figure 5.11. UV spectrum of compound 5.5.

#### 5.2.1.7. Dioctyl phthalate – contaminant

During the isolation of natural compounds from *G. caudiculata*, a large amount of the contaminant compound dioctyl phthalate (40 mg) was isolated from a non-polar fraction of the dichloromethane *G. caudiculata* extract. The molecular structure was determined as  $C_{24}H_{38}O_4$  using positive mode Q-ToF MS, where the molecular ion [M+1]<sup>+</sup> was identified as m/z 391.285 ( $\Delta$  = 0 ppm).

To confirm the structure corresponding to the molecular formula, one-dimensional NMR experiments were carried out. The <sup>1</sup>H NMR spectrum exhibited resonances characteristic of a symmetrical phthalic acid diester. In the aromatic region, an orthodisubstituted benzene ring was evident, presenting two distinct doublets of doublets at  $\delta_{\rm H}$  7.46 ppm (H-1, H-1'; J = 5.7, 3.3 Hz) and  $\delta_{\rm H}$  7.64 ppm (H-2, H-2'; J = 5.7, 3.3 Hz), corresponding to four aromatic protons. The aromatic core possessed ester substituents at the 3 and 3' positions. The ester-linked methine protons (H-5, H-5'), deshielded due to their proximity to the electronegative oxygen atoms, resonated as a multiplet between  $\delta_H$  4.09 and 4.21 ppm. A multiplet at  $\delta_H$  1.62 ppm (H-11, H-11'; J = 6.2 Hz) corresponded to the ethyl branch. The subsequent methylene group (H-6, H-6') appeared as a multiplet at  $\delta_{\rm H}$  1.35 ppm (J = 13.6, 7.4 Hz). The remaining methylene groups of the branched octyl chains gave rise to a broad multiplet between  $\delta_H$  1.21 and 1.30 ppm, integrating to twelve protons, consistent with long saturated aliphatic chains. Finally, the terminal methyl groups of the octyl chains and ethyl branches appeared as a doublet of triplets at  $\delta_{\rm H}$  0.84 ppm (H-10, H-10', H-12, H-12'; J = 12.4, 7.3 Hz), resulting from coupling with adjacent methylene protons (Table 5.6).

The  $^{13}$ C NMR spectrum supported these observations, with the deshielded ester carbonyl carbon atoms resonating at  $\delta_{\rm C}$  167.9 ppm (C-4, C-4'). The aromatic ring carbons directly bonded to the ester groups appeared further downfield at  $\delta_{\rm C}$  132.6 ppm (C-3, C-3'), while the remaining protonated aromatic carbons were observed at  $\delta_{\rm C}$  123.0 ppm (C-2, C-2') and  $\delta_{\rm C}$  131.0 ppm (C-1, C-1'). The methylene carbons adjacent to the ester oxygen atoms (C-5, C-5') were shifted downfield to  $\delta_{\rm C}$  68.3 ppm due to the electron-

withdrawing influence of the oxygen. The internal methylene carbons of the branched octyl chains (C-6 to C-9) gave rise to resonances between  $\delta_{\rm C}$  23 and 38 ppm. The terminal methyl carbons resonated upfield at  $\delta_{\rm C}$  14.2 ppm, while the ethyl branch methyl groups appeared at  $\delta_{\rm C}$  11.1 ppm (Table 5.6). The chemical shift values and symmetry of the signals were in full agreement with previously reported data, confirming the identity of the compound as bis(2-ethylhexyl) phthalate, comprising two identical branched octyl ester chains symmetrically attached to a phthalic acid core <sup>16</sup>.

Bis(2-ethylhexyl) phthalate is a synthetic plasticizer commonly used in laboratory plastics, from which it can readily leach. Despite its industrial origin, it has been misidentified on numerous occasions as a natural product. It is therefore important for natural product chemists to be familiar with the characteristic NMR profiles of such ubiquitous contaminants, to avoid investing time and resources into unnecessary structure elucidation. In early-stage investigations, DEHP can be overlooked due to inconclusive or absent mass spectrometric data, particularly when identification relies solely on molecular formulae and natural product-only databases. As a known endocrine disruptor and persistent environmental pollutant, its presence in plant extracts may not only indicate contamination or methodological artifacts, but also serve as a useful bioindicator of environmental or procedural exposure. In some cases, it may even act as a chemical marker reflecting specific extraction or handling conditions <sup>17</sup>.

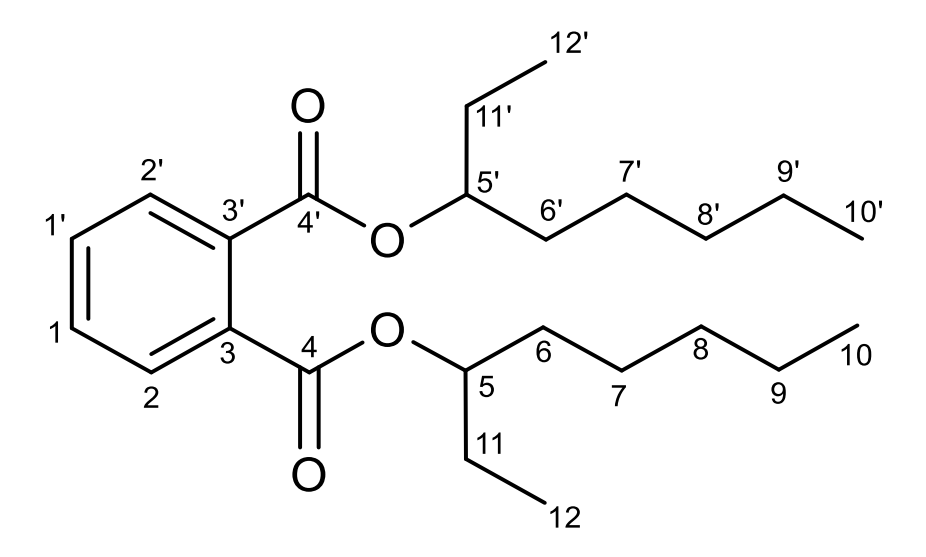
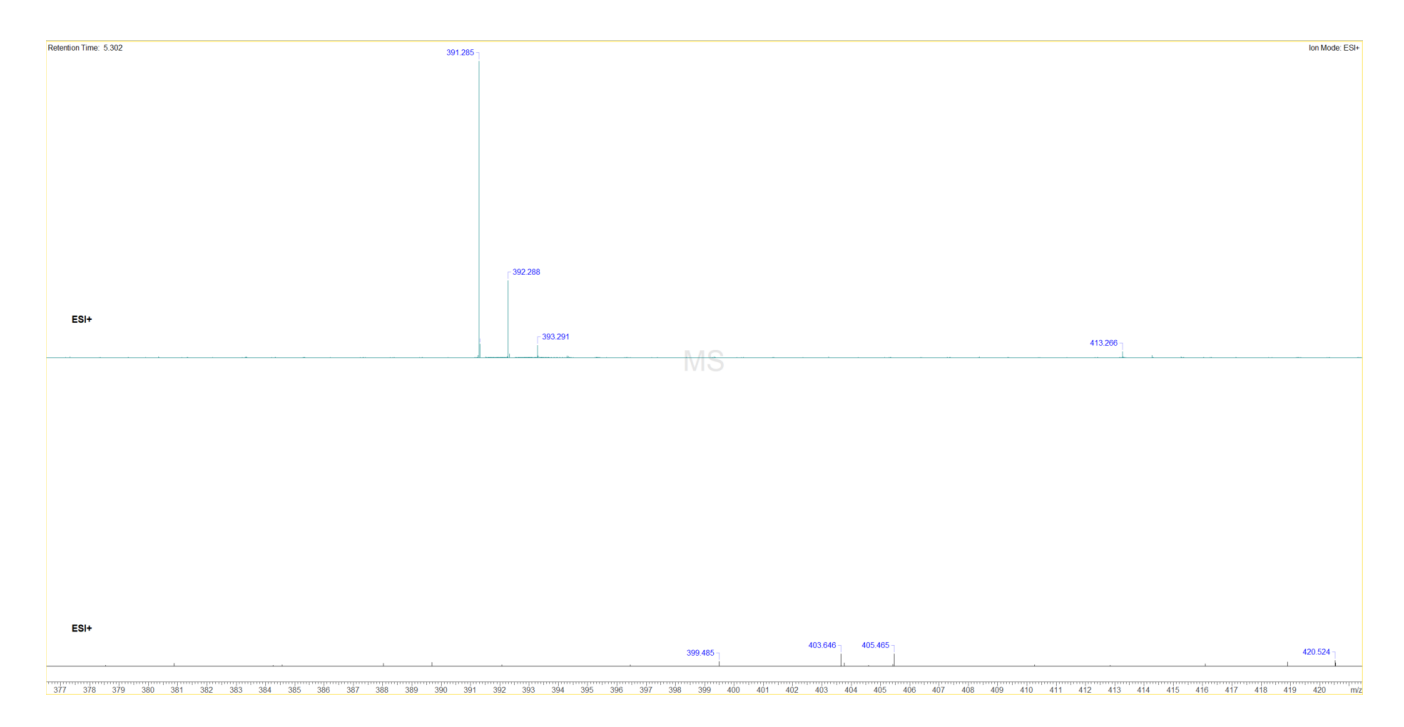


Figure 5.12. Structure of the contaminant dioctyl phthalate.

Table 5.6.  $^{1}$ H,  $^{13}$ C and COSY data of the contaminant dioctyl phthalate compound (CD<sub>3</sub>OD, 500/126 MHz).

Position	$\delta_{\rm C}$ (ppm), type	$\mathbf{\delta}\mathrm{c}^{16}$	$\delta_{\rm H}$ , mult. ( <i>J</i> in Hz)
1, 1'	131.0, CH	131.7, CH	7.46, dd (5.7, 3.3)
2, 2'	129.0, CH	128.7, CH	7.64, dd (5.7, 3.3)
3, 3'	132.6, C	131.8, C	-
4, 4'	167.9, C	167.0, C	-
5, 5'	68.3, CH	67.4, CH	4.09 - 4.21, $m$
6, 6'	38.9, CH <sub>2</sub>	38.1, CH <sub>2</sub>	1.17 – 1.44, m
7,7'	23.9, CH <sub>2</sub>	23.2, CH <sub>2</sub>	1.21 - 1.30, m
8,8'	29.1, CH <sub>2</sub>	28.4, CH <sub>2</sub>	1.21 - 1.30, m
9, 9'	23.13, CH <sub>2</sub>	22.4, CH <sub>2</sub>	1.21 - 1.30, m
10, 10'	14.20, CH <sub>3</sub>	13.9, CH <sub>3</sub>	0.84, dt (12.4, 7.3)
11, 11'	30.5, CH <sub>2</sub>	29.8, CH <sub>2</sub>	1.62, m (6.2)
12, 12'	11.1, CH <sub>3</sub>	10.8, CH <sub>3</sub>	0.84, dt (12.4, 7.3)

<sup>&</sup>lt;sup>16</sup>Reference carbon chemical shifts of chlorogenic acid measured in CD<sub>3</sub>OD.



**Figure 5.13.** Mass spectrum of *Bis*(2-ethylhexyl) phthalate.

#### 5.2.2. Conclusion

This study reports the first phytochemical investigation of *Garcinia caudiculata*, leading to the isolation and structural elucidation of six secondary metabolites, including one previously unreported compound and five known natural products. Comprehensive spectroscopic analysis, including 2D NMR experiments, enabled the structural characterisation of all isolates. This work is the first to report full 2D NMR data for **5.2**, thus building the spectral database for this class of compounds.

This research has expanded the chemical profile of an unstudied *Garcinia* species. The findings emphasise the importance of exploring under investigated species within biodiverse genera such as *Garcinia*, which continue to yield structurally diverse and potentially bioactive metabolites with relevance to drug discovery.

#### 5.2.3. Biosynthetic pathway of Caudiquinol

Meroterpenoid is a term used to describe natural products produced via mixed terpenoid biogenesis. Compound **5.2** is likely biosynthesised through such a mixed pathway, with the aromatic core and lactone ring derived from a polyketide precursor,

and the side chain from a terpenoid intermediate. Both pathways ultimately originate from acetyl-CoA ( $C_2$ ) as a central building block<sup>7,18</sup>.

For the polyketide portion of the molecule, acetyl-CoA undergoes carboxylation by acetyl-CoA carboxylase in a biotin-dependent reaction to form malonyl-CoA, which acts as an extender unit in polyketide synthesis. Sequential Claisen condensations of two malonyl-CoA units form the linear polyketide chain (5.6, Figure 5.14). This undergoes aldol condensation, which forms the phenolic compound 5.7. The hydroxyl at the C-4 position is then reduced to 5.8, followed by the oxidation at C-1 forming 5.9. Intermediate 5.9 undergoes hydrolysis to form either the lactone 5.1 or methyl ester **5.2**<sup>19</sup>. The terpenoid portion is synthesised via the mevalonate pathway, which starts from acetyl-CoA. Two molecules of acetyl-CoA condense to form acetoacetyl-CoA, catalysed by thiolase. A third acetyl-CoA is added by HMG-CoA synthase to produce 3hydroxy-3-methylglutaryl-CoA (HMG-CoA), which is then reduced by HMG-CoA reductase to form mevalonic acid (mevalonate). This is followed by a series of phosphorylation and decarboxylation steps, catalysed by mevalonate kinase, phosphomevalonate kinase, and mevalonate diphosphate decarboxylase, resulting in the formation of isopentenyl pyrophosphate (IPP). IPP is isomerised to dimethylallyl pyrophosphate (DMAPP), and through sequential head-to-tail condensations, forms geranylgeranyl pyrophosphate (5.10) (the  $C_{20}$  precursor used for the prenylation of the polyketide core, Figure 5.14)<sup>20</sup>. This alkylates hydroquinone **5.9** at C6, followed by release of the product 5.1 arising from intramolecular lactone formation or 5.2 by reaction with methanol 19,20.

Figure 5.14. Proposed biosynthetic route of Caudiquinol (5.2).

# 5.2.4. Biological activities of isolated compounds

Following the small-scale extraction and screening of three Clusiaceae species, *G.* caudiculata was the only species to exhibit antibacterial activities against MSSA extractions were scaled up and investigated further due to exhibiting antibacterial effects against MSSA (Table 5.7).

**Table 5.7.** *In vitro* antibacterial activity of Clusiaceae species measured using the broth microdilution assay to obtain the minimum inhibitory concentration (MIC) of each extract.

Species	Extracting solvent	MIC (µg/mL)	
		MSSA 25923	E. coli 10418
Garcinia caudiculata	Hexane	128	>512
	Dichloromethane	64	>512
	Methanol	128	>512
Calophyllum pulcherrimum	Hexane	>512	>512
	Dichloromethane	>512	>512
	Methanol	>512	>512
Mesua calciphila	Hexane	>512	>512
	Dichloromethane	>512	>512
	Methanol	>512	>512

# 5.2.4.1. Antibacterial activities of isolated Clusiaceae compounds

Within the Clusiaceae-derived compounds isolated in this study, **5.1** and **5.2** were the only compounds that had not been previously evaluated for their antibacterial properties. In contrast, the antibacterial activity of **5.3**, **5.4**, **5.5** and **4.7** has been previously reported, therefore such investigations were not repeated during this study. Previous reports of antibacterial as well as other biological activities are described in section **5.2.4.4**.

Compounds **5.1** and **5.2** exhibited no detectable activity against any Gram-positive bacterial strains, with MIC values >128  $\mu$ g/mL (Table 5.8)<sup>6</sup>.

**Table 5.8.** MIC values of compounds **5.1**, **5.2** and ampicillin positive control tested against Gram-negative and Gram-positive bacterial strains.

Bacterial strain	Gram	Compound 5.1	Compound 5.2
MSSA 25923	+	>128	>128
MRSA 13373	+	>128	>128
Staphylococcus aureus RN4220	+	>128	>128
Staphylococcus aureus 1199B	+	>128	>128
Staphylococcus aureus XU212	+	>128	>128
Enterococcus faecalis 12967	+	>128	>128
Enterococcus faecalis 51299	+	>128	>128
Escherichia coli 10418	-	>128	>128
Escherichia coli G69	-	>128	>128
Salmonella typhimurium 14028S	-	>128	>128
Pseudomonas aeruginosa 10662	-	>128	>128
Klebsiella pneumonia CPE16	-	>128	>128
Ampicillin		0.5	0.5

#### 5.2.4.2. Anticancer activities of isolated Clusiaceae compounds

This study partially aimed to assess the anticancer potential of compounds isolated from the Myristicaceae and Clusiaceae families. While anticancer activity was not the primary focus of the phytochemical investigations, pure compounds were tested *in vitro* against common cancer cell lines by Dr Salonee Banerjee in Dr. Sobolewski's laboratory at the School of Chemistry, Pharmacy, and Pharmacology, University of East Anglia.

As the anticancer properties of 5.3 - 5.5 isolated from the Clusiaceae family have been previously studied, only 5.1 and 5.2 were initially screened at concentrations of  $10~\mu\text{M}$  and  $100~\mu\text{M}$  against A549, SK-MEL28, HL60, and RAW264.7 cell lines. Both compounds demonstrated growth inhibition of A549 cells at  $100~\mu\text{M}$ , prompting further investigation. Subsequent determination of their IC<sub>50</sub> values revealed significantly higher fluorescence intensity values compared to the cisplatin control, indicating that these compounds exhibit minimal to no cancer cell inhibitory activity (Table 5.9).

During a previous study, two similar compounds to **5.1** and **5.2** (differing in that these possessed a 10-carbon geranyl chain) were isolated from *Magnolia denudate* (Magnoliaceae). In concurrence with this study, the closed ringed lactone displayed lower  $IC_{50}$  values than the open ringed structure, similar to **5.2**. However, these *in vitro* assays were performed against the non-cancer cell line SFME and the cancer cell line r/mHM-SFME-1, and the  $IC_{50}$  values for a positive control were not mentioned, therefore comparison of structure-activity relationships between these compounds and those isolated in this thesis are hard to infer. Although, the study does state that cytotoxic activity of both was observed, suggesting that the 10-carbon chain may offer this activity<sup>21</sup>.

Previously isolated compounds conservative in the 20-carbon geranylgeranyl chain have also been isolated and tested for their anticancer abilities. Research shows that compounds possessing this side chain have displayed cytotoxic activities against P-388 leukaemia cells. Data from both previous studies show that the 20-carbon chain alone may offer cytotoxic effects, however the aromatic parts of these structures may be responsible for the observed activity too<sup>9</sup>. Given that neither compounds containing the lactone moiety nor those with the 20-carbon side chain individually exhibit potent cytotoxic activity, and considering the lack of activity in compounds possessing both moieties in this study, these findings confirm the absence of cytotoxic potential in either moiety alone or in combination, limiting their relevance for future anticancer studies.

**Table 5.9.** Cytotoxic activity of compounds **5.1** and **5.2** against A549 lung cancer cells, displaying IC<sub>50</sub> values obtained using an AlamarBlue *in vitro* assay.

Compound	IC <sub>50</sub> (μΜ)
5.2	451.50
5.1	157.60
Cisplatin	18.57

# 5.2.4.3. Antifungal activities of isolated Clusiaceae compounds

The antifungal properties of compounds **5.1** and **5.2** isolated from the Clusiaceae family during this study were examined through an *in vitro* AlamarBlue cell viability assay against critical priority pathogens *Aspergillus fumigatus* and *Candida albicans*. This evaluation aimed to determine the potential cytotoxic effects of these compounds on fungal cells. Results showed no decrease in cell viability of fungal species (Appendix C, Figure C1).

# 5.2.4.4. Previous reports of biological activities

# Previously studied biological activities of 5.1

The antibacterial activities of **5.1** were described for the first time during this study, however Gu *et al.*, previously reported its anti-HIV activities. Here, **5.1** significantly suppressed HIV-1 replication, with EC<sub>50</sub> and CC<sub>50</sub> values of 3.7 and 12.1  $\mu$ M, respectively, and displayed a low therapeutic index. This compound was later found to inhibit HIV-1 replication in chronically infected H9 cells, however did not inhibit cell-cell fusion between C8166 cells and HIV-1IIIB infected cells at the entry step of HIV, inferring that this compound targets the later part of the HIV-1 life cycle<sup>22</sup>.

# Previously studied biological activities of 5.5

Compound **5.5** has been sourced from multiple genera and is a well-studied, widely used natural product which has several pharmacological properties including immunomodulatory, hypoglycemic, anticardiovascular and antimicrobial. Chlorogenic acid is used clinically to treat acute bacterial infections and has been proven to inhibit biofilm development of several clinically significant microorganisms including *P. aeruginosa*, *Yersinia enterocolitica* and *A. fumigatus*<sup>23</sup>. Reported MIC values for various bacterial pathogens range from 10 to 80 µg/mL<sup>24,25</sup>. The inhibitory effects of chlorogenic acid have been studied, particularly in relation to its mechanism of action against *E. coli* and *S. aureus*<sup>26</sup>. In addition, **5.5** works synergistically with (and can have additive effects on) the majority of commonly used antibiotics. Such studies demonstrate this compound as a potential candidate in a new class of antibiotics<sup>27</sup>.

This compound has also been investigated for its antimutagenic and anticancer effects, being proven to inhibit genetic mutations, cancer cell proliferation and promote apoptosis of multiple cancer cell lines<sup>28-31</sup>.

#### Previously studied biological activities of 5.4

Due to the numerous previous reports on its variety of biological activities including, but not limited to, anticancer and antimicrobial, compound 5.4 was not biologically studied during this work<sup>32</sup>. Disc diffusion assays have proven this compound to inhibit growth of both Gram-positive and -negative bacteria, including *Bacillus subtilis*, *S. aureus* and *P. aeruginosa*, all with zones of inhibition over 18 mm, comparable to that of the antibiotic standard<sup>33,34</sup>. However, a more qualitative study by Adamczak *et al.*, showed weak activity of 5.4 against Gram-positive strains (MIC = >1000 μg/mL) and moderate activity against Gram-negative (MIC = 500 μg/mL)<sup>35</sup>. In concurrence with this, 5.4 displayed weak activity against *S. aureus* during a disc diffusion assay. However, this compound has been shown to decrease adhesion of *S. aureus* biofilms<sup>36</sup>. Recent mechanistic studies have demonstrated that although 5.4 does not interfere with *S. aureus* growth, it does inhibit activities of *S. aureus* coagulase and sortase A, potentially decreasing pathogenesis and persistent infection<sup>37,38</sup>. Rammohan *et al.*, also demonstrated that this compound inhibits pathogenic fungal growth including that of *C. albicans, Candida tropicalis, Penicillium notetum* and *Aspergillus niger*<sup>34</sup>.

**5.4** has been investigated for its anticancer effect in multiple cell lines and has demonstrated its ability to suppress cancer cell stemness and promote apoptosis<sup>39-43</sup>. Mechanistic studies have been undertaken and well-reviewed, illustrating that **5.4** should be considered as a prospective candidate for cancer prevention and treatment<sup>44</sup>.

#### Previously studied biological activities of 5.3

**5.3** is an abundant and biologically active isoform of vitamin E, which is well studied as an antioxidant<sup>45</sup>. This compound has been shown to offer preventative measures against chronic diseases including Parkinson's, arthritis and cardiovascular diseases<sup>46</sup><sup>48</sup>. However, studies have demonstrated a lack of antibacterial activity against the

resistant *S. aureus* RN4220 and 1199B strains (also used during this thesis)<sup>49</sup>. Although, such strains possess efflux-pumps, which **5.3** has been proven to inhibit, thereby enhancing antibiotic activity. For example, by reducing MIC values of fluoroquinolone against *Campylobacter jejuni* and *C. coli*<sup>50</sup>.

Although lack of activity of 5.3 alone was also demonstrated in P. aeruginosa, E.coli and susceptible S. aureus strains, synergistic effects were also recorded with the combination of 5.3 and aminoglycosides, such studies illustrate its potential as an antibiotic adjuvant<sup>51</sup>. *In vivo* experiments have investigated the effect of **5.3** during *P*. aeruginosa-induced pneumonia in rats, showing that pre-treatment with 5.3 inhibits the bacterial increase in endothelial paracellular permeability, and blocks specific bacterial exoenzymes into alveolar epithelial cells, preventing bacterial pathogenesis<sup>52</sup>. **5.3** demonstrates potential in prevention and antibiotic enhancement, particularly against clinically significant multidrug resistant strains, however further in-depth experimental studies are required to clearly illustrate this compound's antimicrobial capabilities<sup>53</sup>. Alpha tocopherol has been investigated for its potential in the treatment of cancers too. However, no encouraging results have been obtained. In fact, a clinical trial found 5.3 to actually increase the risk of prostate cancer in healthy individuals compared to the placebo<sup>54-56</sup>. Hence, later studies have been undertaken to assess other forms of vitamin E, including structurally related molecules such as beta-, gamma-, delta-tocopherol and gamma- and delta-tocotrienol. These have displayed promising cancer preventative results in mechanistic and preclinical cancer model studies<sup>57-60</sup>.

# **Previously Studied Biological Activities of 4.7**

*In vitro* antibacterial studies of **4.7** have been carried out, demonstrating lack of antibacterial properties of this compound. Ling *et al.*, assessed antibacterial activities against Gram-positive and -negative bacteria including *B. subtilis, Micrococcus tetragenus, E. coli* and *P. fluorescens* with MIC values >1000 μg/mL<sup>61</sup>. However, moderate antibacterial activity was observed in another study with **4.7** displaying an MIC of 25 μg/mL against *Mycobacterium tuberculosis*<sup>62</sup>. A more recent study determined

the MIC value of **4.7** against *S. aureus*, *Bacillus subtili*s and *Mycobacterium smegmatis* and determined this compound inactive against these strains<sup>63</sup>.

Regarding anti-cancer activities, **4.7** has displayed moderate *in vitro* cytotoxicity against lung, breast, bladder, cervical and pancreatic cancer<sup>64</sup>.

#### 5.3. Conclusion

This study presents the first antimicrobial evaluation of **5.1** and **5.2**. Neither compound displayed significant antibacterial or antifungal activity, with MIC values exceeding 128  $\mu$ g/mL and no observed cytotoxicity against *C. albicans* or *A. fumigatus*. Anticancer screening against common human cancer cell lines revealed limited activity, with IC<sub>50</sub> values notably higher than cisplatin, indicating low therapeutic potential.

Comparison with structurally related natural products from previous studies highlights the nuanced and often unpredictable nature of structure-activity relationships in natural product research. The absence of activity amongst compounds containing either the lactone moiety or long-chain substitutions (features often associated with bioactivity) suggests that these structural elements alone are insufficient to confer bioactivity. This reinforces the importance of evaluating entire molecules, rather than relying on individual functional groups or motifs, when assessing pharmacological relevance.

Revealing the negative data of the antibacterial, anticancer and antifungal activities of the tested compounds, these data are valuable in refining the chemical space of bioactive natural products, thus preventing redundancy in future screening efforts.

#### 5.4. References

- 1 A. Zamri and J. W. F. Slik, *SciBru*, 2018, **17**, 6–122.
- 2 S. Katagiri, T. Yamakura and S. H. Lee, *Jpn J Southeast Asian Stud*, 1991, **29**, 35–48.
- 3 GBIF, Garcinia caudiculata Ridl., www.gbif.org/species/3715253, (accessed 9 April 2025).
- 4 Q. Gu, R. R. Wang, X. M. Zhang, Y. H. Wang, Y. T. Zheng, J. Zhou and J. J. Chen, *Planta Med*, 2007, **73**, 279–282.
- 5 P. C. Vieira, O. R. Gottlieb and H. E. Gottlieb, *Phytochemistry*, 1983, **22**, 2281–2286.
- 6 M. Valmiki, S. P. Teo, P. E. de Resende, S. Gibbons and A. Ganesan, *Molecules*, **29**, 3613.
- M. Nazir, M. Saleem, M. I. Tousif, M. A. Anwar, F. Surup, I. Ali, D. Wang, N. Z. Mamadalieva, E. Alshammari, M. L. Ashour, A. M. Ashour, I. Ahmed, Elizbit, I. R. Green and H. Hussain, *Biomolecules*, 2021, 11.
- 8 V. Rukachaisirikul, M. Kamkaew, D. Sukavisit, S. Phongpaichit, P. Sawangchote and W. C. Taylor, *J Nat Prod*, 2003, **66**, 1531–1535.
- 9 L. Voutquenne, C. Lavaud, G. Massiot, T. Sevenet and H. A. Hadi, *Phytochemistry*, 1999, **50**, 63–69.
- 10 G. W. Reynolds and E. Rodriguez, *Phytochemistry*, 1981, **20**, 1365–1366.
- 11 J. K. Baker and C. W. Myers, *Parm Res*, **8**, 1991, 763–770.
- 12 L. C. V. Cuong, D. T. Trang, N. T. Cuc, N. X. Nhiem, P. H. Yen, H. L. T. Anh, L. M. Huong, C. Van Minh and P. Van Kiem, *Vietnam J Chem*, 2015, **53**, 94–97.
- L. Velkoska-Markovska, M. S. Jankulovska, B. Petanovska-Ilievska and K. Hristovski, *Acta Chromatogr*, 2020, **32**, 34–38.
- M. Leonor Suarez-Quiroz, A. A. Campos, G. V. Alfaro, O. Gonzalez-Rios, P. Villeneuve, M. C. Figueroa-Espinoza, M. L. Suá Rez-Quiroz and O. Gonzá Lez-Ríos, *J Food Compos Anal*, 2014, **33**, 55–58.
- M. Yüzbaşıoğlu Baran, S. Özlem Şener, Ş. Kanbolat, M. Badem and U. Özgen, *Int J Second Metabolite*, 2025, **12**, 158–165.
- 16 J. Wu, J. Ye, J. Cen, Y. Chem and J. Xu, *Mar drugs*, 2024, **22**, 332–340.
- 17 T. Thiemann, *Open Chem J*, 2020, **8**, 1–36.
- 18 Y. Matsuda and I. Abe, *Nat Prod Rep*, 2016, **33**, 26–53.
- 19 C. Hertweck, *Angew Chem Int Ed*, 2009, **48**, 4688–4716.
- 20 Y. Huang, F. J. Xie, X. Cao and M. Y. Li, *Biotechnol Biotechnol Equip*, 2021, **35**, 1800–1809.
- T. Noshita, H. Kiyota, Y. Kidachi, K. Ryoyama, S. Funayama, K. Hanada and T. Murayama, *Biosci Biotechnol Biochem*, 2009, **73**, 726–728.
- 22 R. R. Wang, Q. Gu, Y. H. Wang, X. M. Zhang, L. M. Yang, J. Zhou, J. J. Chen and Y. T. Zheng, *J Ethnopharmacol*, 2008, **117**, 249–256.
- 23 K. Chen, C. Peng, F. Chi, C. Yu, Q. Yang and Z. Li, Front Microbiol, 13, 885092.
- A. Karunanidhi, R. Thomas, A. Van Belkum and V. Neela, *Biomed Res Int*, 2013, **2013**, 392058.
- 25 Z. Lou, H. Wang, S. Zhu, C. Ma and Z. Wang, *J Food Sci*, 2011, **76**, 398–403.
- L. Wang, C. Bi, H. Cai, B. Liu, X. Zhong, X. Deng, T. Wang, H. Xiang, X. Niu and D. Wang, *Front Microbiol*, 2015, **6**, 1031.
- 27 S. Feng, Y. Zhang, S. Fu, Z. Li, J. Zhang, Y. Xu, X. Han and J. Miao, *Int Immunopharmacol*, 2023, **114**, 109536.
- A. A. Neamţu, T. A. Maghiar, V. Turcuş, P. B. Maghiar, A. M. Căpraru, B. A. Lazar, C. A. Dehelean, O. L. Pop, C. Neamţu, B. D. Totolici and E. Mathe, *Curr Issues Mol Biol*, 2024, **46**, 6783–6804.
- 29 M. Miao and L. Xiang, *Adv Pharmacol*, 2020, **87**, 71–88.
- 30 W. Tian, Y. Dou, H. Wang, J. Zhu, Y. Dai and H. Xiang, *J Prev Med Chin People's Liber Army*, 2017, **34**, 854–857.

- N. Cinkilic, S. K. Cetintas, T. Zorlu, O. Vatan, D. Yilmaz, T. Cavas, S. Tunc, L. Ozkan and R. Bilaloglu, *Food Chem Toxicol*, 2013, **53**, 359–363.
- 32 M. He, J. W. Min, W. L. Kong, X. H. He, J. X. Li and B. W. Peng, *Fitoterapia*, 2016, **115**, 74–85.
- 33 M. E. Hosen, S. Jahan Supti, S. Akash, M. E. Rahman, M. O. Faruqe, M. Manirujjaman, U. K. Acharjee, A. R. Z. Gaafar, L. Ouahmane, B. Sitotaw, M. Bourhia and R. Zaman, *Front Chem*, 2023, 11.
- A. Rammohan, B. V. Bhaskar, N. Venkateswarlu, V. L. Rao, D. Gunasekar and G. V. Zyryanov, *Microb Pathog*, 2019, **136**, 103667.
- 35 A. Adamczak, M. Ożarowski and T. M. Karpiński, J Clin Med, 2019, 9, 109–126.
- G. V. Awolola, N. A. Koorbanally, H. Chenia, F. O. Shode and H. Baijnath, *Afr J Tradit, Complement, Altern Med*, 2014, **11**, 124–131.
- 37 H. Xiang, P. Yang, L. Wang, J. Li, T. Wang, J. Xue, D. Wang and H. Ma, *J. Microbiol Biotechnol*, 2021, **31**, 1350–1357.
- 38 D. Mu, H. Xiang, H. Dong, D. Wang and T. Wang, J. Microbiol Biotechnol, 2018, 28, 1426–1432.
- 39 C. Xu, X. Cao, X. Cao, L. Liu, Y. Qiu, X. Li, L. Zhou, Y. Ning, K. Ren and J. Cao, *Anticancer Agents Med Chem*, 2020, **20**, 1654–1663.
- 40 C. C. Guimarães, D. D. Oliveira, M. Valdevite, A. L. F. Saltoratto, S. I. V. Pereira, S. de C. França, A. M. S. Pereira and P. S. Pereira, *Food Chem Toxicol*, 2015, **86**, 88–94.
- 41 T. K. Girish, K. A. Kumar and U. J. S. Prasada Rao, *Toxicol Rep.*, 2016, 3, 652–663.
- 42 F. Conforti, F. Menichini, D. Rigano and F. Senatore, ZNaturforsch CJBiosci, 2009, 64, 490–494.
- 43 Y. gang Zu, X. lei Liu, Y. jie Fu, N. Wu, Y. Kong and M. Wink, *Phytomedicine*, 2010, 17, 1095–1101.
- 44 K. Ganesan and B. Xu, *Ann N.Y. Acad Sci*, 2017, **1401**, 102–113.
- J. M. Tucker and D. M. Townsend, *Biomed Pharmacother*, 2005, **59**, 380–387.
- E. W. Karlson, N. A. Shadick, N. R. Cook, J. E. Buring and I. M. Lee, *Arthritis Rheum*, 2008, **59**, 1589.
- M. Wallert, M. Ziegler, X. Wang, A. Maluenda, X. Xu, M. L. Yap, R. Witt, C. Giles, S. Kluge, M. Hortmann, J. Zhang, P. Meikle, S. Lorkowski and K. Peter, *Redox Biol*, 2019, **26**, 101292.
- 48 X. Hao, H. Li, Q. Li, D. Gao, X. Wang, C. Wu, Q. Wang and M. Zhu, *Front Nutr*, 2023, **10**, 1289238.
- 49 S. R. Tintino, C. D. Morais-Tintino, F. F. Campina, R. L. Pereira, M. do S. Costa, M. F. B. M. Braga, P. W. Limaverde, J. C. Andrade, J. P. Siqueira-Junior, H. D. M. Coutinh, V. Q. Balbino, T. C. Leal-Balbino, J. Ribeiro-Filho and L. J. Quintans-Júnior, *EXCLI J*, 2016, **15**, 315–322.
- 50 A. A. Abd El-Tawab, A. M. Ammar, H. A. Ahmed and A. A. Hefny, *Microb Drug Resist*, 2019, **25**, 203–211.
- J. C. Andrade, M. F. B. Morais-Braga, G. M. M. Guedes, S. R. Tintino, M. A. Freitas, I. R. A. Menezes and H. D. M. Coutinho, *Biomed Pharmacother*, 2014, **68**, 1065–1069.
- B. M. Wagener, N. Anjum, C. Evans, A. Brandon, J. Honavar, J. Creighton, M. G. Traber, R. L. Stuart, T. Stevens and J. F. Pittet, *Am J Respir Cell Mol Biol*, 2020, **63**, 234–243.
- 53 M. S. Hartmann, M. M. Heimesaat, S. Bereswill and S. Mousavi, *Eur J Microbiol Immunol*, 2020, **10**, 193–201.
- E. A. Klein, I. M. Thompson, C. M. Tangen, J. J. Crowley, S. Lucia, P. J. Goodman, L. M. Minasian, L. G. Ford, H. L. Parnes, J. M. Gaziano, D. D. Karp, M. M. Lieber, P. J. Walther, L. Klotz, J. K. Parsons, J. L. Chin, A. K. Darke, S. M. Lippman, G. E. Goodman, F. L. Meyskens and L. H. Baker, *JAMA*, 2011, **306**, 1549–1556.
- 55 Q. Jiang, S. Christen, M. K. Shigenaga and B. N. Ames, *Am J Clin Nutr*, 2001, **74**, 714–722.
- J. Ju, S. C. Picinich, Z. Yang, Y. Zhao, N. Suh, A. N. Kong and C. S. Yang, *Carcinogenesis*, 2010, 31, 533–542.
- 57 M. T. Ling, S. U. Luk, F. Al-Ejeh and K. K. Khanna, *Carcinogenesis*, 2012, **33**, 233–239.
- 58 Q. Jiang, Free Radic Biol Med, 2014, 72, 76–90.

- 59 S. Das Gupta, S. Sae-Tan, J. Wahler, J. Y. So, M. J. Bak, L. C. Cheng, M. J. Lee, Y. Lin, W. J. Shih, J. D. Shull, S. Safe, C. S. Yang and N. Suh, *Cancer Prev Res (Phila)*, 2015, **8**, 807–816.
- 60 Q. Jiang, *Adv Nutr*, 2017, **8**, 850–867.
- 61 T. J. Ling, W. W. Ling, Y. J. Chen, X. C. Wan, T. Xia, X. F. Du and Z. Z. Zhang, *Molecules*, 2010, **15**, 8469–8477.
- 62 J.-J. Chen, W.-J. Lin, P.-C. Shieh, I.-S. Chen, C.-F. Peng and P.-J. Sung, *Chem Biodivers*, 2010, 7, 717–721.
- 63 H. T. Nguyen, D. V. Ho, H. Q. Vo, A. T. Le, H. M. Nguyen, T. Kodama, T. Ito, H. Morita and A. Raal, *Pharm Biol*, 2017, **55**, 787–791.
- A. Hamed, M. El Gaafary, L. F. Yamaguchi, H. G. Stammler, L. M. Salih, D. Ziegler, T. Syrovets and M. J. Kato, *Nat Prod Res*, 2024, 1–7.

## **Chapter 6 – Conclusions**

The urgent global demand for novel antibacterial and anticancer agents continues to intensify, driven by rising resistance and unmet therapeutic needs. Despite their high medicinal potential, less than 10% of plant species have been investigated in this context, leaving many sources of untapped chemical diversity within plants. As described in the outlined aims and objectives in sections 1.5.1 and 1.5.2, this thesis constitutes a focused investigation into the chemical and biological potential of previously uncharacterised plant species endemic to Borneo, undertaken with the dual aim of expanding phytochemical knowledge and identifying novel bioactive metabolites. This work prioritised taxonomically and ethnobotanically significant genera within the Myristicaceae and Clusiaceae families which have remained largely unexplored. The aim was to build metabolite profiles for selected species while evaluating their constituents for antibacterial, antifungal, and anticancer activities.

Objective 1 was addressed in the second chapter, which presents a systematic review of the phytochemical and pharmacological literature pertaining to 44 plant species from the Myristicaceae and the Clusiaceae families which had been previously sampled from Borneo. This analysis was undertaken to identify unexplored species, which possessed potential phytochemical significance, and to therefore guide the selection of species for subsequent investigations. Here, a significant research gap was revealed, with several species showing no prior published chemical or biological evaluation. Based on these findings, objective 2 was addressed, by selecting nine species for preliminary antibacterial screening: *Gymnacranthera contracta, Horsfieldia polyspherula, Horsfieldia splendida, Knema elmerii, Knema latifolia* and *Knema membranifolia* (Myristicacaea), and *Calophyllum pulcherimum, Garcinia caudiculata* and *Mesua calciphila* (Clusiaceae). This initial study directed the project into a more focused phytochemical investigation of *K. membranifolia, G. contracta* and *G. caudiculata*. Here, compounds were extracted, purified, and characterised primarily using mass spectrometry and 1D and 2D NMR

techniques (objectives 3 and 4). Chapters Four and Five address objectives 5 and 6, presenting the structural elucidation and biological evaluation of isolated metabolites from each plant family.

Chapter Four presented the first phytochemical investigation of *K. membranifolia* and G. contracta (Myristicaceae), resulting in the structural characterisation of fourteen secondary metabolites, including a previously undescribed salicylic acid derivative, differing in alkane chain length (summarised in Figure 6.1). Amongst these findings, α-tocopherol quinone was reported here from the Myristicaceae family for the first time, revealing the presence of potential biosynthetic routes within the family. A structurally distinctive 12-carbon salicylic acid analogue bearing a terminal phenyl ring (4.2) exhibited exceptional antibacterial activity against MRSA, with an MIC of 2 µg/mL, placing it as the most potent natural analogue of its class described to date, revealing the importance of the terminal phenyl group as well as optimal chain length and saturation of salicylic acid derivatives. In addition, 4.2 was found to be amongst the most potent antibacterial plant derived compounds. Interestingly, 4.2 displayed reduced activity against MSSA, alluding to a potential mechanism of action which evades PBP interactions. Mechanistic evaluation, including MBC determination, confirmed the bactericidal nature of 4.2 (MBC =  $2 \mu g/mL$ ), displaying its potential to not only inhibit growth, but kill pathogens. As outlined in Chapter Four, a comprehensive structure-activity relationship investigation, encompassing a broader spectrum of salicylic acid, cardol and acetophenone derivatives with varied alkyl chain lengths and functional group modifications, is essential to elucidate the precise structural determinants of antibacterial potency across different bacterial strains.

The fifth chapter of this thesis revealed the phytochemistry and biological activities of *G. caudiculata* for the first time. This yielded six secondary metabolites, including one previously undescribed open ringed lactone (**5.2**) which is the first of this compound type to be described in this family (Figure 6.1). The biological evaluation of these compounds revealed a lack of antibacterial, antifungal, or cytotoxic activity

across a broad panel of microbial and cancer cells, delineating inactive chemical space. This newly described compound was published in the journal *Molecules*. Despite the observed negative biological results of compounds, particularly amongst those containing traditionally bioactive motifs such as lactones and terpenoid chain substituents, these data challenge conventional assumptions in natural product pharmacology. Such findings reinforce the complex and non-linear relationship between structure and activity within plant metabolites and highlight the necessity of holistic molecular evaluation rather than reliance on predictive structural features alone.

While this study led to the identification of some new natural products, it also involved the re-isolation of previously known compounds. Importantly, many of these compounds underwent biological evaluation for the first time, revealing impressive activity which would likely have remained undocumented. Thus, this thesis emphasises the importance of building metabolic profiles for unexplored plants. The re-identification of bioactive compounds from these species reinforces their pharmacological relevance, therefore supporting their inclusion in future drug discovery efforts.

**Table 6.1.** Structures of all compounds identified in this study, indicating the plant source.

Identifier	Source	Structure
4.1	Knema	O <sub>S</sub> _OH
	membranifolia	
	(Myristicaceae)	HO 10
4.2		OVOH
		HO 12

4.3

O OH HO 16

4.4

HO 8 OH

4.5

HO 10 OH

4.6

HO 10 OH

4.7 Knema

membranifolia
(Myristicacea)

and Garcinia

caudiculata
(Clusiaceae)

4.8 Gymnacranthera contracta (Myristicacea)

4.14

5.1 Garcinia caudiculata (Clusiaceae)

OH 4

5.2

5.3

5.4

## 6.1. Future Outlooks

Given that only approximately only half of Borneo's original forest cover remains (due to deforestation and replacement with monocultures for farming), demonstrating the biochemical value of native flora may contribute to broader conservation arguments. Identifying pharmacologically promising compounds from these ecosystems highlights the medicinal potential embedded within biodiversity, providing a compelling incentive for preservation. However, such bioprospecting must proceed with a conservation-conscious mindset which considers the historical and ongoing tensions between medicinal plant harvesting and habitat degradation. This work also reaffirms the significance of ethnomedicinal knowledge, particularly that of the Dayak communities. Many of the species investigated here have long-standing traditional uses, yet have remained chemically and biologically underinvestigated. By integrating traditional ecological knowledge with phytochemical and pharmacological approaches, this study not only strengthens the foundation for future scientific discovery but also recognises and validates the deep cultural knowledge held by Indigenous communities.

Collectively, this thesis demonstrates the importance of investigating chemically uncharacterised plant species, particularly within the Myristicaceae and Clusiaceae families, in an approach which considers ethnobotany, phytochemistry and pharmacology. The isolation of novel and minimally studied metabolites, including a structurally unique salicylic acid analogue with exceptional bactericidal activity against MRSA, expands the known chemical space of these species and advances

our understanding of natural product pharmacophores. This provides a valuable basis for future structure-activity optimisation studies. More broadly, this thesis demonstrates the relevance of phytochemical exploration as an important foundation for antimicrobial drug discovery. In an era of rising resistance and diminishing antimicrobial resources, the future of drug discovery significantly depends on exploring the potential of plant natural products.

## **Appendices**

## Appendix A: Spectral data of natural products isolated from Myristicaceae

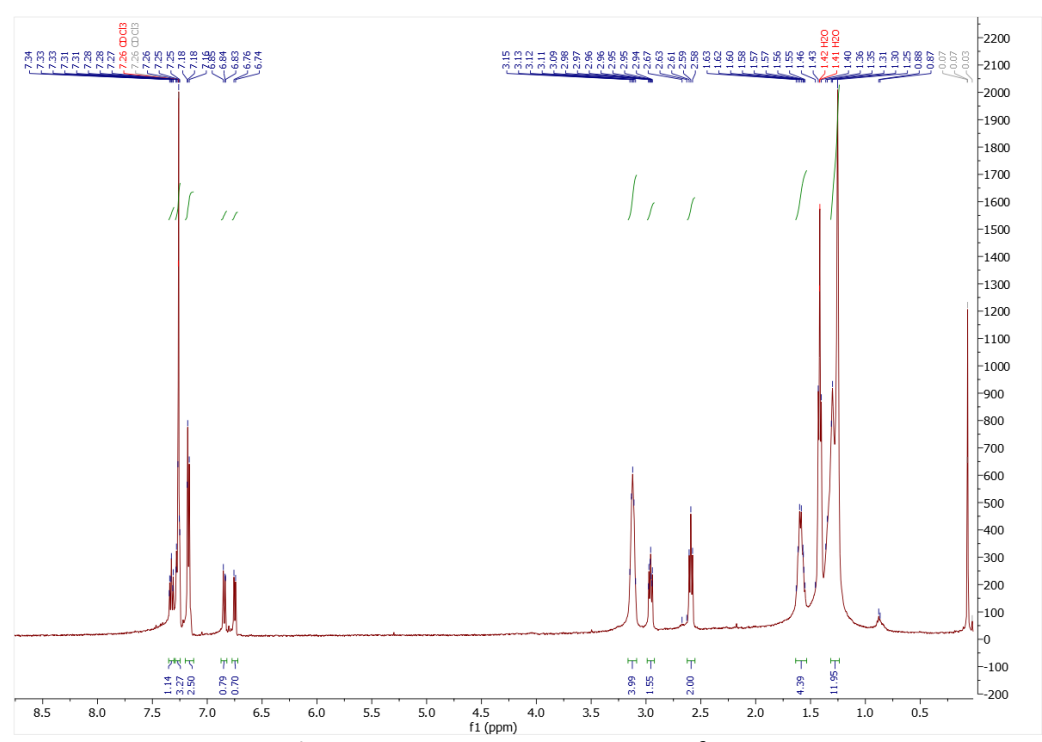


Figure A1. 1H NMR spectrum of 4.1.

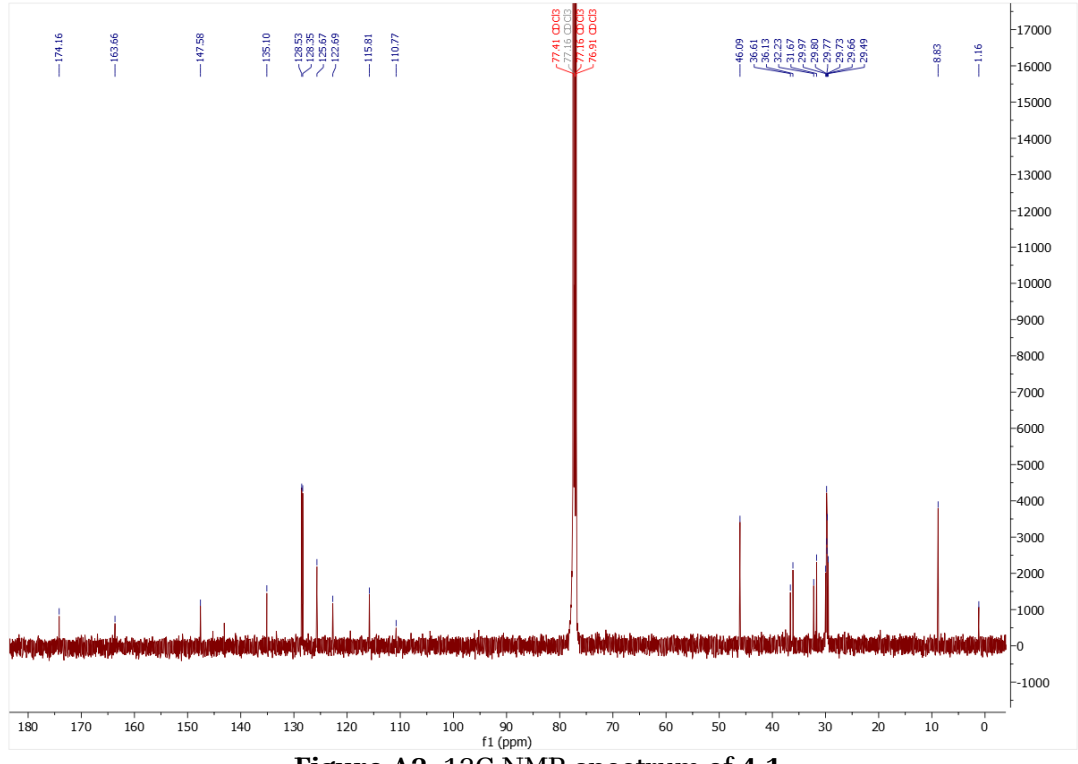


Figure A2. 13C NMR spectrum of 4.1.

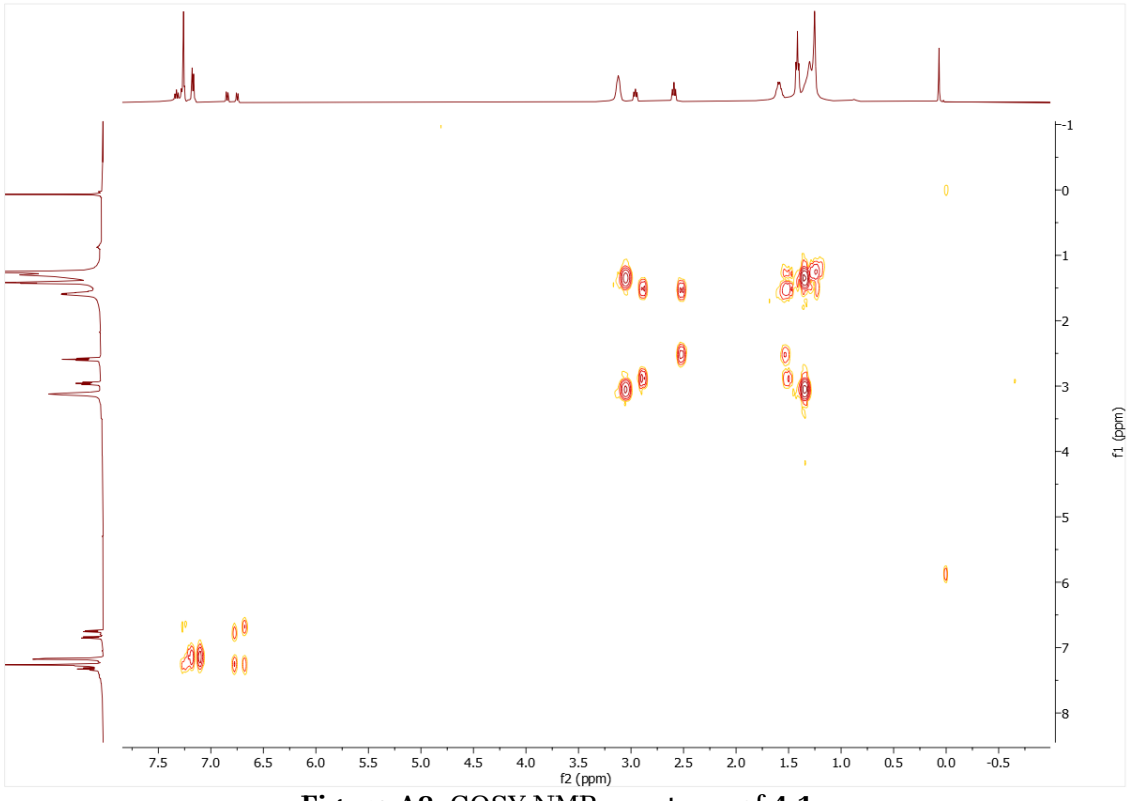
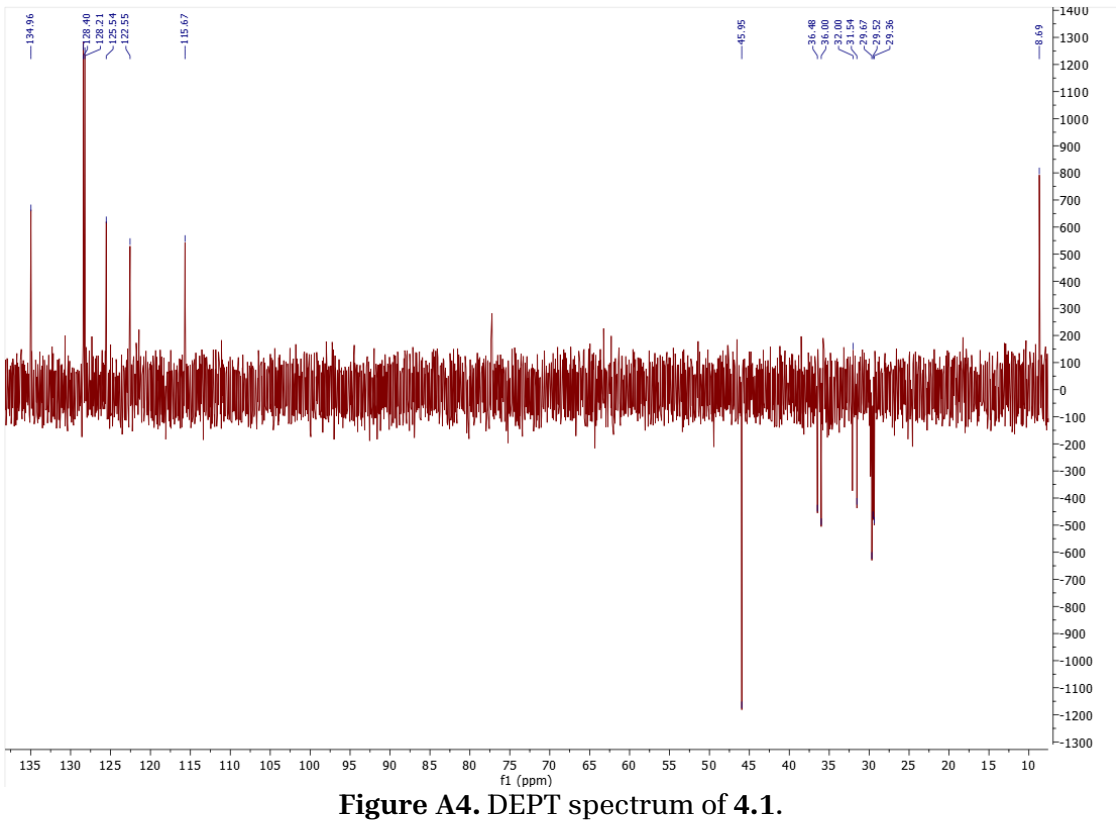


Figure A3. COSY NMR spectrum of 4.1.



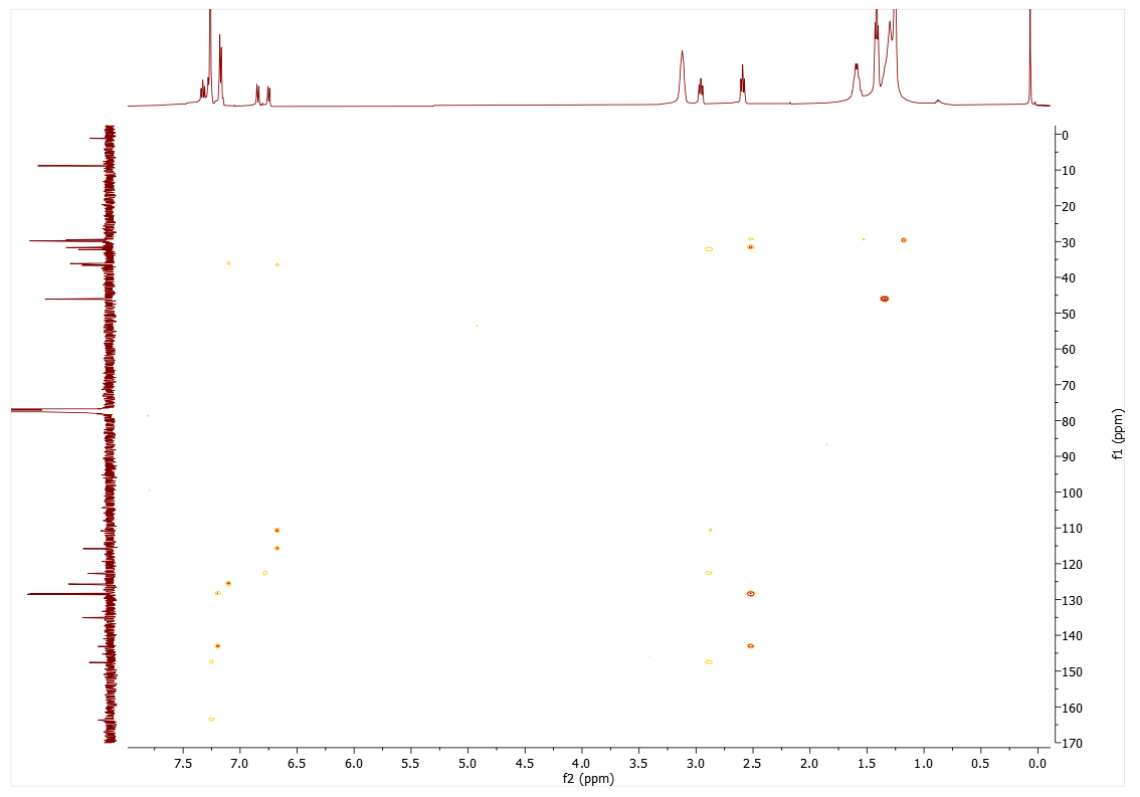
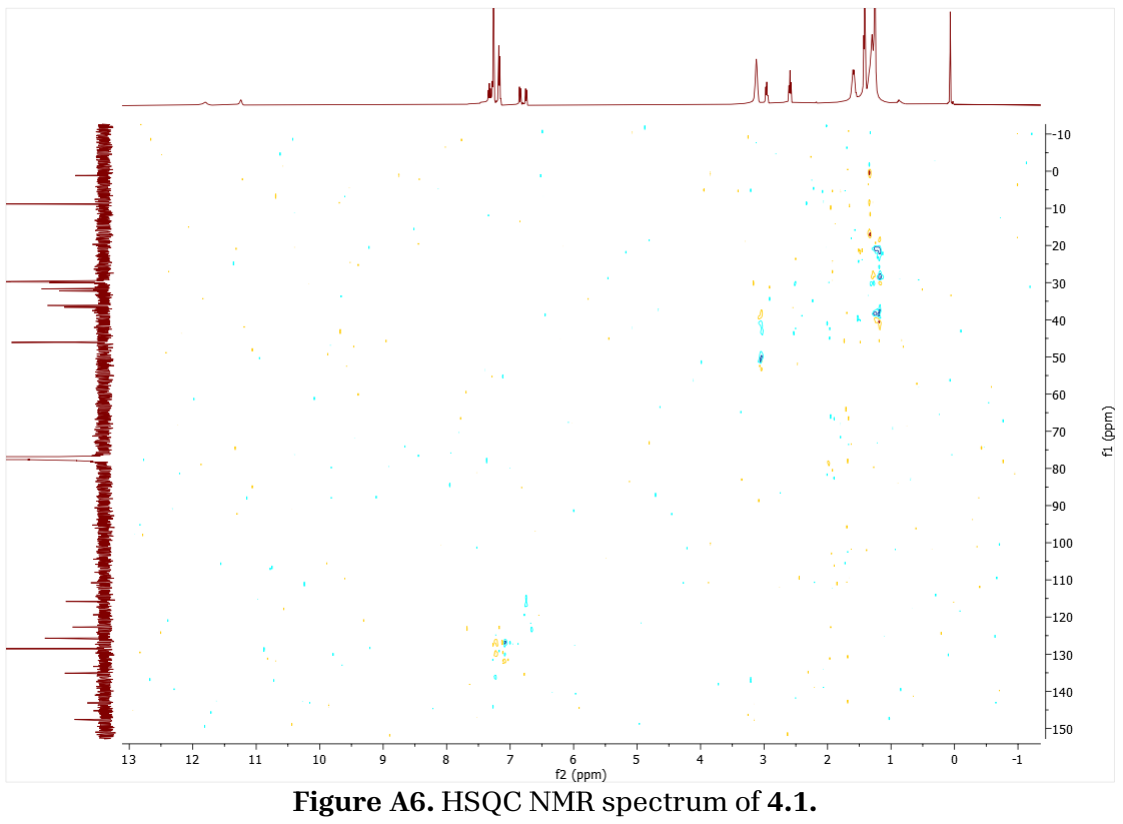


Figure A5. HMBC NMR spectrum of 4.1.



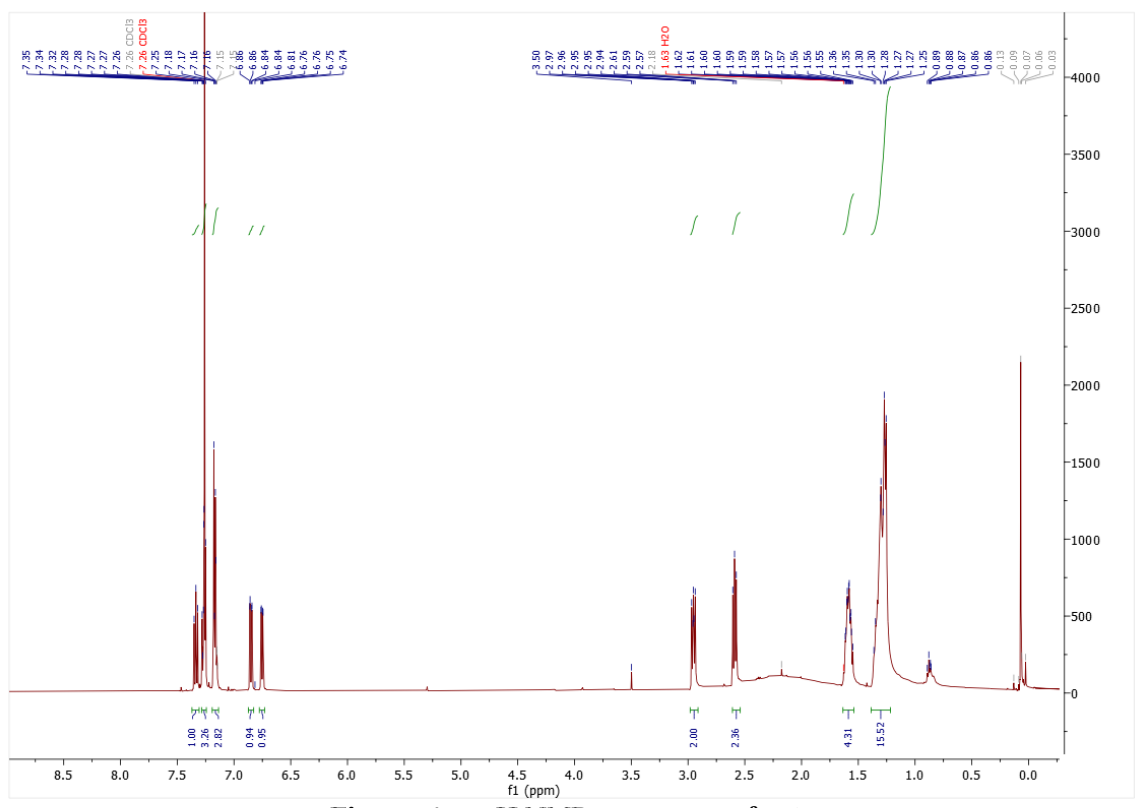


Figure A7. 1H NMR spectrum of 4.2.

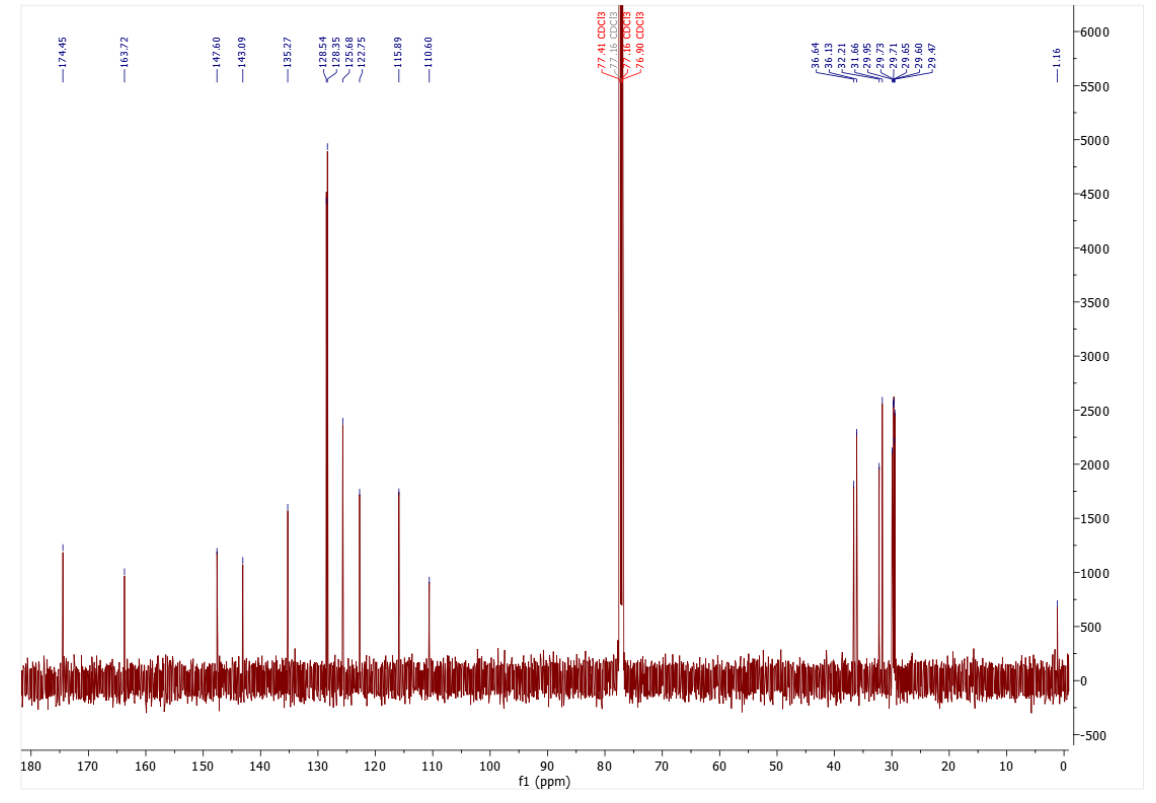


Figure A8. 13C NMR spectrum of 4.2.

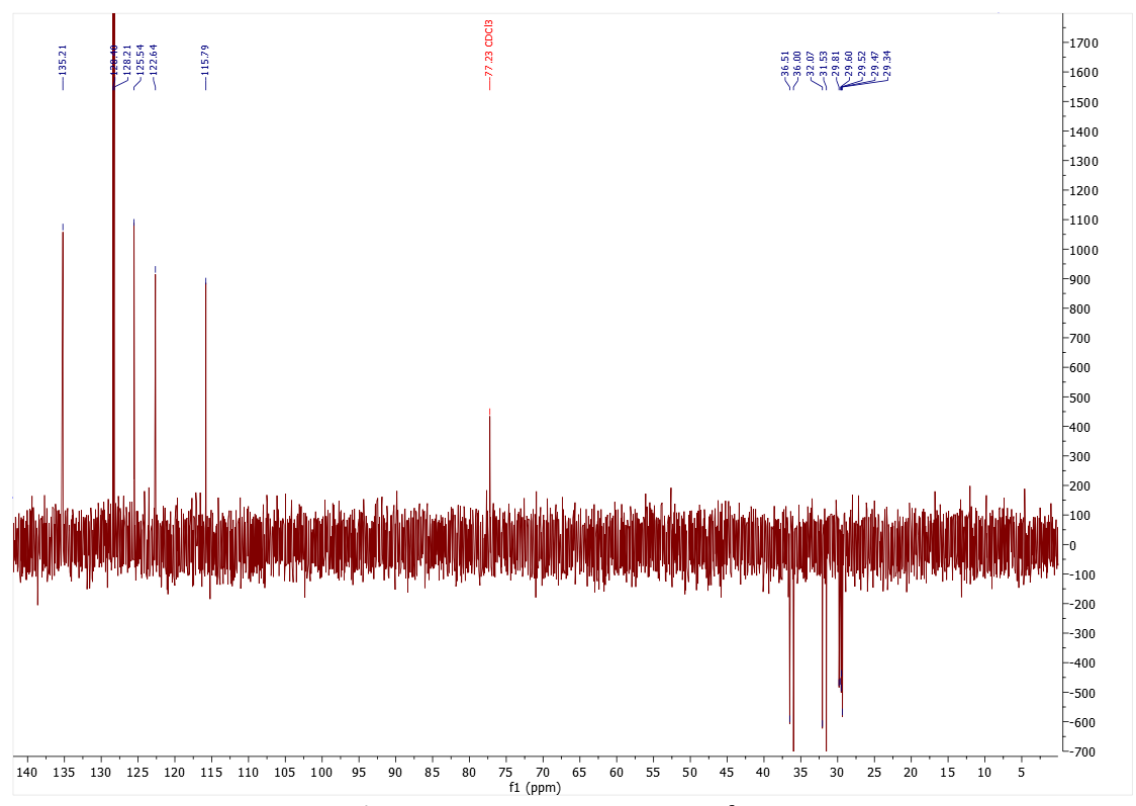


Figure A9. DEPT spectrum of 4.2.

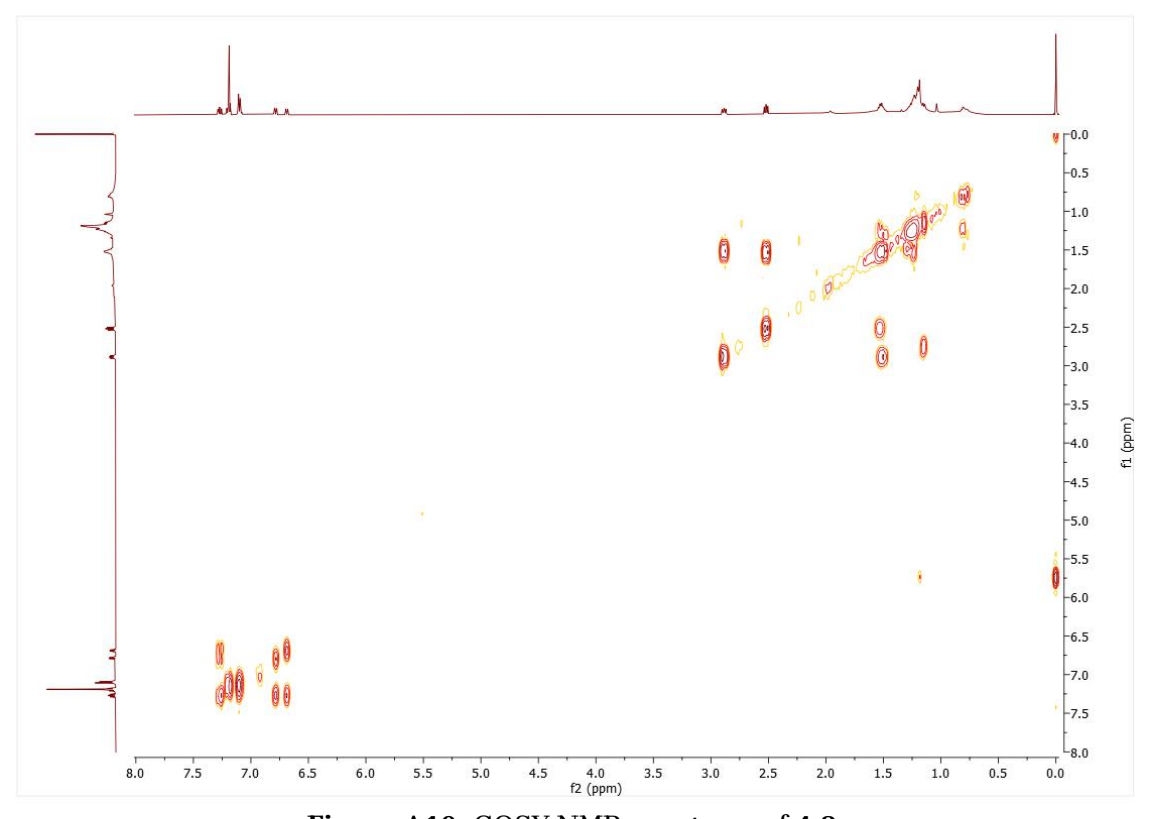


Figure A10. COSY NMR spectrum of 4.2.

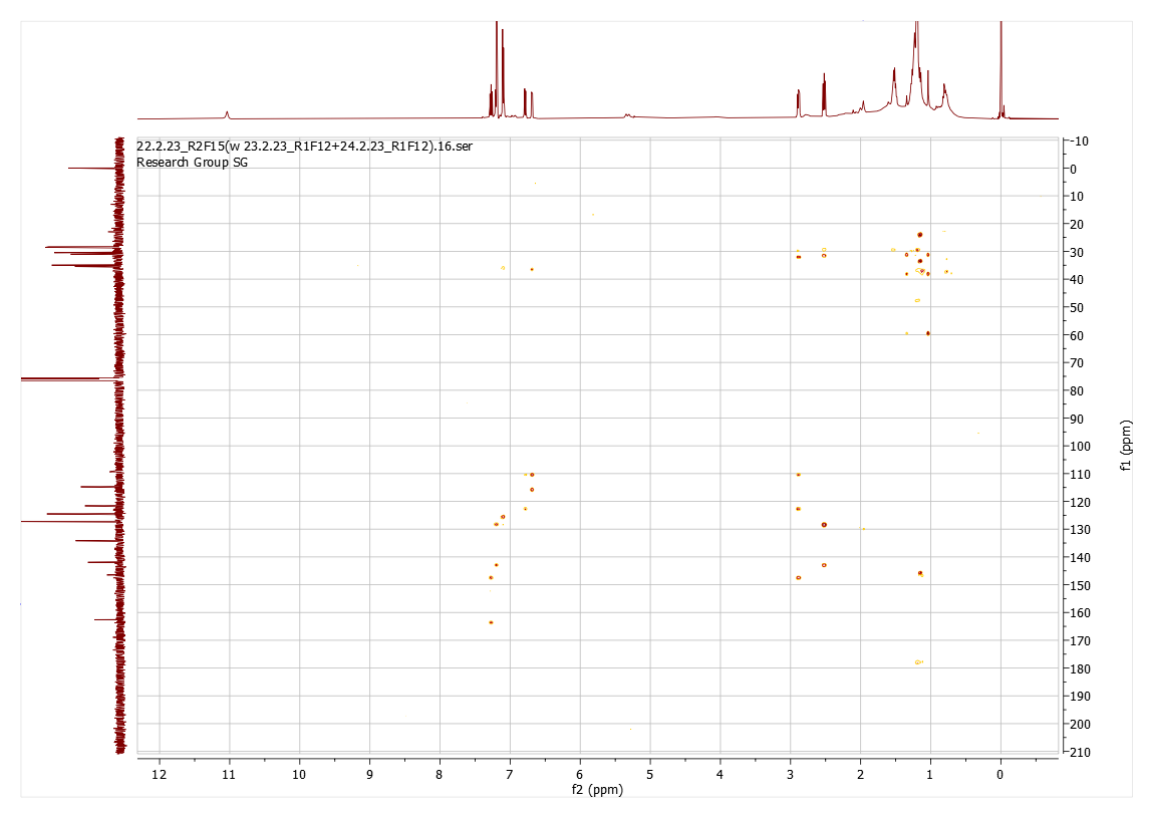


Figure A11. HMBC NMR spectrum of 4.2.

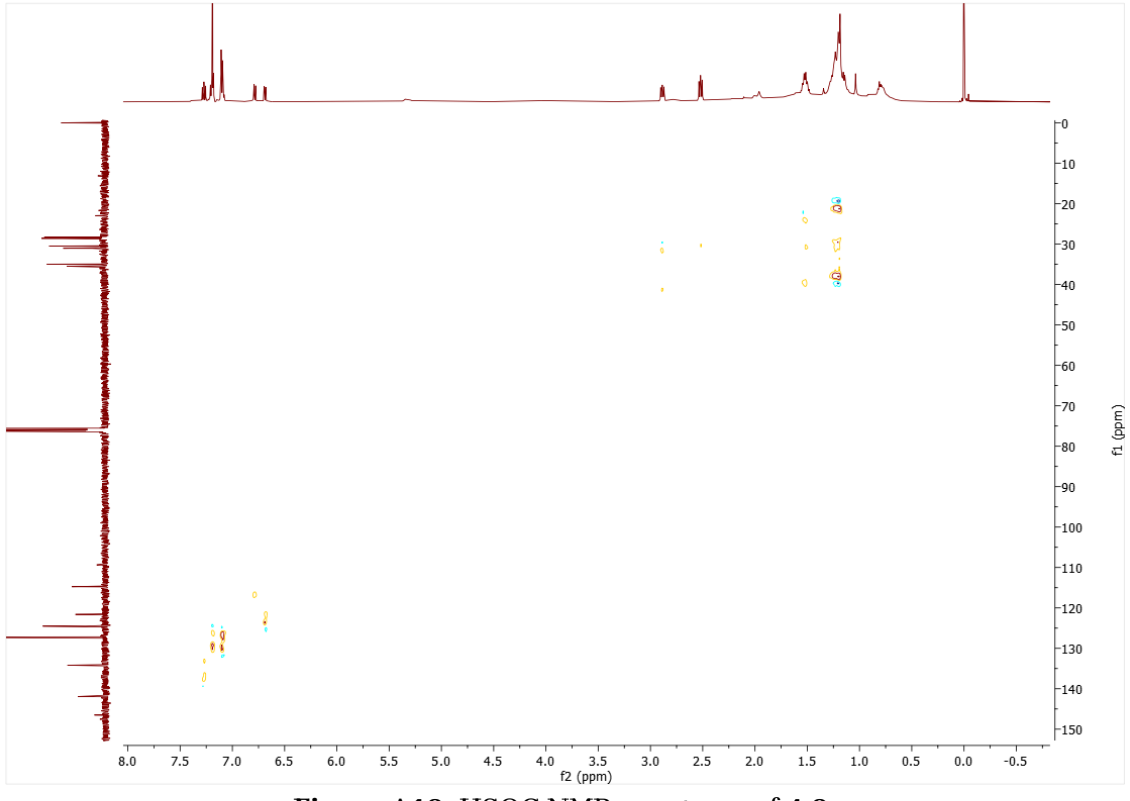


Figure A12. HSQC NMR spectrum of 4.2.

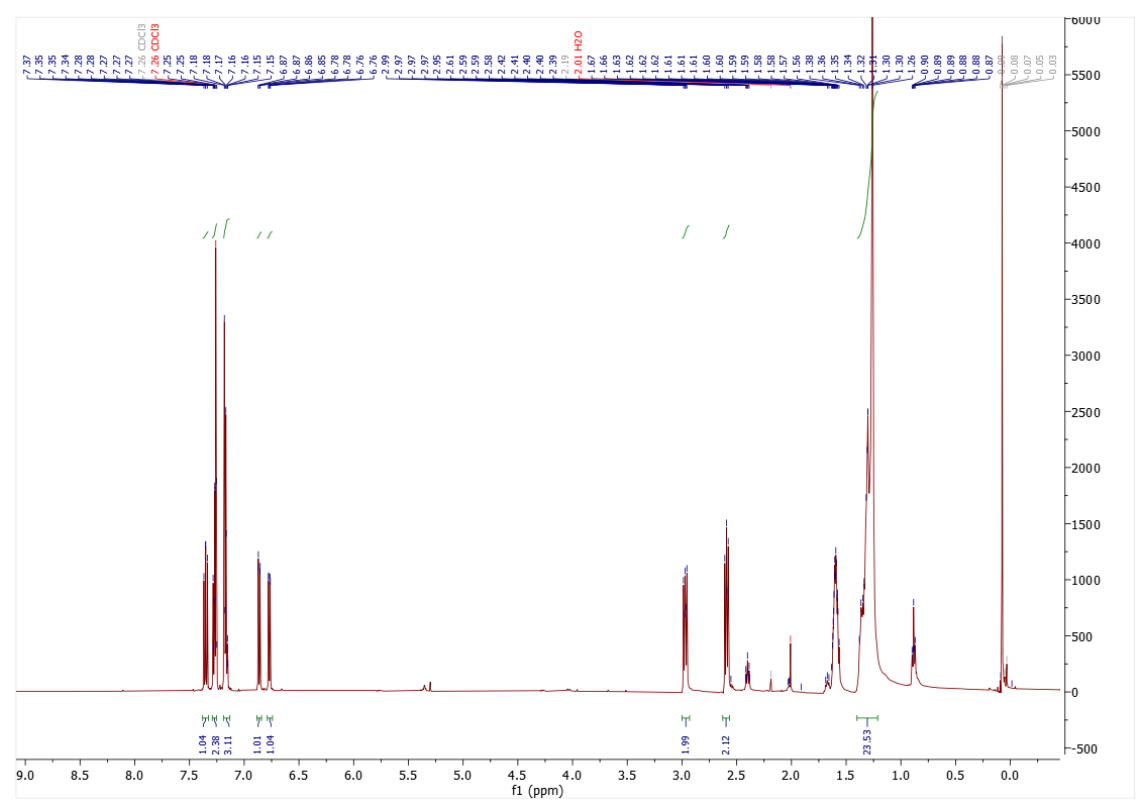


Figure A13. 1H NMR spectrum of 4.3.

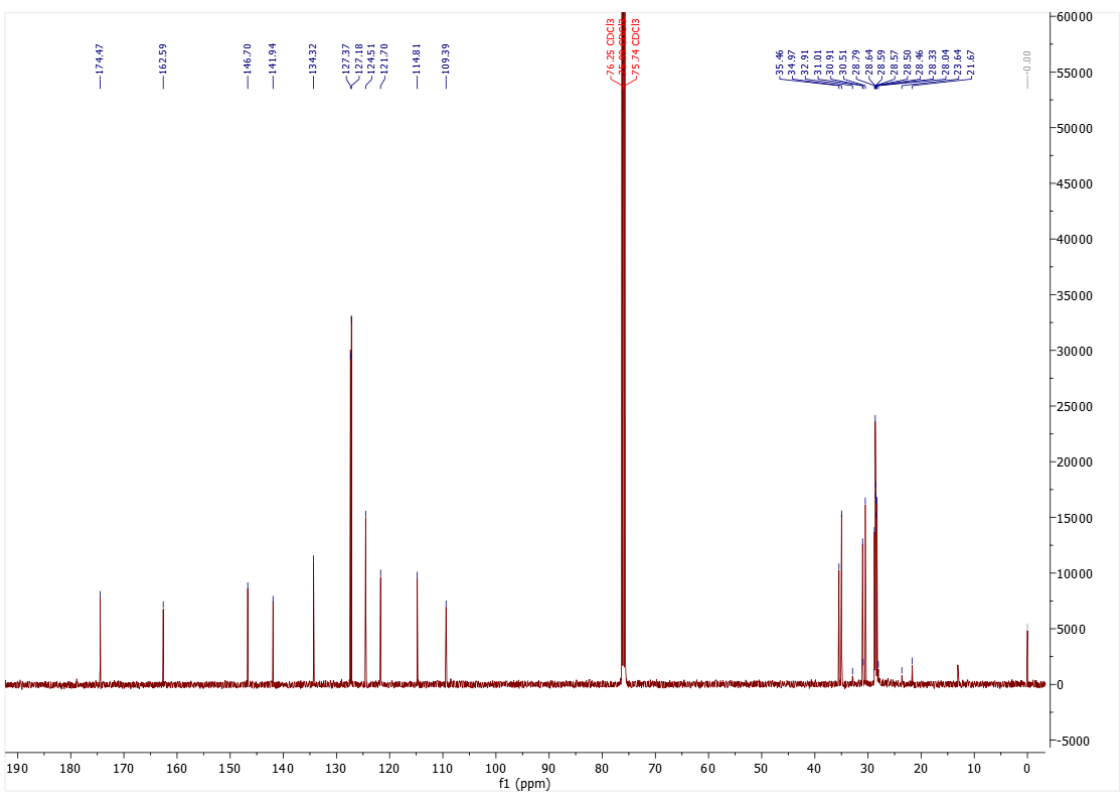


Figure A14. 13C NMR spectrum of 4.3.

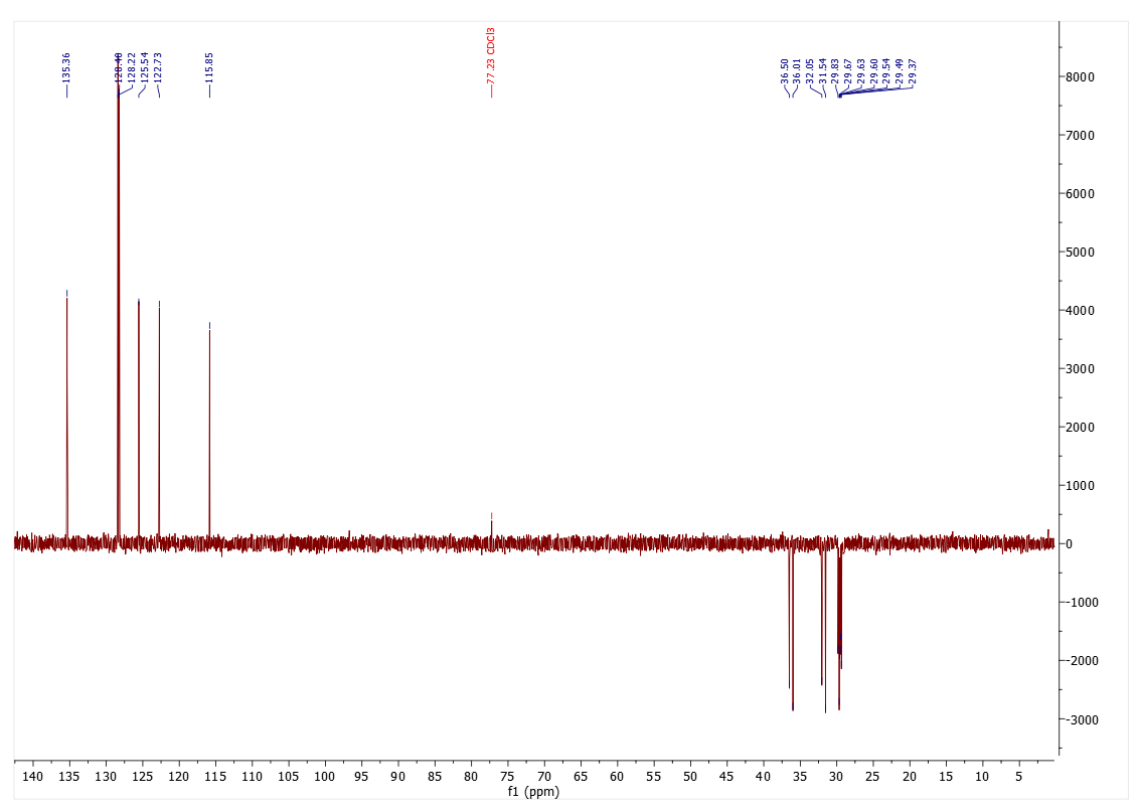


Figure A15. DEPT spectrum of 4.3.

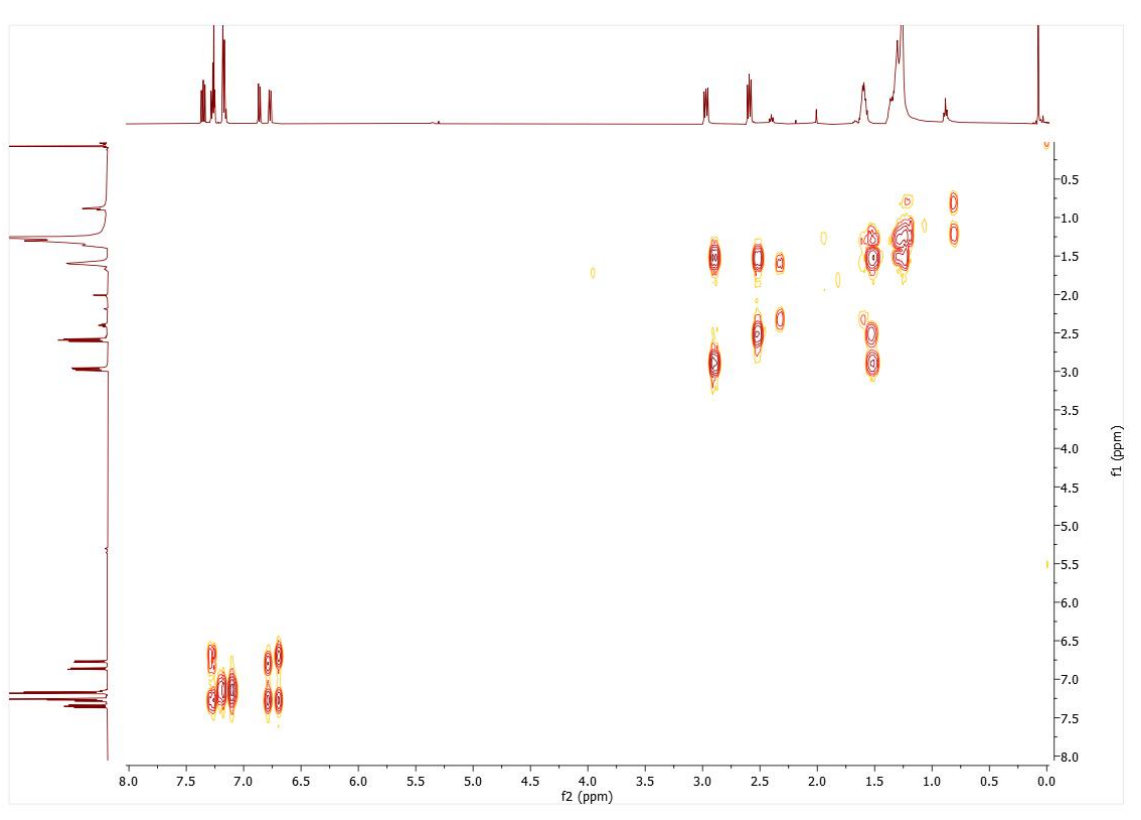


Figure A16. COSY NMR spectrum of 4.3.

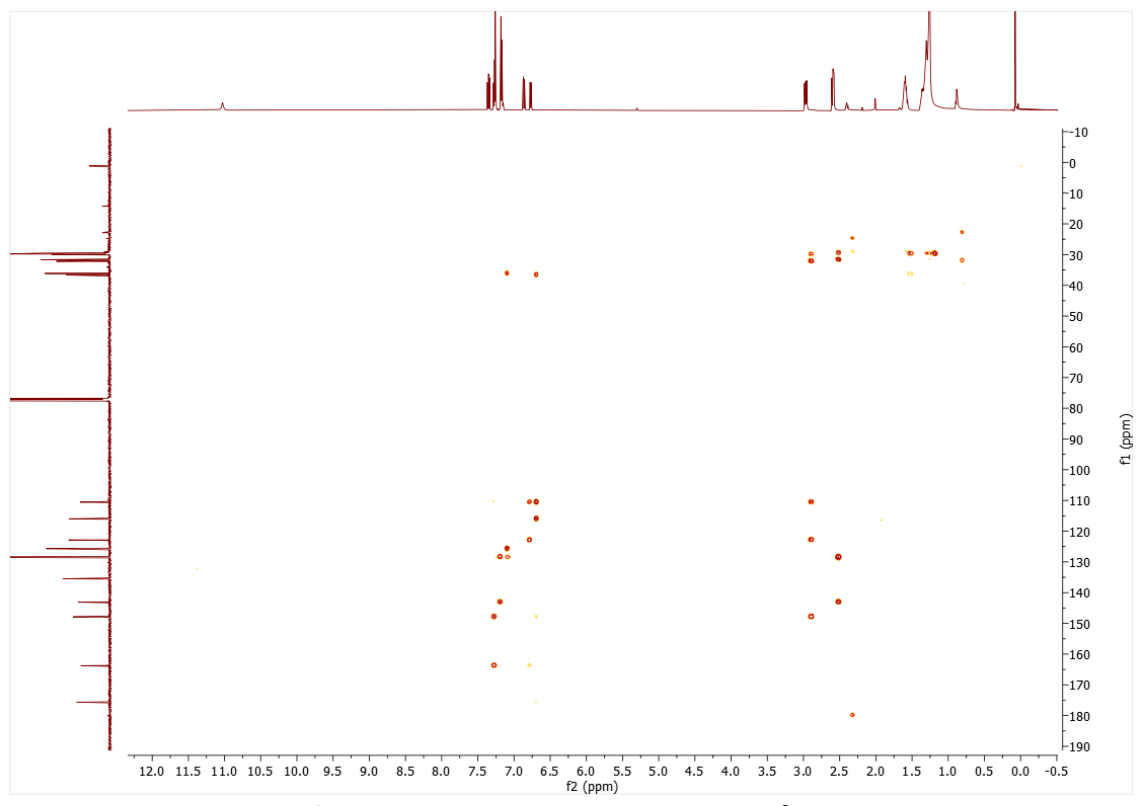


Figure A17. HMBC NMR spectrum of 4.3.

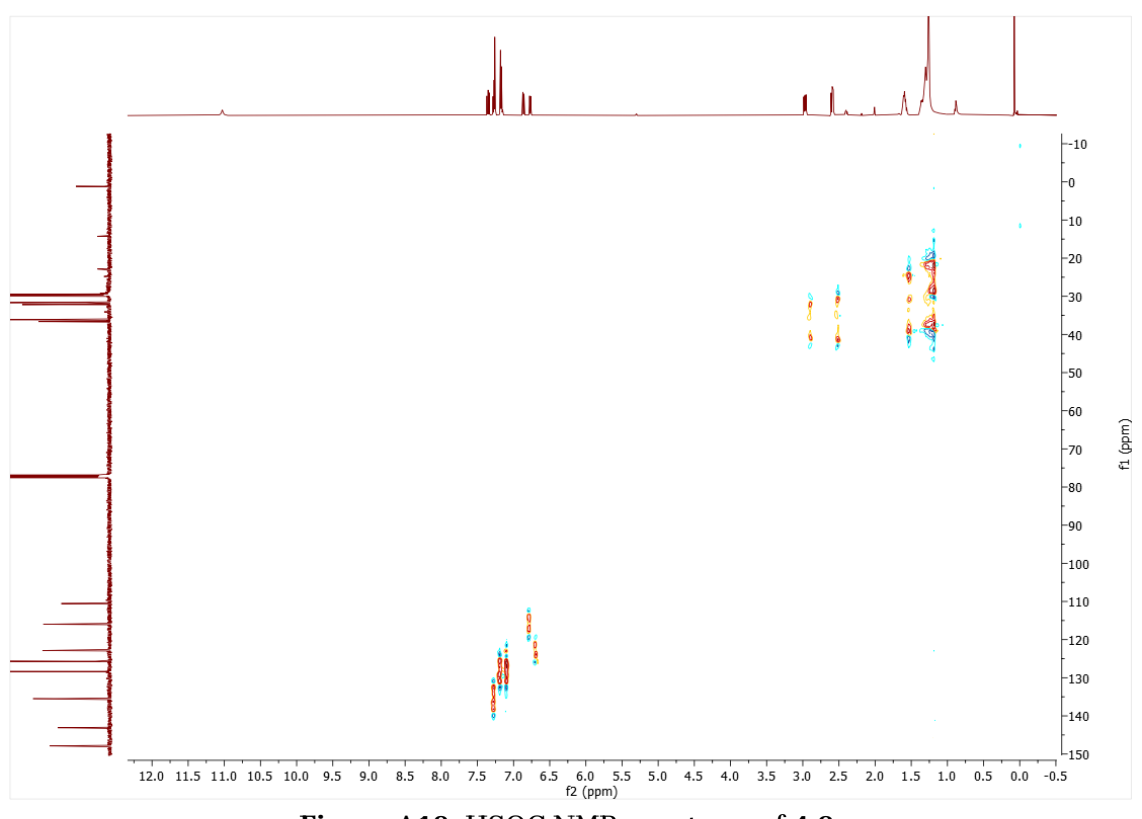


Figure A18. HSQC NMR spectrum of 4.3.

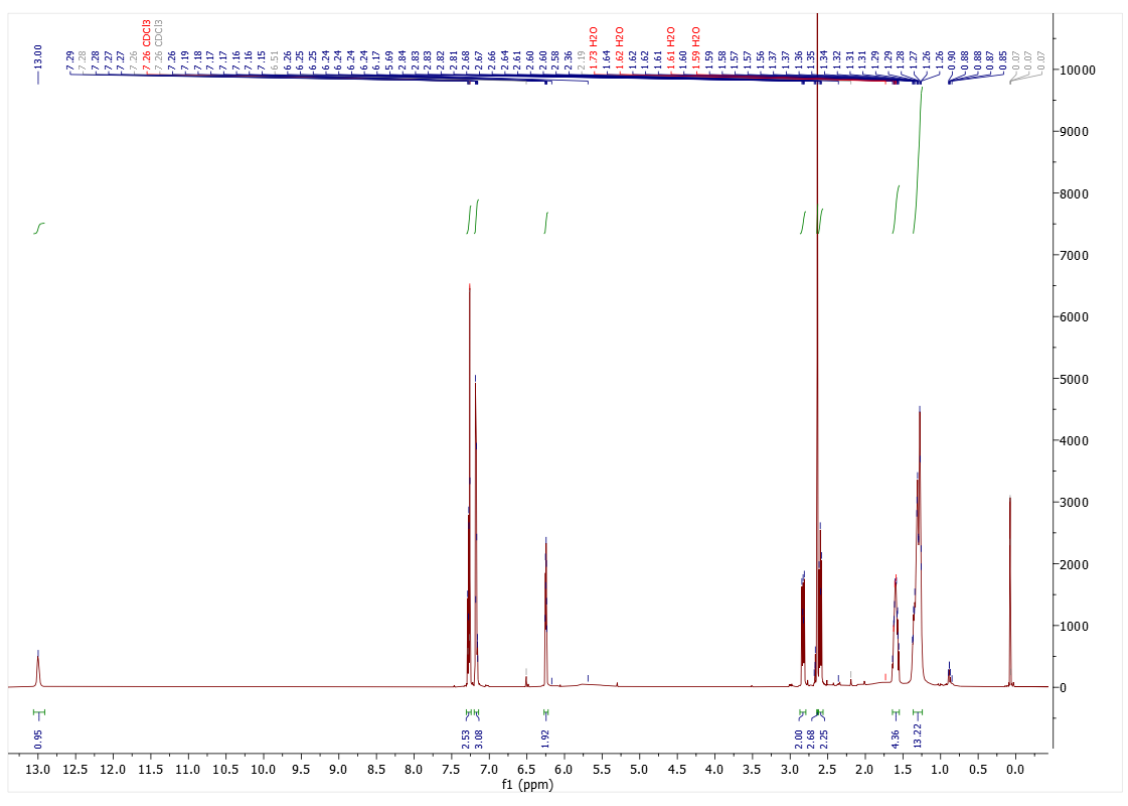


Figure A19. 1H NMR spectrum of 4.4.

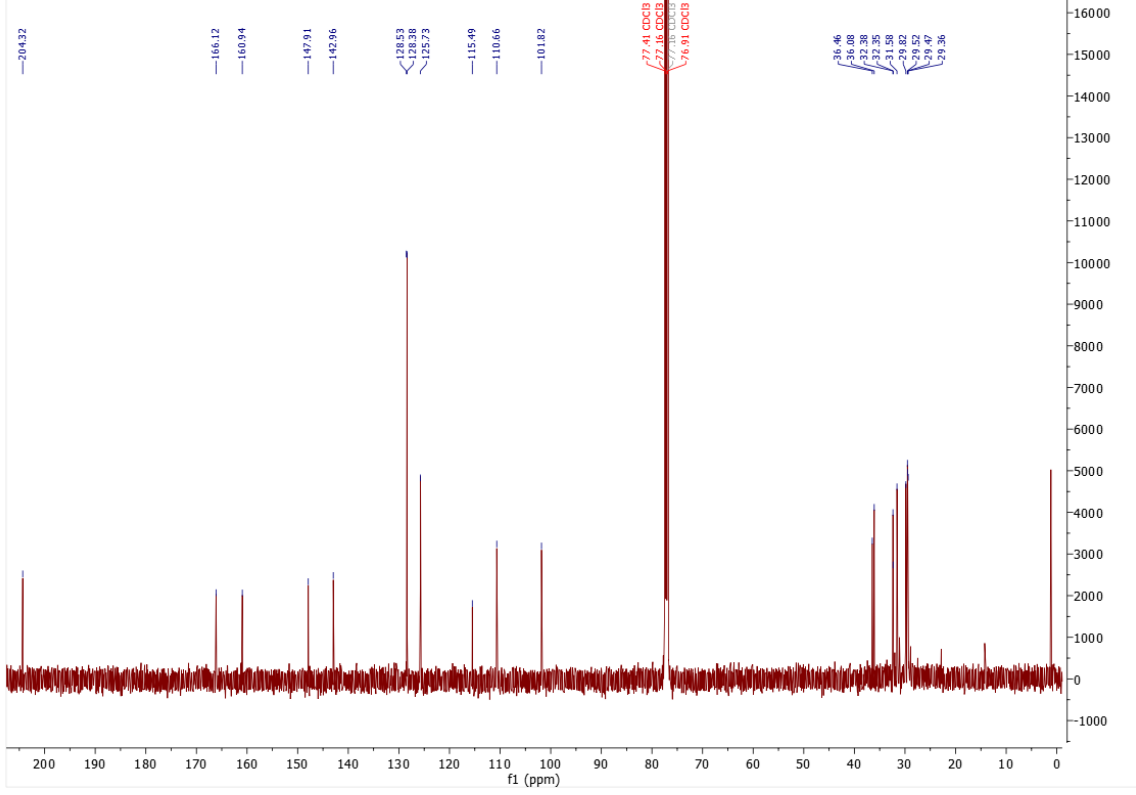


Figure A20. 13C NMR spectrum of 4.4.

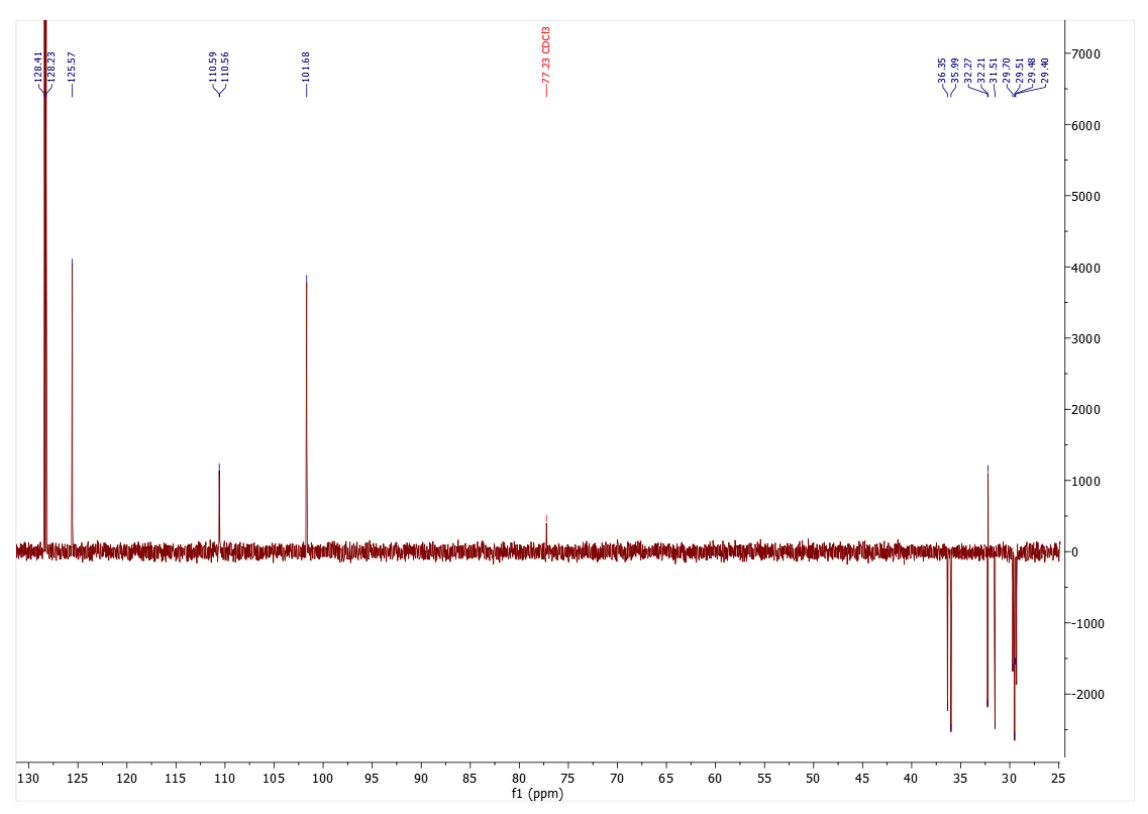


Figure A21. DEPT spectrum of 4.4.

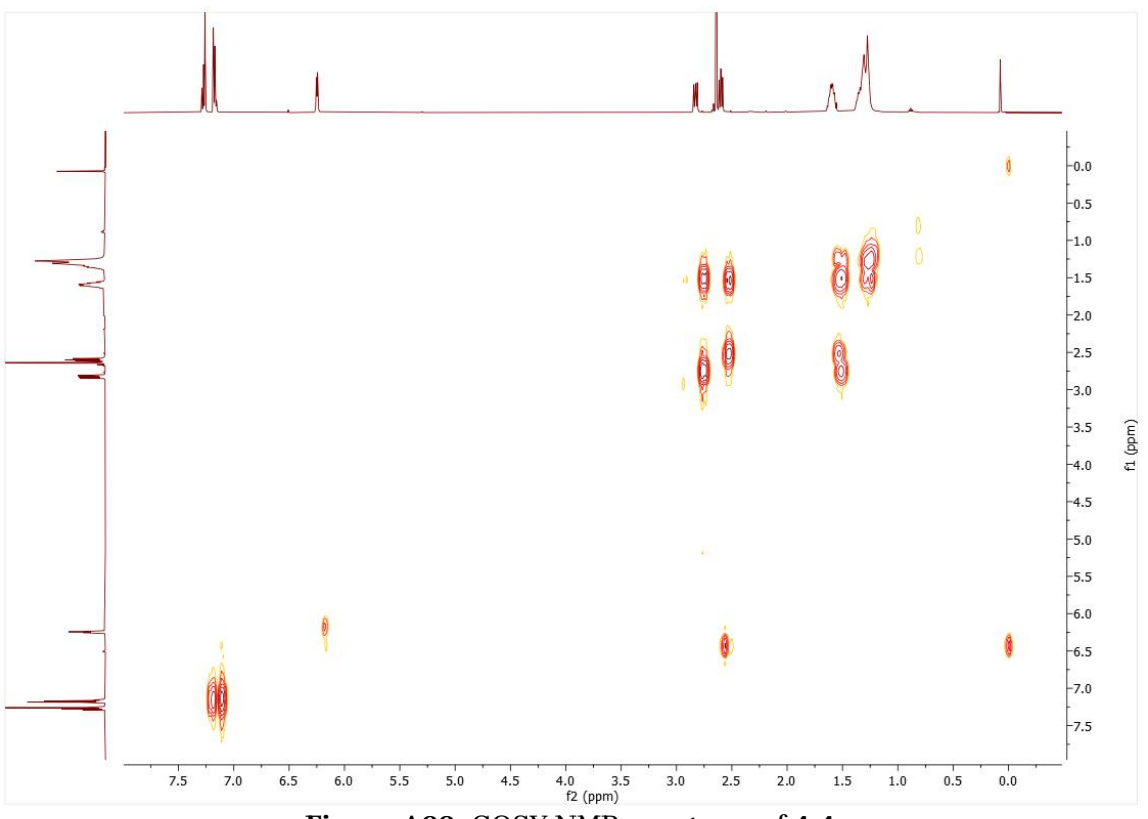


Figure A22. COSY NMR spectrum of 4.4.

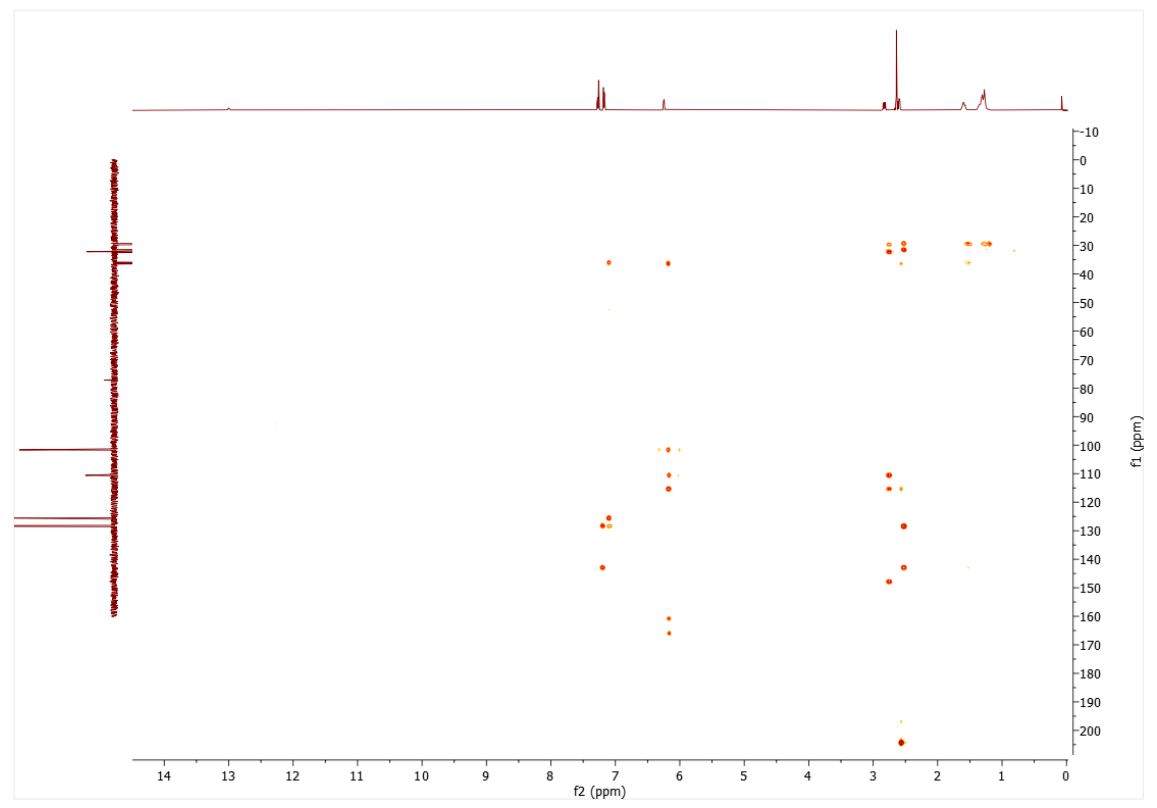


Figure A23. HMBC NMR spectrum of 4.4.

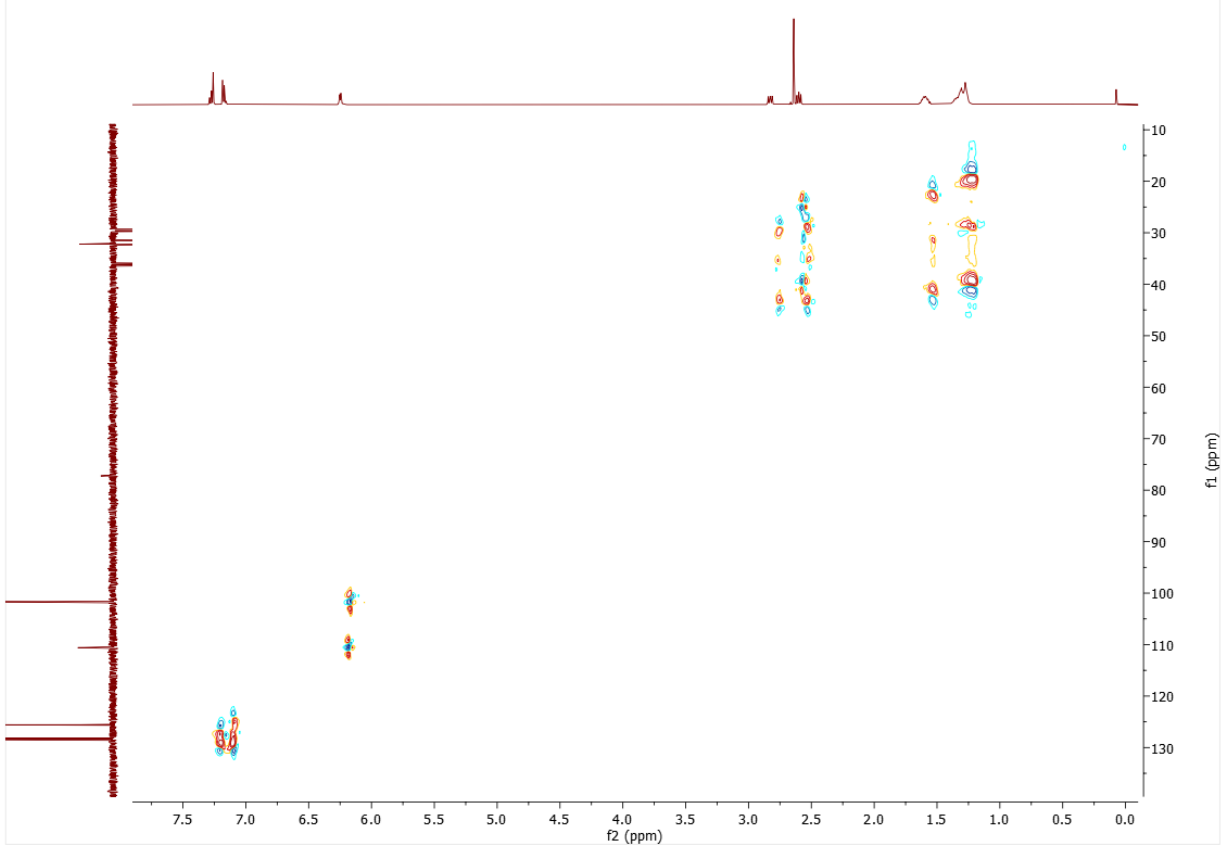


Figure A24. HSQC NMR spectrum of 4.4.

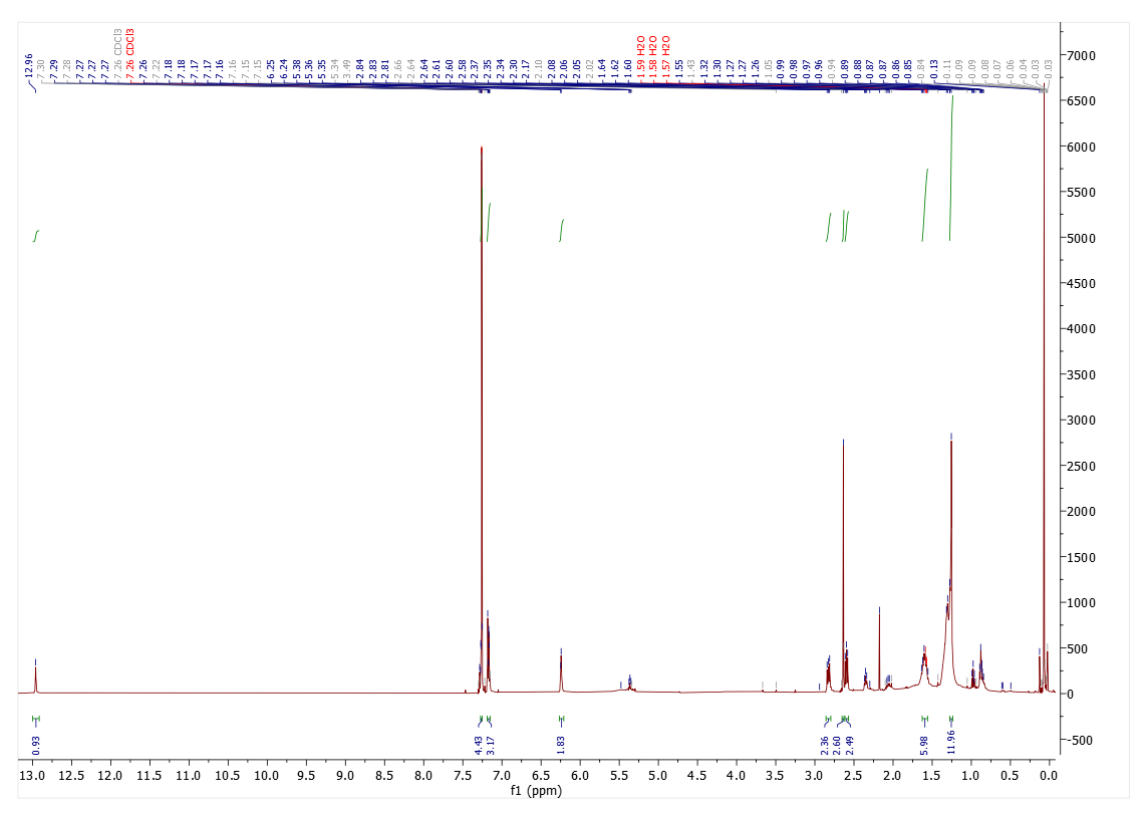


Figure A25. 1H NMR spectrum of 4.5.

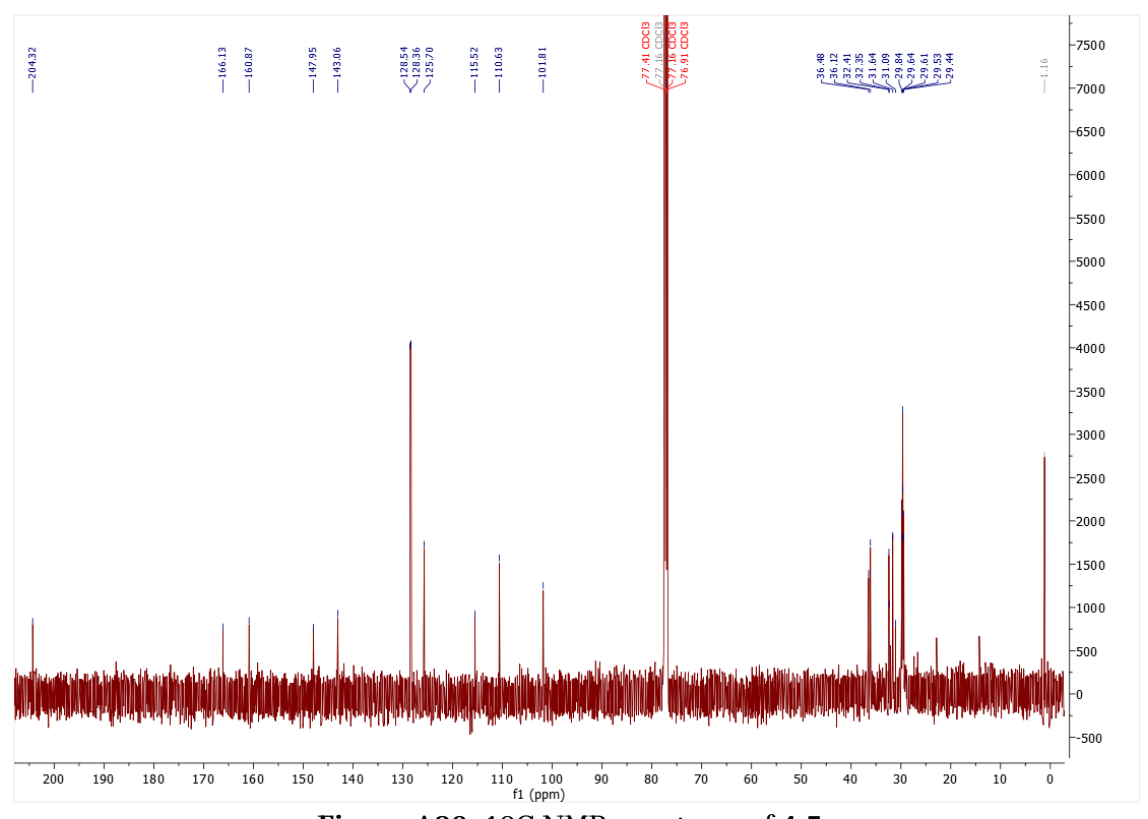


Figure A26. 13C NMR spectrum of 4.5.

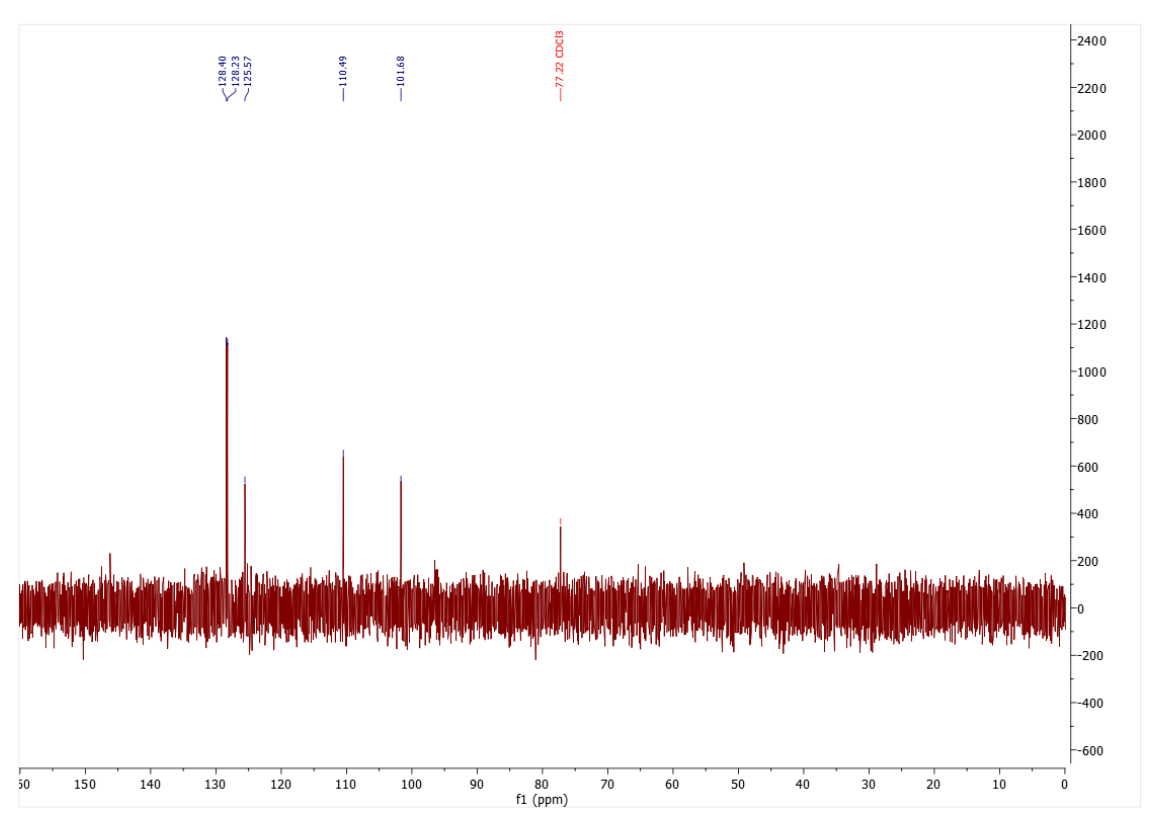


Figure A27. DEPT spectrum of 4.5.

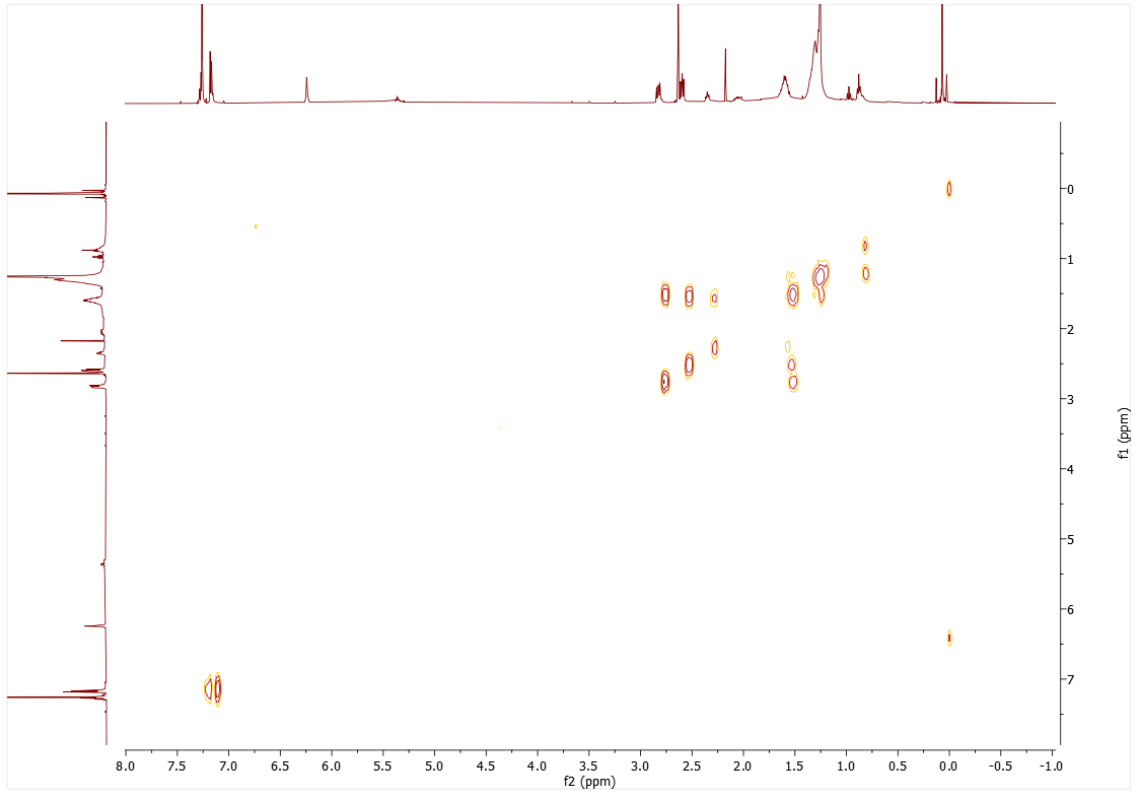
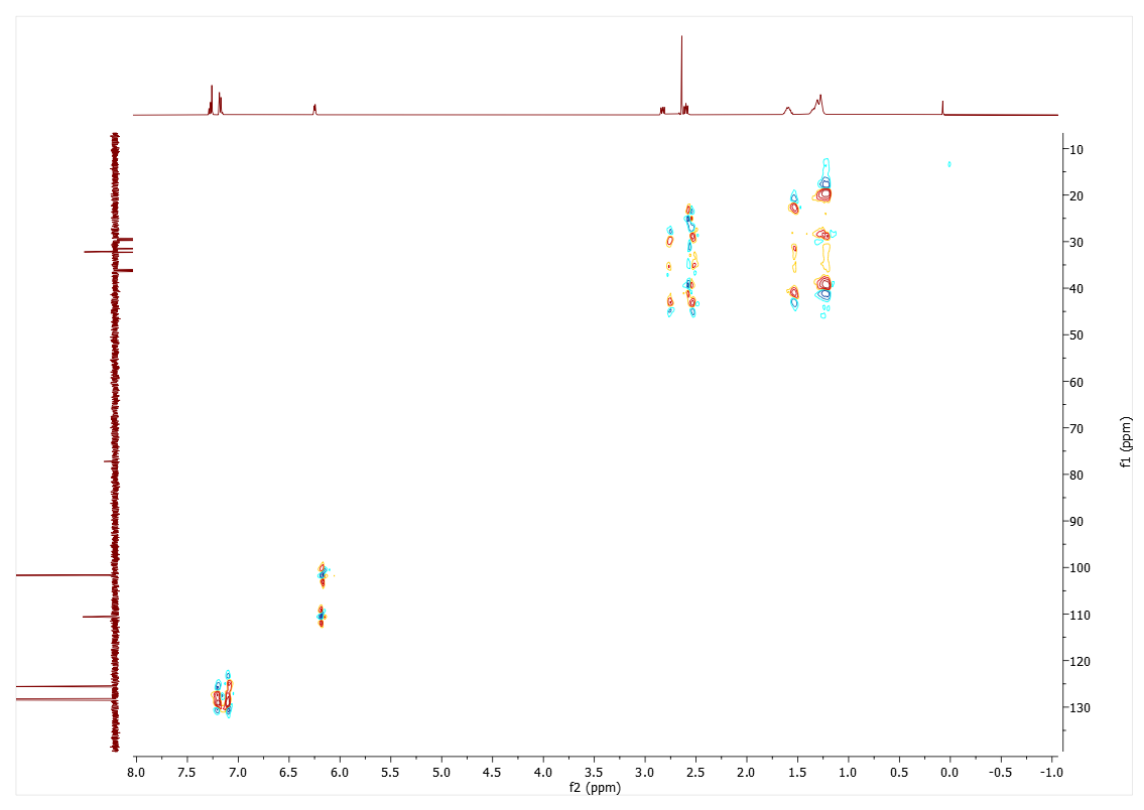


Figure A28. COSY NMR spectrum of 4.5.



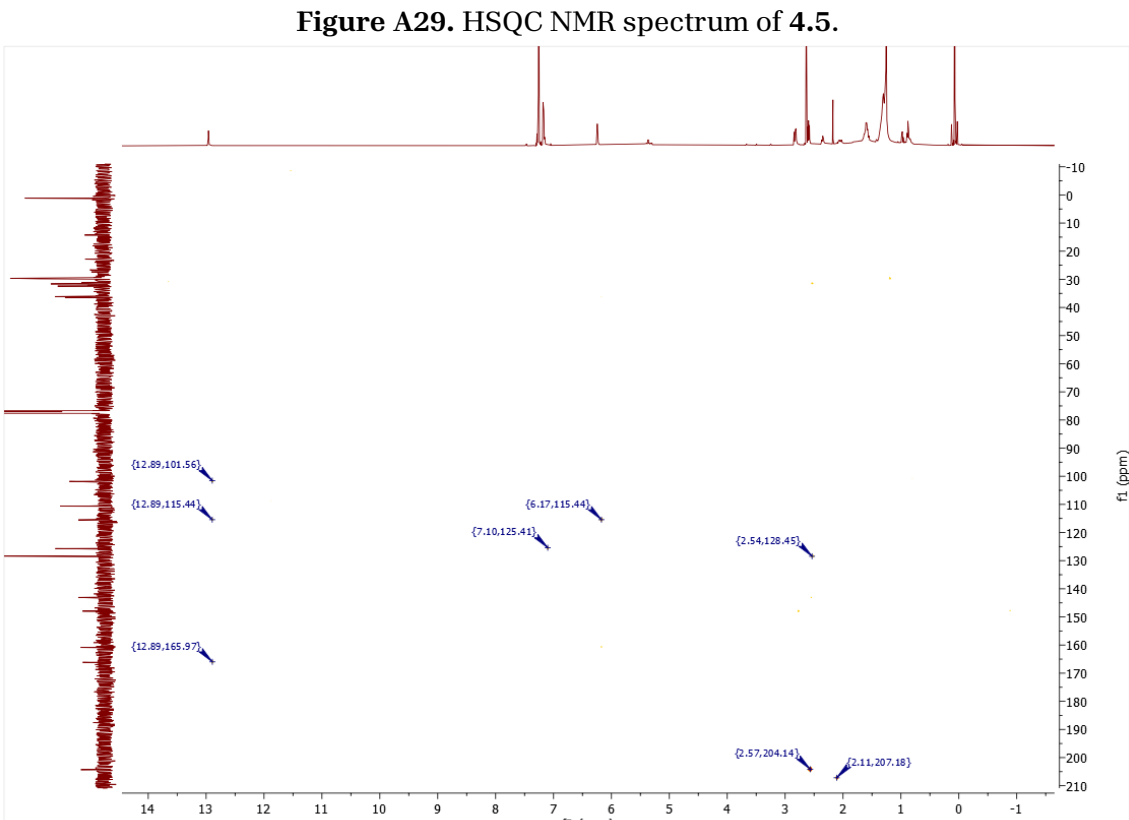


Figure A30. HMBC NMR spectrum of 4.5.

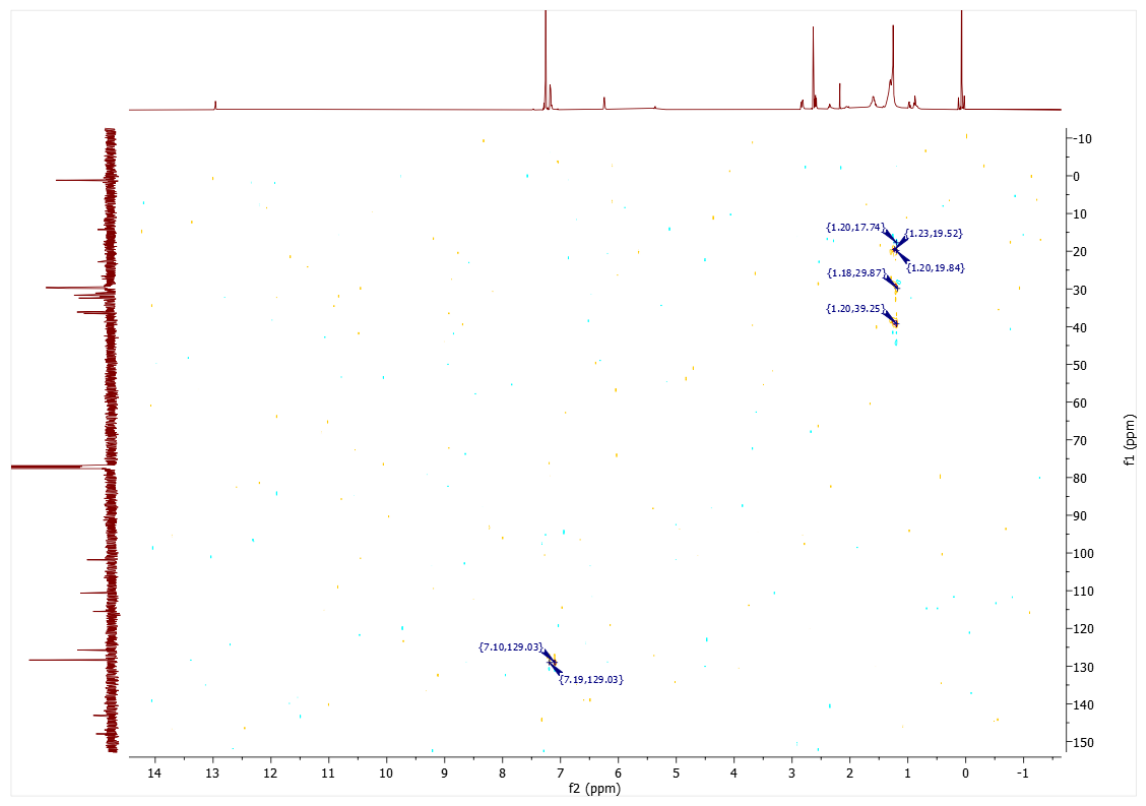


Figure A31. HSQC NMR spectrum of 4.5.

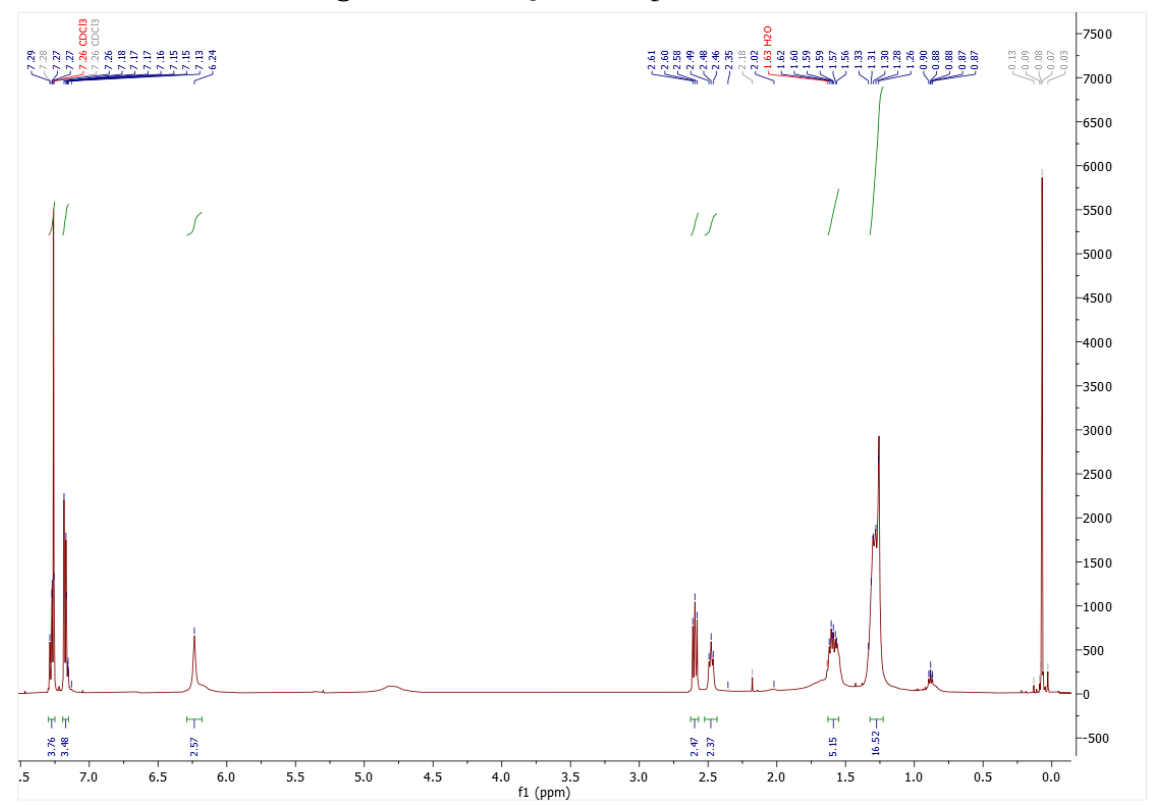


Figure A32. 1H NMR spectrum of 4.6.

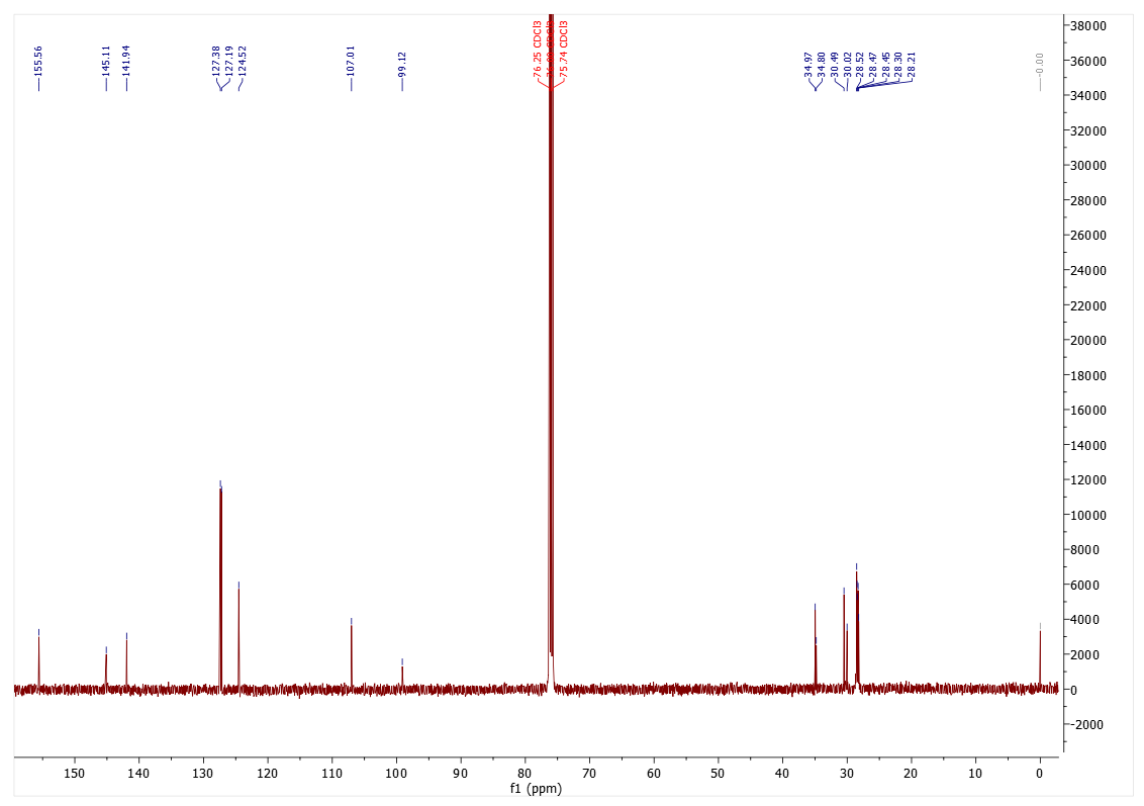


Figure A33. 13C NMR spectrum of 4.6.

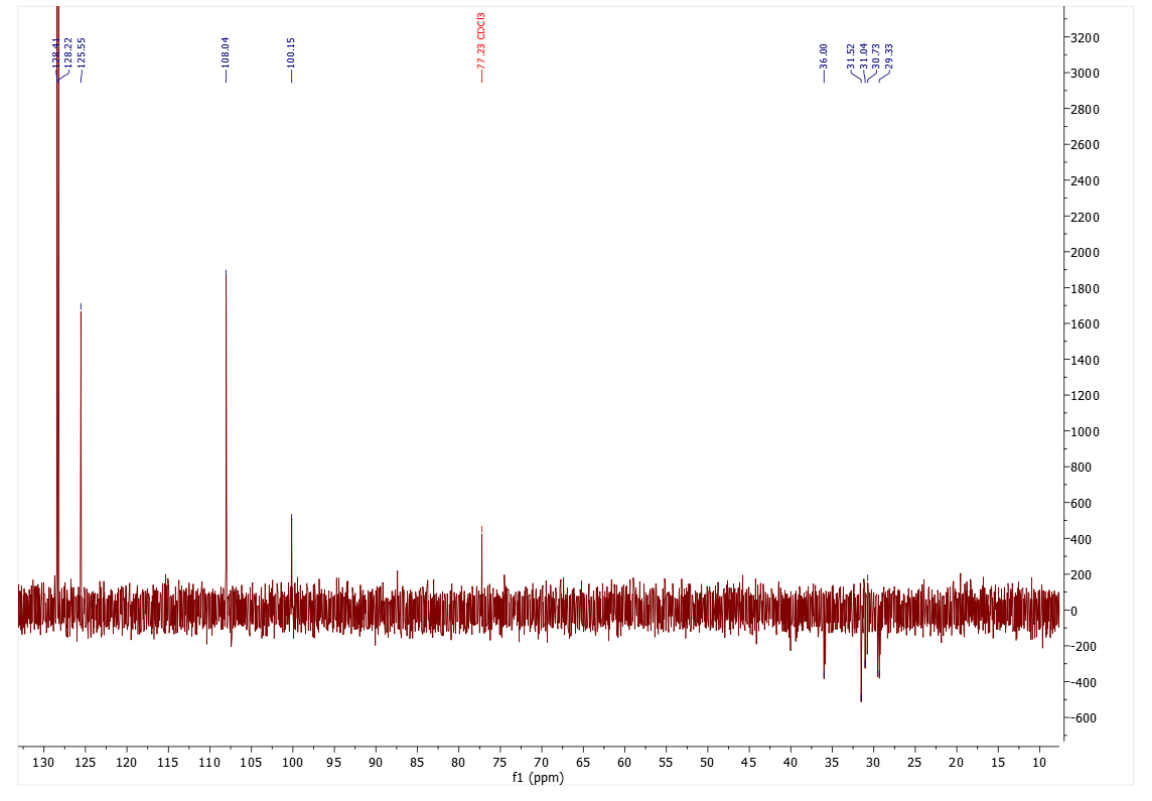
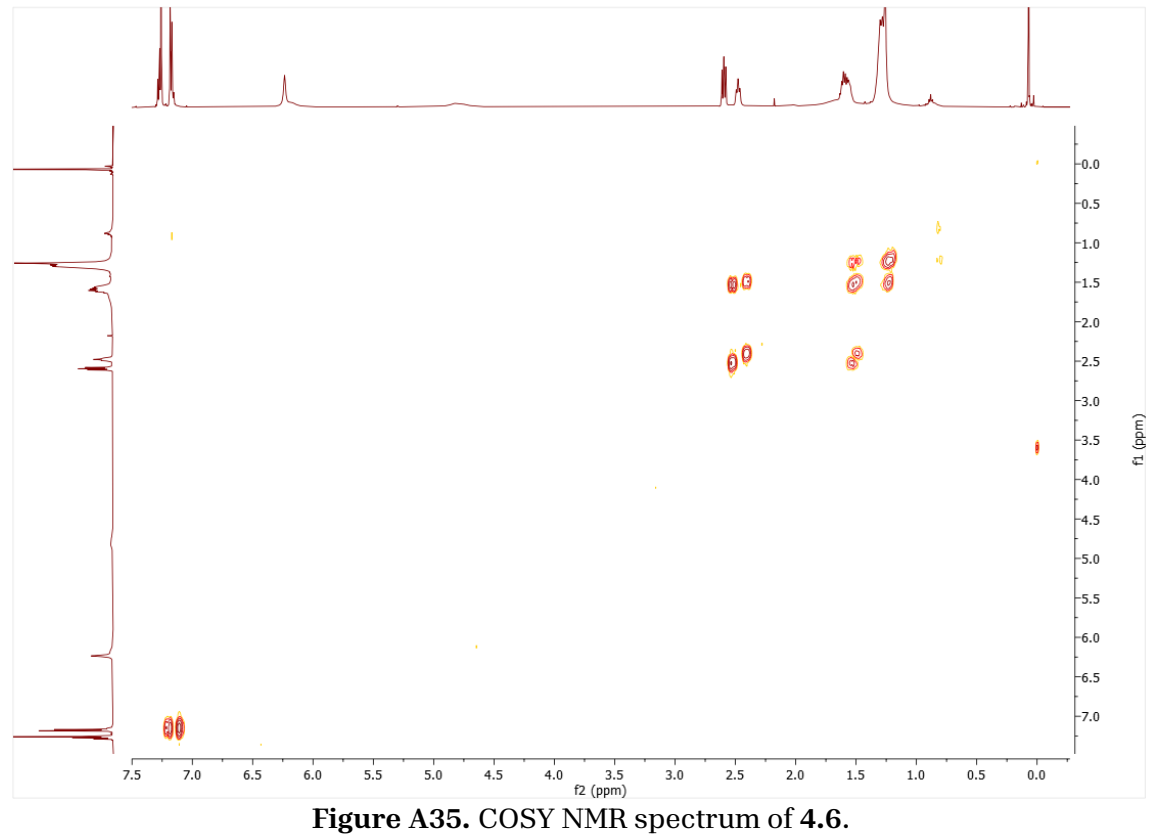


Figure A34. DEPT spectrum of 4.6.



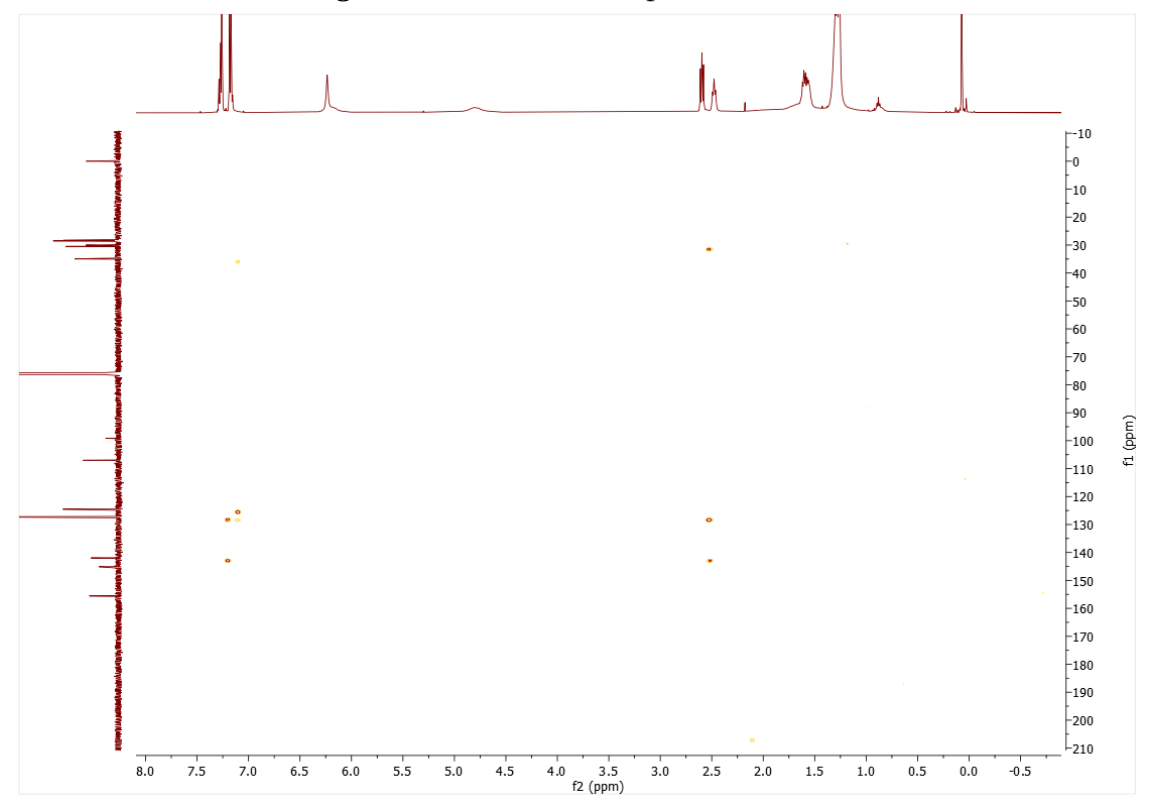


Figure A36. HMBC NMR spectrum of 4.6.

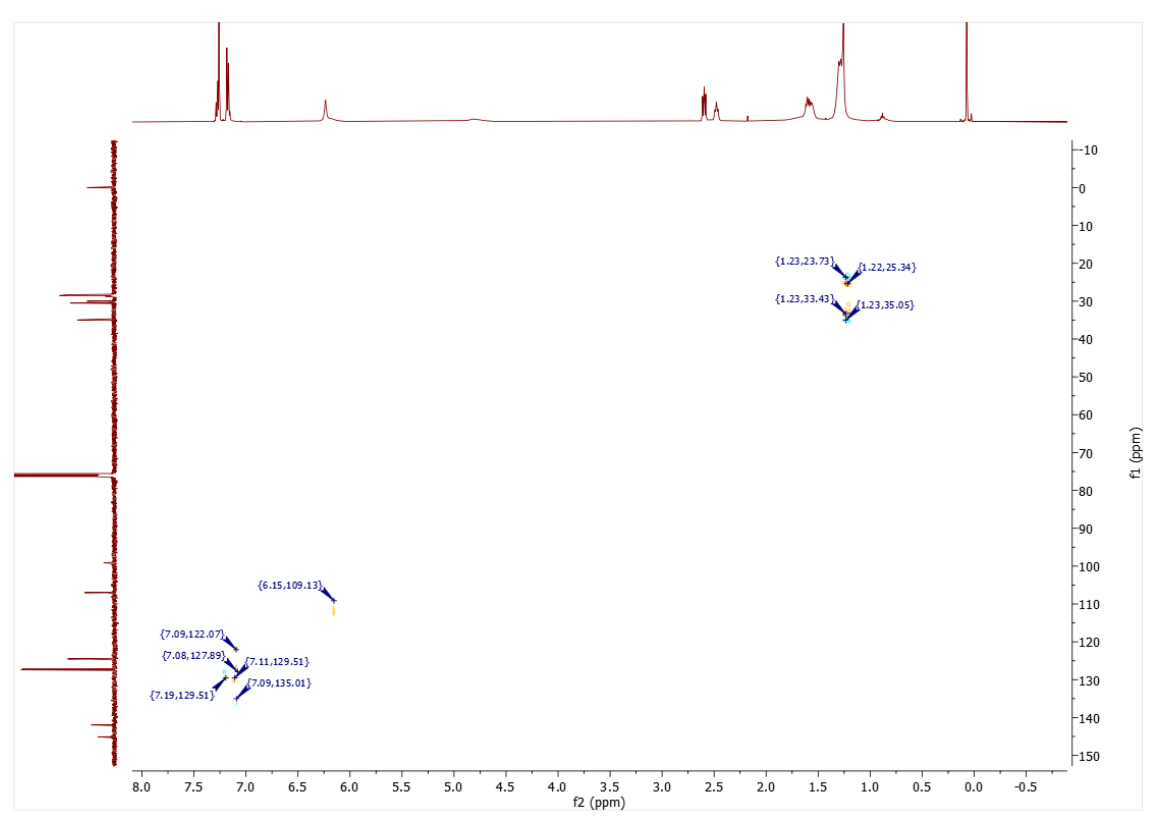


Figure A37. HSQC NMR spectrum of 4.6.

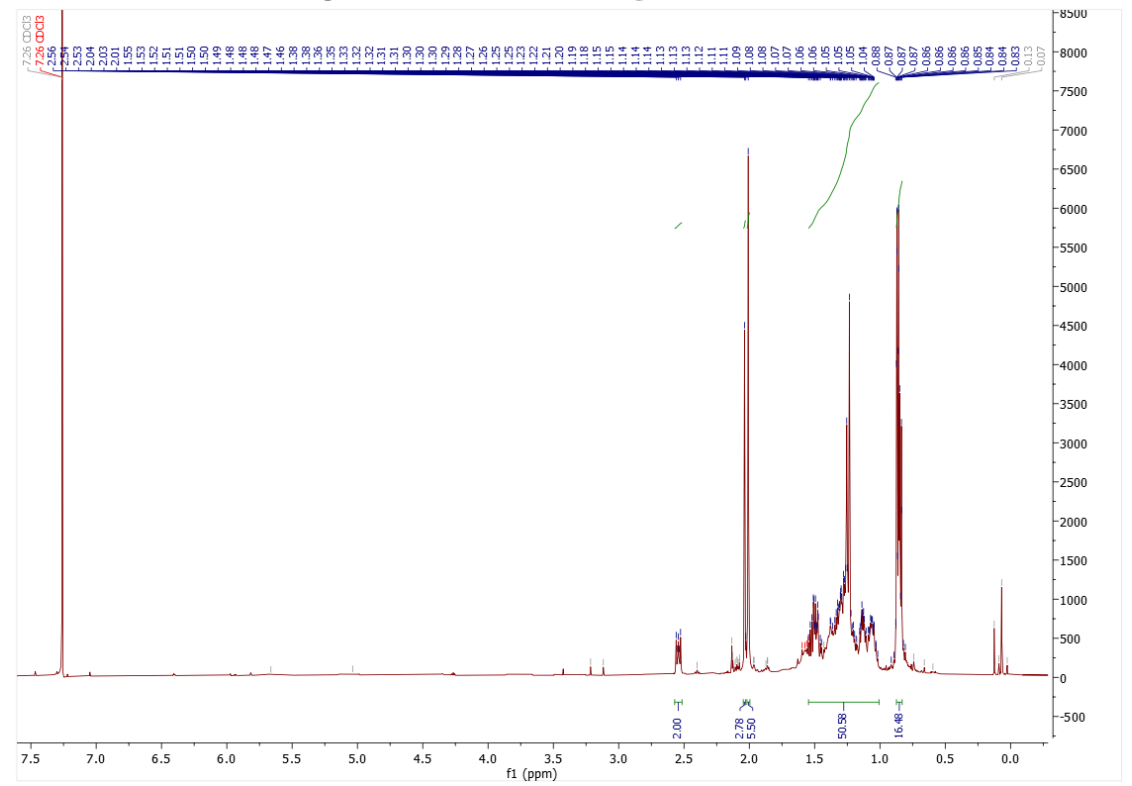
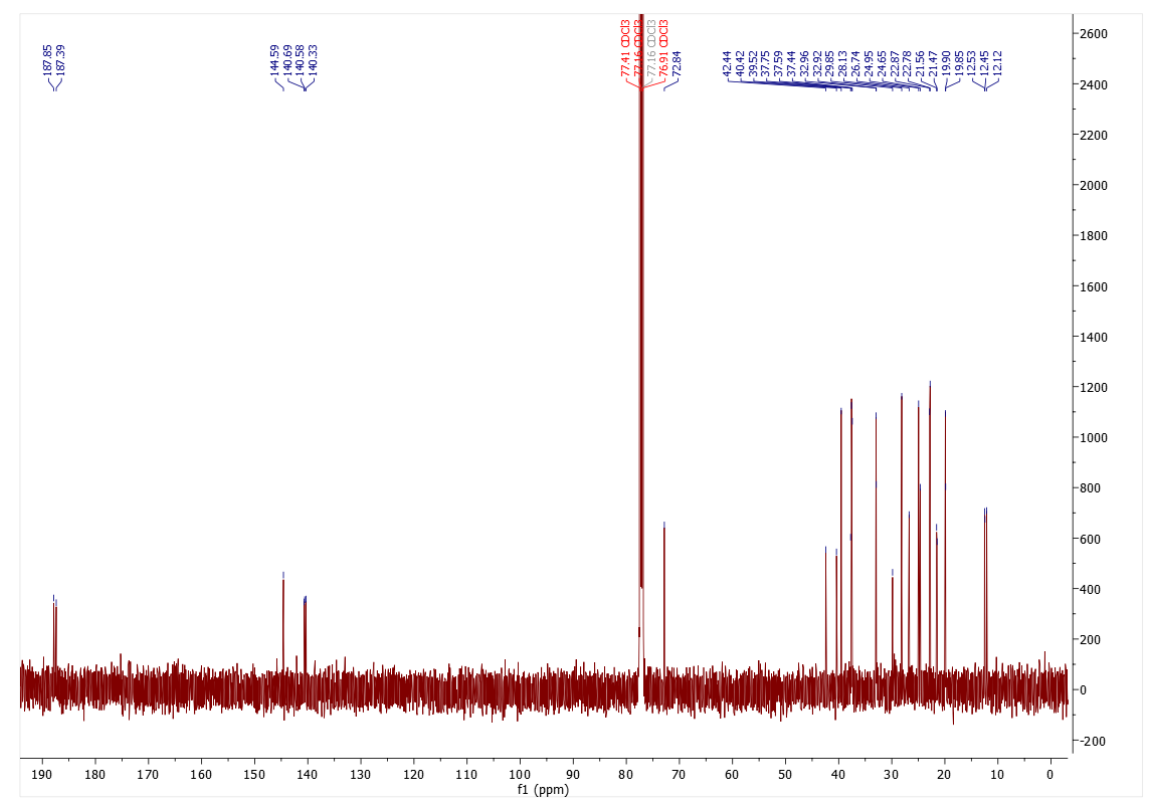


Figure A38. 1H NMR spectrum of 4.7.





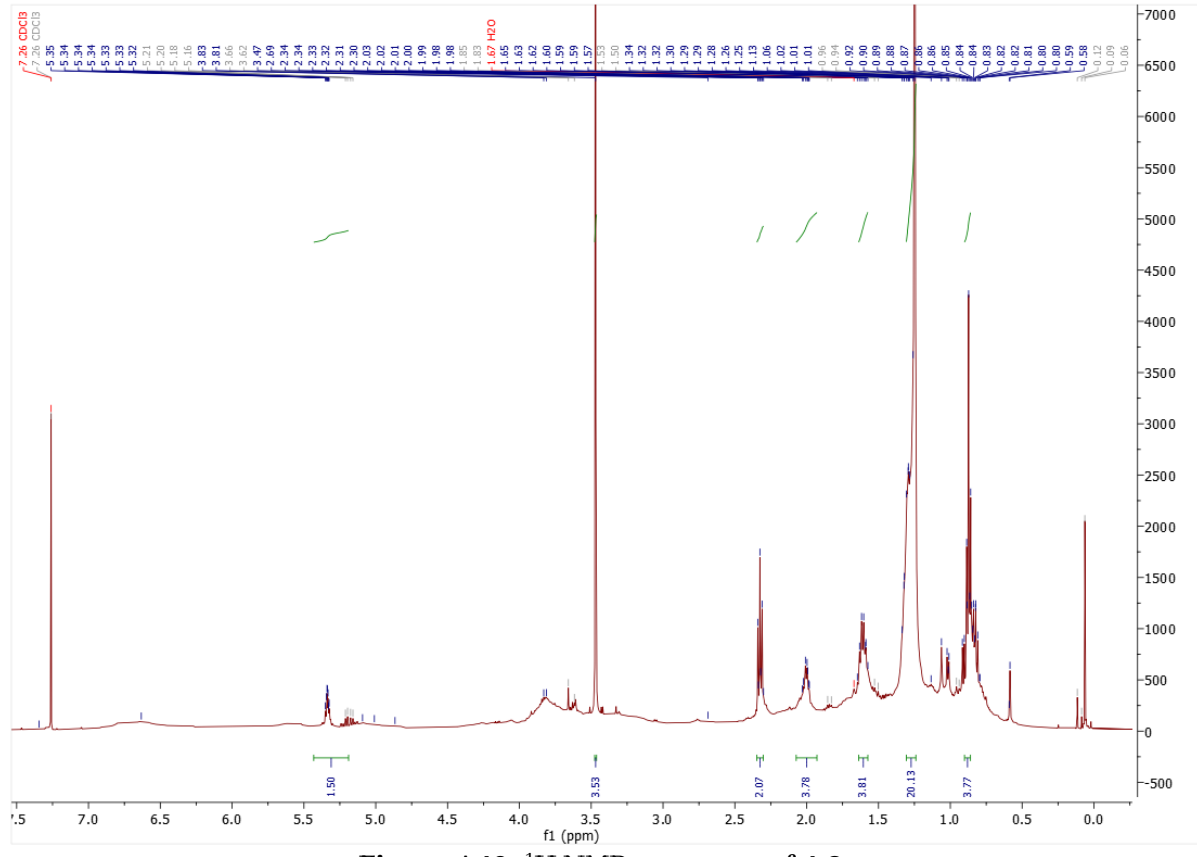
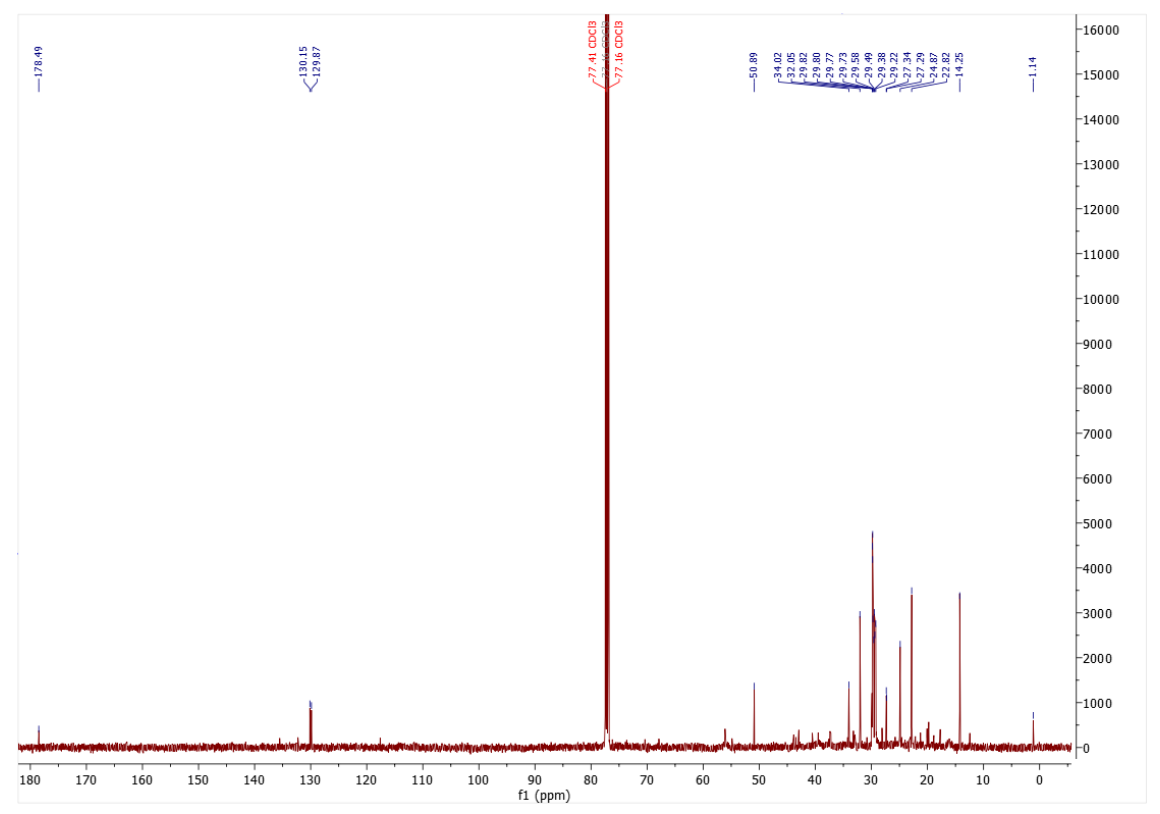


Figure A40. <sup>1</sup>H NMR spectrum of 4.8.





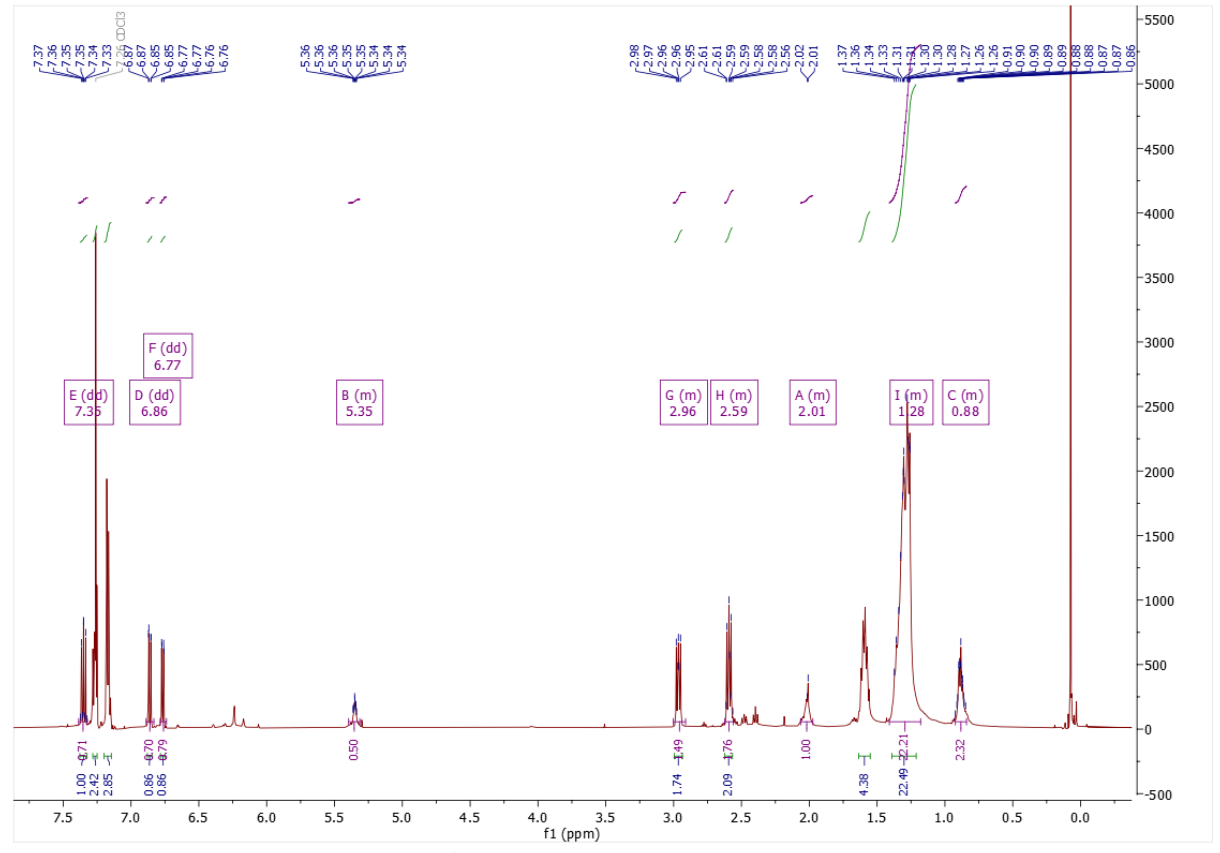


Figure A42. <sup>1</sup>H NMR spectrum of 4.1/4.9 mixture.

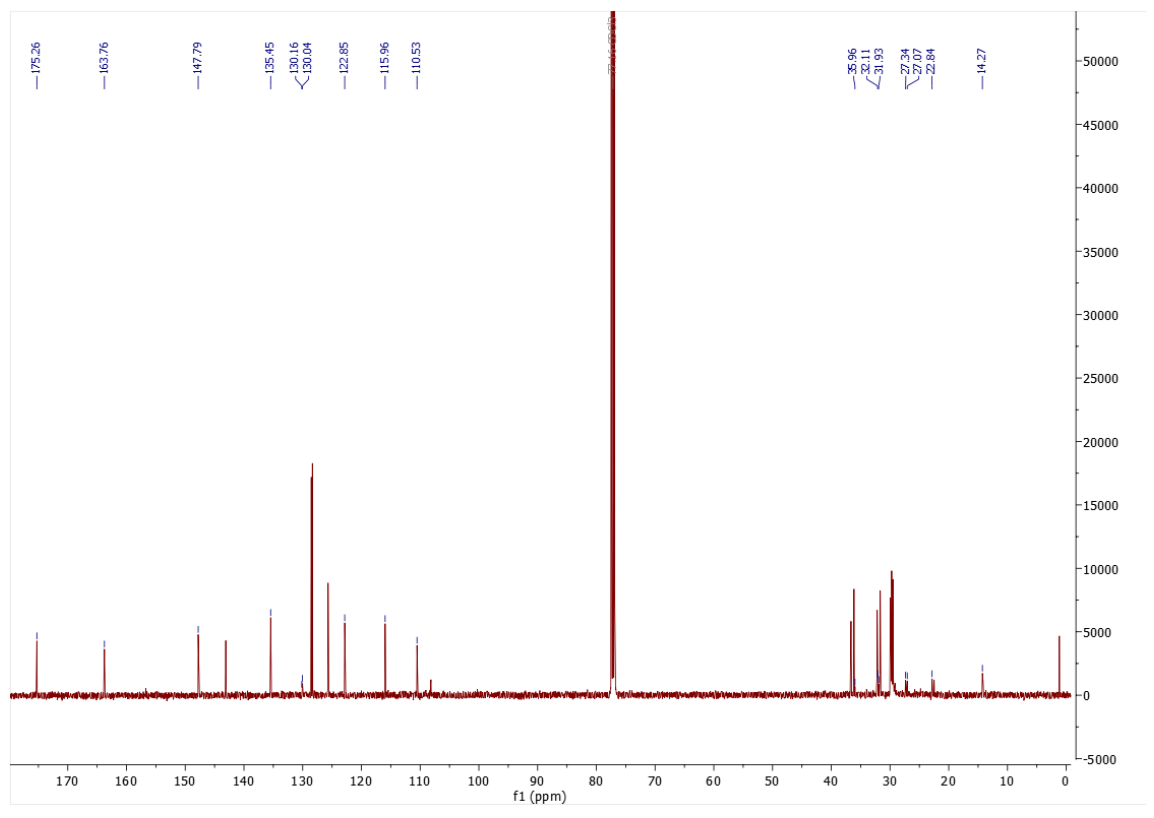


Figure A43. <sup>13</sup>C NMR spectrum of 4.1/4.9 mixture.

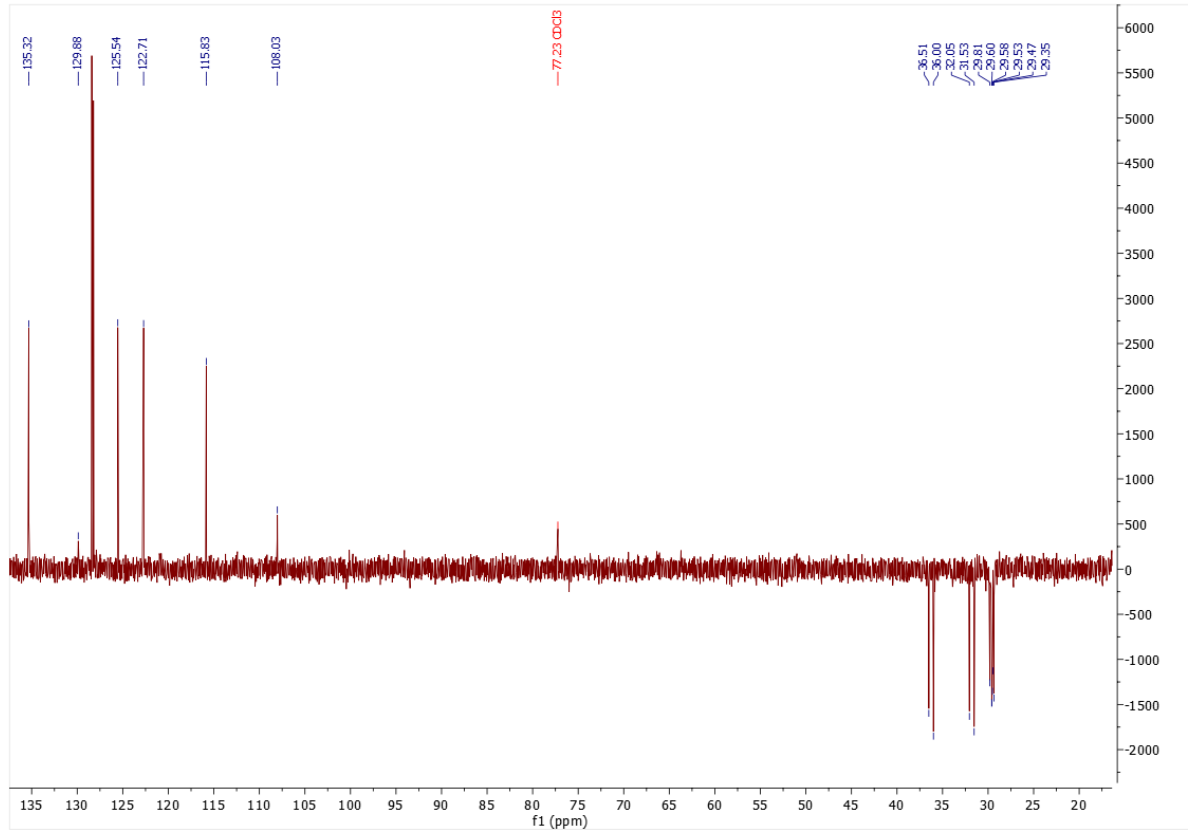
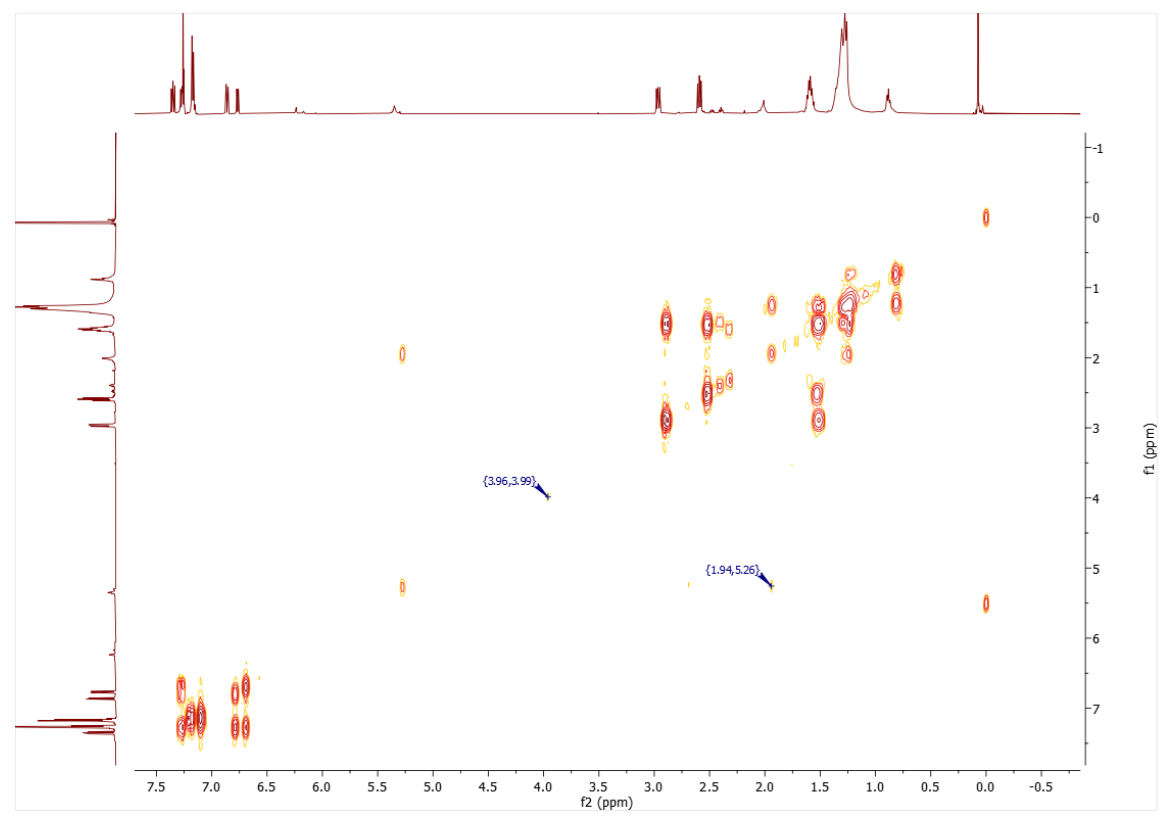


Figure A44. DEPT NMR spectrum of 4.1/4.9 mixture.





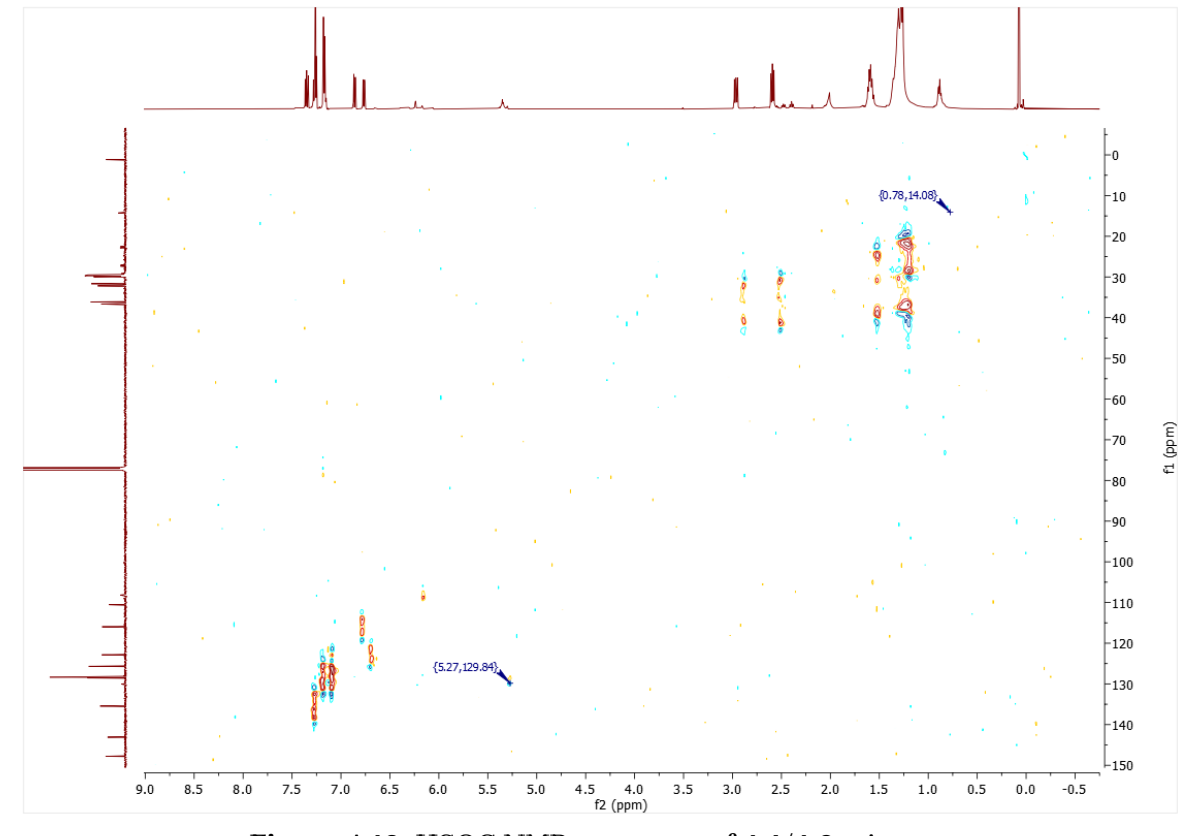
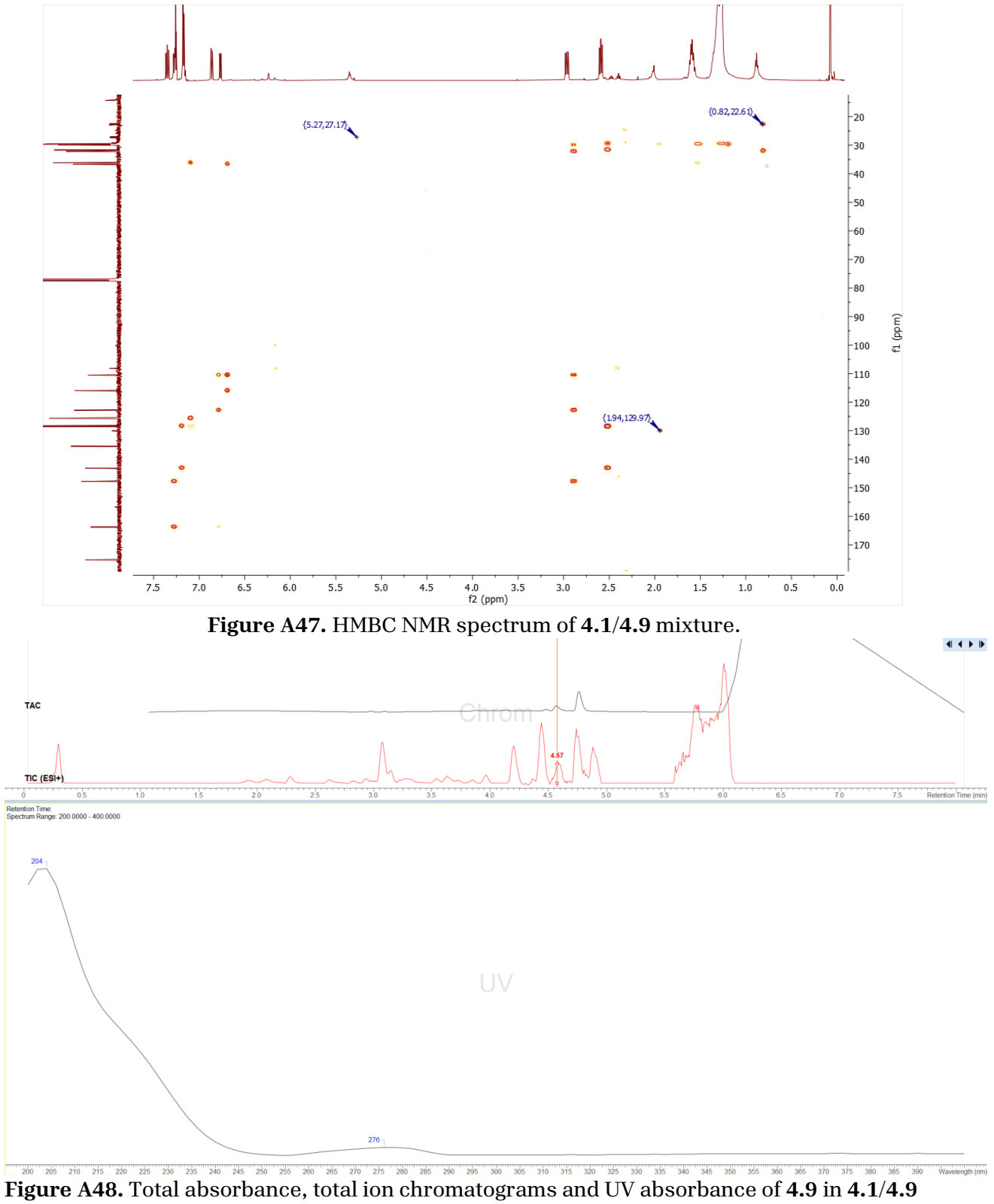
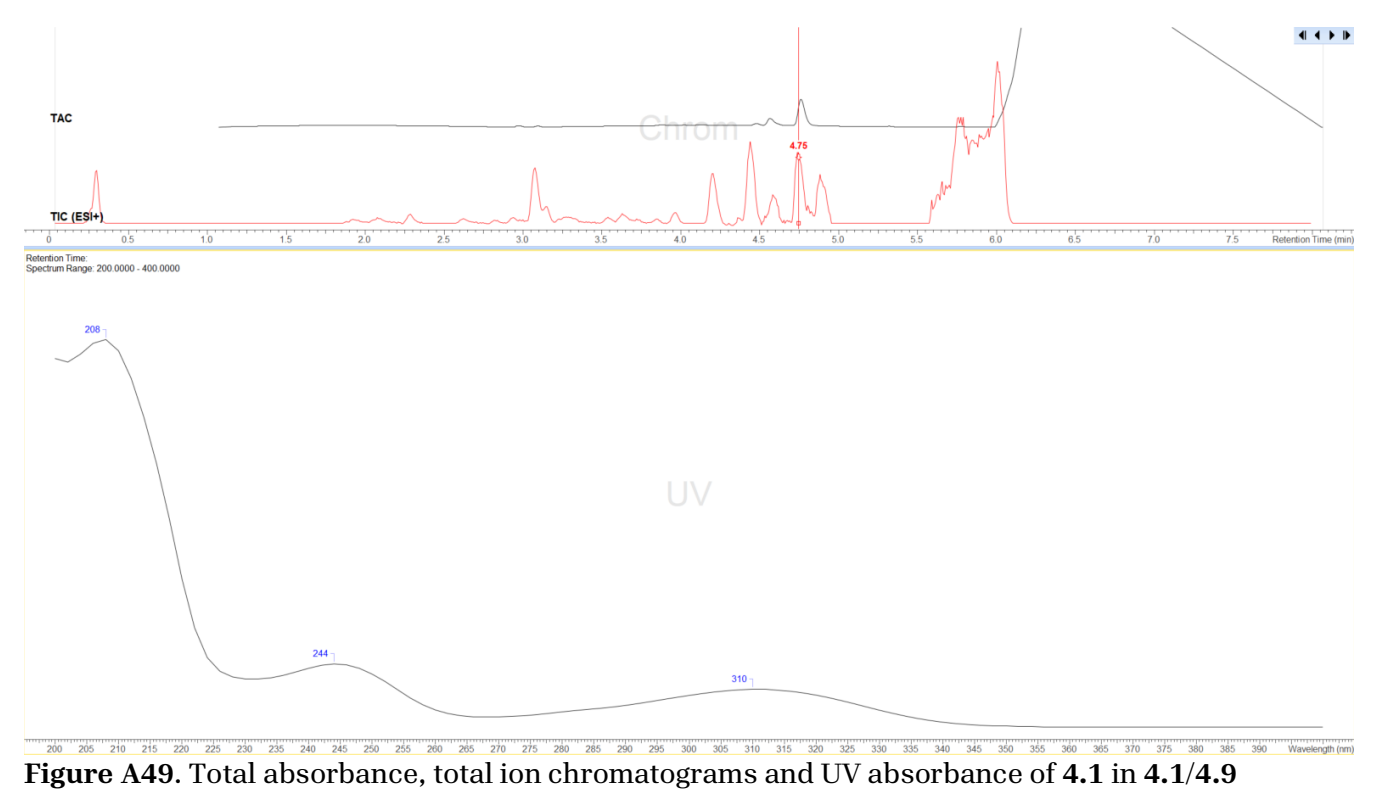


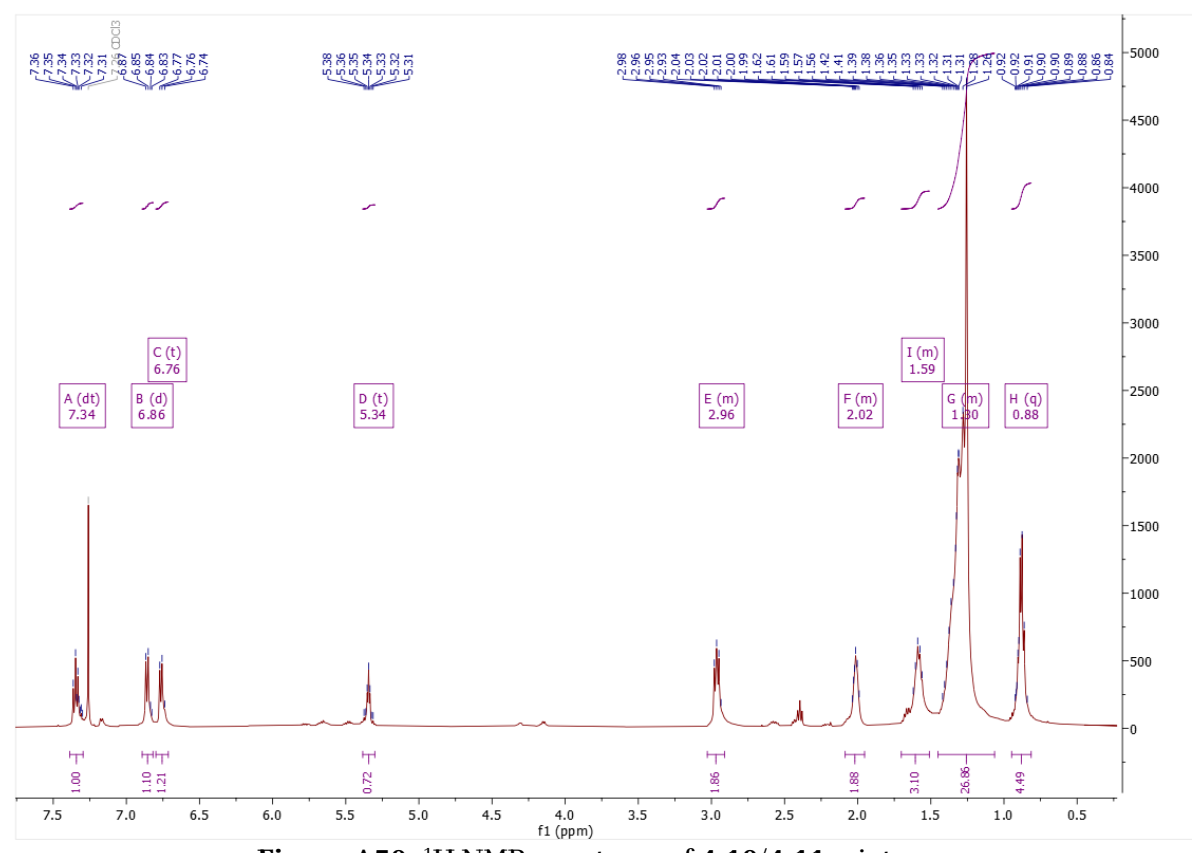
Figure A46. HSQC NMR spectrum of 4.1/4.9 mixture.



mixture.



mixture.



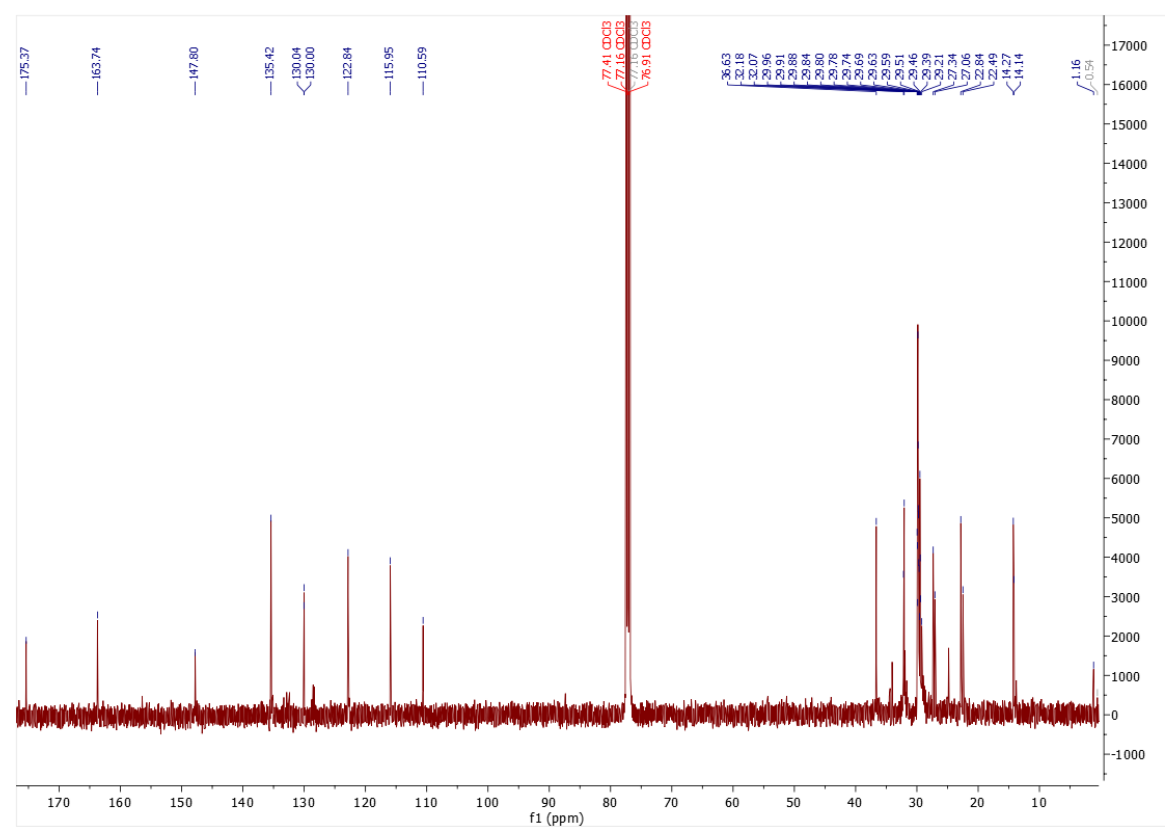


Figure A51. <sup>13</sup>C NMR spectrum of 4.10/4.11 mixture.

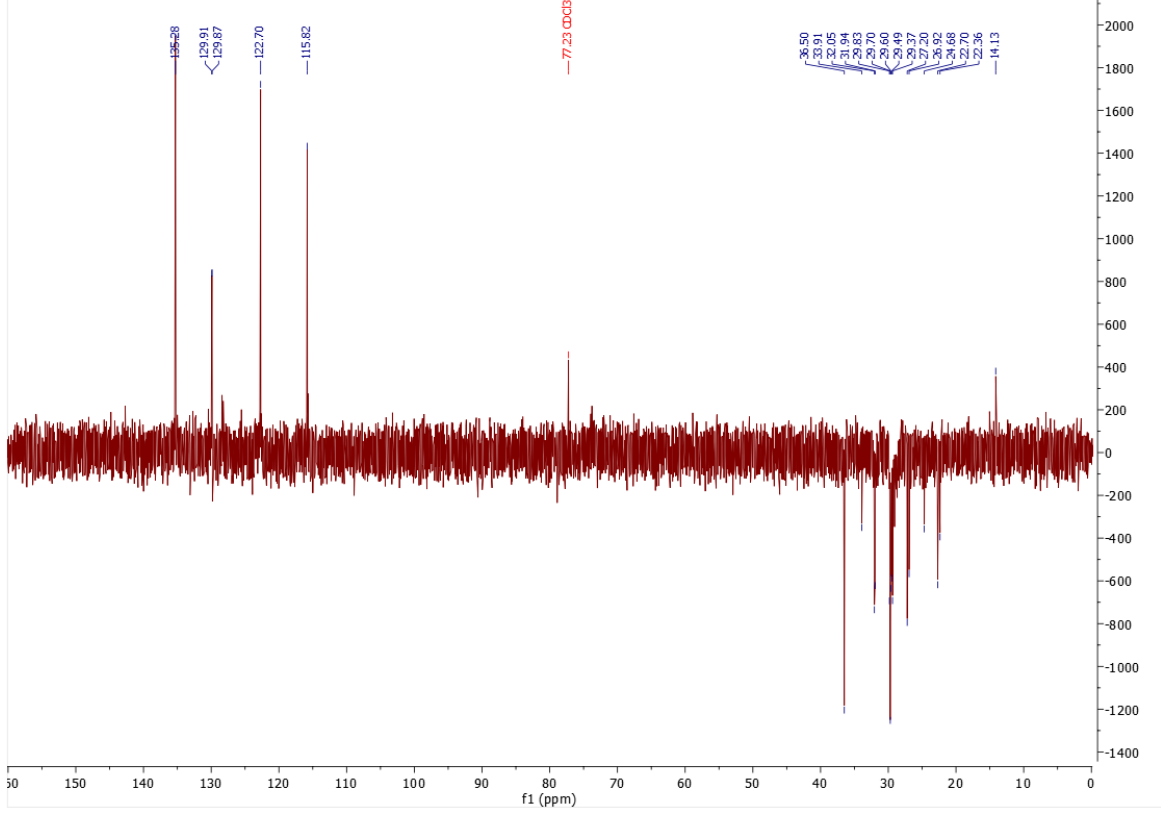


Figure A52. DEPT NMR spectrum of 4.10/4.11 mixture.

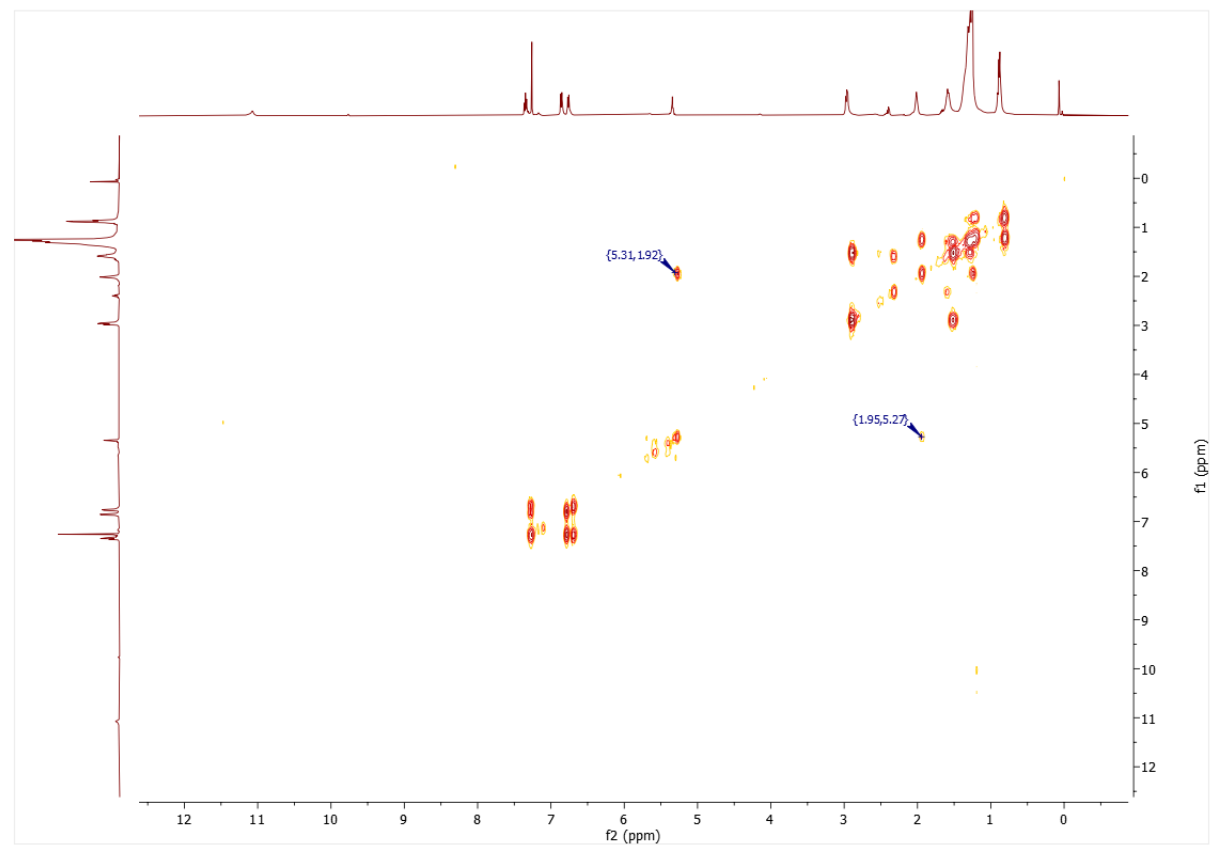
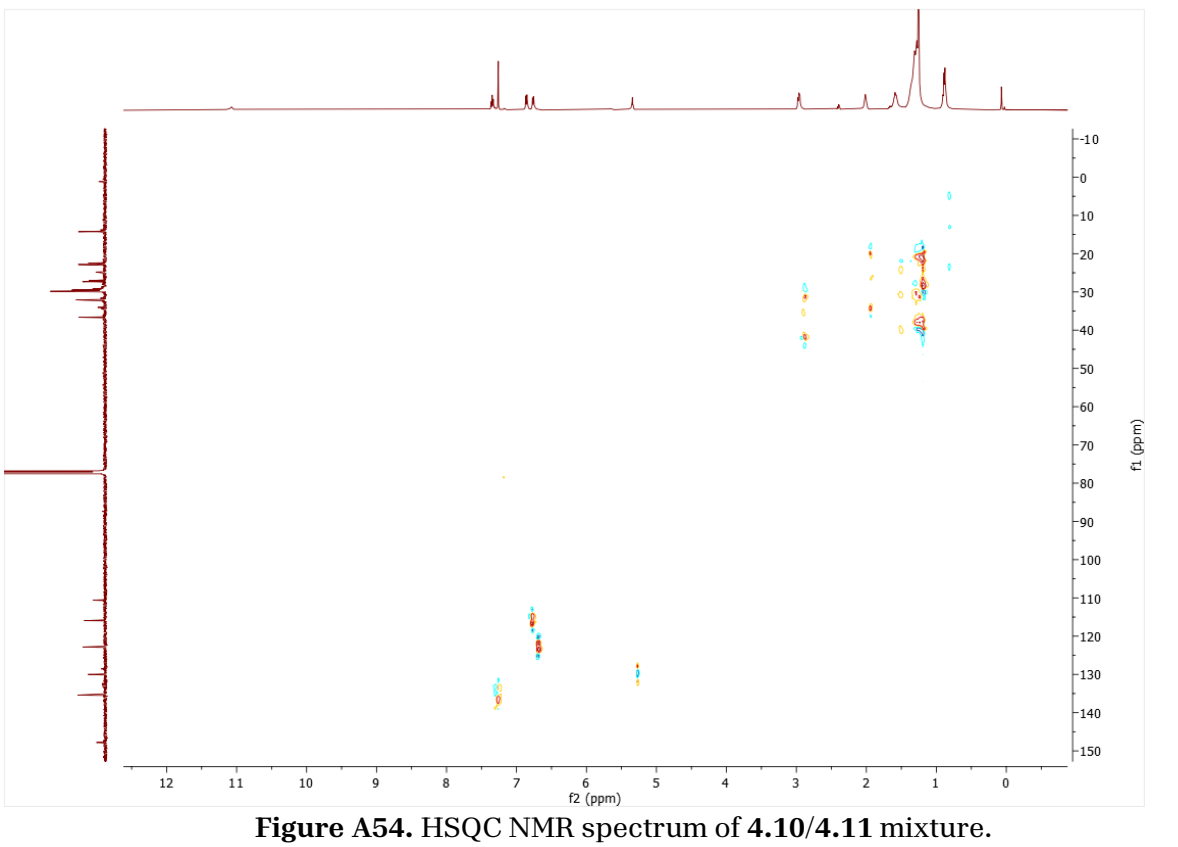


Figure A53. COSY NMR spectrum of 4.10/4.11 mixture.



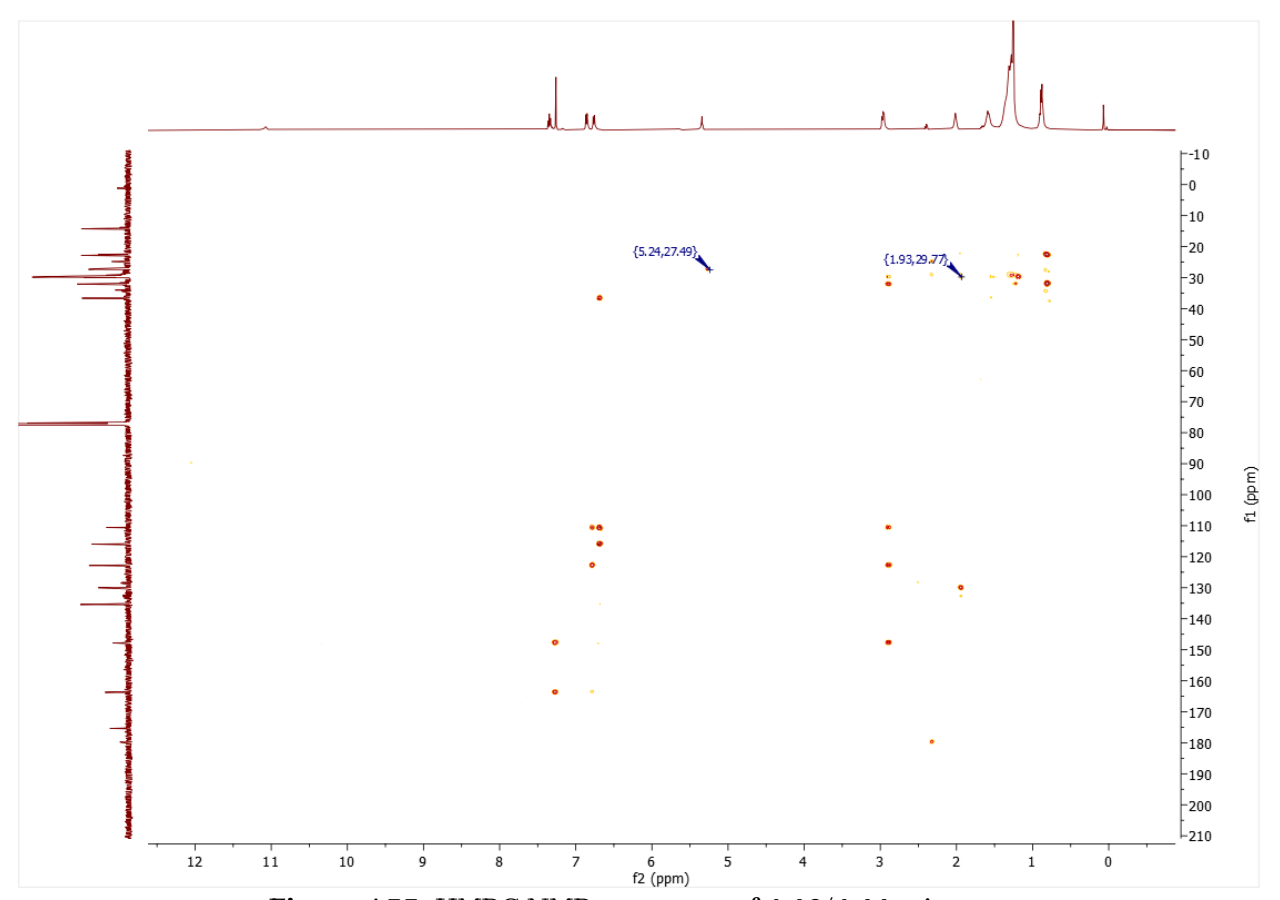


Figure A55. HMBC NMR spectrum of 4.10/4.11 mixture.

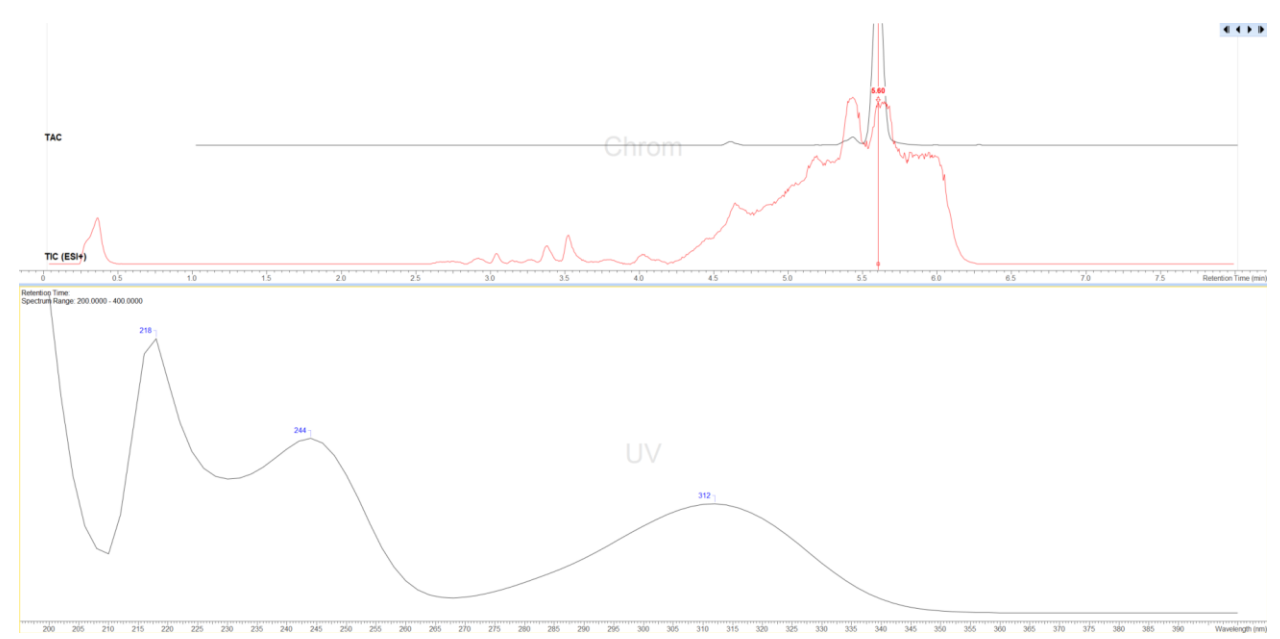


Figure A56. Total ion, total UV absorbance and UV absorbance spectrum of **4.10/4.11** mixture.

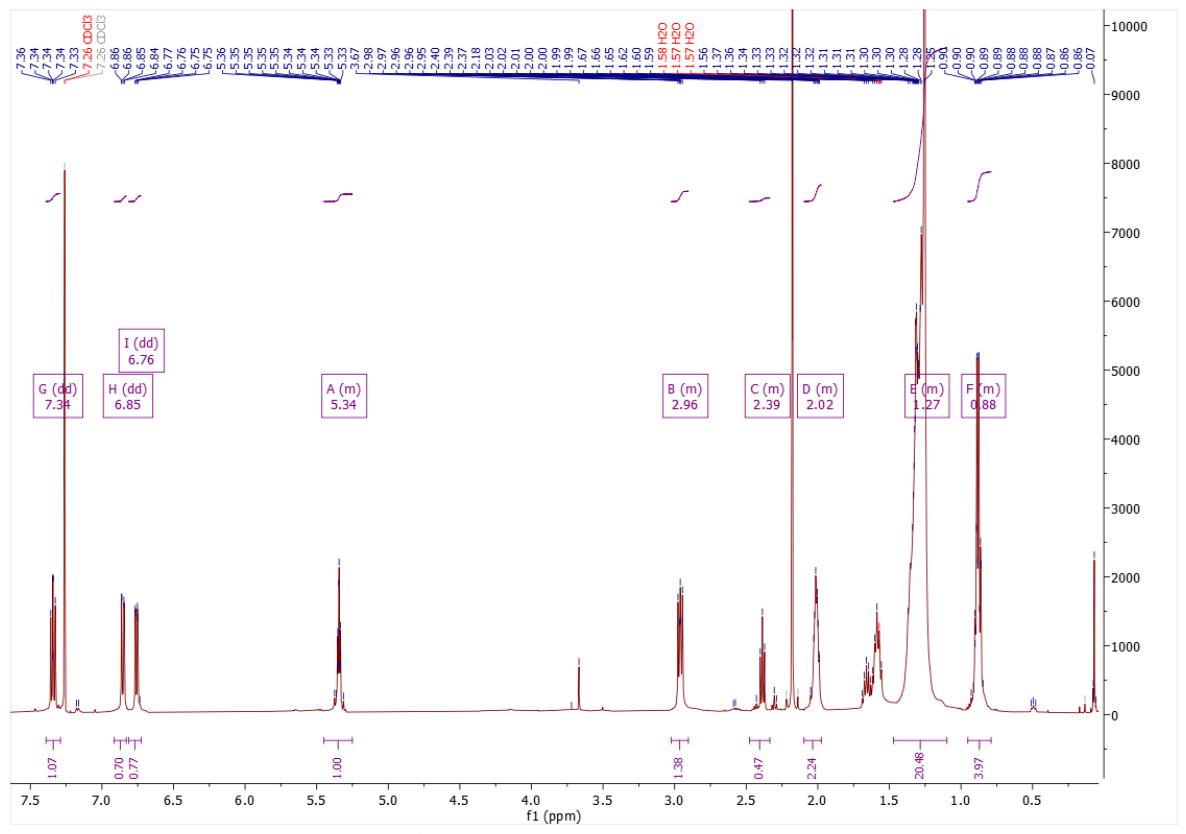


Figure A57. <sup>1</sup>H NMR spectrum of 4.11/4.12 mixture.

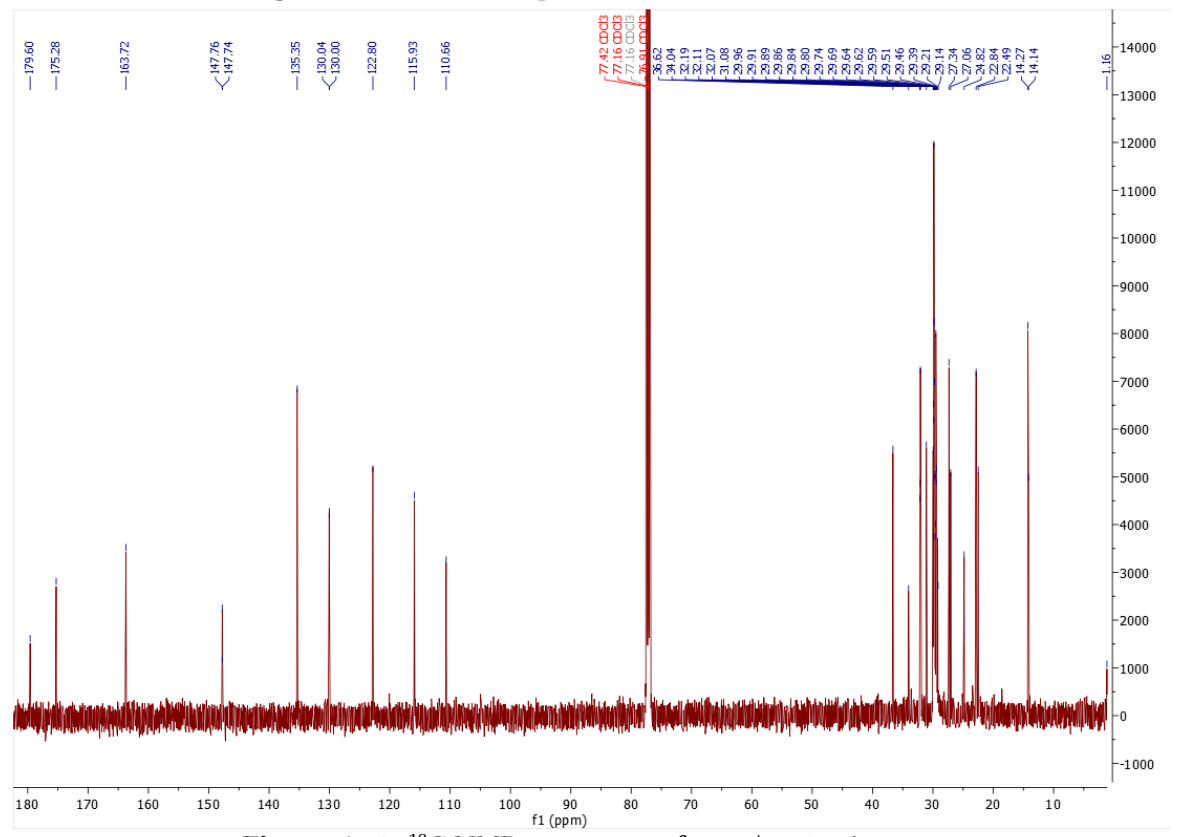


Figure A58. <sup>13</sup>C NMR spectrum of 4.11/4.12 mixture.

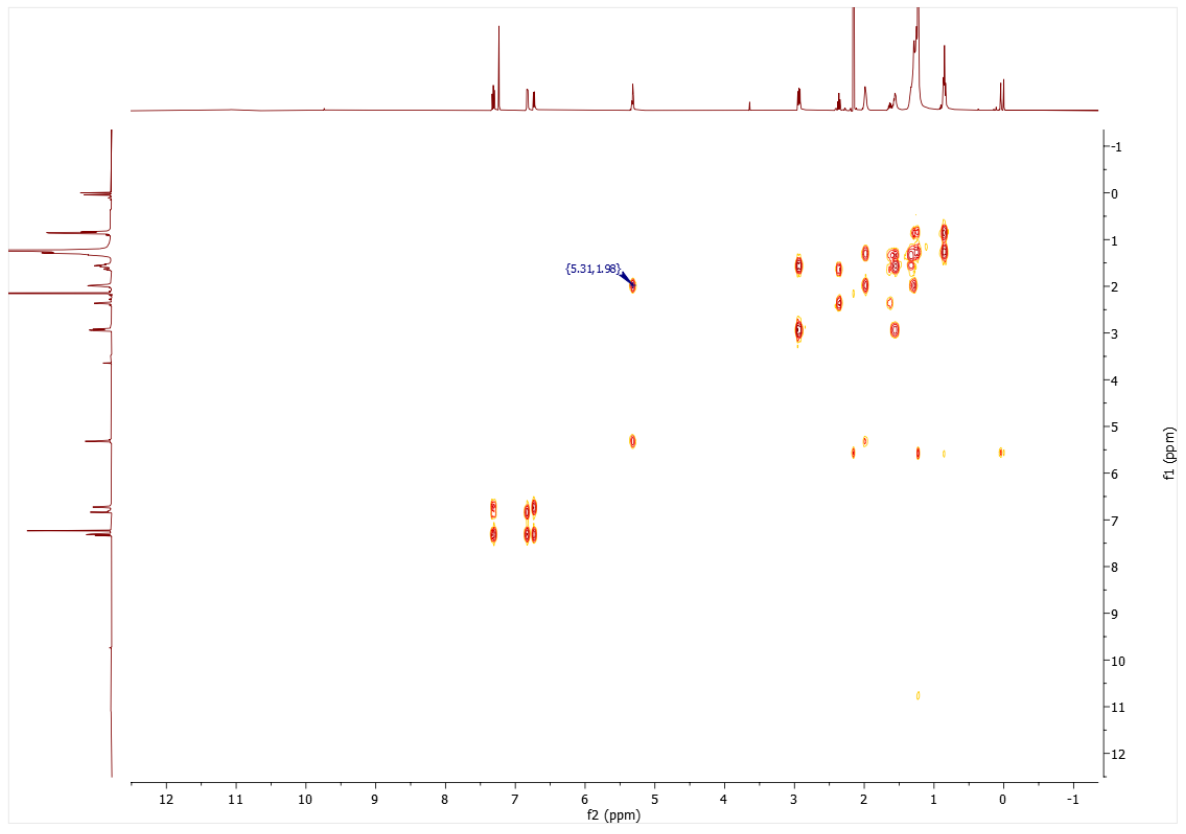


Figure A59. COSY NMR spectrum of 4.11/4.12 mixture.

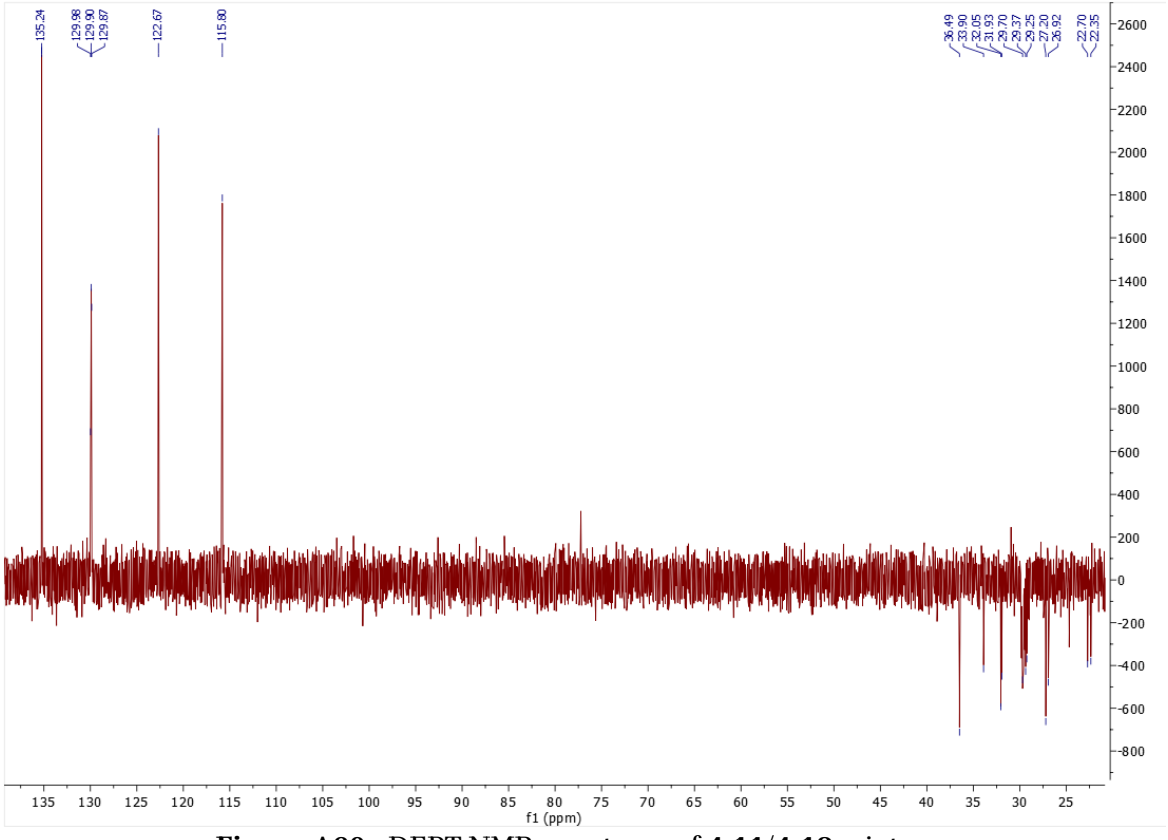
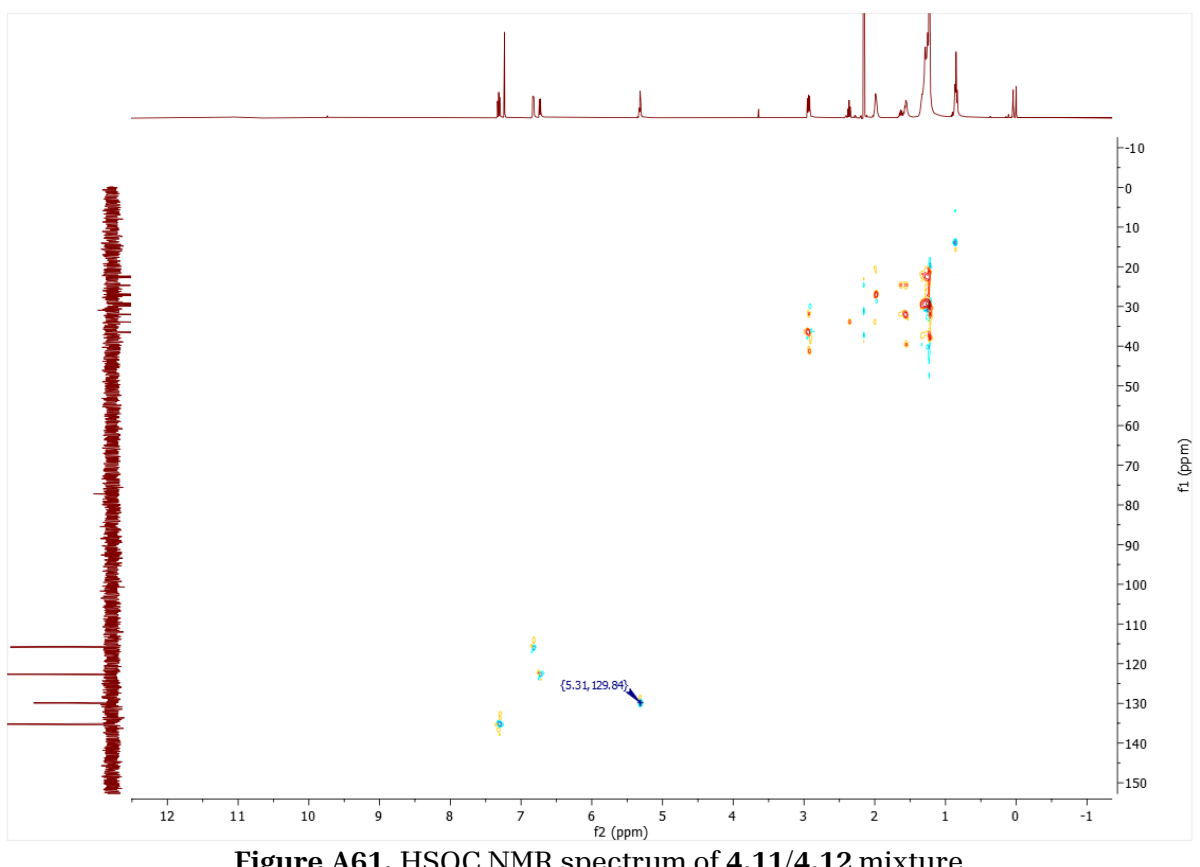


Figure A60. DEPT NMR spectrum of 4.11/4.12 mixture.



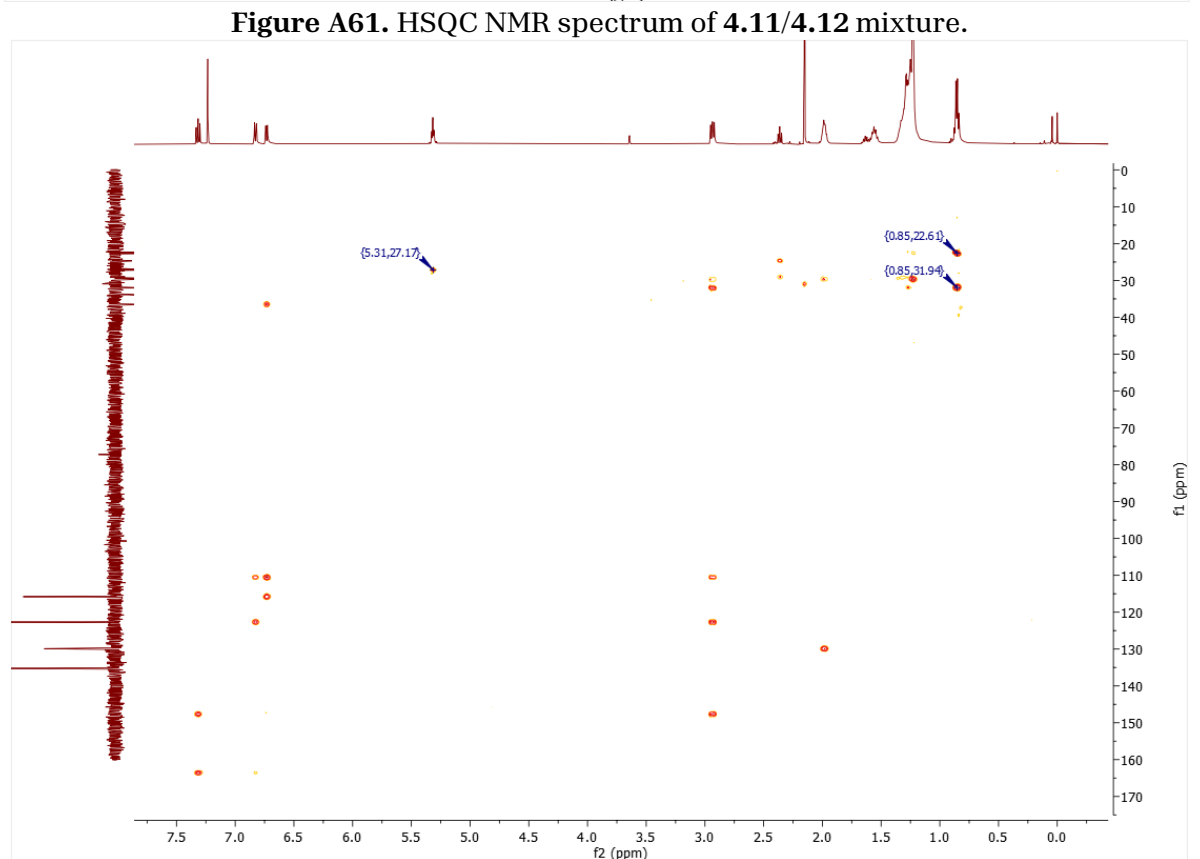


Figure A62. HMBC NMR spectrum of 4.11/4.12 mixture.

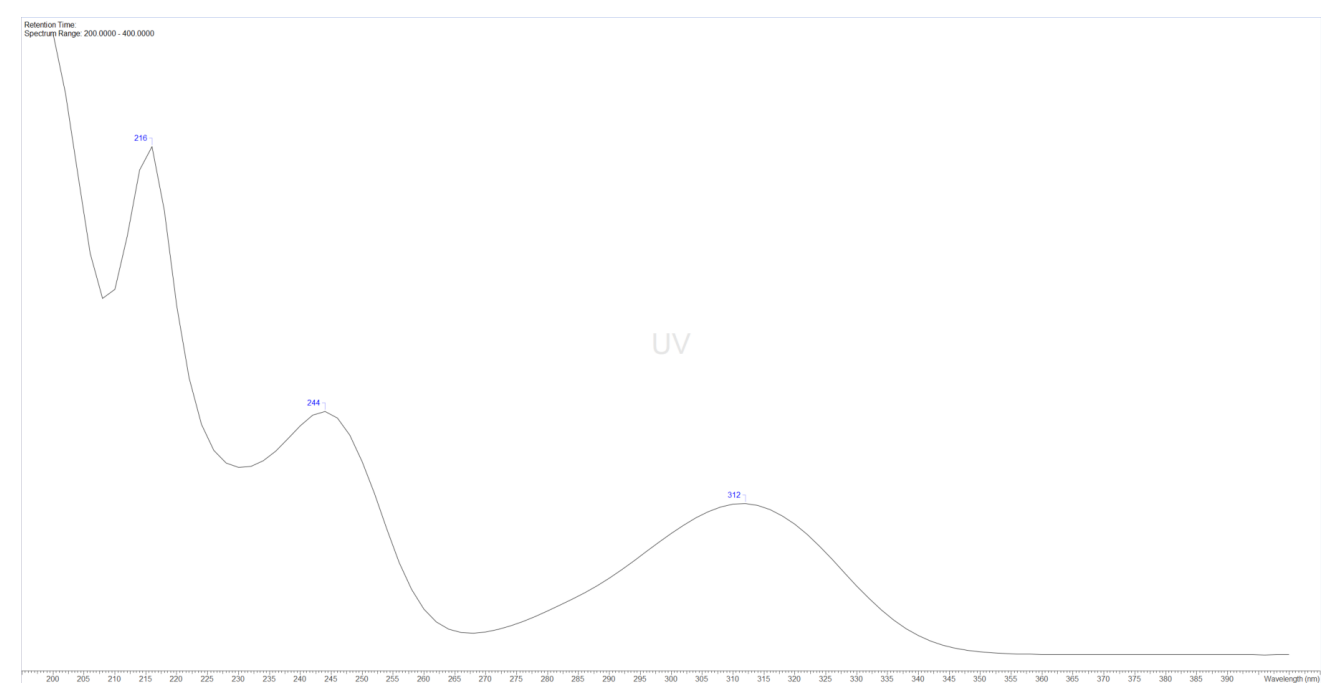
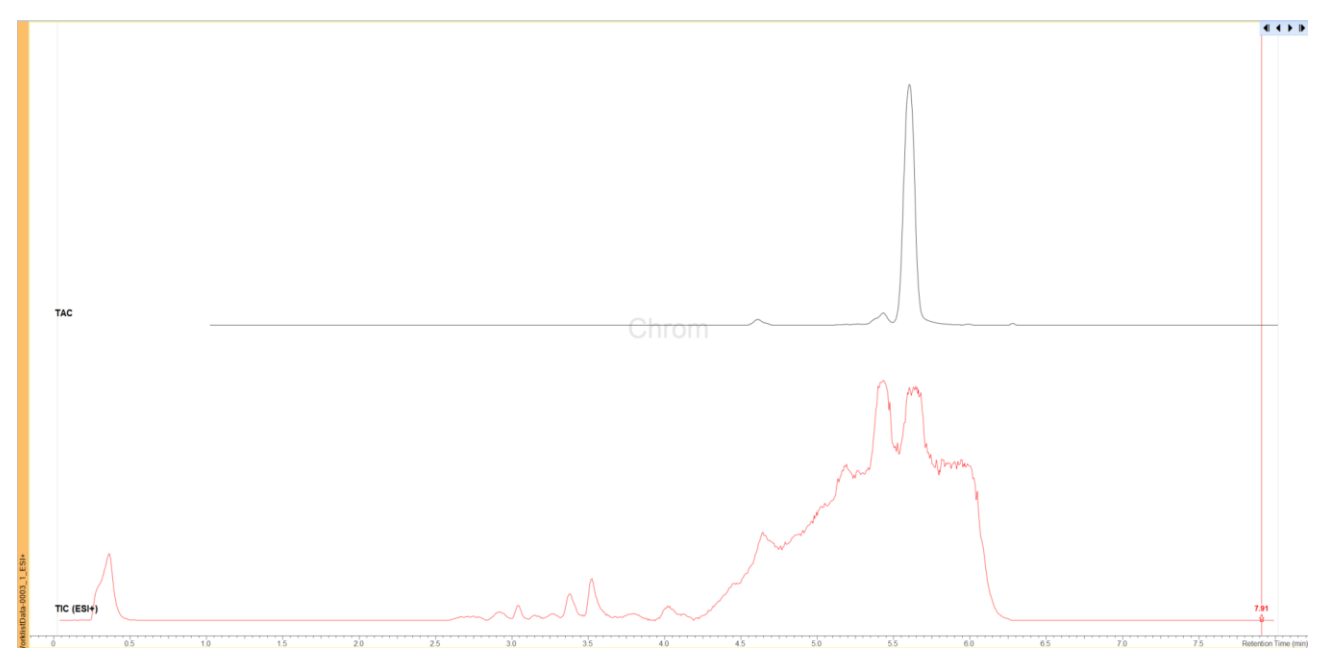


Figure A63. UV-vis absorbance of 4.11/4.12 mixture.



**Figure A64.** Total ion and total absorbance chromatogram of alkene 4.11/4.12 mixture.

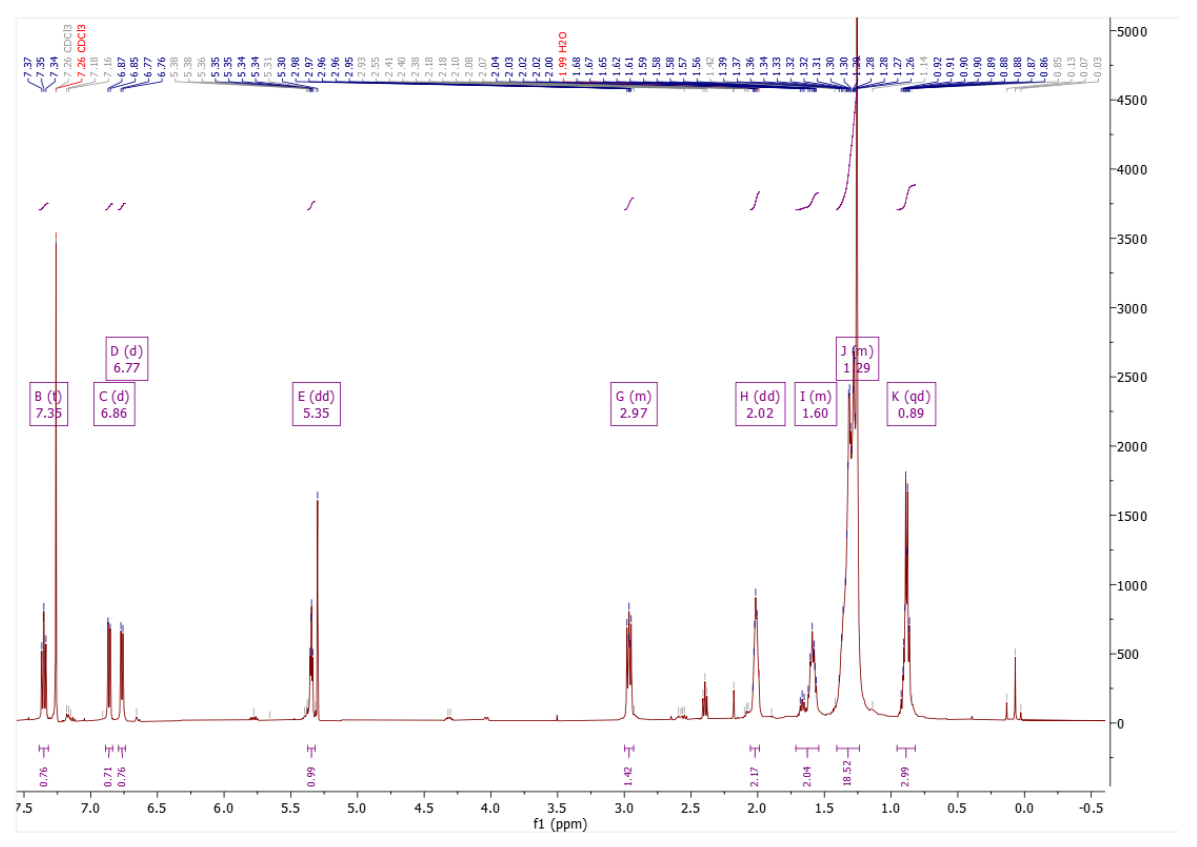


Figure A65. <sup>1</sup>H NMR spectrum of 4.13/4.13 mixture.

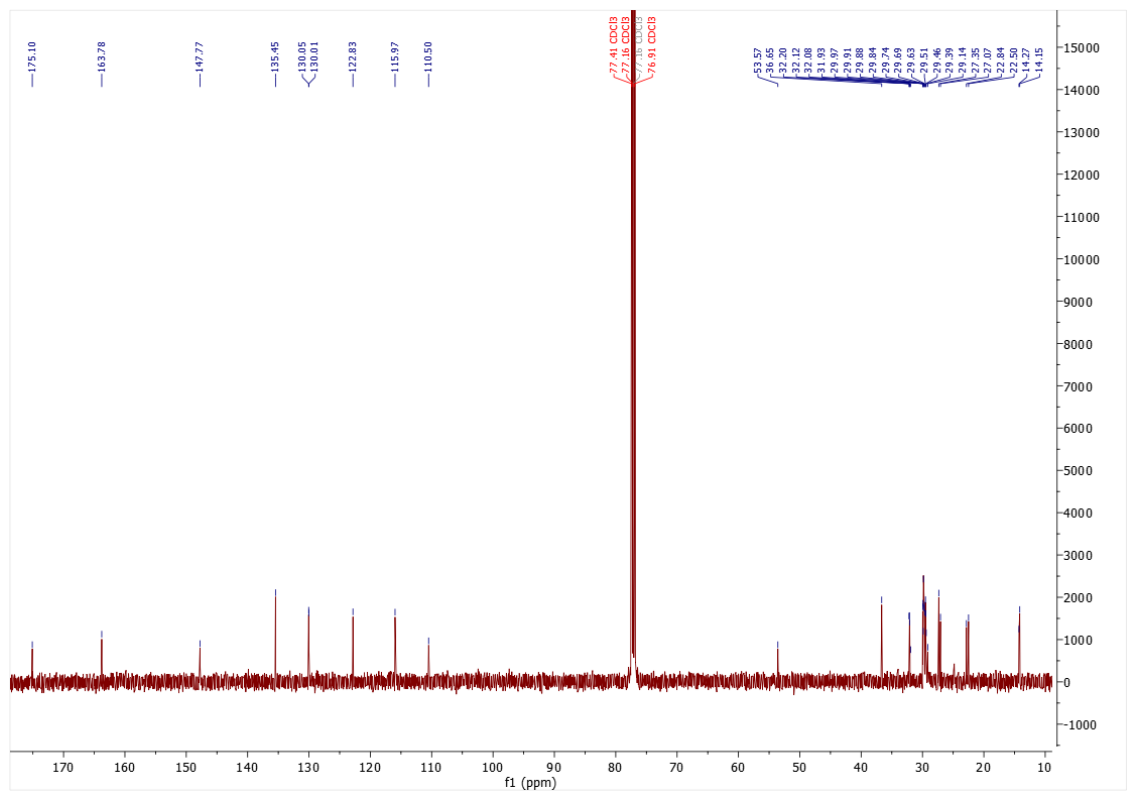
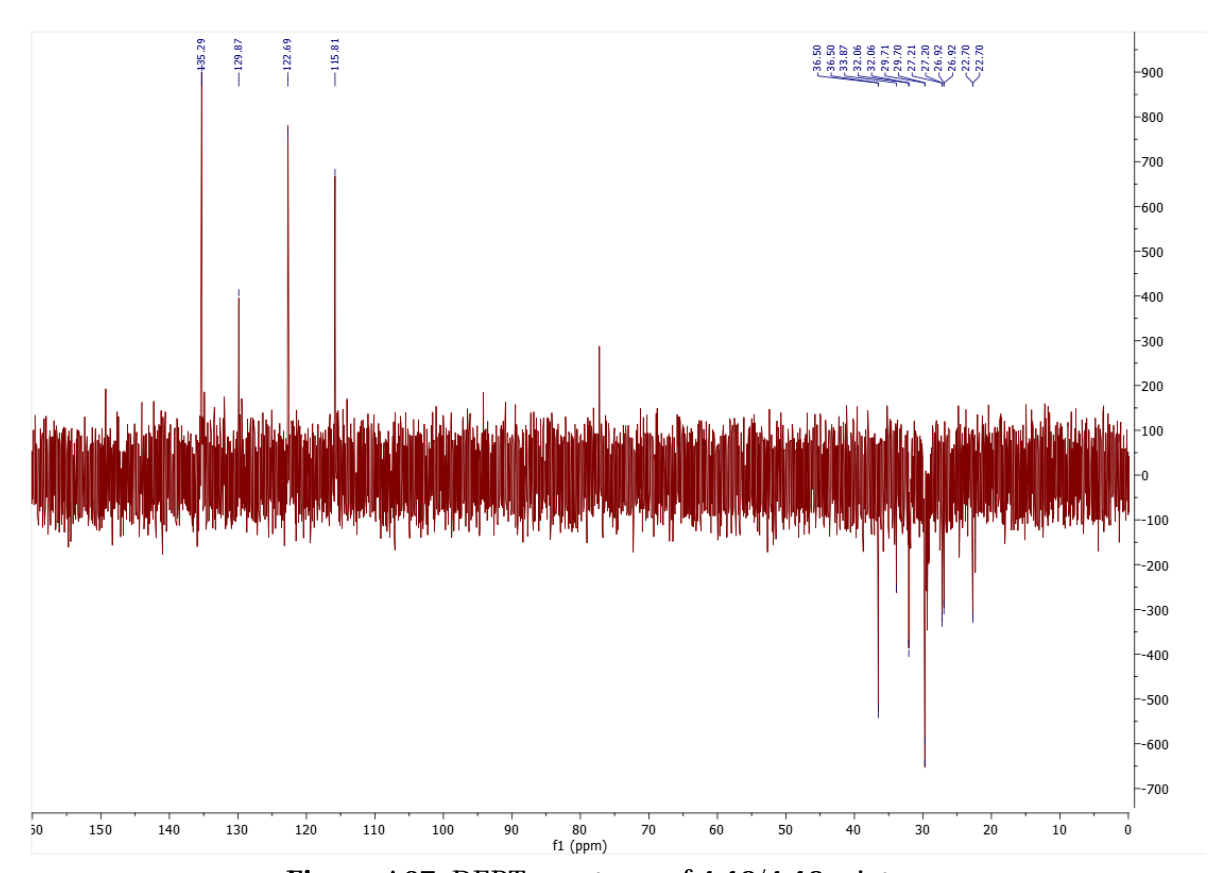
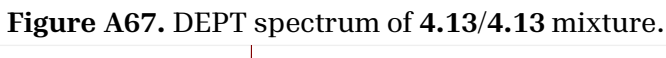


Figure A66.  $^{13}$ C NMR spectrum of 4.13/4.13 mixture.





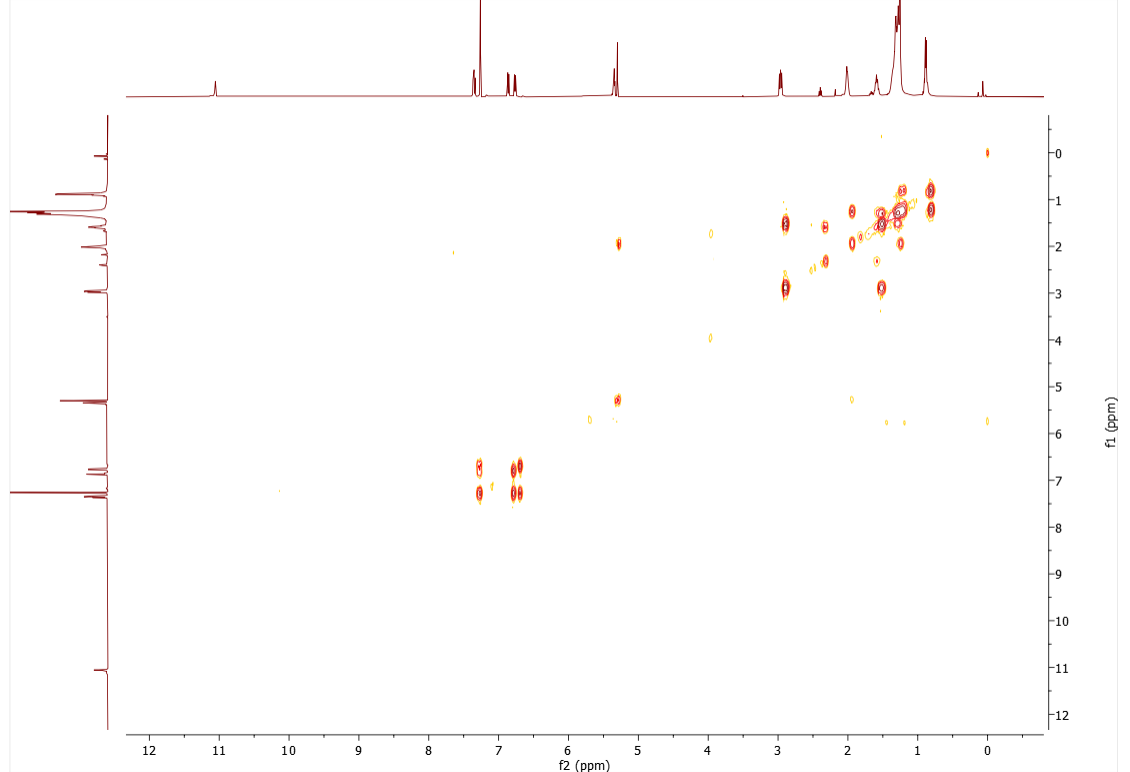


Figure A68. COSY spectrum of 4.13/4.13 mixture.

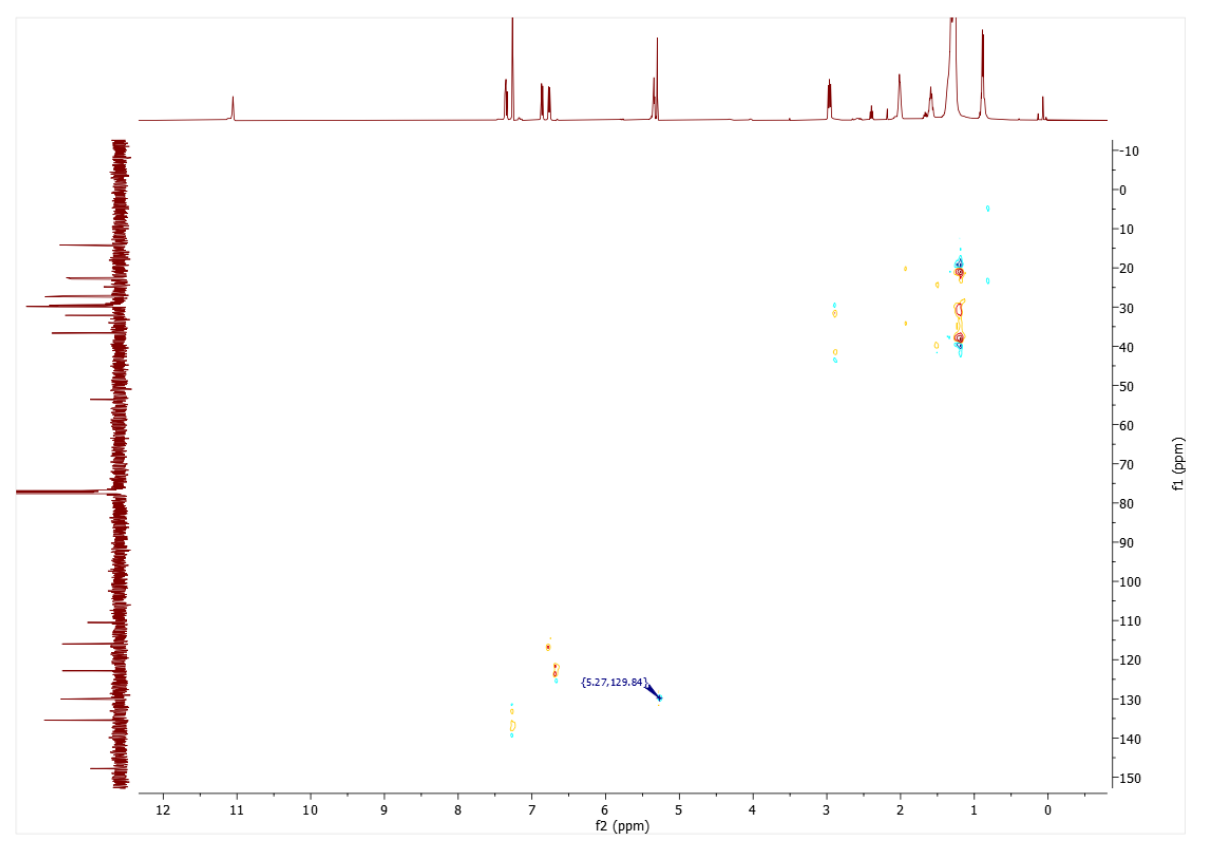


Figure A69. HSQC spectrum of 4.13/4.13 mixture.

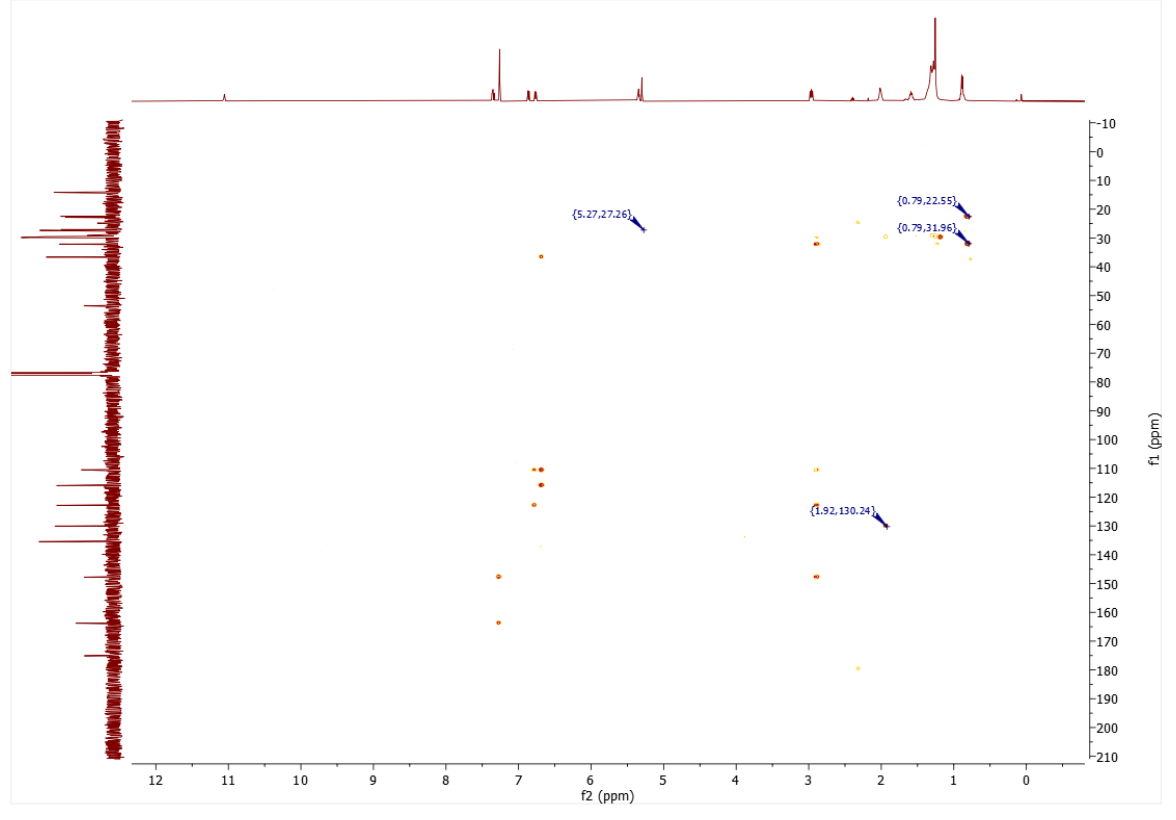
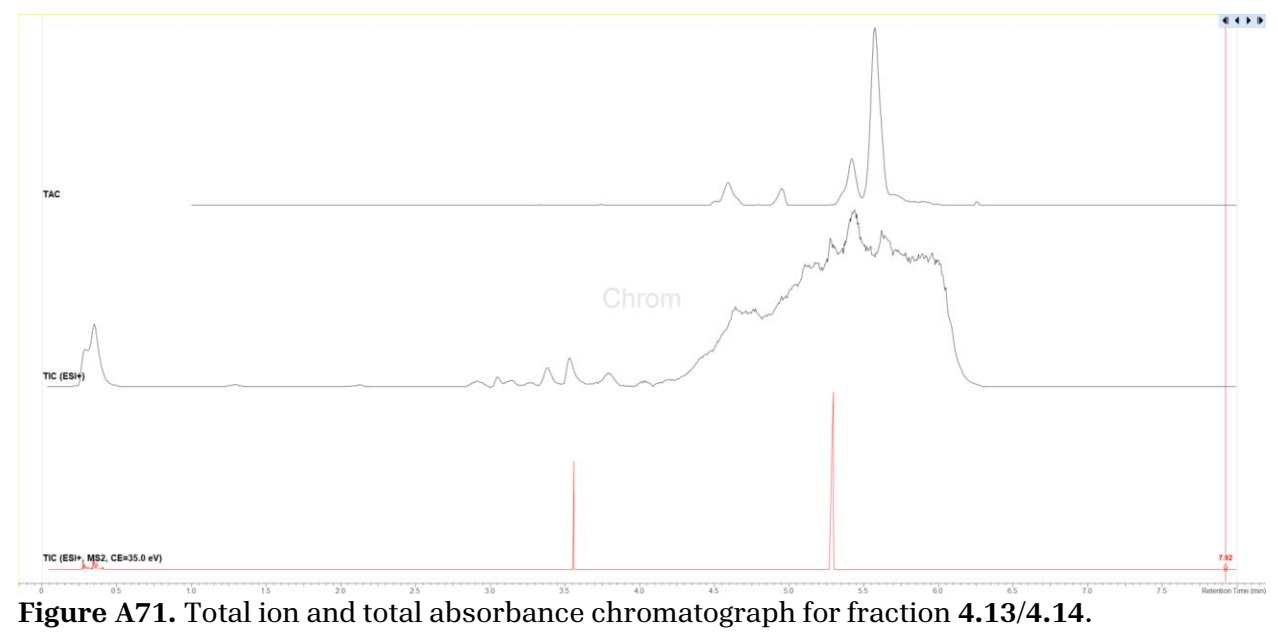
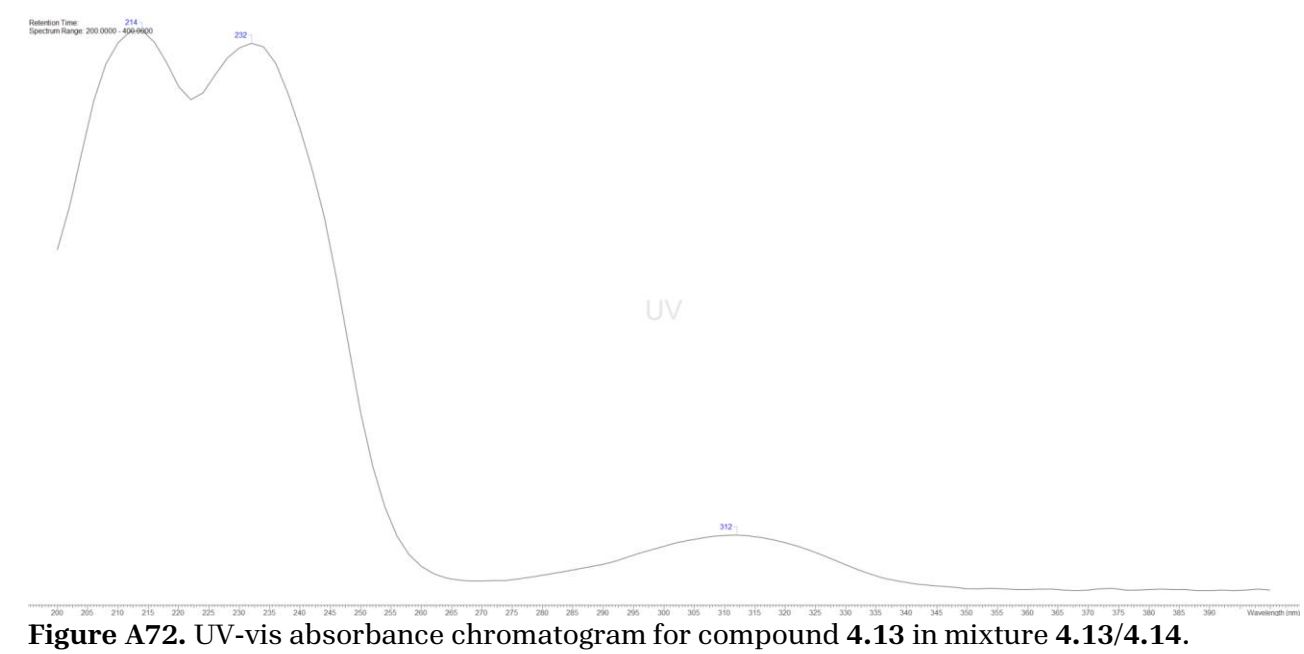


Figure A70. HMBC spectrum of 4.13/4.13 mixture.





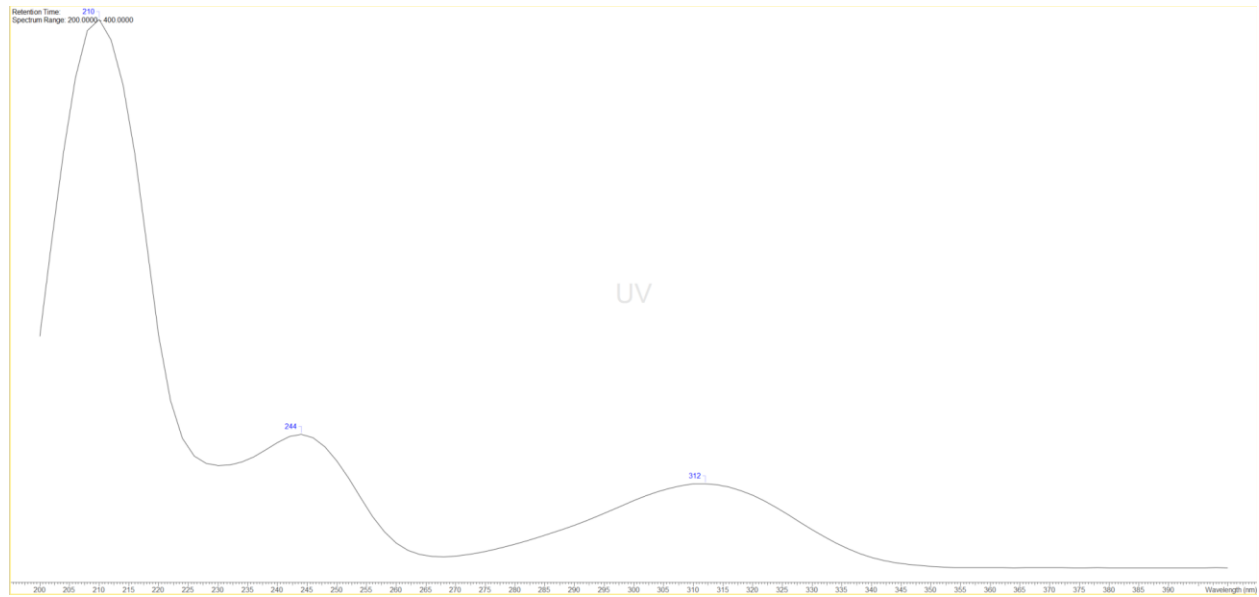


Figure A73. UV-vis absorbance chromatogram for compound **4.14** in mixture **4.13/4.14**.

# Appendix B: Spectral data of natural products isolated from Garcinia caudiculata

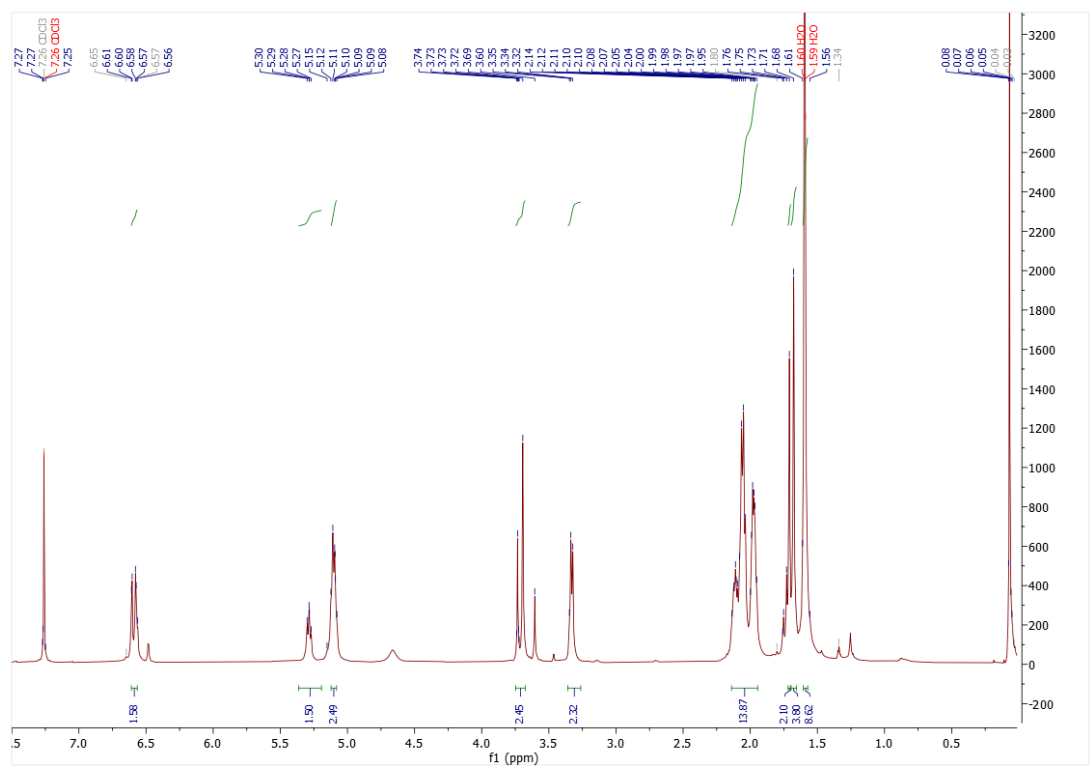


Figure B1. 1H NMR spectrum of 5.1.

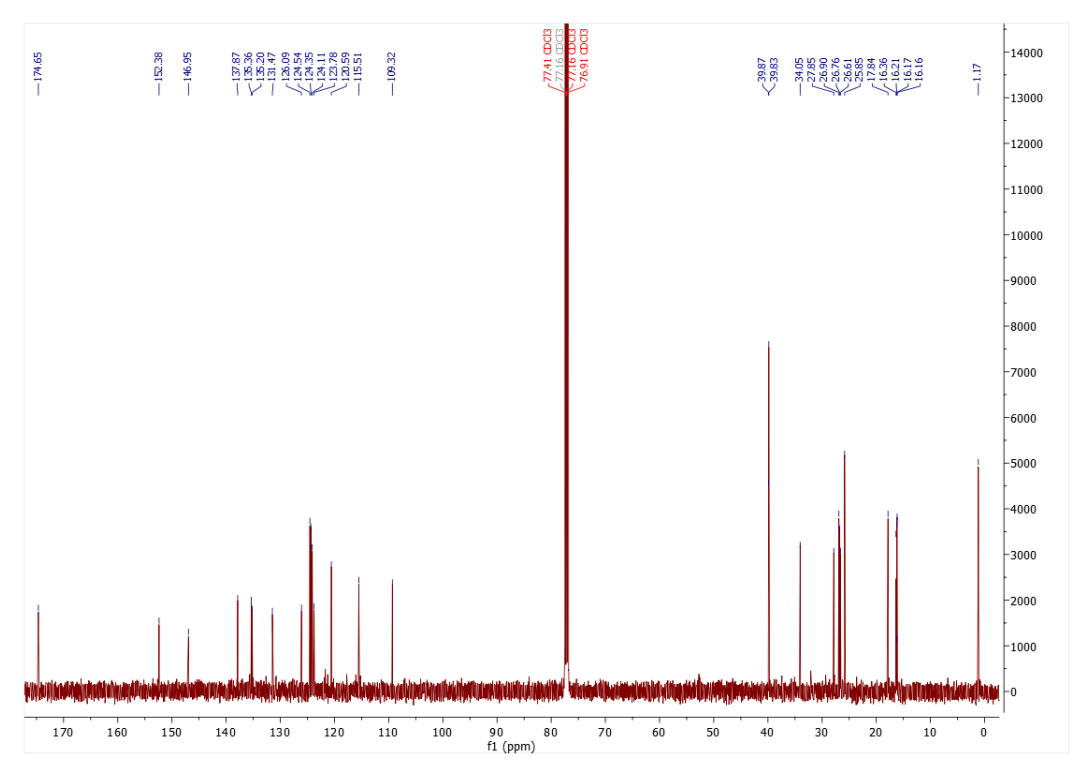
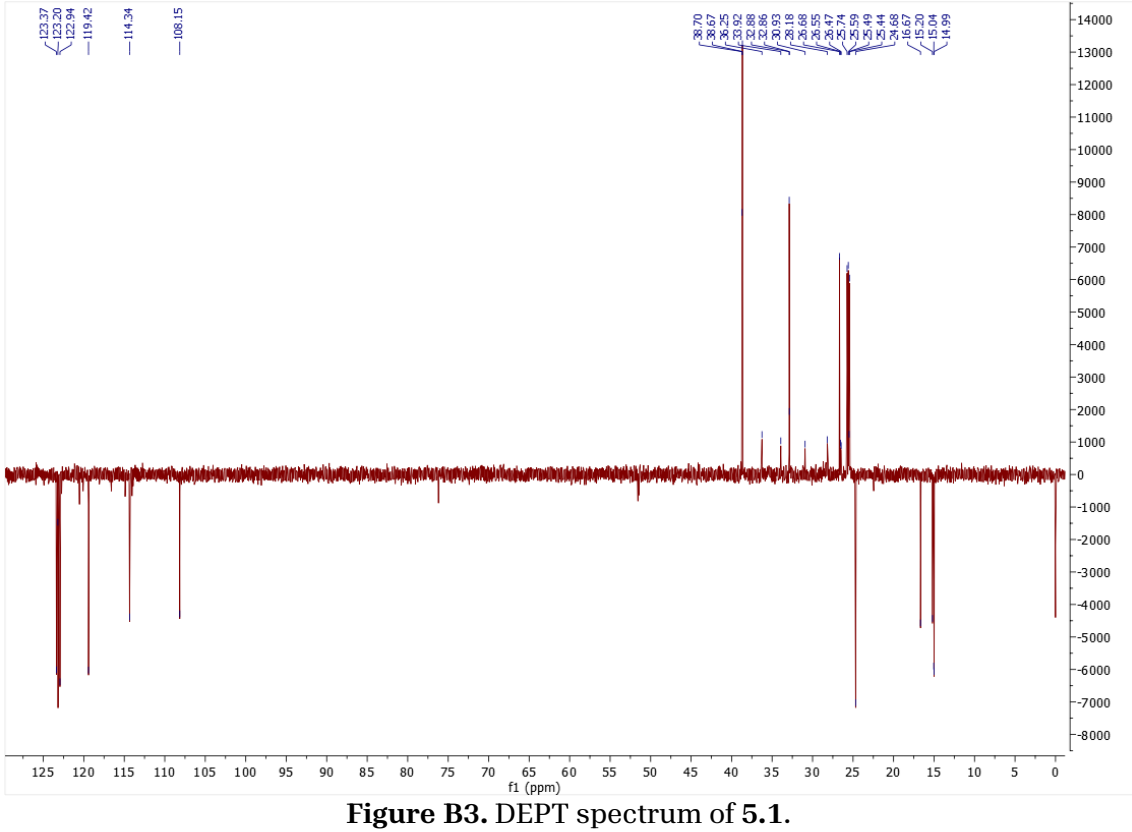


Figure B2. 13C NMR spectrum of 5.1.



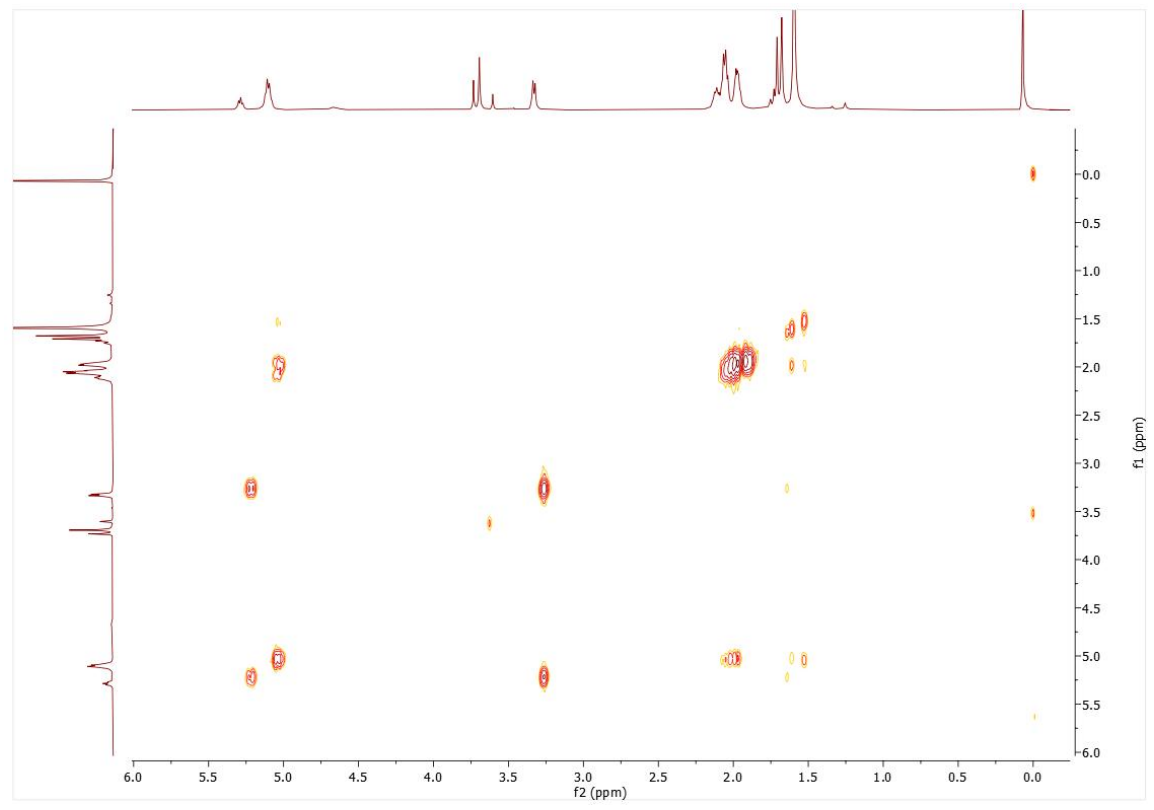


Figure B4. COSY NMR spectrum of 5.1.

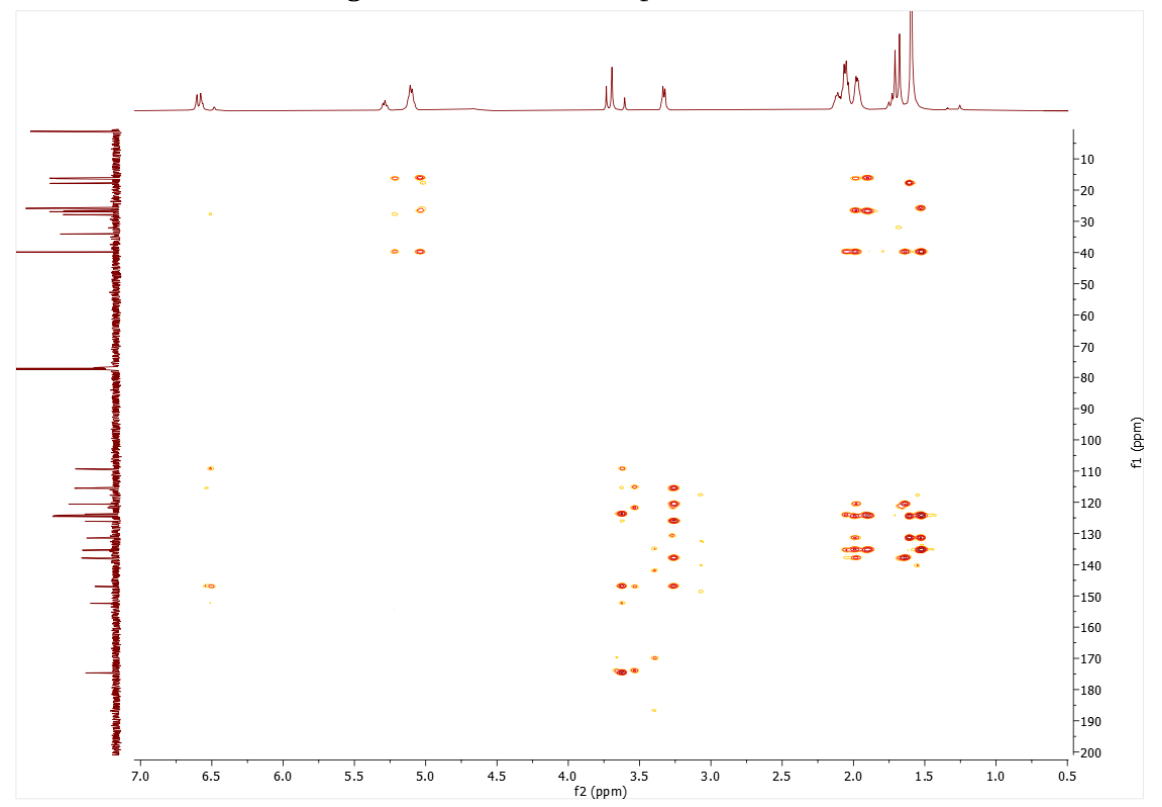


Figure B5. HMBC NMR spectrum of 5.1.

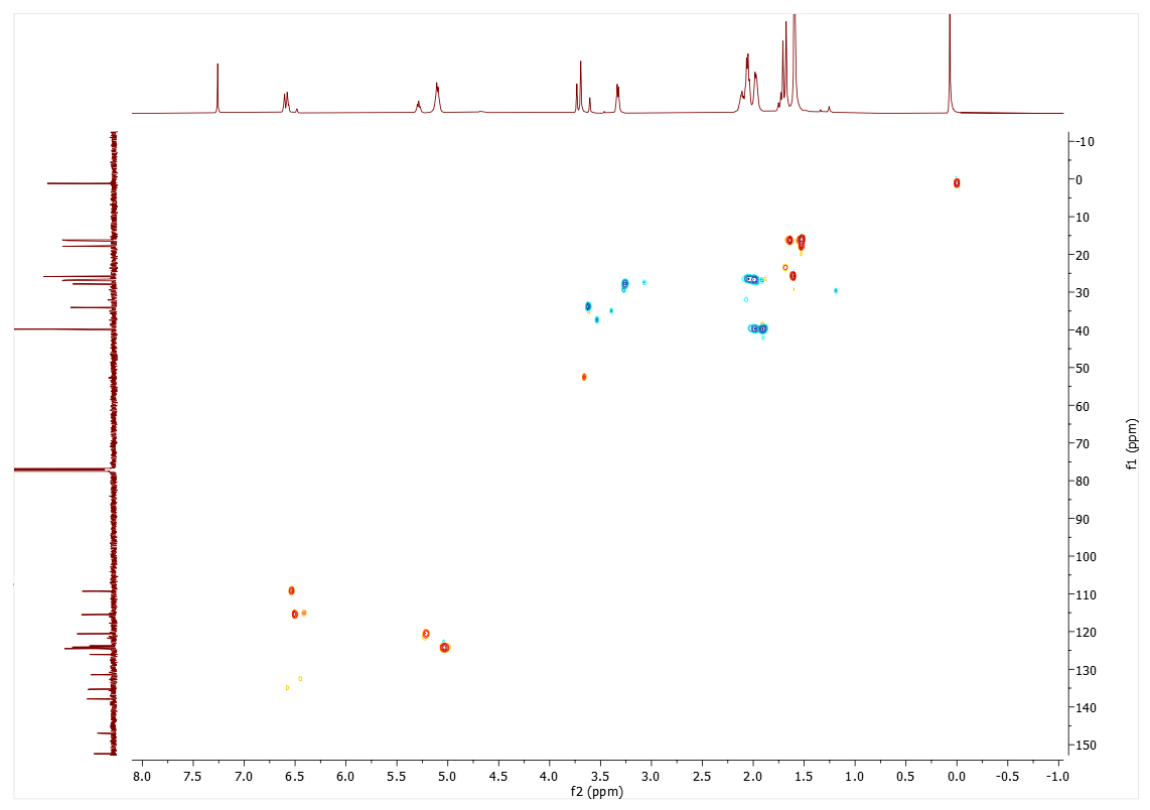


Figure B6. HSQC NMR spectrum of 5.1.

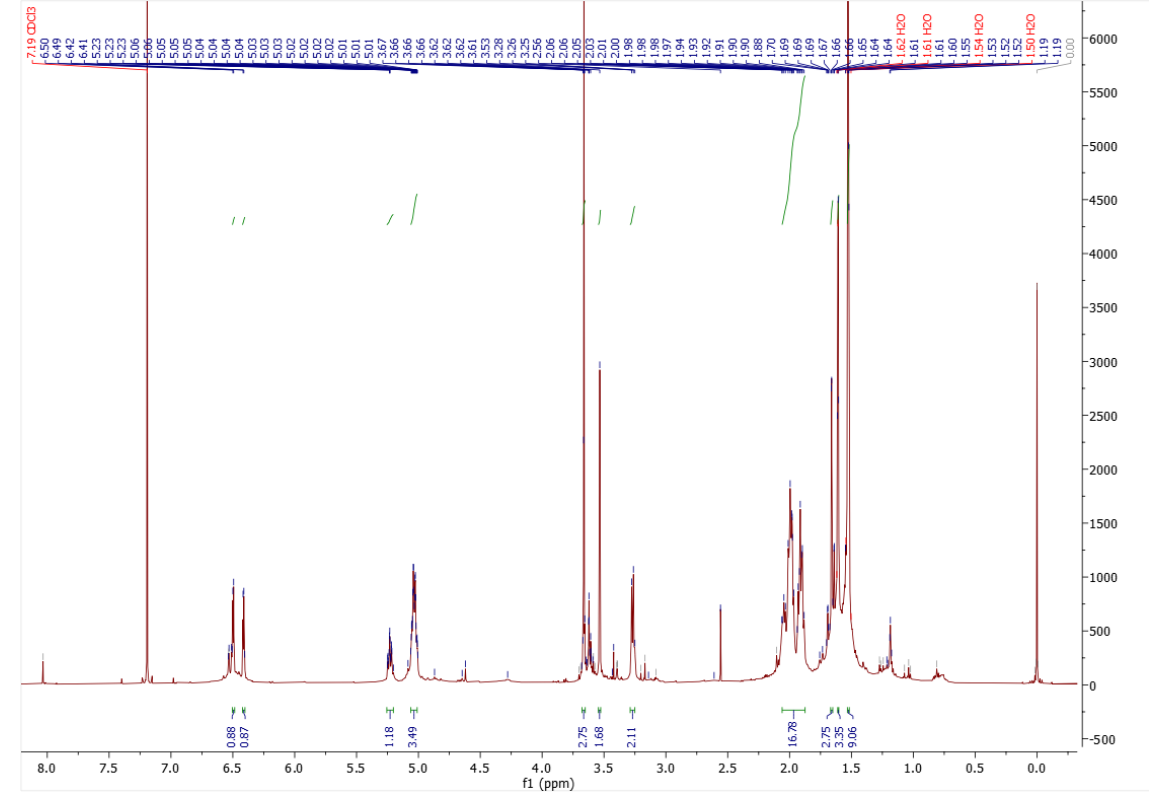
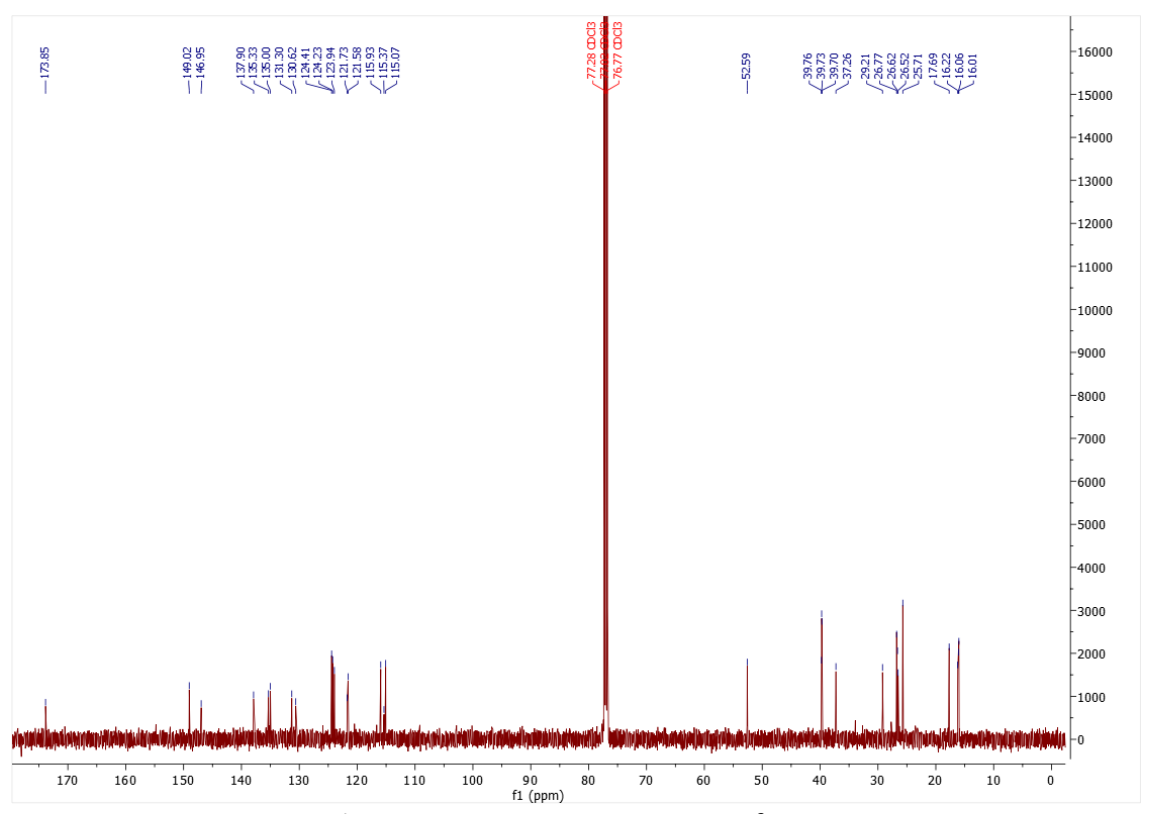


Figure B7. 1H NMR spectrum of 5.2.





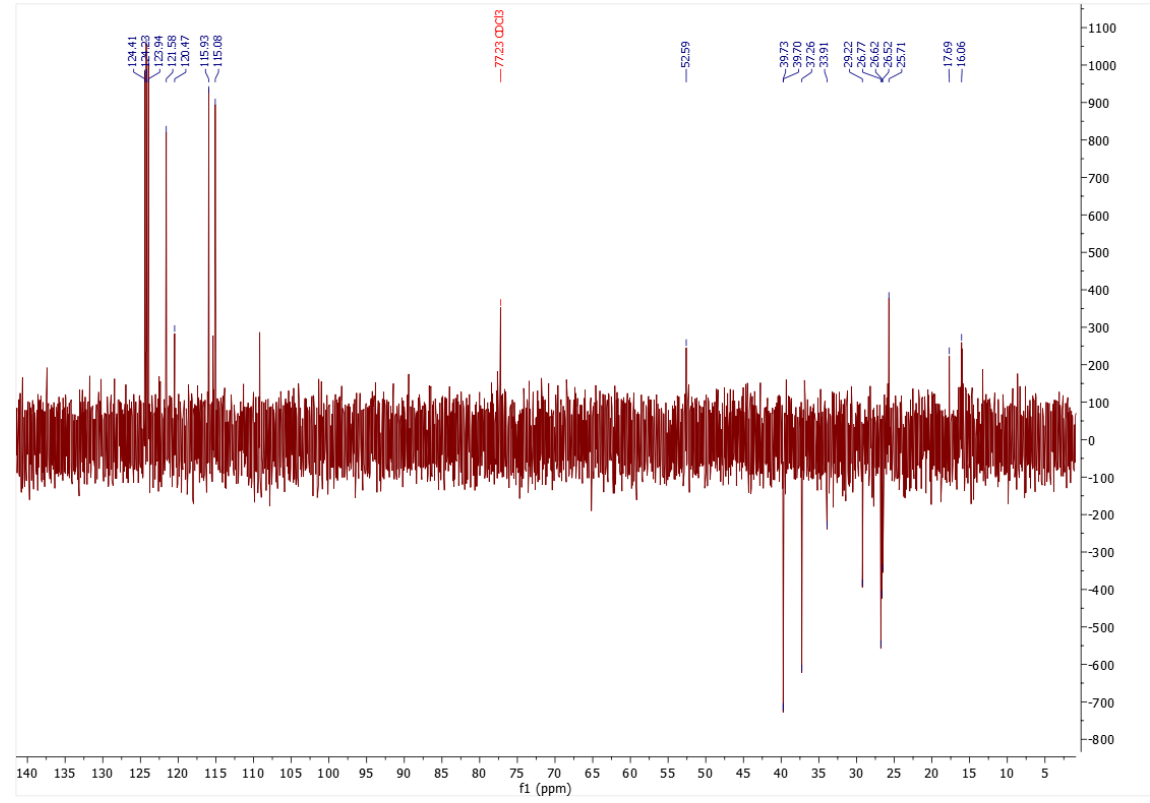
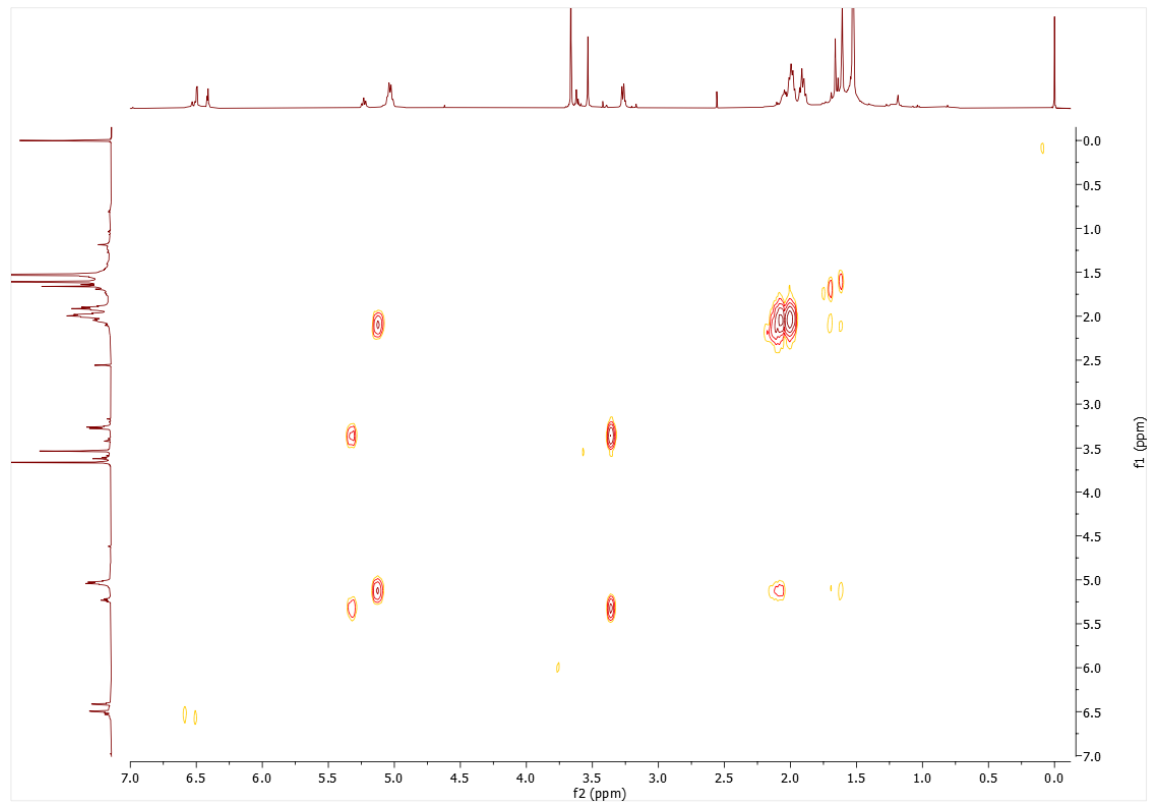
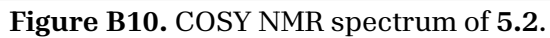


Figure B9. DEPT spectrum of 5.2.





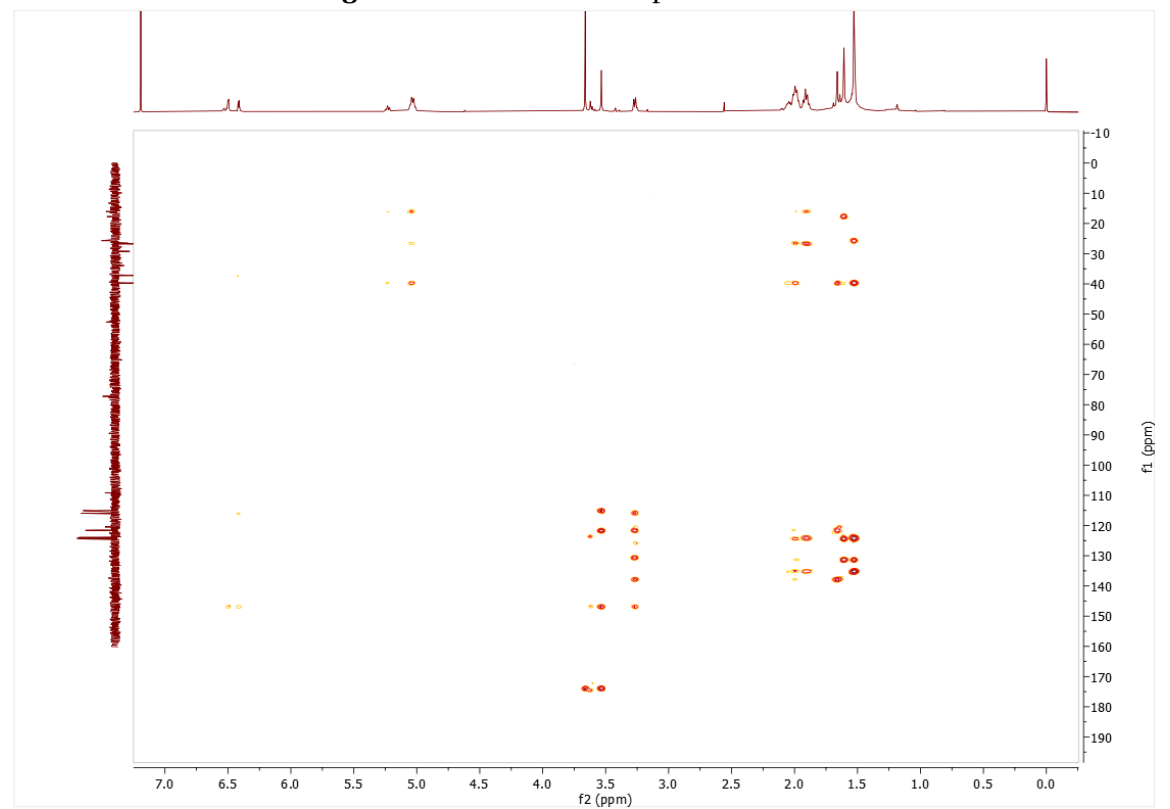


Figure B11. HMBC NMR spectrum of 5.2.

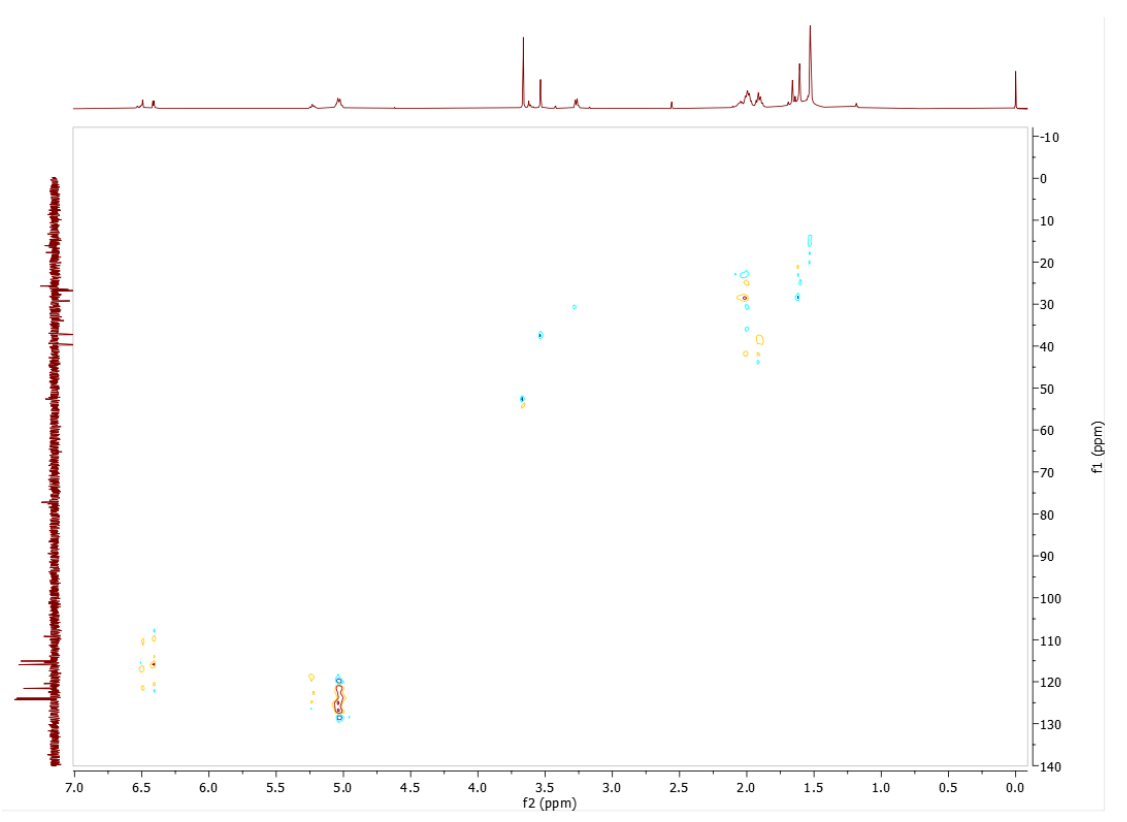


Figure B12. HSQC NMR spectrum of 5.2.

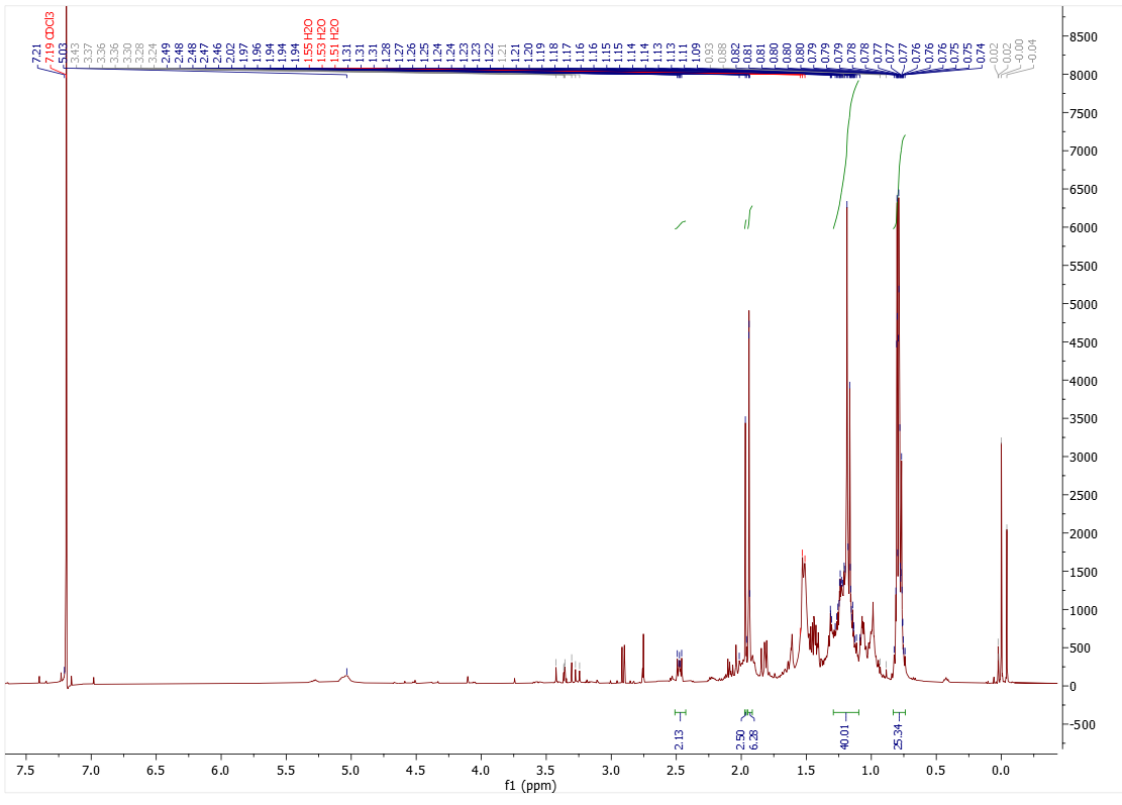


Figure B13. 1H NMR spectrum of 4.7 (second isolation).

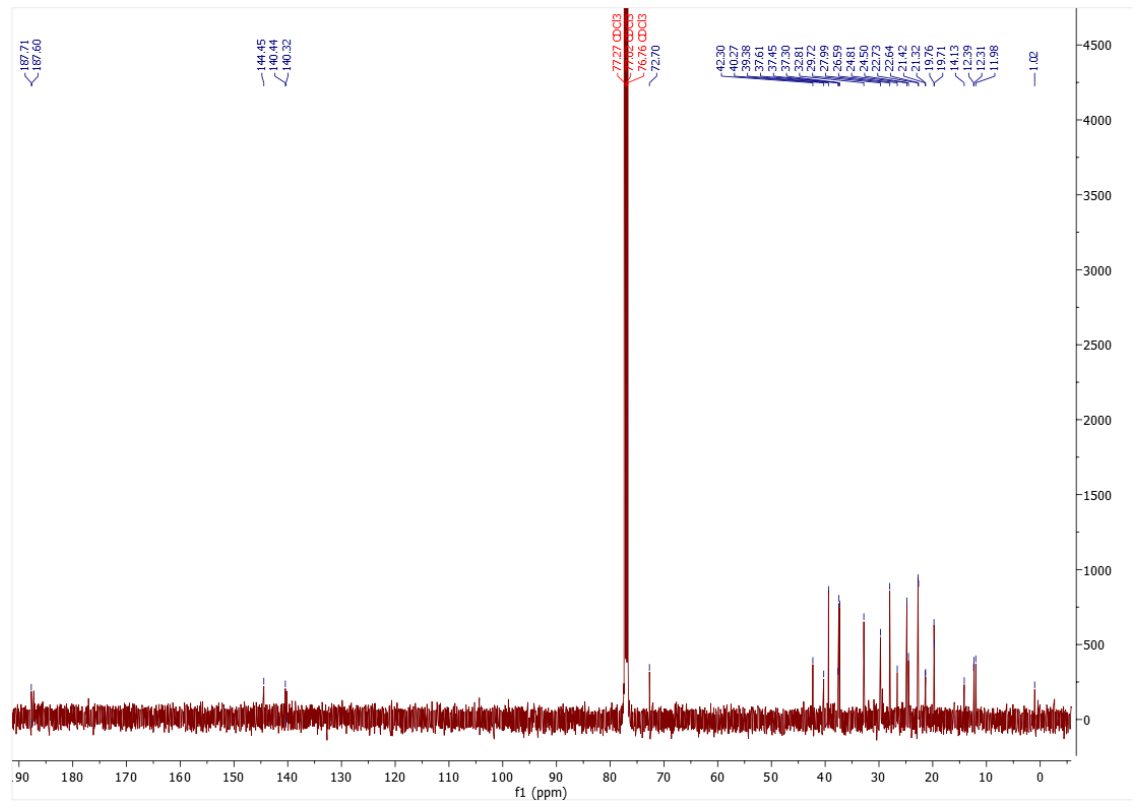


Figure B14. 13C NMR spectrum of 4.7 (second isolation).

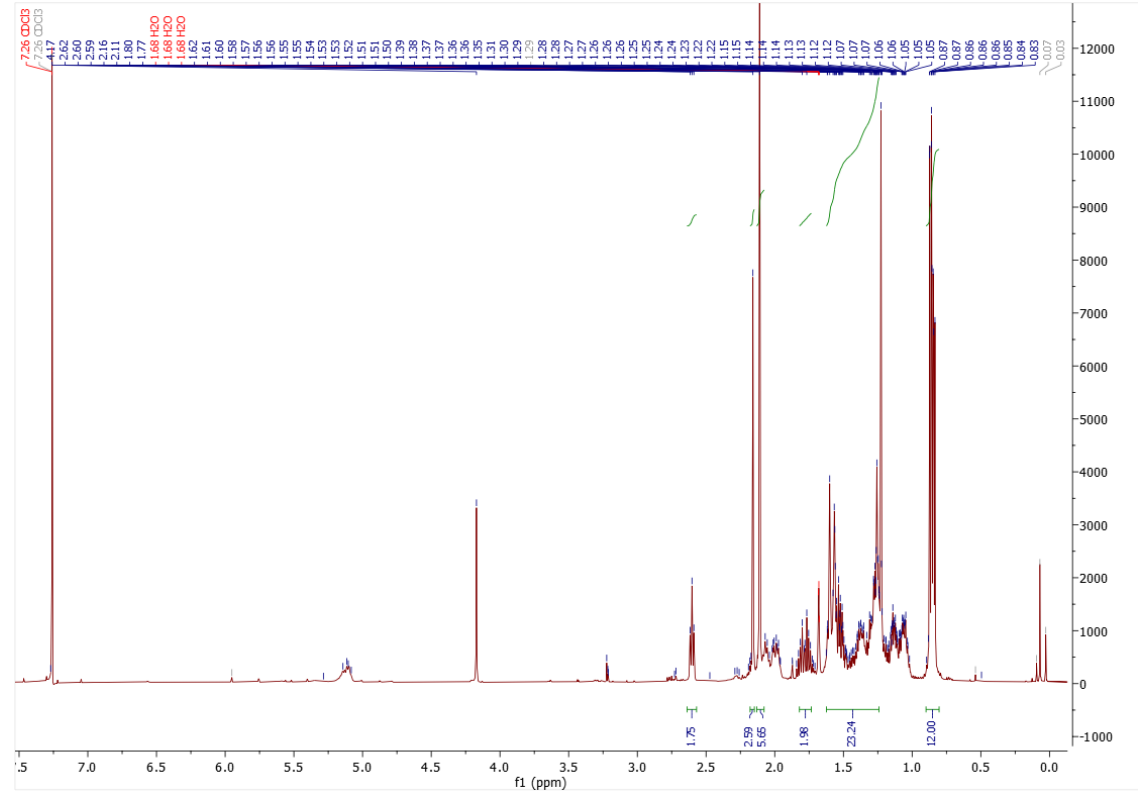


Figure B15. 1H NMR spectrum of 5.3.

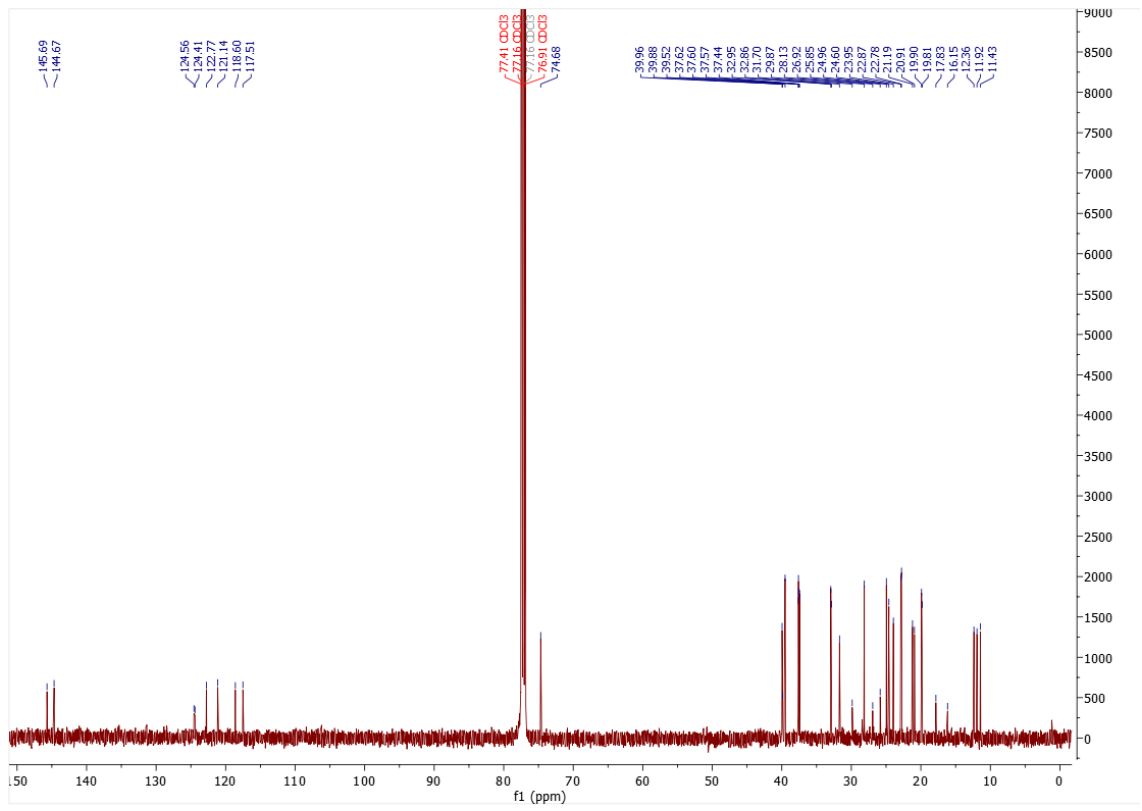


Figure B16. 13C NMR spectrum of 5.3.

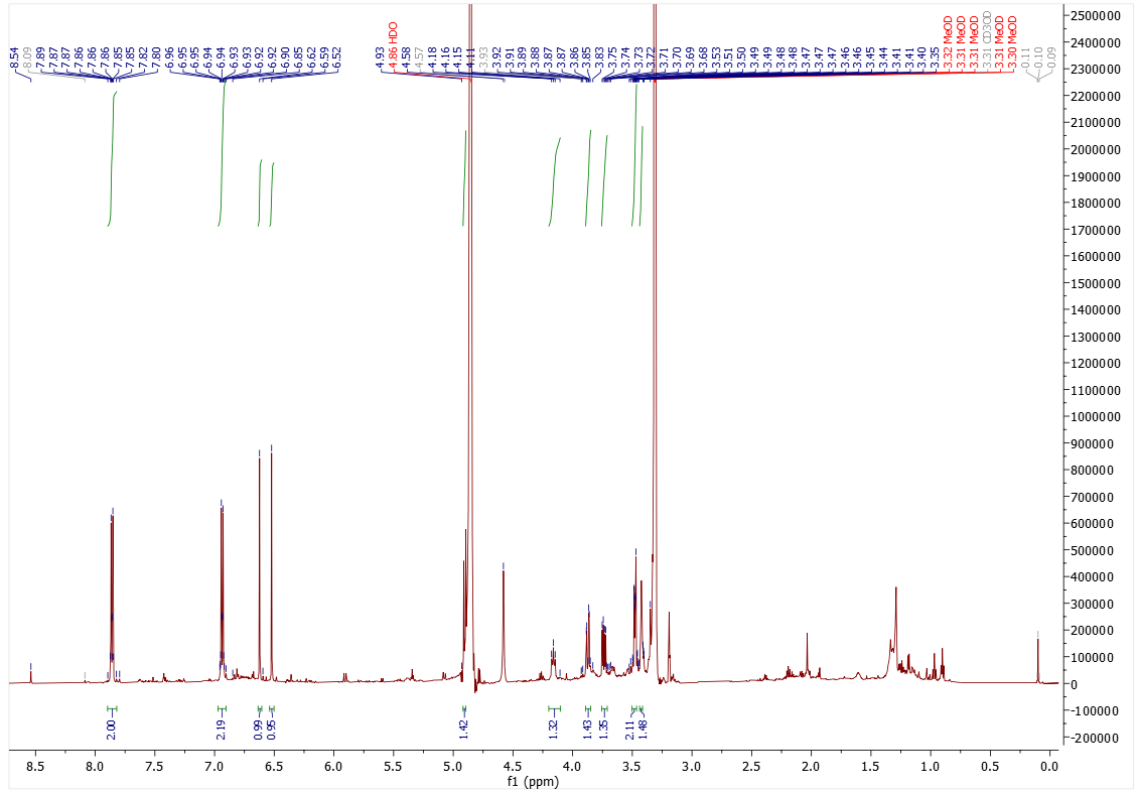
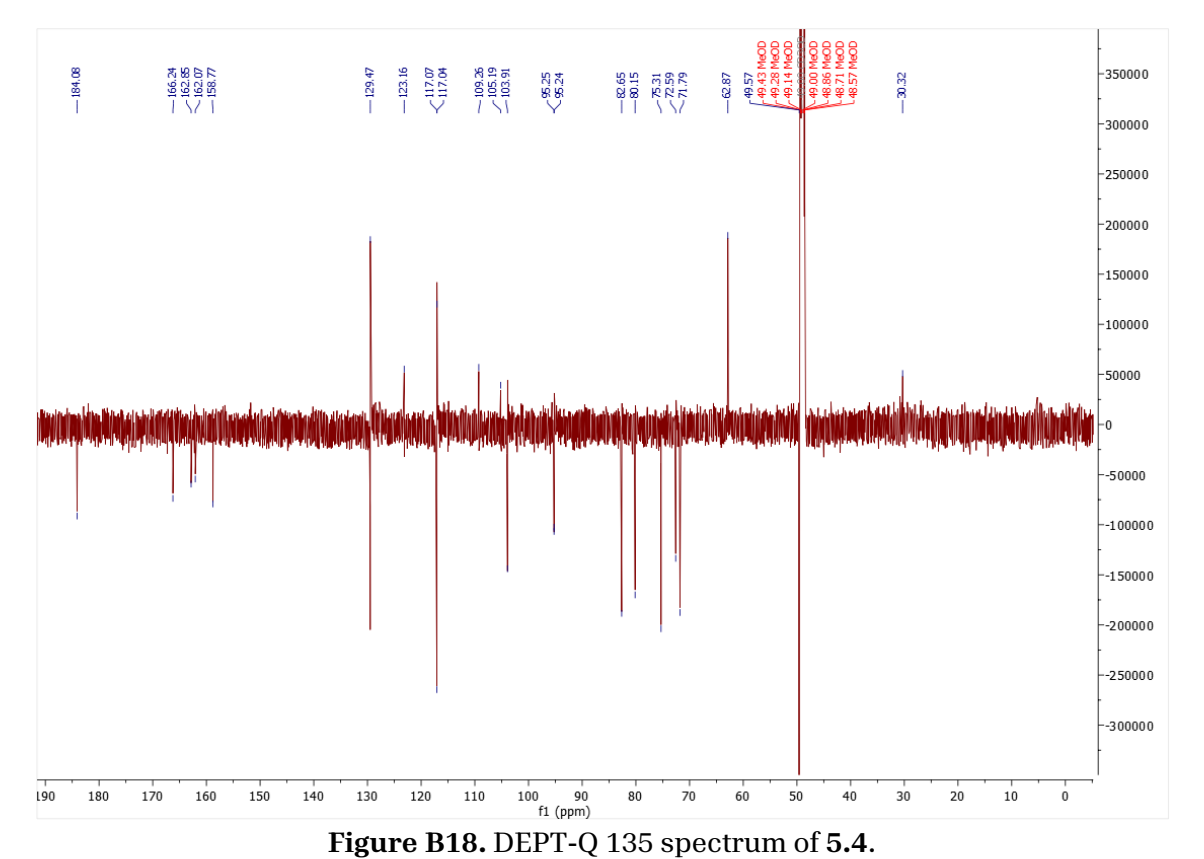
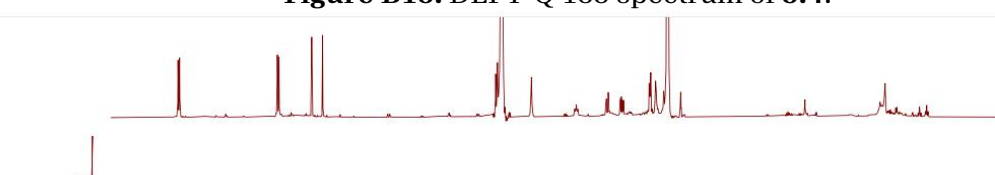


Figure B17. 1H NMR spectrum of 5.4.





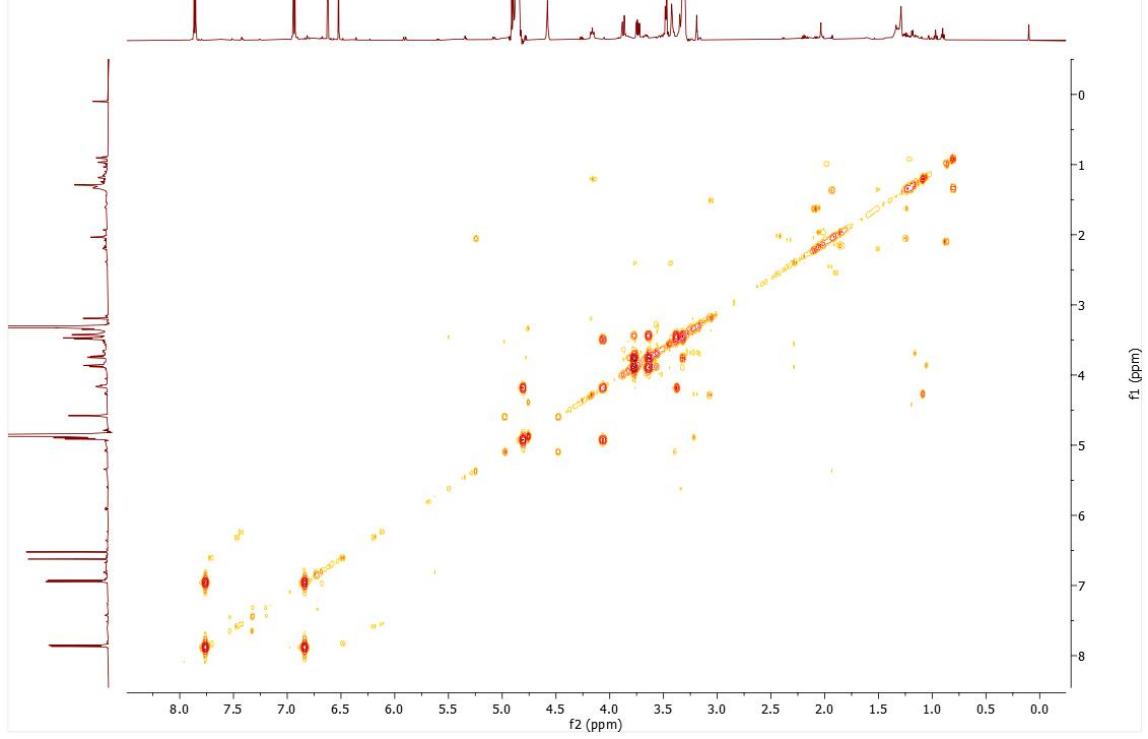


Figure B19. COSY NMR spectrum of 5.4.

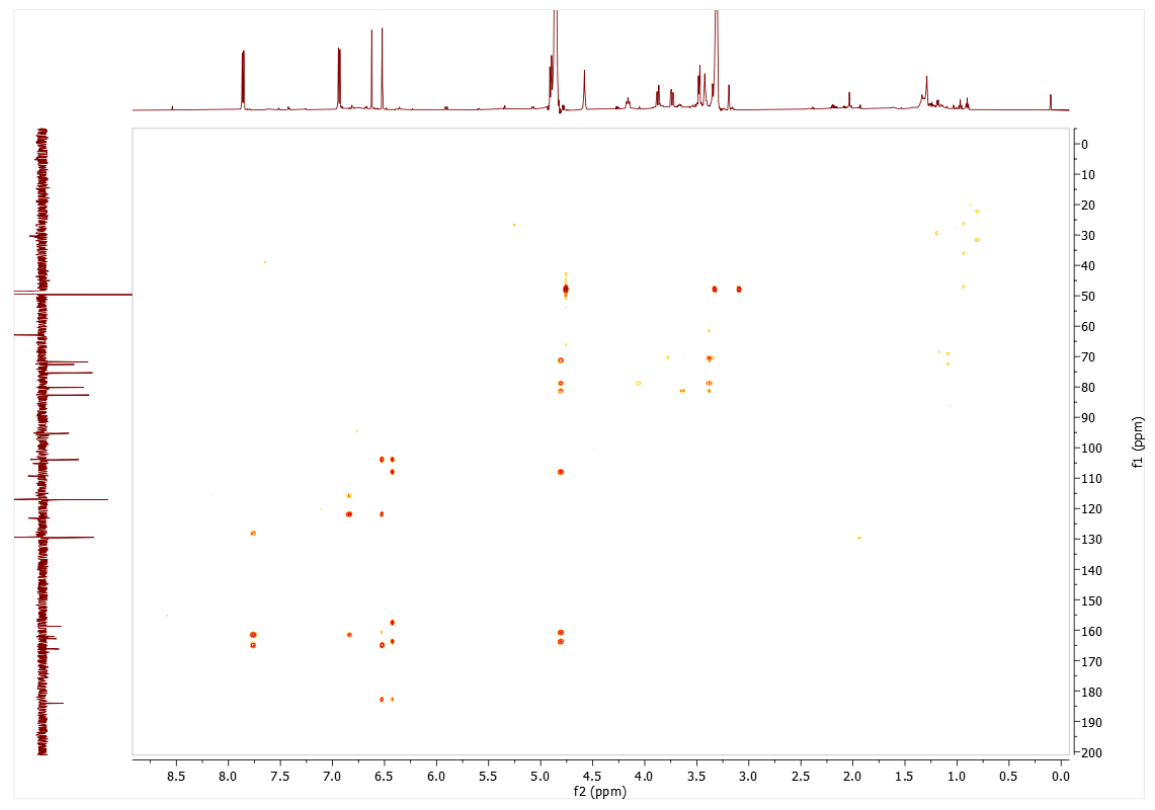


Figure B20. HMBC NMR spectrum of 5.4.

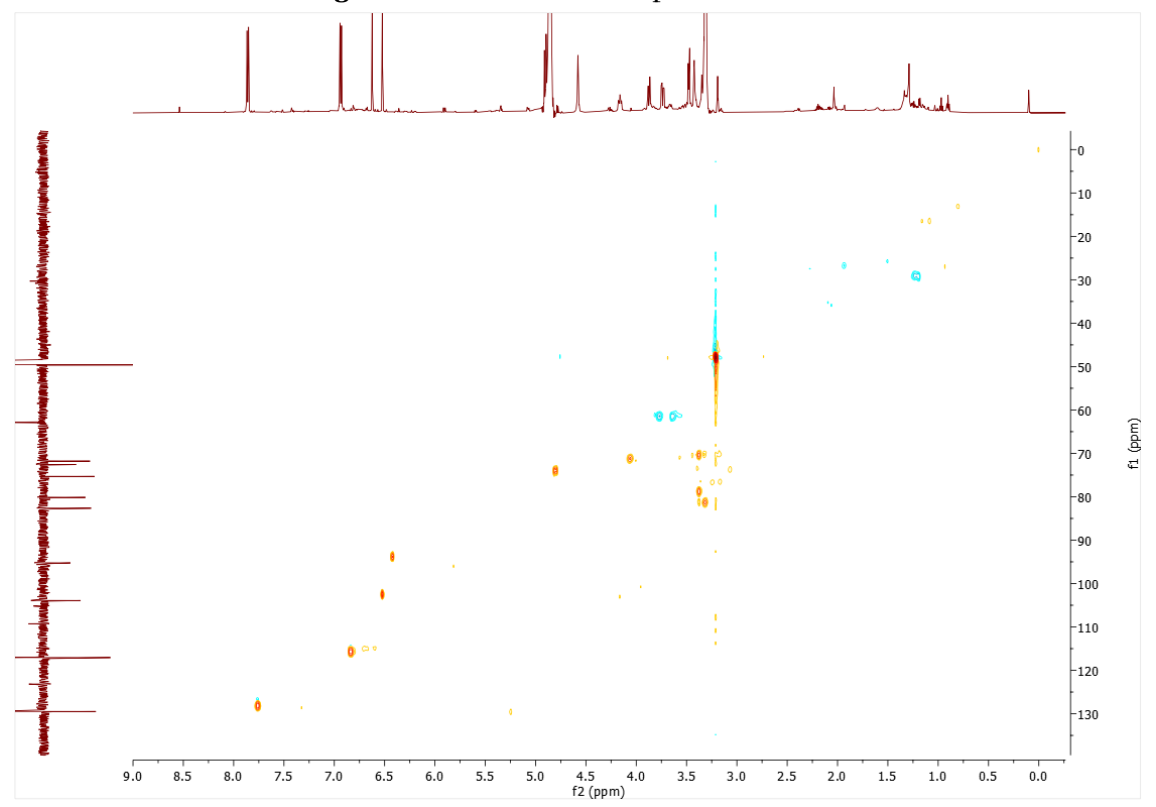


Figure B21. HSQC NMR spectrum of 5.4.

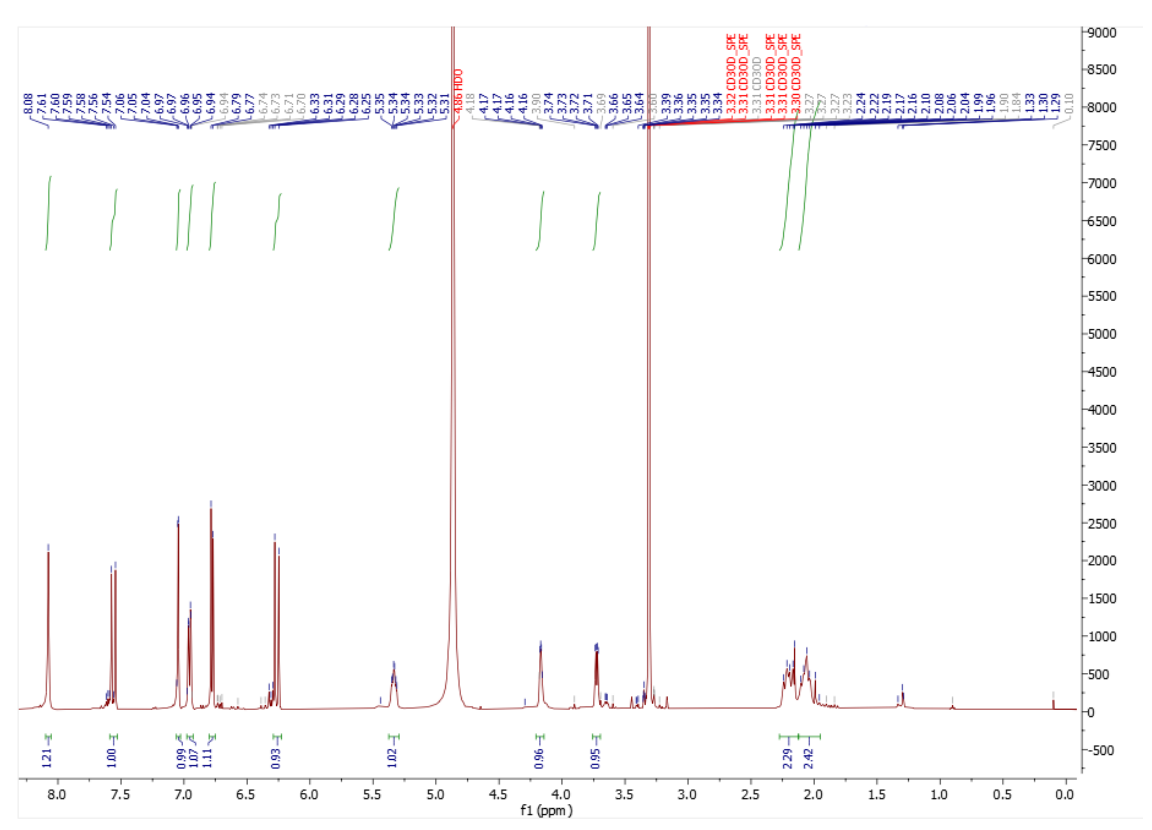


Figure B22. 1H NMR spectrum of 5.5.

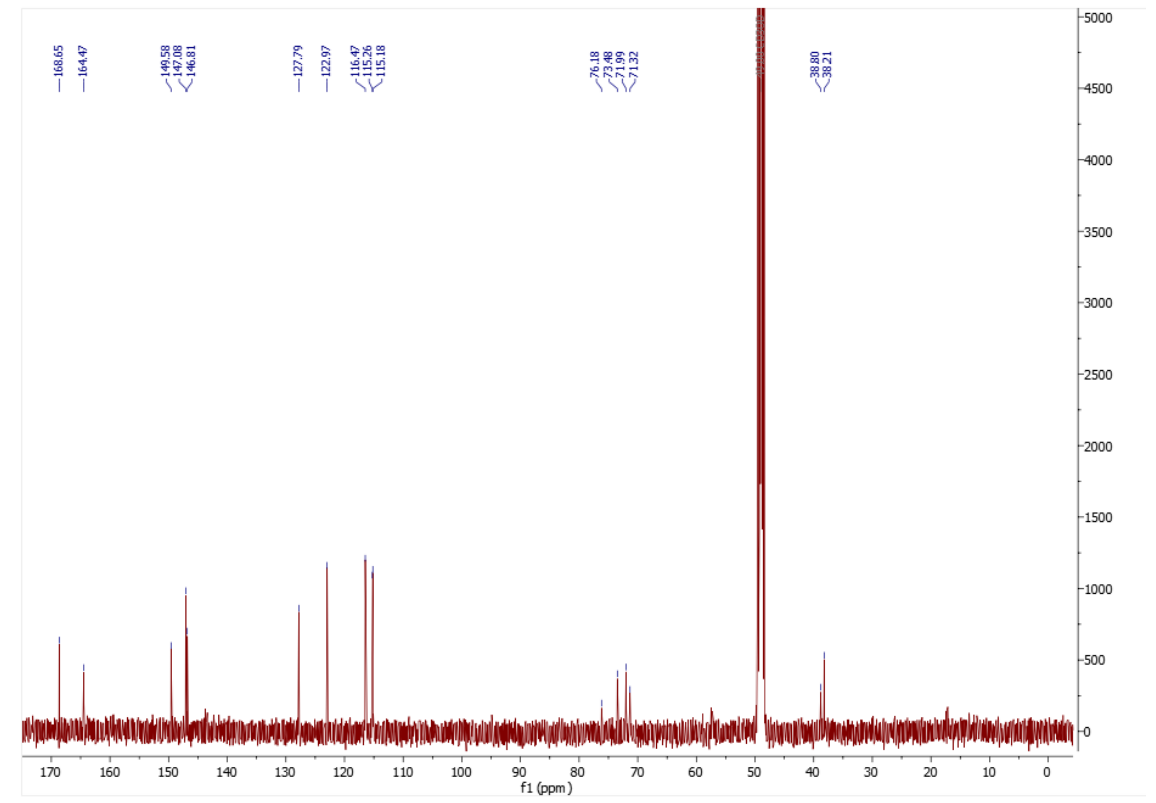


Figure B23. 13C NMR spectrum of 5.5.

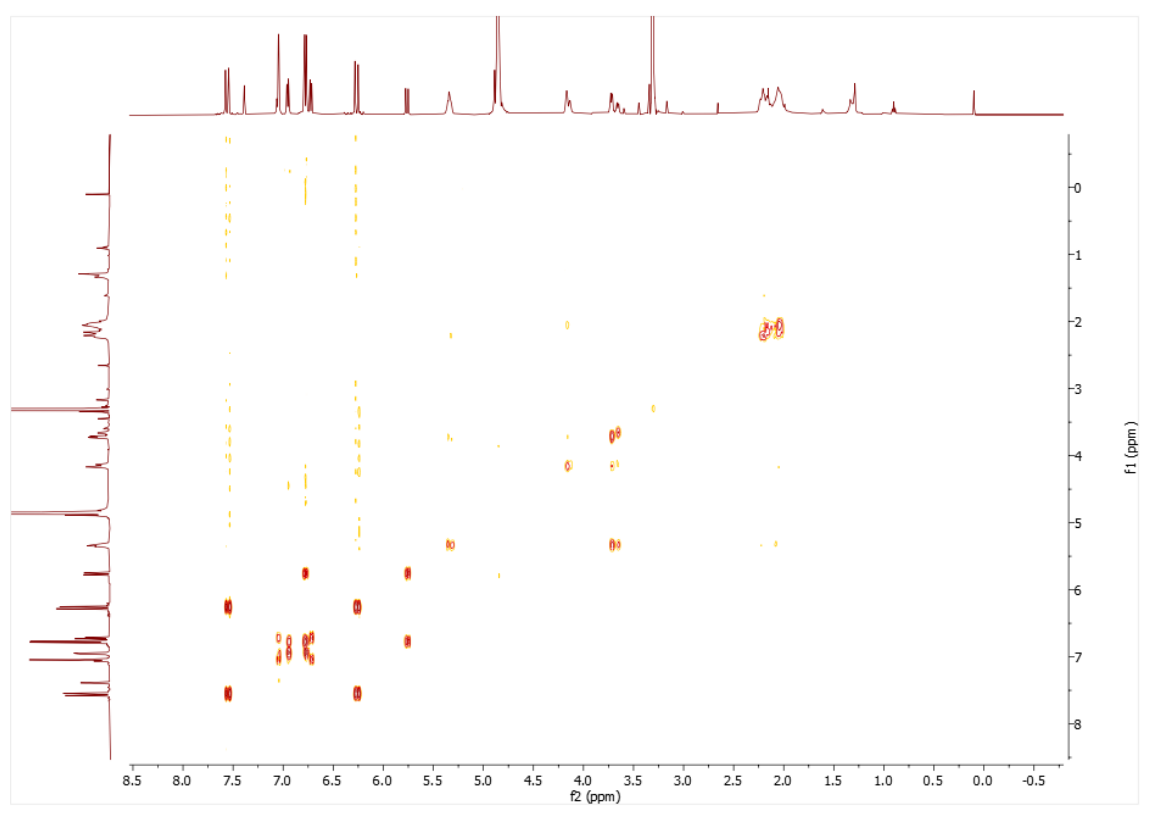
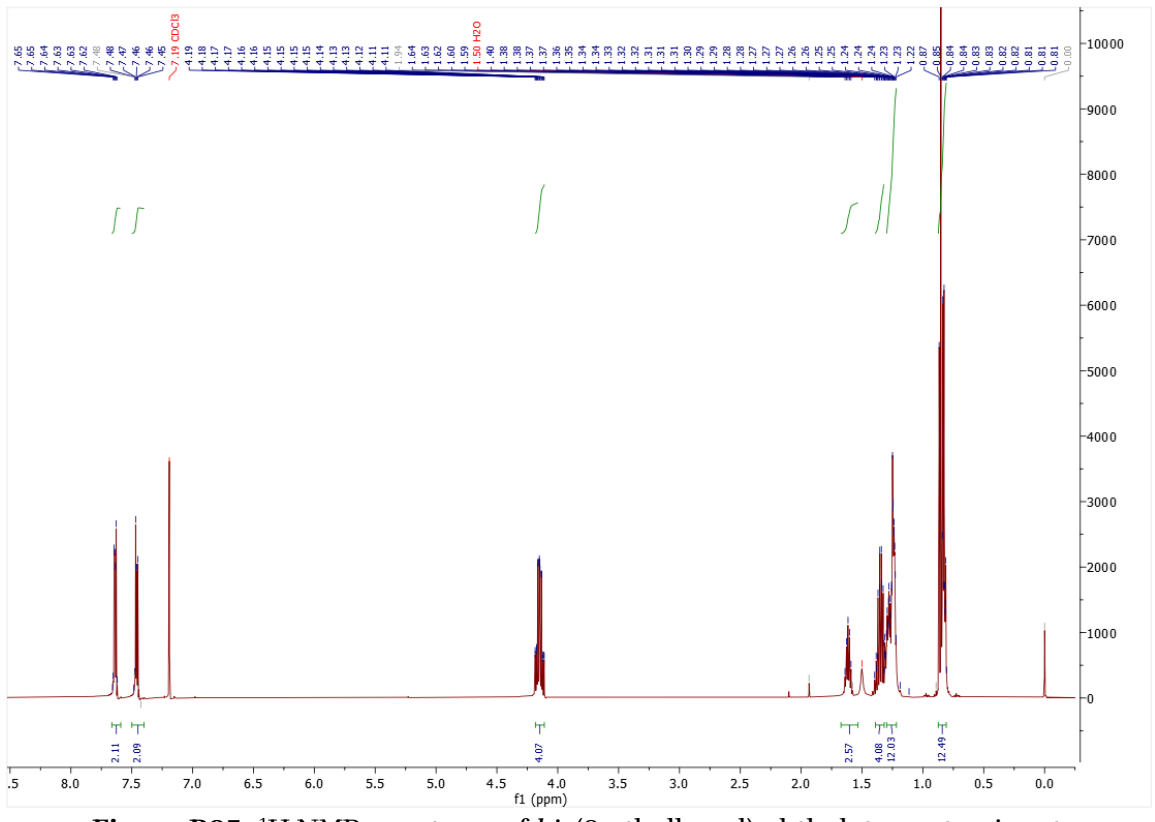


Figure B24. COSY NMR spectrum of 5.5.



**Figure B25.** <sup>1</sup>H NMR spectrum of *bis*(2-ethylhexyl) phthalate contaminant.

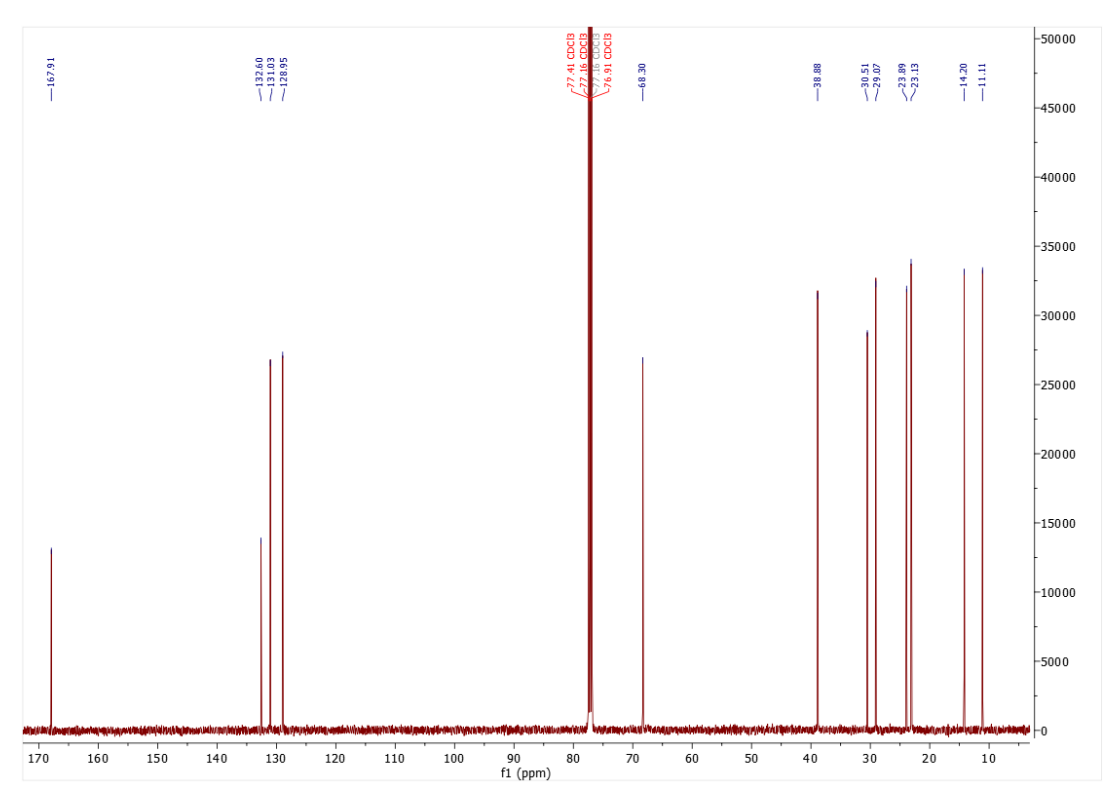
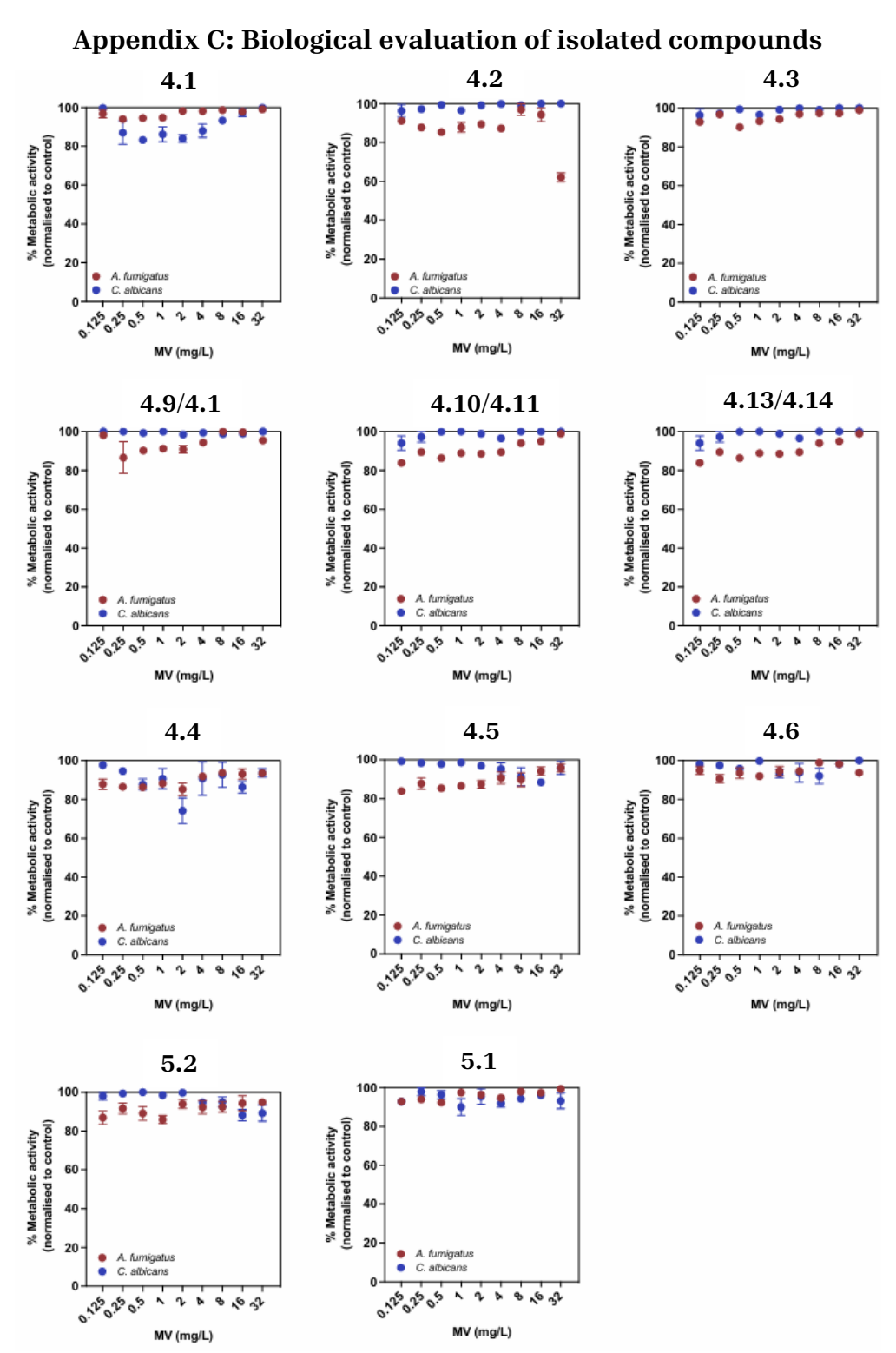
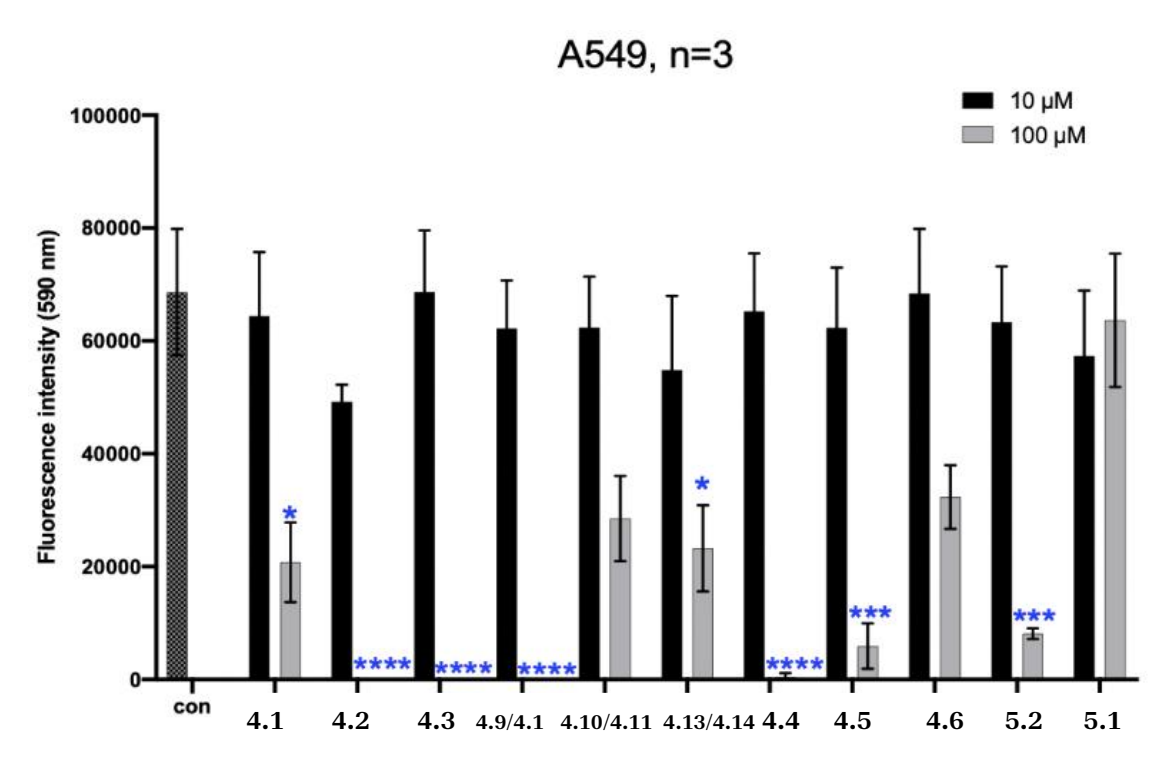


Figure B26.  $^{\rm 13}{\rm C}$  NMR spectrum of bis (2-ethylhexyl) phthalate contaminant.



**Figure C1.** Negative results for antifungal AlamarBlue assay against *A. fumigatus* and *C. albicans*.



**Figure C2.** AlamarBlue screening results for isolated compounds against A549 cells. All values are expressed as mean +/- standard deviation; n = 3; \*\*\*\* p < 0.0001, \*\*\* p < 0.001, \*\*p < 0.01 and \*p < 0.05 at each concentration point when compared to untreated control cells.

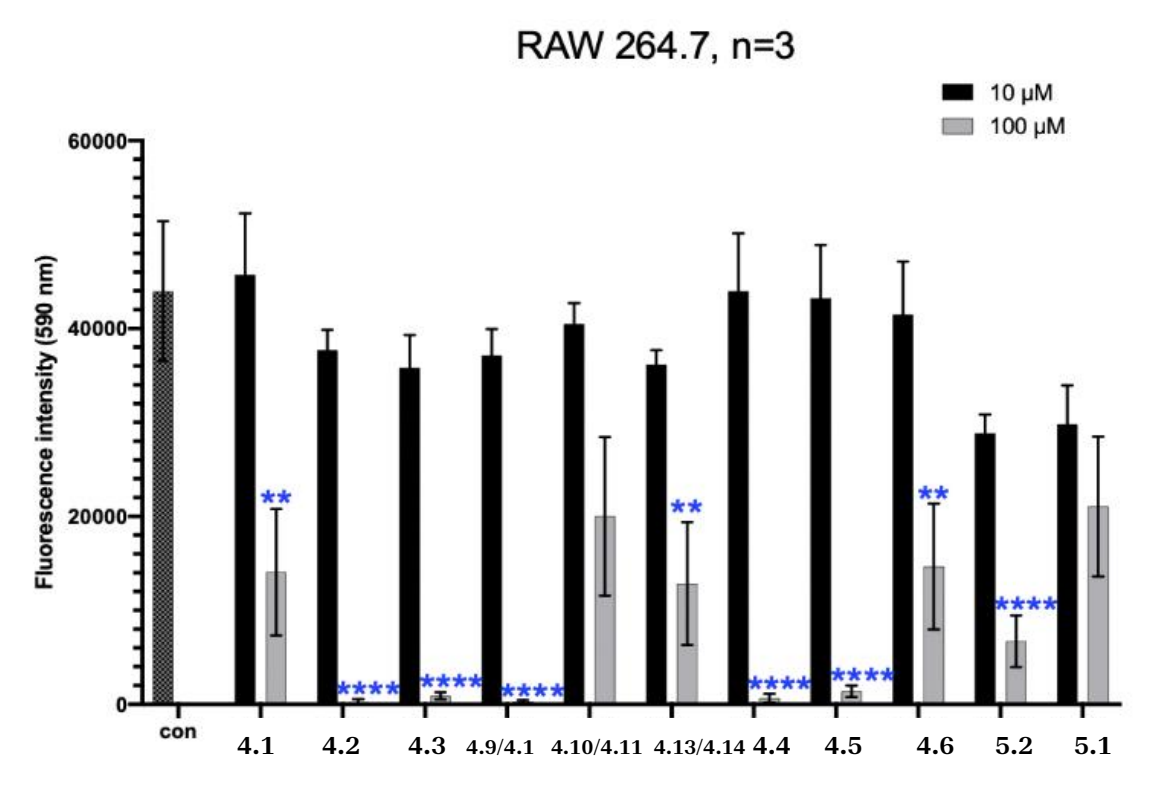


**Figure C3.** AlamarBlue screening results for isolated compounds against RAW 264.7 cells. All values are expressed as mean +/- standard deviation; n = 3; \*\*\*\* p < 0.0001, \*\*\* p < 0.001, \*\*p < 0.01 and \*p < 0.05 at each concentration point when compared to untreated control cells.

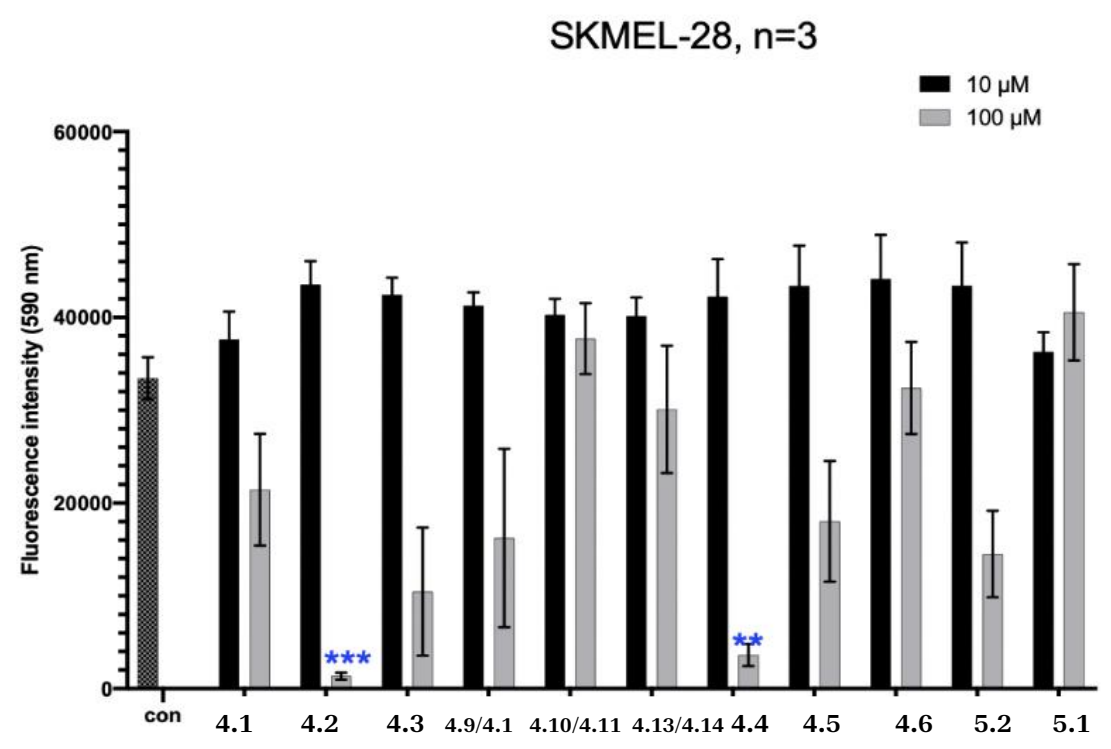


**Figure C4.** AlamarBlue screening results for isolated compounds against SKMEL-28 cells. All values are expressed as mean +/- standard deviation; n = 3; \*\*\*\* p < 0.0001, \*\*\* p < 0.001, \*\*\* p < 0.001 and \*p < 0.05 at each concentration point when compared to untreated control cells.

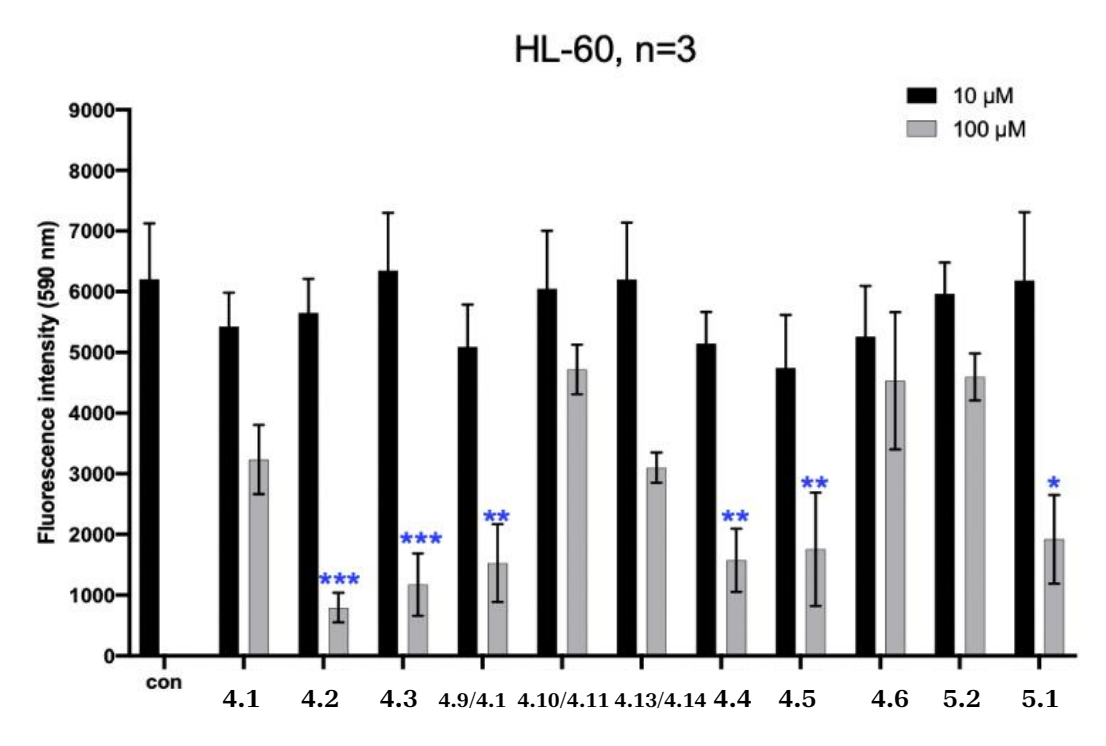


**Figure C5.** AlamarBlue screening results for isolated compounds against HL-60 cells. All values are expressed as mean +/- standard deviation; n = 3; \*\*\*\* p < 0.0001, \*\*\* p < 0.001, \*\*p < 0.01 and \*p < 0.05 at each concentration point when compared to untreated control cells.

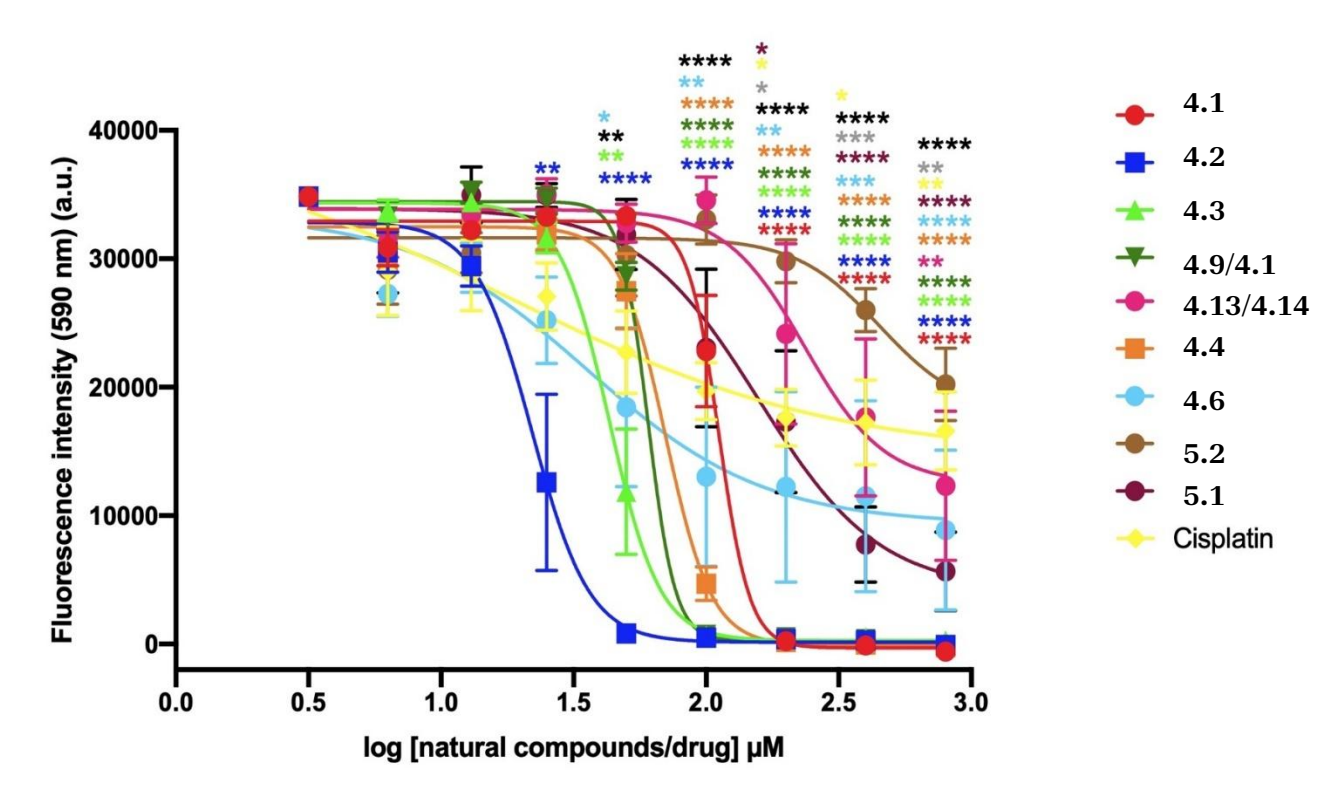


**Figure 6C.** Dose-response curves of compounds against A549 lung cancer cells in comparison to cisplatin. All values are expressed as mean +/- standard deviation; n = 3; \*\*\*\* p < 0.0001, \*\*\* p < 0.001, \*\*p < 0.01 and \*p < 0.05 at each concentration point when compared to untreated control cells.





Communication

## Caudiquinol: A Meroterpenoid with an Intact C20 Geranylgeranyl Chain Isolated from Garcinia caudiculata

Maya Valmiki 1, Stephen Ping Teo 200, Pedro Ernesto de Resende 300, Simon Gibbons 400 and A. Ganesan 1,\*00

- School of Pharmacy, University of East Anglia, Norwich Research Park, Norwich NR4 7TJ, UK; m,valmiki@uea.ac.uk
- Forest Department Sarawak Headquarters, Medan Raya, Petra Jaya, Kuching 93050, Sarawak, Malaysia; stephetp@sarawak.gov.my
- The John Innes Centre, Norwich Research Park, Norwich NR4 7UH, UK; pedro.de-resende@jic.ac.uk
- <sup>4</sup> Natural and Medical Sciences Research Center, University of Nizwa, PC 616, Birkat Al-Mauz, Nizwa P.O. Box 33, Oman; simon@unizwa.edu.om
- \* Correspondence: a.ganesan@uea.ac.uk

Abstract: The tropical Garcinia genus of flowering plants is a prolific producer of aromatic natural products including polyphenols, flavonoids, and xanthones. In this study, we report the first phytochemical investigation of Garcinia caudiculata Ridl. from the island of Borneo. Fractionation, purification, and structure elucidation by MS and NMR resulted in the discovery of two meroterpenoids. One was a benzofuranone lactone previously isolated from Iryanthera grandis and Rhus chinensis, and the second was a new hydroquinone methyl ester that we named caudiquinol. Both natural products are rare examples of plant meroterpenoids with an intact geranylgeranyl chain.

Keywords: natural products; meroterpenoids; hydroquinones; Garcinia species



Citation: Valmiki, M.; Teo, S.P.; de Resende, P.E.; Gibbons, S.; Ganesan, A. Caudiquinol: A Meroterpenoid with an Intact C20 Geranylgeranyl Chain Isolated from Garcinia caudiculata. Molecules 2024, 29, 3613. https:// doi.org/10.3390/molecules29153613

Academic Editors: Radosław Kowalski and Tomasz Baj

Received: 18 June 2024 Revised: 29 July 2024 Accepted: 29 July 2024 Published: 31 July 2024



Copyright: © 2024 by the authors. Licensee MDPI, Basel, Switzerland. This article is an open access article distributed under the terms and conditions of the Creative Commons Attribution (CC BY) license (https:// creativecommons.org/licenses/by/ 4.0/).

#### 1. Introduction

The Garcinia genus of saptrees within the Clusiaceae family comprises several hundred species of flowering shrubs and trees that are widely distributed in tropical regions around the world [1]. In addition to producing edible fruit, such as the mangosteen from Garcinia mangostana, Garcinia species are a prolific source of biologically active secondary metabolites, including polyphenols, flavonoids, and xanthones [2–4]. Within this genus, Ridley classified the bunau tree found on the island of Borneo as a new species, G. caudiculata, nearly a century ago [5]. However, no phytochemical investigations have appeared until the present work, where we report two meroterpenoids with a geranylgeranyl sidechain: the benzofuranone lactone 1 (Figure 1), previously isolated from two other plant genera, and a new quinol 2 that was given the name caudiquinol.

Figure 1. Benzofuranone (1) and caudiquinol (2), geranylgeranyl meroterpenoids isolated from Garcinia caudiculata.

Molecules 2024, 29, 3613. https://doi.org/10.3390/molecules29153613

https://www.mdpi.com/journal/molecules

Molecules 2024, 29, 3613 2 of 5

#### 2. Results

Leaves of *G. caudiculata* Ridl. were collected from Lundu, Sarawak, Malaysia, and air-dried before being ground into a powder and extracted with dichloromethane. In a minimum inhibitory concentration (MIC) antibacterial assay, the crude extract was active against methicillin-susceptible *Staphylococcus aureus* (MSSA) 25923 at a level of 128 μg/mL. A portion of this extract of 5 g was subjected to vacuum liquid chromatography (VLC), eluting with a gradient of hexane/ethyl acetate (100:0 to 0:100) to provide 16 fractions. Upon evaporation, the most abundant yellow fractions 10 and 11, each containing ~0.5 g of residue, were selected for further purification. By recycling preparative HPLC, we ultimately obtained 7 mg of 1 from fraction 10 and 6 mg of 2 from fraction 11. Based on the spectroscopic and mass spectrometric data (Supporting Information), we assigned 1 as a benzofuranone lactone (Figure 1) with a C20 geranylgeranyl sidechain. This lactone was first identified in *Iryanthera grandis* of the Myristicaceae family [6] and later, in *Rhus chinensis* of the Anacardiaceae family [7]. It was the subject of a recent total synthesis due to its anti-HIV activity [8].

Compound 2 was isolated as a yellow oil with IR absorptions at 3387 and 1714 cm<sup>-1</sup> suggesting the presence of OH and C=O functional groups. The 1H and 13C NMR chemical shifts of 2 (Table 1) indicated a carbonyl group at  $\delta_C$  173.9, a tetrasubstituted aromatic benzene ring with two proton signals in a meta relationship at  $\delta_H$  6.50 and 6.41 (J = 3 Hz), and an unsaturated terpenoid chain with four double bonds and five methyl groups at  $\delta_C$ 16.2, 16.2, 16.3, 17.8, and 25.6. All these features were common to both 1 and 2. However, 2 uniquely contained a singlet at δ<sub>H</sub> 3.66 (3H) that correlated with a signal at δ<sub>C</sub> 52.5. Furthermore, the pseudo-molecular ion of m/z 455.316 observed in the positive-mode ESI MS of 2 was higher than that of 1 by 32 Da. We concluded that the two natural products differed by the addition of a methoxy group. Since the geranylgeranyl moiety and the two aromatic protons within 1 were preserved in 2, we deduced that the methoxy group was attached as either a phenolic ether or as an ester of the ring-opened lactone. In the HMBC spectrum (Supporting Information), an absence of correlations between the methoxy group and the aromatic ring ruled out the ether structures. Meanwhile, a 3J coupling observed between the methyl group and the carbonyl (Figure 2) enabled us to conclusively elucidate 2 as the methyl ester that we named caudiquinol.

Table 1. 1H NMR (500 MHz) and 13C NMR (126 MHz) data for compound 2 in CDCl<sub>3</sub>.

Position	δ <sub>C</sub> , Type	δ <sub>H</sub> , Type
1	147.0, C	
2	121.5, C	
3	115.0, CH	6.50, d
4	149.0, C	
5	115.9, CH	6.41, d
6	131.3, C	
7	29.2, CH <sub>2</sub>	3.27, d
8	121.6, CH	5.20-5.25, m
9	138.0, C	
10	37.2, CH <sub>2</sub>	1.90-2.02, m
11	26.5, CH <sub>2</sub>	1.90-2.02, m
12	123.9, CH	5.00-5.09, m
13	135.3, C	
14	39.69, CH <sub>2</sub>	1.90-2.02, m
15	26.6, CH <sub>2</sub>	1.90-2.02, m
16	124.2, CH	5.00-5.09, m
17	135.0, C	
18	39.73, CH <sub>2</sub>	1.90-2.02, m
19	26.7, CH <sub>2</sub>	1.90-2.02, m
20	124.4, CH	5.00-5.09, m

Molecules 2024, 29, 3613 3 of 5

-		-	
Tabl	0	(792	۰

Position	δ <sub>C</sub> , Type	δ <sub>H</sub> , Type
21	130.6, C	
22	25.6, CH <sub>3</sub>	1.54, s
1'	39.75, CH <sub>2</sub>	3.53, s
2'	173.9, C	
3'	52.5, CH <sub>3</sub>	3.66, s
1"	16.3, CH <sub>3</sub>	1.66, s
2"	16.2, CH <sub>3</sub>	1.61, s
3""	16.2, CH <sub>3</sub>	1.54, s
4"	17.8, CH <sub>3</sub>	1.54, s
		The state of the s

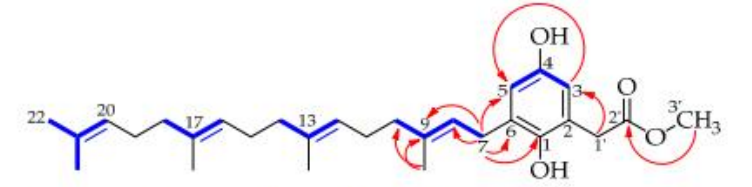


Figure 2. Observed COSY (blue; bold) and HMBC (red arrows) correlations in caudiquinol.

#### 3. Discussion

The lactone versus methyl ester relationship between meroterpenoids 1 and 2 was precedented by a shorter C10 geranyl sidechain by the pair of natural products denudalide (3) and denudaquinol (4) (Figure 3) isolated from fruits of *Magnolia denudata* of the Magnoliaceae family [9]. Although denudalide could give rise to denudaquinol, in principle, by methanolic hydrolysis, the authors could not demonstrate this conversion in the laboratory. Similarly, given our mild HPLC conditions (aq MeOH; pH 7; rt), we believe that caudiquinol is an authentic natural product.

Figure 3. The geranyl meroterpenoids denudalide (3) and denudaquinol (4).

Meroterpenoids that contain units larger than the simple C5 prenyl (dimethylallyl) group typically undergo further transformations, such as oxidation or cyclization, whereas 1–4 feature unmodified C10 or C20 sidechains. The discovery of 1–4 from four different tree families suggests a common biosynthetic pathway to such meroterpenoids within the plant kingdom, and that congeners with an intermediate C15 sidechain are also likely to be found in nature. Furthermore, in addition to 1 and 2, we are aware of only four other meroterpenoids (5–8 (Figure 4)) of plant origin with an intact C20 geranylgeranyl unit [7,10–12].

Purified 1 and 2 were inactive against seven Gram-positive bacterial strains assayed (MSSA 25923, methicillin-resistant *S. aureus* (MRSA) 13373, SA XU212, SA 1199B, SA RN4220, *Enterococcus faecalis* 12967, and *E. faecalis* 51299) with MIC values of >250  $\mu$ M or against the A549 lung cancer cell line at 100  $\mu$ M. We did not have access to the HIV virus or the SFME cell line against which 1, 3, and 4 were reported to be active. We conclude the original antibiotic activity of the crude extract arises from other components within the mixture.

Molecules 2024, 29, 3613 4 of 5

Figure 4. Plant meroterpenoids, other than 1 and 2, with an intact geranylgeranyl sidechain.

### 4. Materials and Methods

General experimental procedures: Vacuum liquid chromatography (VLC) was performed using dry silica gel 60 PF $_{254+366}$  (Merck, London, UK). LC-QToF-MS/MS data were acquired using an Agilent (Santa Clara, CA, USA) 6546 Quadrupole/Time-of-Flight (Q-ToF) mass spectrometer with 1290 UHPLC, equipped with a Phenomenex Kintex C $_{18}$  column (100 × 2.1 mm, 2.6 µm, 100 Å) using deionized H $_2$ O/MeCN (95:5 to 5:95 gradient with 0.1% HCO $_2$ H over 5 min 50 s) eluent mixture. Preparative HPLC was performed using a recycling LaboACE LC-5060 series HPLC instrument fitted with a C18 column (20 × 500 mm, 10 µm, 120 Å) (JAI, Tokyo, Japan) and a flow rate of 10 mL/min. One- and two-dimensional (1D and 2D) NMR spectra were recorded with a 500 MHz spectrometer (Bruker, Billerica, MA, USA) using a chloroform-d solvent. The spectra were processed using the MestReNova 14.1 software. UV–visible absorption spectra were recorded with a Perkin Elmer (Shelton, CT, USA) UV/Vis Lambda 365 spectrophotometer. IR absorbance spectra were recorded with a Perkin Elmer FT-IR System Spectrum BX.

Plant material: Leaves of Garcinia caudiculata Ridl. were collected at Lundu, Sarawak, Malaysia (1°37′15″ N, 109°45′57″ E). The samples were taxonomically identified by one of the authors, Stephen Ping Teo, and deposited as a voucher specimen STP86 at the Forest Herbarium (SAR), the Forest Department Sarawak. The leaves were air-dried and ground into a fine powder before storage.

Extraction and isolation: The dry, powdered leaves (100 g) were extracted by macerating them with  $CH_2Cl_2$  at room temperature (1 L  $\times$  3 times for 24 h each). The extracts were filtered, and the supernatant was concentrated under reduced pressure at 40 °C to obtain the combined crude extract (10 g). Half of the crude extract (5 g) was separated using VLC via silica gel into 16 fractions using a mixture of two solvents (hexane and ethyl acetate) of increasing polarity. Of these, fractions 10 (554 mg) and 11 (459 mg), eluted with 50% and 30% hexane, respectively, were purified by preparative HPLC, using 1 mL volume injections. Fraction 10 was injected at 10 mg/mL and was eluted using 100% MeOH to yield compound 1 (7.4 mg). Fraction 11 was injected at 12 mg/mL and eluted using a gradient of deionized  $H_2O/MeOH$  of 20%:80% for 10 min followed by a linear gradient reaching 100% MeOH at 15 min to yield caudiquinol 2 (6.0 mg).

Molecules 2024, 29, 3613 5 of 5

Methyl 3-[(2E, 6E, 10E, 14E)-3,7,11,15-tetramethyl-2,6,10,14-hexadecatetraen-1-yl]-2,5-dihydroxybenzeneacetate (caudiquinol 2). 6.0 mg; yellow oil; UV  $\lambda_{max}$  (MeOH): 220, 232, and 294 nm; IR: 3387, 2914, 1714, and 1435 cm<sup>-1</sup>; m/z 455.316 [M + H]<sup>+</sup> (calcd. for C<sub>29</sub>H<sub>43</sub>O<sub>4</sub>; 455.316; Δ = 0 ppm); <sup>1</sup>H NMR (500 MHz): δ 6.50 (d, J = 3.1 Hz, 1H), 6.41 (d, J = 3.1 Hz, 1H), 5.20–5.25 (m, 1H), 5.00–5.09 (m, 3H), 3.66 (s, 3H), 3.53 (s, 2H), 3.27 (d, J = 7.0 Hz, 2H), 1.90–2.02 (m, 12H), 1.66 (s, 3H), 1.61 (s, 3H), and 1.53 (s, 9H). <sup>13</sup>C NMR (126 MHz): δ 173.9, 149.0, 147.0, 138.0, 135.3, 135.0, 131.3, 130.6, 124.4, 124.2, 123.9, 121.5, 121.6, 115.9, 115.0, 52.5, 39.75, 39.73, 39.69, 37.2, 29.2, 26.7, 26.6, 26.5, 25.6, 17.8, 16.3, 16.20, and 16.15.

Supplementary Materials: The following supporting information can be downloaded at https://www.mdpi.com/article/10.3390/molecules29153613/s1. Characterization data for 1 and 2 comprising NMR, MS, IR, and UV spectra.

Author Contributions: Conceptualization, S.P.T., S.G. and A.G.; methodology, all; investigation, M.V.; resources, S.P.T., S.G. and A.G.; data curation, M.V.; writing—original draft preparation, A.G.; writing—review and editing, M.V., S.P.T., P.E.d.R., S.G. and A.G.; visualization, M.V.; supervision, P.E.d.R., S.G. and A.G.; project administration, S.P.T., P.E.d.R., S.G. and A.G.; funding acquisition, S.P.T., S.G. and A.G. All authors have read and agreed to the published version of the manuscript.

Funding: This research received no external funding. We thank the University of East Anglia for awarding a studentship to M.V.

Institutional Review Board Statement: Not applicable.

Informed Consent Statement: Not applicable.

Data Availability Statement: The data are contained within this article and the Supplementary Materials.
Conflicts of Interest: The authors declare no conflicts of interest.

## References

- Garcinia L. Plants of the World Online. Available online: https://powo.science.kew.org/taxon/urn:lsid:ipni.org:names:19345-1 (accessed on 24 May 2024).
- Espirito Santo, B.L.S.D.; Santana, L.F.; Kato Junior, W.H.; de Araújo, F.O.; Bogo, D.; Freitas, K.C.; Guimarães, R.C.A.; Hiane, P.A.; Pott, A.; Filiú, W.F.O.; et al. Medicinal Potential of *Garcinia* Species and Their Compounds. *Molecules* 2020, 25, 4513. [CrossRef] [PubMed]
- Brito, L.C.; Marques, A.M.; da Camillo, F.C.; Figueiredo, M.R. Garcinia Spp: Products and by-products with potential pharmacological application in cancer. Food Biosci. 2022, 50, 102110. [CrossRef]
- Nchiozem-Ngnitedem, V.-A.; Mukavi, J.; Omosa, L.K.; Kuete, V. Phytochemistry and antibacterial potential of the genus Garcinia. In Advances in Botanical Research; Kuete, V., Ed.; Academic Press: London, UK, 2023; Volume 107, pp. 105–175.
- Ridley, H.N. Additions to the Flora of Borneo and Other Malay Islands: VI. Bull. Misc. Inf. (Royal Gardens Kew) 1938, 1938, 110–123.
   [CrossRef]
- Vieira, P.C.; Gottlieb, O.R.; Gottlieb, H.E. Tocotrienols from Iryanthera grandis. Phytochemistry 1983, 22, 2281–2286. [CrossRef]
- Gu, Q.; Wang, R.R.; Zhang, X.M.; Wang, Y.H.; Zheng, Y.T.; Zhou, J.; Chen, J.J. A New Benzofuranone and Anti-HIV Constituents from the Stems of Rhus chinensis. Planta Med. 2007, 73, 279–282. [CrossRef] [PubMed]
- Li, T.Z.; Geng, C.A.; Chen, J.J. First total synthesis of rhuscholide A, glabralide B and denudalide. Tetrahedron Lett. 2019, 60, 151059.
   [CrossRef]
- Noshita, T.; Kiyota, H.; Kidachi, Y.; Ryoyama, K.; Funayama, S.; Hanada, K.; Murayama, T. New Cytotoxic Phenolic Derivatives from Matured Fruits of Magnolia denudata. Biosci. Biotechnol. Biochem. 2009, 73, 726–728. [CrossRef] [PubMed]
- Reynolds, G.W.; Rodriguez, E. Prenylated hydroquinones: Contact allergens from trichomes of *Phacelia minor* and *P. parryi*. *Phytochemistry* 1981, 20, 1365–1366. [CrossRef]
- Voutquenne, L.; Lavaud, C.; Massiot, G.; Sevenet, T.; Hadi, H.A. Cytotoxic polyisoprenes and glycosides of long-chain fatty alcohols from Dimocarpus fumatus. Phytochemistry 1999, 50, 63–69. [CrossRef] [PubMed]
- Rukachaisirikul, V.; Kamkaew, M.; Sukavisit, D.; Phongpaichit, S.; Sawangchote, P.; Taylor, W.C. Antibacterial Xanthones from the Leaves of Garcinia nigrolineata. J. Nat. Prod. 2003, 66, 1531–1535. [CrossRef] [PubMed]

Disclaimer/Publisher's Note: The statements, opinions and data contained in all publications are solely those of the individual author(s) and contributor(s) and not of MDPI and/or the editor(s). MDPI and/or the editor(s) disclaim responsibility for any injury to people or property resulting from any ideas, methods, instructions or products referred to in the content.